UNITED STATES DEPARTMENT OF THE INTERIOR

GEOLOGICAL SURVEY

NATIONAL EARTHQUAKE HAZARDS REDUCTION PROGRAM, SUMMARIES OF TECHNICAL REPORTS VOLUME XXIX

Prepared by Participants in

NATIONAL EARTHQUAKE HAZARDS REDUCTION PROGRAM

December 1989

OPEN-FILE REPORT 90-54

Menlo Park, California

1989

DIRECTIONS FOR PREPARATION OF REPORTS

1. Use 8 1/2 x 11" paper for both text and figures.
2. Leave at least 1" margins at top, sides and bottom.
3. Type all text single-spaced.
4. Type only on one side of the paper.
5. Draft figures in black ink (color, weak or grey lines will not photo-reproduce) and make them simple and legibly lettered.
6. Type figure captions on the same page as the figure.
7. Please do not use staples.
8. Do not number pages.
9. Send original copies of text and figures. Do not send xerox copies as they do not photo-reproduce clearly. Do not send oversize photos. They should be able to be placed on regular sized paper and the caption must fit under it.
10. Do not type headings such as "Technical Report" or "Summary".
11. Do not use scotch tape. Use paste.
12. If you use photographs please send a glossy print of each.

UNITED STATES
DEPARTMENT OF THE INTERIOR
GEOLOGICAL SURVEY

NATIONAL EARTHQUAKE HAZARDS REDUCTION PROGRAM, SUMMARIES OF TECHNICAL REPORTS VOLUME XXIX

Prepared by Participants in

NATIONAL EARTHQUAKE HAZARDS REDUCTION PROGRAM

Compiled by

Muriel L. Jacobson

The research results described in the following summaries were submitted by the investigators on October 13, 1989 and cover the period from April 1, 1989 through October 1, 1989. These reports include both work performed under contracts administered by the Geological Survey and work by members of the Geological Survey. The report summaries are grouped into the five major elements of the National Earthquake Hazards Reduction Program.

Open File Report No. 90-54

The data and interpretations in these progress reports may be reevaluated by the investigators upon completion of the research. Readers who wish to cite findings described herein should confirm their accuracy with the author.

CONTENTS

Earthquake Hazards Reduction Program

Southern California Seismic Arrays

Cooperative Agreement No. 14-08-0001-A0613

Clarence R. Allen and Robert W. Clayton
Seismological Laboratory, California Institute of Technology
Pasadena, California 91125 (818-356-6912)

Investigations

This semi-annual Technical Report Summary covers the six-month period from 1 April 1989 to 30 September 1989. The Cooperative Agreement's purpose is the partial support of the joint USGS-Caltech Southern California Seismographic Network, which is also supported by other groups, as well as by direct USGS funding to its own employees at Caltech. According to the Agreement, the primary visible product will be a joint Caltech-USGS catalog of earthquakes in the southern California region; quarterly epicenter maps and preliminary catalogs have been submitted as due during the Agreement period. About 250 preliminary catalogs are routinely distributed to interested parties.

Results

During the reporting period, the joint Caltech-USGS Southern California Seismographic Network located 5,145 events (Fig. 1), including 62 of magnitude 3.0 and larger. Five of these were of magnitude 4.0 or larger. The most significant events were:

(1) On 4 April, a ML 4.5 event appears to have been centered on the Newport-Inglewood fault beneath Newport Beach. It showed a pure strike-slip focal mechanism, with the dextral movement plane parallel to the strike of the Newport-Inglewood fault. The event occurred only 1 to 2 km south of the estimated epicenter of the ML 6.3 Long Beach earthquake of 1933.

(2) An ML 4.5 shock occurred on 4 June near the Lenwood fault about 40 km southeast of Barstow in the Mojave Desert, followed by 6 aftershocks. These events occurred about 50 km west-northwest of the 1979 Homestead Valley sequence (ML 5.2, 5.0, 4.8).

(3) On 12 June, two earthquakes of ML 4.4 and 4.1 near Montebello created significant public interest throughout the Los Angeles area. Both focal mechanisms represented thrusts, indicating that the events were probably associated with the east-trending Elysian Park fold and thrust system. The two events were located about 5 km southwest of the 1987 Whittier Narrows earthquake but had approximately the same depth of 14-15 km. Since the thrust system is thought to dip north, it is unlikely that the same fault strand was responsible. Twenty small aftershocks of the Montebello events occurred over the following two weeks, and three small events also occurred on the nearby Raymond fault within 5 days of the events. Movement on the Raymond fault probably caused the ML 4.9 shock on 3 December 1988--the so-called "Rose Bowl earthquake."

(4) On 12 August and 15 September, ML 3.0 and ML 3.6 events occurred very near the San Andreas fault in Cajon Pass, northwest of San Bernardino, and both events showed reverse-fault focal mechanisms. These events occurred in the same area as the 1970 Lytle Creek earthquake, of ML 5.4.

Aside from the above events, seismicity in the southern California region was relatively low for the entire 6-month reporting period. In particular, only 598 locatable earthquakes occurred during July, compared to a long-term monthly average of 800 to 1000 shocks. Activity in the Los Angeles basin continued with only a minor enhancement in the number of small events, whereas since March 1986, this area has experienced about three times its normal level of activity. It remains to be seen whether this July slow-down represents an end to the episode of markedly increased activity in the Los Angeles basin.

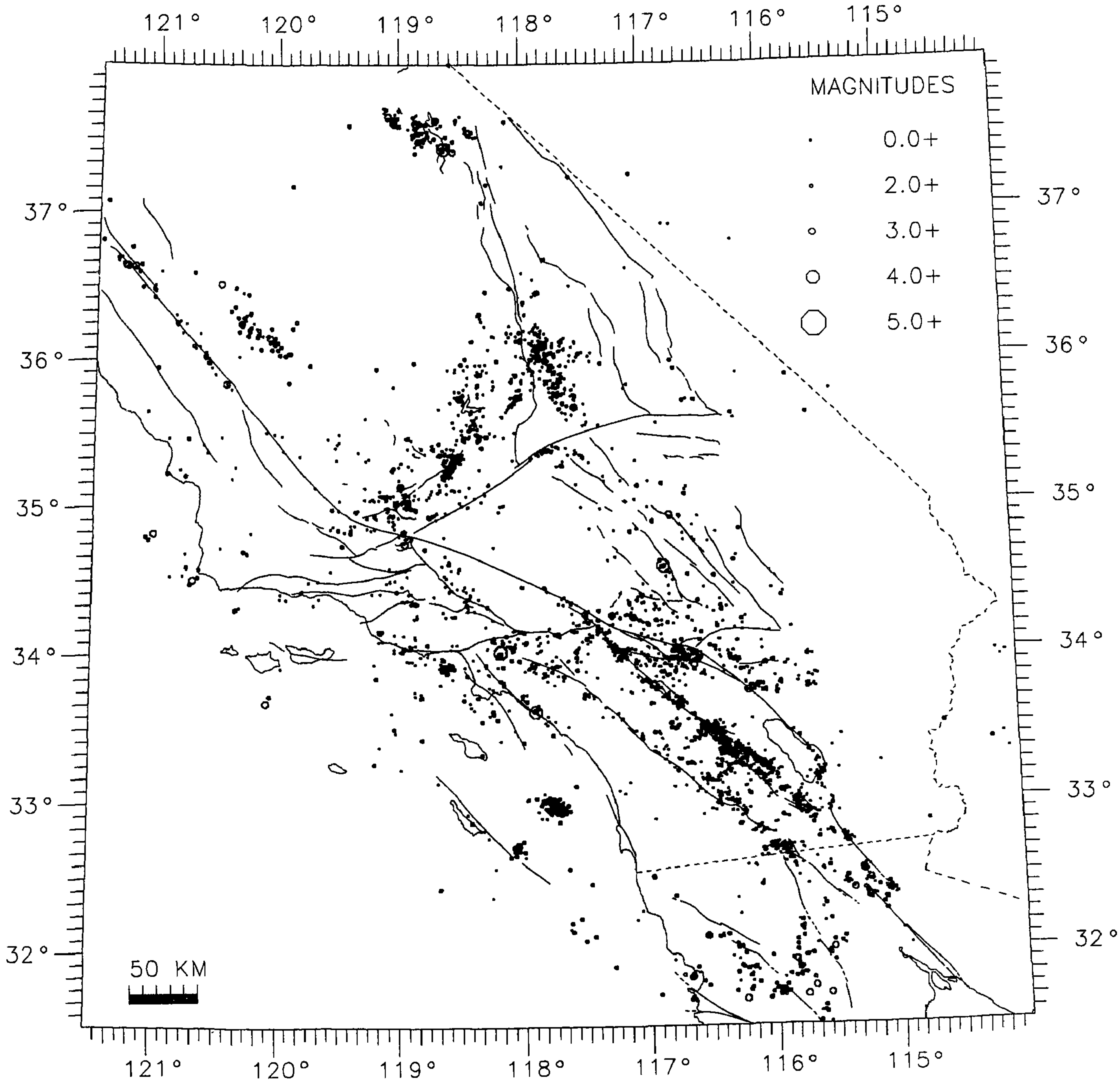

Fig. 1.--Map of epicenters of earthquakes in the southern California region, 1 April 1989 to 30 September 1989.

Regional Seismic Monitoring Along The Wasatch Front Urban Corridor And Adjacent Intermountain Seismic Belt

14-08-0001-A0621

W. J. Arabasz, R.B. Smith, J.C. Pechmann, and S. J. Nava
Department of Geology and Geophysics
University of Utah
Salt Lake City, Utah 84112
(801) 581-6274

Investigations

This cooperative agreement supports "network operations" associated with the University of Utah's 80-station regional seismic telemetry network. USGS support focuses on the seismically hazardous Wasatch Front urban corridor of north-central Utah, but also encompasses neighboring areas of the Intermountain seismic belt. Primary products for this USGS support are quarterly earthquake catalogs and a semi-annual data submission, in magnetic-tape form, to the USGS Data Archive.

During the report period, significant efforts were made in: (1) ongoing *in situ* calibration of remote telemetry stations, including seven stations recently upgraded to four-component recording (high- and low-gain vertical components and high-gain horizontal components); (2) development of a major initiative to the Utah state legislature for modernizing seismic-network instrumentation in Utah as part of a state-federal partnership; and (3) installation and operation of two temporary telemetered seismograph stations in and around the source zone of an M_L4.8 earthquake in the Blue Springs Hills of north-central Utah.

Results

Network Seismicity: April 1, 1989 - September 30, 1989

Figure 1 shows the epicenters of 477 earthquakes ($M_L \leq 4.8$) located in part of the University of Utah study area designated the "Utah region" (lat. 36.75°-42.5°N, long. 108.75°-114.25°W) during the six-month period April 1, 1989 to September 30, 1989. The seismicity sample includes 15 shocks of magnitude 3.0 or greater (labeled with date and magnitude on Figure 1) and 13 felt earthquakes.

The largest earthquake during the six-month report period was a shock of M_L4.8 on July 3 at 22:44 UTC, located 16 km W of Tremonton, Utah, in the Blue Springs Hills. The earthquake was felt throughout north-central Utah with a maximum Modified Mercalli intensity of V (USGS, PDE No.27-89). Ten foreshocks for this earthquake were recorded during the two-week period preceding the main shock (Figure 2). The largest of these occurred occurred on June 21 at 21:54 UTC, and had an M_L of 4.1. Through September 30, 1989, 217 aftershocks were located in the Blue Springs Hills area, including 12 of magnitude 2.0 and larger. The largest aftershock, of M_L4.6, occurred on July 5 at 22:51

UTC and was widely felt in north-central Utah.

A preliminary focal mechanism for the Blue Springs Hills main shock indicates normal faulting with a right-lateral strike-slip component on a fault that dips moderately to the NE or, alternatively, normal faulting with a left-lateral strike-slip component on a fault that dips moderately to steeply to the WNW (Figure 3). The preliminary focal mechanism for the largest aftershock shows normal faulting on a fault that dips moderately in a direction that is either between WSW and WNW or between E and SE. The focal mechanism for the aftershock has a smaller strike-slip component of motion than the focal mechanism for the main shock. The T axes for both focal mechanisms trend approximately E-W. First motion data currently available for the largest foreshock match the first motion data for the main shock, but are inadequate to constrain the focal mechanism.

Other felt earthquakes in Utah of magnitude 3.0 or larger during the report period include: an M_L 3.1 event on April 9 at 11:24 UTC, felt in Tabiona; an M_c 3.7 event on May 1 at 18:35 UTC, felt in Santa Clara; and an M_L 3.7 event on July 23 at 10:39 UTC, felt in the Richfield area.

Reports and Publications

Nava, S. J., Utah earthquake activity, January through March, 1989, *Survey Notes (Utah Geological and Mineral Survey)*, v. 23, no. 1, p. 26, 1989.

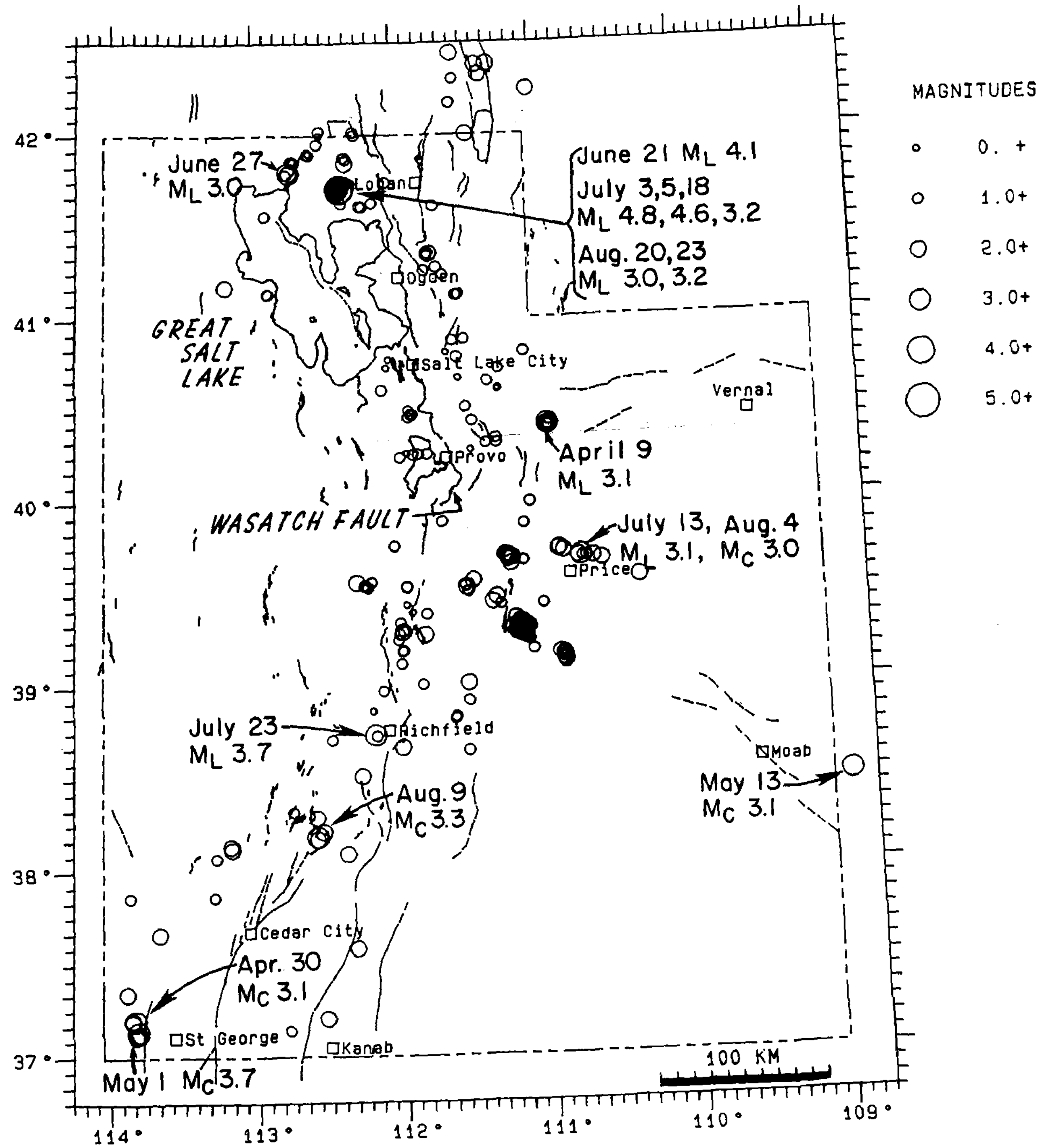

Figure 1. Utah Earthquake Activity, April 1, 1989, through September 30, 1989.

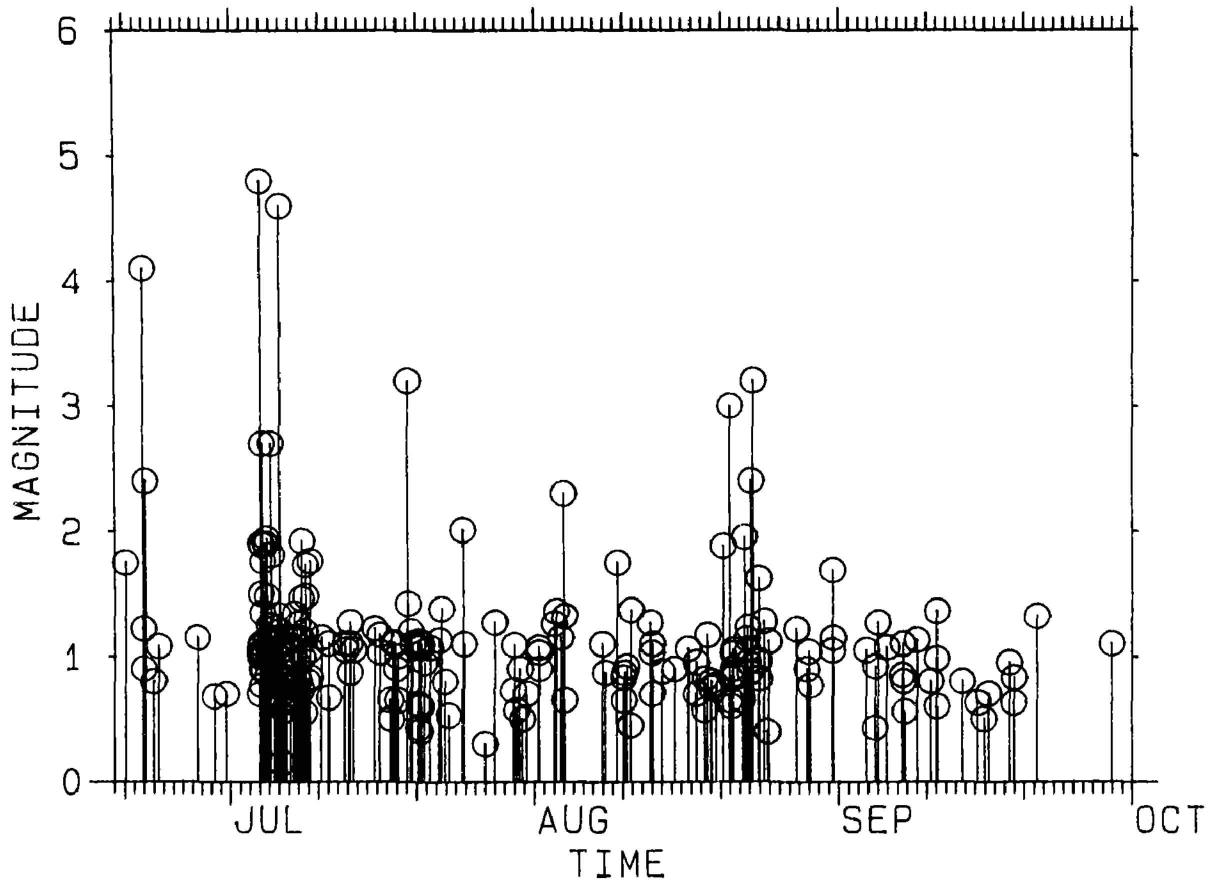

Figure 2. Magnitude as a function of time for the Blue Springs Hills, Utah, earthquake and its associated foreshocks and aftershocks (complete at least for $M_L \geq 2.0$). Ten foreshocks and 217 locatable aftershocks were recorded from June 20 through September 30, 1989.

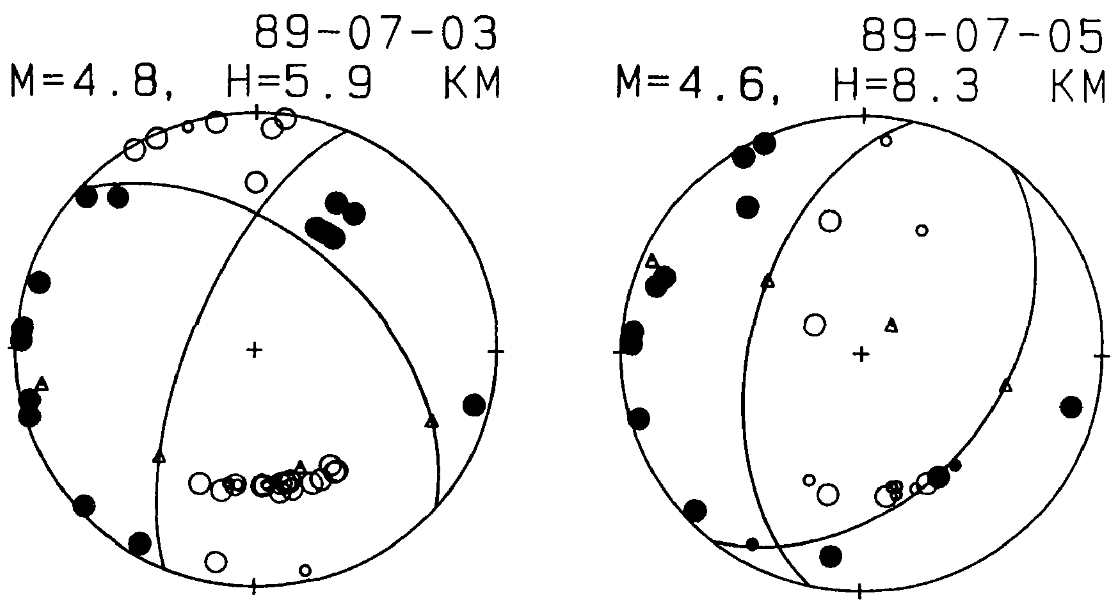

Figure 3. Preliminary focal mechanisms (lower hemisphere projections) for the Blue Springs Hills earthquake and its largest aftershock. Solid circles show compressions and open circles show dilatations, with the smaller circles indicating readings of lower confidence. The triangles represent slip vectors and P and T axes.

Regional Seismic Monitoring in Western Washington

14-08-0001-A0622
14-08-0001-A0623

R.S. Crosson
S.D. Malone
R.S. Ludwin
Geophysics Program
University of Washington
Seattle, WA 98195
(206) 543-8020

Investigations

Operation of the western portion of the Washington Regional Seismograph Network (WRSN) and routine preliminary analysis of earthquakes in western Washington are carried out under these contracts. Quarterly bulletins which provide operational details and descriptions of seismic activity in Washington and Northern Oregon are available from 1984 through the second quarter of 1989. Final catalogs are available from 1970, when the network began operation, though 1986. The University of Washington operates approximately 80 stations west of 120.5°W, 28 of which are supported under A0622, and 40 under A0623. This report includes a brief summary of significant seismic activity. Additional details are included in our Quarterly bulletins.

Excluding blasts, probable blasts, and earthquakes outside the U. W. network, 808 earthquakes west of 120.5°W were located between April 1 and September 30, 1989. Of these, 395 were located near Mount St. Helens, which has not erupted since October of 1986. Twelve earthquakes were felt in western Washington during the period covered by this report. East of 120.5°W 76 earthquakes were located, one of which was felt.

Notable seismicity and related phenomena during this reporting period includes 3 unusual episodes at Mt. St. Helens in late August, which lasted as long as 45 minutes (as recorded on the crater station helicorder record). These episodes consisted of complex signals containing slightly elevated levels of shallow seismicity accompanied by high-frequency background noise. These sequences left no surface deposits, such as might be expected from steam and ash emissions, rockfalls, or mudflows. After each episode, seismicity rapidly returned to background levels.

During the summer of 1989 two new seismic stations were installed on the west and northeast sides of Mt. Rainier to improve our location resolution for earthquakes on the volcano, and to investigate lahars on the flanks of the mountain caused by glacial outburst floods. This proved to be fortuitous timing, since on August 16 a significant rockfall (more than 1 million cubic meters) occurred on Mt. Rainier originating at Russell Cliff, and traveling 4 km down the Winthrop Glacier. We were able to accurately locate the rockfall and alert the Park Service on a day when bad weather and poor visibility prevented visual observation. We also recorded a small lahar on one of the newly installed stations in late September. Elsewhere in western Washington on June 18th a notable deep earthquake, magnitude 4.4, was widely felt in the Puget Basin and was located at a depth of 45 km beneath the Kitsap Peninsula.

In Oregon, a cluster of activity near the summit of Mt. Hood in August and September included over a dozen shallow (depth less than 10 km) earthquakes larger than magnitude 1.0. Five of these were magnitude 2.0 or larger, with the largest being a magnitude 3.5 on September 15. A similar sequence occurred in September, 1978 (Weaver et al., 1982). In Portland, Oregon a magnitude 3.8 earthquake was felt on August 1. Its depth was about 15 km, and it was followed immediately by one aftershock.

East of 120.5°W, a very interesting magnitude 4.5 earthquake, at 15 km depth occurred on May 9th in the North Cascades about 40 km southwest of Okanogan and was felt in Omak, Washington. This is the largest earthquake we have located in this area since beginning instrumental recording in 1970. Very little seismicity is seen in the North Cascades, although it is believed to be the source region for the 1872 earthquake, the largest earthquake known to have occurred in Washington or Oregon.

Publications

Havskov, J., S. Malone, D. McClurg, and R.S. Crosson, 1989, Coda Q for the state of Washington, BSSA, V. 79, pp. 1024-1038.

Ludwin, R. S., S.D. Malone, R.S. Crosson, A.I. Qamar, 1989 (in press), Washington Earthquakes 1985, in U.S. Earthquakes, National Earthquake Information Service.

Ludwin, R. S., S.D. Malone, R.S. Crosson, A.I. Qamar, 1989 (in press), Washington Earthquakes 1986, in U.S. Earthquakes, National Earthquake Information Service.

Ludwin, R. S., C.S. Weaver, and R.S. Crosson, 1989 (in press), Seismicity of Washington and Oregon, in: Slemmons, D.B., E.R. Engdahl, D. Blackwell and D. Schwartz, editors, Decade of North American Geology associated volume CSMV-1; Neotectonics of North America.

McCrumb, D.R., R.W. Galster, R.S. Crosson, R.S. Ludwin, D.O. West, W.E. Hancock, and L.V. Mann, 1989, Tectonics, Seismicity, and Engineering Seismology in Washington, in Association of Engineering Geologists, Washington State Centennial Volume, Washington State Department of Natural Resources, Division of Geology and Earth Resources, Bulletin 78.

Neri, G. and S.D. Malone, 1989 (in press), An analysis of the earthquake time series at Mt. St. Helens, Washington, in the framework of recent volcanic activity, Jour. Volcan. Geother. Res.

Thompson, K.I., 1989 (submitted), Seismicity of Mt. Rainier - a detailed study of events to the west of the mountain and their tectonic significance, BSSA.

Univ. of Wash. Geophysics Program, 1989, Quarterly Network Report 89-B on Seismicity of Washington and Northern Oregon

Univ. of Wash. Geophysics Program, 1989 (in preparation), Quarterly Network Report 89-C on Seismicity of Washington and Northern Oregon

Abstracts

Jonientz-Trisler, C., C. Driedger, and A. Qamar, 1989 (in press), Seismic signatures of debris flows on Mt. Rainier, WA, EOS, Fall 1989 PNAGU.

Jonientz-Trisler, C., and A. Qamar, 1989 (in press), Debris flow seismograms from Mt. Rainier and Mt. Adams, EOS, Fall 1989 AGU.

Miyamachi, H;, and S.D. Malone, 1989 (submitted), Relocation of earthquakes at Mount St. Helens using a three-dimensional velocity model, EOS.

Nielson, E.A., R.B. Waitt, and S.D. Malone, 1989, Eyewitness accounts and photographs of the 18 May, 1980 eruption of Mount St. Helens, Wash., I.A.V.C.E.I. General Assembly Program.

SEISMOLOGICAL DATA PROCESSING

9930-03354

John Evans, Greg Allen, Moses Smith

U.S. Geological Survey
345 Middlefield Road
Menlo Park, Ca.

(415) 329-4695

INVESTIGATIONS

The purpose of this project is to provide for both general purpose and specialized computer systems and data communications required by the branch of Seismology and its research collaborators. Some systems are required to meet the general computing needs of scientists in the earthquake prediction program. Other specialized systems monitor earthquakes in northern and central California, in real-time around the clock, or perform specific data acquisition and processing.

To meet the stated project goals, this project has responsibility for maintaining and enhancing existing computer systems and computer communication networks in addition to planning and purchasing new systems. Existing systems include a DEC PDP 11/70 UNIX system, an ISI Motorola 68020 UNIX system, a SUN 4/280 (sparc) UNIX system, two SUN 3/50 UNIX workstations, and nine SUN 3/60 UNIX workstations. All of these systems are connected to networking facilities, which include wide area networks (internet), a campus wide local area network (ethernet), a digital data switch (ROLM), and phone links (public and dedicated).

Recent work has focused on: increasing disk storage on the SUN 4/280; providing a tape back up system for the SUN 4/280; installing a data communication network for the administrative personel's computers; moving the PDP 11/70's RTP data aquisition functions to another computer system.

RESULTS

A new disk (1234 megabytes) and a new tape system (2.3 gigabyte per cartridge) have been purchased for the SUN 4/280. Both the disk and tape system should be installed by the first week of October, 1989.

The hardware and software for a PC network, to service the administrative personnel's computers, has been ordered and should be installed during October 1989.

Moving the PDP 11/70's RTP data aquisition functions to another computer system is in a research and planning mode.

Central California Network Operations

9930-01891

Wes Hall
Branch of Seismology
U.S Geological Survey
345 Middlefield Road-Mail Stop 977
Menlo Park, California 94025
(415)329-4730

Investigations

Maintenance and recording of 346 seismograph stations (447 components) located in Northern and Central California. Also recording 68 components from other agencies. The area covered is from the Oregon border south to Santa Maria.

"Drop outs" of seismic data in J120 discriminators during large events.

Results

1. Bench Maintenance Repair
   - A. seismic VCO units 251
   - B. summing amplifier 18
   - C. seismic test units 5
   - D. VO2H/JO2L VCO Units 15
   - E. FBA VCO Units 6

2. Production/Fabrication
   - A. J512A VCO units 37
   - B. J512B VCO units 9
   - C. summing amplifier units 10
   - D. dc converter/regulators 24
   - E. seismic test units 1

3. Modifications
   JJ501/502 22

4. Discriminator Tuning
   J120 239

5. Increased clamping circuit time constants of 48 ea J120 discriminators. 46 of 48 modified discriminators did not drop out during 9/21/89 Mendocino event.

6. Equipment Shipped
   A. 76ea, J120 tuned discriminators to University of Utah
   B. 60ea, J601 dc-dc converters to Cal Tech
   C. 60ea, J120 discriminators to Cal Tech

7. New seismic stations: LSH, MMIN, MMIV,MMT

8. Stations deleted: PGHA, PGHB, PGHC, LBM, MNPN, MNPV, MSLN.

9. Tuned the Corp of Engineer (San Francisco Division) microwave system to manufacture specifications.

10. Refurbished the Reason Peak Receiver site to accomadate data receivers/transmitters for Miami and Tom's mountain.

11. Connected 64 channel input to Willie Lee's portable IBM based computer monitor.

Central Aleutians Islands Seismic Network

Agreement No. 14-08-0001-A0259

Carl Kisslinger and Sharon Kubichek
Cooperative Institute for Research in Environmental Sciences
Campus Box 216, University of Colorado
Boulder, Colorado 80309

(303)492-6089

Brief Description of Instrumentation and Data Reduction Methods

The Adak seismic network (Figure 1) consists of 13 high-gain, high-frequency, two-component seismic stations and one six-component station (ADK) located at the Adak Naval Base. Station ADK has been in operation since the mid-1960s; nine of the additional stations were installed in 1974, three in 1975, and one each in 1976 and 1977.

Data from the stations are FM-telemetered to receiving sites near the Naval Base, and are then transferred by cable to the Observatory on the Base. Data were originally recorded by Develocorder on 16 mm film; since 1980 the film recordings are back-up and the primary form of data recording has been on analog magnetic tape. The tapes are mailed to CIRES once a week.

At CIRES, the analog tapes are played back into a computer at four-times the speed at which they were recorded. This computer then digitizes the data, automatically detects events, demultiplexes each event, and writes them to disk. These events are edited to eliminate spurious triggers, and a tape containing only seismic events is created. All subsequent processing is done from this tape. Times of arrival and wave amplitudes are read from an interactive graphics display terminal. The earthquakes are located using a program developed for this project originally by E. R. Engdahl which has been modified several times since then.

Data Annotations

A major maintenance trip was conducted during mid-July through September, 1988. Of the 28 short-period vertical and horizontal components, 16 were operating for most of the time period May through July, 1988. By the end of the 1988 summer field trip to Adak, all 28 components were operating. Our field team was able to obtain use of a Coast Guard helicopter, at no cost to the project, and brought up AK2 and AK3, which had been down for about 6 years due to difficult access. A lightning strike at the end of the summer field trip brought AD1Z and AD6H down again and we were unable to repair them. However, due to the combined efforts of our observers on Adak and Sean Morrissey over the past year, the network status is more complete than it has been for many years. Table 1 shows the status of the network for the time period October 1988 to the present. The minor winter maintenance trip has not yet been done for this year but is planned in the near future.

Current Observations

In late 1987, the network purchased a Sun 3/50 work-station, Sun 1600/6250 bpi tape drive and controller, and two 141 Mbyte hard disks to replace our PDP 11/70. Currently, the tape drive and Versatec are driven by a Sun 3/260 belonging to CIRES, free of charge, while all of our computing is done on the Sun 3/50. We have installed and customized the data analysis package developed at Lamont-Doherty Geological Observatory and have been using it to locate earthquakes since August 29, 1988. Due to the down time associated with our move to a new building and installation of the above system, we have modified our locating strategy in order to maintain a sampling of seismicity after the May 7, 1986 major event (M_S 7.7), and also remain as current as possible. As a result, we have a research assistant locating the first week of every month after the May 7, 1986 event through June 1987, one locator working in 1988, and one locator working in 1989.

In November, 1988, the PDP 11/34 used to digitize our analog data tapes died and all affordable attempts to repair it failed. In the spring of 1989 we began testing a new digitizing device on loan from Mr. Reese Cutler of Cutler Digital Design, and software provided by Dr. Peter Ward of Menlo Park. This device is linked to a Sun 3/50 workstation and the combination can be used to replace the PDP 11/34. Dr. Peter Ward of Menlo Park is currently using such a system to digitize his network data on a real-time basis. We have more stations than Dr. Ward and are digitizing at four times his rate (38 channels at 300 sps) but the Sun 3/50 and Cutler Digital Design Data Sampler are able to handle this and produce high quality data compatible with the PDP 11/34. We began digitizing June, 1989 data in late August, 1989. Our only problem results from the fact that this Sun 3/50 is also used for locating earthquakes and analysis of our data. Such a small machine cannot handle both our tasks, digitizing at 300 sps and analysis, at the same time without the operating system hanging and requiring a re-boot to clear the system. As a result we are two months behind in digitizing, requiring that some data tapes with good film backup and few events be erased before digitizing in order to maintain supply to Adak. The recommended solution is to have two separate machines; one for digitizing and one for analysis so that each task can be done uninterrupted. Digitizing and locating both suffer when the one machine used for both is down 2 or 3 times daily. We are hopeful that a CPU and memory upgrade to a Sun 3/60 will allow us to digitize and analyze at the same time with fewer problems, since we cannot afford two machines.

The location work has proceeded well; 67 earthquakes were located during November 1 - 8 and December 1 - 7, 1986; 136 earthquakes were located during October, November, and December, 1987; and 61 earthquakes during June, 1989. No more events have been located in 1988 at this time. The grand total for all three time periods located since May, 1989 is 274, about half the rate of last period due to the interference with the digitizing process.

Epicenters of *all* the located events for 1986, 1987, and 1989 are shown in Figures 2a, 2b, and 2c and vertical cross-sections are given in Figures 3a, 3b, and 3c.

Two of the events located with data from the Adak network for 1986 were large enough to be located teleseismically (USGS PDEs). A number of other teleseismically located aftershocks within the network region are difficult for us to locate due to their arrivals being masked by the codas of other aftershocks. Also, 10 of the events located with data from the Adak network for the specified dates in 1987 and 4 in 1989 were large enough to be located teleseismically (USGS PDEs). Because of the large number of aftershocks of May 7, 1986, a decision was made to not locate earthquakes with duration magnitudes (M_d) of less than 2.3 for 1986 and 1987. However, *all* events are being located for 1988 and 1989.

A catalog has been complied of the located events which occurred in 1986, 1987, and 1989. The catalog is complete for events within the specified time intervals with $M_d \geq 2.3$ for 1986 and 1987, and is complete for all events in 1989.

More detailed information about the network status and a catalog of the hypocenters determined for the time period reported here are included in our semi-annual data report to the U.S.G.S. Recent research using these data is reported in the Technical Summary for U.S.G.S. Grant No. G1368.

Improvements in Analysis Techniques

In the past, the Central Aleutians Seismic Network duration magnitudes have been smaller than USGS m_b value for larger events by approximately one unit of magnitude. Recent research has exposed some additional inconsistencies with the traditional method of determining magnitude for events in the central Aleutians. To correct these problems we are developing a new formula which has been scaled to agree with the magnitudes reported in the Preliminary Determination of Epicenters, but yields the same value for small events. The resulting preliminary formula is:

$$M_d=1.0+.63[\log_{10}{}^2\tau+.003\Delta+.003z]$$

where M_d is the duration magnitude, τ is the duration measured from the S arrival, Δ is the epicentral distance, and z is the depth. As yet, this formula is not being used routinely for magnitude calculations. A discussion of research on this problem can be found in the report of Grant No. G1368 elsewhere in this volume.

Due to the manner in which the new digitizer determines the user-supplied sampling rate, our sampling rate was increased from 75 sps to 84 sps for all data digitized since August, 1989. This represents a slight increase in resolution and a slight increase in storage requirements, but has not otherwise effected analysis.

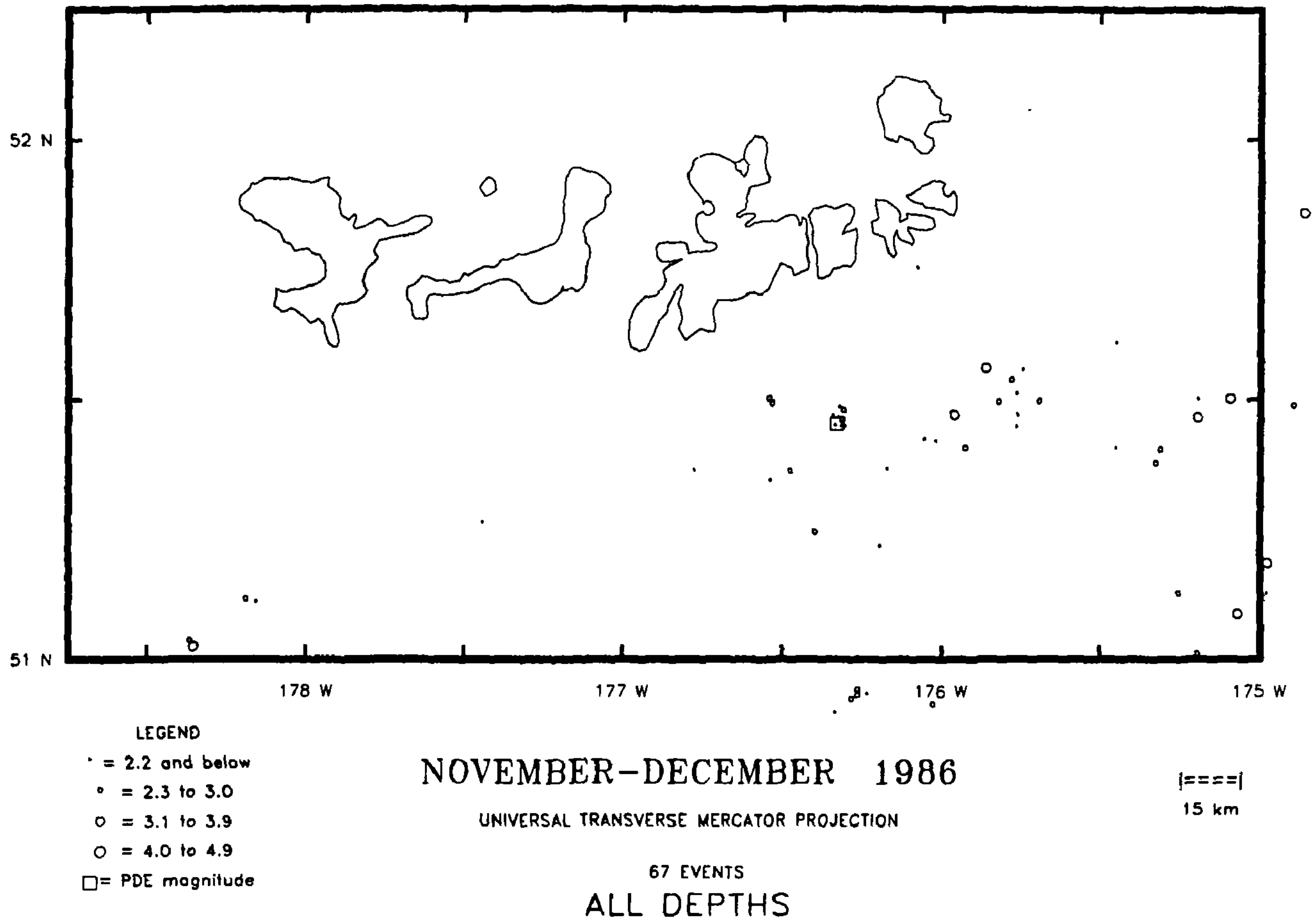

Figure 1a: Map of seismicity which occurred November 1 - 8 and December 1 - 7, 1986. All epicenters were determined from Adak network data. Events marked with squares are those for which a teleseismic body-wave magnitude has been determined by the USGS; all other events are shown by symbols which indicate the duration magnitude determined from Adak network data. The islands mapped (from Tanaga on the west to Great Sitkin on the east) indicate the geographic extent of the Adak seismic network.

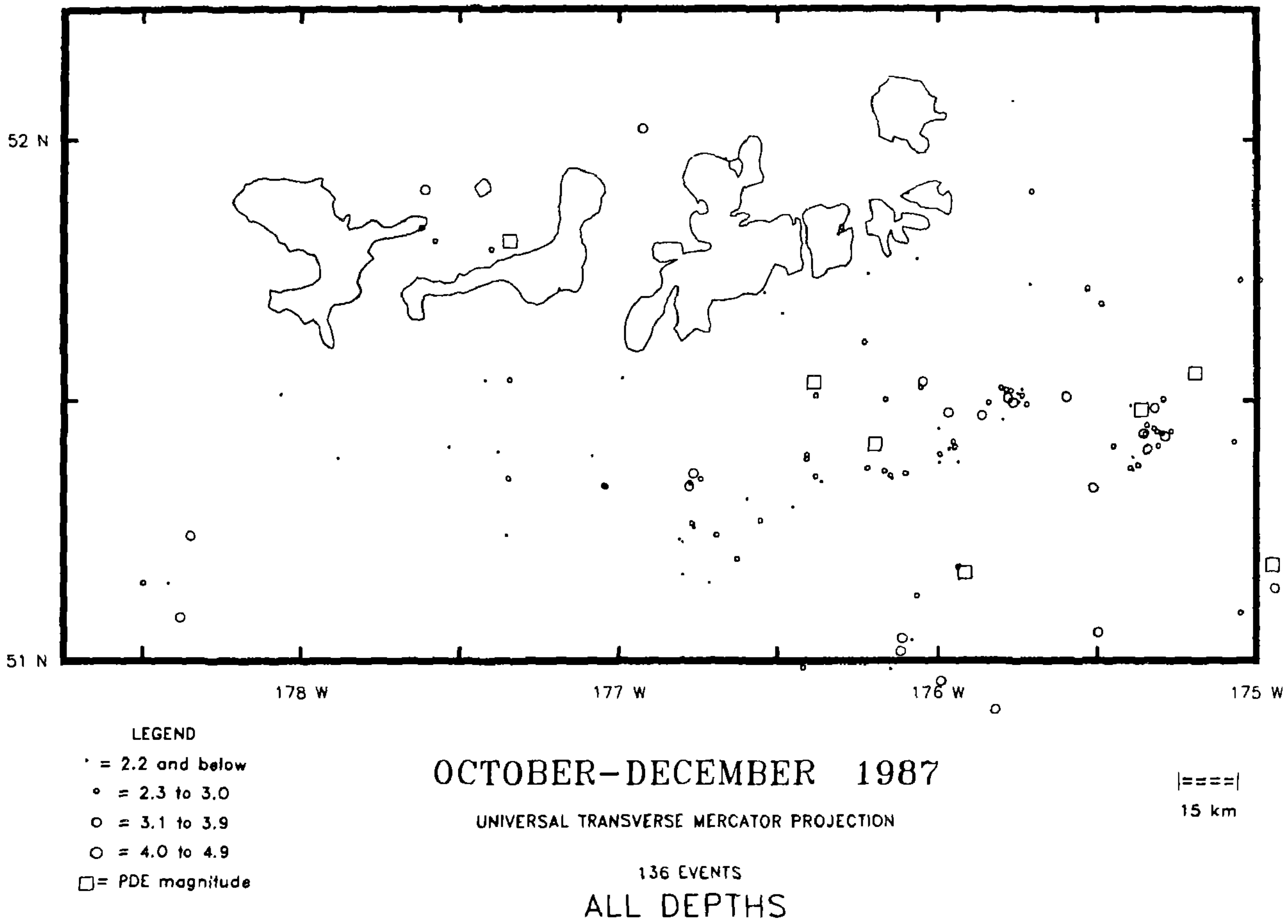

Figure 1b: Map of seismicity which occurred October, November, and December, 1987. Symbols as in Figure 1a.

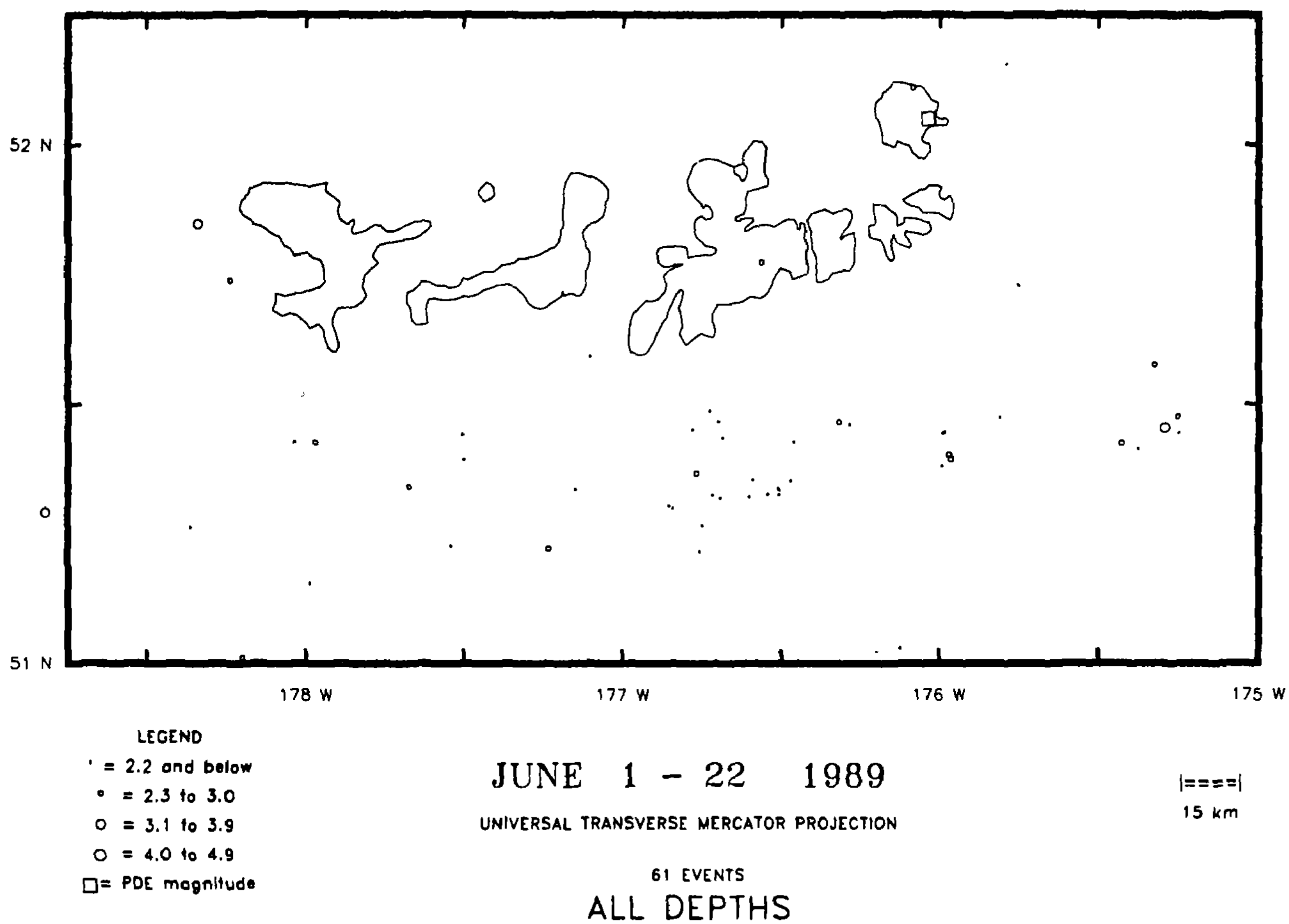

Figure 1c: Map of seismicity which occurred June 1 - 22, 1989. Symbols as in Figure 1a.

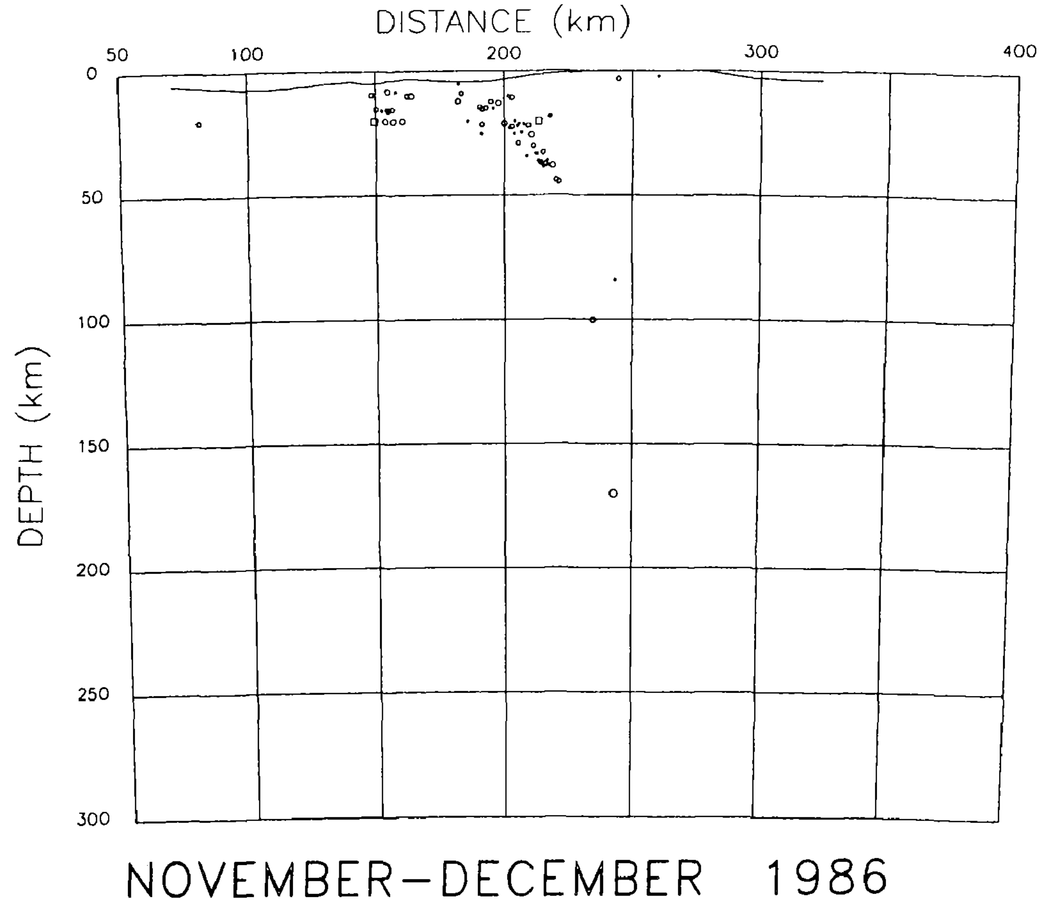

Figure 2a: Vertical cross section of seismicity which occurred November 1 - 8 and December 1 - 7, 1986. Events are projected according to their depth (corresponding roughly to vertical on the plot) and distance from the pole of the Aleutian volcanic line. The zero-point for the distance scale marked on the horizontal axis of the plot is arbitrary. Events marked with squares are those for which a teleseismic body-wave magnitude has been determined by the USGS; all other events are shown by symbols which indicate the duration magnitude determined from Adak network data. The irregular curve near the top of the section is bathymetry.

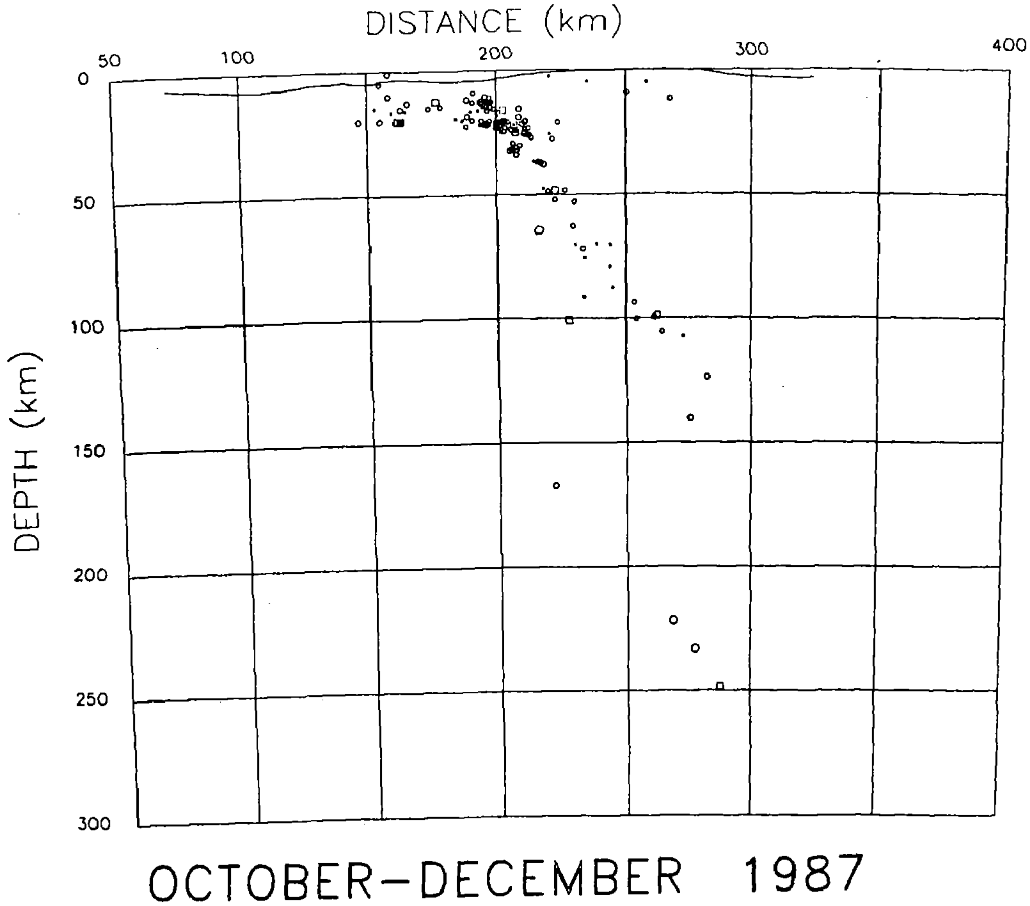

Figure 2b: Vertical cross section of seismicity which occurred October, November, and December, 1987. Projection and symbols as in Figure 2a.

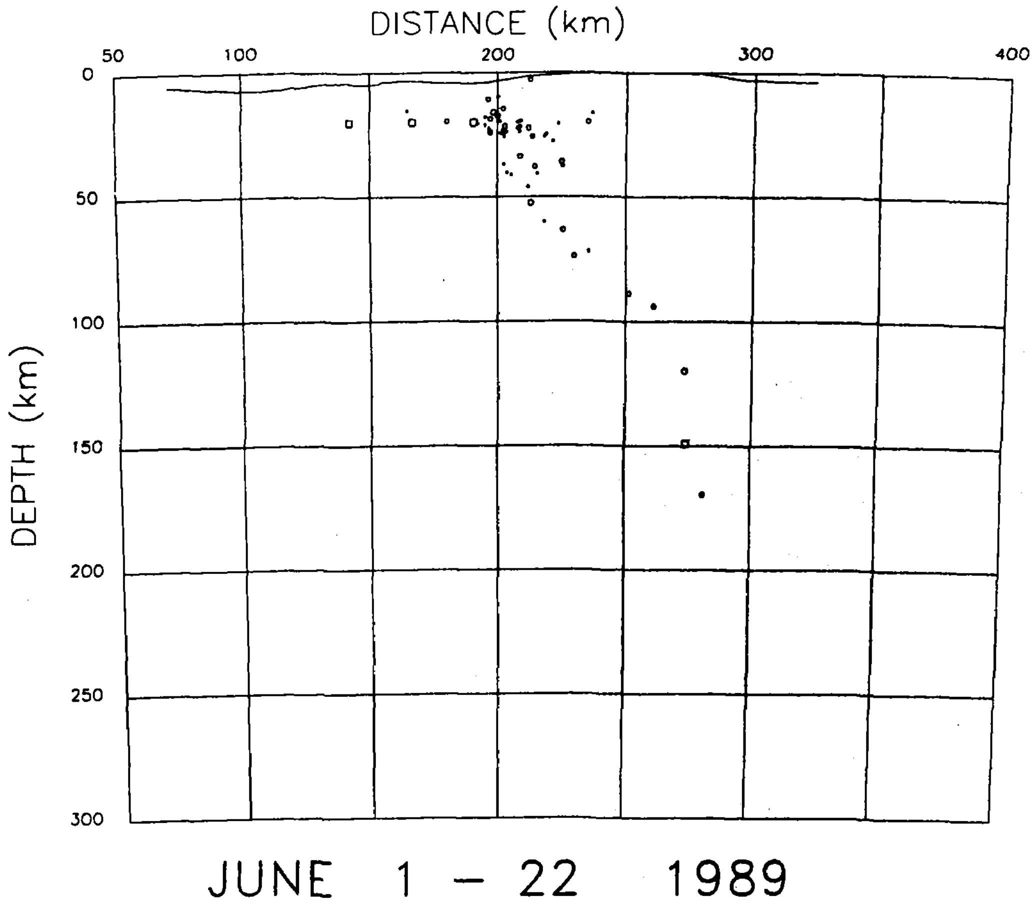

Figure 2c: Vertical cross section of seismicity which occurred June 1 - 22, 1989. Projection and symbols as in Figure 2a.

Alaska Seismic Studies

9930-01162

John C. Lahr, Christopher D. Stephens,
Robert A. Page, Kent A. Fogleman
Branch of Seismology
U. S. Geological Survey
345 Middlefield Road, Mail Stop 977
Menlo Park, California 94025
(415) 329-4744

Investigations

1) Continued collection and analysis of data from the high-gain short-period seismograph network extending across southern Alaska from the volcanic arc west of Cook Inlet to Yakutat Bay, and inland across the Chugach Mountains. This region spans the Yakataga seismic gap, and special effort is made to monitor for changes in seismicity that might alter our assessment of the imminence of a gap-filling rupture.

2) Cooperated with the USGS Branch of Alaskan Geology, the Geophysical Institute of the University of Alaska (UAGI), and the Alaska Division of Geological and Geophysical Surveys in operation the Alaska Volcano Observatory (AVO). Under this program, our project monitors seismicity near Mt. Spurr and Mt. Redoubt with a 16-station network that includes 6 stations near each of these volcanoes.

3) Cooperated with the Branch of Engineering Seismology and Geology in operation of 15 strong-motion accelerographs in southern Alaska, including 11 between Icy Bay and Cordova in the area of the Yakataga seismic gap.

Results

1) The number of shallow earthquake hypocenters in southern Alaska determined for the period January - June 1989 (Figure 1) is nearly twice that of the first six-month period of 1988. Similarly, the number of subcrustal shocks (Figure 2) is nearly three times greater. These changes are attributed primarily to systematic effects related to implementation of the digital event detection system that incorporates data from both the USGS and UAGI seismograph networks. In particular, many more events from the area north of about latitude 62.5° N and from southwest of the Kenai Peninsula are included in the processing, and the magnitude threshold for including events from within the Wadati-Benioff zone is lower than previously applied. Although preliminary, these new data suggest that the level of crustal seismicity along and adjacent to the Denali fault system west of about longitude 147° W is comparable to that in the northern Cook Inlet region.

Despite the large increase in the number of located shocks, the general features in the spatial distribution of seismicity within areas monitored by the USGS network (roughly between latitudes 58°-62.5°N, and beneath the northern Gulf of Alaska) are similar to those over the past few years. Important features of the shallow seismicity include continuing aftershocks from the 1987/1988 sequence of large (Ms 7.0,Ms 7.6,Ms 7.6) earthquakes in the northern Gulf of Alaska, persistent seismicity beneath Waxell Ridge near the center of the Yakataga seismic gap and within the aftershock zone of the 1979 St. Elias earthquake east of the gap, clustered activity beneath Prince William Sound and along the Castle Mountain-Caribou fault system north and northeast of Anchorage, and activity along the volcanic arc west of Cook Inlet. It is interesting to note that beneath northern Cook Inlet, where two bursts of seismicity were observed in the previous six month period, the rate of activity continues to be high. However, the significance of any apparent changes in rates of seismicity is uncertain at this time because current procedures for determining magnitudes have not been calibrated against previous methods.

On July 16, a M 4.1 (m_b 4.4) shallow earthquake occurred in the aftershock zone of the August 1984, m_b 5.7, Sutton earthquake. The latter event involved dextral slip at 13- to 20-km depth on the Talkeetna segment of the Castle Mountain fault system (Lahr and others, 1986). Three aftershocks with magnitudes of 1.9, 2.0, and 2.6 were located. The focal mechanism for the July shock is very similar to that of the 1984 earthquake. This event is the largest to occur in the aftershock zone since 1984.

2) An extensive review of the literature was completed for the DNAG paper, Seismicity of continental Alaska (Page and others, 1989). This paper reviews the seismicity of Alaska and discusses this activity in the context of the current tectonic regime. The seismicity is dominated by the intense activity that occurs along the Pacific coast, and results primarily from the interaction of the Pacific and North American lithospheric plates. Most of the 30 earthquakes of magnitude equal to or larger than 7.0 that have occurred in continental Alaska since 1899 are located along this coast. The largest instrumentally recorded interior shocks are of magnitude 7.3, two near Fairbanks and one in western Alaska.

3) In addition to the routine maintenance of the high-gain seismograph network, three new stations, including two that are solar-powered, were installed within 13 km of the summit of Mt. Spurr. These new sites were added to aid in the investigation of the nature of shallow, swarm-like activity that occurs near this volcano. A new station was also installed at Cape Yakataga with a high-power VHF transmitter to improve coverage and detection within the gap and to improve the reliability of data transmissions. Reconfiguration of the telemetry circuits required the installation of several new repeater sites on the Kenai Peninsula, and modifications were made at other sites to interface with state microwave facilities. A heavy-duty VHF whip antenna installed last year at PWL survived the winter, thus offering a relatively inexpensive solution to the long-standing problem of

damage to Yagi-style antennas at sites that become buried by snow each year.

4) A joint UAGI/USGS seismic center, the Alaska Earthquake Information Center (AEIC), has been established at the UAGI Seismology Laboratory in Fairbanks for recording and analyzing Alaskan earthquake data and for disseminating information about Alaskan earthquakes. By May, 1989, most of the USGS seismic stations were being recorded at the UAGI and the seismic recording equipment operated for the USGS by the Alaska Tsunami Warning Center (ATWC) at Palmer, Alaska was dismantled during June. During August the capacity of the UAGI digital system was increased from 64 to 128 channels, allowing all of the stations being telemetered to Fairbanks to be recorded. The AEIC will provide an improved data base for studying Alaskan earthquakes, assessing their hazards, and disseminating earthquake information and advisories to government agencies and to the public. The expanded data set will facilitate joint research projects and stimulate cross-fertilization of ideas.

5) Seven of the strong-motion sites were visited, but no event triggers occurred at these sites during the past year. The SMA1 located at the FAA in Yakutat was moved to the USGS building in Yakutat.

References

Lahr, J. C., Page, R. A., Stephens, C. D., and Fogleman, K. A., 1986, Sutton, Alaska earthquake of 1984: evidence for activity on the Talkeetna segment of the Castle Mountain fault system, Bulletin of the Seismological Society of America, v. 76, p. 967-983.

Reports

Fogleman, K. A., 1989, Catalog of earthquakes in southern Alaska for 1986, U. S. Geological Survey Open-File Report [submitted to Branch Chief].

Page, R. A., N. N. Biswas, J. C. Lahr, and Hans Pulpan, 1989, Seismicity of continental Alaska, [submitted for DNAG volume Neotectonics of North America].

Page, R. A., George Plafker, J. N. Davies, and Hans Pulpan, 1989, Block Rotation and Seismicity in East-Central Alaska, EOS, Trans. Amer. Geophys. Union, [abs., in press].

Stephens, C. D., R. A. Page, and J. C. Lahr, 1989, Reflected and mode-converted seismic waves within the shallow Aleutian subduction zone, southern Kenai Peninsula, Alaska, [submitted to J. Geophys. Res.; Dir. Approv. 08/09/89].

Figure 1. Epicenters of 1,024 shallow earthquakes that occurred between January and June 1989. Magnitudes are determined from coda duration or maximum amplitude. The magnitude threshold for completeness varies across the network. Dashed contour outlines inferred extent of Yakataga seismic gap. Neogene and younger faults shown as solid lines.

Figure 2. Epicenters of 1,242 intermediate and deep shocks that occurred between January and June 1989. PWS - Prince William Sound. See figure 1 for details about magnitudes and map features.

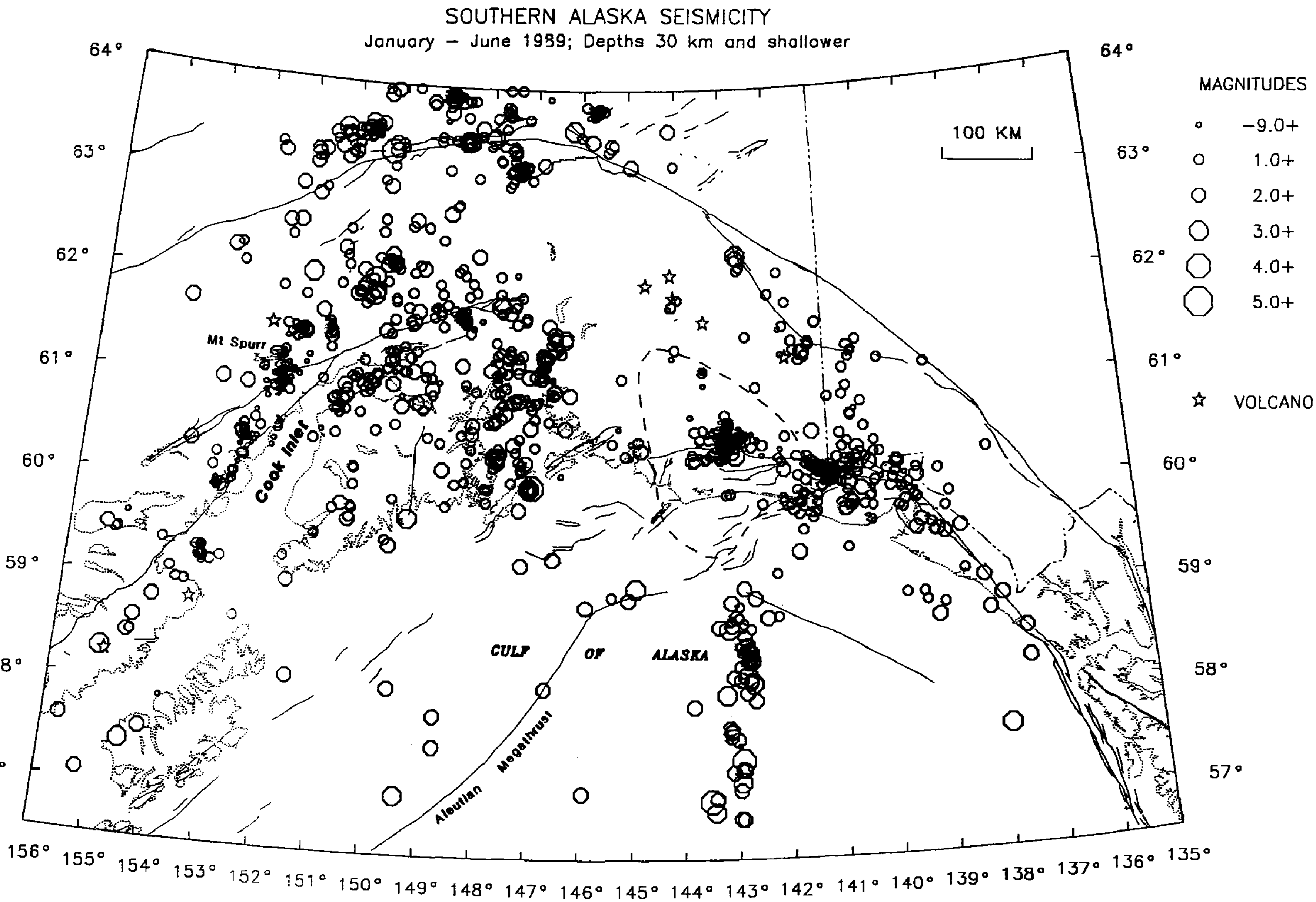

Figure 1. Epicenters of 1,024 shallow earthquakes that occurred between January and June 1989. Magnitudes are determined from coda duration or maximum amplitude. The magnitude threshold for completeness varies across the network. Dashed contour outlines inferred extent of Yakataga seismic gap. Neogene and younger faults shown as solid lines.

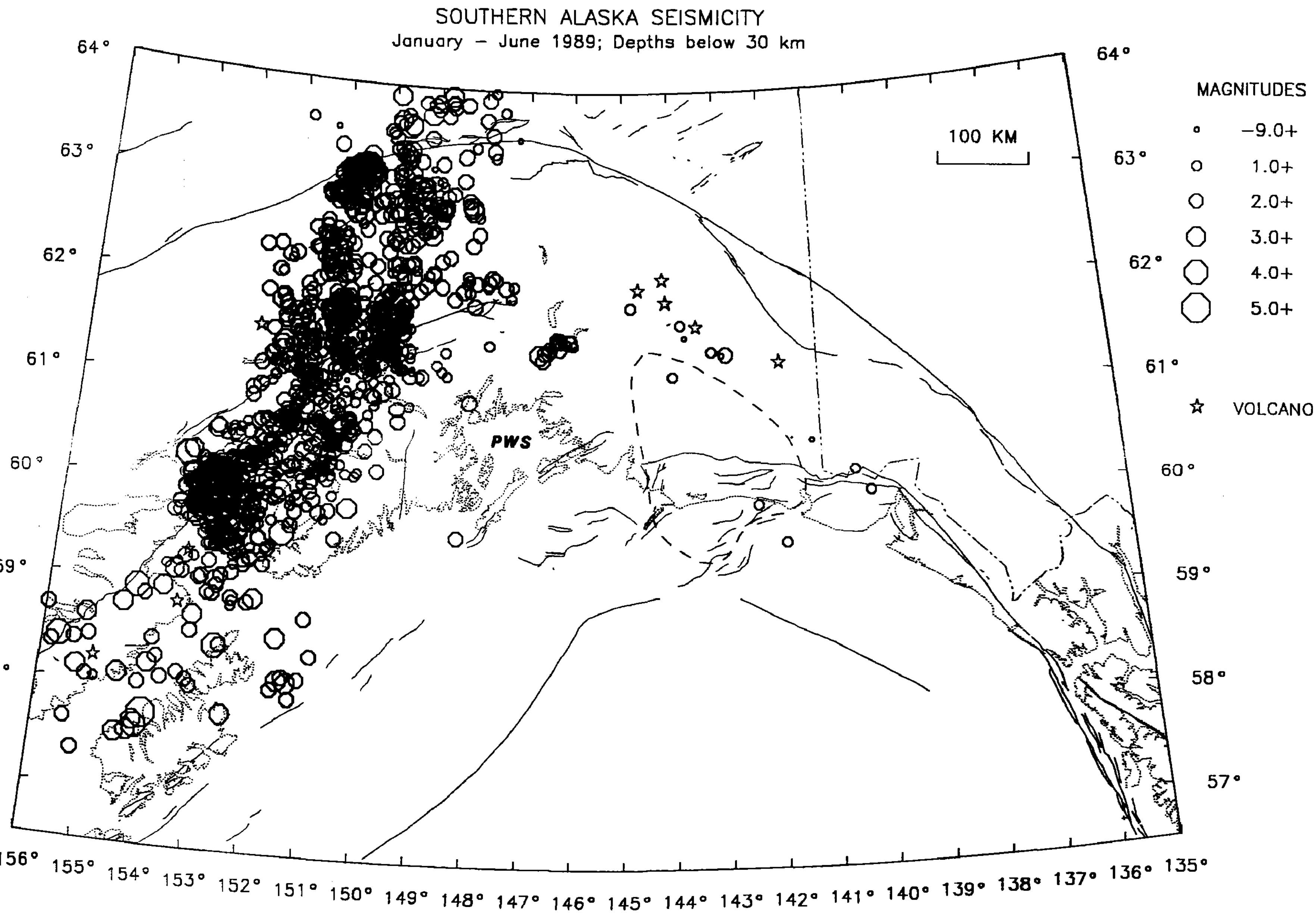

Figure 2. Epicenters of 1,242 intermediate and deep shocks that occurred between January and June 1989. PWS - Prince William Sound. See figure 1 for details about magnitudes and map features.

Northern and Central California Seismic Network Processing

9930-01160

Fredrick W. Lester
Branch of Seismology
U.S. Geological Survey
345 Middlefield, MS 977
Menlo Park, CA 94025
(415) 329-4747

Investigations

1. In 1966 a seismographic network was established by the USGS to monitor earthquakes in central California. In the following years the network was expanded to monitor earthquakes in most of northern and central California, particularly along the San Andreas Fault, from the Oregon border to Santa Maria. In its present configuration there are over 500 single and multiple component stations in the network. The primary responsibility of this project is to monitor, process, analyze, and publish data recorded from this network.

2. This project continues to maintain the primary seismic data base for the years 1969 to the present on both computers and magnetic tapes for those interested in doing research using the network data. As soon as older data are complete and final the preliminary data base is updated with the final phases and locations.

3. For nearly two decades this office monitored the earthquakes in Yellowstone National Park and vicinity. The data from these earthquakes have been collected and processed, and approximately 7000 events have been located for the time period 1959 to 1986. These data are currently being used to produce a map of epicenters for the region. This map will compliment both the recently published catalog of earthquakes for 1973 to 1984, and a map and cross sections for 1964 to 1981, covering the same area.

4. As time permits some research projects are underway on some of the more interesting or unusual events or sequences of earthquakes that have occurred within the network.

Results

1. Figure 1 illustrates 8353 earthquakes located in northern and central California and vicinity during the time period April through September 1989. This level of seismicity is normal for a six month period as a staff of nine technicians and professionals typically processes 35 to 45 events per day. The largest earthquake during that time was a magnitude 5.2 event that occurred on August 8, 1989. It was located approximately 15 kilometers north-northeast of Santa Cruz and was probably on the San Andreas fault. It was preceded by a magnitude 5.0 earthquake on April 3 that occurred on the Calaveras fault approximately 14 kilometers northeast of San Jose. On September 21 we recorded another magnitude 5.0 earthquake. This one was located just off the the northern California coast, approximately 70 kilometers southwest of Eureka.

   Seismic data recorded by the network are being processed using the CUSP (Caltech USGS Seismic Processing) system. CUSP was designed by Carl Johnson in the early 1980's and has since undergone some revisions for the Menlo Park operation. As of September 1, 1989 we have begun using revised CUSP software in a generic format. This new format will make CUSP more universally acceptable to groups that are using or plan to use it in the future because the commands are relatively non-specific to any particular group operation.

In the near future we plan to begin publishing, probably on a monthly basis, a preliminary catalog of earthquakes for northern and central California. The format is not yet established but it will probably be some type of listing of events accompanied by a text explaining the processing and what is in the catalog, and a map showing the epicenters. The catalog will be approximately complete at the magnitude 1.5 in the central core of the network and something approaching M2.0 in the more remote portions of the net.

2. The current catalog is relatively complete and correct through January 1989. The data from March 1989 through August 1989 are complete, but some work remains to make corrections on some problem events and identify the quarries that have been located. Data from September 1989 are still incomplete and some errors still remain to be identified and corrected.

3. The map of earthquake locations for Yellowstone Park and vicinity for 1959 to 1986 is now undergoing final revisions. It is expected to be finished and at the publisher by October or November 1989.

4. Steve Walter has been investigating the seismicity in the Medicine Lake region. A magnitude 4.0 earthquake occurred in that area on September 30, 1988 followed by many aftershocks. The aftershocks have continued until the present and there has been renewed interest in this region because of this activity and the possible implication of associated volcanic activity. Steve has submitted an abstract for a talk to be presented at the Fall 1989 AGU meeting in San Francisco. He will be describing the Medicine Lake swarm and related topics.

Reports

Klein, Fred, Lindh, Allan, and Walter, Steve, 1989, Central California earthquake animation January - June 1989, U.S.G.S. Open-File Report 89-308 (video).

Walter, Steve, and Dzurisin, Dan, 1989, The September 1988 Earthquake Swarm at Medicine Lake Volcano, Northern California (abstract), EOS, (in press).

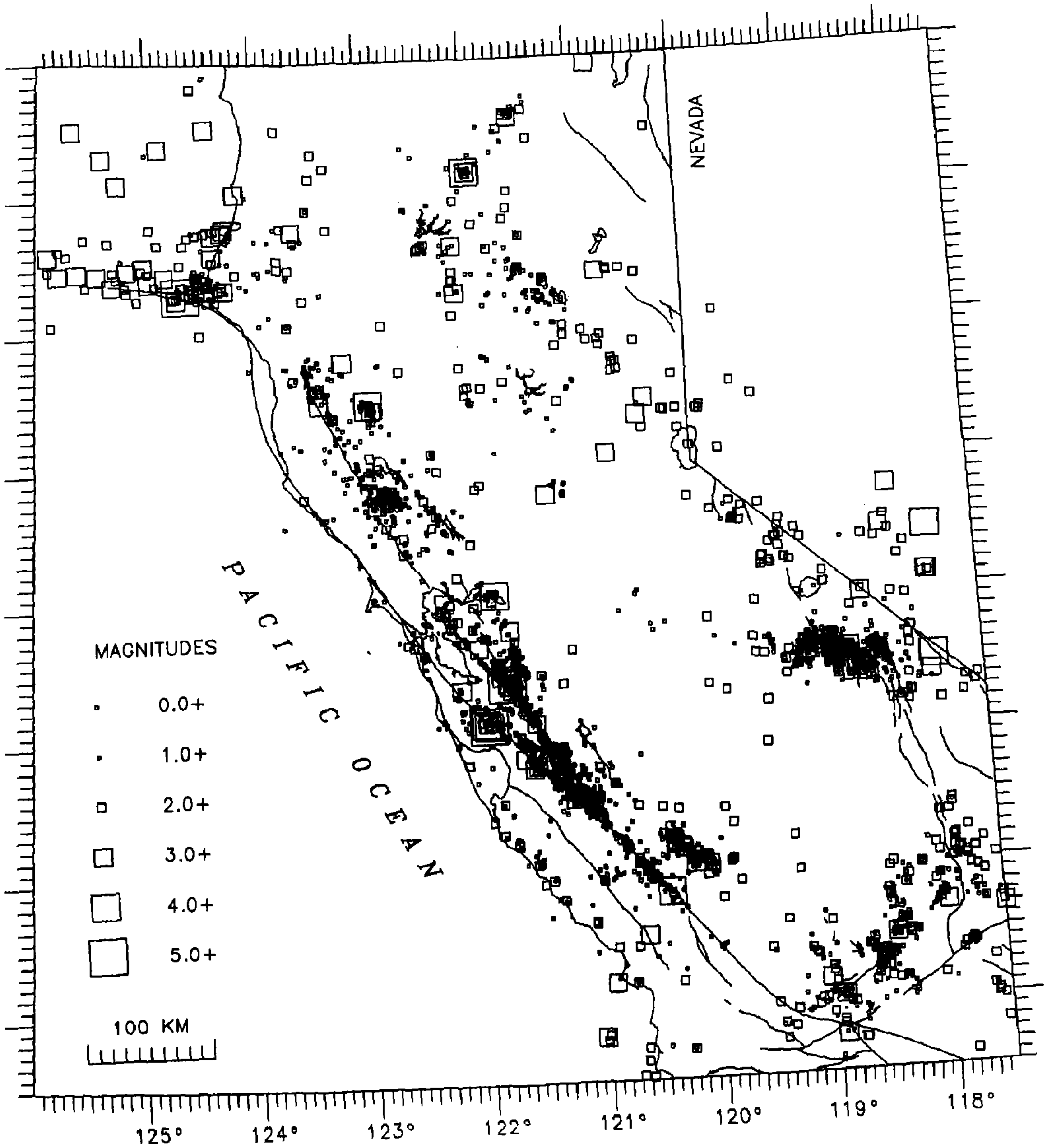

FIGURE 1. Seismicity for northern and central California and vicinity during April - September 1989

WESTERN GREAT BASIN-EASTERN SIERRA NEVADA SEISMIC NETWORK

USGS Cooperative Agreement 14-08-0001-A0618

Principal Investigators: M. K. Savage and W.F. Nicks
Seismological Laboratory
University of Nevada
Reno, NV 89557
(702) 784-4315

Investigations

This contract supported continued operation of a seismic network in the western Great Basin of Nevada and eastern California, with the purpose of recording and locating earthquakes occurring in the western Great Basin, and acquiring a data base of phase times and analog and digital seismograms from these earthquakes. Research using the data base was performed under USGS contract 14-08-0001-G1524 and is reported elsewhere in this volume.

Results

Development of the network

A new computer system, based around a Microvax II running VAX/VMS and the Caltech -U.S.G.S. Seismic Processing (CUSP) software is now in full operation and replaces the former array of three computers which were being used in support of network operations (a PDP 11/34 computer recording real-time short-period signals; a PDP 11/23 computer recording a continuous data stream of asynchronous digital data from four three-component wideband (0.1 to 25 Hz) outstations; and a PDP 11/70 computer.) Essentially all of the software has been brought over from the PDP 11/70, including a sizeable library of C programs. Pickfiles created on the 11/70 have been relocated on the Microvax, and we plan to continue creation of pickfiles which are strictly compatible with these (the picking software writes ASCII pickfiles from the MEM and GRM files created by CUSP). Although the VMS system has a UNIX tar emulation, we have not completed software as yet to read the binary header and seismogram files written on the 11/70, but understand that such software is available. Readers of this report should note that the new system makes calibrated three-component digital data available with the standard network data stream, and that software is now available to access this data quite easily and efficiently. Also, the array of digital stations has been expanded to nine, giving quite widespread coverage of Nevada by these digital stations.

The digital signals are mixed with the incoming analog data as follows. Incoming data is converted to analog data (16-bit accuracy D to A converter) and redigitized along with the analog data, thus making the time base common to all recorded stations, and allowing us to intermix data from digital stations with disparate sampling rates. These signals are recorded intermittently as dictated by the CUSP program SPIDER, which detects events and directs event recording to disc.

In addition, the digital data are brought into the computer exactly as they arrive from the field in a continuous, asynchronous data stream through a second DRV11-W parallel port. They are then recorded on an Exabyte streaming tape device. 0.01-second time stamping is placed on every digital sample that is written on the tape, together with station i.d. and error detection bits. These Exabyte tapes are VMS COPY tapes accessible either via the CUSP software or directly transportable to the Sun/UNIX system through the UNIX utility "dd", where George Randall has written software to unpack the data and convert it to

SAC format for analysis on that system. Direct comparison of the data recorded either way shows that almost no loss of resolution occurs in the D to A to D process: the digital traces being recorded on triggered events overlay the actual digital data recorded down to the level of individual counts apart from noise of about one bit.

Seismicity during report time

From 1 April 1989 through 31 September 1989 the University of Nevada Seismological Laboratory located 1,566 earthquakes (fig 1, 2), most near Long Valley caldera as has been the case for the last ten years. Of these, 27 were magnitude 3 or greater. The most significant activity has been the ongoing swarm of earthquakes under Mammoth Mountain, which has now been going on for five months without interruption, far longer than any of the previous swarms at that site.

More detailed monthly reports of seismicity can be obtained by contacting the laboratory.

Seismicity

April 1, - September 30, 1989

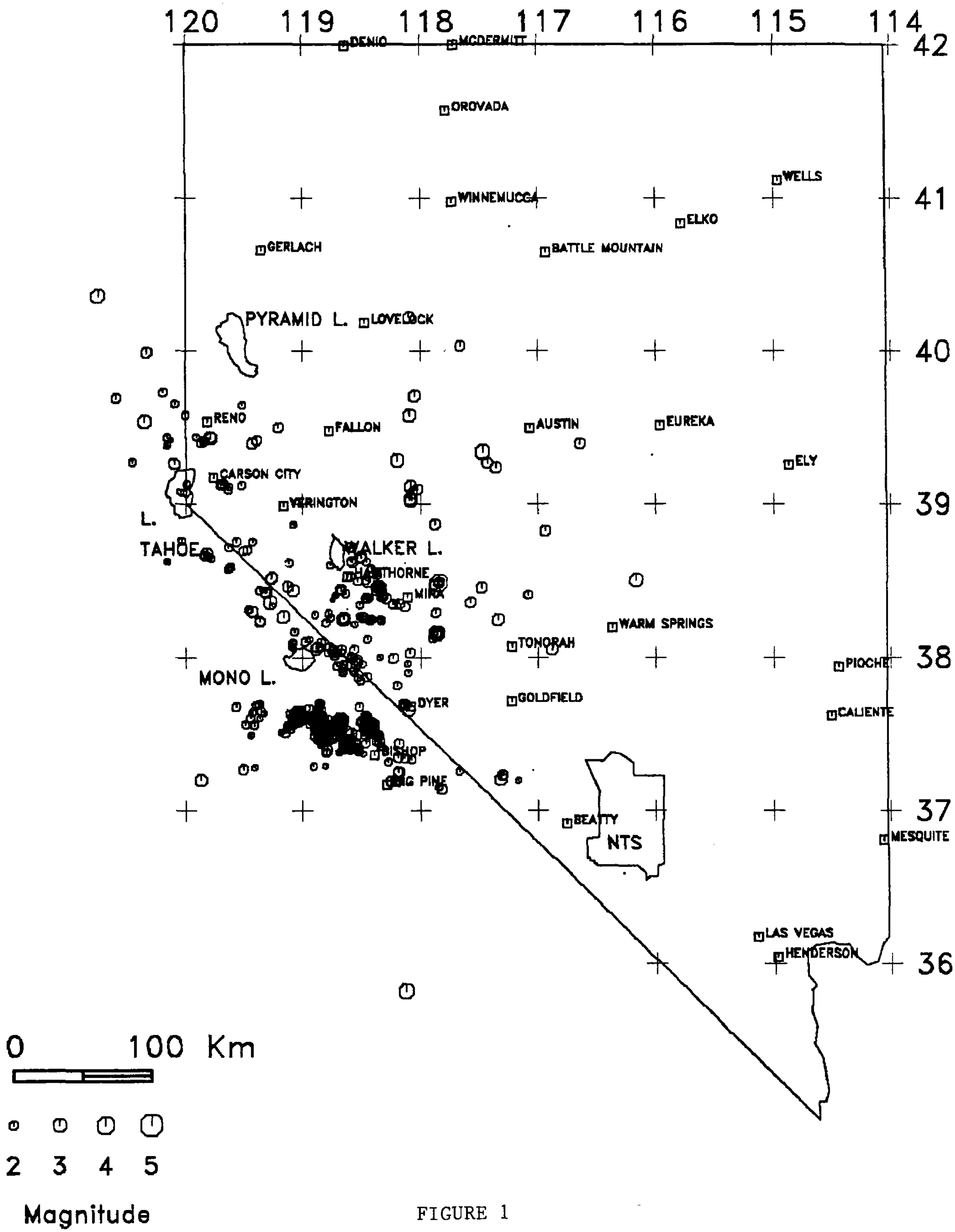

FIGURE 1

Mammoth Earthquakes
April 1, – September 30, 1989

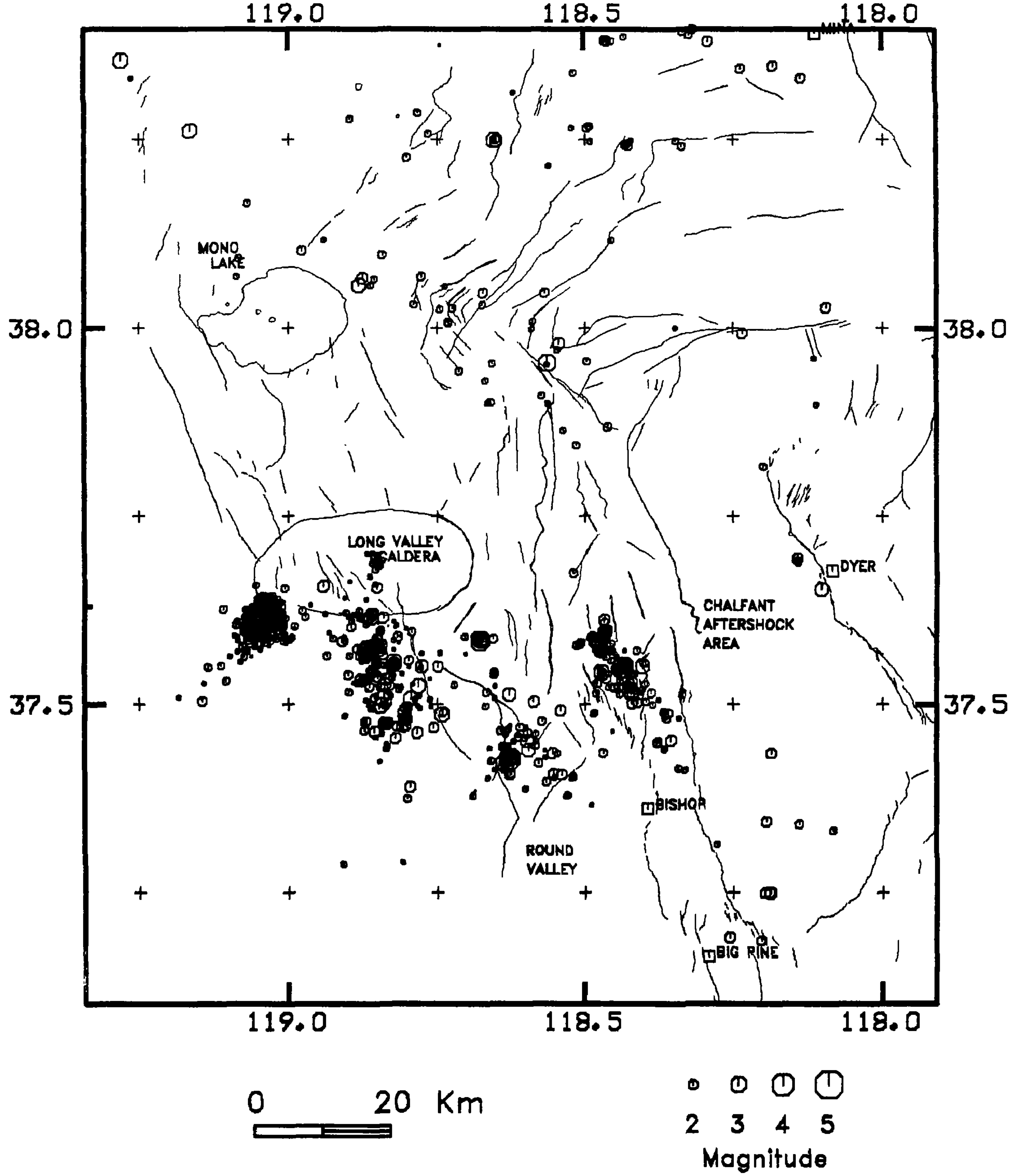

Figure 2

Regional Microearthquake Network in the Central Mississippi Valley

14-08-0001-A0263

William V. Stauder and Robert B. Herrmann
Department of Earth and Atmospheric Sciences
Saint Louis University
3507 Laclede
St. Louis, MO 63103
(314) 658-3131

Investigations

The purpose of the network is to monitor seismic activity in the Central Mississippi Valley Seismic zone, in which the large 1811-1812 New Madrid earthquakes occurred. The following section gives a summary of network observations during the first six months of the year 1989, as reported in Network Quarterly Bulletins No. 59 and 60.

Results

In the first six months of 1989, 41 earthquakes were located by the 42 station regional telemetered microearthquake network operated by Saint Louis University for the U.S. Geological Survey and the Nuclear Regulatory Commission. Figure 1 shows 41 earthquakes located within a 4° x 5° region centered on 36.5°N and 89.5°W. The magnitudes are indicated by the size of the open symbols. Figure 2 shows the locations and magnitudes of 34 earthquakes located within a 1.5° x 1.5° region centered at 36.25°N and 89.75°W.

In the first six months of 1989, 63 teleseisms were recorded by the PDP 11/34 microcomputer. Epicentral coordinates were determined by assuming a plane wave front propagating across the network and using travel-time curves to determine back azimuth and slowness, and by assuming a focal depth of 15 kilometers using spherical geometry. Arrival time information for teleseismic P and PKP phases has been published in the quarterly earthquake bulletin.

The significant earthquakes occurring in the first six months on 1989 include the following:

1. April 27 (1647 UCT). New Madrid, Missouri. m_{bLg} = 4.7 (BLA). Slight damage (VI) at Steele, Missouri. Felt (V) at Gobler, Hayti, Kennett and Senath, Missouri and at Blytheville AFB, Arkansas. Felt (IV) in parts of Missouri, Arkansas, Tennessee, Kentucky and Illinois.
2. May 14 (0016 UCT). New Madrid, Missouri. m_{bLg} = 3.7 (NEIS). Felt (IV) at Canalou and Matthews. Felt (III) at Cooter, Doniphan, Fredricktown, Grayridge, Kewanee, New Madrid, Risco and Senath. Also felt (III) at Pollard, Arkansas and Bardwell, Hikman and Kevil, Kentucky.

In addition to servicing the network project personnel have been involved in installation and bringing on-line the IRIS station at the Cathedral Cave site. This station is located on the northwest border of the network and will provide significant data for location and source characteristics studies, particularly for events which occur in the Ozark uplift region of southeast Missouri.

With a view toward the evolution of network hardware and processing, several important software developments have been made. First, present PDP 11/70 analysis software, PING, has been ported to a SUN Sparc Station in such a manner that permits the use without modification of archive tapes acquired since 1980. The other effort has been directed toward the implementation of a data base management scheme for analyzing seismic traces and locating earthquakes. This is an implementation of the Center for Seismic Studies data base and will work on UNIX machines and on PC's under DOS. Thus a single package works both at the university and in the field.

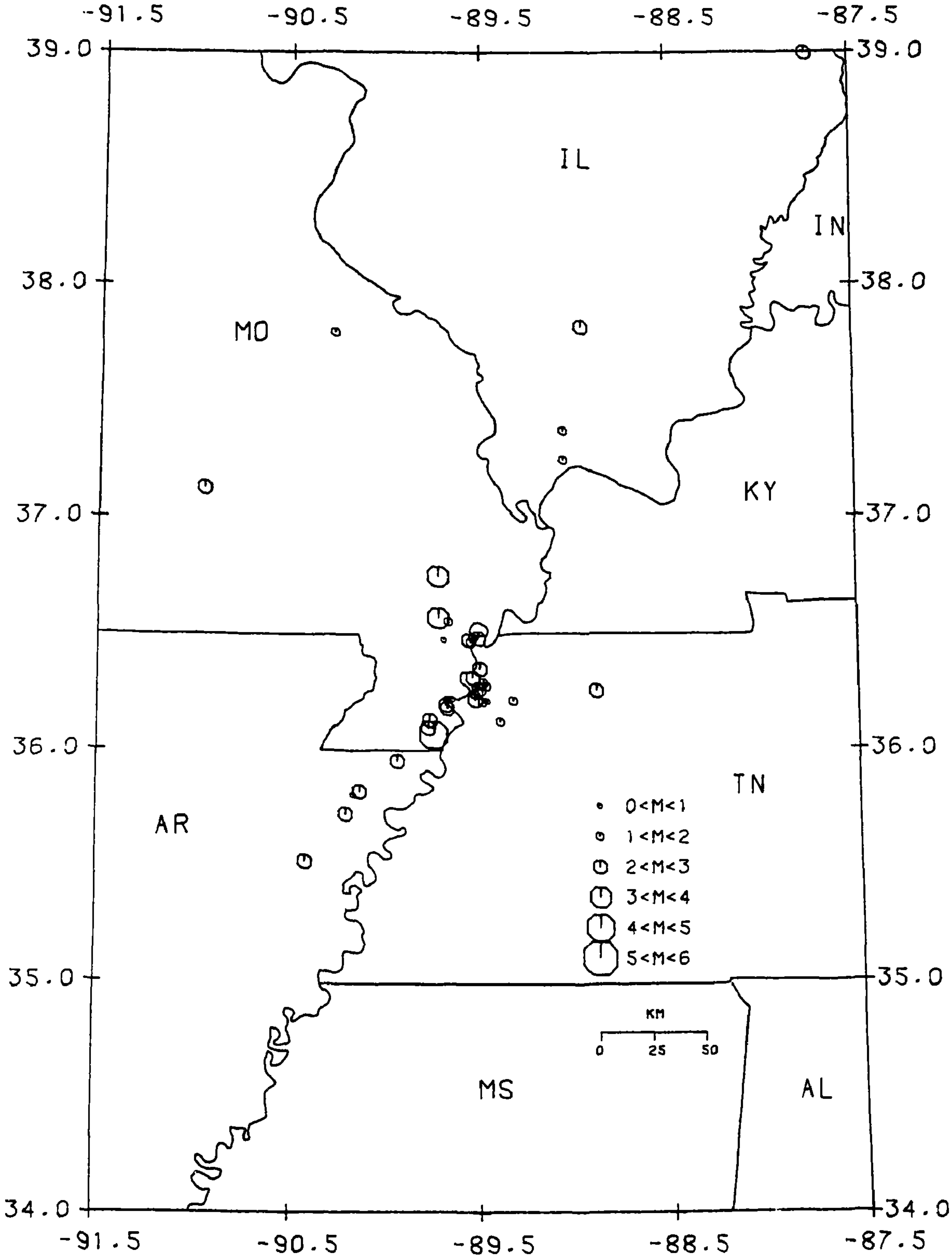

FIGURE 1. CUMULATIVE EVENTS 01 JAN 1989 TO 30 JUN 1989
LEGEND . ◎ EPICENTER

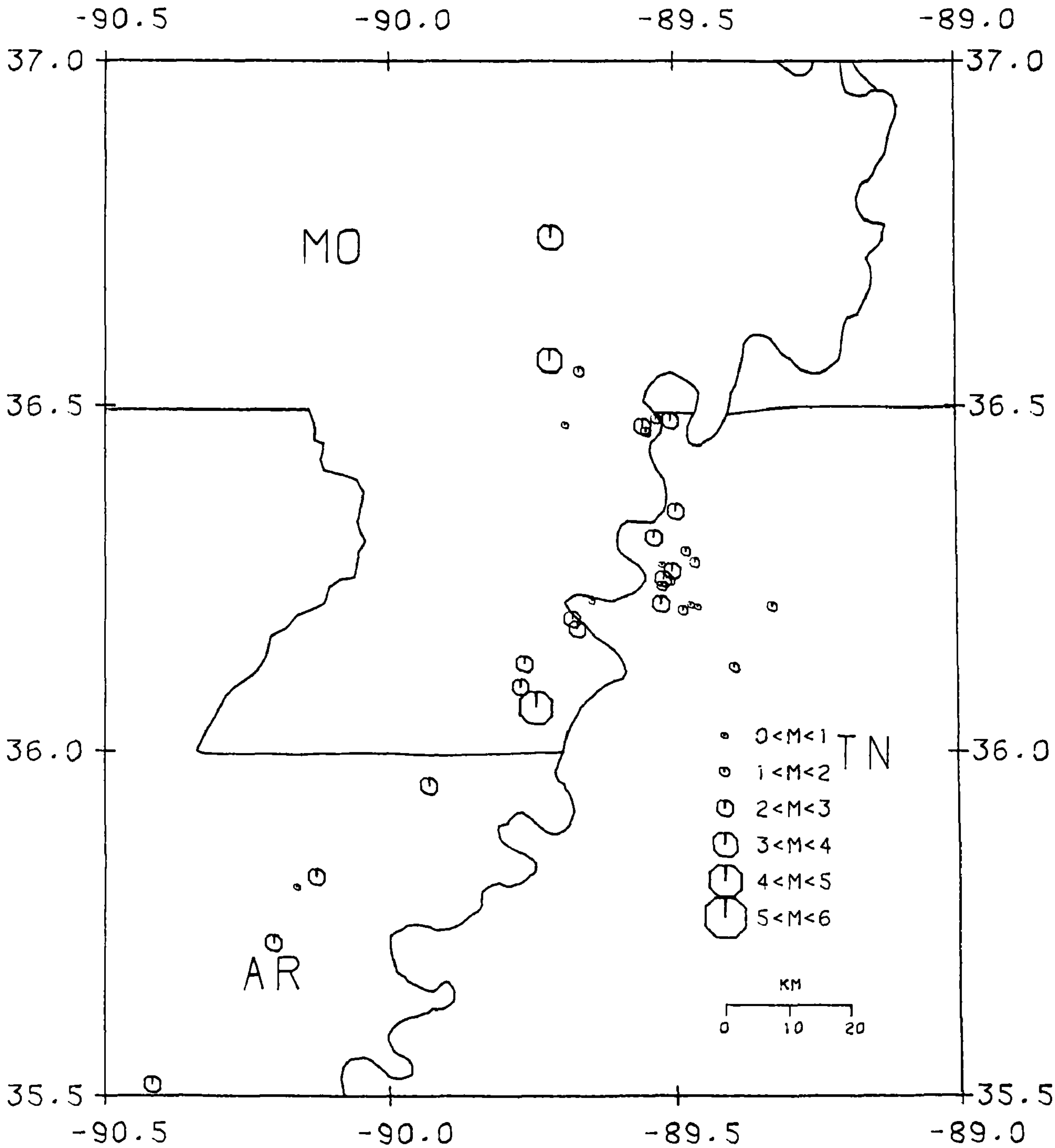

FIGURE 2. CUMULATIVE EVENTS 01 JAN 1989 TO 30 JUN 1989
LEGEND . EPICENTER

Consolidated Digital Recording and Analysis

9930-03412

Sam Stewart
Branch of Seismology
U. S. Geological Survey
345 Middlefield Road Mail Stop 977
Menlo Park, California 94025

Investigations.

On February 1, 1989 the operational functions of this project, along with appropriate personnel, were transferred to the "North and Central California Seismic Network Processing" project (9930-01160). See Rick Lester's report in this volume for a summary of the CUSP network processing function.

The "Consolidated Recording and Analysis " project now has as its primary goal the design, development and support of computer-based systems for processing earthquake data recorded by large, telemetered seismic networks. This includes (1) realtime systems capable of monitoring up to 512 stations and detecting and saving waveforms even from earthquakes registering just slightly above background noise level, (2) near-realtime and offline graphics systems to analyze, catalog and archive the detected waveforms, (3) support and documentation for the users of the system.

Hardware for these systems is based upon Digital Equipment Corporation (DEC) VAX series of micro-computers. Currently, this includes the VAX 750, microVAX II, and VAXstations 2000 and 3200.

Software is based upon the DEC/VMS operating system, the CUSP database system, and the GKS graphics system. VMS is a major operating system, well documented and developed, and has a rich variety of system services that facilitate our own system development. CUSP is a state-driven data base system specifically designed and developed by Carl Johnson of the USGS.
GKS is an international-standard graphics analysis package that provides interactive input facilities as well as graphical output to a workstation. We use the DEC implementation of GKS.

Results.

1. Realtime Data Acquisition: system development and support.

Realtime earthquake detection and data acquisition systems are running at the Varian site and Halliburton site in Parkfield, CA. The Varian site has been running throughout this report period. The Halliburton site began useful work in June, 1989. At that site a Vaxstation II computer is monitoring an array of 3-component seismometers in each of 9 boreholes. Digitizing rate is 500 samples/sec per component.

The CUSP realtime system operating at the University of Nevada (Reno) was modified to accept digital data directly. It now collects the usual analog signals that are digitized at the computer interface, and telemetered digital data.

The CUSP realtime system, as well as the Generic CUSP data processing system, was installed at the Idaho National Electronics

Laboratory in September, 1989. Signals are input to the Vaxstation 3200 computer via a Camac Crate programmable interface.

Asynchronous DECNET software/hardware was installed and now works between Menlo Park and Parkfield, and Menlo Park and Pasadena. One use of it is to transfer waveforms from the Parkfield Halliburton site to Menlo Park.

2. Data processing with the (Generic) CUSP system: development and support.

The (Generic) CUSP data analysis system is now developed to the point where all the pieces are in place, and now fine tuning and elimination of bugs is underway. The CALNET seismic network processing group in Menlo Park started using it with data beginning September 1, 1989. (See Rick Lester's project cited above.) We provide development and support services to the CALNET project, to equivalent network projects at Pasadena and Reno, and to the Menlo Park Parkfield Earthquake Prediction project.

3. Documentation of the Generic CUSP system.

Online documentation of the CUSP system commands is available on the Branch VAX/750 in Menlo Park. When you are working in a CUSP environment, by typing CHELP (Cusp HELP) you enter into a help-file structure that contains detailed descriptions of nearly all CUSP commands, with many examples. There are options to make hard copies as well. The online CHELP documentation feature allows CUSP users quick access to syntax of various commands and processes, as well as a presentation of nearly all available CUSP commands.

4. Interactive seismic trace processing using the GKS system.

The GKS-based inter-active graphics system (TMIT) for mass processing of seismic waveform data has now started initial 'live' testing. (A serious system bug that caused TMIT to 'hang' in a tight instruction loop seems to have been eliminated by going to a combination of VAX/VMS operating system 4.7, DEC/GKS Version 4.0, and VWS 3.2.) TMIT runs on our VAXstation 2000 and 3200 computers.

Reports.
None.

Seismic Monitoring of the Shumagin Seismic Gap, Alaska

USGS 14-08-0001-A0260

John Taber
Lamont-Doherty Geological Observatory of Columbia University
Palisades, New York 10964
(914) 359-2900

Investigations

Seismic data from the Shumagin seismic network were processed to obtain origin times, hypocenters, and magnitudes for local and regional events. The processing resulted in files of hypocenter solutions and phase data, and archive tapes of digital data. These files are used for the analysis of possible earthquake precursors, seismic hazard evaluation, and studies of regional tectonics and volcanicity (see Analysis Report, this volume). Yearly bulletins are available starting in 1984.

Results

The Shumagin network was used to locate 135 earthquakes from January through June 30, 1989. The seismicity of the Shumagin Islands region for this time period is shown in map view in Figure 1 and in cross section in Figure 2. There were a total of 4 events over magnitude 4 during the time period. The largest event in this period within the network occurred on 5/19/89, had a m_b of 5.0, and was located just south of the Shumagin Islands at 53.34N, 165.14W.

The overall pattern over this time period is similar to the long term seismicity. Concentrations of events occur at the base of the main thrust zone and in the shallow crust directly above it. The continuation of the thrust zone towards the trench is poorly defined. West of the network (which ends at 163°), the seismicity is more diffuse in map view and extends closer to the trench. Below the base of the main thrust zone (~45 km) the dip of the Benioff zone steepens.

Unusually bad weather this winter caused severe damage to a number of remote sites, which resulted in only 135 events recorded during the first half of the year. Servicing of the network was successfully completed in July, most sites were visited, and neccessary repaires were made . The network is capable of digitally recording and locating events as small as M_l=0.4 with uniform coverage at the 2.0 level. Events are picked and located automatically at the central recording site in Sand Point, Alaska and the results, along with subsets of the digital data, can be accessed via telephone modem. Onscale recording is possible to ~M_s=6.5 on two telemetered 3 component force-balance accelerometers. Larger events are recorded by one digitally recording accelerometer and on photographic film by 10 strong-motion accelerometers.

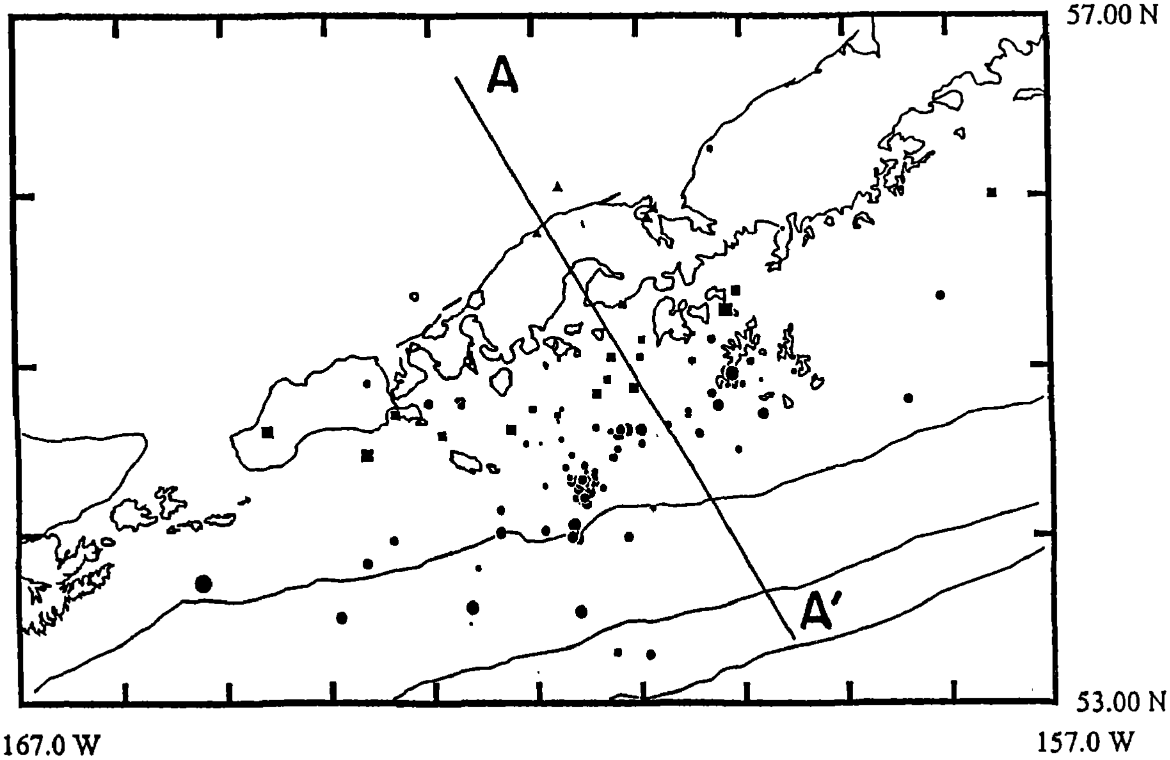

Figure 1. Seismicity located by the Shumagin seismic network from January through July, 1989. Squares are events between 50 and 150 km; triangles are events below 150 km.

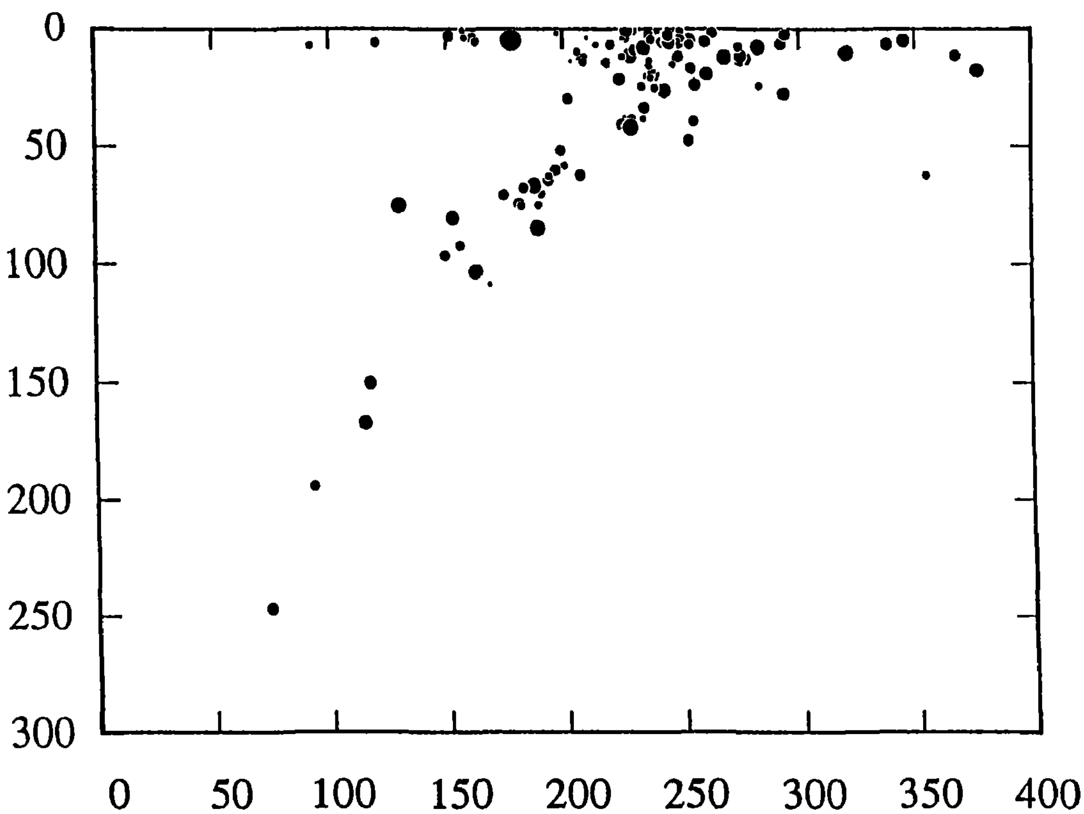

Figure 2. Cross-section of Shumagin network seismicity along line A-A' in previous figure.

Earthquake Hazard Research in the Greater Los Angeles Basin and Its Offshore Area

#14-08-0001-A0620

Ta-liang Teng
Egill Hauksson
Thomas L. Henyey

Center for Earth Sciences
University of Southern California
Los Angeles, CA 90089-0740
(213) 743-6124

INVESTIGATIONS

Monitor earthquake activity in the Los Angeles Basin and the adjacent offshore area. Upgrade of instrumentation for onscale recording of waveforms from local earthquakes.

RESULTS

The 01 January - 30 September, 1989 Los Angeles Basin Seismicity

In addition to numerous single shocks during 01 January- 3 September 1989 two events of M_L=5.0 and M_L=4.6 were recorded (Figure 1). The first mainshock of January 19 was located 15 km south of Malibu and was followed by several hundred aftershocks. The mainshock fault plane solution showed pure thrust faulting, similar to the solution for the 1979 Malibu earthquake. The second mainshock of April 7 was located on the Newport-Inglewood fault, near Newport Beach. This event was located 2-3 km south of the epicenter of the 1933 Long Beach earthquake. The Newport Beach earthquake that showed pure strike-slip movement was only followed by six recorded aftershocks. Two earthquakes of M=4.4 and 4.1 occurred on June 12 beneath the Montebello Hills, approximately 10 km to the southwest of the 1987 Whittier Narrows earthquake. Both events showed pure thrust faulting on east striking planes. In addition, during this time period enhanced activity is observed along the Elysian Park fault, to the west of the Whittier Narrows.

These and other sequences recorded during 1988-1989 indicate an unusually high level of seismicity in the Los Angeles basin. Jones et al. (1989) have shown that the present rate is anomalously high compared with the rate recorded from 1975 to March 1986.

Crustal Velocity Models for the Los Angeles Basin.

As a part of our analysis of the local earthquake data, we have determined four sets of one-dimensional velocity models and corresponding sets of station delays using the computer code VELEST. These models have been published by Hauksson [1987], Hauksson and Jones [1989], Hauksson and Saldivar [1989], and Hauksson [in preparation].

The 1988 and 1989 seismicity was located using the four pairs of new velocity models. These models are listed in Table 1 and areas where each pair of models applies are shown in Figure 2. Each pair of models has a corresponding set of station delays. A new version of the computer program Hypoinverse (Klein, 1989) was used to calculate the improved hypocenters. If a hypocenter falls within the area of a model pair, one model (even numbered models in Table 1) is used for stations in the Los Angeles basin and an alternative regional model (odd numbered model in Table 1) is used for stations located outside of the basin. At the model boundaries the models are tapered off over a buffer zone indicated by the dashed line in Figure 2. If the earthquake is located outside the model pairs the average or generic southern California model is used (model 1 in Table 1). In general the new models provide more accurate hypocenters than were available before.

PUBLICATIONS

Hauksson, E. and L. M. Jones, The 1987 Whittier Narrows earthquake sequence in Los Angeles,southern California: Seismological and tectonic analysis, J. Geophys. Res., 94, 9569-9590, 1989.

Hauksson E. and G. V. Saldivar, Seismicity (1973-1986) and active compressional tectonics in the Santa Monica Bay, southern California, J. Geophys. Res. , 94, 9591-9606, 1989.

Hauksson, E. and R. S. Stein, The 1987 Whittier Narrows earthquake: a metropolitan shock, J. Geophys. Res., 94, 9545-9547, 1989.

Jones, L. M., K. E. Sieh, E. Hauksson and L. K. Hutton, The December 3, 1988 Pasadena, California Earthquake: Evidence for Strike-slip Motion on the Raymond fault, Bull. Seism. Soc. Amer.., to appear in February 1990.

Hauksson, E., Earthquakes, active faulting,and stress in the Los Angeles Basin, submitted to J. Geophys. Res., August 1989.

REPORTS

Hauksson, E., T. L. Teng, T. L. Henyey, M. Robertson, J. K. McRaney and L. Hsu, Earthquake hazard research in the Los Angeles basin and its offshore area, Annual Technical Report submitted to the U.S. Geological Survey, December 1988, 90 pp.

Hauksson, E., Comparison of broad-band waveforms of local earthquakes recorded at crystalline and sedimentary rock sites in the Los Angeles basin, submitted to fall AGU meeting, 1989.

Robertson, M. C., and E. Hauksson, Three-dimensional fine velocity structure of the Los Angeles basin, submitted to fall AGU meeting, 1989.

TABLE 1
LOS ANGELES BASIN VELOCITY MODELS

VELOCITY KM/S	DEPTH TO TOP OF LAYER KM	VELOCITY KM/S	DEPTH TO TOP OF LAYER KM
SOUTHERN CALIFORNIA MODEL			
C model	1		
5.50	0.00		
6.30	5.50		
6.70	16.00		
7.80	32.00		
NEWPORT-INGLEWOOD FAULT			
NIL	model 2	NIS	model 3
4.11	0.00	5.52	0.00
5.55	4.00		
5.73	5.50	6.23	5.50
6.66	16.00	6.62	16.00
7.80	32.00	7.73	32.00
WHITTIER NARROWS			
WNL	model 4	WNS	model 5
3.31	0.00	4.10	0.00
5.16	2.00	4.09	2.00
6.02	5.50	6.35	5.50
6.37	13.00		
6.68	16.00	6.54	16.00
7.80	30.00	7.87	32.00
SANTA MONICA BAY			
SBL	model 6	SBS	model 7
3.30	0.00	4.04	0.00
4.14	2.00	5.22	2.00
6.04	5.50	6.18	5.50
6.25	13.00		
6.72	16.00	6.57	16.00
7.80	32.00	7.80	32.00
PALOS VERDES AND SAN PEDRO BAY			
PV1	model 8	PV2	model 9
3.43	0.00	4.28	0.00
4.39	2.00	5.46	2.00
6.24	5.50	6.25	5.50
6.47	13.00		
6.48	16.00	6.62	16.00
7.80	32.00	7.80	32.00

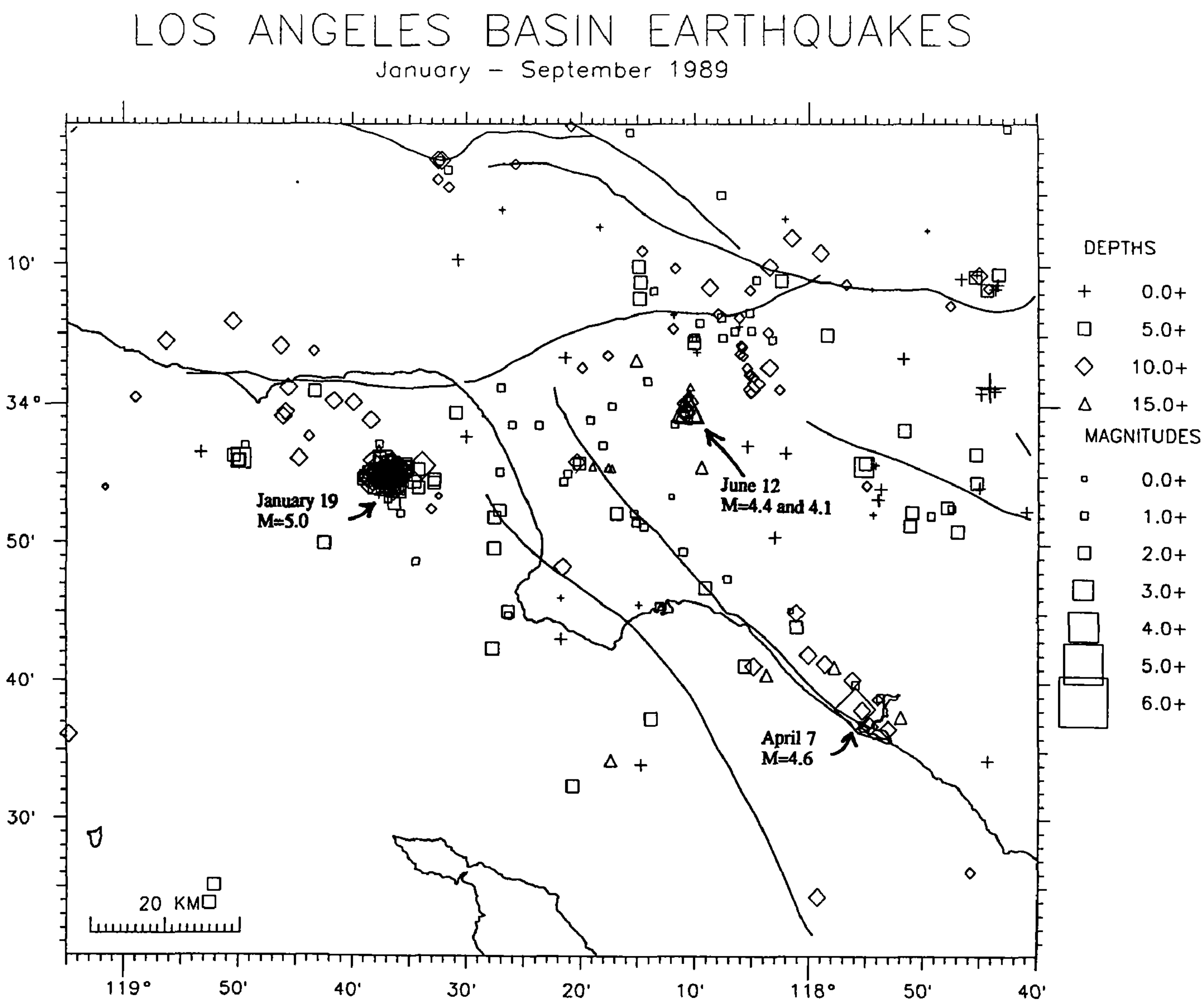

Figure 1. Seismicity recorded during 01 January - 30 September 1989 by the USC Los Angeles basin network.

LOS ANGELES BASIN VELOCITY MODELS

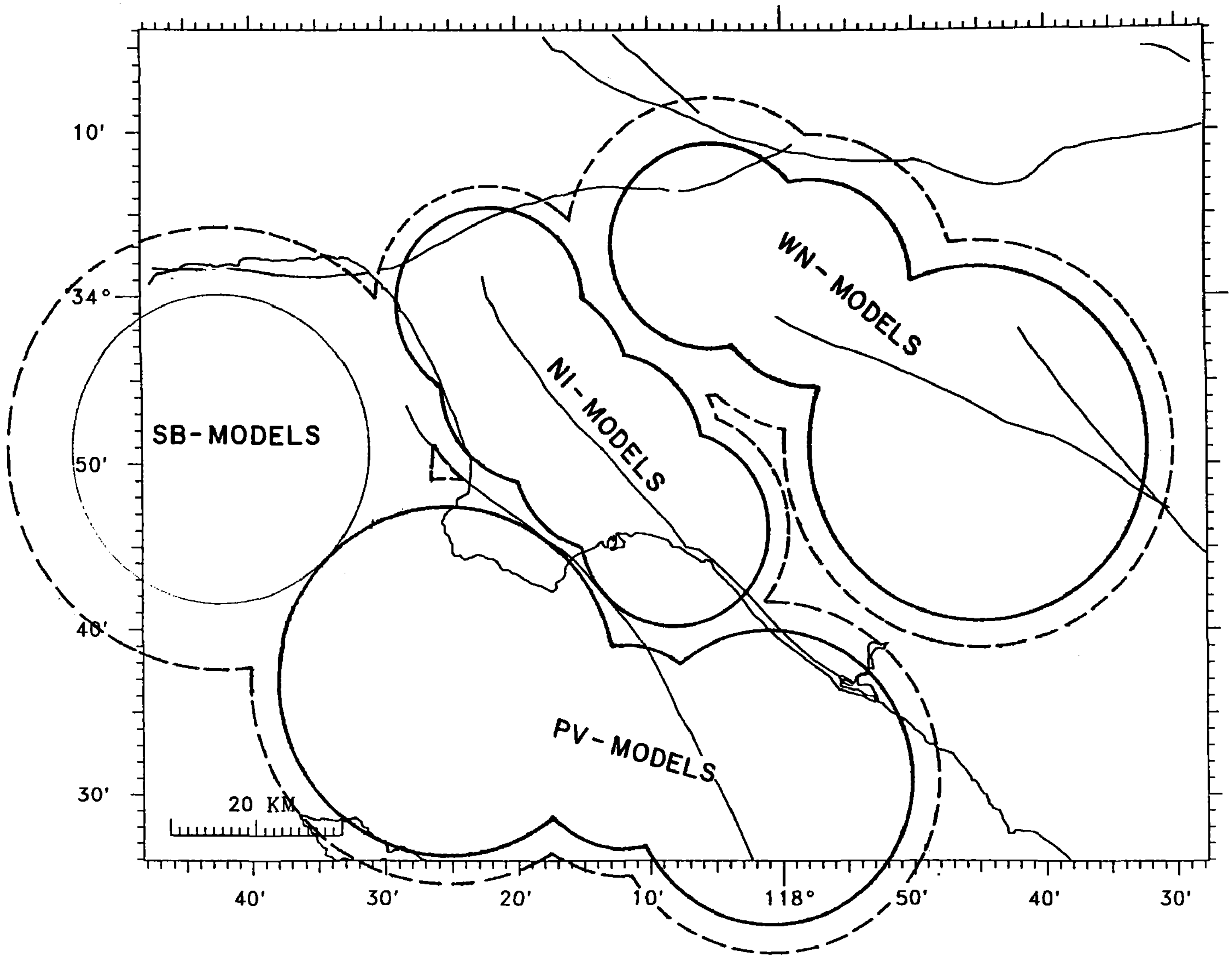

Figure 2 Four pairs of velocity models (WN, NI,PV, and SB) have been determined for the Los Angeles basin. Each pair of models applies to earthquakes located within the encircled area. The dashed outer circles indicate a zone of tapering off for the model pairs. Earthquakes located outside the circles are located with the generic southern California model.

Field Experiment Operations

9930-01170

John Van Schaack
Branch of Seismology
U. S. Geological Survey
345 Middlefield Road MS-977
Menlo Park, California 94025
(415) 329-4780

Investigations

This project performs a broad range of management, maintenance, field operation, and record keeping tasks in support of seismology and tectonophysics networks and field experiments. Seismic field systems that it maintains in a state of readiness and deploiys and operates in the field (in cooperation with user projects) include:

a. 5-day recorder portable seismic systems.
b. "Cassette" seismic refraction systems.
c. Portable digital event recorders.

This project is responsible for obtaining the required permits from private landowners and public agencies for installation and operation of network sensors and for the conduct of a variety of field experiments including seismic refraction profiling, aftershock recording, teleseism P-delay studies, volcano monitoring, etc.

This project also has the responsibility for managing all radio telemetry frequency authorizations for the Office of Earthquakes, Volcanoes, and Engineering and its contractors.

Personnel of this project are responsible for maintaining the seismic networks data tape library. Tasks includes processing daily telemetry tapes to dub the appropriate seismic events and making playbacks of requested network events and events recorded on the 5-day recorders.

Results

Seismic Refraction

Personnel from this project assisted Mr D. Okaya of U. C. Berkeley in a small seismic reflection project in southeast California. Personnel also selected shotpoints in Arizona for the Pacific Arizona Crustal Experiment and wrote environmental assessment reports for this same project. The cassette recorders were used in a cooperative program with the Canadian Geological Survey in Western Canada. This project provided explosive handlers and shooters.

Portable Networks

The 5-day portable tape recorders were used in two small experiments during the summer; one in southern Alaska and the other in southwest Oregon.

Geothermal Seismotectonic Studies

9930-02097

Craig S. Weaver
Branch of Seismology
U. S. Geological Survey
at Geophysics Program AK-50
University of Washington
Seattle, Washington 98195
(206) 442-0627

Investigations

1. Continued analysis of the seismicity and volcanism patterns of the Pacific Northwest in an effort to develop an improved tectonic model that will be useful in updating the geothermal potential of the Cascade Range and earthquake hazards in the region. Funded by Geothermal and Volcano Hazards. (Weaver)

2. Continued acquisition of seismicity data along the Washington coast, directly above the interface between the North American plate and the subducting Juan de Fuca plate. Funded by Geothermal and Volcano Hazards. (Weaver, Yelin, UW contract)

3. Continued seismic monitoring of the Mount St. Helens area, including Spirit Lake (where the stability of the debris dam formed on May 18, 1980 is an issue), Elk Lake, and the southern Washington-Oregon Cascade Range (north of Newberry Volcano). The data from this monitoring is being used in the development of seismotectonic models for southwestern Washington and the interaction of the Basin and Range with the Oregon Cascades. Funded by Volcano Hazards. (Weaver, Zollweg, Grant, Norris, Yelin, UW contract)

4. Study of Washington seismicity, 1960-1989. Earthquakes with magnitudes greater than 4.5 are being re-read from original records and will be re-located using master event techniques. Focal mechanism studies are being attempted for all events above magnitude 5.0, with particular emphasis on the 1962 Portland, Oregon event. Emphasis is being placed on developing the seismotectonic framework of the Portland basin, in order to further models of segment boundaries defined by the pattern of late Cenozoic volcanism. Funded by Geothermal. (Yelin, Weaver)

5. Detailed analysis of the seismicity sequence accompanying the May 18, 1980 eruption of Mount St. Helens, including about 500 deep earthquakes (>3 km) that occurred prior to May 18. Earthquakes are being located in the ten hours immediately following the onset of the eruption, and the seismic sequence is being compared with the detailed geologic observations made on May 18. Re-examination of the earthquake swarms that followed the explosive eruptions of May 25 and June 13, 1980, utilizing additional playbacks of 5-day recorder data. Funded by Volcano Hazards. (Zollweg--volunteer, Norris, UW contract)

6. Study of earthquake catalogs for the greater Parkfield, California region for the period 1932-1969. Catalogs from the University of California (UCB) and CalTech (CIT) are being compared, duplicate entries noted, and the phase data used by each reporting institution are being collected. The study is emphasizing events greater than 3.5, and most events will be relocated using station corrections determined from a set of master events located by the modern networks. Funded by the Earthquake Program. (Meagher, Weaver, with Lindh in Menlo)

7. Study of estuaries along the northern Oregon coast in an effort to document probable subsidence features associated with paleosubduction earthquakes. Funded by Geothermal and Earthquake Programs. (Grant).

Results

A crustal refraction profile across the Columbia Plateau through the Pasco Basin of Washington has given us the opportunity to compare details of the crust and upper mantle with the distribution of seismicity. This refraction line (C-C' in Fig. 1) crossed the series of post-Miocene east-west striking thrust faults at acute angles and passed through the center of the Pasco Basin where the flows of the Columbia River Basalt Group are thought to be thickest.

East of the Cascade crest in Washington and northern Oregon, all earthquakes locate within the mid to upper crust. More than ninety percent of the earthquakes occur at depths less than 8 km and there are no events located deeper than 25 km. Although several magnitude 4+ earthquakes have been located in the Columbia Plateau east of the northern Oregon Cascade Range, the great majority of earthquakes occur around the Pasco Basin (Fig. 1). The shallow depths of most earthquakes in eastern Washington mean that their hypocenters lie within the Columbia River Basalt Group, a sequence of flood basalts of Miocene age that thickens to a maximum depth of 6 km in the central Pasco Basin.

The shallowest events frequently occur in earthquake swarms isolated in both space and time. Swarms occur in restricted volumes only a few kilometers in diameter and last a few weeks to several months. Some swarms appear spatially associated with east-west trending anticlines, such as the steeply dipping north limb of the Saddle Mountains anticline (Fig. 1), possibly along short segments of a high-angle reverse fault. There are few other associations of seismicity with mapped surface structures and no indication of horizontal alignments of earthquakes that would indicate major segments of near-vertical fault systems (Fig. 1). At depths greater than 8 km, earthquakes occur as isolated events, rather than in swarms.

Throughout the Columbia Plateau in eastern Washington thrust or reverse focal mechanisms are common. These mechanisms suggest that movement occurs on east-west trending faults, although no earthquake has been correlated to a specific mapped fault. P-axes of these focal mechanisms are roughly horizontal and oriented north-south, and the direction of maximum principal stress has been inferred to be north-south [Malone and others, 1975]. This stress direction is consistent with the east-west trending anticlines mapped in the area (shown in Fig. 1)

The crustal structure (Fig. 2) interpreted by Catchings and Mooney [1988] along line C-C' contains four features of interest with respect to the earthquake distribution: 1) a series of alternating layers of high and low velocity (5.85 and 5.3 km/s respectively) that comprise the Columbia River Basalt Group. The high velocity represents the Miocene basalts whereas the low velocity represents sedimentary deposits between flows [Catchings and Mooney, 1988]. This integrated structure reaches its maximum depth near the center of the Pasco Basin (Fig. 2). 2) A low velocity layer beneath the Columbia River Basalt Group that is interpreted by Catchings and Mooney as a pre-Miocene sedimentary basin. 3) The low velocity layer is contained within a graben structure defined in the mid and upper crust (Fig. 2). The graben structure is about 70 km wide and has a vertical offset of about 4 km between the central axis and either side; the low velocity sedimentary fill is thickest within the graben axis. 4) A lower crustal upwelling of velocity 7.5 km/s occurs beneath the entire graben structure, but reaches its highest crustal level of about 25 km directly beneath the center of the graben. Taken together, these four elements are typical of the structure of continental rifts [Catchings and Mooney, 1988].

The earthquake distribution (Fig. 2) shows clearly the concentration of events within the Columbia River Basalt Group. Most of the shallow crustal events within the Columbia River Basalt Group are near the Saddle Mountains which occur over the northeastern edge of the upper crustal graben. The low velocity sediments (of velocity 5.0 km/s) within the graben are nearly devoid of earthquake hypocenters: the deeper crustal events occur in crystalline basement and subbasement layers with velocities of 6.1-6.4 km/s and 6.8 km/sec, respectively [Catchings and Mooney, 1988]. The deepest crustal events at about 22 km occur above the shallowest extent of the lower crustal upwelling. Seismicity seems to be distributed unevenly about the upper crustal graben, with most of the events occurring on the northeast side of the graben. The graben, though pre-dating the Columbia River Basalt Group and the contemporary tectonics, may exert some influence on the shallow crust producing (or localizing) the Saddle Mountain system and contemporary seismicity, although the processes responsible for localizing the shallow thrusts and earthquakes are unknown. Likewise, there is a tendency for most of the earthquakes below the Columbia River Basalt Group to occur beneath the northeastern half of the graben (Fig. 2).

REFERENCES

Catchings, R.D., and W.D. Mooney, 1988, Crustal structure of the Columbia Plateau: Evidence for continental rifting, Journal of Geophysical Research, v. 93, p. 459-474.

Malone, S.D., G.H. Rothe, and S.W. Smith, 1975, Details of microearthquake swarms in the Columbia Basin, Washington, Bulletin of the Seismological Society of America, v. 65, p. 855-864.

Reports

Grant, W. C. and Weaver, C. S., 1989, Seismicity of the Spirit Lake area: Estimates of possible earthquake magnitudes for engineering design, in *The formation and significance of major lakes impounded during the 1980 eruption of Mount St. Helens, Washington, U. S. Geological Survey Professional Paper,* edited by R. L Shuster and W. Meyer, (still in press). Funded by Earthquake, Geothermal, and Volcano Hazards.

Mooney, W. and C. S. Weaver, 1989, Regional crustal structure and tectonics of the Pacific Coastal States: California, Oregon, and Washington, in, *GSA Memoir, Geophysical Framework of the Continental United States,* L. Pakiser and W. Mooney, eds., in press. This project's contribution funded by Geothermal and Earthquake Programs.

Zollweg, J. E., 1989, High frequency earthquakes following the 1985 eruption of Nevada del Ruiz, Columbia, *J. Volcan. and Geotherm. Res.*, 19 pages, 8 figures, (in press). Funded by Volcano Hazards.

Ludwin, R., C. S. Weaver, and R. S. Crosson, Seismicity of Washington and Oregon, *GSA Decade of North American Geology Associated Volume, Neotectonics,* 35 pages, 10 figures, (in press). Funded by Geothermal, Volcano Hazards and Earthquake Programs.

Zollweg, J. E. and P. Johnson, The Darrington seismic zone in northwestern Washington, *Bull. Seism. Res. Amer.*, 19 pages, 10 figures, (in press). Funded by Earthquake Program.

Shedlock, K. M. and C. S. Weaver, Rationale and outline of a program for earthquake hazards assessment in the Pacific Northwest, in *U.S. Geol. Surv. Open-File Report 89-xxx,* 8 pages, 1 figure, (in press), 1989. Funded by Geothermal and Earthquake Programs.

Weaver, C. S. and K. M. Shedlock, Potential subduction, probable intraplate, and known crustal earthquake source areas in the Cascadia subduction zone, in *U.S. Geol. Surv. Open-File Report 89-xxx,* 8 pages, 8 figures, (in press), 1989. Funded by Geothermal and Earthquake Programs.

Fournier, R. O. and C. S. Weaver, Heat flow from the Washington Cascades and adjacent regions estimated using variations in depth of the seismogenic crust, submitted to *J. Geophys. Res.*, 21 pages, 8 figures. Funded by Geothermal Program.

Finn, C., Weaver, C. S., and W. D. Stanley, Relation of earthquakes and aeromagnetic anomalies to crustal structure of western Washington, (abs), *EOS, Trans. Amer. Geophys. Union, 71,* in press.

Grant, W. C., Atwater, B. F., Carver, G. A., Darienzo, M. E., Nelson, A. R., Peterson, C. D., Vick, G. S., Radiocarbon dating of late Holocene coastal subsidence above the Cascadia subduction zone--compilation for Washington, Oregon and northern California, (abs), *EOS, Trans. Amer. Geophys. Union, 71*, in press.

Shedlock, K. M., Weaver, C. S., Opppenheimer, D., King, G. C. P., Seismic deformation in the Pacific Northwest, *EOS, Trans. Amer. Geophys. Union, 71,* in press.

Yelin, T. S. and H. J. Patton, Seismotectonics of the Portland, Oregon region, (abs), *EOS, Trans. Amer. Geophys. Union, 71,* in press.

Norris, R. D., Seismograms from the 16 August 1989 rockfall from Russell Cliff, Mount Rainier, (abs), *EOS, Trans. Amer. Geophys. Union, xx,* in press (presented at Pacific Northwest AGU section meeting).

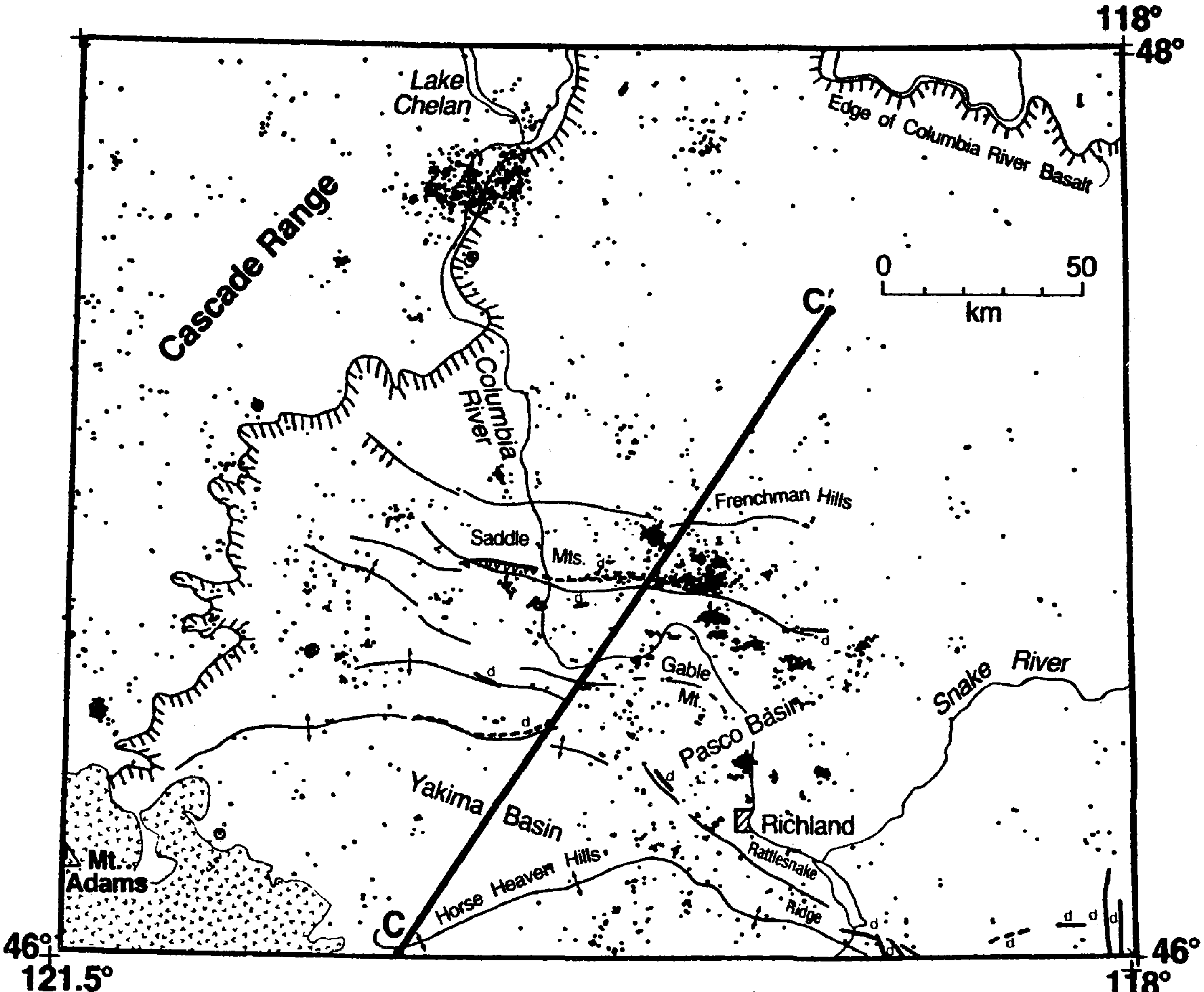

Figure 1. Map view of seismicity in Eastern Washington, 1970-1987, magnitude 1.0 and larger. Earthquakes smaller than magnitude 4 are shown by a single symbol size, while larger events are scaled by whole units of magnitude. Also shown (heavy lines) are mapped faults of post-Miocene age, and (light lines) axes of major anticlines [adapted from Shannon and Wilson, Inc., 1977]. The western margin of the Columbia River Basalt Group is indicated by hachures while Quaternary volcanics near Mt. Adams are shown as a stippled pattern. Cross section line C-C' is indicated.

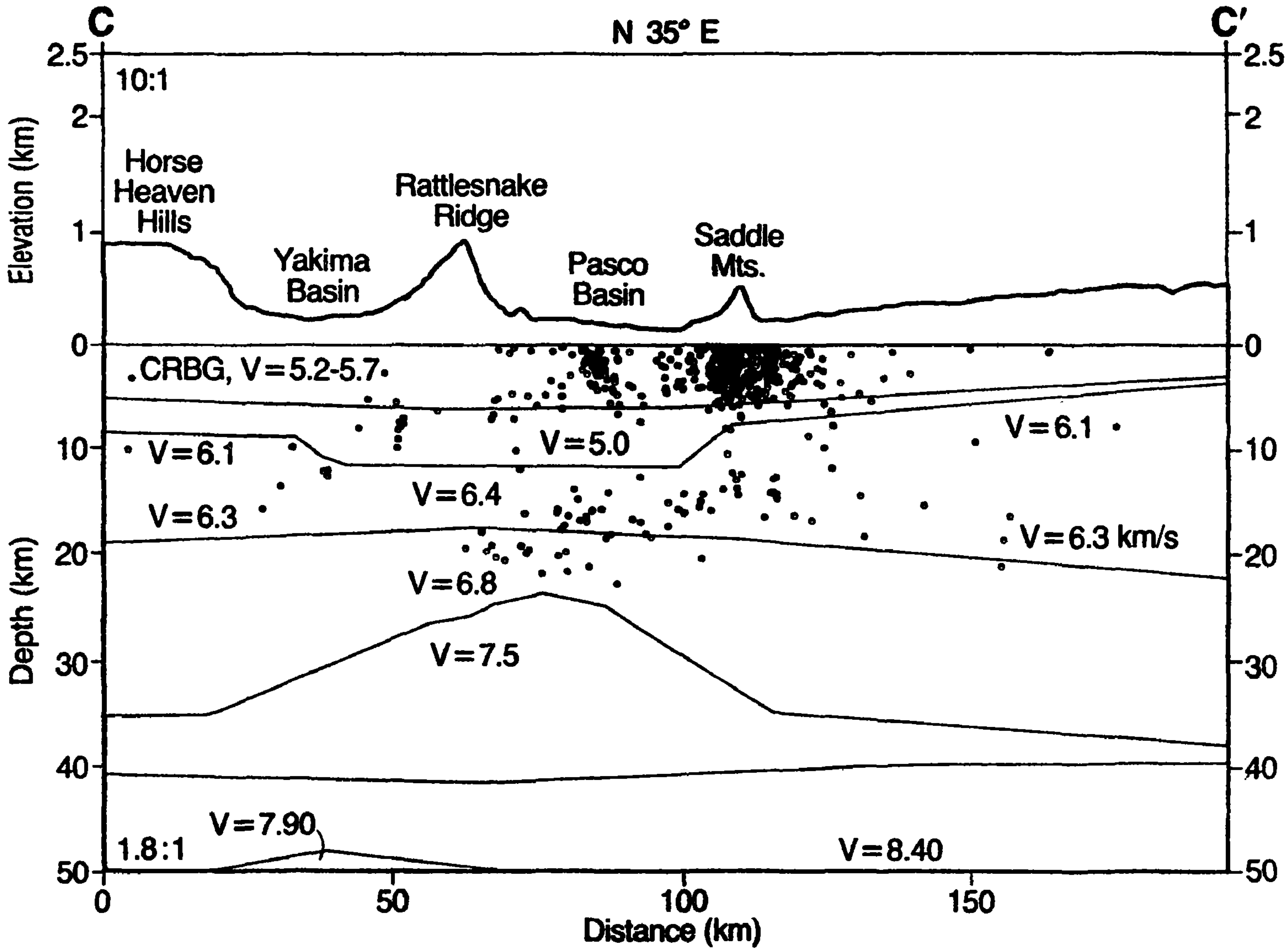

Figure 2. Eastern Washington cross section C-C' (Figure 9); Structural information from Catchings and Mooney [1988]. 10:1 vertical exaggeration of topography; 1.8:1 vertical exaggeration of subsurface. CRBG, Columbia River Basalt Group. Best-located earthquake hypocenters since 1970, regardless of magnitude, are shown by a single symbol size. Earthquakes for 50 km on either side of line C-C' in Figure 1 are projected onto a vertical plane striking N 35° E.

Seismic Source Analysis Using Empirical Green's Functions

9910-02676

J. Boatwright and L. Wennerberg
Branch of Engineering Seismology and Geology
U.S. Geological Survey
345 Middlefield Road, MS 977
Menlo Park, California 94025
(415) 329-5609, 329-5607, 329-5659

Investigations

Theoretical and observational investigations of the earthquake rupture process, with application to locating subevents of a complex rupture, and resolving the spatial and temporal distribution of stress drop in an earthquake.

Results

1. DiBona and Boatwright (1990) have designed, implemented, and tested an iterative inversion scheme which uses positivity constraints to deconvolve recordings of empirical Green's functions from recordings of larger earthquakes, and which minimizes the number of subevents by using an F-test to check the statistical significance of each added subevent. The deconvolutional procedure has been sucessfully used to analyze a suite of aftershock recordings from the 1976 Friuli, Italy, earthquake sequence. In this analysis, DiBona and Boatwright (1990) verified Boatwright's (1988) assertion that asperity waveforms provided more appropriate models for the subevent radiation than crack waveforms. The asperity waveforms were obtained by filtering the empirical Green's functions using a simple mimimum phase filter.

2. Wennerberg (1988 and 1990) has developed a variation of Boatwright's (1988) filtering strategy in which the recordings of small earthquakes a amplified at long periods using a zero-phase shift filter to simulate recordings of large simple earthquakes or large subevents within a complex rupture process. This procedure has proven to be remarkably sucessful not only for scaling small earthquakes, but also for identifying the dominant subevents of a complex earthquake. Where the approach of DiBona and Boatwright (1990), described above, yields Green's functions for the stress release at a single grid point (or discrete sub-event) within a larger rupture process, the analysis of Wennerberg (1990) is designed to model the radiation from coherent sub-events, that is, coherent segments of the rupture process which release stress over a spatially finite area.

References

Boatwright, J., 1988, The seismic radiation from composite models of faulting, Bull. Seism. Soc. Am. 78, 489-508.

Wennerberg, L., 1988, Estimating ground motion with zero-phase scaling filters: EOS 69, 1301.

Publications

DiBona, M., and J. Boatwright, 1990, Single-station decomposition of seismograms for subevent time histories, submitted to Geophys. Jour. of the R.A.S.

Wennerberg, L., 1990, Approximate w^{-2} time series from stochastic summation of empirical Green's functions, submitted to Bull. Seism. Soc. Am.

Earthquake Hazard Investigations in the Pacific Northwest

14-08-0001-G1390

R.S. Crosson and K.C. Creager
Geophysics Program
University of Washington
Seattle, WA 98195
(206) 543-8020

Investigations

The objective of this research is to investigate earthquake hazards in western Washington, including the possibility of a large subduction-style earthquake between the North American and Juan de Fuca plates. Improvement in our understanding of earthquake hazards is based on better understanding of the regional structure and tectonics. Current investigations by our research group focus on the configuration of the subducting Juan de Fuca plate, differences in characteristics of seismicity between the overlying North American and the subducting Juan de Fuca plates, kinematic modeling of deformation of the Juan de Fuca slab, and modeling of lateral velocity variations in the shallow crust. Research during this contract period concentrated on the following topics:

1. Final publication of 3-D crustal velocity models for Puget Sound and southwestern Washington resulting from tomographic inversion of earthquake travel times, and preparation of an article describing a technique for incorporating gravity data as a constraint in the tomographic inversion of earthquake travel times for crustal structure.

2. Development of non-linear inversion techniques for use in an inversion for deep crustal and shallow mantle velocity structure beneath Washington.

3. Investigation of anomalous phase arrivals from sub-crustal earthquakes.

4 Modeling of 3-D kinematic flow of the subducted slab.

Results

1. 3-D structure in western Washington

Final result of our inversions of local earthquake travel-time data for three-dimensional crustal velocity structure have been published or are in press in the form of several journal articles. An additional article on the use of gravity data as a further constraint on the velocity model is being prepared by J. Lees and J. VanDecar.

2. Deep structure of the Cascadia subduction zone

In most subduction regions, the position of the subducting lithosphere is indicated by a Benioff zone. In the Cascadia subduction zone (CSZ), the lack of any well-defined Benioff zone east of the Puget Sound lowland leaves us without detailed knowledge of the plate position. We are studying the deep-crustal and upper-mantle velocity structure of the CSZ by using a large set of teleseismic arrival times which have been recorded on the Washington Regional Seismic Network (WRSN) to invert for velocity structure. Previous teleseismic inversions for velocity structure; Lin and Crosson (1973), Michaelson and Weaver (1986), and Rasmussen and Humphreys (1988); provided low resolution images of the regional velocity structure. The low resolution of these models was due at least in part to the use of (1) small and incomplete data sets, (2) inaccurate, visually chosen arrival times without dependable error estimates and (3) inappropriate linear inversion techniques. In order to obtain a high resolution, well constrained CSZ structure we must improve in each of these areas.

The WRSN has accumulated 9+ years of high-quality digital teleseismic data spanning a nearly complete range of azimuths and distances. To go along with the data set, we have developed a new technique for efficiently extracting both highly accurate relative arrival time and quantitative uncertainty estimates (for use in inversion weighting) from this data. The method combines a multi-channel cross-correlation procedure with adjustment by least squares. A paper on this techniques and its application to the WRSN data will appear shortly in the BSSA. Non-linearity in this inversion arises from the fact that the ray paths depend on the velocity structure. The linear assumption used in past studies significantly distorts ray paths in many parts of the model. This can be dealt with by performing iterative linear inversions, and ray tracing after each iteration to correct the ray paths. The combination of our higher quality data with down-weighting of relatively low quality data (using our quantitative uncertainty estimates) should help to produce a convergent solution.

3. Anomalous Phase Arrivals

Another line of investigation into the deep crustal and upper mantle velocity structure uses phase arrivals from subcrustal earthquakes within the Wadati-Benioff zone under western Washington. Deep structure affects both apparent phase velocities and wave forms. Apparent velocities from these Benioff zone earthquakes show azimuthal dependency at epicentral distance of 100-200 km, with apparent velocities ranging from 7.5 to 8.5 km/sec, with the highest velocities towards the west. This azimuthal dependency could be due to higher velocities in the oceanic lithosphere of the east-dipping subducting slab relative to the surrounding mantle material. Low apparent velocities towards the east in this distance range may give an upper bound of ~7.5 km/sec on the velocity of the wedge of mantle material between the crust and the downgoing slab, lower than the previous estimate of ~7.79 km/s (Zervas and Crosson, 1984). For stations east of the Cascades, at epicentral distances of 200-300 km from the Benioff zone, apparent velocities of 8.25-8.50 km/s are observed. Such high apparent velocities are consistent with the velocity model based on seismic refraction studies (Catchings and Mooney, 1988).

The analysis of subcrustal earthquake waveforms has focused on anomalous phases observed at stations on the Olympic Peninsula, where a high energy arrival is often observed after the initial P-wave, but before the S-wave. This anomalous phase has higher amplitude than the initial P wave, and is not observed on stations towards the east within the same epicentral range. The anomalous phase may represent energy trapped in the low velocity upper crustal layer of the subducting oceanic lithosphere. Such trapped phases have been observed in the subducting Philippine Sea Plate beneath SW Japan (Horai et al., 1985). The anomalous phase arrivals in western Washington show an apparent velocity of 6.0-6.5 km/s, whereas P-arrivals show apparent velocities of 8.2-8.4 km/s in the same western azimuths.

4. Slab Kinematics

As described is the last report, we are attempting to explain the observation that seismicity within the subducting Cascadia slab is concentrated beneath the Puget Sound Basin, along the axis of an apparent east-west trending arch in the slab geometry. The arch extends from an oceanward concave bend in the trench, under the Olympic Mountains, to the Puget Sound Basin. Preliminary calculations of kinematic slab flow suggested that the trench geometry forces along-arc compression in the slab beneath Puget sound, and that an arch in the geometry relieves some of the required in-plane strain rate. During the past six months we have formalized the theoretical description of in-plane strain rates for an arbitrary flow on an arbitrary surface [Creager and Boyd, 1989] and are nearly finished with a new algorithm to calculate the unique flow that globally minimizes the in-plane deformation for an arbitrary surface with boundary conditions imposed on the flow at the trench. A critical part of this calculation is describing realistic slab geometries by smooth continuous surfaces with continuous gradients. We are trying both a taut spline approach and an expansion of the surface in orthogonal polynomials.

Articles

Creager, K.C. and T.M. Boyd, 1989 (revised), The geometry of Aleutian subduction: Three-dimensional kinematic flow modeling, JGR.

Boyd, T.M., and K.C. Creager, 1989 (revised), The geometry of Aleutian subduction: Three-dimensional seismic imaging, JGR.

Lees, J.M. and R.S. Crosson, 1989 (in press), Bayesian ART versus conjugate gradient methods in tomographic seismic imaging: An application at Mount St. Helens, Washington, AMS-SIAM: Conference on spatial statistics and imaging - June, 1988.

Lees, J.M. and R.S. Crosson, 1989, Tomographic inversion for three-dimensional velocity structure at Mount St. Helens using earthquake data, JGR, V. 94, pp. 5716-5728.

Lees, J.M. and R.S. Crosson, 1989 (revised), Tomographic imaging of local earthquake delay times for 3-D velocity variation in western Washington, JGR

Lees, J.M. and J.C. VanDecar, 1989 (in preparation), Seismic tomography constrained by Bouguer gravity anomalies, with application to western Washington, U.S.A..

VanDecar, J.C. and R. S. Crosson, 1989 (in press), Determination of teleseismic relative phase arrival times using multi-channel cross correlation and least squares, BSSA.

Reports

Final Technical Report: 1988, 1989, Earthquake Hazard Research in the Pacific Northwest, USGS Grant #14-08-0001-G1390.

Abstracts

Boyd, T.M., and K.C. Creager, 1989 (submitted), Temperature dependence of seismicity within subducted slabs, EOS, Fall 1989 AGU.

Chiao, L.Y. and K.C. Creager, 1989 (submitted), Kinematic deformation of the subducted Cascadia slab, EOS, Fall 1989 AGU.

Creager, K.C., L.Y. Chiao, and T.M. Boyd, 1989 (submitted), In-plane slab deformation and seismic moment distributions, EOS, Fall 1989 AGU.

Crosson, R.S., and J.M. Lees, 1989, Regularization or smoothing in inversion and seismic tomography as a linear filtering operation, EOS, V. 70, p. 601.

Crosson, R.S., 1989 (submitted), Application of spectral constraints in tomography and linear inversion: extension to non-uniformly sampled models, EOS, Fall 1989 AGU.

Mundal, I., M. Ukawa, and R.S. Crosson, 1989 (submitted), Evidence of subducting Juan de Fuca plate in apparent velocities observed from subcrustal earthquakes, EOS, 1989 PNAGU.

Ukawa, M. and R.S. Crosson, 1989 (submitted), Investigation of deep crustal and uppermost mantle structure in the Pacific Northwest through subcrustal earthquakes, EOS, Fall 1989 AGU.

Source Characteristics of Earthquakes Along the Southern San Jacinto and Imperial Fault Zones (1937 to 1954)

14-08-0001-G1683

Diane I. Doser
Department of Geological Sciences
University of Texas at El Paso
El Paso, Texas 79968-0555
(915) 747-5501

Objective: Between 1937 and 1954 four large earthquakes with local magnitudes of 6.0 to 6.7 occurred along the southern San Jacinto and Imperial fault systems. Waveform modeling of region and teleseismic body waves is being used to determine the faulting processes of these earthquakes. Data from available geological and geophysical studies provides additional constraints on fault geometry. Information on faulting processes obtained in this study will be compared to the rupture processes of post-1960 earthquakes occuring along the fault zones in an attempt to better determine the factors that control the nucleation and termination of rupture along the faults.

Progress to Date: The past six months of this project have been devoted to data acquisition and analysis. Tasks completed during this time period include:

1. In July a trip to Caltech was made to collect additional regional and teleseismic data for waveform analysis and first motion studies for the four earthquakes of interest. On the return trip the PI stopped at San Diego State University to discuss geological aspects of the study area with Dr. Tom Rockwell.

2. Preliminary analysis of the waveforms of the 1954 Arroya Salada and 1942 Borrego Valley earthquakes has been completed. The results suggest that the 1954 event occurred at a depth of 10 km along a right-lateral strike-slip fault with a strike similar to the Clark fault, in agreement with previous aftershock studies that suggested the earthquake ruptured to the southeast from a point near the mapped termination of the Clark fault. The moment of the 1954 event is estimated to 3 x 10**25 dyne-cm, equivalent to a moment-magnitude of 6.3. The local magnitude of the event (6.2) is comparable to this estimate. The 1942 event appears to have occurred along a northeast trending strike-slip fault, similar to the trend of structures mapped to the southwest of the southern San Jacinto fault. The largest aftershock of the 1942 sequence appears to have a similar mechanism. Results of the analysis will be presented at the fall meeting of the American Geophysical Union.

3. The digitization of seismograms for the 1940 Imperial Valley and 1937 Buck Ridge earthquakes are nearly complete. Seismograms have also been collected for the 1918 and 1923 earthquakes along the northern San Jacinto fault and are currently being digitized.

4. Gravity data for the southern San Jacinto and Imperial fault region is currently being extracted from the university's extensive gravity data base. Of particular interest is the gravity data in the region southwest of the southern San Jacinto fault where the 1942 earthquake may have occurred. It is hoped the data may reveal whether there are prominent northeast trending structures in the region.

Spatial and Temporal Patterns of Seismicity in the Garm Region, USSR: Applications to Earthquake Prediction and Collisional Tectonics

14-08-0001-G1382

Michael W. Hamburger, Gary L. Pavlis
Daniel Sarewitz, Bingjun Zheng, and Margaret Thomas
Department of Geology, Indiana University
Bloomington, Indiana 47405
(812) 855-2934

Investigations

This program focuses on the highly active seismic zone between the Pamir and Tien Shan mountain belts in Soviet Central Asia. The Garm region, shown in Figures 1 and 2, is located directly atop the collisional boundary between the Indian and Eurasian plates, and is associated with a dense concentration of both shallow and intermediate-depth earthquakes. Since the early 1950's, Garm has been the home of the Complex Seismological Expedition (CSE), whose primary mission is the prediction of earthquakes in the USSR (Nersesov *et al.*, 1979). Beginning in 1975, the USGS, in cooperation with the CSE, has operated a telemetered seismic network nested within a stable CSE network that has operated in the area for over thirty years. The fundamental aims of the present research project are: (1) to elucidate the structures and processes involved in active deformation of the broad collisional plate boundary, and (2) to examine the temporal variations in seismicity near Garm, in the form of changing spatial, depth, and stress distribution of microearthquakes that precede larger events. The data base for this study includes the combined resources of the global, regional, and local seismic networks.

Results

The research reported here is based on two main data sources: (1) the *Soviet regional catalog* ("Earthquakes in the USSR," Acad. Sci. USSR), which covers an area of approximately 15° by 25° and includes over 30,000 events since 1962 (compiled in collaboration with D.W. Simpson, Lamont-Doherty Geol. Obs.), and (2) the *CSE network catalog,* which covers an area of about 2° square surrounding Garm, and includes over 70,000 events since the early 1950's. Earthquakes located by these networks are compared to the teleseismic seismicity catalog in Figure 1.

Earthquake Relocations. We have continued our work on relocation of earthquakes from the CSE and USGS seismic networks. We have now obtained all available arrival time from the dense telemetered USGS network (for the period 1975-1982) and have merged arrival times with those obtained by the CSE network. Using revised station location information, we have relocated all events recorded by the two networks for the 18-year period 1969-1987. Over 55,000 events recorded by the two networks have now been relocated, and are shown in Figure 3. This earthquake list includes over 2500 events common to the two catalogs; this data set will provide the basis for new inversions for three-dimensional velocity structure beneath the network. The new seismicity map shows the dense concentration of crustal activity extending along strike of the high ridge of the Peter the First Range, notable spatial clusters of activity within the Tien Shan to the north, and a marked decrease in activity approaching the Pamir Range in the south. Several marked cross-strike features are visible, and the town of Garm (near 39°N, 70.2°E) appears to be surrounded by a distinct zone of reduced seismicity.

Geological Investigations. During the summer of 1989, we began a program of field investigations in the Garm region that included four weeks of reconnaissance field mapping, using Landsat Multispectral Scanner (MSS) imagery as a map base. The excellent exposure in the area, combined with characteristic topographic expression and reflectivity of the sedimentary strata in the region, permitted use of the satellite imagery to extend key units between exposures directly observed in outcrop. We also relied heavily on previous detailed mapping by V.I. Shevchenko (Institute of Physics of the Earth), although our tectonic interpretation differs substantially from his (see Lukk and Shevchenko, 1986). The geological field work permitted us to compile a preliminary geological map of the Garm region (Figure 2), as well as a geometrically constrained geological cross section (Figure 4). The well constrained hypocenters (grades A, B, and C) located within a 20-km wide rectangle surrounding the section (shown on Figure 3) have been superimposed on the geological cross section. Our preliminary results (Hamburger and Sarewitz, 1989) can be summarized as follows.

The Peter the First Range (PFR) south of Garm represents a deformed segment of a large intracontinental basin, the Tadjik Depression, which is actively uplifting and shortening in response to the north-south convergence between two crystalline blocks, the Pamir and the Tien Shan ranges. The stratigraphy of the PFR comprises a sedimentary section of shallow marine to non-marine sediments deposited in a broad, restricted intracontinental basin. The lower part of the section, which accumulated from Late Jurassic through Paleogene time, includes fine-grained clastic, carbonate, and evaporitic sediments. These rocks were deposited in a tectonically quiescent basin, close to sea level, probably in the absence of significant syndepositional relief. These sediments depositionally overlie Paleozoic units of the Pamir to the south and the Tien Shan to the north. Starting in Miocene time, the progressive uplift of the Pamir massif is indicated by the appearance of alluvial sandstone and conglomeratic units that coarsen upwards through the entire Neogene section and thin toward the north. Subsequent shortening within the PFR is recorded by km-scale isoclinal, upright-to-recumbent folds, and imbricate, north-verging thrusts that emerge near the northern edge of the range, and mark the active tectonic boundary with the Tien Shan. Thrust faults consistently exhume a sequence of Late Jurassic evaporites, which may provide a regional decollement at depth.

The seismicity within the PFR is dominated by low-magnitude earthquakes that extend from the surface to approximately 12 km depth. A subhorizontal zone of relatively low activity at this depth may mark the location of a basal detachment that underlies a structurally thickened sedimentary section; this horizon may coincide with the basal zone of Jurassic evaporites. This aseismic zone is in turn underlain by a south-dipping belt of seismicity that extends from 17 km to as much as 35 km depth, and which can be traced updip to the seismogenic crystalline basement of the Tien Shan range to the north. We interpret this south-dipping structure as a zone of intracontinental subduction that may be a continuation of the enigmatic intermediate-depth Wadati-Benioff Zone beneath the Pamir Range to the south. Upper crustal shortening observed within the PFR may be resolved at greater depths along this structure. The geology of the region suggests a progressive northward migration of the Himalayan deformation front in Cenozoic time, beginning with the Eocene suturing in the Indus-Kohistan region, developing into the Miocene uplift and deformation of the Pamirs, and culminating in the progressive closure of the Tadjik Depression, uplift and shortening within the PFR, and reactivation of the Tien Shan range in the north.

Aftershock Properties of Intermediate-Depth Earthquakes. We have used the twenty-two year regional seismicity record to examine the characteristics of aftershock sequences following 89 moderate and large ($M_L \geq 5.5$) earthquakes in the Central Asian region. Our study (Thomas, 1989; Pavlis *et al.,* 1989) includes 49 intermediate-depth earthquakes from the active Pamir-Hindu Kush region. We identified aftershocks using a statistical approach that considers the average background seismicity rate within a rigid spatial window ($1° \times 1°$ square) surrounding each mainshock. The sequence begins at the mainshock and ends when the smoothed seismicity rate falls below the 95% confidence level above the mean rate. This method allows for a consistent, objective method of aftershock identification that accounts for the enormous differences in background seismicity among the various source areas.

In sharp contrast to other intermediate-depth earthquake zones (e.g., Isacks *et al.*, 1967; Page, 1968), we found that well defined aftershock sequences are commonly associated with larger earthquakes in the Pamir-Hindu Kush zone. 32 of 39 earthquakes with $M_L \geq 5.5$ were followed by bursts of smaller magnitude earthquakes in which the rate exceeded the background rate (at the 95% confidence level), extending for periods ranging from 9 to 192 days. The nature of individual sequences, however, is highly variable and the number of aftershocks shows no clear correlation with magnitude. 17 of the 39 sequences had more than 10 aftershocks, and 4 had over 100. The most dramatic sequence followed a magnitude 6.7 event that occurred on 30 December 1983, at a depth of 210 km. This event was followed by a marked aftershock sequence unambiguously defined by a cluster of activity surrounding the mainshock in space and time. The sequence exceeded the background for 102 days, yielding a count of 632 aftershocks above background level, and showed the classic power law decay in time. We hypothesize that the reason for the anomalous behavior of these deep earthquakes is that the source region for these events is more heterogeneous than that found in subduction zones. This provides circumstantial evidence to support Roecker's (1982) hypothesis that this unusual intracontinental deep earthquake zone is associated with subducted continental, rather than oceanic, lithosphere.

References

Hamburger, M.W. and D.R. Sarewitz, 1989, Geology and seismicity of the Peter the First Range, a deformed intracontinental basin in Soviet Central Asia [abstract], *Geol. Soc. Amer. Abs. w/ Prog.*, *21*, A148.

Isacks, B.L., L.R. Sykes and J. Oliver, 1967, Spatial and temporal clustering of deep and shallow earthquakes in the Fiji-Tonga-Kermadec region, *Bull. Seismol. Soc. Amer.*, *57*, 935-958.

Lukk, A.A. and V.I. Shevchenko, 1986, Character of the deformation of the earth's crust in the Garm region (Tadjikistan) from geological and seismic data, *Izvestiya, Phys. Solid Earth, 22*, 527-539.

Nersesov. I.L., Yu, P. Skovorodkin, and T.V. Guseva, 1979, Results of complex studies in the Garm geodynamic polygon, *Izvestiya, Physics of the Solid Earth, 15:4*, 47-55.

Page, R., 1968, Focal depths of aftershocks, *J. Geophys. Res.*, *73*, 12-16.

Pavlis, G.L., M.W. Hamburger and M.W. Thomas, 1989, Aftershock sequences associated with intermediate-depth earthquakes in the Pamir-Hindu Kush region [abstract], *EOS Trans. Am. Geophys. Un.*, in press.

Thomas, M.W., Temporal distribution of seismic activity within the Soviet regional earthquake catalog, Central Asia, M.S. thesis, Indiana University, 149 pp.

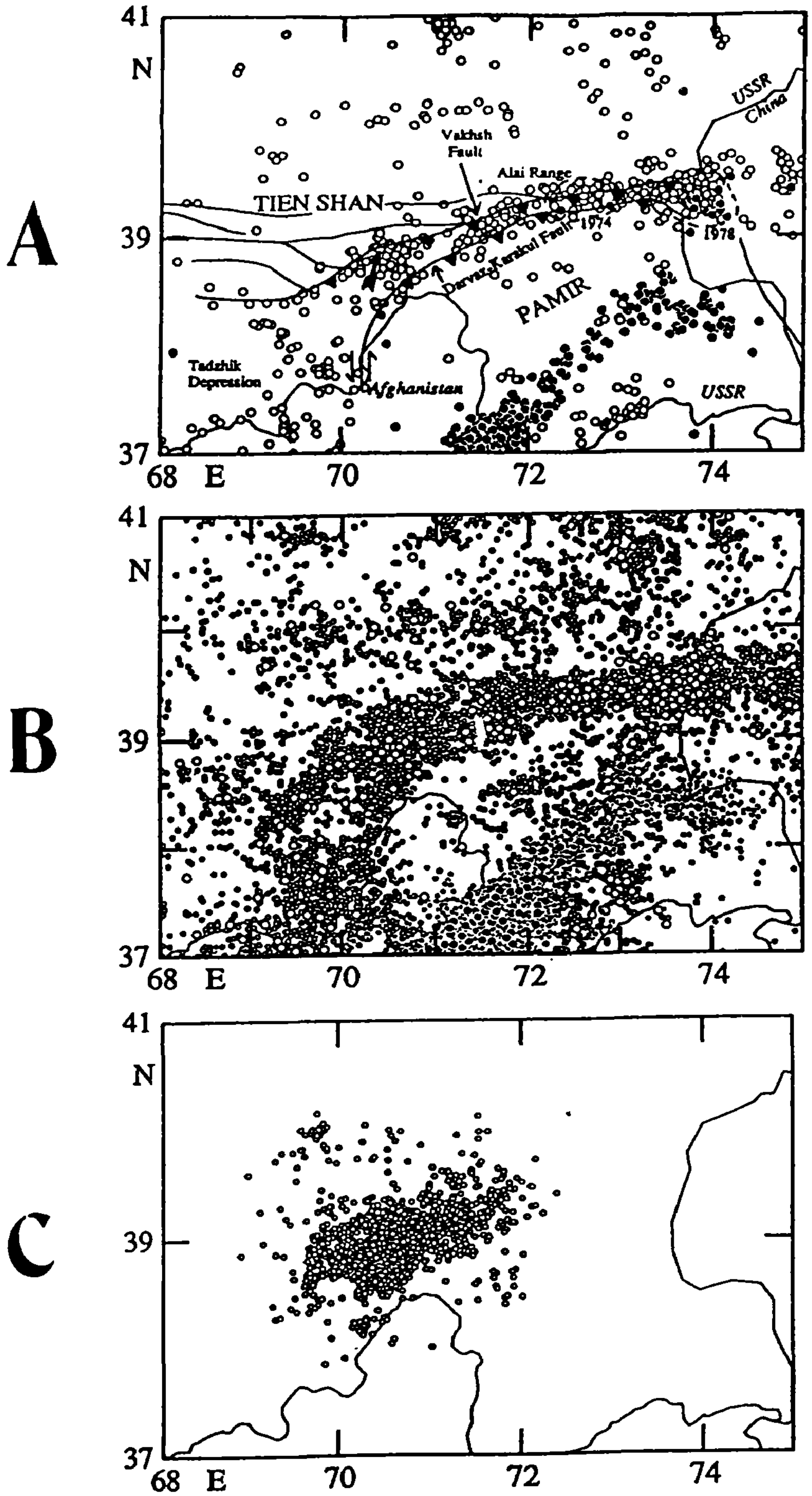

Figure 1. Comparison of earthquake data bases for the Garm region. (A) Teleseismic locations (from ISC catalog). Open circles: $h \leq 70$ km; filled circles: $h > 70$ km. Fault maps are adapted from *Atlas of the Tadjik SSR* (Acad. Sci. Tadj. SSR, 1968). Dashed ellipses indicate aftershock zones of 1974 Markansu and 1978 Alai Valley earthquakes. Heavy arrow shows the location of Garm. (B) Locations from the Central Asia regional network, 1964-1980. Focal depths as in (A); small symbols: $M_L \leq 4.0$; large symbols: $M_L > 4.0$. We have arbitrarily "randomized" the coordinates of poorly located events on the margins of the seismic network. (C) Earthquake locations for the CSE network at Garm. We have plotted all epicenters for a one-year recording period (1986).

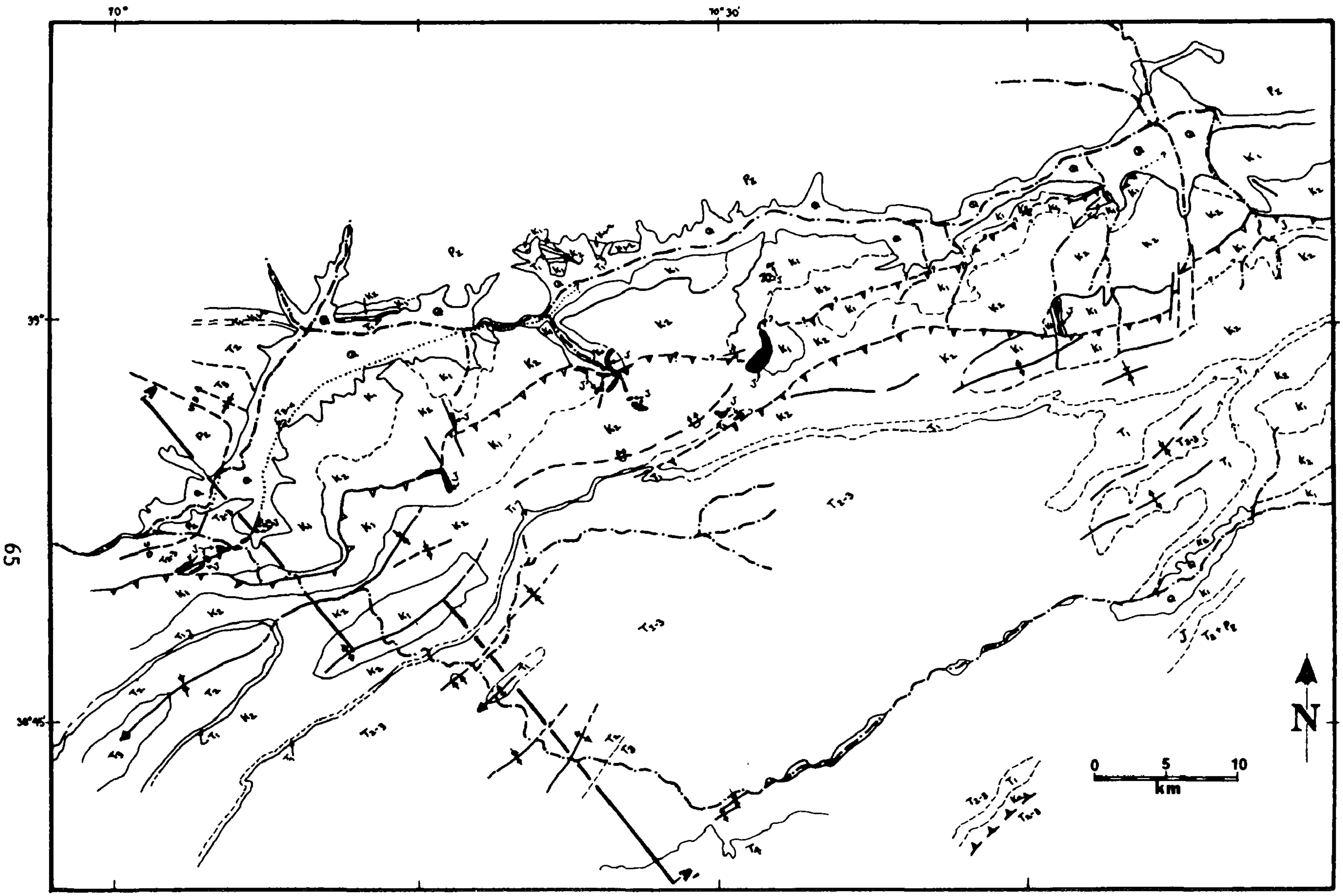

Figure 2. Preliminary geological map of the Garm region, based on reconnaissance field mapping, analysis of satellite imagery, and field data collected by V.I. Shevchenko [pers. comm., 1989]. Contacts and structures are shown in solid symbols where well constrained by field observation or imagery interpretation, dashed where approximate, queried where uncertain, and dotted where inferred. Heavy dot-dash line indicates drainage network of the Surkhob and Obi-Khingou rivers. Black areas indicate exposures of Jurassic evaporites, primarily gypsum. Heavy solid line labelled A - A' indicates position of geological cross section shown in Figure 4. Note that the section is offset along an anticlinal axis.

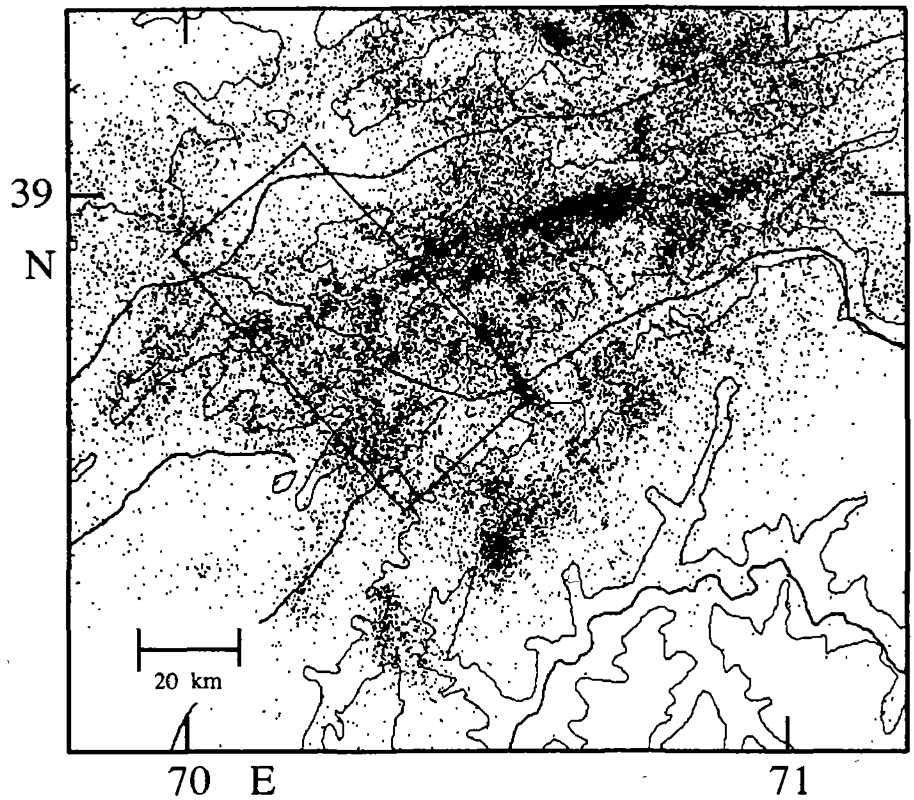

Figure 3. Map of seismicity of the Garm region, 1969-1987. Relocated epicenters, obtained using HYPOELLIPSE, are shown as dots. Heavy lines indicate drainage network; light lines indicate 9000-foot topographic contours. Rectangle indicates area included in seismicity cross section shown in Figure 4.

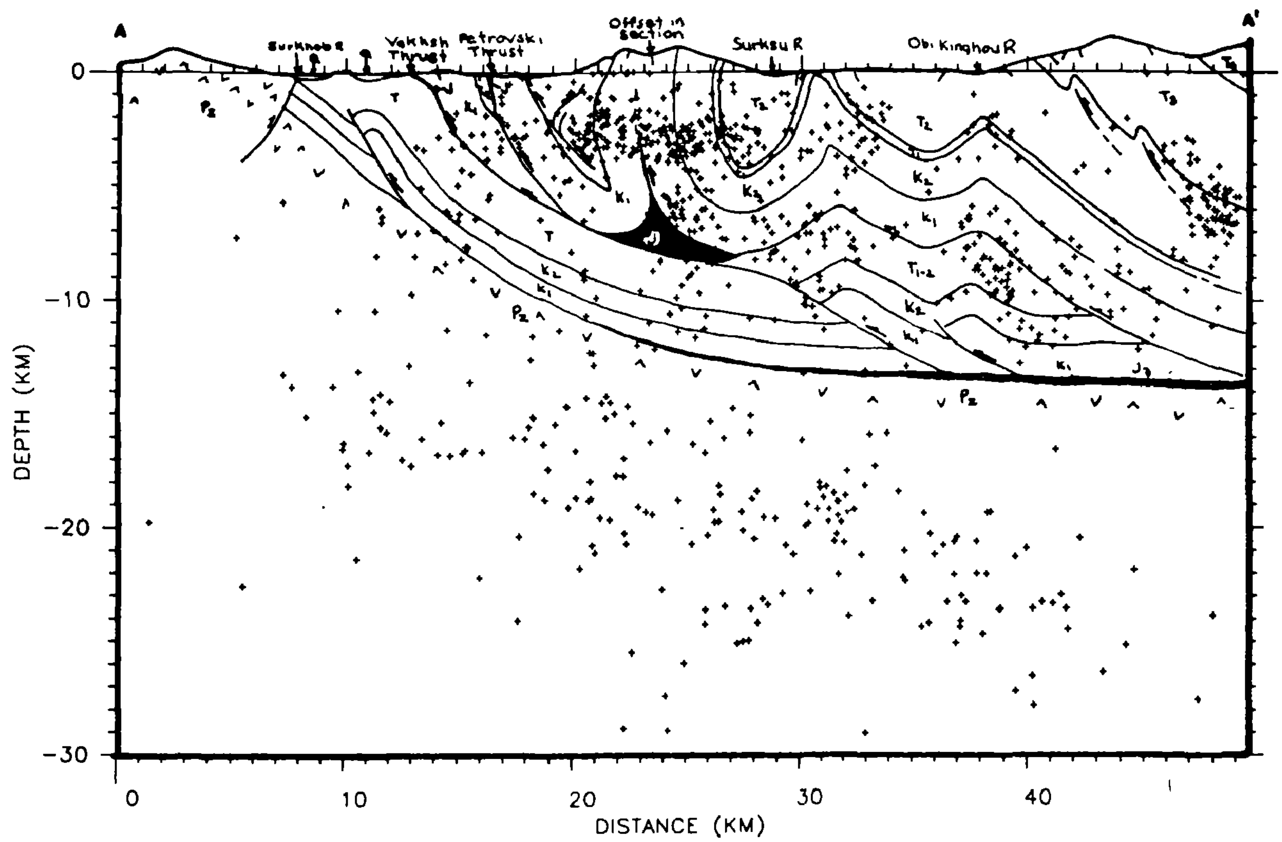

Figure 4. Geological cross section A - A' (location shown in Figure 2) across the Peter the First Range. Data sources as in Figure 2. Earthquake hypocenters, graded "B" or better, for the period 1975-1982, are shown projected onto the same vertical plane (location shown in Figure 3). Note the dense concentration of events within the axial zone of the Peter the First Range, zone of reduced activity near the base of the sedimentary section, and the south-dipping zone of midcrustal seismicity occurring within the Paleozoic basement rocks.

Analysis of Earthquake Data from the Greater Los Angeles Basin and Adjacent Offshore Area, Southern California

#14-08-0001-G1328

Egill Hauksson
Ta-liang Teng
Center for Earth Sciences
University of Southern California
Los Angeles, CA 90089-0740

INVESTIGATIONS

Seismotectonic analysis of earthquake data recorded by the USC and CIT/USGS networks during the last 15 years in the greater Los Angeles basin. Improve models of the velocity structure to obtain more accurate earthquake locations including depth and to determine focal mechanisms. Studies of the earthquake potential and the detailed patterns of faulting along major faults in the metropolitan area and adjacent regions.

A comprehensive study entitled: *Earthquakes, faulting and stress in the Los Angeles basin* , has been submitted for publication in Journal of Geophysical Research.

RESULTS

Since 1920 fourteen moderate-sized (M_L=4.9-6.6) earthquakes have been reported in the Los Angeles basin. These events are associated with both mappable surficial faults and buried faults beneath the basin sediments. To determine the style of faulting and state of stress in the basin, single-event focal mechanisms for 244 earthquakes of M≥2.5 since 1977 have been determined.

59% of the events are strike-slip and are mostly located near the three major, northwest striking right-lateral strike-slip faults in the basin, the Whittier fault, the Newport-Inglewood fault and the northern end of the Palos Verdes fault (Figure 1). In addition to the Pasadena 1988 earthquake that showed left-lateral slip on the Raymond fault, numerous small earthquakes show left-lateral strike-slip faulting and form a seismicity trend extending from Yorba Linda toward the northeast. The northeast trending depth cross section AA' in Figure 1 shows that the strike-slip faulting earthquakes are scattered in the depth range from the near surface down to depths of 14-17 km. The most prominent feature on the map in Figure 1 is the cluster of strike-slip mechanisms along the Newport-Inglewood fault, which was pointed out previously by Hauksson [1987]. The largest event (M_L=4.5) to rupture the Newport-Inglewood fault since the 1940's showed strike-slip movement and occurred on April 7, 1989 near Newport Beach, just 2-3 km to the south of the epicenter of the 1933 Long Beach earthquake [Richter, 1958]. The depth section in Figure 1 also shows the enhanced activity along the Newport-Inglewood fault.

The 32% of the events that have thrust or reverse mechanisms are distributed along two broad zones (Figure 2). The first zone coincides with anticlines along the eastern and northern flank of the Los Angeles basin extending into Santa Monica Bay forming the Elysian Park fold and thrust belt. The second zone that extends from offshore Newport Beach to the northwest into Santa Monica Bay coincides with anticlines mapped on the southwest flank of the basin forming the Torrance-Wilmington fold and thrust belt. Oblique faulting that is required by the regional stresses does not occur in the basin. Instead, the coexistence of zones of thrusting and large strike-slip faults in the basin suggests that the thrust and strike-slip movements are decoupled.

As can be seen in Figure 2, the thrust focal mechanisms are not located adjacent to the north dipping surficial reverse faults, such as the Santa Monica and Sierra Madre faults that define the north edge of the sedimentary basin. Instead the thrust or reverse focal mechanisms are mostly located to the south of these reverse faults and form broad clusters along the flanks of the basin. Most of the folding of the basin sediments also occurs along the flanks of the basin. This spatial coincidence of the folding and thrust faulting can be explained with Suppe's [1985] fault-bend or fault-propagation folding models, where the thrust faulting earthquakes at depth cause folding of the cover sequence. The 1987 Whittier Narrows earthquake that showed thrust faulting and caused coseismic uplift in the Whittier Narrows, demonstrated how the folding and faulting are causally related [Lin and Stein, 1989; Davis et al., 1989]. Thus, when the geological evidence for folding and the seismological evidence for thrust faulting are combined, two fold and thrust belts can be identified along the flanks of the basin (Figure 2). These belts are called here the Elysian Park and the Torrance-Wilmington fold and thrust belts and are located along the east and north, and southwest flanks of the basin, respectively.

A few normal faulting mechanisms appear to be related to faulting orthogonal to the axes of plunging anticlines(Figure 3). The normal faulting is observed in 9% of the earthquakes analyzed, which is a small fraction of the ongoing faulting. The normal faulting events analyzed here all have small magnitudes with the largest event of M_L=3.9. The normal faulting mechanisms that are shown in Figure 3 are distributed adjacent to the Newport-Inglewood fault and offshore in the San Pedro Bay. The offshore events may be less well constrained than the onshore events because the distance to the nearest station is in some cases larger than one focal depth. Some normal faulting is expected in this region of intense crustal deformation and may be associated with extensional bending moments that can cause extensional faulting during the growth of anticlines [e.g., Ramsey and Huber, 1987]. Alternatively, the normal faulting events that have nodal planes trending northwest to north-northwest could be related to faulting on planes orthogonal to the axes of anticlines. Because the anticlines usually plunge at the ends, normal faulting could occur to accommodate this deformation as is often seen in seismic reflection profiles [personal communication, J. Suppe, 1989].

PUBLICATIONS and REPORTS

Hauksson, E. and L. M. Jones, The 1987 Whittier Narrows earthquake sequence in Los Angeles,southern California: Seismological and tectonic analysis, J. Geophys. Res., 94, 9569-9590, 1989.

Hauksson E. and G. V. Saldivar, Seismicity (1973-1986) and active compressional tectonics in the Santa Monica Bay, southern California, J. Geophys. Res. , 94, 9591-9606, 1989.

Hauksson, E. and R. S. Stein, The 1987 Whittier Narrows earthquake: a metropolitan shock, J. Geophys. Res., 94, 9545-9547, 1989.

Jones, L. M., K. E. Sieh, E. Hauksson and L. K. Hutton, The December 3, 1988 Pasadena, California Earthquake: Evidence for Strike-slip Motion on the Raymond fault, Bull. Seism. Soc. Amer.., to appear in February 1990.

Hauksson, E., Earthquakes, active faulting,and stress in the Los Angeles Basin, submitted to J. Geophys. Res., August 1989.

Hauksson, E. and T. L. Teng, Analysis of earthquake data from the greater Los Angeles basin and adjacent offshore area, southern California, Annual Technical Report submitted to the U.S. Geological Survey, March 1989, 60 pp.

Hauksson, E., Comparison of broad-band waveforms of local earthquakes recorded at crystalline and sedimentary rock sites in the Los Angeles basin, submitted to fall AGU meeting, 1989.

Robertson, M. C., and E. Hauksson, Three-dimensional fine velocity structure of the Los Angeles basin, submitted to fall AGU meeting, 1989.

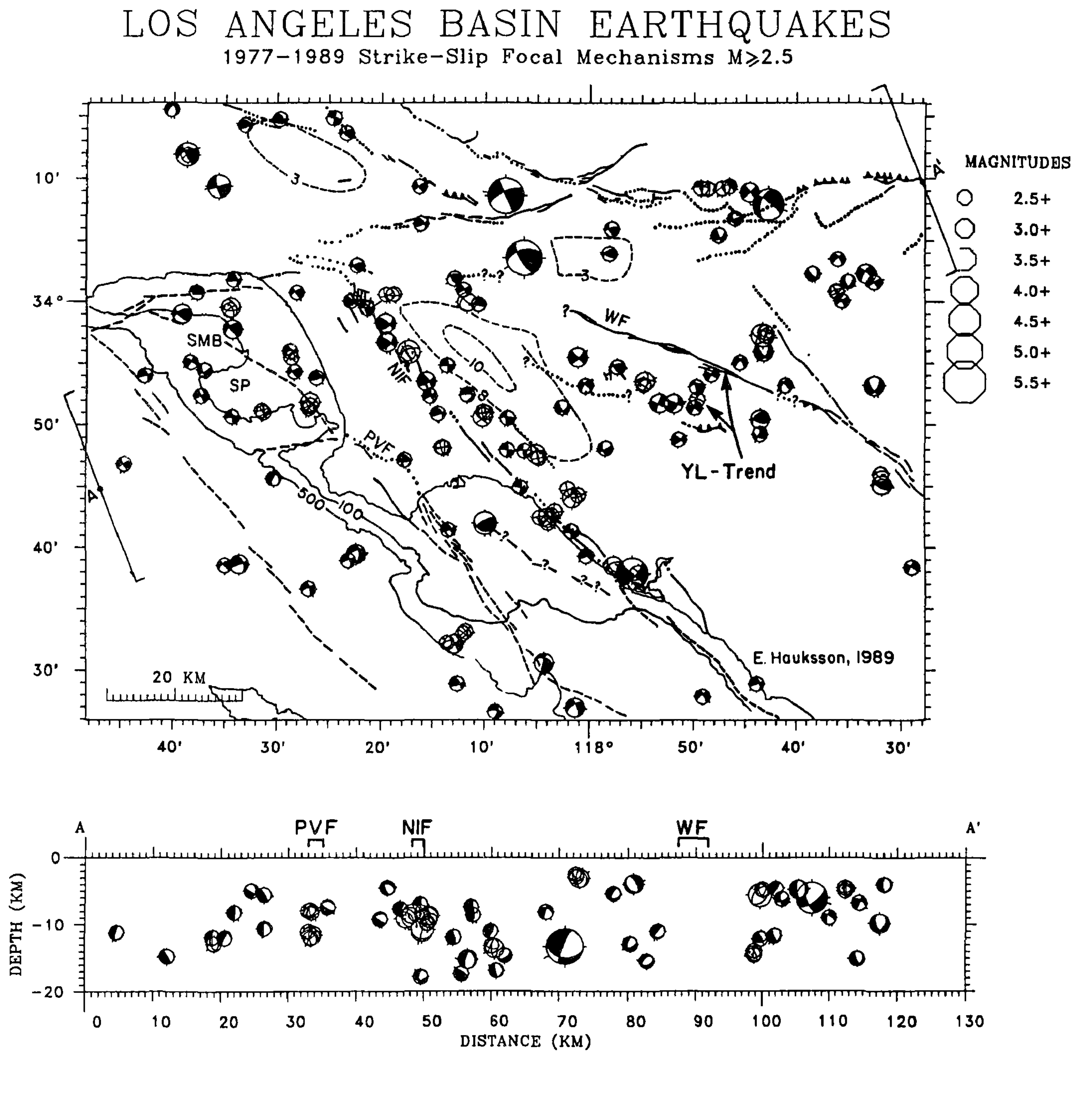

Figure 1. (Top) Map of late Quaternary faults and strike-slip focal mechanisms. Compressional quadrants are shaded. Mechanisms that overlapp significantly are not shaded. WF-Whittier fault, NIF-Newport-Inglewood fault, PVF-Palos Verdes fault, SMB-Sant Monica Bay, SP-Shelf Projection and YL-trend is the Yorba Linda seismicity trend. (Bottom) a northeast trending depth section A-A'.

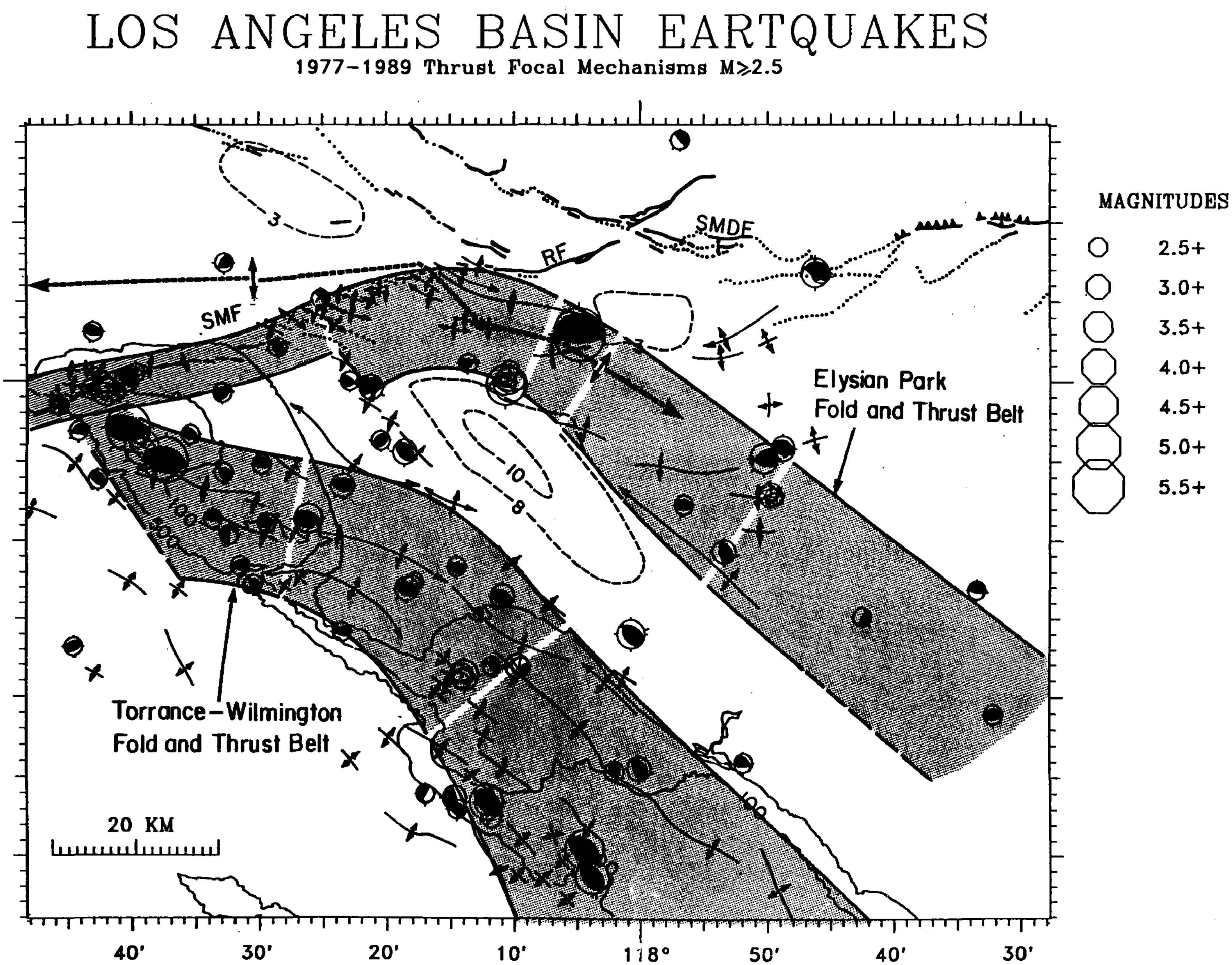

Figure 2. Map of fold axes and thrust focal mechanisms. The Elysian Park and Torrance-Wilmington fold and thrust belts are shaded with breaks in the shading at segmentation boundaries. RF- Raymond fault, SMDF-Sierra Madre fault, and SMF-Santa Monica fault.

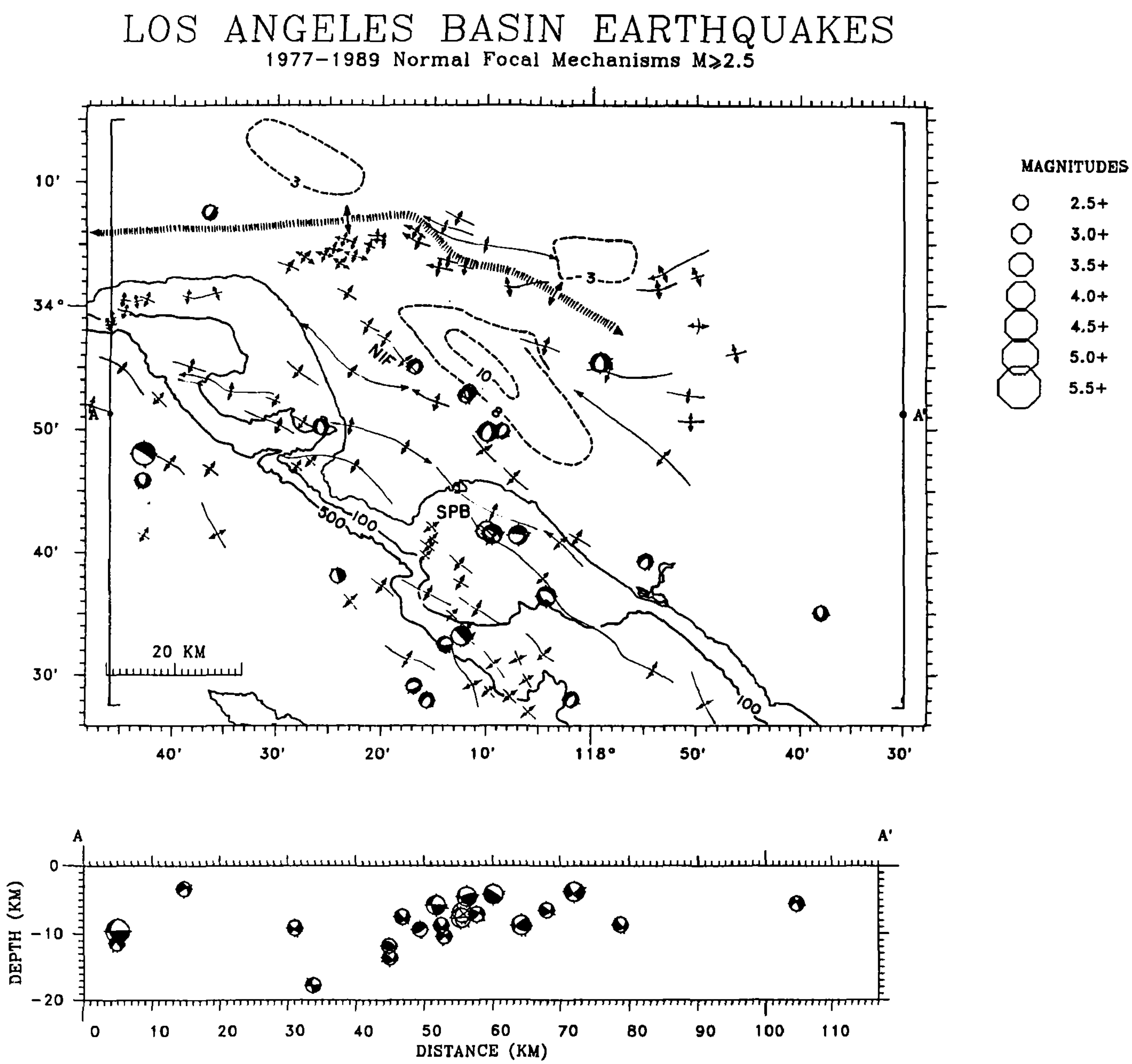

Figure 3. (Top) Map of fold axes and normal faulting focal mechanisms. (Bottom) an east trending depth section A-A'. NIF-Newport-Inglewood fault, and SPB-San Pedro Bay.

Geologic Mapping of the Island of Hawaii - Kaoiki Fault Zone

Program Task No. I.2

Marie D. Jackson
Branch of Igneous and Geothermal Processes
U. S. Geological Survey
P. O. Box 51
Hawaii National Park
Hawaii, 96718
(808) 967-7982

Investigations

1. Field and mechanical study of ground cracks associated with the 1974 M_L=5.5 and 1983 and M_L=6.6 Kaoiki earthquakes.

Results

1. *Importance of the Kaoiki Fault Zone.* The Kaoiki seismic zone, a young tectonic feature of Mauna Loa volcano, Hawaii, is the site of recurrent moderate- to large-magnitude earthquakes that cause serious damage. The Kaoiki is the subject of a forecast for a M_L=6 earthquake before the turn of the century (Wyss, 1986). Investigation of the relation between volcano-seismic processes and faulting within the Kaoiki zone will increase our ability to predict earthquake hazards within this area.

   In the past 15 years, the November 30, 1974 M_L=5.5 and November 16, 1983 M_L=6.6 earthquakes generated zones of left-stepping, echelon ground cracks on the lower SE flank of Mauna Loa. Most large magnitude earthquakes occur along preexisting faults; in contrast, the major Kaoiki earthquakes propagate new ruptures, at least in their surface expression. Geologic mapping by this project and by Endo (1985) shows that at least four ground-rupture zones are concentrated within a 30 km^2 area. The Kaoiki seismic zone is unique because its ground ruptures record the initial stages of development of a strike-slip fault zone: future earthquake ground ruptures should be expected to merge into a mature fault.

   General Objectives. This work provides important information on the history and mechanisms of faulting within the Kaoiki zone that will form the basis for seismic hazard evaluations for the Island of Hawaii. This study investigates 1) the faulting and earthquake mechanisms involved in the 1974 and 1983 Kaoiki events and 2) the deformation of the Mauna Loa and Kilauea volcanic edifices resulting from the mutual inflation of their summit magma chambers and the seaward migration of Mauna Loa's SE flank. Field work undertaken by this study includes 1) the preparation of a 1:10,000 geologic map of the entire rupture zone generated by the 1983, 1974, and 1962 earthquakes, and another, much older, undated earthquake and 2) detailed outcrop-scale mapping (<1:1000) of three critical exposures of the 1983 ground cracks and one excellent exposure of the oldest crack set. (Endo (1985) mapped the 1974 ground cracks at 1:1360). Analytical work includes mechanical analysis of the nature and depth of faulting underlying the 1974 and 1983 cracks and will include analysis of sparse geodetic data spanning the epicentral region.

Mapping Results, 1:10,000 scale. Geologic mapping on 1:5,000 aerial photography by M. Jackson and E. Endo in April 1989 produced a reconnaissance map of the 1983 rupture zone and identified several critical areas for more detailed field work. In the past 5 months, Jackson has transferred much of this mapping to a 1:10,000 topographic base map using the PG-2 plotter, and has completed the field work necessary for the compilation of this map and four detailed maps of the cracks.

Ground ruptures from the 1983 M_L=6.6 earthquake, the 1974 M_L=5.5 earthquake and an older, undated earthquake trend N48°-55°E, a direction nearly parallel to nodal planes of the 1983 and 1974 main shocks' focal mechanisms. The ground ruptures do not lie along a single trend. Individual ruptures consist of long arrays of left-stepping, en echelon cracks, with predominantly opening displacements, which strike roughly EW, about 30°-50° clockwise from the overall trend of the zones. The orientation and geometry of the cracks are consistent with right-lateral shear and they strike parallel to a transect joining the summit magma chambers of Mauna Loa and Kilauea volcanoes.

- Exposures of the 1983 cracks begin about 4.3 km NE of the mainshock epicenter and continue for over 7 km to the NE, along the SE flank of Mauna Loa at about 2000 m elevation. Three detailed maps of the cracks are described below.

- The 1974 cracks (Endo, 1985) extend for 2.2 km, about 3.5 km downslope to the SW from the 1983 rupture zone. Left-stepping, echelon ground cracks from the 1974 M_L=5.5 event may have reactivated 2 large cracks associated with the 1962 M_L= 6.2 event (Endo, 1985).

- Exposures of much older ground cracks crop out within a 1.6 km long zone located about 0.5 km upslope from the western termination of the 1983 fractures. The cracks are deeply weathered with thick growths of lichen; small trees and bushes grow within wider cracks. Jim Jacobi, an expert on the vegetation and microclimates of Mauna Loa, suggests that the shrubs and lichens in the cracks have been established for at least 30 years, and certainly predate the 1962 Kaoiki earthquake. Major Kaoiki earthquakes in 1941, 1918, or 1868 (Wyss, 1986) may have generated this rupture. The cracks have been disrupted at least twice by subsequent earthquakes. A N65°W trending, 100 m long array of large, moderately-weathered rubble piles traverses the older crack zone. Freshly broken rubble and spalled blocks within some older cracks and prominent mole tracks with only slightly weathered surfaces that occur at the tips of some of the older cracks indicate strong shaking or reactivation of these surfaces by right-lateral shear, perhaps during the 1983 event.

Mapping Results, 1983 Rupture Zone, <1:1000 scale. Marie Jackson has completed mapping of three well-exposed outcrops of 1983 ground cracks that include a 2-km-long exposure of cracks located at the NE terminus of the 1983 rupture zone, near the Mauna Loa Strip Road, and small exposures of narrow left-stepping cracks in pahoehoe near the western edge of the 1880 flow and within the Kea Poomoku flow near the SW terminus of the the zone. These maps show how 1) individual cracks form hierarchial arrays that coalesce at depth, 2) crack segments link to form continuous arrays that accomodate right-lateral shear, and 3) displacements vary along the strike of the zone.

•The cracks apparently represent a breakdown zone above a parent fault (Pollard et al., 1982; Jackson et al., 1988). With depth, cracks segments coalesce to form progressively longer, left-stepping arrays of twisted surfaces that become progressively more parallel to the overall trend of the rupture zone. The geometry of the 1983 rupture appears to confirm the self-similarity of earthquake produced fractures in the hierarchial arrays that range in length from several kilometers to a few meters.

•Although most en echelon cracks within the 1983 rupture step to the left with little overlap, some segments are linked by zones of rubble breccia and have small (<15 cm) right-lateral displacements. In contrast, the 1974 cracks have greater components of right-lateral slip, and crack segments are commonly linked by zones of uplift. These features indicate coalescence at depth. They may result from reactivation of yet another zone of cracks, perhaps associated with a 1962 M_L=6.2 event, or they may be a result of the 1974 event's shallower hypocenter, 4 to 5 km deep (compared with 9 to 10 km depth in 1983), that allowed the tip of the underlying parent crack to propagate closer to the earth's surface and form a more continuous zone of strike-slip ground breakage.

•Displacements along the 1983 cracks are predominantly opening-mode. Some of the narrowest cracks, with < 2 cm displacement, are purely dilatant. Wider cracks that have linked to form rubbley left-stepping arrays, have small to moderate components of right-lateral shear. Measurements of total displacement across the zone have been made along the 7 km length of the 1983 rupture; displacements are greatest, up to 1 m in a northerly direction, within the central part of the zone.

References cited

Endo, E. T., 1985, Seismotectonic framework for the southeast flank of Mauna Loa volcano, Hawaii: Ph.D. Thesis, Univ. of Wash., Seattle.

Jackson, M. D., E. T. Endo, P. T. Delaney, 1988, Ground rupture from the 1983 Kaoiki earthquake, Mauna Loa volcano, Hawaii (abs.): Seismological Research Letters, v. 59, p.35.

Pollard, D. D., P. Segall, P. T. Delaney, 1982, Formation and interpretation of dilatant echelon cracks: Geological Society of America Bulletin, v. 93, p. 1291-1303.

Wyss, M., 1986, Regular intervals between Hawaiian earthquakes: Implications for predicting the next event: Science, v. 234, p. 726-728.

Reports

Jackson, M. D., and E. T. Endo, in press, Genesis of a strike-slip fault zone: the 1974 and 1983 Kaoiki ground ruptures, Mauna Loa Volcano, Hawaii (abs): Transactions of the American Geophysical Union, Fall Meeting. To BWTR 8/89.

COMPETITIVE CONTINUATION OF "NEXT GENERATION SEISMIC STUDIES OF THE NEW MADRID SEISMIC ZONE"

14-08-0001-G1534

Arch Johnston and Jer-Ming Chiu
Center for Earthquake Research and Information (CERI)
Memphis State University, Memphis, TN 38152
(901)-678-2007

Robert B. Herrmann
Dept. Earth and Atmospheric Sciences
Saint Louis University
Saint Louis, MO 63156
(314)-658-3120

This project aims to support a 9-month deployment of the PANDA seismic array (Portable Array for Numerical Data Acquisition) to monitor seismic activities around the central arm of the New Madrid seismic zone (NMSZ). The PANDA array consists of 40 three-component stations. High- and low-gain seismic signals from each station are telemetered directly or repeated through an inner station to a central recording site for multi-group, multi-station trigger detection and on-line real-time digital recording. Synchronized sampling of 256 channels and centralized timing system and the above mentioned features will guarantee considerably higher quality data to be collected in the NMSZ which are not available from regional seismic networks.

After two years deployment in San Juan and Jujuy regions of Argentina, the PANDA array returned to Memphis in late July. Upon its return, the entire PANDA system has subjected to very extensive software and hardware modifications and upgrade. A deployment plan has been outlined and executed. Figure 1. shows the central recording site in the Tiptonville and selected PANDA station locations. In average, station spacings are around 4 to 8 km in this preliminary plan with smaller spacings around the intersections of the central NMSZ with the other two branches. The newly updated MASSCOMP MC6600 data acquisition system is installed immediately after the first two stations were installed in the second week of October, 1989. Field installation of the entire PANDA array is expected to be completed by the end of October, 1989.

Several fundamental data processing are planned in a regular basis at the central recording site. These processing include (1) accurate P and S picking; (2) document any interesting features from each seismogram, (3) earthquake locations, (4) epicenter map, (5) cross sectional display, (6) daily Vp/Vs analysis, (7) focal mechanism and regional stress pattern recognization, and many others. On-site processing will not only provide information necessary for immediately modification of the array configuration but will also significantly reduce time required for advanced studies.

The fundamental objective of this research project - that of gaining a better understanding of seismogenesis in the NMSZ - may be subdivided into a number of specific targets.

- Characterization of shallow structure effects. The thick alluvial cover in the region makes this study particular important.
- Determination of source parameters. Single-event focal mechanisms from well-located events should provide new constraints on the faulting mechanisms of this complex zone.
- Study of high frequency spectral characteristics Does the NMSZ produce the enriched high frequency spectra observed from other less active eastern North American seismic zones ?
- Crustal inversion studies. Considerably higher resolution of 3-D attenuation and crustal velocities than were previously available should be possible with PANDA data.
- Development of a structural and dynamic faulting model. A synthesis, not previously possible for the central zone of the NMSZ.

REPORT. Chiu, J.-M., R. Smalley, G. Steiner, and A. Johnston (1989) The PANDA seismic array - a simple but working system for portable array experiment, *Bull. Seismol. Soc. Amer.*, (in press).

NEW MADRID SEISMIC ZONE

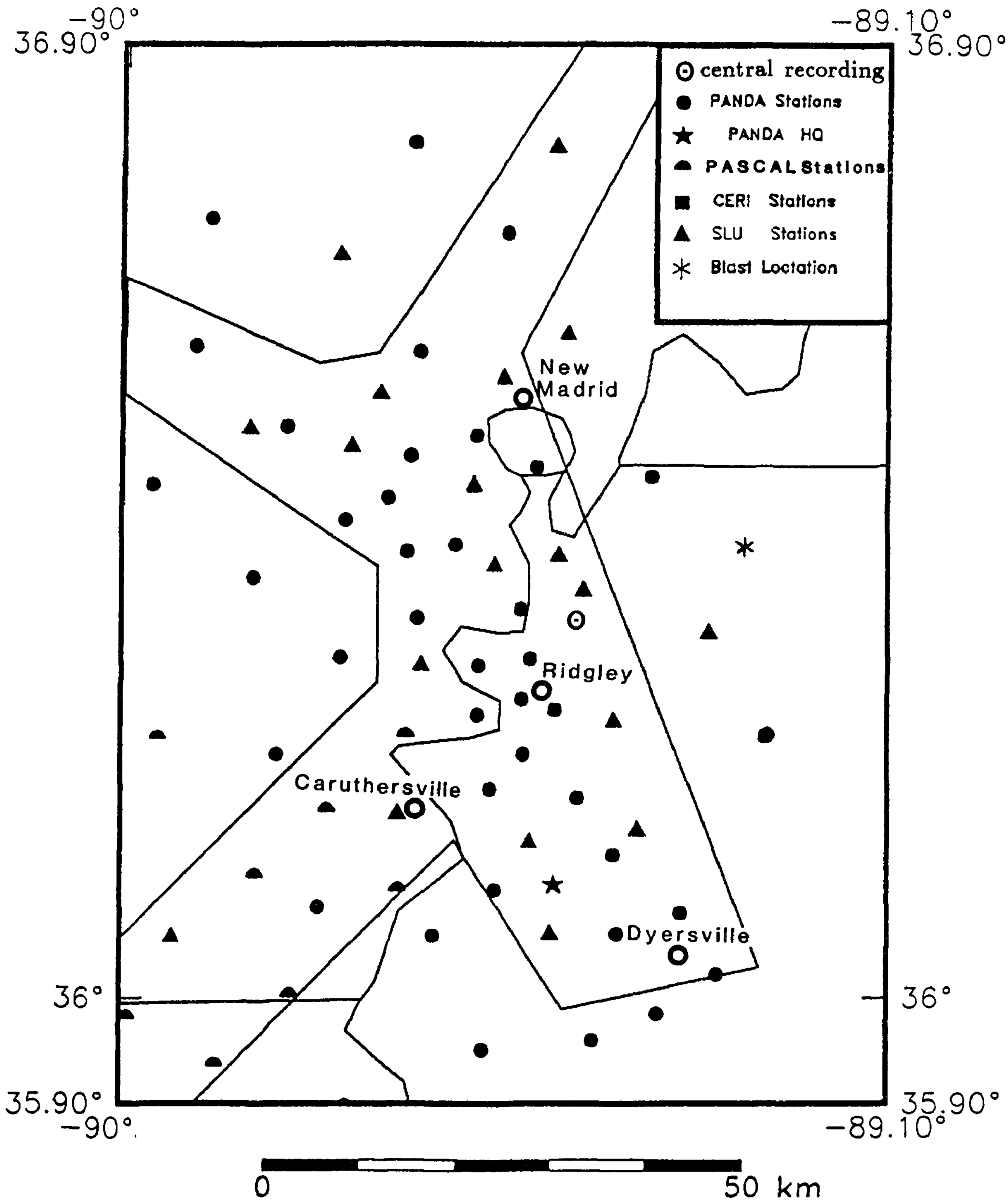

Figure 1. A close view of the planned PANDA deployment in the central segment of the New Madrid seismic zone. Central recording site is located in the Tiptonville near Ridgley.

Seismicity Patterns and the Stress State in Subduction-Type Seismogenic Zones

Grant Number 14-08-0001-G1368

Carl Kisslinger
Cooperative Institute for Research in Environmental Sciences
Campus Box 216, University of Colorado
Boulder, Colorado 80309-0216
(303)-492-6089

Research during May through October, 1989 was focused on the following topics: (1) analysis of earthquake doublets for evidence of changes in material properties associated with preparation for and occurrence of a strong earthquake; (2) further research on methods for determining magnitudes from regional network data; (3) subduction-zone seismotectonics from the characteristics of aftershock sequences.

Doublet Analysis

Progress has been made on the method of analysis of earthquake doublets for the detection of velocity changes, including possible anisotropic velocity changes, associated with the preparation of a strong earthquake. Doublets are defined as earthquakes that occur at essentially identical locations, i.e. within .01 degree of each other, and give rise to almost identical seismograms at each station. They may be separated in times of occurrences and the main interest for this study are those doublets that have members occurring before and after a major earthquake. As reported earlier, several doublets have been found in a small zone close to the hypocenter of the May 7, 1986 mainshock. Methods of correcting these data for all instrumental types of errors have already been established and reported earlier.

The analysis of doublets involves fitting a line to the phase of the cross-spectrum of the two doublet members. The slope of the line then yields the relative delay of one with the other. This is done for a small window (about 1.0 sec width) that is moved along the seismograms so as to obtain delays of one seismogram relative to the other as a function of running time along the seismogram. These delays, in turn, reflect any velocity changes that may have occurred in the path of travel between the times of occurrences of the two doublet members.

Fig. 1 shows the two seismograms from a doublet pair in the area of interest and below them is shown the delays calculated by a standard technique as a function of running time along the seismograms. As evident, the delays appear to be stable in parts and quite unstable in others. This prompted a closer scrutiny of the actual calculations of delays of each individual window. Fig. 2 shows the Cross-Spectrum (top), Coherence (middle) and Phase (bottom) of one window of the seismograms in Fig.1. The Cross-Spectrum shows signal power in a range of frequencies and the Coherency also appears to be good in that range. When fitting the straight line to the phase, however, the method forces a 0 phase at 0 frequency. However, from the phase itself, it is obvious that, at least for this window, this assumption does not hold and the the delay we obtain thus is not sensible. We, therefore, decided to drop this assumption and obtain delays by getting the best fit straight line to the linear part of the phase. This resulted in delays that were more reasonable but the fits were also yielding arbitrary intercepts on the phase axis at 0 frequency. Since this is unphysical, we tried to analyze the problem and determine the reason for this apparent discrepancy. It turned out that the intercepts on the phase axis were not as arbitrary as previously thought. In fact, the majority of them were some multiple of π, in particular they were mostly 2π. This would solve the problem right away since a phase difference of 2π is the same as 0.

An intriguing aspect is the fact that it appears that whenever there is a notch in the Cross Spectrum, there is an associated abrupt change in the slope of the phase. This can be observed in Fig. 2 and is quite common in the database so that it is not an artificial effect. The reason for this behavior is not clear and is still being investigated. In particular, synthetics are being created and artificial delays being introduced. These are then run through the method of analysis to see if there are any deficiencies in the method itself. The results from these studies will be shown in the next report.

It was also decided to try and use properties of the cross-correlation of the doublet pair (in time domain) to support the delays calculated from the slope of the phase. For an ideal doublet, the cross correlation would have a sharp peak at the right lag, which in turn would be the relative delay between the two windows. Furthermore, the cross-correlation should also be symmetric around the maximum peak and so the symmetry of the cross correlation would yield information about how coherent the the two windows are. We were interested to pursue this approach because the delays in our studies appear often to be larger than the digitization interval. However, this technique by itself, would not be able to give us the desired information. In the first place, this method would only detect delays in multiples of digitization interval and would therefore yield step changes in delays rather than smooth transitions. Secondly, in the presence of even moderate noise, the cross-correlation properties break down very fast, whereas in the frequency domain moderate noise would still leave a part of the phase to be linear from which the delay can be calculated. Fig. 3 shows the Cross-correlation of one of the windows in Fig. 1 for which the delay was calculated to be 58 msec. The delay suggested by the offset of the peak of the Cross-spectrum is 53 msec. which, to within its limit, is a perfect match. Note that 13 msec is the digitization interval so that this time domain approach can only yield delays in multiples of 13 msec.

The next step was to change the method of analysis so that the intercept of the phase slope is no longer restricted to 0 at 0 frequency. However, instead of just getting the best fit with an arbitrary intercept , it was decided to search for the best fit that would yield an intercept which is a multiple of pi. This is an iterative method and till now has been done by repeated manual fits. The present aim is to try and automate this so that, given a choice of the intercept desired (usually apparent after seeing the phase behavior), the computer will automatically find the best fit to the slope that yields the desired intercept. This is underway and should be completed very soon.

Fig. 4 shows the delays calculated by the modified method for the same doublet shown in Fig. 1. Obviously, the delays are much more stable than in Fig. 1. Note that there are some windows which do not show any delays. This is because the Coherency and the symmetry of the Cross-Correlation in those windows suggest that they are not coherent enough to yield meaningful results. The most important feature to note is the fact that there appears to be a distinct increase in the delays observed along the coda of the S-wave. If the coda wave has traveled through longer distances in the medium in which the velocity has decreased, then this makes very good sense. Previous experience with synthetic modeling of waveforms from the area has indicated that there are probably converted and reflected phases observed in our data. If this is the case, then it also makes sense to observe longer delays for reflected phases. It should be noted that this increase in delays along the coda of the S-wave for this doublet is observed in all the stations that have good data for the events.

It is hoped that results from studying multiple doublets may yield some systematic pattern to the delays associated with the occurrence of the May 7, 1986 earthquake. The results from such studies will be tested by analyzing a multiplet which has at least two events occurring close in time and one after the big earthquake. The two events close in time should show little or no delay whereas the ones before and after the main earthquake should show the observed delay pattern.

A paper on this study has been submitted to BSSA under the title: A note on the correction for time drift of digital data converted from analog tapes, by W. Kazi and C. Kisslinger.

Magnitude Determination

Since its inception in 1974, the Central Aleutians Seismic Network has determined magnitude using the formula $M_D = -1.15 + 2.0 \log_{10}\tau + .0035\Delta + .007z$ where M_D is the duration magnitude, τ is the coda duration measured from the P arrival, Δ is the epicentral distance, and z is the depth. This formula was developed in 1978 for earthquakes in southern Alaska and was adopted unchanged. The Central Aleutians Seismic Network duration magnitudes have been smaller than USGS m_b values for large events by approximately one unit of magnitude. Recent research has exposed some additional inconsistencies in our traditional method of determining magnitudes. A significant dependence of magnitude bias upon epicentral distance has been discovered. Near stations consistently report smaller magnitudes than distant stations. This effect can be satisfactorily removed by measuring duration from the S arrival. We also found that the depth coefficient was too large. 47 earthquakes with $M_D \geq 4.0$ were found in our catalog which did not have magnitudes reported in the PDE catalogs. All of these events had depths greater than 90 kilometers.

In the last semi-annual technical report we reported these findings as well as a preliminary formula: $M_D = 0.8 + 0.7[\log_{10}^2\tau + .003\Delta + .003z]$ where M_D is the duration magnitude, and τ is the duration measured from the S arrival. This formula has since been further examined and several changes have been made. It was discovered that the epicentral distance coefficient was not constant for different regions of the network. We suspected that this was due to differences in the gains of our stations. Therefore, station corrections have been determined. Using these station corrections the epicentral distance coefficient was recalculated and it is now constant for all regions of the network. For our preliminary formula, we used $\log^2\tau$. This was because Bakun (1984) reported that using $\log^2\tau$ provided a good magnitude estimate over a wider magnitude range than $\log\tau$ for earthquakes in central California. We have now compared $\log\tau$ to $\log^2\tau$ for our data and determined that the differences in magnitude estimate are minor in the magnitude range for which we are interested ($2 \leq M_D \leq 5$). We have therefore decided to use the simpler $\log\tau$. Our resulting formula is: $M_D = -2.1 + 2.7\log_{10}\tau + .006\Delta + .002z + \alpha_i$ where α_i is the station correction.

Aftershock Studies

The comparison of two intermediate-depth aftershock sequences, one under the central Aleutians, the other under northern Honshu Island, Japan, has been completed. The principal findings are: (1) both sequences have numerous aftershocks, contrary to conventional wisdom concerning intermediate depth earthquakes; (2) in both cases, the aftershocks fill in a region of low seismicity prior to the mainshock; (3) in both cases, the sequences behave initially according to the modified Omori relation, but in both cases a surge of activity, similar to a secondary aftershock sequence, occurred, but in neither case could the surge be associated with a strong aftershock or a strong earthquake in the vicinity. A speculative explanation of this phenomenon, not yet supported by other data, is that a major creep event occurred, either in the main thrust zone updip from the aftershock area, or within the Wadati-Benioff zone itself, and the surges were triggered by a stress step due to the creep event.

A paper on this study was presented at the IASPEI Scientific Assembly in Istanbul, Turkey, in

August, 1989, under the title: Seismotectonics of Intermediate Depth Earthquakes from Properties of Aftershock Sequences, by C. Kisslinger and A. Hasegawa. The paper is in preparation for publication.

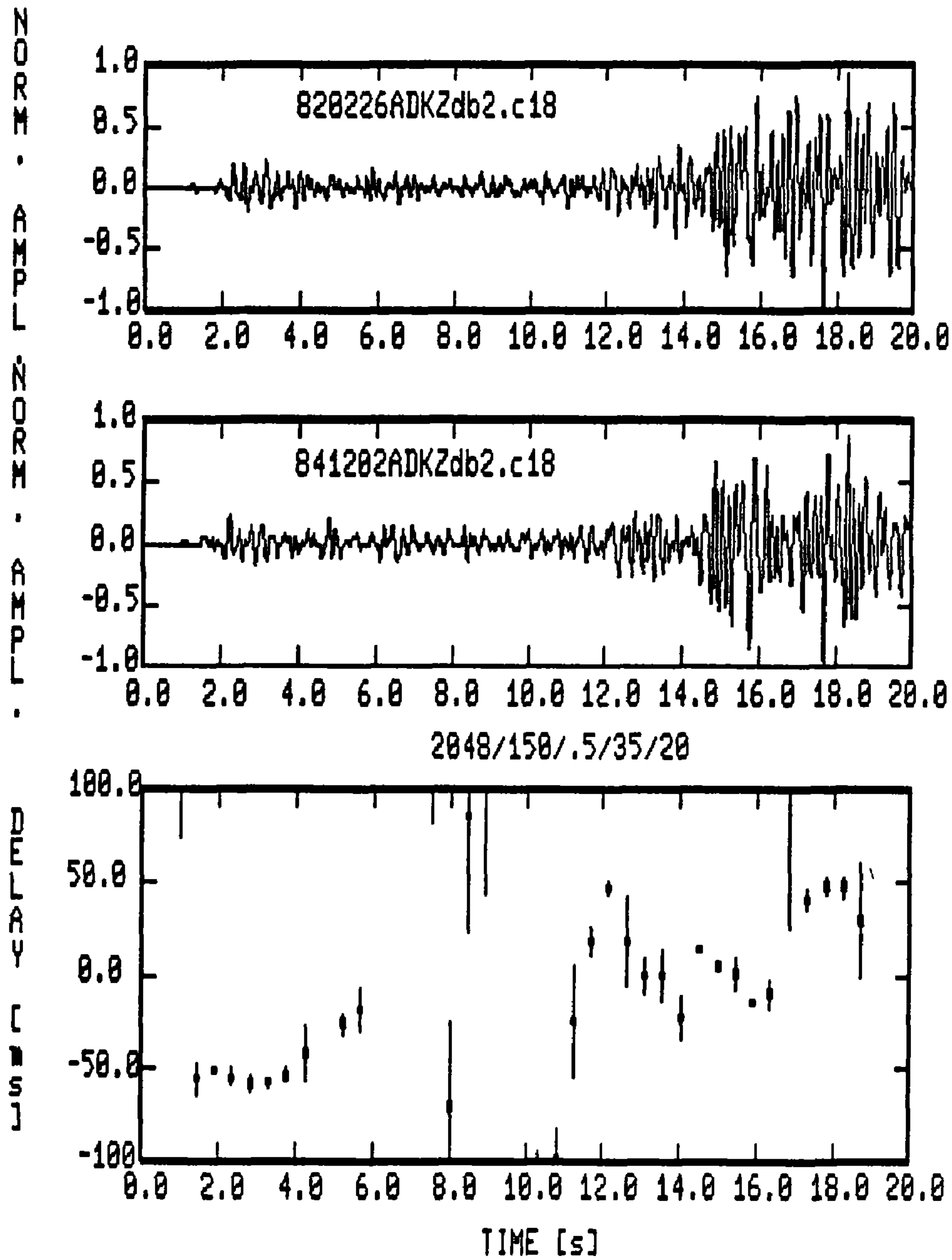

Figure 1

Doublet Analysis by Standard Technique.

From top to bottom:

Vertical component seismogram recorded at station ADK of Adak network for event on Feb. 26,1982.

Vertical component seismogram recorded at station ADK of Adak network for event on Dec. 2, 1984.

(Both of above have been band pass filtered from 1 to 8 Hz. and redigitized to remove time drift.)

The delay as function of running time along the seismograms calculated by standard technique with 0 phase at 0 frequency.

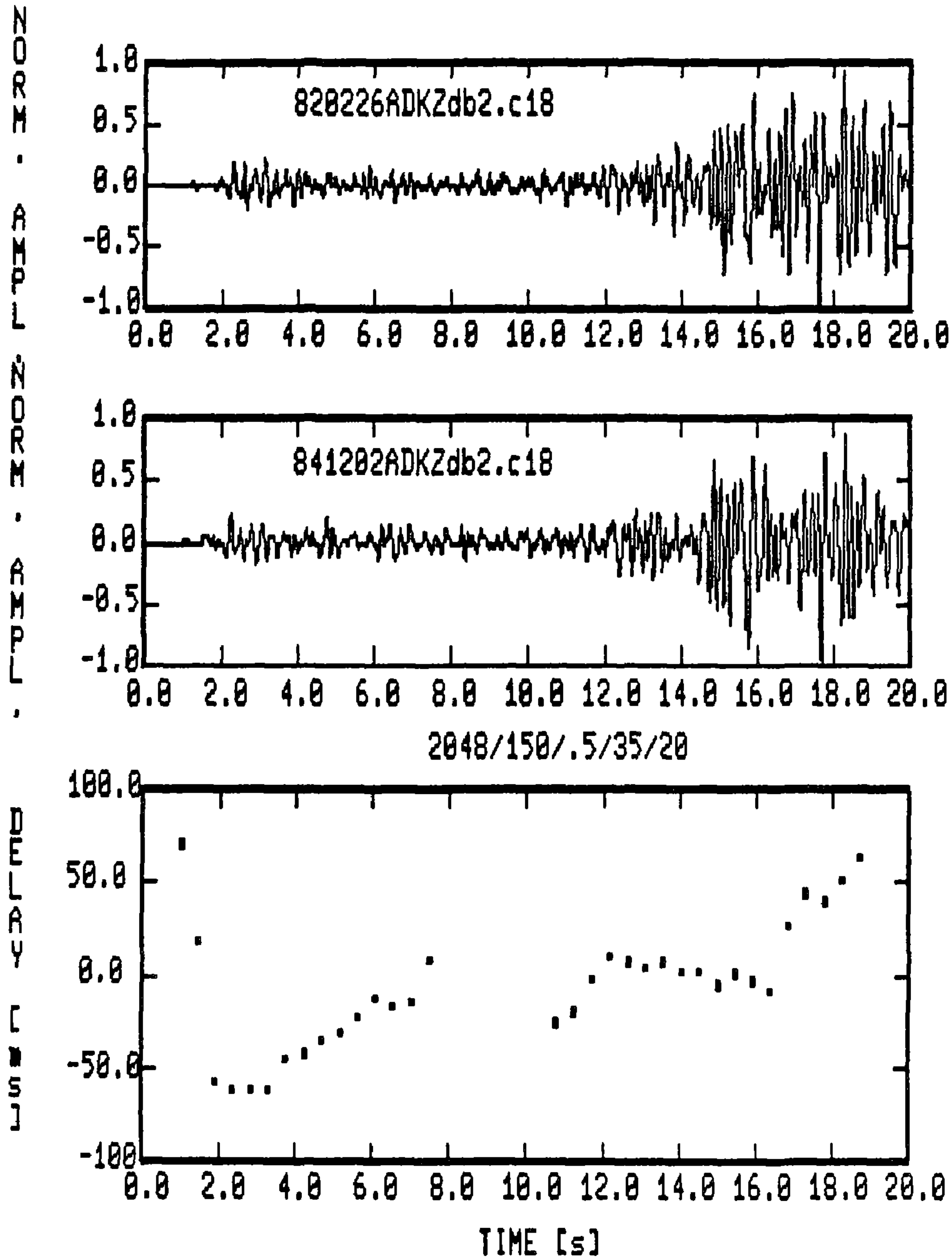

Figure 2

Doublet Analysis by Modified Technique.

From top to bottom:

Vertical component seismogram recorded at station ADK of Adak network for event on Feb. 26,1982.

Vertical component seismogram recorded at station ADK of Adak network for event on Dec. 2, 1984.

(Both of above have been band pass filtered from 1 to 8 Hz. and redigitized to remove time drift.)

The delay as function of running time along the seismograms calculated by revised technique with phase intercept set at some multiple of π at 0 frequency.

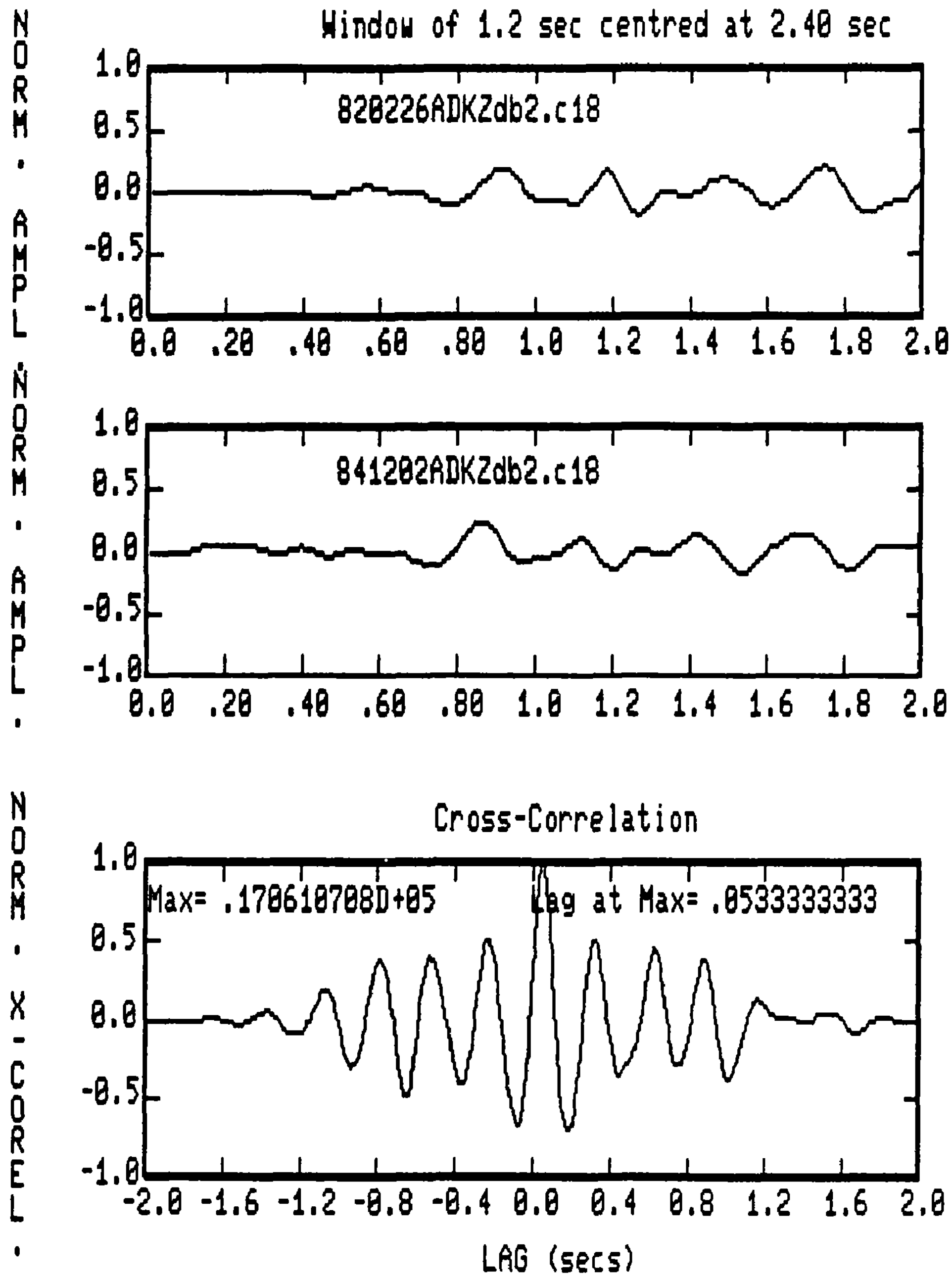

Figure 3

Cross-Correlation Analysis.

From top to bottom:

Window of 1.2 sec centred at 2.40 sec from upper seismogram in figure 1.

Window of 1.2 sec centred at 2.40 sec from lower seismogram in figure 1.

Cross-Correlation of the above windows (calculated as inverse of Cross-Spectrum) exhibiting lag of 53 msec. at maximum peak. The symmetry around the peak suggests good coherency between the two windows.

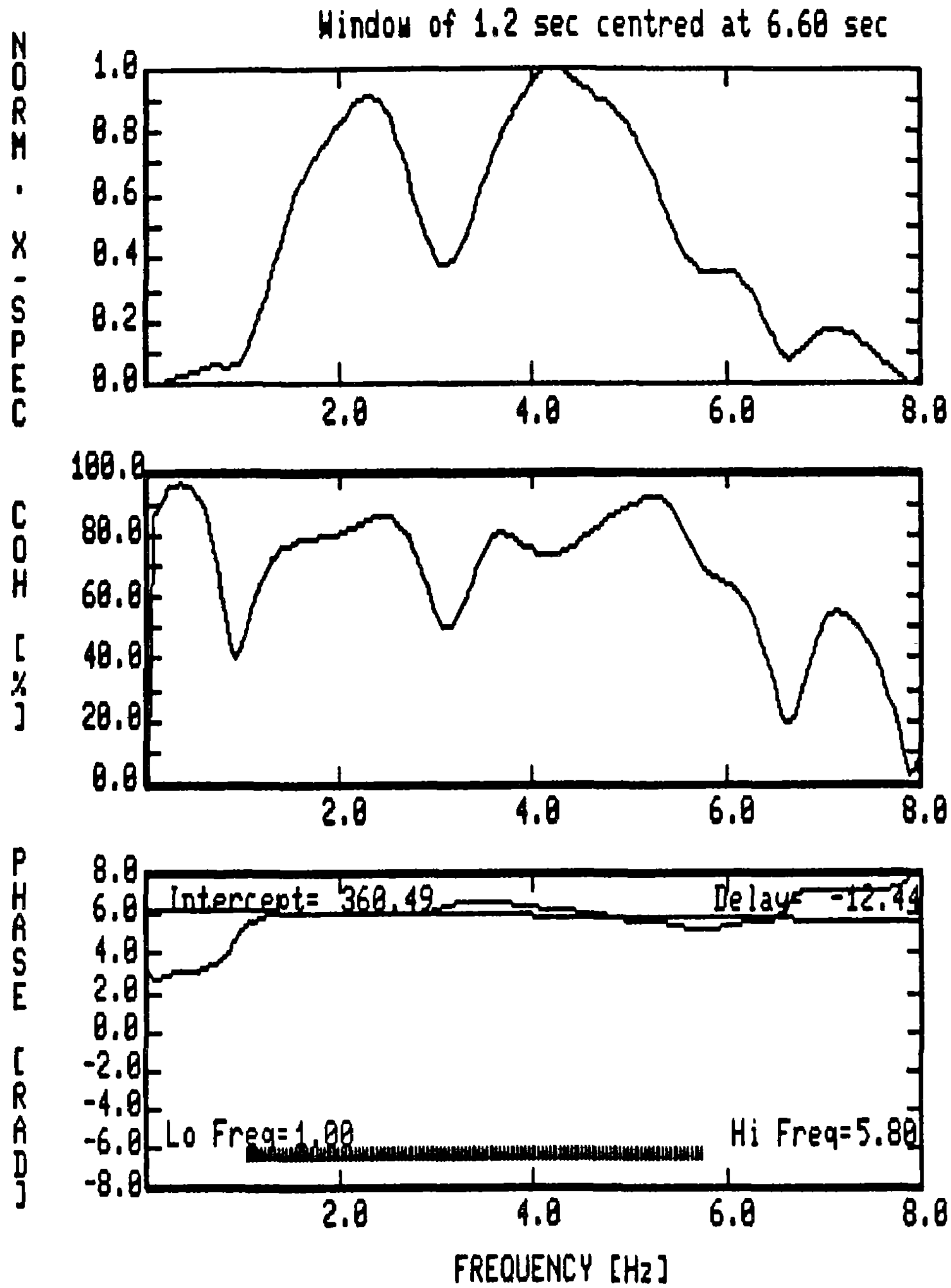

Figure 4

Revised Method of obtaining fit for phase.

From top to bottom:

Cross-Spectrum of windows of 1.2 sec centred at 6.60 sec from the two seismograms in figure 1.

Coherency of windows of 1.2 sec centred at 6.60 sec from the two seismograms in figure 1.

Phase of Cross-Spectrum of windows of 1.2 sec centred at 6.60 sec from the two seismograms in figure 1. The fit to the phase is the best fit which gives an intercept of 2π.

SEISMOLOGICAL FIELD INVESTIGATIONS

9950-01539

Charley J. Langer
Branch of Geologic Risk Assessment
U.S. Geological Survey
Box 25046, Denver Federal Center, MS 966
Denver, CO 80225
(303) 236-1593

Investigations

1. Armenian earthquake--Investigation of the December 7, 1988 earthquake of M(S) - 6.9 located near Spitak, Armenia, S.S.R.

2. Q study--Estimated Q for the Wasatch front in Utah.

Results

1. A 13-day period of aftershock monitoring, commencing 16 days after the December 7, 1988 Armenian earthquake, was conducted by a U.S. Geological Survey (USGS)/Lamont-Doherty field team in cooperation with groups from the Institute of Physics of the Earth, Moscow, and the Armenian Institutes of Geology and Seismology. Twelve portable, analog short-period vertical seismographs and eight portable three-component digital recording systems were deployed in a network some 55 km long (E-W) and 35 km wide (N-S). Of the several thousand recorded events, hypocentral locations have been determined for 327 aftershocks. A selected subset containing 284 best located events define an arcuate pattern of seismicity (fig. 1) about 55-60 km in length. The pattern has a rather broad bend centered near its mid-point at the town of Spitak, changing from an east-west alignment west of the bend to a S. 45-50^{o} E. trend.

   Aftershocks in the western half of the zone occur mainly along a narrow E-W trend, but activity extends over a volume about 25 km long (E-W), 25 km wide (N-S), and between about 5 and 15 km in depth. Events in the central and eastern parts of the zone are shallower with depths ranging from near surface to about 8 km. The central part, at the bend in seismicity near Spitak, extends over an area 10 km long and 10 km wide. The eastern end of the aftershocks defines a narrow southeasterly striking zone less than 5 km wide and about 20 km long. Hypocentral cross sections indicate a complex pattern in the depth distribution of aftershocks suggesting that more than a single fault plane was activated during the aftershock sequence.

2. This Q study developed estimates for the attenuation of peak vertical ground motions using a conventional, least-squares regression applied to unfiltered and band-pass-filtered ground-motion data. The input data are from 88 earthquakes (1.0 <= M <= 3.3; epicentral distance range 10-250 km) located along the Utah-Idaho border and propagating Sg/Lg waves southward to seismograph stations along the Wasatch front in Utah. The regression model includes parameters to account for geometic spreading, anelastic attenuation with a power-law-frequency dependence, source size, and station-site effects.

   The maximum ground-motion amplitudes are derived from waves arriving some 2-4 sec after the S-wave arrivals and are interpreted to be Sg in close (roughly 100 km or two crustal thicknesses) and Lg at greater distances.

   Accordingly, geometric spreading coefficients of 1.0 and 0.9 for body waves (Sg) and 0.83 (5/6) for higher-mode Airy-phase surface waves (Lg) are chosen for testing. Similarly, a range of initial values of the power dependence of the attenuation (0.5-0.9) are also tested. The suite of estimates that result from regressing the amplitude data while employing the family of fixed parameter values, leads to the following model:

$$Q(f) = 90f^{0.86}$$

   for 3Hz <= f <= 10 Hz and 10 km <= R <= 250 km.

   Attenuation comparable to that in southern California is indicated. That pronounced level of attenuation for the study area has been reported in previous investigations which analyzed PSRV spectra, intensity attenuation, and fall-off of Wood-Anderson seismogram amplitudes.

Reports

Brockman, S.R., and Bollinger, G.A., 1990, Q estimates along the Wasatch front in Utah derived from Sg/Lg wave amplitudes: Seismological Society of America Bulletin. (In press).

Langer, C.J., Simpson, David, Pacheco, J.F., Cranswick, E., Glassmoyer, G., and Andrews, M., 1989, Aftershock of the December 7, 1988 Armenian earthquake (abs.): EOS, AGU, 1989 Fall Meeting.

Pacheco, J.F., Simpson, D., Chistoffel, J., Nabelek, J., and Langer, C.J., 1989, Teleseismic, near field and aftershock analysis of the 1988 Spitak, Armenia, earthquake (abs.): EOS, AGU, 1989 Fall Meeting.

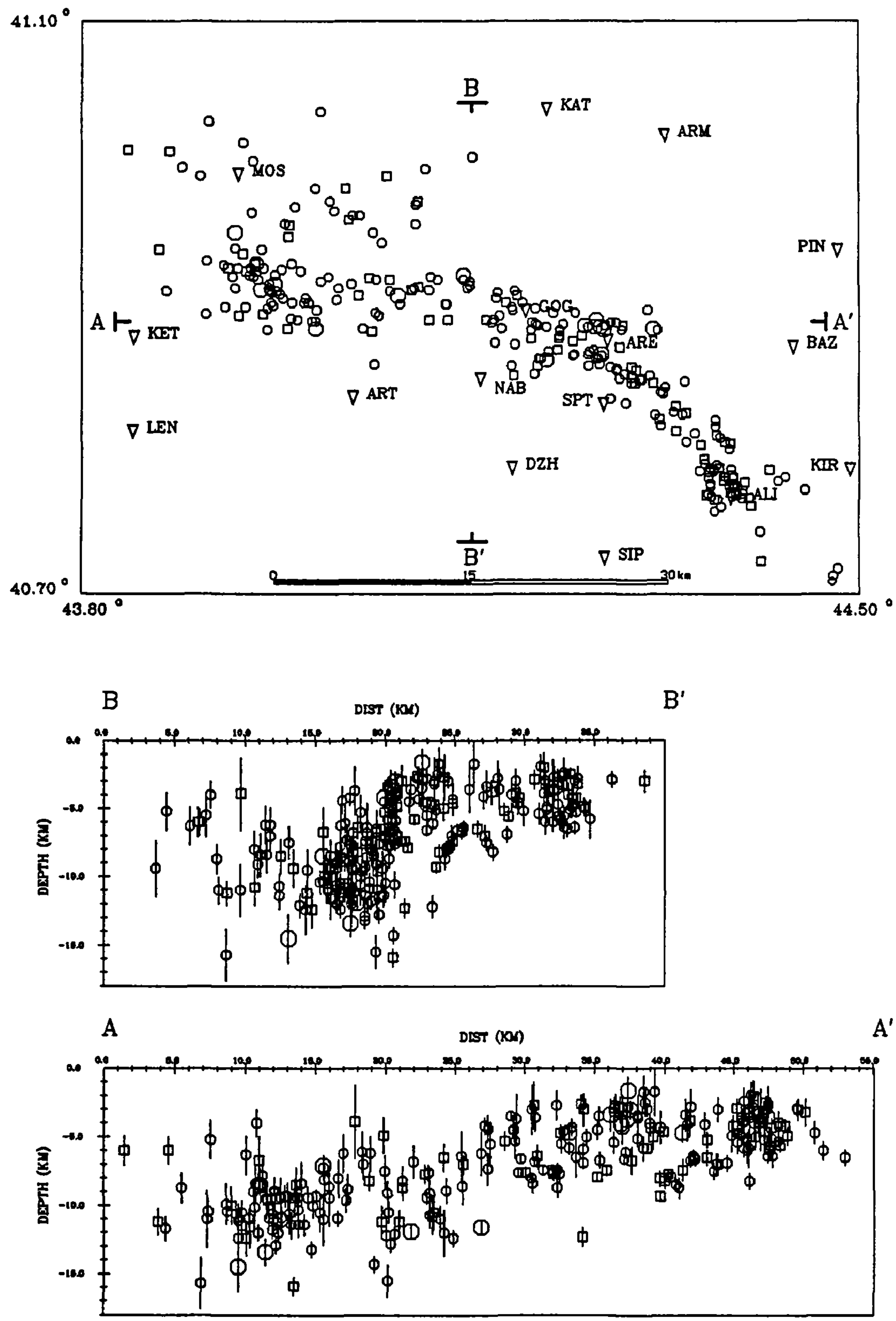

Figure 1. Preliminary distribution of aftershock epicenters (top) and hypocentral cross sections (middle and bottom), Armenian earthquake of December 7, 1988. Inverted triangles = station locations (station SPT was in Spitak); aftershock symbols indicate estimated magnitudes where small octagon is M < 3.0, square is 3.0 < = M < 4.0, and large octagon is M > 4.0.

Slip History of San Andreas and Hayward faults

9910-04192

J. J. Lienkaemper
Branch of Engineering Seismology and Geology
U.S. Geological Survey
345 Middlefield Road, MS 977
Menlo Park, California 94025
(415) 329-5642

Investigations

Determine slip rates and earthquake recurrence intervals on the San Andreas and Hayward faults. Compare rates of geologically determined surface slip to rates of historic creep and geodetically determined deep slip. Analyze the effects of structural complexity and fault segmentation upon inferring recurrence times from slip rate.

Results

1. Previous Work. A joint trenching effort, by the U.S. Geological Survey and California Division of Mines and Geology (USGS/CDMG) in Fremont 1986-1987, yielded a minimum slip rate of 5.5 ± 0.5 mm/yr for the the last 8040 yr from an offset buried channel unit [*Borchardt et al., in prep.*]. The full amount of right slip during that period could not be determined for a 200-m-wide zone of distributed deformation eastward from the site, either by further paleomagnetic or piercing point investigation.

Along the 70-km length of the creeping trace of the Hayward fault, offset curbs, fences, and buildings indicate that the creep rate over several decades has averaged 5-6 mm/yr, except for southern Fremont where it has been 8-10 mm/yr [*Lienkaemper and Borchardt, in prep.*] The Holocene slip rate of 5.5 mm/yr measured in central Fremont may be too low because of local structural complications, thus the 8-10 mm/yr creep rate measured by us in southern Fremont may better represent the full amount of long-term slip rate on the fault. To test this possibility, we began trenching at the Masonic Home site in Union City where the Holocene-active fault zone appears to be narrower.

2. Holocene and Late Pleistocene Slip Rates, Masonic Home, Union City. (Location shown in Figure 1). A small vertical component of slip at the Masonic site makes this an ideal location to investigate the variability of slip rate over most recent geologic time, because it creates the conditions for preserving and dating evidence of accumulated right slip. A small perrenial stream in the hillside northeast of the Hayward fault has cut a narrow bedrock channel (canyon trend in Figure 1) that has meandered little during the late Quaternary. Southwest of the fault, the stream has formed an alluvial fan showing a right-lateral offset of 40-50 m. In April-May 1989, the USGS/CDMG jointly funded the excavation of a 130 m long by 4-6 m deep trench into this alluvial fan and parallel to the fault at a distance of 20 m. Analysis of detailed logs of both walls of the trench reveals a series of gravel-filled channels (shown as dashed lines in Figure 1) and associated silty overbank strata. From the orientation of these many channels, we reconstruct the positions along the fault of at least six beheaded and subsequently buried fan apexes. The values of total slip inferred from these offset apexes shown in Figure 1 are: C) 20 ± 5 m, E) 46 ± 5 m, G) 66 ± 5 m, I) 88 ± 5 m, K) 131 ± 6 m, and M) 167 ± 6 m. Pleistocene camel and horseteeth appear within apex K deposits. We have submitted 24 radiocarbon samples (all charcoal) for dating. Thus far only one date is available, 7435 ± 60 yr BP (radiocarbon yr, ± 1 standard dev.), which dates the onset of deposition from apex G, thus indicating an average slip rate of 8.8 ± 0.7 mm/yr over the last 7475 yr (including 1989-1950 AD ≈ 40 yr).

More parallel trenching in 1990 will verify and improve both stratigraphic control and accuracy of inferred offsets. Possibly more apexes will be located, particularly in the Pleistocene part of the fan (*i.e.*, pre-apex I) where many broad channels could not yet be used reliably to infer the location of apexes. A major change in both overbank composition and channel morphology took place sometime in early Holocene while apex I was active. Pleistocene overbank deposits are composed of yellow brown sandy silt; in Holocene dark gray brown clayey silt dominates. Pleistocene channels generally have a broader form, up to 10 m wide; Holocene ones are mostly narrower, 1-2 m wide. The form of the canyon northeast of the fault may help explain this change in fan channel morphology. Northeast of the fault the present thalweg is narrow, 1-2 m wide, and is bordered by a narrow flat terrace within the canyon. Above the canyon walls to the southeast lies a much broader terrace that we suspect correlates with our latest Pleistocene broader channel deposits. Our knowledge will be improved by a 0.25-m contour topographic map of the site that is being compiled. If time and funding permit, we may test these assumptions about terrace ages by trenching. If correlative Pleistocene channels are found in the upper terrace, our estimates of Pleistocene slip are low. Alternatively, the terrace may be a strath; if so our estimates are correct. This problem does not affect our Holocene slip estimates although they may be slightly improved by the detailed mapping of the modern thalweg.

Based on our Holocene slip rate discussed above, 8.8 mm/yr, I tentatively conclude that the Hayward fault has a surface slip deficit rate of 3-4 mm/yr. Deficit rate is defined here as the difference between long-term slip rate and historical creep rate. If one accepted the commonly used value of 3 feet (90 cm) for maximum surface slip in the 1868 earthquake, then recurrence times would range 225-300 yr. However there is little justification for using the 90 cm assumption: it's source, *Lawson* [1908], did not know if it represented right slip, scarp height, or simply the width of a gaping crack. More physically realistic perhaps is to estimate coseismic slip from general earthquake scaling relations as was done by the *Working Group on California Earthquake Probabilities* [1988]. For both northern (1836?) and southern (1868) segments of the Hayward fault they adopted 1.4 ± 0.4 m for coseismic slip (not necessarily surficial) in M 7 earthquakes. At a rate of 8.8 mm/yr, simple recurrence assumptions for such events gives an interval of 159 ± 47 yr between magnitude 7 earthquakes. Because it has been at least 153 yr since the northern segment has ruptured (possibly in 1836?), it seems especially appropriate now to search for direct evidence of timing and size of both historic and prehistoric events in the geologic record.

3. Other project work. I continue to compile a strip map of the 70-km-long creeping trace of the Hayward fault, and to monitor slip along it (at 6-km spacing). Status of work on the San Andreas fault follows: 1) the Parkfield paper [*Lienkaemper and Prescott*] is in press, 2) Cholame I [*Lienkaemper and Sturm*, 1989] is published, and 3) Cholame II [*Lienkaemper*] is in preparation.

Reports

Borchardt, G., J. J. Lienkaemper, and K. Budding, ----, Holocene slip rate of the Hayward fault at Fremont, California: manuscript in preparation for J. Geophys. Res.

Bonilla, M. G., and J. J. Lienkaemper, in press, The visibility of fault strands in exploratory trenches and timing of rupture events: *Geology*,.

Lienkaemper, J. J., 1989, Field trip guide to the Hayward fault, *U.S. Geol. Surv., Open-File Report 89-500*, 23 p.

Lienkaemper, J. J., ----, Amount of slip along the San Andreas fault near Cholame, California, associated with the great 1857 earthquake: evidence from offset stream channels: manuscript in preparation.

Lienkaemper, J. J., and G. Borchardt, ----, Historic slip on the Hayward fault, northern California: manuscript in preparation

Lienkaemper, J. J., G. Borchardt, J. F. Wilmesher, and D. Meier, 1989, Holocene slip rate along the Hayward fault, northern California (abs.): *EOS, Abstr. Am. Geophys. Union*, Fall Meeting.

Lienkaemper, J. J., and W. H. Prescott, in press, Surface slip along the San Andreas fault near Parkfield, California: *J. Geophys. Res.*

Lienkaemper, J. J., and T. A. Sturm, 1989, Reconstruction of a channel offset in 1857(?). on the San Andreas fault near Cholame, California: *Bull. Seismol. Soc. Am. 89*, 901-909.

References

Lawson, A. C., 1908 [reprinted 1969], The Earthquake of 1868, *in* The California Earthquake of April 18, 1906, *Report of the State Earthquake Investigation Commission, v. I*, (A.C. Lawson, chairman), Carnegie Institution of Washington, Washington, D.C., 434-438.

Working Group on California Earthquake Probabilities, 1988, Probabilities of large earthquakes occurring in California on the San Andreas fault: *U.S. Geol. Surv., Open-File Report 88-398*, 62 p.

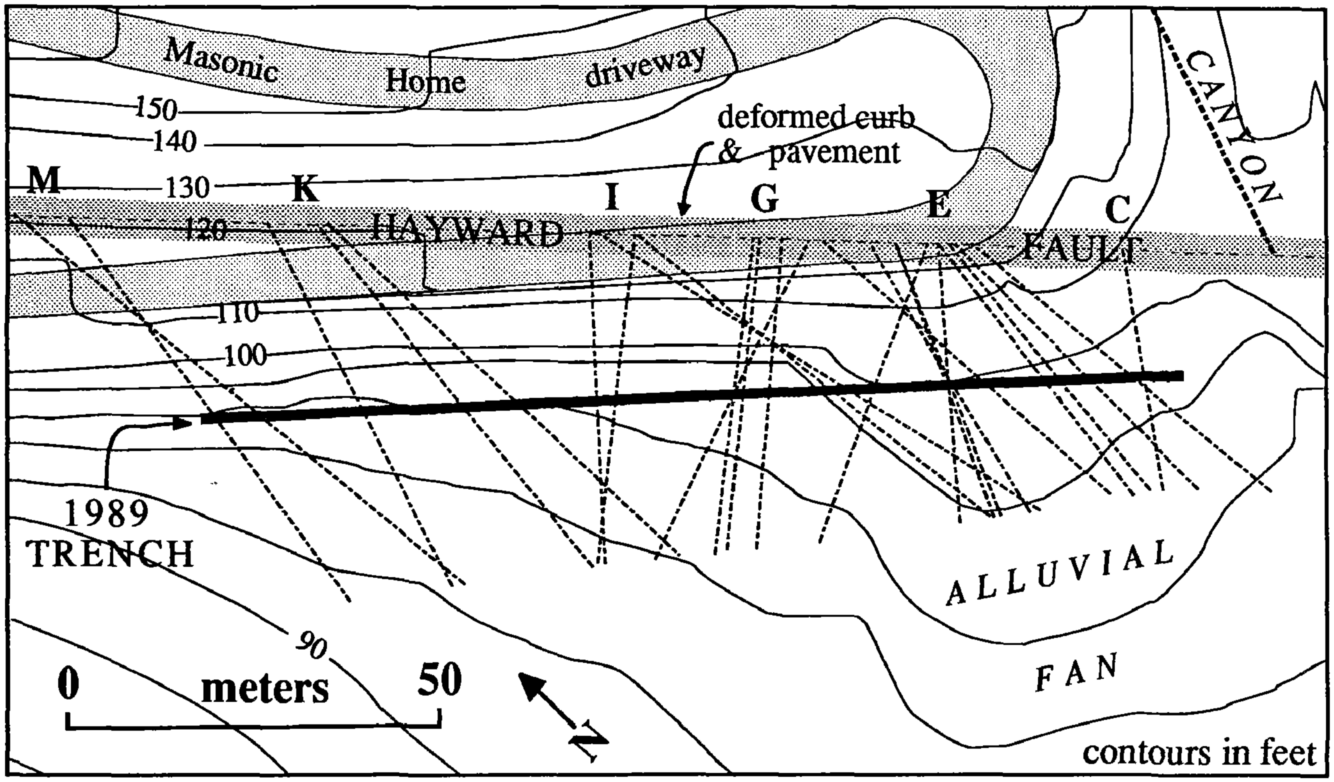

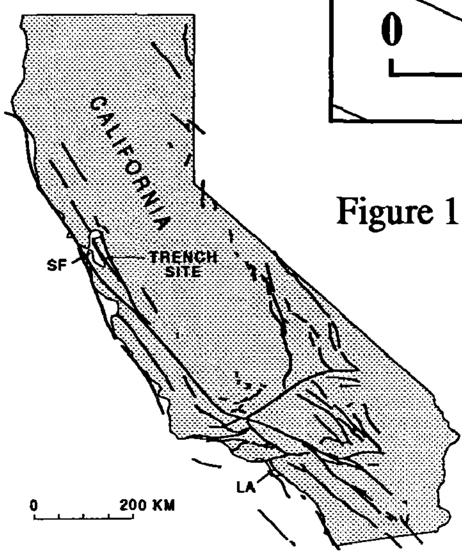

Figure 1. Masonic Home trench site, Union City, California.

Paleoseismic Liquefaction Studies

9950-03868

Stephen F. Obermeier
Branch of Geologic Risk Assessment
US Geological Survey
M.S. 922, National Center
Reston, Virginia 22092
703-648-6791

Investigations

1. Used borehole data (from more than 1000 holes) in the vicinity of Charleston, S.C., to look for evidence of tectonic ground deformations. Parameters that were examined included variations in thickness of Pleistocene deposits, surface warping of the ground, and warping of the base of near-shore, marine depostis.

2. Examined field data which I have collected primarily from New Madrid seismic zone and from the Charleston area, for the purpose of developing criteria to distinguish between short-term, artesian spring fluidization features and earthquake-induced liquefaction features.

3. Worked on manuscript which discussed geologic, geotechnical and seismological criteria for evaluation of liquefaction potential caused by large earthquakes in the New Madrid seismic zone.

Results

1. In the Charleston area, no conspicuous regions of Pleistocene deformation are apparent. A few candidate areas have been located, but borehole data are needed for verification. A manuscript, in part discussing results, has been submitted for technical review.

2. A listing of criteria, some still tentative, has been developed to distinguish between artesian fluidization features and earthquake-induced liquefaction features. For verification of the criteria, excavations need to be made into known spring-induced sand boils.

3. A study set of photographs and slides has been completed, which show earthquake induced liquefaction features and features with which they might be confused. The study set is available for loan upon request to me.

4. Received approval for publication , as a USGS Bulletin, the text and maps showing regions of liquefaction potential caused by earthquakes in the New Madrid seismic zone.

Reports

Obermeier, S. F., Wingard, N. E., Jibson, R. W., and Hopper, M. G.: Regional assessment of liquefaction potential for M_s-8.6, -7.6, and -6.7 earthquakes originating in the New Madrid seismic zone, received Branch Chief approval as USGS Bulletin.

Weems, R. E. and Obermeier, S. F.: The 1886 Charleston Earthquake--An Overview of Geological Studies, submitted for technical review for publication in Proceedings of 17th Water Reaction Information Meeting sponsored by the Nuclear Regulartory Commission, October 25, 1989.

Determination of Earthquake Hypocenters, Focal Mechanisms, and Velocity Structures in the Morgan Hill/Coyote Lake and Bear Valley/Stone Canyon areas of Central California through the use of Fast, Accurate Three-Dimensional Ray Tracing.

14-08-0001-G1697

Steven W. Roecker
Department of Geology
Rensselaer Polytechnic Institute
Troy, New York 12180-3590
(518)-276-6773

Objectives: This project will apply a new three-dimensional ray tracing technique to determine earthquake hypocenters, focal mechanisms, and velocity structures in the Morgan Hill/Coyote Lake and Bear Valley/Stone Canyon areas of central California. The primary objectives of the study are two: (1) to address the importance of, and to develop an algorithm for, routine determination of earthquake locations and fault plane solutions using three-dimensional ray tracing in these areas, and (2) to refine the locations and mechanisms of previously recorded earthquakes in these areas and improve the definition of their P and S wave velocity structures. Both of these objectives will improve our understanding of the seismic activity, the nature of faulting, and the tectonic environment in which these earthquakes occur. A fast, accurate, and robust three-dimensional ray tracing technique recently developed by the PI will be used to analyze the data. The speed and robustness of the technique will make the analysis of large volumes of data feasible, and will allow it to be used in a routine application. The ability of the algorithm to trace rays through large gradients makes it particularly useful for examining locations and structures in Morgan Hill/Coyote Lake and Bear Valley/Stone Canyon, because previous studies have suggested large velocity gradients in these areas.

Progress to Date: In the seven months that we have been working on this project, we have accomplished the following:

1. We have completed development and testing of the software. The ray tracing and inversion routines have been tested both with synthetic data and with real data from another region (Taiwan). We have completed writing a technical manual for this software, and are preparing a short paper for BSSA. We have also already been contacted by several other investigators who are interested in applying this method to different regions, and have distributed the software to them.

2. The PI spent the month of June at the USGS in Menlo Park collecting suitable datasets for this project. The following data sets have been compiled:

(a) A general dataset of arrival times recorded by the USGS regional network from earthquakes that occurred in the regions between the Morgan Hill and Bear Valley/Stone Canyon areas. This data set contains 8000 of the best recorded events that occurred between 1/1984 and 4/1989. Nearly all of the data in this set has been read either by an automatic picker or by the CUSP system, and is therefore likely to be of much higher quality than arrival times reported before this time.

(b) A collection of aftershock data from the Morgan Hill earthquake that was previously analyzed by A. Michael.

(c) A collection of aftershock data from the Coyote Lake earthquake that was previously analyzed by C. Thurber.

(d) The data collected by the 1974 "Centipede" array in Bear Valley area.

3. Since June we have been running this data through our relocation routine, using various structural models based on previous work in the area. Our principal objective to this point has been to cull a working data set of a few hundred of the very well constrained hypocenters from the thousands that we are starting with. This objective is nearing completion and we will begin inversion for structure in the next few weeks.

EARTHQUAKE RESEARCH IN THE EASTERN SIERRA NEVADA-WESTERN GREAT BASIN REGION

Contract 14-08-0001-G1524, October 1989

M. K. Savage, W.A. Peppin, U.R. Vetter, J.N. Brune, and K.F. Priestley
Seismological Laboratory
University of Nevada
Reno, NV 89557
(702) 784-4315

Investigations

This contract supports continued research focused on the eastern Sierra Nevada and the western Great Basin region. We have focused on three areas: (1) seismicity, tectonics and earthquake potential, and (2) rupture mechanics and high frequency radiation Some of the new results are described below.

Results

(1) Seismicity and Tectonics

Che Norliza Lat has completed a Master's thesis on the seismicity of the Garfield Hills area of the Excelsior Mountains, Nevada (Lat, 1989). Arrival times taken from the UNR seismic network were combined with aftershock recordings of the 19 September 1988 Garfield Hills earthquake (M 5.0) were processed using master-event analyis to provide a refined look at seismicity at a resolution of one or two km. One purpose of this effort was to investigate whether the occurrence of seismicity in this region was related to the intersections of visible faults at the surface, as has been suggested by various investigators at the Seismological Laboratory for the last twenty years, and which appears to be the case for the a cluster of earthquakes near Mina (Smith and others, 1988) and for the 1986 Chalfant sequence. If such a correlation exists in the vicinity of Garfield Hills, then it only occurs for seismicity clusters with largest magnitude about 5 or greater: only the 19 September 1988 event is so related, the other 15 clusters showing no such relationship.

In general, seismicity of this area has been occurring in small clusters, with greatest magnitude less than 5 and usually less than 4, and with the dimension of the cluster zone quite small, a few km in extent. The occurrence of these clusters is random, and the record of seismicity extending back to 1852 shows no evidence of a deviation from this pattern (e.g., no earthquake larger than the 1934 Excelsior Mountains sequence, and bursts of seismicity occurring randomly over the area in space and time).

Overall, this study provides no reason to question the suggestion by Savage(1972) and Ryall and Priestley (1974) that this is an area of continuing moderate seismicity with more or less constant strain release through small to moderate earthquakes rather than repeating major earthquakes.

Pre-S Observations at Station SLK

Work on the SLK observations has been finalized with the completion of a Master's thesis by Scott Lewis and the submittal of a paper in press (Peppin and others, 1989). The thesis gives detailed descriptions of efforts made to determine the character of seismic waves arriving at station SLK based on a miniarray deployed near that site. The SLK phase is unambiguously identified as having longitudinal particle motion; consequently, it is almost certainly the same phase seen by Luetgert and Mooney (1985) and Zucca and others (1987). Both of these papers interpret this phase as a deep reflection from deep (presumed magma-related) sources in the caldera, but if their observations are the same phenomenon as the SLK phase, then our observations definitely preclude such interpretations. Lewis presents the model of Peppin and others (1989) with fairly minor modification as the one which best fits the observations: an S to P conversion across a two-dimensional surface in the vicinity of Inyo Craters NW of the caldera. He goes on to describe drillhole and geologic results which suggest the physical cause of such a conversion to be related to fluid-filled dykes which trend NE along the Inyo - Mono Craters trend.

(2) Rupture Mechanics and High Frequency Radiation

An earthquake swarm began under Mammoth Mountain beginning in May of 1989. This swarm has produced thousands of events, and is probably the single swarm of greatest temporal duration of any that have occurred in the entire sequence since 1978. As Mammoth Mountain is strategically placed relative to the populous Mammoth Lakes resort, the U.S.G.S. and UNR deployed temporary instruments around the mountain. The epicenters define a nebulous NE trend at fairly shallow depths (many events 2 to 6 km deep).

An array of three-component widerange digital event recorders were deployed near the mountain during two separate periods, and over 1,000 records obtained. The specific purpose of this effort was to obtain close-in records for use in waveform inversion to determine the focal mechanism of these events; we would presume that these earthquakes, probably related to geothermal or magmatic processes, would have a chance to have a non-couple component to the mechanism. The data obtained includes ten events for which a station west, north, and east of the epicenter triggered the digital instruments. Efforts are now underway to invert these waveforms for the seismic moment tensor (Stump and Johnson, 1977).

Reports published, in press, or submitted during this period

Lat, Che Norliza, 1989. Seismicity and Tectonics of the Garfield Hills Area, Nevada, *M.S. thesis, University of Nevada, Reno*, 154 pp.

Lewis, J. Scott, 1989. Observations Preceding S at the Station SLK, NW of Long Valley, California and a Real Physical Model, *M.S. thesis, University of Nevada, Reno*, 225 pp.

Peppin, W.A., W. Honjas, T.W. Delaplain, U.R. Vetter, 1989. The case for a shallow-crustal anomalous zone (magma body?) near the south end of Hilton Creek fault, California including new evidence from an interpretation of pre-S arrivals. *Bull. Seism. Soc. Am.*, **79**,805-812.

Priestley, K.F. and R. Robinson, 1989. The Edgecumbe, New Zealand earthquake: An analogue to an expected Yucca Mountain event, *Late Cenozoic Evolution of the Southern Great Basin*, in press.

Rogers, A., S. Harmsen, E. Corbett, K. Priestley, and D. dePolo, 1989. The seismicity of Nevada and adjacent areas of the Great Basin, Geol. Soc. Am. vol *Decade of North American Geology*, in press.

Savage, M.K., W.A. Peppin, and U.R. Vetter, 1989. Shear-wave anisotropy and stress direction in and near Long Valley Caldera, California, 1979-1988. *J. Geophys. Res.*, accepted.

Savage, M.K., X.R. Shih, R.P. Meyer, and R.C. Aster, 1989. Shear-wave anisotropy of active tectonic regions via automated shear-wave polarization analysis, *Tectonophysics*, **165**, 279-292.

Savage, M.K., 1988. Report of the State of Nevada to the Western States Seismic Policy Council, 1987. *Proceedings of the annual meeting of the Western States Seismic Policy Council, Nov. 3-6, 1987* 15-17.

Savage, M.K. and P.G. Silver, 1989. Observations of teleseismic shear wave splitting in the Basin and Range from portable and permanent stations, *Geophys. Res. Letters*, accepted.

Savage, M.K., W.A. Peppin, and U.R. Vetter, 1988. Stress measurements in the Long Valley Caldera, California: comparison of focal mechanisms, stress tensors, and shear-wave splitting. *EOS, Trans. A.G.U.*, vol. 69, no. 44, p. 1462.

Smith, K.D., J.N. Brune and K.F. Priestley, 1989. Seismic Energy, Spectrum, and the Savage and Wood Inequality for complex Earthquakes, *submitted to Tectonophysics.*

Smith, K.D., W.R. Walter, R.R. Castro, K.F. Priestley, and A.R. Anooshepoor, 1989. Earthquake clustering near Mina, Nevada, July and August, 1987, *Late Cenozoic Evolution of the Southern Great Basin*, in press.

Vetter, U.R., 1988. Characterization of regional stress patterns in the western Great Basin using grouped earthquake focal mechanisms, *Tectonophysics, 152*, 239-251.

Vetter, U.R., 1989. Regional variation of the stress tensor in the western Great Basin boundary region from the inversion of earthquake focal mechanism, *Tectonics*, accepted.

Salton Trough Tectonics and Quaternary Faulting

9910-01292

Robert V. Sharp
Branch of Engineering Seismology and Geology
345 Middlefield Road, MS 977
Menlo Park, California 94025
(415) 329-5652

Investigations

1. Post-seismic slip on the Superstition Hills fault zone following the November 1987 earthquakes.

2. Nearfield leveling across the northern Imperial fault.

Results

1. Remeasurement in May 1989 of 46 sets of semipermanent monuments straddling the Superstition Hills fault zone, documents continuing afterslip of the 1987 surface faulting event for the period 338 ± 2 to 541 ± 2 postearthquake days. The largest right-lateral movement, 1.7 cm, was recorded near Imler Road, which is the location of the maximum "final" cumulative slip for the Superstition Hills fault predicted by a damped power-law fitting of earlier slip measurements. Despite the smallness of the new increments of slip, the shape of the longitudinal profile of them continues to mimic the form of the longitudinal profile of cumulative slip. This shows that after 1.5 years of post-seismic movement, there is little evidence of "catch up" behavior - i.e., more rapid slip at these sites with smaller early displacement.

   The longitudinal extent of afterslip on the Superstition Hills fault for this period nearly matches the full length of initial rupture, and there has been no evidence of increasing length of the rupture with time. Afterslip on the Wienert fault, which lies to the southwest of the Superstition Hills fault, may also extend the full length of that initial surface rupture, but the density of observation points along it is insufficient for proof.

2. The profile of elevation change along the 0.5 km nail array in pavement at Harris Road is unusual for the period October 1988 to May 1989. The profile is a nearly linear tilt of about 6μ radians, and it is unusual because its sense, downward on the west side of the fault, is opposite to the cumulative sense of vertical

displacement on the fault there. In the 13-year record of elevation changes at this location, only twice before has a reversed sense of tilt been observed. Apparently, relaxation has occurred at depths greater than about 0.2 km but retrograde movement of the fault at the ground surface is not indicated by the data. Retrograde vertical surface displacement has never been recorded here or at other sites on the northern Imperial fault.

Reports

Sharp, Robert V., 1989, Surface faulting: a preliminary view, *in* Wyllie, L.A., Jr. and J.R. Filson (eds.), Armenia earthquake preliminary report: E.E.R.I. Earthquake Spectra Spec. Supplement, p. 13-22.

Seismotectonic Framework and Earthquake Source Characterization (FY89) Wasatch Front, Utah, and Adjacent Intermountain Seismic Belt

14-08-0001-G1349

R.B. Smith, W.J Arabasz, and J.C. Pechmann*
Department of Geology and Geophysics
University of Utah
Salt Lake City, Utah 84112-1183
(801) 581-6274

Investigations: April 1 - September 30, 1989

1. Source parameters of aftershocks of the 1983 Borah Peak, Idaho, earthquake.
2. An assessment of source parameters of earthquakes in the Cordillera of the western United States.
3. Relocation of the 1987-1988 Lakeside, Utah, earthquakes.

Results

1. The highest quality data available for studies of earthquake source properties in the Intermountain seismic belt are USGS 3-component digital recordings of aftershocks ($M_L \leq 5.6$) of the 1983 M_S 7.3 Borah Peak, Idaho, earthquake. We used these data to investigate relations between seismic moment (M_0) and stress drop and between M_0 and local magnitude (M_L). M_0 and fault radii for 53 aftershocks were calculated from measurements of areas and widths of SH-wave displacement pulses, assuming a circular source model. Our estimates of these parameters generally agree within a factor of two with estimates made by Boatwright (1985) from spectral analyses of P and S waves. M_L determinations from synthetic Wood-Anderson seismograms do not differ systematically from determinations made using Wood-Anderson seismograms recorded in Utah at $\Delta = 390-430$ km and Richter's distance corrections. This agreement in M_L values suggests that attenuation in the Wood-Anderson passband ($0.3-10$ Hz) in S. Idaho and N. Utah may not be significantly different from that in California.

Static stress drops range from 1 to 50 bars and do not vary systematically with moment for aftershocks of $M_0 \geq 10^{21}$ dyne-cm (Figure 1). For smaller events, pulse widths decrease with M_0 at a rate much slower than that predicted by constant stress drop scaling, and could be interpreted to have a nearly constant value of 0.23 ± 0.10 sec. This observation cannot be easily explained by attenuation, since correction for attenuation using an average whole-path t^* value of 0.025 measured by Boatwright (1985) has a negligible effect on the waveforms. Linear regression of log M_0 versus M_L yields the following relations:

*D.I. Doser and J.E. Shemeta also contributed significantly to the work reported here.

$$\log M_0 = (1.2 \pm 0.1) M_L + 16.8 \pm 0.3 \qquad (2.3 \leq M_L \leq 3.7)$$
$$\log M_0 = (1.5 \pm 0.1) M_L + 15.7 \pm 0.4 \qquad (3.5 \leq M_L \leq 5.6)$$

These $M_0 - M_L$ relations are very similar to those found for California earthquakes, but differ from those found in two previous studies of earthquakes in the Utah-Idaho-Wyoming region (Figure 2).

2. In a cooperative study with D. Doser of the University of Texas at El Paso, source parameters of 50 earthquakes occurring between 1915 and 1988 have been used to examine the faulting characteristics of magnitude 5.5 to 7.8 earthquakes within the western U. S. Cordillera. The study area extends from the eastern Sierra Nevada to the Great Plains and from northwestern Montana to Trans-Pecos Texas. Source parameters used in this study include seismic information from first motion analyses, body and surface waveform modeling, geodetic studies, and geological studies of surface faulting. The principal results of this analysis include: (1) all earthquakes occurred on faults dipping 38° or more, and no evidence for listric or low-angle planar faulting was found, (2) all $M \geq 7.0$ earthquakes occurred at depths ≥ 12 km and were composed of multiple subevents, (3) most earthquakes (>70%) had unilateral ruptures, and (4) no individual subevent had a rupture length > 21 km.

3. From September 1987 through March 1988, an earthquake sequence which included eight events of $3.8 \leq M_L \leq 4.8$ occurred beneath a desert basin west of Utah's Great Salt Lake. Calculation of high precision locations for these earthquakes has proven difficult because the earthquakes were outside the boundaries of the Utah regional network. We have used P-wave arrival time data and a computer program written by W. Nagy of the University of Utah to solve simultaneously for hypocentral locations of 170 of the Lakeside earthquakes and station delays for 21 stations. The 21 stations include 13 selected regional network stations at epicentral distances of 60 to 125 km and 8 portable stations (up to 4 at any one time) operated by the University of Utah during the Lakeside activity at epicentral distances of 1 to 25 km. The station delays were then used together with the location program Hypoinverse written by F.W. Klein of the USGS to relocate all 222 Lakeside earthquakes for which there are at least five P-wave arrival times. The resulting hypocentral distribution is similar to that found previously, but has less scatter and a more restricted depth range. The best-located hypocenters clearly delineate a 6-km-square zone between 6 and 12 km depth that is nearly vertical and trends SSE. This zone is parallel to a nodal plane of the main shock focal mechanism that shows right-lateral strike-slip motion.

Reports and Publications

Arabasz, W.J. and S.J. Nava (1989). Historical seismographic recording in Utah, *Seism. Res. Lett. 60*, 33.

Bjarnason, I.T. and J.C. Pechmann (1989). Contemporary tectonics of the Wasatch front region, Utah, from earthquake focal mechanisms, *Bull. Seism. Soc. Am. 79*, 731-755.

Doser, D.I. and R.B. Smith (1989). An assessment of source parameters of earthquakes in the Cordillera of the western United States, *Bull. Seism. Soc. Am.*, in press.

Nava, S.J., J.C. Pechmann, and W.J. Arabasz (1989). A swell earthquake in the Colorado Plateau, *Seism. Res. Lett. 60,* 30.

Shemeta, J.E. and J.C. Pechmann (1989). New analyses of three-component digital data for aftershocks of the 1983 Borah Peak, Idaho, earthquake: Source parameters and refined hypocenters, *Seism. Res. Lett. 60,* 30.

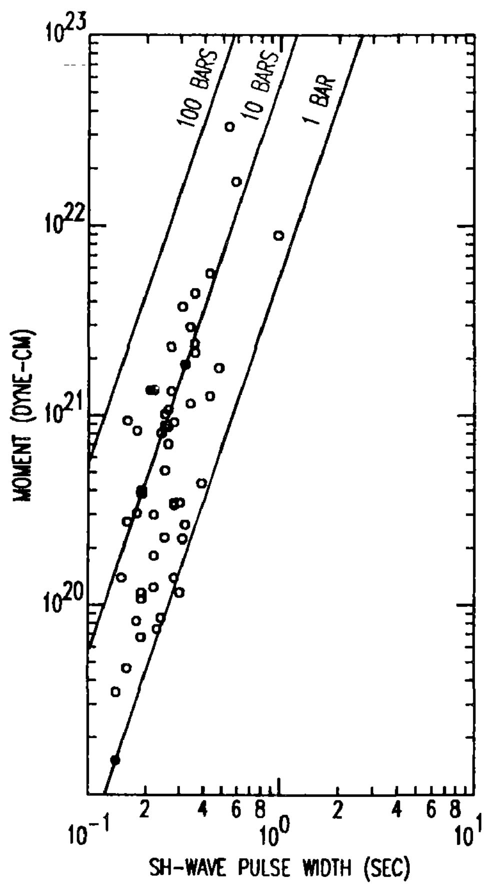

Figure 1. Seismic moment versus SH-wave pulse width for aftershocks of the 1983 M_S 7.3 Borah Peak, Idaho, earthquake. Each of the data points represents an average of two or more measurements for both moment and pulse width. Lines of constant stress drop calculated using the circular source model of Cohn et al. (1982, *JGR,* v. 87, p. 4585-4594) are shown for 1, 10, and 100 bars. Note the apparent change in the relation between moment and stress drop at $M_0 \approx 10^{21}$ dyne-cm.

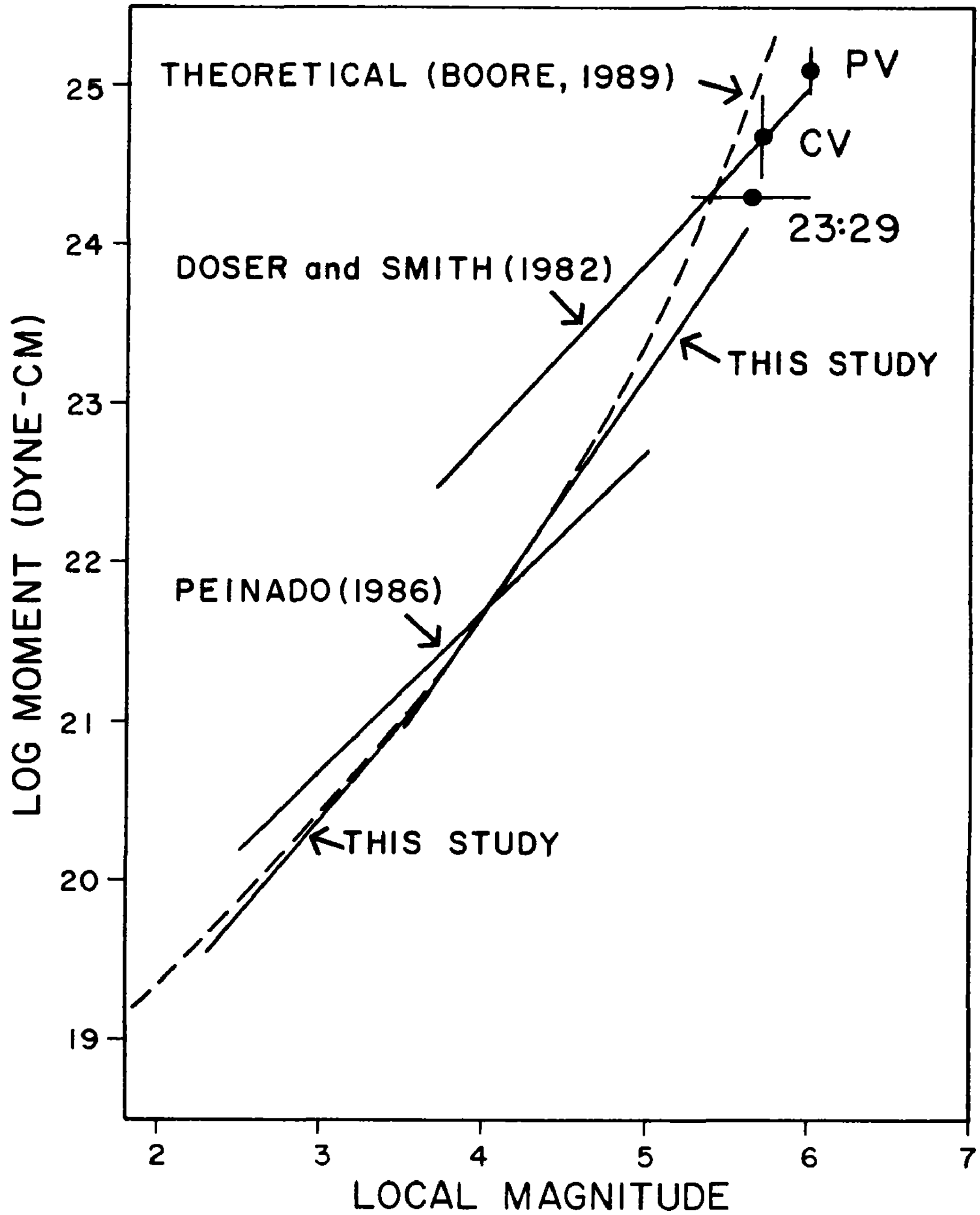

Figure 2. Comparison of moment-local magnitude relations derived for Borah Peak aftershocks ("This study") with those derived by Doser and Smith (1982, *BSSA*, v. 72, p. 525-551) for earthquakes in the Utah region and by Peinado (1986, *M.S. thesis*, University of Utah) for earthquakes in Utah, SE Idaho, and W Wyoming. Also shown is a theoretical M_0 - M_L relation from Boore (1989, *Tectonophysics*, v. 166, p. 1-14), which provides an excellent fit to M_0 and M_L measurements for California earthquakes of $0 \leq M_L \leq 6$. The solid circles with error bars (one standard deviation) represent data points for the 1962 Cache Valley, Utah, earthquake (CV), the 1975 Pocatello Valley, Idaho, earthquake (PV), and the October 29, 1983 23:29 (UTC) Borah Peak aftershock. The close agreement between the M_0 - M_L relations found for the Borah Peak aftershocks and the theoretical relation of Boore (1989) suggests that the M_0 - M_L relation for earthquakes in the Intermountain seismic belt does not differ significantly from that for California earthquakes.

EARTHQUAKE STUDIES: SOUTH CAROLINA

Semi-Annual Report
May 1, 1989 through September 30, 1989

Robert E. Weems
Branch of Eastern Regional Geology
U.S. Geological Survey
National Center, MS 928
Reston, Virginia 22092
(703) 648-6930

Investigations

Spent two weeks in the Charleston region finishing up stratigraphic correlation work for the middle to late Tertiary sequences. Began investigation of the influence of lunar and solar gravity on the timing of aftershock sequences following the 1886 Charleston earthquake.

Results

Compiled a summary report of progress toward resolving the Charleston earthquake problem for the 17th Water Reactor Safety Information Meeting in October 1989. This paper integrates stratigraphic, geophysical, and paleoliquefaction data to give our present best estimate of the location of the fault that caused the 1886 earthquake and the probabilities that it, or related faults, may cause future earthquakes.

A study of lunar and solar gravitational efforts on aftershocks of the 1886 Charleston earthquake revealed that the gravitational triggering mechanism changed markedly around the middle of 1897. Prior to the middle of 1897, the overwhelming majority of aftershocks occurred between 22:00 and 3:00 hours. After the middle of 1897, the time distribution of aftershocks became almost evenly distributed between day time and night time. Because the main shock of August 31, 1886, occurred just before 22:00 hours, and thus seems to have been similar in its timing to the main aftershock sequence up until mid-1897, it is likely that the aftershock sequence until the middle of 1897 was directly related to the fault that produced the main shock. Events after the middle of 1897 show none of the characteristics of the earlier events, and thus seem to have occurred on some other fault or fault set. Thus the aftershock sequence of the 1886 Charleston earthquake can be considered to have ended in the middle of 1897.

Reports

Weems, R.E., and Perry, W.H., Jr., 1989, Strong correlation of major earthquakes with solid-earth tides in part of the eastern United States: Geology, v. 17, p. 661-664.

Weems, R.E., and Obermeier, S.F., in review, The 1886 Charleston earthquake -- An overview of geological studies: 17th Annual Water Reactor Safety Information Meeting.

Geologic studies for seismic zonation of the Puget Sound lowland

9540-04004

Brian F. Atwater
U.S. Geological Survey at Department of Geological Sciences
University of Washington AJ-20
Seattle, WA 98195
(206) 442-2927 FTS 399-2927

INVESTIGATIONS AND RESULTS

Precise radiocarbon dating in coastal southwestern Washington

Sudden tectonic movement of late Holocene age is now known to have involved the coast above the Cascadia subduction zone at many sites in northern California, Oregon, and Washington. Most of this known movement was subsidence--widespread in southern Washington and Oregon, localized farther south. Conventional ^{14}C ages show that the most recent subsidence in all areas took place in the range of 200-400 years ago, probably about 300 years ago. But earthquake scenarios consistent with this evidence span a tremendous range--from a series of many earthquakes of magnitude 7 or 8 distributed through an interval of 100-200 years, to a single earthquake of magnitude 9 (Grant and others, 1989). Chief culprits are the large (100-200 yr) two-standard-deviation uncertainty in conventional ^{14}C ages, and the inadvertant dating of materials whose true age differs by decades or centuries from the age of the subsidence.

Precise radiocarbon dating of subsidence-killed Sitka spruce should greatly reduce both these kinds of error. Precise radiocarbon ages have two-standard-deviation counting errors in the range of 20-30 years--that is, 3-10 times less than errors of conventional ages. Sitka spruce was the chief arboreal casualty of sudden late Holocene subsidence in northern California, Oregon, and Washington. The stumps of subsidence-killed spruce readily yield 60-g samples needed for precise dating. Gary Carver (oral communication, 1989) has already begun to obtain precise radiocarbon ages on such samples from northern California. Moreover, standard deviations can be further reduced by dating rings that formed during centuries of rapid increase in atmospheric ^{14}C.

In August 1989 Atwater began a test of the precise radiocarbon dating of Sitka spruce. To do so he sampled spruce stumps rooted in the uppermost buried lowland soil at estuarine sites in coastal southwestern Washington. Also rooted in this soil are snags of western redcedar that died soon after A.D. 1687 according to ring-width pattern matching by David K. Yamaguchi and his coworkers (abstract in press, for AGU meeting in December, 1989). The salt-water intrusion, prolonged inundation, and rapid burial brought about by sudden subsidence should have killed both the redcedar and, except perhaps in chiefly freshwater areas, the Sitka spruce. Hence the test: precise radiocarbon ages on Sitka spruce from the uppermost buried lowland should indicate that many spruce died soon after A.D. 1687.

If Sitka spruce passes this test, precise radiocarbon dating of additional spruce samples can be used with confidence to look for asynchrony larger than about 30 years in sudden coastal movement above the Cascadia subduction zone about 300 years ago. If such asynchrony exists, and if none of the areas of apparent synchrony exceeds 100 km in coastwise extent, the most recent Cascadia earthquake did not approach magnitude 9 and probably did not exceed magnitude 8. At the other extreme, if they reveal no asynchrony from Washington through Oregon into northern California, precise ages on Sitka spruce would greatly increase the odds that a Cascadia earthquake about 300 years ago attained magnitude 9.

Sand blows in Puyallup

John Shulene, a retired junior-high-school science teacher now working with Atwater and Stephen Obermeier as a USGS volunteer, began a survey of liquefaction effects of the magnitude-7.1 earthquake that struck the southern Puget Sound region in 1949. One of his informants provided black-and-white photographs of sand volcanoes that erupted in Puyallup, which is near Tacoma. These photographs, which he plans to publish in a state geologic newsletter, appear to be the first for sand blows from the 1949 earthquake.

REPORTS (both abstracts)

Atwater, B.F., 1989, Net late Holocene emergence in the subsidence belt of the giant 1960 earthquake, southern Chile: EOS (in press)

Grant, W.C., Atwater, B.F., Carver, G.A., Darienzo, M.E., Nelson, A.R., Peterson, C.D., and Vick, G.S., 1989, Radiocarbon dating of Holocene coastal subsidence above the Cascadia subduction zone--compilation for Washington, Oregon, and California: EOS (in press)

29 September 1989

Surface Faulting Studies

9910-02677

M.G. Bonilla
Branch of Engineering Seismology and Geology
U.S. Geological Survey
345 Middlefield Road, MS 977
Menlo Park, CA 94025
(415) 329-5615

Investigations

1. Variation in surface slip along historical ruptures

2. The appearance of faults in exploratory trenches

Results

1. Study of the small-scale variations in surface slip along historical ruptures was continued, and 21 events have been examined so far. The average surface slip compared to the maximum surface slip has a wide variation in these events. The average slip, based on the area under the displacement-distance plots, ranges from 12 percent to 49 percent of the maximum slip. The position of the point of maximum slip along the rupture also varies widely, ranging from 3 percent to 49 percent of the total length. These numbers may change as more data are analyzed.

2. Editorial and other changes were made in the text, and final copies of several of the tables were prepared for a USGS bulletin on factors affecting recognition of faults exposed in exploratory trenches. Revisions in text and figures were made for a journal report on the visibility of fault strands as related to the timing of faulting events.

Reports

Thatcher, Wayne, and Bonilla, M. G., 1989, Earthquake fault slip estimation from geologic, geodetic and seismologic observations: implications for earthquake mechanics and fault segmentation, in Proceedings of Workshop XLV, Fault Segmentation and Controls of Rupture Initiation and Termination, Palm Springs, California, March 6-9, 1989: U. S. Geological Survey Open-File Report 89-315, p. 386-399.

Bonilla, M. G., and Lienkaemper, J. J., [in press], Visibility of fault strands in exploratory trenches and timing of rupture events: Geology.

10/89

Northern San Andreas Fault System

9910-03831

Robert D. Brown
Branch of Engineering Seismology and Geology
U.S. Geological Survey
345 Middlefield Road, MS 977
Menlo Park, California 94025
(415) 329-5620

Investigations

1. Continuing research and compilation of data on Quaternary deformation in the San Andreas fault system, to update chapter for a planned volume summarizing current geologic and geophysical knowledge of the fault system.

2. Research and review of work by others on the tectonic setting and earthquake potential at Diablo Canyon Power Plant (DCPP), near San Luis, Obispo, California. Activities are in an advisory capacity to the Nuclear Regulatory Commission (NRC) and are chiefly to review and evaluate data and interpretations obtained by Pacific Gas and Electric Company (PG&E) through its long-term seismic program.

3. Serve as chairman of Policy Advisory Board, Bay Area Earthquake Preparedness Project (BAREPP). A joint project of the State of California and the Federal Emergency Management Agency, BAREPP seeks to further public awareness of earthquake hazards and to improve mitigative and response measures used by local government, businesses, and private citizens.

Results

1. Continued reviews of geologic and geophysical data related to DCPP and provided oral and written review comments to NRC. Coordinated USGS review and data acquisition efforts related to DCPP.

2. Provided informal oral and written data, analysis, and recommendations to BAREPP and other Policy Advisory Board members on geologic, seismologic, and management issues relating to earthquake hazard mitigation in California.

Reports

None

9/89

CHARACTERISTICS OF ACTIVE FAULTS

9950-03870

Robert C. Bucknam, Anthony J. Crone, Michael N. Machette
Branch of Geologic Risk Assessment
U.S. Geological Survey
Box 25046, MS 966, Denver Federal Center
Denver, Colorado 80225
(303) 236-1604

INVESTIGATIONS

1. Organized and conducted the final project meeting of IGCP Project 206 (A Worldwide Comparison of the Characteristics of Major Active Faults) which was held June 29-July 7, 1989 (R.C. Bucknam and K.M. Haller).

2. Continued research on segmentation and late Quaternary history of major range-front normal faults in northern Basin and Range province of east-central Idaho and southwestern Montana in collaboration with David P. Schwartz, USGS-Menlo Park, CA (A.J. Crone and K.M. Haller).

RESULTS

1. The project meeting and associated field trip was attended by 45 scientists from 8 countries. The field trip began in San Francisco, Calif., and visited sites of historic and late Holocene faulting along the San Andreas fault, the Garlock fault, and in Owens Valley. The meeting was held mid-way through the field trip at Mammoth Lakes, California. The field trip continued north from Mammoth Lakes along the west margin of the Great Basin, east and north through the Nevada seismic zone, and across the Basin and Range to the Wasatch fault zone at Salt Lake City, Utah. Bucknam, Haller, Crone, and Machette all participated in the meeting and field trip. Many of the papers presented at the meeting will be submitted for publication in a special issue of the *Journal of Structural Geology*. In addition, work synthesized under this project is to be submitted to Cambridge University Press for publication.

Presented two papers at IGCP meeting and prepared two manuscripts for submission to *Journal of Structural Geology*, which will publish special issue of the proceedings of the workshop. A.J. Crone and K.M. Haller discussed "Segmentation and the coseismic behavior of Basin-and-Range normal faults as illustrated by examples from east-central Idaho and southwestern Montana, U.S.A." M.N. Machette presented a poster session describing the Quaternary geology of the Wasatch fault zone, Utah.

2. The logging of two trenches at the southeastern end of the Mackay segment of the Lost River fault in east-central Idaho has been nearly completed. The trenches were excavated across a major scarp and an adjacent antithetic scarp that are formed on outwash gravels believed to be ~150,000 yr old ("Bull Lake" in age). A detailed topographic survey of the site indicates about 5-5.5 m of net tectonic displacement across the fault. Preliminary interpretation of the trench stratigraphy indicates three surface-faulting events. Two volcanic ashes were found in one of the trenches; these ashes have been identified as a Glacier Peak ash (~11,300 yr old) and the Mazama ash (~6,800 yr old). Both ashes are displaced by the most recent event. Fragments of charcoal from the base of youngest colluvial wedge will establish a minimum age for last surface-faulting event. The timing of older events may be constrained by thermoluminescence dating of selected samples. Our studies of the Mackay segment tentatively indicate a strong temporal clustering of paleoearthquakes during the late Quaternary.

REPORTS

Bucknam, R.C., and Haller, K.M., 1989, Examples of active faults in the western United States A field guide: U.S. Geological Survey Open-File Report 89-528, 140 p.

Machette, M.N., 1989, Slope-morphometric dating, *in* Forman, S.L., ed., Dating methods applicable to Quaternary geologic studies in the Western United States: Utah Geological and Mineral Survey Miscellaneous Publication, p. 30-42.

Machette, M.N., Nelson, A.R., Personius, S.F., Lund, W.R., and Schwartz, D.P., Lengths of segments, recurrence intervals, and Holocene history of the Wasatch fault zone, Utah: Submitted to Journal of Structural Geology, 20 ms. p., 2 tables, 4 figures.

Characterization of Quaternary Deformation Associated with Concealed Thrust Faulting

14-08-0001-G1680

Thomas F. Bullard and William R. Lettis
Geomatrix Consultants, Inc.
One Market Plaza
Spear Street Tower, Suite 717
San Francisco, California 94105
(415) 957-9557

OBJECTIVES

Recent moderate-to-large earthquakes in the southwestern and southern San Joaquin Valley (Coalinga, 1983, M_L 5.5; Arvin-Tehachapi, 1952, M_L 7.3) and the Los Angeles Basin (Whittier Narrows, 1987, M_L 5.9) have focused attention on the presence of previously unidentified active thrust faults that may underlie areas of late Quaternary fold deformation without surface expression. Analyses of focal mechanisms and distributions of aftershocks suggest that these earthquakes occurred on thrust faults at mid-to-lower crustal depths (6 to 12 km) (Eaton, 1985; T. Heaton, oral presentation, EERI-Whittier Narrows Earthquake, 1987). General spatial coincidence of the earthquake epicenters with anticlinal fold axes (Coalinga earthquake with Anticline Ridge; Avenal earthquake with Kettleman Hills; Arvin-Techachapi earthquake with Wheeler Ridge; and Whittier Narrows earthquake with Elysian Park Anticline) and geodetic data that document coseismic fold growth (Stein, 1985; Stein, personal communication, 1987; Lin and Stein, 1988) strongly suggest a genetic association between these active blind faults and shallow-crustal anticlinal fold growth.

Two primary concerns associated with blind faults are our ability (or inability) to: 1) identify the presence of these faults beneath surface folds and to evaluate whether or not they are active; and 2) characterize the behavior of these faults as seismic sources (e.g., maximum magnitude, recurrence, etc.). Conventional geomorphic, paleoseismic, and geodetic techniques and criteria, which are aimed at identifying and characterizing active surface faults (e.g., geologic mapping, trenching, geomorphic analyses), may not lead to the recognition of these blind earthquake sources. Geologists in private industry and with state and federal agencies are confronted with the task of evaluating seismic hazards in areas of potential blind seismogenic sources without the benefit of industry standards, regulatory criteria, or conventional methodologies for characterizing these sources.

The purpose of this study is to conduct a detailed Quaternary geological evaluation of the Elysian Park anticline. Geodetic observations indicate that coseismic uplift of the anticline occurred during and/or immediately following the 1987 Whittier Narrows earthquake. Quantification of the Quaternary physical and behavioral characteristics of this anticline, therefore, will provide data necessary to assess the kinematic and geometric relationship of the fold to the underlying fault and to assess the Quaternary rate of activity on this fault.

DATA ACQUISITION AND ANALYSIS

During the past six months, Quaternary investigations in the Whittier Narrows area focused on office-based morphometric analyses and field investigations in the Monterey Park and Montebello Hills region of the Elysian Park anticline. Data acquisition and analyses included obtaining and evaluating information from topographic maps, aerial photography, and field mapping.

1. Turn of the century and early 1900s topographic maps were acquired to provide information on the study region prior to widespread urbanization. These early maps enhance our ability to confidently recognize geomorphic features in the field. Topographic maps acquired include the 1900 Pasadena 15' quadrangle (1:62,500), and 6' quadrangles (1:20,000) for Whittier (1925), El Monte (1926), Los Angeles and Glendale (1928), and Alhambra and Bell (1936); the 6' quadrangles have contour intervals of 5, 10, and 25 feet and offer the potential to construct topographic profiles of fluvial terrace remnants that may record tectonic deformation as young as mid-Holocene.

2. Aerial photographs from the 1928 Fairchild Collection were acquired for the area. The early photographic coverage allowed identification and mapping of surficial deposits which existed prior to intense urban development. Based on interpretation of the photography and inspection of the early topographic maps, we developed and mapped a preliminary Quaternary stratigraphy in the area. Our ability to map Quaternary geology and to evaluate urban landscape modification from early topographic maps and aerial photographs is supported by field observations and has enabled us to identify, target, and select optimal sites for stratigraphic and soil profile descriptions.

3. Office-based morphometric analyses were performed to evaluate tectonic activity in the study area. To date, these analyses have included: construction of a generalized topographic map to illustrate regional slope; analysis of drainage net maps; construction of subenvelope, envelope, and residual maps to quantify areas of maximum relief; and drainage basin asymmetry analyses to detect tectonic tilting.

4. Field investigations were conducted to field check existing geologic maps and our interpretation of aerial photography; evaluate unmapped stratigraphic units adjacent to mapped areas; map pre-Quaternary bedrock; recognize regional unconformities between Quaternary and Tertiary units; make preliminary reconnaissance field descriptions of soils and Quaternary stratigraphy; select locations for future soil descriptions and drill-hole sites; and search for datable materials.

PRELIMINARY RESULTS

<u>Morphometric Analysis</u>

A regional slope map was constructed using elevations obtained at the center-points of a 1-cm-square grid overlain on a 1:100,000 scale topographic map. The slope map indicates that the regional piedmont slope is predominantly southeast toward the San Gabriel River. This slope orientation suggests that

Rio Hondo and San Gabriel River did not play a significant role in the development of prominent wind gaps at Monterey Pass Road (Coyote Pass), Atlantic Boulevard, and Garfield Avenue as suggested by Lin and Stein (1989). More likely candidates for the development of these wind gaps are the Arroyo Seco and Alhambra Wash drainages. Drainage network examination suggests that the present location of Rio Hondo may represent a former course of San Gabriel River from a point about 12 km upstream from the Whittier Narrows.

Construction of a subenvelope map, using second-order streams only, is more objective and quantitative than the method described by Stearns (1967) for depicting the landscape if it were eroded to the level of the second-order streams. Subtracting the subenvelope from the envelope (surface tangent to ridges and hillslopes) gives a topographic residual that we interpret to represent a quantification of relief due to stream incision as a result of tectonic uplift (Figure 1). The residuals can then be contoured to produce a map that illustrates spatial variations in uplift across a region. Based on the envelope, subenvelope, and residual maps constructed in the study region, we interpret that maximum uplift in the study area occurs in the area between Atlantic Boulevard and Laguna Channel, well to the west of the area of maximum coseismic uplift associated with the 1987 Whittier Narrows earthquake as reported by Lin and Stein (1989) and Hauksson and Stein (1989). Long-term magnitude of uplift generally decreases eastward. A prominent right step occurs in both the axis of inferred Quaternary uplift and position of the range front from the Monterey Park hills to the Montebello Hills. The right step is accompanied by a slight increase in uplift from west to east that is nearly coincident with the surface projection of the western margin of the concealed thrust fault proposed by Lin and Stein (1989).

Tectonic tilting will tend to force stream systems toward one side of their drainage basin, resulting in a disproportionate distribution of basin area to the right or left of the trunk stream. This type of areal distribution is referred to as drainage basin asymmetry. Drainage basin asymmetry can be measured using a simple area method where the area of the downstream right side of the drainage basin is divided by the total basin area and multiplied by 100 to give an asymmetry factor (A.F.) (Gardner et al, 1987). This defines the system as right (A.F. < 50) or left (A.F. > 50) asymmetric, or symmetric (A.F. = 50). Preliminary results for several south-flowing systems across the Elysian Park anticline (down-dip and transverse to regional strike) indicate that a slight westward tilting has occurred in addition to overall vertical uplift. Completion of the asymmetry analysis may elucidate any structural block segmentation that may be occurring along the axis of uplift or tilting of individual tectonic blocks.

Field Mapping

A total of five fluvial terraces associated with the San Gabriel River has been identified on aerial photographs and confirmed in the field. These terraces can be correlated to terrace sequences in the wind gaps of Potrero Grande, Garfield Avenue, Atlantic Boulevard, Laguna Channel, Eastern Boulevard, and along the piedmont south and west of the Montebello and Monterey Park hills. The correlations are tentative based primarily on topographic position relative to a regionally extensive geomorphic surface. Final

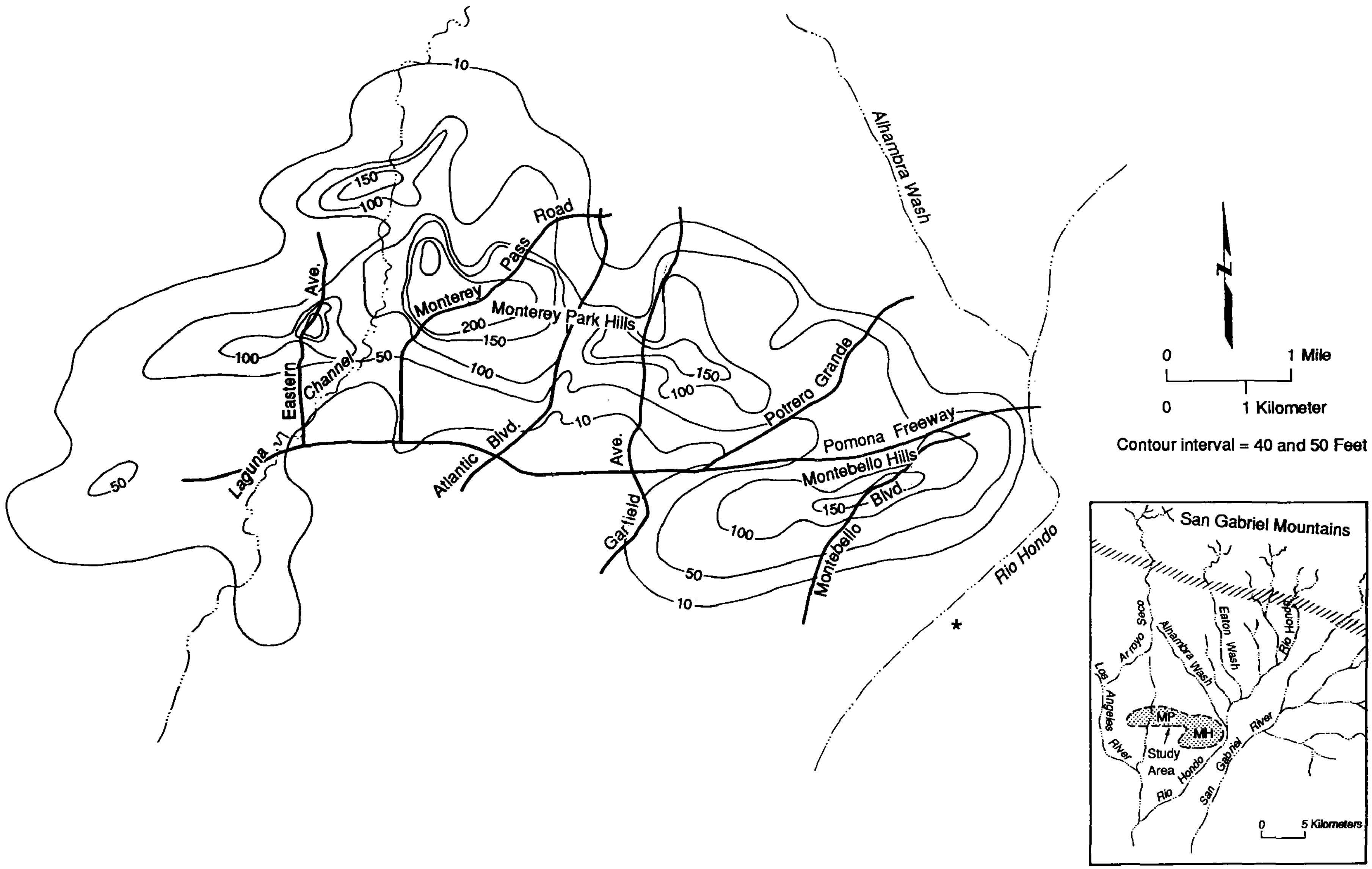

Figure 1. Generalized contour map of subenvelope and envelope residuals showing areas of maximum uplift. Inset shows regional location. MH = Montebello Hills, MP = Monterey Park; ∗ = location of maximum coseismic uplift for 1987 Whittier Narrows earthquake.

terrace correlations both within and between drainages will be made pending assessment of soil-profile development.

Field mapping to date has also identified: 1) a prominent 10-20° angular discordance between coarse, cross-bedded gravels and underlying fine-grained silts and sands of the Pliocene Fernando Formation exposed along the south flanks of the Monterey Park and Montebello hills. We interpret the gravel as remnants of a regional pediment surface; and 2) a thick gravel body that trends northeast and cuts across regional strike of bedding through the Potrero Grande area. We interpret the gravel to be a valley fill deposit associated with a former course of the ancestral San Gabriel River.

The gravel unit that unconformably overlies the fine-grained Fernando Formation on the south flanks of the hills has been mapped by Lamar (1970) and Dibblee (1989) as a conglomerate member of the Fernando, yet the angular discordance in our study area is much greater than the angular discordance reported by Yerkes (1972) and Dibblee (1989) for the upper and lower Fernando in the region east of Montebello. Lithology and angular discordance suggest that the gravel unit may be better associated with the Pleistocene San Pedro, Coyote Hills, or La Habra formations of Yerkes (1972). If we assume that topographic relief on the Fernando Formation represents a minimum amount of vertical uplift above sea level (probably much more since the Fernando is a deep to shallow marine unit) and assume that uplift was coincident with the onset of Pliocene north-south shortening across the Los Angeles Basin as indicated by angular unconformities and proposed by Davis and Namson (1989), a long-term uplift rate of < 0.1 mm/yr (0.2-0.5 μrad/yr) is obtained. To produce the 10-20° of angular discordance between the pediment gravels and the fine-grained deposits of the Fernando Formation, therefore, requires approximately 1 my, which indicates that the gravel is probably early- to mid-Pleistocene in age. Various possible explanations for the pronounced unconformity and confusion over the age of the conglomerate unit include: a dramatic, local change in uplift rate; local structural complexities; uplift that began earlier than suggested by Davis and Namson (1989); or the gravel unit is younger than thought. We interpret the gravel, therefore, to be the remnant of a former pediment surface that covered much of the region during the early- to mid-Pleistocene.

The second gravel deposit that we recognized in the field is about 50 m thick and forms a 1- to 2-km-wide, northeast-trending swath between the Montebello Hills and Monterey Park hills. The gravels are inset into the Fernando Formation and dip gently (< 5°) south to southwest, in contrast with dips on the Fernando Formation that range from 30-75°. Based on its lateral distribution and abrupt erosional margins, we interpret the gravel to represent the course of an ancestral San Gabriel River.

Remnants of relatively undisturbed geomorphic surfaces and fluvial terraces are preserved in the region and are promising for the development of a local chronosequence. The chronosequence can be used to establish correlation of terrace deposits in the area as well as to correlate with existing dated chronosequences in the Los Angeles Basin (McFadden, 1982). We have identified potential sites for soil-profile analysis on all major terrace sequences where preserved surfaces exist, as well as additional sites for potential drilling activities.

Establishing numerical age control for Quaternary deposits in the Los Angeles Basin is a problem due to the general absence of promising datable materials. In the study area, one megafossil site has been identified (G. Jefferson, Los Angeles County Museum, pers. comm., 1989) and may provide material for Uranium-series dating. The fossil locality is within what we infer to be mid-to late-Pleistocene deposits and may provide a useful date from which to calibrate the local and regional chronosequences and assess rates of late Quaternary deformation.

Preliminary Interpretation

Morphometric and stratigraphic analyses define at least two en echelon Quaternary anticlines in the region, one centered beneath the Monterey Park hills and one below the Montebello Hills. The anticlines appear to be asymmetric with steep, linear south flanks and more gentle, deeply dissected northern flanks. The Montebello Hills anticline is about 7 km long and 1.5 km wide; the Monterey Park anticline is about 11 km long and 3 km wide. Late Cenozoic uplift occurs within the Montebello Hills several km west of the point of maximum coseismic uplift of the 1987 Whittier Narrows earthquake and west of the surface projection of the fault plane associated with the 1987 event as reported by Lin and Stein (1989). The residual maps suggest that maximum uplift has been at least 80 m during an as yet undefined period of Quaternary time.

Changes in the amount of uplift along the hills and the apparent right en echelon step in the anticlinal axis and front of the Monterey Park-Montebello Hills may reflect possible segmentation of the underlying thrust fault defined by Davis and Namson (1989), Lin and Stein (1989), and Hauksson and Jones (1989). North-trending lineaments are evident on the residual maps and aerial photography and may be the surface expression of one or more tear faults that segment the underlying thrust fault.

REFERENCES

Dibblee, T.W., Jr., 1989, Geologic map of the Los Angeles quadrangle, Los Angeles County, California: Dibblee Geological Foundationm, Santa Barbara, California, scale 1:24,000.

Davis, T.L., and Namson, J., 1989, A cross section of the Los Angeles area: seismically active fold and thrust belt, the 1987 Whittier Narrows earthquake, and earthquake hazard: Journal of Geophysical Research, v. 94, no. B7, p. 9644-9664.

Gardner, T.W., Hare, P.W., Pazzaglia, F.J., and Sasowsky, I.D., 1987, Evolution of drainage systems along a convergent plate margin, Pacific coast, Costa Rica: in Graf, W.L., ed., Geomorphic systems of North America, Geological Society of America, Centennial Special Volume 2, p. 357-372.

Hauksson, E., and Jones, L.M., 1989, The 1987 Whittier earthquake sequence in Los Angeles, southern California: seismological and tectonic analysis: Journal of Geophysical Research, v. 94, no. B7, p. 9569-9589.

Hauksson, E., and Stein, R.S., 1989, The 1987 Whittier Narrows, California, earthquake: a metropolitan shock: Journal of Geophysical Research, v. 94, no. B7, p. 9545-9547.

Lamar, D.L., 1970, Geology of the Elysian Park-Repetto Hills area, Los Angeles County, California: California Division of Mines and Geology, Special Report 101, 45 p.

Lin, J., and Stein, R.S., 1989, Coseismic folding, earthquake recurrence, and the 1987 source mechanism at Whittier Narrows, Los Angeles Basin, California: Journal of Geophysical Research, v. 94, no. B7, p. 9614-9632.

McFadden, L.D., 1982, The impacts of temporal and spatial climatic changes on alluvial soils genesis in southern California: Ph.D. thesis, Tucson, Arizona, University of Arizona, 430 p.

Stearns, R.G., 1967, Warping on the Western Highland Rim Peneplain in Tennessee by groundwater sapping: Geological Society of America Bulletin, v. 78, p. 1111-1124.

Yerkes, R.F., 1972, Geology and oil resources of the Western Puente Hills area, southern California: U.S. Geological Survey Professional Paper 420-C, 62 p.

Sedimentological Analysis of Postulated Tsunami-Generated Deposits from Great-Subduction Earthquakes Along Washington's Outer Coast

14-08001-1532

Joanne Bourgeois and Mary A. Reinhart
Dept of Geological Sciences AJ-20
University of Washington
Seattle, Washington, 98195
(206) 545-2443

INVESTIGATION: The goal of this project is to determine the genesis of 300-year old sand sheets in coastal Washington, in particular, whether these sheets were deposited by a tsunami generated by a great-subduction earthquake at the Cascadia subduction zone. The tsunami hypothesis is being tested by: 1) developing a sediment-transport model for the sand sheet and comparing it to possible depositional mechanisms, and 2) calibrating the model through the study of Chilean sand sheets known to have been laid down by the tsunami from the great 1960 earthquake (Mw 9.5) in south-central Chile. A summary of Chilean field work was presented in our previous progress report.

From field mapping and laboratory analysis already completed on the Washington coast, we have reconstructed the depositional event of 300 years ago: the event was of regional scale, depositing sand similarly over a distance of at least 200 km; the force of the event was landward-directed, comprised several discrete pulses, and propagated inland at least 3 km via coastal rivers (Copalis R) and embayed estuaries (Willapa Bay and Grays Harbor) and their tidal channels; sediment was deposited onto former marsh/point bar surfaces from suspension, rather than from bedload; within Willapa Bay and Gray's Harbor the greatest number of pulses are recorded in the river/tidal channels adjacent to and just south of each entrance. This reconstruction eliminates from consideration all seaward-directed mechanisms and helps establish the required depositional conditions from which we can test the remaining landward-directed mechanisms.

SEDIMENT-TRANSPORT MODELING: We have chosen to construct a sediment-transport model for the sand sheet as preserved along the Niawiakum River, Willapa Bay (as described in progress report of May, 1988). The conditions required to transport sand and silt over three buried marsh/point bar surfaces of the Niawiakum River are: 1) overbank flow depths and velocities must be sufficient to transport suspended sand and silt across marsh surfaces, and 2) the boundary shear stress in the channel must be high enough to suspend a volume of sediment in the overbank part of the flow sufficient to deposit laminae 2-10 mm thick.

Results of calculations include:

1) Overbank discharges of 4200-7600 cm^3/s are required to transport sand and silt across the bar nearest the mouth, and 3000-5500 cm^3/s for the bars upstream.

2) Shear stresses in the channel required to generate such overbank discharges depend upon flow depth and bottom roughness. For example, for overbank flow depths of 1, 2, 2.5, and 3 meters for the bar nearest the mouth (Bar 1), calculated stresses vary from 1.90 to 9.80 $dynes/cm^2$, 0.47 to 2.35 $dynes/cm^2$, 0.30 to 1.50 $dynes/cm^2$, and 0.19 to 1.00 $dyne/cm^2$ respectively (see Table 1).

3) We estimate that overbank flow depths were no greater than about 2 m. For greater flow depths, the calculated Rouse number indicates insufficient suspension of sediment required for transport across the marsh surface (see Table 2).

4) The volume of sediment in each of the basal sandy laminae requires that at least 3000-5000 mg/l of sediment was suspended in the overbank part of the flow. We estimate that entrainment (erosion) of 5-10 cm of the channel floor adjacent to each bar was required for each lamina. Only the larger shear stresses are capable of mobilizing and suspending such volumes of sediment.

We are evaluating the ability of landward-directed mechanisms (tsunami, storm, and seiche) to meet our depositional model. Preliminary results include:

1) Storm surge amplified by flood tides appears to be insufficient to exert the necessary shear stresses or overbank flow velocities.

2) Initiation of seiching in Willapa Bay is very difficult. The long fundamental period of oscillation and the shallow and irregular bathymetry of the bay serve to damp excitation.

3) A crude routing model for a tsunami wave train predicts a water particle velocity of 60-100 cm/s generated by a wave propagating up a bank-full channel (wave speed approximately 6 m/s), predicts high shear stresses sufficient to entrain and suspend the required volume of sediment, and appears to predict the geographic distribution of the deposit within Willapa Bay.

TABLE I

SHEAR VELOCITIES AND SHEAR STRESSES CALCULATED FOR CHANNEL ADJACENT TO BAR I, NIAWIAKUM RIVER, WILLAPA BAY

FLOW DEPTH OVER MARSH cm	SURFACE VELOCITY cm/s	Z_0	U_* cm/s	T_b dynes/cm^2
100	42	10^{-3}	1.37	1.90
		10^{-2}	1.69	2.91
	76	10^{-3}	2.51	6.43
		10^{-2}	3.10	9.8
200	20.8	10^{-3}	0.68	0.47
		10^{-2}	0.83	0.70
	38	10^{-3}	1.24	1.57
		10^{-2}	1.52	2.35
250	16.8	10^{-3}	0.54	0.30
		10^{-2}	0.66	0.44
	30.4	10^{-3}	0.98	0.98
		10^{-2}	1.21	1.50
300	13.9	10^{-3}	0.44	0.19
		10^{-2}	0.55	0.32
	25.3	10^{-3}	0.81	0.67
		10^{-2}	1.00	1.00

Overbank velocity computed by dividing flow discharge (4200-7600 cm^3/s) by overbank flow depths; Z_o defines the channel bed roughness parameter (10^{-3} defines a smooth bed, 10^{-2} defines a surface with small bed-forms and/or small woody debris); U_* = shear velocity in the channel; T_b = shear stress ($T_b = pU_*^2$, where p is water density). Maximum discharge provides the best fit to the distribution of sand and silt sizes over the 300-yr-old surface and $Z_0 = 10^{-2}$ better suits the modern channel bottom of the Niawiakum River.

TABLE II
CALCULATED ROUSE NUMBERS (P_S) FOR 0.125 mm (3 phi) (BASAL SAND LAMINA) IN SAMPLES FOR FOUR OVERBANK FLOW DEPTHS, BAR 1

FLOW DEPTH OVER MARSH cm	SHEAR VELOCITY (in channel) cm/s	ROUSE # (P_S)
100	1.37	1.13
	1.69	0.92
	2.51	0.62
	3.10	0.50
200	0.68	2.28
	0.83	1.87
	1.24	1.25
	1.52	0.61
250	0.54	2.87
	0.66	2.34
	0.98	1.58
	1.21	1.28
300	0.44	3.52
	0.55	2.82
	0.81	1.91
	1.00	1.56

$P_S = W_S/U_*k$ (where W_S = settling velocity and k = 0.4 (von Karman's constant)), and is an indicator of transport mode of a given grain size at specified shear velocities (P_S < 0.8-1.5 indicates entrainment and transport by suspended load and P_S > 3.0 indicates transport as bedload). Grain size analysis of basal sand lamina consistently show that sand sizes equal to and larger than 0.18 mm in diameter comprise less than 1% of the size distribution, and that 0.125 mm sand (8% volume near channel edge and 5.5% volume 67 m from channel edge in the estimated direction of paleo-flow) represents the coarstest grain size delivered to the marsh. In order for 0.125 mm sand to be elevated from the channel floor to the marsh level, the Rouse number must have been less that 1.5; if P_S is greater than 1.5 the sand is unlikely to be suspended into the overbank part of the flow.

Late Quaternary Slip Rates on Active Faults of California

9910-03554

Malcolm M. Clark
Branch of Engineering Seismology and Geology
345 Middlefield Road, MS 977
Menlo Park, California 94025
(415) 329-5624, FTS 459-5624

Investigations

1. Recently active traces of Calaveras fault zone at Tres Pinos Creek and San Felipe Creek, California (K.J. Kendrick [Harms], J.W. Harden, M.M. Clark).

2. Recently active traces of Owens Valley fault zone, California (Sarah Beanland [NZGS], Clark).

3. Degradation of fluvial terrace risers along Lone Pine Creek, San Bernardino County. (Kendrick, in conjunction with J.B.J. Harrison, L.D. McFadden (UNM), and R.J. Weldon (University of Oregon)).

4. Revision of slip-rate table and map of late-Quaternary faults of California (Clark, Kendrick, J.J. Lienkaemper, K.R. Lajoie, C. Prentice, M.J. Rymer, D.P. Schwartz, R.V. Sharp, J.D. Sims, J.C. Tinsley, R.J. Weldon).

Results

4. We are in the process of revising, updating, and publishing (as a USGS Bulletin) the slip-rate table and map of late-Quaternary faults of California (USGS OFR 84-106). Our aim is to review all entries in OFR 84-106 and add all new data generated since its release. We welcome any relevant unpublished data from workers in this field.

9/89

DETECTION OF BLIND THRUSTS IN THE WESTERN TRANSVERSE RANGES AND SOUTHERN COAST RANGES

14-08-0001-G1687

DAVIS AND NAMSON
CONSULTING GEOLOGISTS
1545 NORTH VERDUGO ROAD, SUITE 9
GLENDALE, CA 91208
(818) 507-6650

I. Objectives

A. Detection of seismically active blind thrusts in the western Transverse Ranges and southern Coast Ranges.

B. Determination of the geometry, kinematics, and slip rate of blind thrust faults.

C. Calculation of regional convergence rates across the western Transverse Ranges and southern Coast Ranges.

II. Approach:

Compilation of surface and shallow subsurface geology using detailed maps and well data, regional seismicity, earthquake focal mechanisms and seismic reflection data for the construction of retrodeformable cross sections.

III. Results

A. A series of 8 cross sections across the western Transverse Ranges and southern Coast Ranges are either completed or under construction (Figure 1). The cross sections identify the major anticlinoria of the the area and thrust faults (mostly concealed) are interpreted to cause the regional folds. The interpretations provide an estimate of the slip on thrust faults as well as the regional shortening of area west of the San Andreas fault. The slip and shortening estimates from these cross sections are being integrated on maps to further understand the distribution of fault slip, slip rates, shortening and shortening rates in the region. The status of these cross sections is as follows:

1. Cross section 1 through the southern Coast Ranges near San Luis Obispo has been completed and accepted for publication (Namson and Davis, in press). The cross section has 26.8 km of shortening from the edge of the continental margin to the San Andreas fault. Based on numerous geologic relationships, region-wide shortening began at ≈4.0 Ma which yields a regional convergence rate of 6.7 mm/yr.

2. Cross section 2 extends across the western edge of the onshore Santa Maria basin and has been accepted for publication (Namson and Davis, in press). The Pliocene and

Quaternary convergence across the onshore Santa Maria basin is 9.2 km and the convergence rate is 2.3 mm/yr.

3. Cross section 3 extends from the western Santa Barbara Channel near Point Conception to the San Andreas fault. The cross section is completed but the section has not been restored.

4. Cross section 4 extends from the central Santa Barbara Channel to the San Andreas fault. All the surface and subsurface data are compiled for this section, and the section is in the interpretation phase.

5. Cross section 5 extends from the eastern edge of the Santa Barbara Channel to the Big Pine fault and has been published (Namson, 1987). The interpretation suggests 35 km of convergence and using 3.0 Ma for the onset of deformation yields a convergence rate of 11.7 mm/yr.

6. Cross section 6 extends from the coast at the southwest edge of the Santa Monica Mountains to the San Andreas fault. The data for this cross section have been compiled and the section is in the construction phase.

7. Cross section 7 extends from the coast near Santa Monica to the San Gabriel fault. The cross section has been completed but the restoration is incomplete. The cross section has approximatly 15 km of convergence and a preliminary version was published in Davis and Namson (1988).

8. Cross section 8 extends offshore near Palos Verdes to the San Andreas fault and has been published (Davis et al., 1989). The cross section has 21.4-29.7 km of convergence and a convergence rate of 3.8-13.5 mm/yr.

B. Reports

1. Namson, J. and Davis, T.L., in press, Late Cenozoic Fold and Thrust Belt of the Southern Coast Ranges and Santa Maria Basin, California: American Association of Petroleum Geologists Bulletin.

2. Davis, T.L., Namson, J., and R.F. Yerkes, 1989, A Cross Section of the Los Angeles Area: Seismically Active Fold and Thrust Belt, the 1987 Whittier Narrows Earthquake, and Earthquake Hazard: Journal of Geophysical Research, v. 94, p. 9644-9664.

3. Namson, J., and T. Davis, 1989, Reply on Structural transect of the western Trranverse Ranges, Califronia: Implications for lithospheric kinematics and seismic risk evaluation: Geology, v. 17, p.670-671.

4. Namson, J., and T. Davis, 1989, Reply on Structural transect of the western Trranverse Ranges, Califronia: Implications for lithospheric kinematics and seismic risk evaluation: Geology, v. 17, p.672-673.

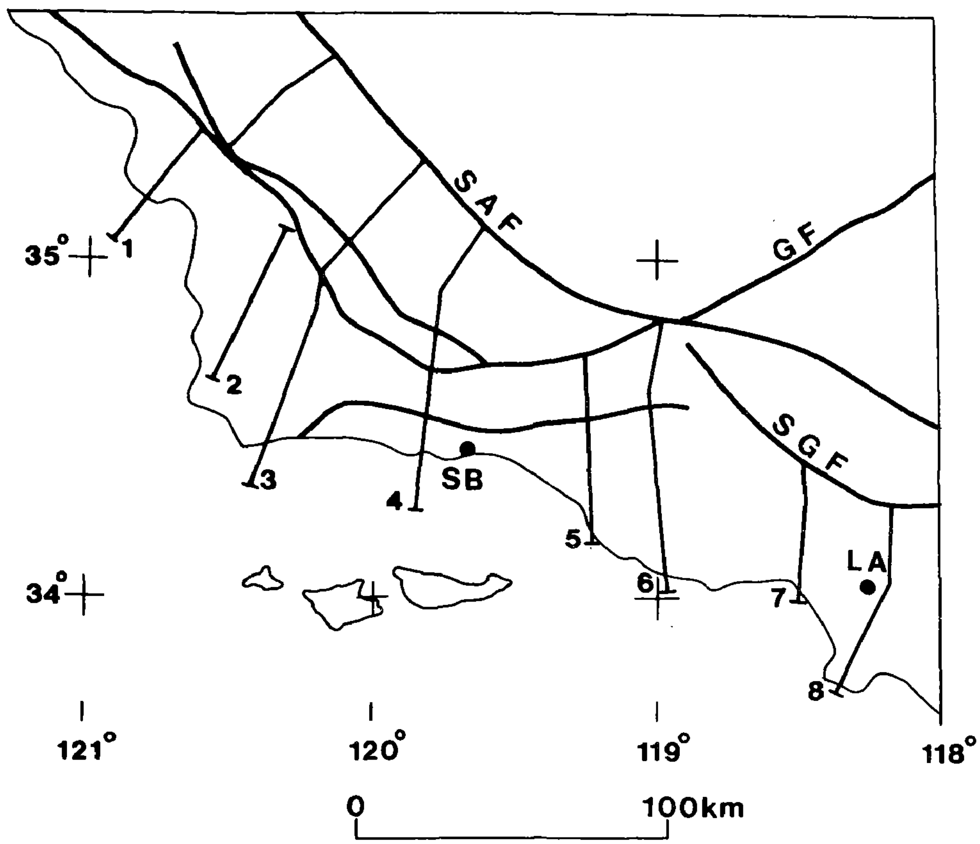

Figure 1. Map of southern and central California showing the location of regional balanced cross sections completed or in the construction phase. GF- Garlock fault, LA- Los Angeles, SAF- San Andreas fault, SB- Santa Barbara, SGF- San Gabriel fault.

Evaluation of Late Quaternary Rate of Slip, Whittier Fault Zone, Southern California

14-08-0001-G1696

Eldon M. Gath
Leighton and Associates, Inc.
1470 South Valley Vista Drive, Suite 150
Diamond Bar, California 91765
(714) 860-7772

Objective: Previous investigations have provided evidence that the Whittier fault has had Holocene activity, and recorded microseismicity shows that this activity is continuing. Preliminary results appeared to indicate a Holocene slip rate loosely constrained between 1.7-5.7 mm/yr. The purpose of this study is to determine a better constrained slip rate, and provide data on the slip history of the Whittier fault for seismic hazard evaluation to the Los Angeles Basin. One of the most important pieces of data needed is a determination of the timing of the last earthquake, and the amount of slip that occurred during that event.

Data Acquisition and Initial Analysis: The project authorization was obtained in late February 1989. Due to the timing of the project authorization, the trenching portion of the study was postponed to late in the year in order to complete the air photo analysis needed to select the best and yet accessible site. The following discussion presents the study's current status and any preliminary conclusions.

1. Procurement of suitable topographic coverage for the fault zone. For purposes of the project, 1:24,000 scale quadrangle sheets were utilized for the aerial photographic mapping of tectonic geomorphic features and offsets that were resolvable at that scale.

2. Procurement and review of stereo aerial photographs to map the fault location from offset geomorphic features.

3. Procurement of 200 scale topographic maps where the initial photographic mapping indicated a high probability of surviving geomorphic offsets that would be better resolved at the smaller scale (much of the Whittier fault has been either extensively urbanized, or modified due to oil exploration and production).

4. Oblique, low altitude, aerial photographs in color infrared, were flown in late June. Although a complete interpretation is still in progress, these images are providing a refinement of the fault trace location within those areas where access is restricted, and only high altitude aerial photographs are available. They have also proven useful in the preliminary selection of trenching sites for the detailed paleoseismic investigation scheduled for this November.

Completed Research: The following discussion will present preliminary results of current investigations.

1. Air photo strip mapping of tectonic geomorphic features has been completed.

2. Characterization of offset geomorphic features have been compiled into a histogram to group and quantify individual events, but the data have not been screened to remove the impacts of multiple strands or physical deflections. The smallest deflections located are about 3 meters, and are preliminarily concluded to have been caused by the last event. Larger deflections of 6, 12, 20, 40, 400, and 1500 meters are also common. Except for the 3 meter deflection, all offsets are from topographic map and aerial photograph measurements, taken at various scales.

3. Detailed mapping and logging of two separate exposures of faulted alluvial sediments within a canyon east of Fullerton Road in the La Habra Heights area of the Puente Hills. At this location, the fault splits into two parallel traces, separated by approximately 500 meters. The alluvial sediments were ponded behind a shutter ridge along the southernmost trace, and behind a canyon-damming landslide on the northernmost fault trace. The canyon has been captured to the east (apparent left lateral) of the shutter ridge, and downcutting of the channel has exposed and drained the ponded sediments. The landslide dam has also been breached, and the ponded sediments preserved on the protected lateral flanks of the canyon, in immediate proximity to the residual landslide materials.

a. Detailed stratigraphic mapping of the southern alluvial exposure determined that there was a time stratigraphic progression to the amount of tilting of the alluvial beds, with the older units progressively more deformed. Liquefaction features were identified, several peat layers were sampled for C-14 analysis, and a detailed log of the exposure was produced. A charcoal sample from one of the older peats has been submitted for accelerator dating, with the results expected in early November. At this time, preliminary age estimates for the alluvial sediments range from 30,000-100,000 years B.P. due to the degree soil development, and the amount of geomorphic alteration of the site.

b. Detailed stratigraphic mapping of the ponded alluvial sediments behind the old landslide dam were not as successful as the southern exposures. Well bedded, highly deformed alluvium was mapped in fault contact with the Puente Formation bedrock. Charcoal samples from several interbedded peats were obtained. The stratigraphically lowest peat sample was submitted for C-14 analysis, and resulted in a 12,200 age. Continued logging of the exposure began to indicate a very pervasive influence of landsliding within the alluvial sediments. It was subsequently determined that the exposure was too limited to isolate the effects of fault slip from landslides, and as a consequence, the site was abandoned.

4. Access to two of the previously identified trenching sites (within Arroyo San Miguel and off Fullerton Road in the Puente Hills) was denied by the property owner due to pipeline obstructions at the specific location needed for the study. Three additional sites have been identified (within Carbon or Tonner Canyons, or above Telegraph Canyon) and landowner negotiations are again underway.

5. The development of the soil chronosequence is proceeding in the Yorba Linda area and working northward. Several well developed soils upon elevated fluvial terraces are being logged and clay fractions quantified.

6. Trench excavations should be underway by December 1, 1989.

Tectonics of Central and Northern California

9910-01290

William P. Irwin
Branch of Engineering Seismology and Geology
U. S. Geological Survey
345 Middlefield Road
Menlo Park, CA 94025
(415) 329-5639

Investigations

Preparation and revision of manuscripts pertaining to the geology and tectonics of northern California and southwestern Oregon.

Results

A geologic compilation of the Klamath Mountains province, planned for publication as an I-series map at a scale of 1:500,000, was extensively revised following reviews by the Geologic Names Unit and the Geologic Map Editor. Writing of a report describing the geology and tectonic development of the Klamath Mountains and adjacent regions continued during the report period and is planned for publication in the Bulletin series. The Klamath Mountains province is of particular interest because of its large number and variety of accretionary terranes and its long history of tectonic development of the Pacific coastal region of North America. A review of paleomagnetic results from the Klamath Mountains, Blue Mountains, and Sierra Nevada, co-authored with E.A. Mankinen, is being revised following technical review. Page proof for a contribution to the Richard H. Jahns Memorial Volume was reviewed and returned to the publisher. Proposed field work for a collaborative study of the distribution of Lower Jurassic chert, which occurs sparsely in the Franciscan assemblage on both sides of the San Andreas fault, was postponed because of scheduling problems.

Reports

Irwin, W.P., 1989, Terranes of the Klamath Mountains, in Tectonic evolution of northern California: *28th International Geological Congress Field Trip Guidebook T108*, p. 19-32.

Mankinen, E.A., Irwin, W.P., and Gromme, C.S., 1989, Paleomag-netic study of the Eastern Klamath terrane, California, and implications for the tectonic history of the Klamath Mountains province: *Journal of Geophysical Research*, v. 94, no. B8, p. 10400-10472.

Schweickert, R.A., and Irwin, W.P., 1989, Extensional faulting in southern Klamath Mountains, California: *Tectonics*, v. 8, no 1, p. 19-32.

Very Precise Dating of Prehistoric Earthquakes in California using Tree-ring Analysis

14-08-001G1329
EAR88-05058

Gordon C. Jacoby
Tree-Ring Laboratory
Lamont-Doherty Geological Observatory
Palisades, New York 10964
(914) 359-2900

San Andreas Fault, Southern California

Analysis of previously collected samples from this area yielded preliminary tree-ring evidence that the length over which trees were disturbed by surface rupture by the 1812 earthquake may be extended. Our previous research determined that trees were disturbed over a length of approximately 12 km. (Jacoby et al. 1988). Samples from just northwest of Jackson Lake indicate response to the event and thus extend the length of probable surface rupture another 1.5 kilometers toward the Pallett Creek site (about 16 km to the northwest) where displacement for the event is estimated at 6 meters (Sieh,1984). More importantly, samples of California white oak [*Quercus lobata* Nee] from about 80 km. northwest of the Pallett Creek site also indicate probable disturbance by the 1812 event. At both of the tree-sampling sites the evidence of disturbance is much more subtle than for the trees in the Wrightwood area. In the vicinity of the oaks even a tree sited right on the fault trace shows only minor effects from the documented 1857 event. The oaks are a much stronger wood than the conifers sampled in the Wrightwood area and are also of a much more compact growth form. A major problem is the occurence of drier years to extreme drought in both the 1812-13 and the 1856-57 years. At the Jackson Lake and the oak sites the fault line trees appear to show trauma beyond the drought effect but this response needs to be carefully modeled before definitive results can be confirmed.

San Andreas Fault, Northern California

More extensive collections of tree samples have been made in this area. Previously we collected cores from dead redwood stumps logged around 1900. We have now collected slabs from the same area along about 5 km of the fault trace. We have obtained cores from a few living old-aged trees and slabs from recently cut (1986 and 1988) old growth. These latter samples are away from the fault but are necessary to establish a master chronology for dating the cores and the slabs from the older stumps along the fault. Analysis of previous samples indicated that trees inland of the first range of hills are better for crossdating than the coastal trees. Slabs were taken from the stumps of logged old growth at the inland location and are now in the laboratory for analysis. Maximum ages for the samples approach 1,000 years.

Cascadia Subduction Zone, Northern California

Grand fir [*Abies grandis* (Dougl. ex D. Donn) Lindl.] and Douglas fir [*Pseudotsuga menziesii* (Mirb.) Franco] were sampled in Redwood National Park and a chronology was developed that crossdated with the same inland sites that crossdated with the cores from the Catfish Lake landslide site near Arcata. Unfortunately the length of the grand fir chronology is too short to directly crossdate with the Catfish Lake trees which dated to 1741 B. P. In addition to the landslide site samples we also have core samples from stumps growing in and near the trace of the Little Salmon Creek thrust fault. Many of these cores have over 500 rings. In October of 1989 we obtained some 300 to 500 year old Douglas fir slabs from a timber company to aid in developing a long-term chronology for better crossdating of the material from the stumps and dead trees. The paleoseismic interpretation of any tree-ring disturbance will result from composite analysis of fault-line trees, landslide trees and undisturbed trees nearby. A the present time we have just transported about two and one half tons of tree slab samples to the Tree-Ring Lab. from all California sites and analyses will progress through the winter months.

The area being studied near Eureka, California is very complex tectonically. It is near a triple junction and there is subsidence, strike-slip and thrust faulting in the region. There are also landslides which may or may not be related to seismic events. Recent paleoseismic investigations are producing dates for events in the region (e. g. Jacoby et al. 1989, Grant et al. 1989, Williams and Jacoby, 1989 and Yamaguchi et al. 1989). As those studies and our studies progress there should be convergence of some dates for large events and distinct dates for smaller events. The eventual seismic prehistory of the region will result from a composite of all of these studies.

References:

Grant, W. C., Atwater, B. F., Carver, G. A., Darienzo, M. E., Nelson, A. R., Peterson, C. D., and Vick, G. S. 1989. Radiocarbon dating of late Holocene coastal subsidence above the Cascadia subduction zone--Compilation for Washington, Oregon and Northern California. EOS, abst. (in press).

Jacoby, G. C., Sheppard, P. R. and Sieh, K. S. 1988. Irregular recurrence of large earthquakes along the San Andreas fault: evidence from trees. Science 241, pp 196-99.

Jacoby, G. C. Sheppard, P. R. and Carver, G. A. 1989. Dating of earthquake-induced landslides using tree-ring analysis. GSA meeting of Cordilleran and Rocky Mountain Sections. abst.

Sieh, K. S. 1984. Lateral offsets and revised dates of large prehistoric earthquakes at Pallett Creek, Southern California. J. Geophys. Res. 89, 7641-70.

Williams, P. L. and Jacoby, G. C. 1989. Testing of postulated seismic triggering of giant landslides in seattle, Washington. EOS, (in press).

Yamaguchi, D. K., Woodhouse, C. A. and Reid, M. S. 1989. Tree-ring evidence for synchronous rapid submergence of the Southwestern Washington coast 300 years B. P. EOS, (in press).

Coastal Tectonics

9910-01623

Kenneth Lajoie
Branch of Engineering Seismology and Geology
345 Middlefield Road, M/S 977
Menlo Park, California 94025
(415) 329-5641/5747

Investigations

1. Age and deformation of Pleistocene marine strandlines and sediments in the Los Angeles basin.

2. Paleosea-level as a tectonic datum.

3. Earthquake history, southern Alaska (assistance provided to G. Plafker, Alaskan Branch).

Results

1. Topographic and stratigraphic data indicate that the Bolsa Chica, Huntington Beach and Newport mesas, which lie along the coastline of the southern Los Angeles basin, represent a broad anticline (Huntington Beach anticline) that extends northwestward from the northern end of the San Joaquin Hills. Amino acid data on marine shells tentatively date the sediments that underlie these mesas at 200-300 ka. Amino acid dating also tentatively dates the marine terrace cut into western flanks of these mesas at 120 ka. Both the sediments and a fluvial terrace graded to the marine terrace are warped over the anticline, indicating that folding is continuous.

2. To derive a long-term tectonic history (primarily uplift from a sequence of emergent marine strandlines, the Paleosea-level history must be known. Presently the most detailed and best dated Paleosea-level curve is based on U-series dated coral reefs on the Huon Peninsula of Papua, New Guinea (Chappell, 1983; Chappell and Shackleton, 1986). U-series ages on emergent coral reefs from many other places are similar to those from the Huon sequence, indicating the general ages and relative elevations of the major sea-level highstands on the Huon curve are, for the most part, universal. U-series ages of soutary corals from several erosional terraces along the central and southern California coastline (research in progress with Stein and Wasserberg, Cal Tech.) agree well with the broader data set from the emergent coral reefs. However ages from one late-Pleistocene California locality indicate that sea level stood

slightly above its present position for at least twice as long as previously indicated. If correct, this modification to the sea-level curve might change interpreted uplift rates at a few localities.

3. Shallow (3-8 m hand-auger holes in the sediments of the Copper River delta reveal a sequence of several earthquake cycles (rapid uplift followed by gradual subsidence) in the last few thousand years. Radiocarbon analysis of organic materials from these sediments will provide a fairly detailed Paleo-earthquake history for this region.

Publications

Lajoie, K.R., Ponti, D.J., Powell, C.L., II, Mathieson, S.A., and Sarna-Wojcicki, A.M., in press, Emergent marine strandlines and associated sediments, coastal California.

ACTIVE MARGIN TECTONICS, PACIFIC NORTHWEST REGION

9910-04492

P. A. McCrory

Branch of Engineering Seismology and Geology
U.S. Geological Survey
345 Middlefield Road, MS 977
Menlo Park, California 94025
(415) 329-5677 or (FTS) 459-5677

Investigations

Document recent tectonic deformation in the vicinity of the Puget Sound metropolitan area and relate it to the earthquake potential in this region.

Results

1. FY89 field work focused on sediments exposed along the coast of the Quinault Indian Reservation, Washington. Three key stratigraphic sequences within the Quinault Formation have been measured and sampled: the Point Grenville, Taholah, and Duck Creek sections. Field reconnaissance has been conducted for the remaining sequences: the Cape Elizabeth, Pratt Cliff, and Raft River sections. This field work yielded some promising leads, in the youthful folding of the sedimentary units exposed in the sea cliffs along the coast, in the extreme tilting and angular discordance of Pleistocene gravels near the mouth of the Raft River, and in the liquifaction features preserved in the sediments. The next task will be to determine the age of this tectonic deformation, so as to understand the rates at which the sediments are being compressed and tilted.

2. Rock samples collected in FY89 are being processed for analyses of age and uplift data.

Reports

McCrory, P. A., *in press*, Neogene paleoceanographic events recorded in an active-margin setting: Humboldt basin, California: Palaeogeography, Palaeoclimatology, Palaeoecology.

McCrory, P. A., *in press*, Depositional history of an uplifted trench-slope basin: The Neogene Humboldt basin, California: Sedimentology.

STRUCTURAL FRAMEWORK OF THE PENINSULAR RANGES
9540-04040

Douglas M. Morton

Branch of Western Regional Geology
U.S. Geological Survey
University of California
Riverside, California 92521
(714) 351-6397

Investigations:

The project goal to understand the geologic history of the northern part of the Peninsular Ranges Province and its interaction with the Transverse Ranges Province to the north with emphasis on the Neogene tectonic history. Field mapping was continued in the northern Perris Block area of the Peninsular Ranges.

Results:

A number of low east facing scarps were discovered and mapped in an area west of the town of Perris. This is in an area of Cretaceous batholithic rocks which had been considered to be virtually free of faults. The low scarps offset Pleistocene alluvial deposits.

Reports:

Morton, D. M. and Cox, B. F., 1988, Geologic map of the Riverside East 7.5' quadrangle: U.S. Geological Survey Open-file Report 88-753.

Morton, D. M. and Cox, B. F., 1988, Geologic map of the Riverside West 7.5' quadrangle: U.S. Geological Survey Open-file Report 88-753.

Morton, D. M., and Matti, 1989, A vanished Late Pliocene to Early Pleistocene alluvial-fan complex in the northern Perris Block, southern California: in Colburn, I. P., Abbott, P. L., and Minch, J., eds., Conglomerates in basin analysis: a symposium dedicated to A. O. Woodford: Pacific Section, Society of Economic Paleontologists and Mineralogists, Book, 62, p. 73-80.

Morton, D. M., Campbell, R. H., Jibson, R. W., Wesson, R. L., and Nicholson, Craig, 1989, Landslides and ground fractures produced by the July 8, 1986, North Palm Springs California earthquake: Geological Society of America Abstracts with Programs, v. 21, n. 5, p. 119.

NORTHERN SAN ANDREAS FAULT SYSTEM: PALEOSEISMIC AND SLIP RATE STUDIES IN NORTHERN AND CENTRAL CALIFORNIA

9910-04483

CAROL PRENTICE

BRANCH OF ENGINEERING SEISMOLOGY AND GEOLOGY
345 MIDDLEFIELD RD, MS 977
MENLO PARK, CA 94025
415-329-5690

Investigations

Investigations of the San Andreas and related faults in northern and central California to determine timing of prehistoric earthquakes and average Quaternary slip rates.

Results

Three trench sites were identified and evaluated for their potential to yield slip-rate and paleoseismic data: 1) along the Maacama fault near Ukiah, CA, 2) on the Carrizo Plain along the San Andreas fault in central California, and 3) along the northern San Andreas fault near Gualala, California. Excavations at the first two of these sites demonstrated potential for yielding paleoseismic information. An excavation at the third locality, near Gualala, revealed no potential for further work at this site. The excavations near Ukiah and on the Carrizo plain are described briefly below:

1) The excavation at the City of Ten Thousand Buddhas, in Talmage, near Ukiah, California, exposed a sequence of marsh, fluvial and lacustrine deposits overlying a paleosol developed on Pleistocene (?) gravel. The Maacama fault, clearly expressed in the older gravels, has not caused any brittle deformation of the overlying Late Holocene section. Radiocarbon dating of peat in the lower Holocene section will allow determination of the time elapsed since the last ground-rupturing event on this segment of the Maacama fault.

2) Excavations along the Carrizo plain at the Bidart site done in conjunction with Kerry Sieh at Caltech have revealed stratigraphic evidence for five earthquakes along this segment of the San Andreas fault. Radiocarbon dating will allow limits to be placed on the timing of these events.

<u>Reports</u>

Prentice, C.S., and Sieh, K.E., A Paleoseismic Site Along the Carrizo Segment of the San Andreas Fault, Central California: *abs*. EOS, *in press*.

9/89

Latest Quaternary Surface Faulting in the Northern Wasatch to Teton Corridor (NWTC)

14-08-0001-G1396

James McCalpin
Department of Geology
Utah State University
Logan, UT 84322-4505
(801) 750-1220

Objective: This project attempts to date the latest surface-faulting earthquakes on the Holocene faults bounding Bear Lake Valley (Utah and Idaho) and Star Valley (Wyoming). These faults are part of an en echelon belt of six Holocene or Late Pleistocene normal faults which traverse the region between the northern end of the Wasatch fault and the Teton fault. The ultimate objective of the study is to determine if prehistoric surface-rupturing events in the belt have been clustered in time.
If paleoseismic events do cluster in "pulses", then future events in the relatively unpopulated NWTC may imply an increased probability of faulting in the more populated Wasatch Front.

Results: 1) Two large trenches were excavated in June and July, 1989, across the eastern Bear Lake fault at North Eden Canyon. Trenches were logged by the PI and Zhang Liren of the State Seismological Bureau, Beijing, China as part of a cooperative exchange and training exercise. The western trench (Fig.1) exposed a 5 meter-wide complex zone of normal faults. Two colluvial wedges were identified (units 5 and 6 in Fig.1) suggesting that the 8 meters of stratigraphic displacement was produced by two surface-faulting events. Radiocarbon samples JM89-08, JM89-11, and JM89-13 were concentrated by Rolf Kihl at INSTAAR, University of Colorado and submitted to Beta Analytic Inc. for dating. Results are expected by Nov. 5, 1989.

The eastern trench (Fig.2) across a 14 meter-high, somewhat subdued scarp, exposed three separate fault zones with different inferred ages of movement. Earliest movement on the upslope fault occurred when the site was at or very near lake level, and resulted in deposition of a colluvial wedge (unit 3 in Fig. 2). Later faulting occurred on the downslope fault, which accounts for most of the displacement (about 10 meters) in the trench. Colluvial units 4 and 6 were deposited from the free face of the downslope fault. Latest movement occurred on the central fault, the free face of which eroded to form colluvium unit 8 (Fig.2). Age control for faulting events is poor, due to a general lack of organics for radiocarbon dating. A single radiocarbon sample of bulk organics from a buried soil near the base of unit 6 (vertical ruled areas on log) was concentrated at INSTAAR and submitted for dating. Results are pending. In addition I collected a vertical transect of 8 TL samples through the thickest part of the colluvial wedge for possible future dating at INSTAAR.

Preliminary interpretation calls for four to five late Quaternary surface ruptures, the latest of which occurred in the mid to late

Holocene. Pending radiocarbon dates will bracket the latest two events tightly, with broad constraints on the earlier Pleistocene events.

2) Two trenches were excavated across the western Bear Lake fault (Bloomington scarp) 0.8 km east of Bloomington, Idaho in the first week of October. The smaller trench cuts a 1.5 meter-high scarp inferred to represent a single Holocene event, while the larger trench cuts a 4.5 meter-high scarp inferred to represent two paleoseismic events. Preliminary observations reveal faulted monoclinal flexures in the fine-grained alluvial and swamp deposits. These trenches will be logged and sampled during October, 1989, by the PI and Dr. Vladimir Khromovskikh of the Institute of the Earth's Crust, Irkutsk, USSR, as part of a scientific exchange and training program (weather permitting).

3) Trenching on the Star Valley fault has been postponed to May, 1990, because of intransigent landowners.

<u>Reports</u>: none

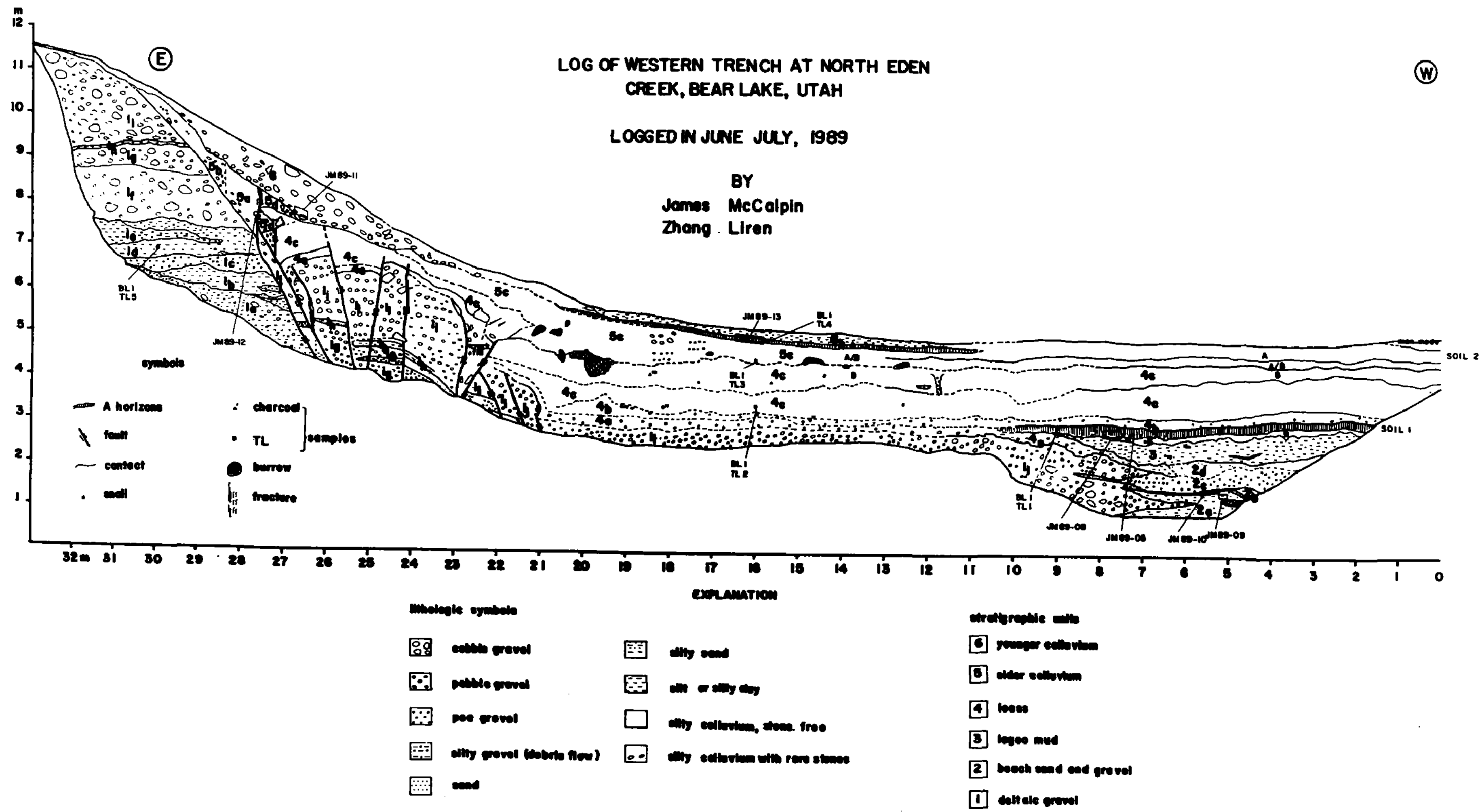

Fig. 1. Log of the western trench across the eastern Bear Lake fault at North Eden Canyon, Utah. The 8 m of stratigraphic displacement were created by two surface-faulting events, the latest of which was in the mid- to late Holocene.

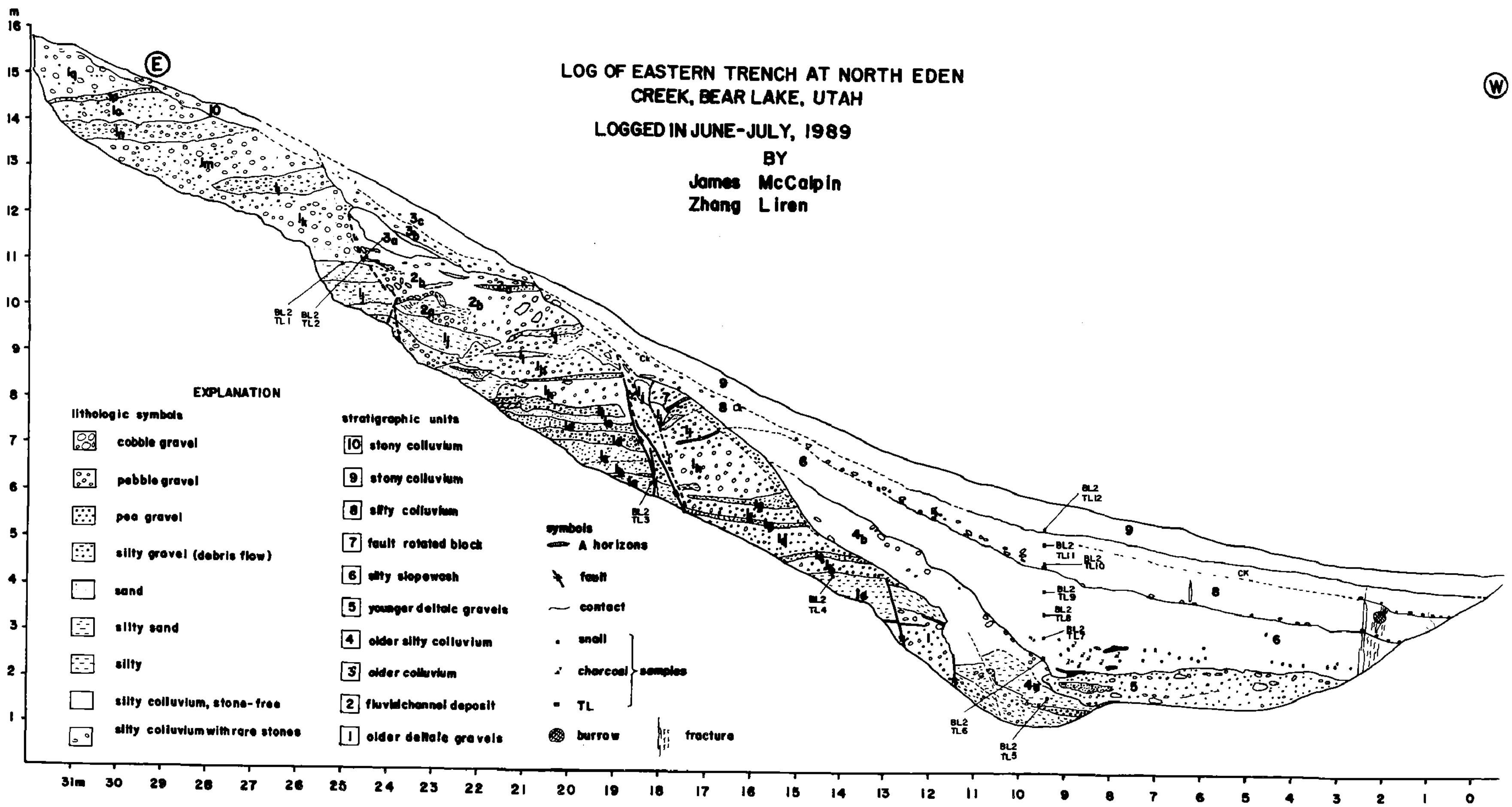

Fig. 2. Log of the eastern trench across the eastern Bear Lake fault at North Eden Canyon, Utah. Oldest fault movement occurred on the upslope fault, followed by up to 10 m of displacement on the downslope fault zone. These movements predate the late Pleistocene (?) younger deltaic gravels (unit 5). Latest faulting occurred in the Holocene on the central fault.

Determination of Slip Rates and Dating Earthquakes for the San Jacinto and Elsinore Fault Zones

14-08-0001-G1669

Thomas Rockwell
Department of Geological Sciences
San Diego State University
San Diego, California 92182
(619) 594-4441

Objectives: There are three primary objectives to this study: 1) to complete trenching studies at Hog Lake along the San Jacinto fault near Anza to determine the timing of prehistorical earthquakes; 2) to redate the peat stratigraphy with high-precision radiocarbon dates at Glen Ivy marsh along the Elsinore fault to better resolve the timing of past earthquakes and assess test earthquake clustering; and 3) to date the several past earthquakes that have been recognized along the southern Elsinore fault in the Coyote Mountains, to resolve the slip distribution for the past two or three events, and to determine a slip rate for this fault segment.

Results to Date: All peat samples from Hog Lake and Glen Ivy Marsh have been submitted for high-precision radiocarbon dating at the laboratory of Minze Stuiver at the University of Washington. All of the Hog Lake analyses are complete, as are most of the Glen Ivy samples.

1. Hog Lake Results. Seven ^{14}C samples from six peats were dated at Hog Lake to constrain the timing of the three earthquakes recognized in the upper 1.5 m of the dewatered sediments. All three events strongly disrupt the stratigraphy, but 3-D trenching was not able to resolve the magnitude of lateral slip. All three events have occurred within the past thousand years, with the most recent event around 1700 A.D. The average recurrence interval is 250-300 years, and they appear to be fairly evenly spaced in time. These data support the idea of a seismic gap in the Anza area and, along with recent estimates of the late Quaternary slip rate, suggest that 2.5-4 m of potential slip may have accumulated.

2. Glen Ivy Results. Eleven peat samples were submitted for high-precision ^{14}C dating, eight of which are final (Table 1). These data, when combined with the previous dates from the University of Arizona, will provide a reasonably well-dated stratigraphy for analysis of the late-Holocene record at Glen Ivy marsh where at least five and probably six events have been recognized in the stratigraphy.

3. Coyote Mountain Results. The distribution of slip in the past two and possibly three slip events has been determined for over half of the length of the fault segment. Previously reported slip for the most recent event at Alverson Canyon was about 1.5 m. This value increases to the northwest to at least 2.3 m, and older events show a similar increase. This invalidates my earlier

estimates about the recurrence interval for this section of the fault because it was predicated on slip at Alverson Canyon and a slip rate farther to the northwest where slip per event is higher.

Attempts at dating these events follow four directions: 1) soil dating of offset alluvium, comparing both physical secondary soil properties (based on field descriptions) and secondary clay/carbonate volume to dated soils in similar environments; 2) direct ^{14}C dating of the secondary soil carbonate, which should provide a solid minimum age in each case; 3) thermoluminesence (TL) dating (with Steve Foreman at the University of Colorado) of eolian and very local (drainage areas of several square meters) fluvial sediments that comprise fissure fillings within the fault zone that can be tied to specific earthquake events; and 4) rock varnish studies of cation ratios (with Charles Harrington at Los Alamos National Laboratory) which, like soils, can provide age control when calibrated. Based on all four separate age dating methods, it should be possible to approximate the timing of the past three or four earthquakes along the southern Elsinore fault zone.

A better slip rate estimate will also be made based on the older members of the soil chronosequence in the Alverson Canyon area. Those deposits are offset several tens to hundreds of meters and should provide a broader perspective within which to evaluate the youngest events.

Table I,

GLEN IVY RADIOCARBON DATES

Sample Number	Lab* Number	13C Corrected Age (Years B.P.)	Dendro-corrected A.D. Age (2 sigma, Method B)		Best Estimated Age Based On Stratrigraphy
				Event 1 -	1910
				Event 2 -	?
P2	A 4029	220 $\pm$80	1660^{+231}_{-154} (.88) or 1931 $\pm$24 (.12)		1660^{+231}_{-154}
P3a	QL 4306	358 $\pm$20	1488^{+36}_{-31} (.59) or 1597 +33 (.41)		
P3b	A 4400	490 $\pm$90	1427^{+100}_{-141} (.89) or 1594 $\pm$38 (.11)		
P3comb	-	364.2 $\pm$19.5	1484^{+38}_{-30} (.69) or 1598^{+28}_{-27} (.31)		1484^{+38}_{-30}
P4a	QL 4307	407 $\pm$34**	1455^{+65}_{-28} (.89) or 1602^{+22}_{-23} (.11)		
P4b	A 4374	590 $\pm$90	1340^{+125}_{-84} (1.00)		
P4comb	-	429.9 $\pm$31.8	1445^{+58}_{-27} (1.00)		1445^{+58}_{-27}
P3+4	-	382.2 $\pm$16.6	1473^{+39}_{-26} (.98) or 1609 $\pm$3 (.02)	Event 3	1473^{+39}_{-26}
P7	A 4401	380 $\pm$150	1474^{+224}_{-184} (.83) or 1770 $\pm$50 (.11) and younger (.06)		1474^{+224}_{-184}
				Event 4	circa 1300
P8a	QL 4308	717 $\pm$21	1275^{+10}_{-11} (1.00)		
P8b	A 4375	820 $\pm$90	1225^{+73}_{-209} (1.00)		
P8c	A 4034	730 $\pm$100	1272^{+138}_{-122} (.89) or 1131 $\pm$16 (.04) or 1072 $\pm$27 (.07)		
P8comb	-	722.6 $\pm$20	1274^{+10}_{-11} (1.00)		1274^{+10}_{-11}
P9 '	QL 4309	688 $\pm$20	1282^{+18}_{-13} (.95) or 1370 $\pm$4 (.05)		1282^{+18}_{-13}
P10a	QL 4310	816 $\pm$34	1227^{+41}_{-63} (1.00)		
P10b	A 4370	630 $\pm$160	1300^{+160}_{-110} (1.00)		
P10comb	-	796.7 $\pm$32.2	1247^{+24}_{-69} (1.00)		1247^{+24}_{-69}
P11a	A 4369	780 $\pm$120	1259^{+141}_{-239} (1.00)		
P11b	A 4033	760 $\pm$50	1265^{+33}_{-100} (1.00)		
P11comb	-	763 $\pm$46.2	1264^{+23}_{-91} (1.00)		1264^{+23}_{-91}
P8-11	-	723.2 $\pm$12.5	1274^{+6}_{-7}	Event 5	1274^{+6}_{-7}
P12	QL 4311	889 $\pm$21	1163^{+50}_{-12} (.38) or 1131 $\pm$18 (.24) or 1068^{+35}_{-34} (.39)		1131^{+82}_{-97}
P15	A 4376	1020 $\pm$80	1012^{+201}_{-154} (.99)		1012^{+201}_{-154}
P20a	QL 4312	931 $\pm$15	1043^{+25}_{-12} (.27) or 1106^{+22}_{-34} (.50) or 1145 $\pm$13 (.22)		
P20b	A 4377	910 $\pm$60	1125 $\pm$111 (1.00)		
P20comb	-	929.8 $\pm$14.6	1043^{+25}_{-11} (.27) or 1104^{+24}_{-32} (.51) or 1150^{+8}_{-18} (.22)		1104^{+54}_{-72}
P22a	QL 4313	pending			
P22b	A 4378	1010 $\pm$70	1015^{+172}_{-130} (1.00)		1015^{+172}_{-130}
P20+22	-	933.1 $\pm$14.2	1042^{+24}_{-12} (.28) or 1109^{+19}_{-36} (.51) or 1145 $\pm$12 (.22)	Event 6	1109^{+19}_{-79}
P24	QL 4314	pending			
P26	QL 4315	1069 $\pm$15	908 $\pm$10 (.06) or 980 $\pm$30 (.94)		980 $\pm$30

EARTHQUAKE GEOLOGY OF THE SAN ANDREAS AND OTHER FAULTS IN CALIFORNIA

Grant Number 14-08-0001-G1370

Kerry Sieh
Division of Geological and Planetary Sciences
California Institute of Technology
Pasadena, CA 91125
(818) 356-6115

During the six month period ending October 1989, I and my graduate students, in collaboration with Carol Prentice of the U. S. Geological Survey and Ken Hudnut, have made progress in several areas:

1) Bidart Site

Knowledge of the dates of the past few great earthquake ruptures in the Carrizo Plain would increase the likelihood of successful forecasts of future great earthquakes along the southern half of the San Andreas fault. Currently, intervals are believed to range from about 250 to 450 years, based upon our knowledge of the long-term slip rate and geomorphic evidence for the amount of slip during the past several earthquakes (Sieh and Jahns, 1984). This suggests that the Carrizo segment of the fault has a very low probability of rupturing in the next few decades. It also suggests that the next few Parkfield earthquakes are unlikely to trigger a great earthquake involving rupture of the Carrizo segment.

Unfortunately, the geomorphic basis of this important conclusion is tenuous. Thus, we have sought to date and characterize the past several earthquakes more convincingly. In May and July, Carol Prentice, Ken Hudnut and I and several graduate students excavated and logged an excavation that revealed superb evidence for six large rupture events. These ruptures are clearly indicated by upward truncations of fault planes and facies variations in alluvial fan and pond deposits. The characteristics of the sediments are such that we are confident that we have a complete record of at least the latest three events. My suspicion is that these are the AD 1100, AD 1480 and AD 1857 events recorded at Pallett Creek (Sieh and others, 1989); radiocarbon analyses of carbon collected from the sediments are now being performed and will confirm or repudiate this speculation.

Prentice and I also excavated and logged trenches across an alluvial fan that is offset 16 meters at the Van Matre Ranch. Radiocarbon analyses of samples from the fan will provide a maximum age for the earthquake that preceded the 1857 event.

2) Phelan Site

Dextral offsets of small stream channels in the Çarrizo Plain occur in rough multiples of 10 meters (Sieh, 1978). This observation is the basis for the interpretation that 10 meters is the magnitude of slip associated with each large earthquake produced by this section of the fault. If this interpretation is correct, this section of the fault must rupture about every 300 years.

Lisa Grant, several graduate students, Ken Hudnut, and I have begun 3-D excavations of an alluvial fan/channel complex that we expect to yield convincing evidence of the amount of dextral slip during each of the past few large earthquakes. Based upon the three excavations we made this summer, the offset across the fault plane in 1857 appears to be about 8 meters, and we believe we may be able to recover the amount of offset that occured during the previous event.

3) Slip in recent earthquakes and a potential slip rate site on the Garlock fault

Graduate student Sally McGill has nearly completed a study of the surface displacements associated with the past few earthquakes on the Garlock fault. Along a 5 km long stretch of the fault located just west of U.S. highway 395, six geomorphic features are left laterally offset between 6.8 and 8.8 m, and two features with less-reliable correlations are offset 3.3 and 3.8 m. The latter set of features were probably offset during the most recent large earthquake produced by this segment of the fault, and the former set of features probably record the surface displacement accumulated during the past two earthquakes.

Along a 26-km-long stretch of the fault in Pilot Knob Valley, 27 features are left-laterally offset between 2.0 and 4.2 m., and 24 features are offset 4.6 to 6.3 m. In addition, 5 features are offset 7.6 to 8.8 m., 2 features are offset 11.7 and 12.4 m., and 7 features are offset 14.0 to 16.5 m. These 5 sets of features suggest that each of the past 5 earthquakes in Pilot Knob Valley has involved 2 to 4 m. of left-lateral slip. The sense of vertical slip within Pilot Knob Valley is consistently up to the north, and its magnitude averages 12% of the horizontal slip.

Along an 0.5-km-long stretch of the fault located 4 km west of Leach Lake, 4 features are left-laterally offset 2.2 to 3.3 m. (presumably in the most recent event), and one feature is offset 5.8 m., (presumably in the past two events). These features also record a north-side-up vertical offset that averages 12% of the lateral offset.

Along the easternmost 15-km of the fault, north of the Avawatz Mountains, 67 features are left-laterally offset from 0.8 to 4.1 m. (the most recent earthquake), and 19 features with less reliable correlations are offset from 4.6 to 7.3 m. (the past two earthquakes combined). Both north-up and south-up vertical displacements are present in this area. The amount of vertical displacement ranges from 0 to 36% of the horizontal displacement. These data suggest an average slip of about 3 m in the latest event.

If the entire 130-km-long eastern half of the fault ruptured with this displacement, the size of the resulting earthquake would have been M=7.3 to 7.6. Using the published 7 mm/yr slip rate, the recurrence interval for such an earthquake would be 430 years.

Sally McGill and I have also discovered a shoreline of latest-Pleistocene Searles Lake that is left-laterally offset 65 to 100 meters across the Garlock fault at the west end of Pilot Knob Valley. We will be documenting this offset by mapping the area and selectively excavating the shoreline. This will yield a precise measurement of the offset and, hopefully, will enable radiocarbon dating of the offset feature. With these data, we should be able to determine a long-term slip rate of the Garlock fault .

4) Burro Flats Site

This site is located near the southeastern termination of the main strand of the the San Andreas fault that passes through San Bernardino. The aim of our study here is to date and characterize earthquakes generated by this segment of the fault. This site may assist attempts to correlate events at Indio, to the southeast, and Wrightwood/Pallett Creek,to the northwest. Geomorphic expression of a single dominant fault trace is clear to the southeast of the marshiest area in Burro Flats. A shutter ridge exists along this trace at the southeast margin of the marsh, marking where the fault cuts the relatively flat marsh deposits.

Along the projection of this trace into the marsh are minor geomorphic features that may represent deformation in the older deposits, but subsequent deposition has generally buried surface expression of the fault. This is evidence for rapid deposition, and so we expect a useful stratigraphic section. We hope to be able to dewater parts of the marsh that are currently too wet to excavate by backhoe. We are in the process of attempting to gain permission from the land owners to excavate through the shutter ridge, and through the low point of a swale northwest of that, to begin dewatering the marsh.

In late June and early July, attempts were made to obtain cores from several sites within the areas we intend to excavate. At a site roughly 3 m northeast of the fault trace, and adjacent to the shutter ridge, we retrieved a continuous 7.5 cm diameter core from a hole that bottomed at a depth of about 1.5 m on a coarse unit of the alluvial fan deposits. The alluvial fans are to northeast and their deposits abut the shutter ridge. Ponding of sediments apparently occurs between deposition of the alluvial fan debris. This ponding is evidenced by accumulation of organic-rich clay beds interlayered with the alluvial fan debris beds.

We are encouraged by the existence of three organic beds within the upper 1.5 m of the section. Until we are more certain of where we will excavate, we do not plan to submit samples of these sediments for radiocarbon dating.

As soon as we acquire permission, we will procede with excavation and logging of the trenches.

Evaluation of the use of compressive growth structure in earthquake hazard assessment

14-08-0001G 1699

John Suppe and R.E. Bischke

Department of Geological and Geophysical Sciences
Princeton University
Princeton, NJ 08540
(609) 258-6769

Investigations:

The primary objective of this work is to evaluate the use of growth fault-bend or fault-propagation theory, to determine long term slip rates on blind thrust faults. The study will concentrate on the heavily populated Los Angeles region.

Results:

We have been able to locate two regions of recent deformation within the Los Angeles basin from proprietary seismic lines. One of these regions parallels the length of the well known Newport-Inglewood Trend (Harding, 1973), while the other parallels the Santa Monica Mountains (Davis et al., 1989). Both regions exhibit compressive growth structures that are related to buried thrust faults, which in the case of the Santa Monica trend produced the 1987 ($M_L = 5.9$) Whittier narrows earthquake (Haunksson and Stein (1989).

Figures A to C show electric well logs that penetrated a growth sedimentary triangle located about 13,000 feet to the east of the Rosecrans oil field, which is part of the Newport-Inglewood trend. We have been able to correlate 28 horizons between these wells and several of these correlations are marked on figures A to C.

Our structural interpretation of the growth features is shown in figure D. This interpretation is constrained by the proprietory seismic data which shows that the active and growth axial surfaces converge to the east of the Pacific Electric well; by the log picks (i.e. correlations), by bed dips in each of the three wells, and by the kink method which requires that the active axial surface roughly bisect the bed dips. The interpretation suggests that some of the beds may change thickness between the Central and Pacific Electric wells, particularly on the level on the number 8 to 16 horizons. While this is not surprising in a fluvial environment the structural interpretation is relatively straight forward.

Provided that two of the horizons can be dated by palaeontological or other methods, the interpretation can now be utilized to predict the long term slip rate on the thrust fault that created the growth panel. For example, if the ages of horizons 1 and 12 are known we can write

R = [Thickness of sedimentary package below active axial surface - thickness of package above growth axial surface] / [sin (fault dip) (age of lower horizon - age of upper horizon)]

or

R = (2200 ft - 1600 ft) / [sin (40^o) (age of horizon 12 - age of horizon 1)]

where

fault dip = as determined from bed dips in the growth triangle. R = long term slip rate.

References

Davis, T.L., J. Namson, R.F. Yerkes (1989). A cross section of the Los Angeles Area: Seismically Active Fold and Thrust Belt, The 1987 Whittier Narrows Earthquake, and Earthquake hazard, Jour. Geophys. Res., v. 94, p. 9644-9664.

Harding, T.P. (1973). Newport Inglewood trend, California - an example of wrenching style of deformation, Am. Assoc. Pet. Geol. Bull., v. 57, p. 97-116.

Haunksson, E. and R.S. Stein (1989). The 1987 Whittier Narrows, California earthquake: A Metropolitan shock, Jour. Geophys. Res., v. 94, p. 9545-9547.

Deviated Well Log Plot

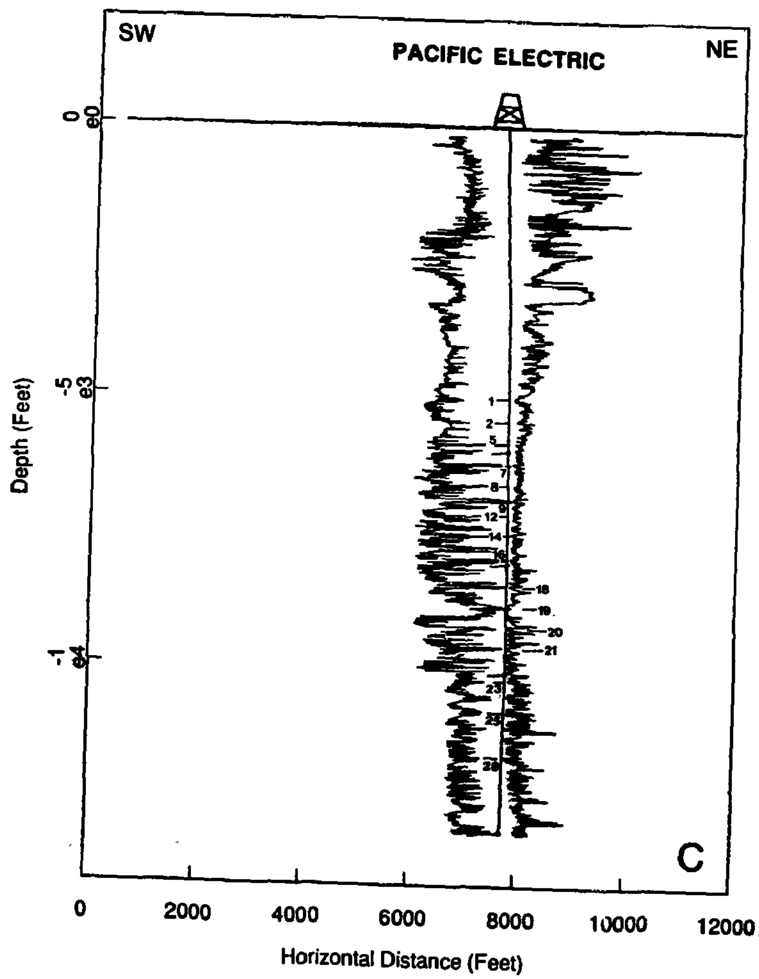

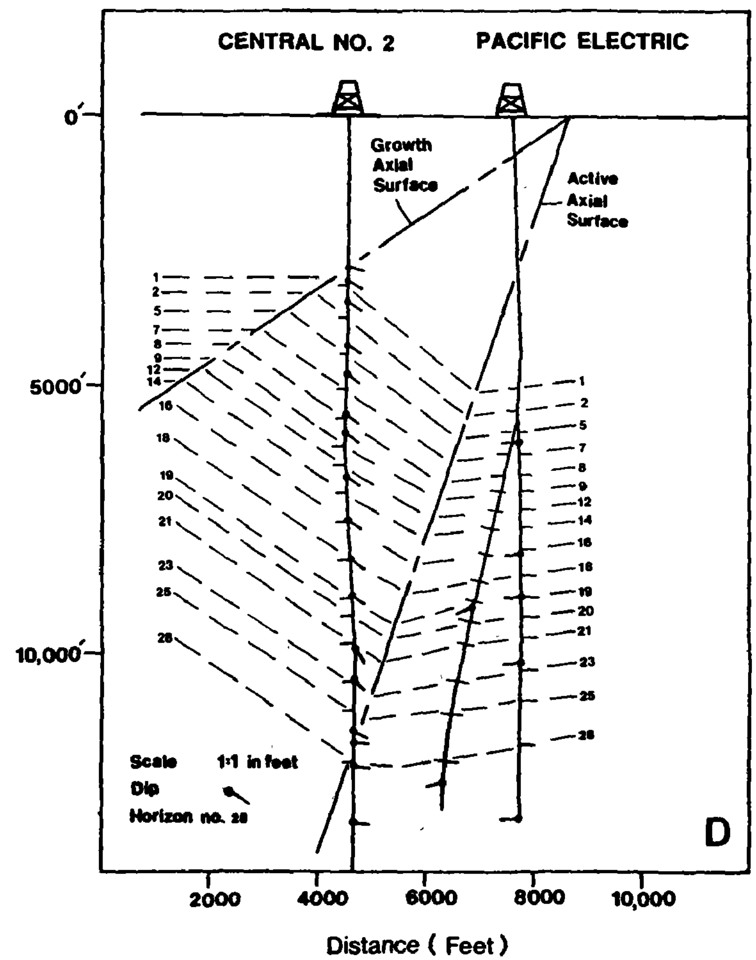

Deviated Well Log Plot

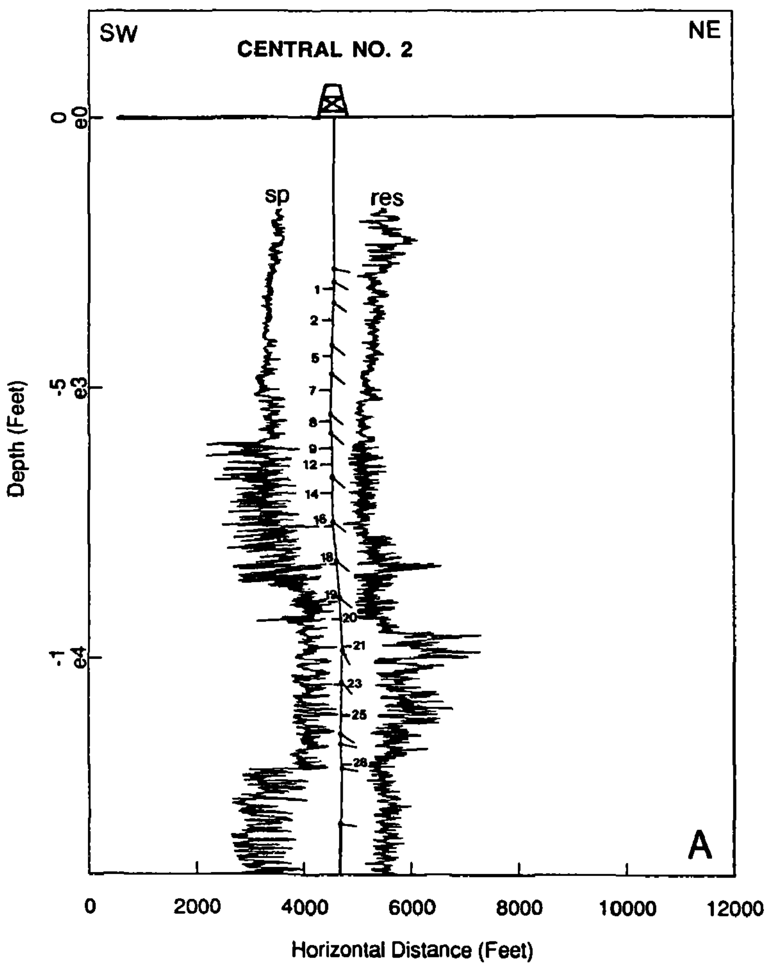

Deviated Well Log Plot

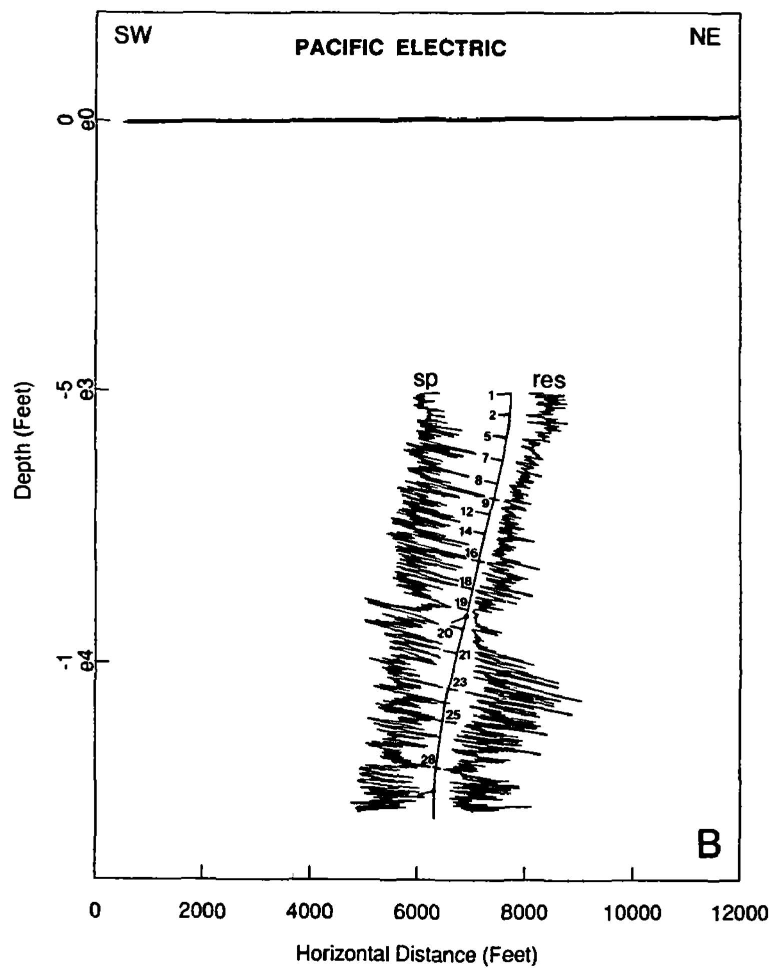

PATTERNS OF OFFSET ALONG SEGMENTED FAULTS NEAR BORAH PEAK, IDAHO: IMPLICATIONS FOR CHARACTERISTIC EARTHQUAKE FAULT BEHAVIOR

USGS contract # 14-08-0001-G1525
Progress report, October 1989

Kirk R. Vincent and William B. Bull
Department of Geosciences, University of Arizona
Tucson, Arizona 85721

Investigation

We are studying spatial patterns of Holocene fault displacements on two contiguous segments of the Lost River Fault in Idaho, in order to elucidate models of fault behavior. Alluvial fans and cones, incised and abandoned at the end of the latest glacial interval, flank the steep and elongate alpine range and record normal-fault displacement from post-glacial earthquakes. Longitudinal profiles of fans and terraces allow measurement of vertical tectonic displacement, and if surveyed at many locations along the range front-fault document the spatial pattern of displacement magnitude.

The northern portion of the study area is the Thousand Springs fault segment, which ruptured during the 1983 Borah Peak Earthquake (Crone and others, 1987) and also once during early to middle Holocene. The southern portion of the study area is the Mackay fault segment which ruptured once just after the end of the latest glacial interval and once after 7 ka (Tony Crone, personal communication 1988). Both segments have independently ruptured twice during the latest Quaternary, thus a total of four earthquakes are under investigation. The central portions of both fault segments are characterized by steep, linear, range-fronts where recent faulting has been restricted to the trace along the foot of the range. Within the 8 km long Elkhorn Creek fault segment boundary, between the fault segments, the strike of the range-front bends forming a spur of hills which stair-step up to the high peaks.

Specifically, our research objective is to evaluate the spatial pattern of post-glacial vertical displacement along the length of the fault, and to evaluate the spatial interaction of faulting within the boundary area. How and how much do surface ruptures, from independent events centered on adjacent segments, overlap within the Elkhorn Creek segment boundary?

Progress and Results

We completed our field work this past summer, and are now in the process of completing our analysis. The research project is outlined below by category of analysis, with brief description of each task, purpose and current results.

1) Previously undocumented surface ruptures from the 1983 earthquake were discovered and mapped, and vertical displacements were measured. Most of these ground cracks and scarps are located at the southern end of the 1983 surface rupture, but occur in bedrock above the range-front fault within the Elkhorn Creek segment boundary. Some of the surface ruptures are the result of ground shaking, some are the result of landsliding caused by both ground shaking and faulting, and some of the surface ruptures are the direct expression of faulting. The newly discovered fault scarps extend through 80% of the width of the segment boundary. Faulting during the 1983 earthquake penetrated the Elkhorn Creek segment boundary along the range-front fault and along a set of faults in the footwall. All of the faults activated during the 1983 earthquake were ruptured previously during the Quaternary. The newly documented surface ruptures are important because they illustrate faulting patterns critical to the understanding of segment boundaries. (Vincent and Bull, 1989a and 1989b)

2) Vertical tectonic displacement measurements document the spatial pattern of displacement magnitude over two seismogenic cycles. Post-glacial cumulative vertical displacement is 4 or 4.5 m at the center of both fault segments, and in each case gradually diminishes about 25% in the direction of the segment boundary. Rupture from all four earthquakes, two centered on each of the segments, penetrated (and stopped within) the Elkhorn Creek fault segment boundary. Faulting on the contiguous segments overlaps. The post-glacial cumulative vertical tectonic displacement at the center of the segment boundary, however, is approximately 2 meters -- half of that at the center of fault segments.

3) Sixty soil profiles in faulted and unfaulted alluvium were sampled for three purposes. First, identical soils above and below a fault scarp would confirm the alluvial surface was continuous previous to faulting, and thus the site would be appropriate for measuring vertical tectonic displacement. Second, we wanted to be certain that all alluvial surfaces used to measure

vertical displacement were abandoned at the same time, which in this case was at the end of the latest glacial about 15 ka. Third, soil development on alluvial surfaces not faulted by prehistoric earthquakes (or faulted by only the 1983 event) would help constrain the timing of these events. The soils data do indeed give us confidence that the pattern of displacement mentioned above reflects cumulative faulting over one time frame.

4) Datable charcoal fragments were collected from alluvial deposits with varying degrees of carbonate soil development. Dating of charcoal is not yet complete, but eventually will allow calibration of Holocene rates of soil development. Dating of calcic soils should allow us to refine estimates of the timing of earthquakes on the Lost River and other faults in the region. Several initial age estimates suggest the Holocene rate of soil carbonate accumulation is linear, and is more rapid than the long term rate integrated over both interglacial and glacial periods.

References

Crone, A.J., Machette, M.N., Bonilla, M.G., Lienkaemper, J.J., Pierce, K.L., Scott, W.E., and Bucknam, R.C., 1987, Surface faulting accompanying the Borah Peak Earthquake and segmentation of the Lost River Fault, central Idaho: Bulletin of the Seismological Society of America, Vol. 77, No. 3, p. 739-770.

Vincent, K.R. and W.B. Bull, 1989a, New evidence of surface rupture from Borah Peak Earthquake: and project summary, in USGS Open-File Report 88-673, National Earthquake Hazards Reduction Program Summaries of Technical Reports Vol. XXVII, p. 178.

Vincent, K.R. and W.B. Bull, 1989b, Newly discovered surface ruptures from the Borah Peak Earthquake: faulting or landsliding?, Geological Society of America, Abstracts with Programs, National Meeting in St. Louis.

Paleoearthquake Study in the New Madrid Seismic Zone.

14-08-0001-G1682

Steven G. Wesnousky
Center for Earthquake Research and Information
Memphis State University
Memphis, TN 38152
(901) 678-2007

Objective: For purposes of flood control and land reclamation, the U.S. Army Corps of Engineers has recently undertaken a major effort to reexcavate and widen an extensive set of drainage ditches within the Saint Francis drainage basin. The majority of the ongoing and planned excavations cut through the meisoseismal zone of the great 1811-12 New Madrid earthquakes. The 1811-12 earthquakes produced extensive liquefaction within the New Madrid Seismic zone at the time of the earthquakes. Evidence of that liquefaction still exists today in the geologic record. As a result, the ditches provide an excellent opportunity to systematically examine and document the geological record of liquefaction in the New Madrid Seismic Zone. The objective of this study is to monitor and document liquefaction phenomena exposed in the ditches and determine whether or not evidence for pre-1811-12 earthquakes exists.

Progress: Initial efforts for this study have concentrated along the banks of Buffalo Creek ditch and Ditch No. 12, each of which cut the interior of the New Madrid Earthquake meisoseismal area and are located near the town of Manilla, Arkansas. Reexcavation of Ditch 29, to the west of New Madrid, Mo is scheduled to be reexcavated during the autumn and winter months of 1989 and 1990, respectively. Ditch No. 12 and Buffalo Creek ditch are situated on a braided terrace deposit associated with the retreat of the last glaciation and, hence, on a surface that has been relatively stable during the last 6 thousand to 10 thousand years. We have currently logged more than 1 km of trench wall along the Buffalo Creek ditch, with the purpose of documenting sites of major liquefaction disturbances near the ground surface. Thus far, major sand blow and fissure deposits have been logged in detail at 3 sites along Buffalo Creek ditch. No evidence suggesting pre-1811-12 earthquakes was documented. Several more sites of liquefaction along Buffalo Creek ditch will be logged in greater detail during October 1989. We have also logged more than 1 km of the walls of ditch no. 12. Several sites along that trench show rupture of surface sediments by liquefied and extruded sands and we will log those sites in detail during October of 1989 to ascertain whether on not evidence exists to indicate the liquefaction occurred before or at the time of the 1811-12 earthquakes. After documenting in detail sites of liquefaction along Ditch No. 12 and Buffalo Creek Ditch, we plan to shift our efforts northward to Ditch 29.

TREE-RING DATING OF LATE HOLOCENE SUBSIDENCE ALONG THE WASHINGTON COAST: A PROGRESS REPORT II

David K. Yamaguchi*, Connie A. Woodhouse*, and Marion S. Reid#

14-08-0001-G1685

*Mountain Research Station & Institute of Arctic and Alpine Research (INSTAAR), Campus Box 450, Univ. of Colorado, Boulder, CO 80309
(303) 492-8841, -8842
#Dept. of Geography, Campus Box 260, Univ. of Colorado, Boulder, CO 80309

Our recent progress is best summarized by the following abstract to be presented at the December 1989 meeting of the American Geophysical Union:

Tree-Ring Evidence for Synchronous Rapid Submergence of the Southwestern Washington Coast 300 Years B.P.[1]

We have been using ring-width pattern matching to determine death dates for western redcedar (Thuja plicata) snags rooted in the uppermost of several buried soils in estuaries along the southwestern Washington coast. Soil burial and tree death are thought to have been caused by coastal subsidence that accompanied a great (M_w 8+) Cascadia subduction zone earthquake about 300 yr ago.

To date, pattern matching between old modern redcedar on Long Island in Willapa Bay and snags at 6 sites, listed north to south, provide the following death dates for individual trees: Copalis R., AD 1664 & 1684; Chehalis R., 1618, 1642, & 1682; Johns R., 1674 & 1678; Bone R., 1684; Palix R., 1655, 1672, 1675, & 1682; Grays R., 1671 & 1687. These dates are limiting minimum dates because sampled snags are missing a small amount of outer wood due to weathering. The outer rings of all dated snags are wide and lack evidence of declining tree vigor before death. Such rings suggest that sampled trees died suddenly rather than gradually.

The general synchroneity of these dates, the wide outer rings of snags, and the spread of the 6 sites along 93 km of coastline provide evidence for synchronous, rapid submergence of the southwestern Washington coast about 300 yr ago. They are thus consistent with a great-earthquake origin for soil burial and tree death.

If we infer that the snags record a single subsidence event, then the youngest snag date from the Grays R. site--1687--revises our earlier minimum date (1684 from the Copalis R. site) for subsidence. However, the 1687 date conflicts with 1666 and 1668 pith (center ring) dates we obtained from 2 modern sitka spruce (Picea sitchensis) stumps at the Grays R. site. It may be that young spruce can survive submergence in brackish water without apparent radial growth effects. Further study is needed to clarify this issue.

[1]Yamaguchi, D. K., Woodhouse, C. A., and Reid, M. S. EOS, in review.

28 September 1989

Convergence Rates Across Western Transverse Ranges

14-08-0001-G1372

Robert S. Yeats and Gary J. Huftile
Department of Geosciences
Oregon State University
Corvallis, Oregon 97331-5506
(503) 737-2484

Investigations

Work is continuing on a residual gravity map of the western Transverse Ranges. We are constructing retrodeformable cross sections across the western San Cayetano fault, the Red Mountain fault, and the Ojai Valley (Figure 1). The residual gravity will be used as an independent data set to verify interpretations. Field checking of surface exposures of the Santa Ynez fault for strain analysis has been completed. Field mapping of the Piru 7 1/2 minute quadrangle is being prepared as an Open-File Report. The Piru quadrangle, together with the adjacent Val Verde quadrangle (Yeats et al., 1985) includes the transfer zone between the San Cayetano and Oak Ridge faults on the west and the Santa Susana fault and the East Ventura basin fold belt on the east.

Results

North dips on the fault surface (Dibblee, 1985) are associated with overturned bedding in the hanging-wall block of the Santa Ynez fault, whereas south dips on the fault are related to normal bedding in the hanging-wall block. This suggests that the fault has been folded along with the overturned strata. Exposures of the Santa Ynez fault near Matilija Creek have slickensides, small folds, and sheared calcite veins which are evidence of left-lateral motion on the fault with σ_1 trending east-northeast. Thus, while reverse movement on the fault is not precluded, the most recent movement on the fault is left-lateral.

Published maps of the Matilija overturn (Dibblee, 1982, 1985, 1986a-b, 1987a-d) reveal that the fold hinge, the change from normal to overturned bedding, can be mapped. This fold hinge has itself been folded, possibly by a blind western extension of the San Cayetano fault beneath Ojai Valley and certainly by a fold or fault beneath and north of the Santa Ynez fault.

References

Dibblee, T. W., Jr., 1982, Geologic map of the Santa Paula Peak Quadrangle: U. S. Geol. Survey, Open-file Report 82-73, Scale 1:24,000.
Dibblee, T. W., Jr., 1985, Geologic map of the Wheeler Springs Quadrangle: Dibblee Foundation, Santa Barbara, California, Scale 1:24,000.
Dibblee, T. W., Jr., 1986a, Geologic map of the Carpenteria Quadrangle: Dibblee Foundation, Santa Barbara, California, Scale 1:24,000.
Dibblee, T. W., Jr., 1986b, Geologic map of the Santa Barbara Quadrangle: Dibblee Foundation, Santa Barbara, California, Scale 1:24,000.
Dibblee, T. W., Jr., 1987a, Geologic map of the Lion Canyon Quadrangle: Dibblee Foundation, Santa Barbara, California, Scale 1:24,000.

Dibblee, T. W., Jr., 1987b, Geologic map of the Matilija Quadrangle: Dibblee Foundation, Santa Barbara, California, Scale 1:24,000.

Dibblee, T. W., Jr., 1987c, Geologic map of the Ojai Quadrangle: Dibblee Foundation, Santa Barbara, California, Scale 1:24,000.

Dibblee, T. W., Jr., 1987d, Geologic map of the White Ledge Peak Quadrangle: Dibblee Foundation, Santa Barbara, California, Scale 1:24,000.

Yeats, R. S., McDougall, J. W., and Stitt, L. T., 1985, Cenozoic structure of the Val Verde 7 1/2 minute Quadrangle and the south half of the Whitaker Peak 7 1/2 minute Quadrangle, California: U. S. Geol. Survey Open-File Report 85-587, 23p., map scale 1:24,000.

Reports

Huftile, G. J., 1989, Thin-skinned tectonics and oil accumulation of the Upper Ojai Valley and Sulphur Mountain area, Ventura basin, California: submitted to American Association of Petroleum Geologists Bulletin.

Huftile, G. J., 1990, Displacement transfer between surface reverse faults and blind thrusts, central Ventura basin, California: to be submitted to Tectonics.

Yeats, R. S., Calhoun, J. A., Nevins, B. B., Schwing, H. F., and Spitz, H. M., 1989, Russell fault: Early strike-slip fault of California Coast Ranges: Am. Assoc. Petrol. Geol. Bull., v. 73, p. 1089-1102.

Yeats, R. S., and Huftile, G. J., 1989, Comment on "Structural transect of the western Transverse Ranges, California: Implications for lithospheric kinematics and seismic risk evaluation": Geology, v. 17, p. 771-772.

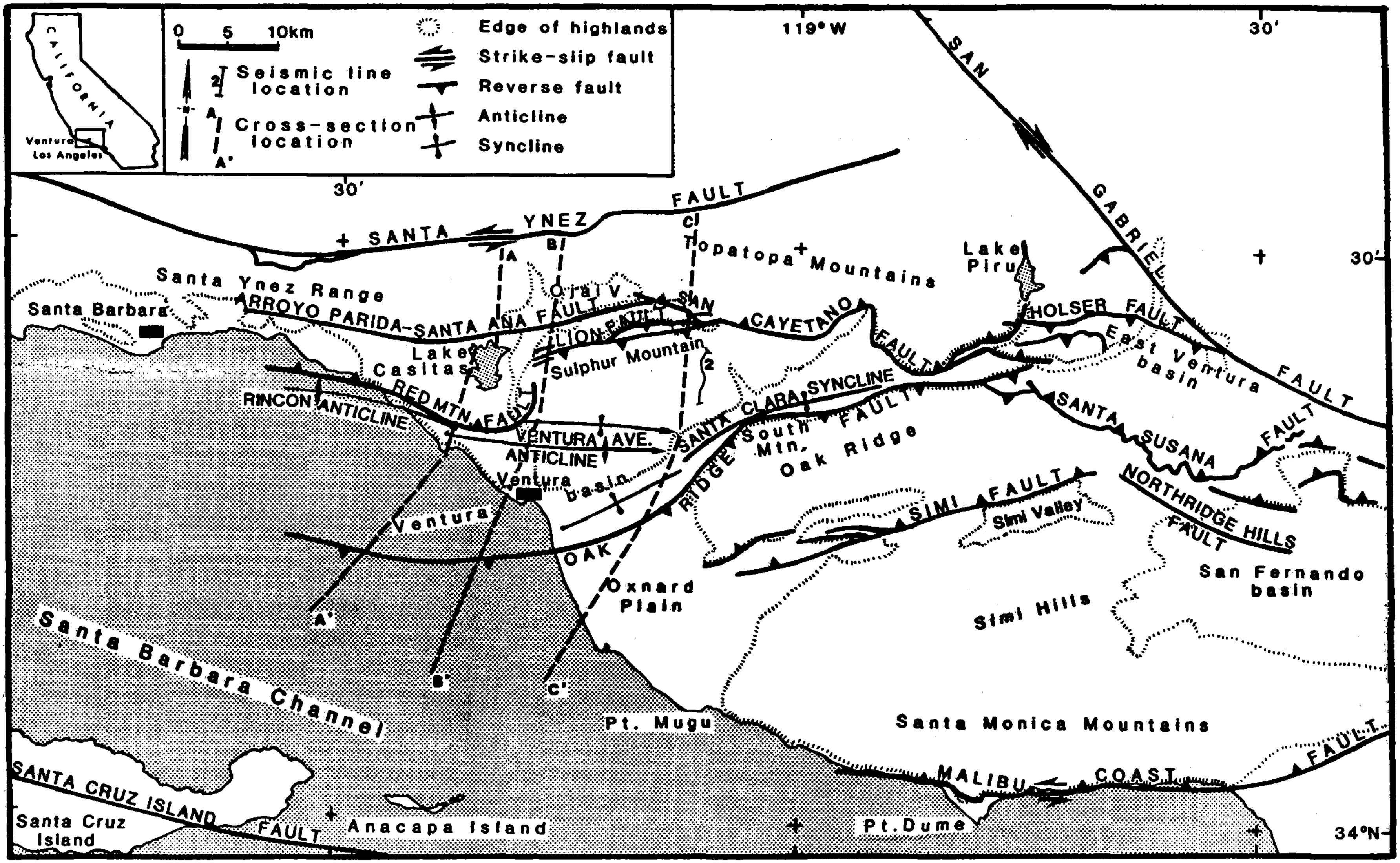

CALIFORNIA
Ventura
Los Angeles
0 5 10km
Seismic line location
Cross-section location
Edge of highlands
Strike-slip fault
Reverse fault
Anticline
Syncline
119° W
30'
SAN GABRIEL FAULT
SANTA YNEZ FAULT
Santa Ynez Range
Santa Barbara
ARROYO PARIDA-SANTA ANA FAULT
Topatopa Mountains
Lake Piru
Ojai V.
SAN CAYETANO FAULT
LION FAULT
Sulphur Mountain
Lake Casitas
HOLSER FAULT
East Ventura basin
RED MTN. FAULT
RINCON ANTICLINE
SANTA CLARA SYNCLINE
VENTURA AVE. ANTICLINE
South Mtn. Oak Ridge
SANTA SUSANA FAULT
Ventura
Ventura basin
OAK RIDGE FAULT
SIMI FAULT
Simi Valley
NORTHRIDGE HILLS FAULT
San Fernando basin
Oxnard Plain
Simi Hills
Santa Barbara Channel
Pt. Mugu
Santa Monica Mountains
MALIBU COAST FAULT
SANTA CRUZ ISLAND FAULT
Santa Cruz Island
Anacapa Island
Pt. Dume
34°N

Figure 1

On-Line Seismic Processing

9930-02940

Rex Allen
Branch of Seismology
U.S. Geological Survey
345 Middlefield Road, MS 77
Menlo Park, California 94025
(415) 329-4731

Investigations and Results

This period has been one of continuing effort toward converting the real-time processor (RTP) to run on INMOS transputer multiprocessors. We have taken delivery of a development system allowing both hardware and software to be prototyped and tested. The basic RTP routines are now running in the new format, and use of simulated data has allowed confirmation of earlier estimates of processor performance. Latest tests indicate that these processors can analyze about fifty stations each at a sample rate of 100 Hz. This works out to a total system requirement of ca. 8 processors for a large seismic net such as the USGS CALNET. It should be emphasized that these figures are for a system operating entirely in FORTRAN floating point with no recourse to speedy but arcane tricks such as fixed point arithmetic or assembly language routines.

We are currently arranging for design of the analog to digital converter system by an outside engineer with extensive experience with these systems. Earlier estimates of early 1990 for an operational system still seem reasonable at this time.

The Mk I RTP's at Menlo Park and the University of Utah have continued to operate satisfactorily, as have the Mk II's at Menlo Park and Caltech.

Crustal Deformation Observatory Part F

14-08-0001-G1355

John Beavan
Lamont-Doherty Geological Observatory of Columbia University
Palisades, New York 10964
(914) 359-2900

Investigations

We operate a 535 m long-baseline half-filled water tube tiltmeter at Piñon Flat Observatory (PFO) in the San Jacinto Mountains of southern California. This is used in conjunction with a similar instrument operated by the University of California, San Diego (UCSD), to investigate:

(1) sources and magnitudes of noise affecting the tilt signal;
(2) water level sensor design and reliability;
(3) methods of referencing tiltmeter to depth;
(4) interpretation of tilt signal.

Results (October, 1989)

1. Tiltmeter Operation and Data Analysis

The L-DGO tiltmeter continues to perform reliably, requiring little maintenance. The remainder of this report concentrates on item (2) above.

2. Absolute Sensor Development

We are developing a low power absolute water level sensor, so that widespread field installation will become possible without the loss-of-datum problems associated with our current interferometer sensor. We are currently operating in the lab a prototype that uses a laser diode beam reflected from the water surface onto a 35 mm CCD sensor with a pixel spacing of about 12 µm (Figure 1). We have overcome the technical problems associated with reading the data out of the CCD and digitising it at the high data rates involved. The laser diode beam is shaped to provide a line source a few hundred µm wide with a gaussian intensity distribution across the width of the beam. Data analysis consists of fitting a gaussian curve to about 100 pixels of the digitised CCD data, centered on the point of highest intensity (Figure 2). The center of the fitted gaussian curve gives the position of the beam which is converted to a measure of water level. A reference beam reflected off the glass top surface of the reservoir is monitored by another CCD whose position is known accurately relative to the first (e.g., by an interferometric measurement in the lab prior to deployment). It is this second beam that ensures the absolute nature of the instrument; the difference in the measurement made by the 2 CCD's essentially gives the height of the water surface relative to the top surface of the reservoir. This arrangement also compensates for small variations in the beam direction, the beam shape, and the heights of the laser and CCD. This ensures that disassembly and reassembly of the instrument (e.g., for cleaning or repair) becomes non-critical.

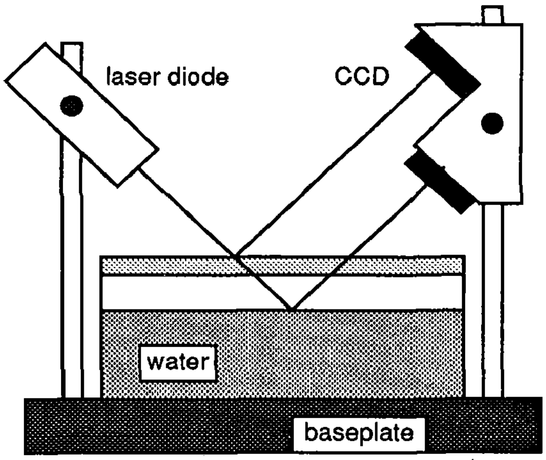

Figure 1. Schematic showing beam reflected off water surface, and reference beam reflected off glass.

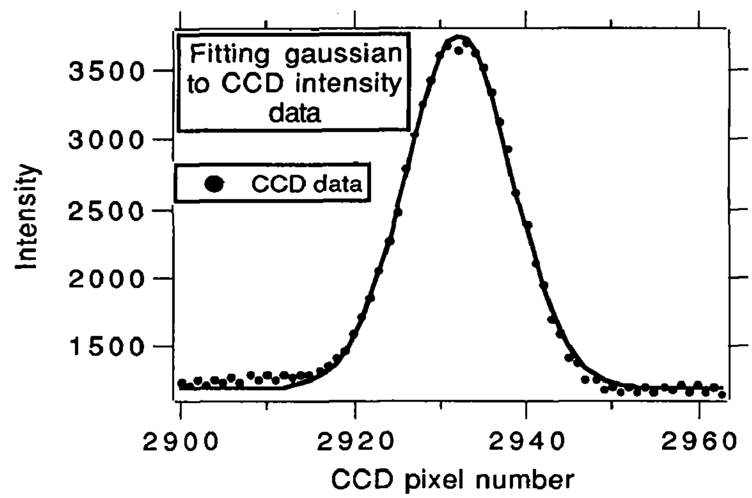

Figure 2. Data recorded by CCD, showing a gaussian curve fit to the intensity pattern.

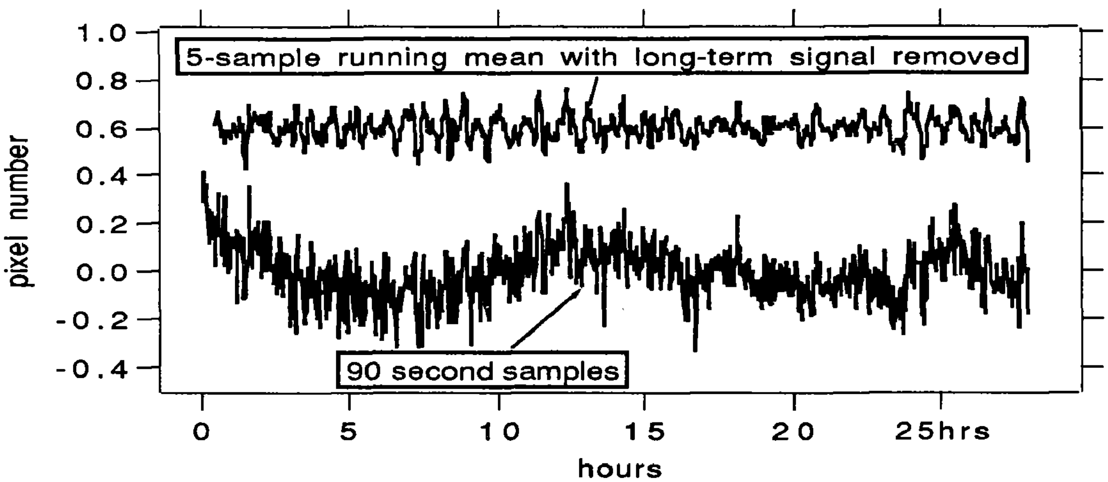

Figure 3. (below) 28 hours data recorded every 90 sec. The rms noise is 0.11 pixel. By taking a 5-term running mean and removing the long term signal (above) the rms noise is reduced to 0.05 pixel.

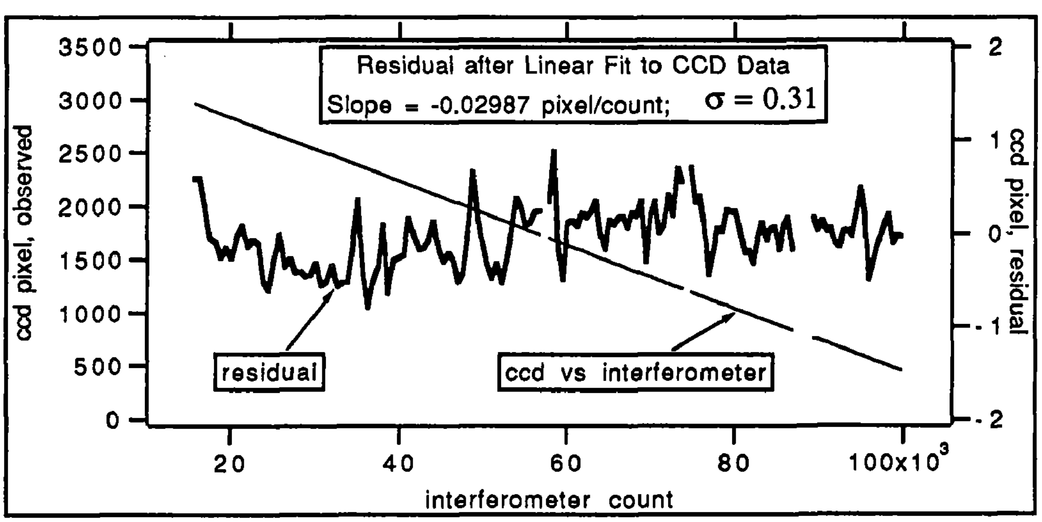

Figure 4. Comparing water level measured by laser interferometer and CCD array. The residual from a straight line fit is shown. The rms of the residual is 0.3 pixels over a range of 2 cm in water height.

An important question is: to what extent is pixel subdivision possible by fitting a gaussian curve to the data rather than, for example, simply selecting the position of the maximum amplitude pixel? Our tests indicate that this is possible to 0.2 pixel or better (Figure 3). This corresponds to a water level measurement with a precision of 1-2 μm. In the current interferometric end sensor, the least count sensitivity is 0.25 μm. The slight reduction in sensitivity in the new design is more than offset by its simplicity and its immunity to ground shaking and power outages. This is particularly so since the main feature of the long base tiltmeter is its high stability at long periods, rather than an inherent high sensitivity.

A second question is: what is the linearity and calibration of the CCD sensor across its full range (> 3 cm), and across smaller parts of its range that are typical of the annual variations in a several hundred metre instrument (i.e., a few mm). We have investigated this by measuring the same water surface using both the CCD sensor and an interferometer sensor. Over the full range the CCD calibration agrees within 0.05% with that calculated from the geometry of the set up and the nominal pixel spacing in the CCD. This agreement is as good as can be expected given the accuracy with which the geometry of the prototype set up is known. The linearity is excellent - the rms deviation from a straight line fit over the entire range is about 0.3 pixels (Figure 4). We have yet to investigate variations in linearity and calibration over smaller ranges.

If the end reservoir itself should tilt then an erroneous signal will be recorded because the top glass surface tilts with the reservoir while the water surface remains on an equipotential. Such a tilt could be introduced by, for example, thermally-induced tilting of the pier on which the instrument is mounted, or by releveling of the end reservoir during repairs or cleaning operations. A final question, therefore, is: how may the effect of this tilting be eliminated. The effect can be reduced by making the instrument smaller since it is directly proportional to the distance from the water surface to the CCD detector. It can be eliminated by operating two independent systems, one pointing in the opposite direction to the other. This is the probably the approach we shall adopt; the cost of the extra laser diode, beam forming optics and CCD sensors is about $2,000; most of the electronics and mounting hardware will be shared by the two independent systems.

We had hoped to have a prototype ready to instal in the field by late 1989, but it now looks as though this will slip to Spring 1990.

Crustal Deformation Measurements in the Shumagin Seismic Gap, Alaska

14-08-0001-G1379

John Beavan
Lamont-Doherty Geological Observatory of Columbia University
Palisades, NY 10964
(914) 359 2900

Investigations

1. Eleven short (~ 1 km) level lines are measured approximately annually within the Shumagin seismic gap, Alaska (Figure 1). Surface tilt data are interpreted in terms of tectonic deformation and earthquake hazard at the Pacific-North American plate boundary.
2. Six absolute-pressure sea-level gauges are operated in the Shumagin Islands in an attempt to measure vertical deformation associated with the Aleutian subduction zone. A two-component short-baseline tiltmeter is operated at one site.
3. Data from the sea-level and tilt sensors are transmitted to Lamont by satellite in near real time, and are examined for possible tectonic signals. Studies of noise level as a function of frequency are used to determine the relative usefulness of different types of measurement, and to evaluate the minimum size of tectonic signal that will be visible above the noise. Our data are compared with other crustal deformation data from the Shumagin gap.

Results (October 1989)

This report will deal principally with the leveling data (see Figure 1). Our measurement and analysis techniques are described by Beavan et al. (1984). The sea level measurement system is described by Beavan et al. (1986); see Beavan (1989) for a recent discussion of these data.

Sea level measurements

Data Continuity, 1988-89

We experienced our best year ever for survival of the sea level gauge network over the 1988/89 winter. Five of the six gauges continued to transmit data throughout the year (though the data from one of these is of rather poor quality due to a progressive leak in the vacuum chamber of the pressure sensor). The sole failure at the sixth site was a blown fuse in the satellite transmitter!

Backup Recording

We installed solid-state backup recorders at three of the sites in order to protect against the type of transmitter failure mentioned above. In 1990 we will upgrade the remainder of the sites: in some cases with backup recorders; in the more exposed sites with self-contained gauges that record more than a year of data in internal solid-state memory. These gauges will be far more robust because they will not require the cable linking the pressure sensor to shore. Their data will not be available in real time; however, the majority of sites will continue to be transmitted in real-time so that detection of possible preseismic anomalies (see Beavan et al., 1984) will still be achievable.

Pressure Sensor Calibration

Five of the six sites were visited, and their sensors exchanged and recalibrated. The recalibration is a necessary step if we are to achieve optimal detection of long-term tectonic tilt; this is because it allows us to monitor and correct for any drift in the pressure sensor itself. The sixth site (chn) was not serviced, because of an unusually extended stretch of very poor weather.

Sea Level Data Analysis

As discussed in recent reports (Beavan, 1988, 1989) we are hoping to use the long term relative vertical displacements measured by the sea level network to help discriminate between various models that explain the surprisingly low horizontal strain rates measured by Lisowski et al. (1988). The analysis is not completed in time for this report, but is being actively worked upon.

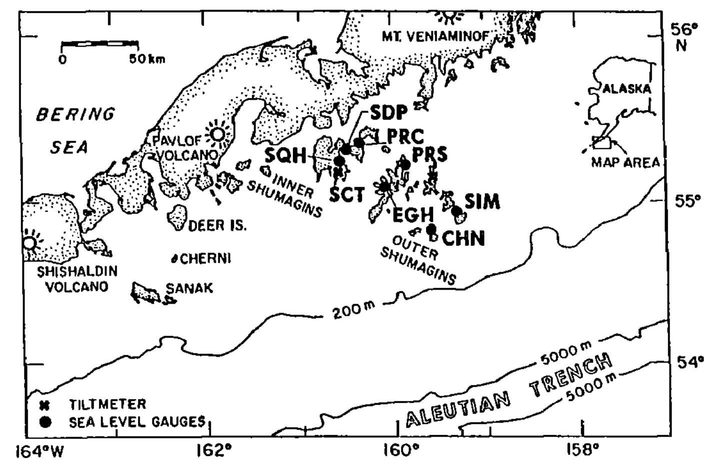

Figure 1a. Location of the Shumagin Islands with respect to the trench and the volcanic arc. Depth contours are in metres. The seismic gap stretches from approximately Sanak Island in the west to about 30 km east of the Shumagin Islands. Also shown are the sites of six sea-level gauges operated by LDGO and one by the National Ocean Survey (at SDP).

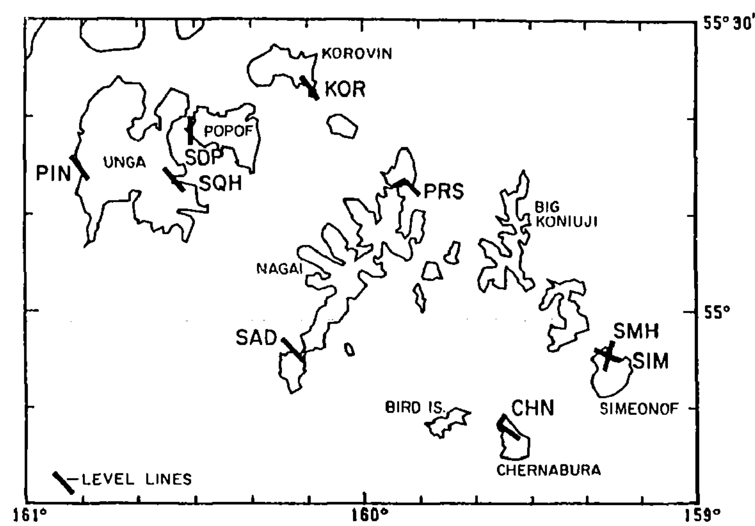

Figure 1b. The Shumagin Islands, showing the locations and directions of first-order level lines, whose lengths vary between 600m and 1200m. The resultant of the data from lines SDP and SQH is used to estimate the tilt direction in the Inner Shumagins. The resultant of SIM and SMH is used for Simeonof Island. The lines at CHN and PRS each consist of two approximately straight sections in different azimuths, with benchmarks at the junction. This non-linear geometry allows tilt direction to be estimated at these sites. Two sets of perpendicular level lines have also been installed on Sanak Island, at the western end of the seismic gap (see Fig. 1a). One of these, at the south-east end of the island was measured in 1988. The other, at the north-west end, has yet to be measured.

Level lines on Sanak

Sanak is located at the western end of the seismic gap, and data from the Sanak level lines will be used to investigate whether deformation is occurring differently in the western and eastern sections of the gap. Such a difference is suggested by seismicity data (Hudnut and Taber, 1987). The two level lines that were installed on southeastern Sanak Island (Fig. 1a) and first measured during the 1988 field season were unfortunately not remeasured during 1989 due to unusually poor weather and an abbreviated helicopter schedule. Remeasurement of these lines will receive highest

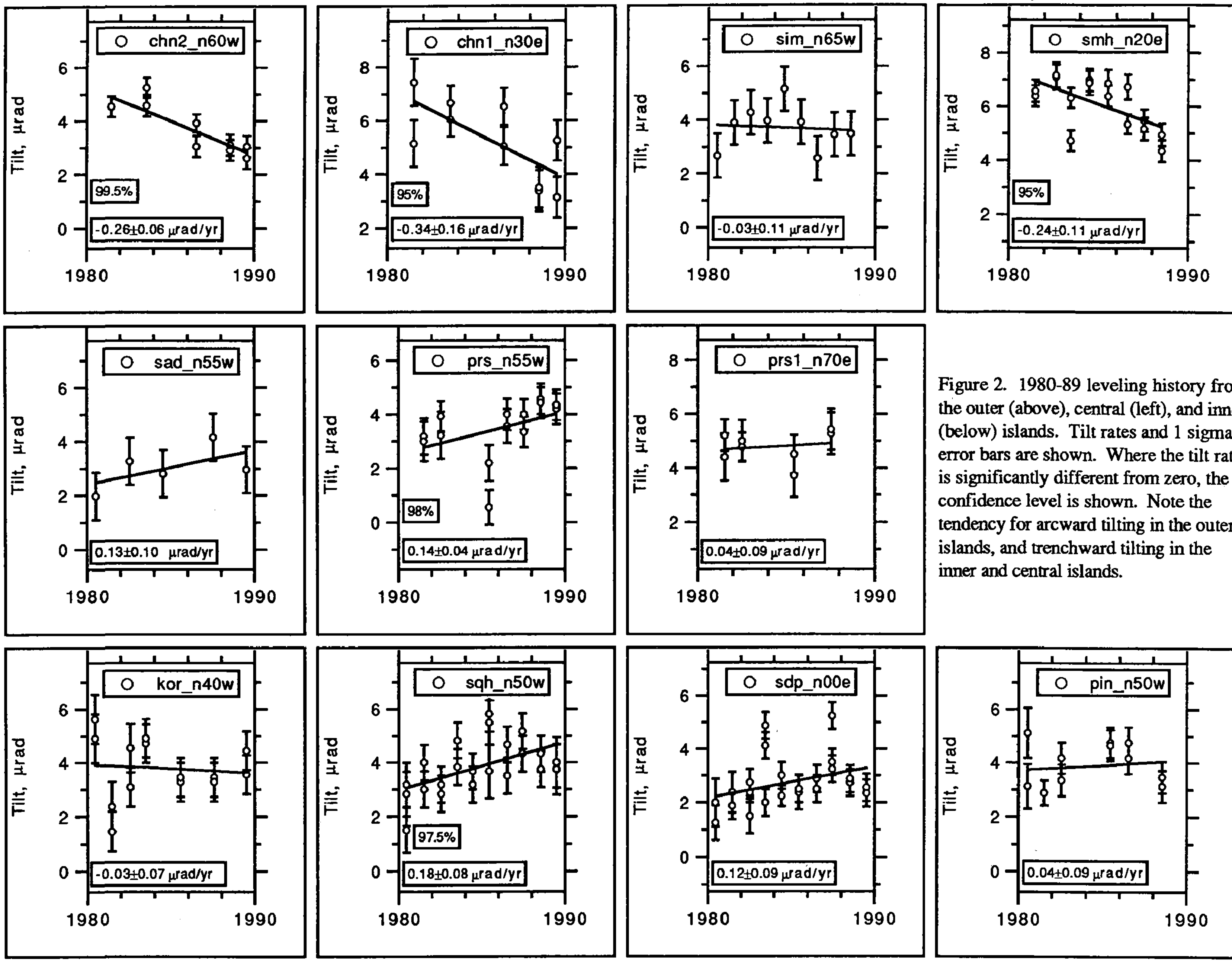

Figure 2. 1980-89 leveling history from the outer (above), central (left), and inner (below) islands. Tilt rates and 1 sigma error bars are shown. Where the tilt rate is significantly different from zero, the confidence level is shown. Note the tendency for arcward tilting in the outer islands, and trenchward tilting in the inner and central islands.

priority in 1990. However, another new pair of lines was installed in 1989 near the northwestern tip of the island; first epoch measurement of these lines will also receive high priority in 1990.

Tilt Accumulation in the Shumagin Islands

Seven of the eleven lines in the Shumagin Islands were remeasured in 1989. The 1980-89 leveling data and inferred tilt rates are shown in Figure 2 and Table 1. Despite the relatively high error estimates on individual data points, consistent trends are shown on most of the lines and several of these are significantly different from zero at high confidence level. Note the pronounced tendency for arcward tilting in the outer islands, and trenchward tilting in the central and inner islands. The addition of the 1989 data points has not changed this pattern significantly since last year, though some of the estimated tilt rates have changed slightly.

Table 1. Shumagin 1980-89 tilt rates

Site	Interval	Rate (μrad/yr)*	Azimuth*	Confidence
Inner Shumagins				
SQH/SDP	1980-89	0.18±0.08	-48°±43°	95%
PIN	1980-88	0.04±0.09	NW†	-
KOR	1980-89	-0.03±0.07	NW†	-
Central Shumagins				
PRS/PRS1	1981-89	0.20±0.09	-9°±22°	95%
SAD	1980-89	0.13±0.10	NW†	-
Outer Shumagins				
SIM/SMH	1980-88	-0.24±0.09	18°±26°	95%
CHN1/CHN2	1980-89	-0.43±0.13	-7°±14°	98%

* Positive rates indicate relative uplift towards the given azimuth
† Level line in only one azimuth, so tilt determined only in that azimuth
Errors quoted are 1 standard deviation

References

Beavan, J., R. Bilham & K. Hurst, 1984. Coherent tilt signals observed in the Shumagin seismic gap; detection of time dependent signals at depth?, J. geophys. Res., 89, 4478-4492.

Beavan, J., K. Hurst, R. Bilham & L. Shengold, 1986. A densely-spaced array of sea-level monitors for the detection of vertical crustal deformation in the Shumagin seismic gap, Alaska, J. geophys. Res., 91, 9067-9080.

Beavan, J., 1988. Crustal Deformation Measurements in the Shumagin Seismic Gap, Alaska, USGS Open File Report, 88-673, 183-188.

Beavan, J., 1989. Crustal Deformation Measurements in the Shumagin Seismic Gap, Alaska, USGS Open File Report, 89-453, 181-184.

Hudnut, K.W. and J.J. Taber, 1987. Transition from double to single Wadati-Benioff seismic zone in the Shumagin Islands, Alaska, Geophys. Res. Lett., 14, 143-146.

Lisowski, M., J.C. Savage, W.H. Prescott and W.K. Gross, 1988. Absence of strain accumulation in the Shumagin seismic gap, Alaska, 1980-1987, J. geophys. Res., 93, 7909-7922.

Error Analysis and Network Design in GPS Measurement of Crustal Deformation

14-08-0001-G1335

Yehuda Bock
Institute of Geophysics and Planetary Physics
Scripps Institution of Oceanography
La Jolla, CA 92093
(619) 534-5292

Objectives:

Understanding the structure and geometry of seismogenic zones is a key element in the prediction of earthquakes. Geodetic measurements contribute to this understanding through the mapping of present-day crustal deformations. Three-dimensional relative-positioning using the Global Positioning System (GPS) appears to be the most accurate and cost-efficient method for measuring crustal deformations over distances of tens to hundreds of kilometers. The objective of our research is to investigate sources of error and optimum analysis techniques for high-precision GPS measurements. Progress in these areas will lead directly to more accurate measurement of deformation in areas of high seismogenic potential.

Investigations undertaken:

Our investigations of the last six months have focused on three primary areas:

(1) continuation of the measurements and analysis of GPS data from a crustal deformation network in central and southern California as described in earlier reports. We have completed the analysis of the data collected in March 1988 and have collected new measurements in March 1989 with our colleagues at Cal Tech, UCSD and UCLA. We have computed preliminary estimates of stations velocities from the data collected between the period December 1987 through March 1988. These estimates agree well with velocities determined from VLBI measurements for baselines crossing the San Andreas fault (Murray et al., 1988; 1989). Analysis of the March 1989 data is currently in progress. We are preparing a journal article describing our results to date including an analysis of crustal deformations [Murray and Bock, in preparation]. This ongoing work is being done in collaboration with investigators at MIT.

(2) analysis of the USGS Parkfield GPS network. We are currently analyzing the two-year GPS time series collected by USGS at four stations in the vicinity of Parkfield (W. Prescott, personal communication). The baselines are several kilometers in length, in a range where modeling of the ionospheric delay should be beneficial in more accurate monitoring of deformations. The baselines are too long to analyze using L1 and L2 frequency data independently (since residual ionospheric delays start becoming significant) and too short to use the ionosphere-free linear combination (since amplification of the phase error in forming the linear combination is larger than the residual ionospheric delay). We are using hybrid observables [Schaffrin and Bock, 1988; Dong and Bock, 1989] which are a combination of L1, L2 observations and constraints on the ionosphere based on ionospheric models, available externally and/or derived from an internal calibration of the GPS data. The solutions using these observables will be compared to the L1 and L2 independent and ionosphere-free solutions, as well as to the solutions by Prescott's group at Menlo Park.

(3) establishment of a continuously monitoring array of GPS observatories in central and southern California. We will elaborate below on this aspect of our research.

Continuous Monitoring of Deformations with GPS

(1) Background

Investigators at four universities (Caltech, MIT, UCLA and UCSD) and JPL, in collaboration with USGS and NGS, are planning to establish and maintain an array of ten or more continuously and remotely operating GPS receivers in central and southern California by early 1990 (Figure 1). In this concept, GPS observations are made continuously for an indefinitely long period of time in search of precursory deformation of some sort, particularly related to the earthquake cycle. If phase lock can be maintained, phase ambiguities on the network baselines need to be resolved only once and relative station positions can be constrained so that deformations can be analyzed continuously at temporal scales as short as several minutes. The original network design consists of primarily Rogue SNR-8 GPS receivers linked to a central data collection and analysis facility by high speed modems.

The scientific motivations for continuous monitoring are (1) establishing a reference network for rapid, frequent resurveys of dense networks in central and southern California; (2) detection and analysis of steady and transient strains; (3) studying strain over a broad spectrum of spatial and temporal scales; and (4) studying the three-dimensional strain tensor (horizontal and vertical). Ultimately, we seek to understand underlying physical phenomena, particularly the physics of the earthquake process.

The technical motivations for continuous monitoring are (1) determining the long-term positional accuracy of GPS geodesy; (2) understanding periodic, non-random signatures in GPS data; (3) determining the "instrument response" of GPS hardware (receivers and antennas); (4) improving the signal-to-noise ratio for baseline estimation; (4) developing optimal and rapid analysis techniques; and (5) studying monumentation and site stability issues. The overall goal is to separate the geophysical signal from the geodetic noise, rapidly and confidently.

(2) Current Activities

We are currently analyzing 14 months of continuously monitored GPS observations collected at a ten station network in the Kanto-Tokai district in Japan by the National Research Center for Disaster Prevention [Fujinawa et al., 1989]. This is the first and currently only such network in the world. We are using this data set as a basis for developing data processing, data handling and data archiving algorithms for use in the California network. The goal is to develop rapid and efficient techniques to handle large quantities of continuously monitored GPS data, and to be able to detect confidently any temporal strain events for time periods as short as several minutes.

As part of the processing, we need to remove systematic errors due to errors in the satellite ephemerides. We have established a data link to the National Geodetic Survey to collect orbit tracking data collected by Mini-Mac 2816 AT GPS receivers in Massachusetts, Florida and California. This data will be analyzed simultaneously with data collected by the continuously monitoring sites in California to eliminate orbital errors as described for example in Dong and Bock [1989]. Therefore, a byproduct of the California network will be accurate orbital ephemerides for use by other investigators in the western United States. Any investigator will be able to do GPS surveys in central and southern California with as little as one receiver and know that there is a continuously recording station within 100 kilometers, and accurate satellite ephemerides available.

Along with many other investigators, we are preparing for a demonstration next month (November 1989) of the continuously monitored GPS network.

References:

Dong, D. and Y. Bock (1989). "Global Positioning System network analysis with phase ambiguity resolution applied to crustal deformation studies in California," J. Geophys. Res., 94, 3949-3966.
Fujinawa Y., S. Shimada, T. Kishii, S. Sekiguchi, T. Eguchi, Y. Okada and S. Watada (1989). "Some results in the preliminary data analysis of the fixed-point GPS baseline determination network in Central Japan," presented at International Association of Geodesy General Meeting, Edinburgh, Scotland, 3 to 12 August.
Murray, M.H., Y. Bock, D. Dong, K.L. Feigl and R.W. King (1988). "Assessing the long-term repeatability and accuracy of GPS: Analysis of four campaigns in California," Eos Trans., 69, 1151.
Murray, M.H., Y. Bock, D. Dong and R.W. King (1989). "Assessing the long-term repeatability and accuracy of GPS: analysis of five campaigns in California," presented at International Association of Geodesy General Meeting, Edinburgh, Scotland, 3 to 12 August.
Schaffrin, B. and Y. Bock (1988). "A unified scheme for processing GPS dual-band phase observations," Bull. Geod., 62, 142-160.

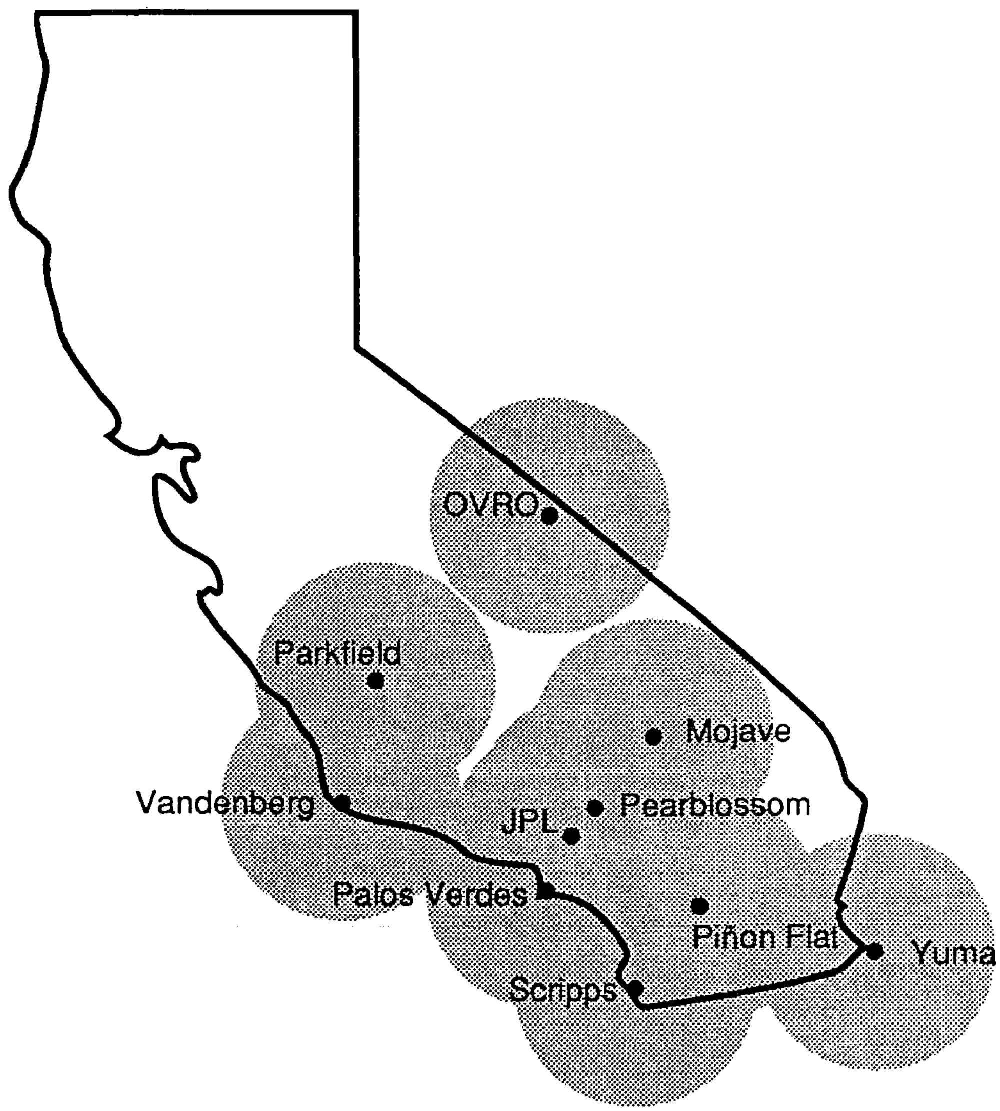

Continuously Monitoring GPS Network in Central and Southern California
(100 kilometer radius indicated for each site)

FAULT ZONE TECTONICS

9960–01188

Sandra Schulz Burford
Branch of Tectonophysics
U.S. Geological Survey
345 Middlefield Road, MS/977
Menlo Park, California 94025
(415) 329–4814

Investigations

1. Directed maintenance of creepmeter and alinement array networks in California.
2. Updated archived creep data on USGS ISUNIX LOW FREQUENCY computer.
3. Monitored creepmeter data for possible earthquake precursors, primarily in the Parkfield, California area, site of the USGS– California State earthquake prediction experiment.
4. Started development of a soil–moisture monitoring system to be deployed at Parkfield creepmeter sites.

Results

1. Currently 30 extension creepmeters, one contraction meter, and 7 strong–motion creepmeters are operating; 22 of the extension meters, the contraction meter, and all 7 strong–motion meters have on–site strip chart recorders. Of the total 38 instruments, data from 29 are telemetered to Menlo Park (Figures 1, 2).

   Due to a combination of budget cuts and the loss of key personnel, surveys of the alinement array network will be discontinued for the foreseeable future.

2. Fault creep data from USGS creepmeters along the San Andreas, Hayward, and Calaveras faults have been updated through September 30, 1989, and stored in digital form (1 sample/day). Telemetry data are also stored in digital form (1 sample/10 minutes), and can be merged with daily–sample data to produce long– or short–term plots.
3. The combination water level drops/creep events at Parkfield's Middle Mountain we described in our semi–annual technical report for October 1, 1988 through March 31, 1989, continue to occur. An effort is now underway to study a possible statistical correlation between these dual events and seismicity in the area.
4. Because creepmeters are buried at shallow depths, rainfall contaminates the instrument signal. However, rainfall effects are not predictable - at some sites, rainfall apparently

will trigger left–lateral movement, while at others it appears to accelerate right–lateral movement. At one site, onset of rainfall coincided with onset of a 3–month cessation of all creep activity. A record of moisture readings taken at regular intervals from near the instrument piers could prove helpful in filtering rainfall noise from the signal.

Toward that end, an electrical circuit was designed by Alan Jones to utilize several recently–acquired soil moisture blocks in an experiment to gather soil moisture data from around the Parkfield creepmeter sites. Several circuit boards have been loaded and are being tested in the lab. When funds permit, several soil moisture blocks will be deployed at the Taylor (XTA1) creepmeter site, and the data sent at 10–minute intervals via satellite telemetry to Menlo Park headquarters.

Reports

No papers were published during the reporting period.

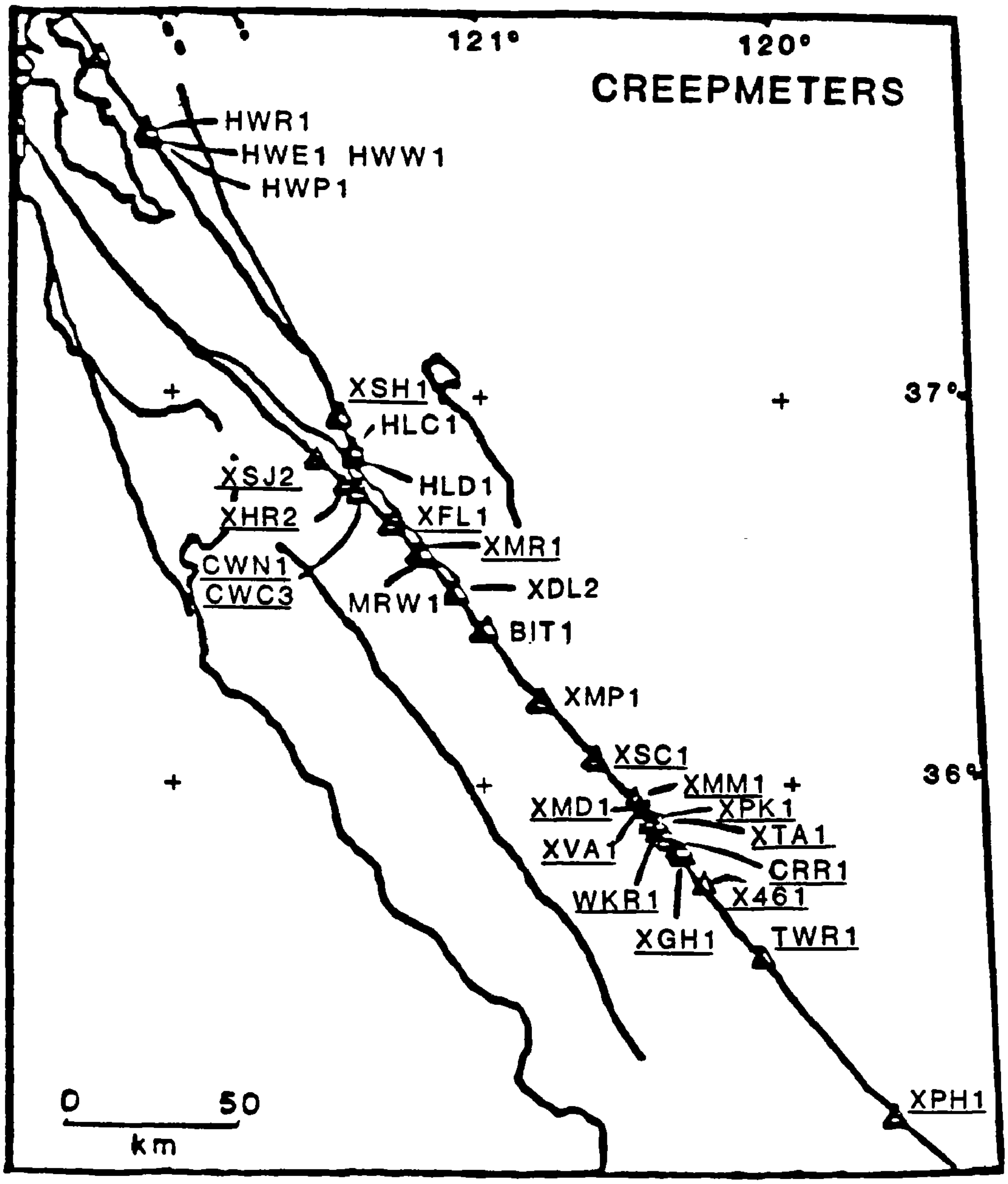

FIGURE 1

USGS creepmeter stations in northern and central California. Instruments with underlined names transmit on telemetry. NOT SHOWN: XRSW, XHSW on the Southwest Fracture near Parkfield (See Figure 2). Strong-motion creepmeters are located in vaults at XMM1, XMD1, XVA1, XTA1, X461, XRSW, and XHSW.

Creep and Alinement : Parkfield, CA

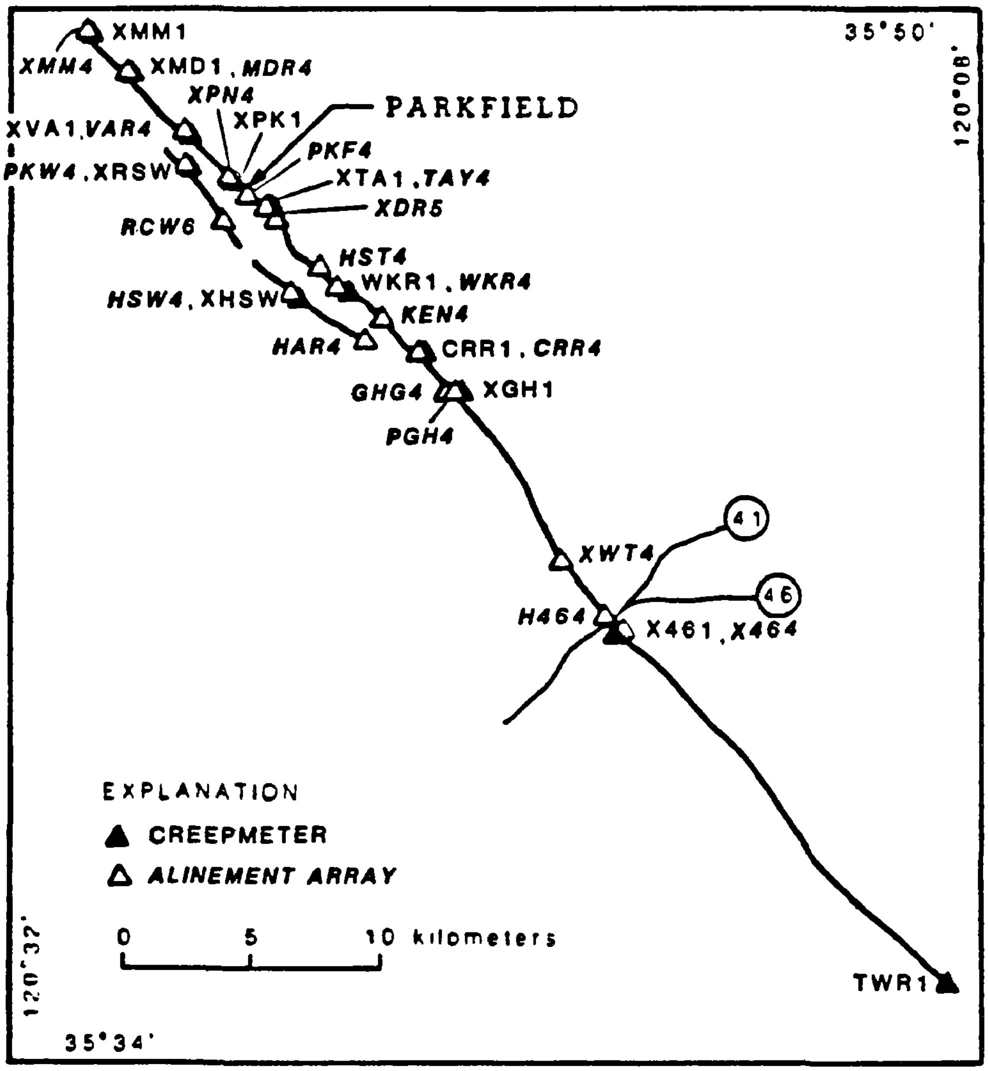

CREEPMETER AND ALINEMENT ARRAY SITES IN PARKFIELD
MARCH 1988

FIGURE 2

Remote Monitoring of Source Parameters for Seismic Precursors

9920-02383

George L. Choy
Branch of Global Seismology and Geomagnetism
U.S. Geological Survey
Denver Federal Center
Box 25046, Mail Stop 967
Denver, Colorado 80225
(303) 236-1506

Investigations

1. NEIC Reporting Services. Broadband data are used routinely to increase the accuracy of some reported parameters such as depth and to compute additional parameters such as radiated energy. These parameters are published in the Monthly Listing of the Preliminary Determination of Epicenters.

2. Rupture Process of Large- and Moderate-Sized Earthquakes. We are using digitally recorded broadband waveforms to characterize the rupture process of selected intraplate and subduction-zone earthquakes. The rupture processes thus delineated are used to complement seismicity patterns to formulate a tectonic interpretation of the epicentral regions.

3. Teleseismic Estimates of Radiated Energy and Strong Ground Motion. On a worldwide basis, the relative paucity of near-field recording instruments hinders the prediction of strong ground motion radiated by earthquakes. We are developing a method of computing radiated energy and acceleration spectrum from direct measurements of teleseismically recorded broadband body waves. From our method, the maximum expectable spectral level of acceleration and lower bounds of stress drops can be made for any event large enough to be teleseismically recorded.

Results

1. Reporting Services. The NEIC now uses broadband waveforms to routinely: (1) resolve depths of all earthquakes with $m_b > 5.8$; (2) resolve polarities of depth phases to help constrain first-motion solutions; and (3) present as representative digital waveforms in the monthly PDE's. In the Monthly Listings of the Preliminary Determination of Epicenters covering the interval October 1988-March 1989, depth phases from broadband data were computed for 31 earthquakes; radiated energies were computed for 29 earthquakes.

2. Rupture Process of Earthquakes. We have modeled the rupture process of three large earthquakes that occurred within an interval of 12 hours at Tennant Creek, Australia on January 22, 1988, by using broadband data, strong constraints on earthquake location (provided by the Warramunga Array) and observed surface deformation. From the derived complexity of rupture and history of stress release, we conclude that the occurrence of multiple main shocks is not an uncommon mode of rupture in intraplate environments. A study of the Armenian earthquake of 7 December 1988 is under way in

collaboration with the German Geological Survey. With broadband data we can resolve the time delays and relative locations of three subevents. From the distribution of aftershocks we infer that the causative faults have different strikes, delineating a fault zone that has a bend.

3a. Subduction-Zone Events. We have compiled the log-averaged P-wave acceleration amplitude spectra from teleseismic data for a set of large, shallow-focus subduction-zone earthquakes. The events range in size from the magnitude 6.2 to 8.1. The acceleration spectra, corrected for frequency-dependent attenuation and the modulation of depth phases, are approximately flat from 10 secs to 2-3 seconds, falling off somewhat at high frequencies. The radiated energies of these earthquakes are proportional to the seismic moments, but the high-frequency acceleration levels are more strongly proportional to the asperity areas than the seismic moments of the earthquakes.

3b. Intraplate Events. We have applied our algorithm for the computation of acceleration spectra to a series of shallow intraplate earthquakes. Most of these events are characterized by a flat spectral level at high frequencies but an intermediate slope before an ω^2 falloff at low frequencies. The high-frequency spectral levels of these intraplate earthquakes are the same as the levels of subduction-zone earthquakes with the same seismic moments, although the spectral shapes are different.

Reports

Boatwright, J., and Choy, G. L., 1989, Acceleration spectra for subduction zone earthquakes: Journal of Geophysical Research (in press).

Boatwright, J., and Choy, G. L., 1989, Source spectra and stress drop of shallow thrust earthquakes obtained from teleseismic recordings [abs.]: in Abstracts of the 25th General Assembly of IASPEI, p. 242.

Choy, G. L., 1989, Interpretation of the earthquake mechanism from analysis of digitally recorded broadband seismograms [abs.]: Abstracts of the 25th General Assembly of IASPEI, p. 312.

Choy, G. L., and Bowman, J. R., 1989, Rupture process of a multiple main shock sequence near Tennant Creek, Australia [abs.]: EOS (American Geophysical Union, Transactions), v. 70, p. 397.

Choy, G. L., and Bowman, J. R., 1989, The rupture process of a multiple main shock sequence--Teleseismic, local and near-field analysis of the Tennant Creek earthquakes of 22 January 1988: Journal of Geophysical Research (submitted).

Choy, G. L., and Kind, R., 1989, A preliminary broadband body-wave analysis of the Armenia S.S.R. earthquake of 7 December 1988 (in preparation).

Sipkin, S. A., and Choy, G. L., 1989, Routine determination of seismic source parameters using digital data at the NEIC [abs.]: Abstracts of the 25th General Assembly of IASPEI, p. 282.

Analysis of Natural Seismicity at Anza

9910-03982

Joe Fletcher and Linda Haar
Branch of Engineering, Seismology, and Geology
U.S. Geological Survey
345 Middlefield Rd.
Menlo Park, CA 94025
(415) 329-5628

Investigations:

A primary objective of the Anza project is to obtain a large data set of 3-component digital seismograms from small earthquakes ranging in size from microearthquakes to large damaging shocks. These data are then used to analyze both the generation and propagation of high-frequency seismic waves. This part of the project centers on the maintenance of the 10-station digital array at Anza, the routine calculation of source parameters from high-quality seismograms, and the updating of the computer data bases that include both the source parameters for local events and the digital time series.

Results:

We have processed 865 events since the array began operation. These events are included in the Anza data base which is now complete through December of 1988. Data base source parameters include origin time, location, moment, source radius, stress drop, apparent stress and energy. Figure 1 shows epicenters for these 865 events. Figure 2 shows the epicenters for the events recorded from August 1988 through December 1988. Activity at the Cahuilla hot spot and uder Torro Peak has resumed in this time period, with much of the remaining seismicity continuing to occur in previously defined clusters (Fletcher *et al.*, 1987). Seismicity has decreased to the south of the array, with a no events occuring between the San Jacinto Fault and the Coyote Creek Fault.

References

Fletcher, J., Haar, L., Hanks, T., Baker, L., Vernon, F., Berger, J., and Brune, J., 1987, The digital array at Anza, Caklifornia: Processing the initial interpretation of source parameters, *Journal of Geophysical Research*, 92, p. 369-382.

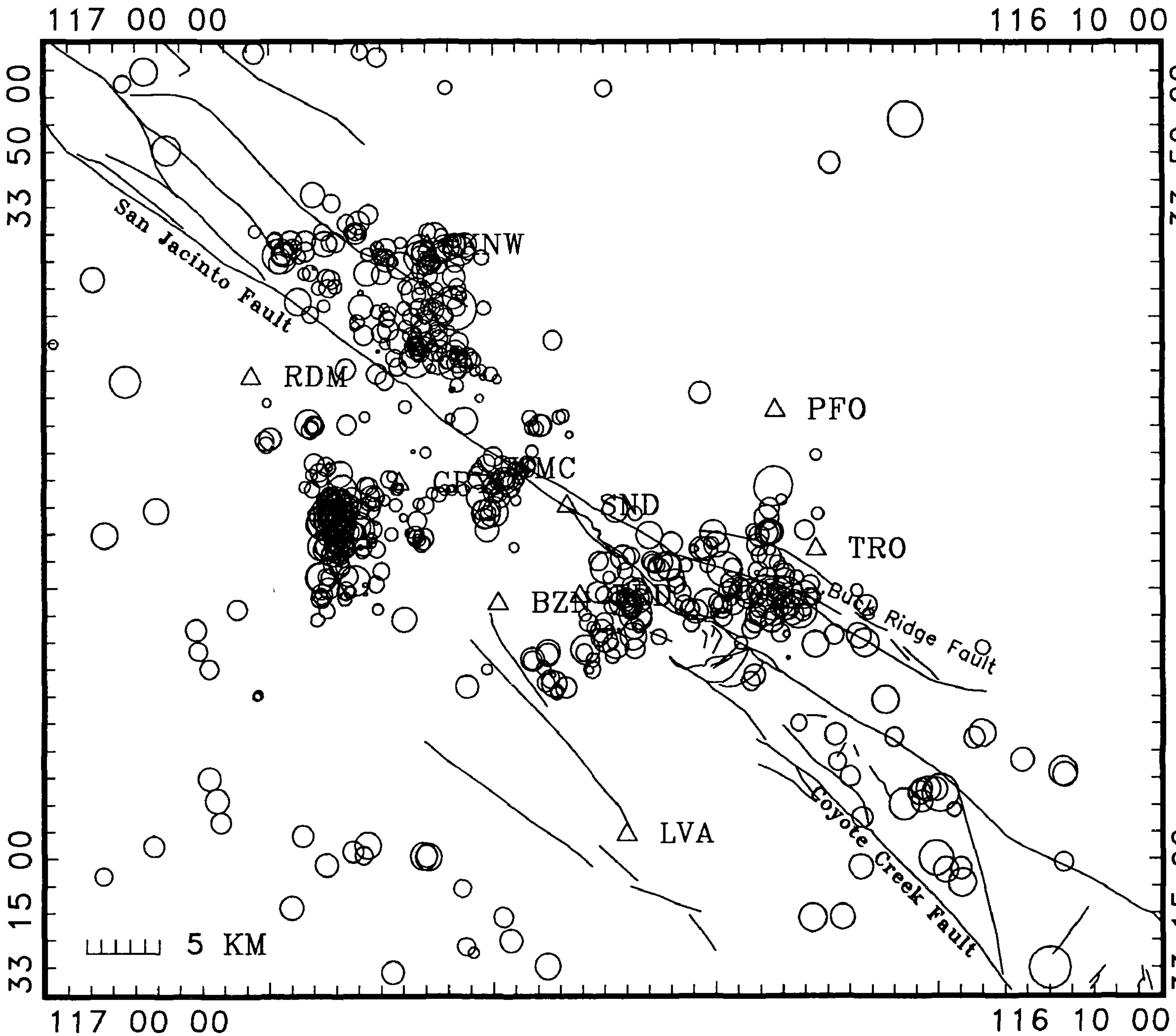

Figure 1. Plot of all epicenters in Anza data-base. Circles are proportional to moment. Anza array stations are shown by triangles.

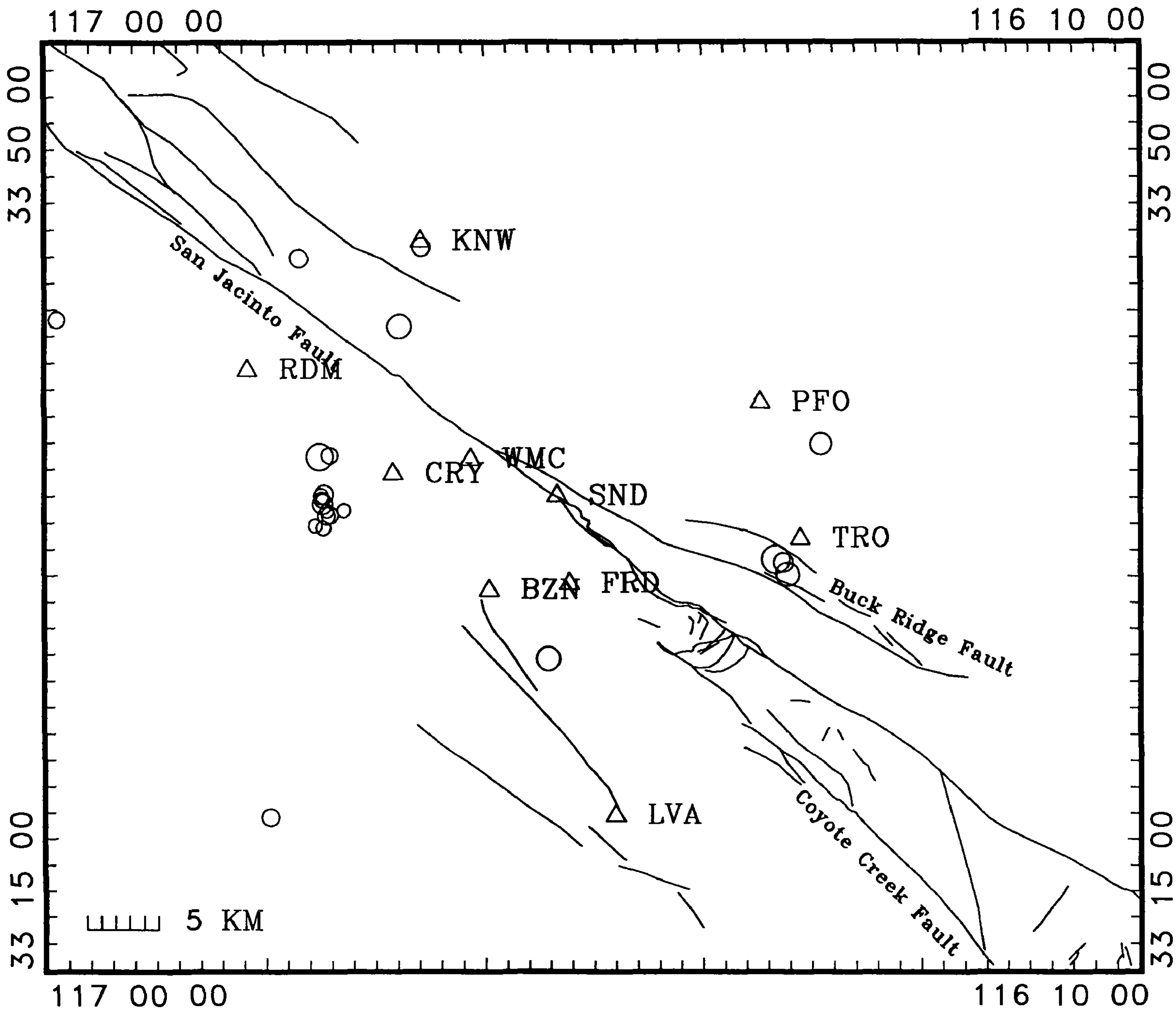

Figure 2. Epicenters for the events recorded from August 1988 through December 1988. Circles are proportional to moment. Anza array stations are shown by triangles.

Southern California Earthquake Project
9-9930-01174

Thomas H. Heaton
Branch of Seismology
U.S. Geological Survey
525 S. Wilson Ave.
Pasadena, CA, 91106
FAX: 818-405-7827

Introduction

This project covers almost all of the activities of the Pasadena Office of the U.S. Geological Survey. For FY89 three preexisting projects have been combined into this one project. The former projects were: 1) the Southern California Co-operative Seismic Network Project 9930-01174 (project chief Charles Koesterer), the Southern California Earthquake Hazard Assessment Project 9930-04072 (project chief, Lucille Jones), and the Seismic Waveform Analysis Project 9930-03790 (project chief Thomas Heaton). The present project is a large and complex project that includes the operation of the 250-station Southern California Seismic Network (SCSN), response to major southern California earthquake sequences, and basic research in earthquake physics.

Investigations

1. Operation, maintenance, development and recording of the Southern California Seismic Network consisting of 208 U.S.G.S. telemetered seismometers and 66 seismometers telemetered from other agencies. All stations are recorded on the CUSP digital analysis system.

2. Routine Processing of Southern California Network Data. Routine processing of seismic data from stations of the cooperative southern California seismic network was continued for the period April 1989 through September 1989 in cooperation with scientists and staff from Caltech. Routine analysis includes interactive timing of phases, location of hypocenters, calculation of magnitudes and preparation of the final catalog using the CUSP analysis system. About 800 events were detected in most months with a regional magnitude completeness level of 1.8. The largest earthquake this recording period was the M_L= 4.5 Montebello earthquake of June 12, 1989 in the Los Angeles basin.

3. Investigation of Southern California Earthquake Sequences. A final report has been completed for the study of the M_L=4.9 Pasadena earthquake of December 3, 1988 and work is continuing on a study of the M_L=5.0 Malibu earthquake of January 19, 1989. The detailed studies include determination of focal mechanisms for $M \geq 3.0$ aftershocks, inversion of these data for changes in the state of stress, and comparison of the results to the geologic structures to better understand

the seismotectonic structure of southern California.

4. Rate of Earthquake Activity in the Los Angeles Basin. Recently, the Los Angeles metropolitan region has experienced numerous felt earthquakes. This apparent increase prompted an analysis of the Caltech/USGS earthquake catalog for the region within 40 km of west Los Angeles (34° 0.0' N, 118° 20.0' W) and for the time period from 1975 to present. The study addresses changes in the rate, b-value and depths of the earthquake activity under Los Angeles, and implications for the regional earthquake hazard.

5. Document programs written by various persons to analyze CUSP data.

6. Examine the nature of Lg and Rg propagation in California using seismograms recorded on the short-period California regional networks.

7. Study of the source complexity of the 1987 Whittier Narrows earthquake by waveform inversion of the strong motion records.

8. Source study of the 1978 Tabas, Iran, intraplate earthquake by the inversion of strong motion and teleseismic records.

9. Modeling of the strong motion records for the 1986 North Palm Springs earthquake using interpolated empirical Green's functions.

10. Waveform Studies of small events in the Imperial Valley. P waveforms of small aftershocks of the Elmore Ranch and Superstition Hills earthquakes were studied for information about velocity structure and source depth. Using numerous aftershocks recorded at several stations, the seismograms can be lined up to form record sections spanning a 10 to 50 km distance range (Fig. 2). The coherent arrivals which can be seen across this distance range are identified as the direct P and the multiple free surface reflections of P (PP, PPP, possibly PPPP). Comparisons of the multiple P waves with synthetics calculated for flat-layered structures, can be used to determine the shallow velocity gradient. The spacing and amplitude of the multiple P waves at the closer distances (10 to 20 km) can be used to help constrain the source depth.

11. Network Instrument Calibrations. There is a continuing effort to obtain and document information on network instrumentation. Randomly recorded calibration pulses have been analyzed for the natural frequency and damping of the seismometer and the overall gain of the system. Reliable calibration information is essential for converting seismic data to true ground motions for various purposes, such as magnitude determinations, moment and stress drop estimates and site response studies.

Results

1. Operation and maintenance of field stations and recording systems continued with little failure during this reporting period. Time varying attributes of the system are completely recorded on a data base (DBASE III). Documentation of the system and changes to the system continued to be developed by the preparation of semi-annual network bulletins (Given et al., 1989).

2. Routine Processing of Southern California Network Data. The projects to upgrade the southern California seismic network are continuing. Documentation of local earthquake analysis programs (LEAP) available at the southern California seismic network facilities has been completed and open filed. To increase the accessibility and research potential of the seismic data, a series of semi-annual Network Bulletins have been issued since 1985. These bulletins provide information about how to access data from the network, problems with the data, details of the processing computer systems, and earthquakes in southern California. As part of this project, documentation of past and present station configurations has been compiled.

3. Investigation of Southern California Earthquake Sequences. The Pasadena earthquake (M_L=4.9) occurred on 3 December 1988, at 34° 8.5' N, 118° 8.0' W, at a depth of 15.6 km, less than 1 km northwest of the Caltech campus. The hypocenters of the earthquake and its aftershocks define a east-northeast-striking, steeply northwest-dipping surface that projects up to the active surface trace of the Raymond fault. The focal mechanism of the mainshock determined from first motion polarities can be interpreted as dominantly left-lateral strike-slip motion on a plane striking N67°E and dipping 75° to the north. A very slight rake of 4° indicates a minor component of reverse slip. This plane parallels the Raymond fault and is consistent with geomorphic and paleoseismic evidence that the Raymond fault is dominantly a left-lateral strike-slip fault. The existence of a component of sinistral slip along the Raymond fault had been suspected prior to the earthquake, but the northward dip of the fault and the prominent scarp along the western portion of its trace had led most workers to conclude that slip along the fault was dominantly reverse. In fact, the geomorphic expression of the fault and shallow exposures of the fault zone provide a strong basis for the argument that the fault is dominantly left-lateral.

4. Rate of Earthquake Activity in the Los Angeles Basin. The rate of background seismicity in Los Angeles, within a circle, 40 km in radius, centered on 34° 0' N, 118° 20' W, in the Baldwin Hills, has been evaluated using the methodology of Matthews and Reasenberg (1988). From 1975 to June 1989, the average rate of magnitude 2.3 or greater earthquake sequences was 22 per year, with variations from 14 events per year to 60 events per year. The only statistically significant variation in rate occurs for an interval ending at the end of the sample (July

1, 1989) and starting 3.3 years earlier in March 1986. The rate since March 1986 has been 1.75 times greater than the rate from 1975 to March 1986. A similar increase has not been seen in the rest of southern California. The increased activity includes the 1987 Whittier Narrows earthquake (M_L=5.9).

Coincident with the change in rate of earthquake activity has been a change in both the depth of the earthquakes and the b-value (the exponent in the magnitude-frequency relationship, $N=10^{-bM}$. The median depth of faulting within this region of increased seismicity has decreased from 7 km to 9.5 km and the third quartile has dropped from 9 km to 13 km. The depths of these earthquakes have been recalculated using all available phase data and regionally appropriate velocity models. Although the median depth of faulting has become deeper, the maximum depth of faulting has not increased significantly. Rather, the maximum depth of faulting has stayed at about 16--17 km but the number of earthquakes occurring between 10 km and 17 km and the magnitudes of those earthquakes has gone up dramatically. In addition, the shallowest parts of the basin (above 4 km) has become quiet with all but 4 of the earthquakes since 1986 occurring below 4.0 km The b-value calculated by the maximum likelihood method over a one year smoothing kernel shows a decrease over the last three years. The b-value has decreased from a 15 year average of 0.91 to 0.72. The first standard deviation of the latest value has just reached the median 0.91.

The greatest concentration of excess earthquakes in the last three years is in the Pasadena--Whittier area (Figure). The rate of activity in this region went from 2 to 8 M≥2.3 events per year, excluding aftershocks but including the Whittier Narrows M_L=5.9, the 1988 Pasadena M_L=4.9 and 1989 Montebello M_L=4.5, 4.3 earthquakes. North of the Los Angeles basin, several smaller earthquakes (largest is M=3.3) were recorded near the aftershock zone of the 1971 San Fernando earthquake leading to increased seismicity in that region. The west side of Los Angeles including the area along the Torrance-Wilmington anticline, offshore in the Santa Monica Bay and along the Palos Verdes Peninsula, has also been particularly active. The largest of these earthquakes was the M_L=5.0 1989 Malibu earthquake, but most of the events in this cluster have been small.

5. Thirty-three programs were documented specifically for researchers and those wishing to use CUSP data. These programs were previously written by various persons to accomplish a variety of tasks from obtaining the digital record from a magnetic tape to plotting the records, making maps, determining focal mechanisms and much more. Each program is briefly described, the input and output files identified, and some common errors and their source mentioned. In addition, an example run of each program is included.

6. We have shown that a short-period regional network can be a valuable source of information with surprising applications. Profiles of Lg and Rg codas, both parallel and perpendicular

to the direction of propagation, were constructed. Groups of records from different regions in California were also observed. Lg and Rg phases react very differently to various crustal changes and heterogeneities in California, Lg being much more sensitive to the propagation path than Rg. Regional variations in the surface wavetrains including amplitudes, coda duration, shape of the energy envelope, frequency content, and sharpness of the phase initiation are clearly seen and can serve to distinguish different geological or structural areas. The amplitudes are low and the coherence poor in the Coast Ranges. The surface waves are amplified by travel through the Great Valley. The Sierra Nevada batholith produces clear, dominant Rg waves in the record, and there is an indication that the Basin and Range region has very large amplitude surface waves. The decreasing Moho depth near the Pacific Coast causes the amplitudes of both types of surface waves to decrease and possibly more high frequency energy to be lost out the bottom of the crust, supporting Kennett's (1986) theoretical results. The most interesting observation is the effect the San Andreas fault has of amplifying the surface waves in the fault zone followed by a decrease of amplitude after crossing the fault zone. This study has served to increase our understanding of the behavior of Lg and Rg waves in California using a dense regional network.

7. Inversion of the strong motion waveforms for the Whittier Narrows earthquake shows a complex source consisting of at least three areas of large slip. One of these regions is associated with the hypocenter and has a source radius of approximately 2 km. This source is surrounded by a region of minimum slip. The aftershocks fall within this minimum slip zone. Flanking the central source to the west and to the east are two other regions of large slip. Together the three large slip areas define a total source region with length 10 km and width 6 km. The maximum slip is close to 1 meter. The best fitting rupture velocity is 2.5 km/sec, and the moment is 1.0×10^{25} dyne-cm.

8. The 1978 Tabas, Iran, earthquake (Ms7.5) is a major intraplate event which was recorded both locally on strong motion instruments and teleseismically. Both of these data sets have been used in an iterative least squares inversion to obtain the best fitting slip distribution and rupture timing on a finite fault. The analysis shows most of the slip is shallow, above 12 km depth. The maximum slip is approximately 1.5 meters and is distributed in a complicated pattern of asperities. The total moment from the modeling of strong motion records and WWSSN P-waves is 5.0×10^{26} dyne-cm. This value is consistent with the results of other investigators, but is 1/3 to 1/2 of the moment estimated from long-period surface waves. These results suggest a heterogeneous stress distribution with the strong motion records and teleseismic body waves mainly sensitive to the high stress regions.

9. Research to date has pointed out the deficiencies of existing computer codes to calculate accurate Green's functions for

complex realistic structures. To avoid this problem work is continuing with Paul Spudich (Ground Motion and Faulting Branch) on the use of interpolated aftershock records as empirical Green's functions in source inversions. Application will be to the 1986 North Palm Springs earthquake. A good set of aftershocks was recorded for this event using GEOS instruments co-located with the existing strong motion stations. The inversion of the source using empirical Green's functions will be compared with previous work using more traditional methods.

10. Record sections were put together using aftershocks of the Elmore Ranch and Superstition Hills events. A comparison of the two sets of data showed P waves with similar time spacings between the multiple surface reflections. The preliminary conclusion is that the velocity gradients are approximately the same for the travel paths to the two faults, and that the source depths for the aftershocks are also about the same. Comparison with synthetic seismograms indicates a velocity gradient that varies from 1.8 to 5.6 km/sec in the upper 5 km. The source depths appear to be fairly shallow, in the 4 to 8 km range.

11. Analysis of random calibration pulses from 68 stations showed that most of the seismometers had acceptable natural frequencies of 1.0 to 1.15 hz. The damping appeared to be in the correct range of 70 to 80% of critical. Gains as determined from the calibration pulses were generally within 30% of the theoretical value for most of the stations, although there were a significant number of stations with larger discrepancies. The stations with unusual seismometers characteristics or large gain differences were inspected and several bad seismometers were found.

Additions were made to the on-line recording system to automatically determine Wood-Anderson amplitudes for larger (3.8 to 5.5) events using data from the low-gain and FBA stations. Synthesized Wood-Anderson records are created by deconvolving the short-period or FBA instrument response from the data and then convolving with the Wood-Anderson response. The Wood-Anderson waveforms from 14 low-gain and 4 FBA stations are available about 10-20 minutes following the event.

The procedure for calculating the Wood-Anderson magnitude was run on 27 previous events (M_L 3.8 to 5.4) of the past 18 months in order to determine stations corrections for all of the stations. Work is being done to incorporate the RTP locations so that the magnitudes can be determined automatically.

Publications

Given, D.G., L.A. Wald, L.M. Jones, and L.K. Hutton, 1989, The Southern California Network Bulletin; July to December, 1987, U.S. Geological Survey Open File Report, in press.

Heaton, T.H., 1989, Evidence for and implications of self-healing pulses of slip in earthquake rupture, manuscript, 42 p.

Hauksson, E. and L. M. Jones, 1989, The 1987 Whittier Narrows earthquake sequence in Los Angeles, southern California: Seismological and tectonic analysis, Journal of Geophysical Research, 94, 9569--9590.

Jones, L. M., K. E. Sieh, E. Hauksson, and L. K. Hutton, 1989, The December 3, 1988 Pasadena, California earthquake: Evidence for strike-slip motion on the Raymond fault, Bull. Seismol. Soc. Am., in press.

Kanamori, H., J. Mori, T H. Heaton, The December 3, 1988 Pasadena Earthquake (M_L 4.9) recorded with the Very-Broad-Band system at Pasadena, submitted to Bull. Seismol. Soc. Am.

Mori, J. and S. Hartzell, Source Inversion of the 1988 Upland, California earthquake: Determination of a fault plane for a small event, submitted to Bull. Seismol. Soc. Am.

Wald, L.A. and L.M. Jones (1989). LEAPing Into CUSP: Local Earthquake Analysis Programs for CUSP Data, U.S. Geol. Surv. Open-File Report 89-479.

Wald, L.A. and T.H. Heaton. Lg and Rg propagation on the California Regional Networks from the December 23, 1985 Nahanni earthquake, to be submitted.

Figure Captions

Figure 1. Contours of the ratio of the rates of seismicity ($M \geq 2.3$) from January 1, 1975 to March 1, 1986 and from March 1, 1986 to June 30, 1989. Each contour represents a 50% increase in the number of earthquakes/yr/km^2 between 3/1/86 and 6/30/89 as compared to the earlier time period, 1/1/75--3/1/86.

Figure 2. Seismograms for 30 events recorded on 1 to 4 stations near the aftershock zone of the Superstition Hills earthquake. This record sections spans a distance range of 15 to 55 km and shows the direct P wave and multiple surface reflections (PP, PPP, PPPP).

Figure 1

1975–Mar 1986 VS Mar 1986–June 1989

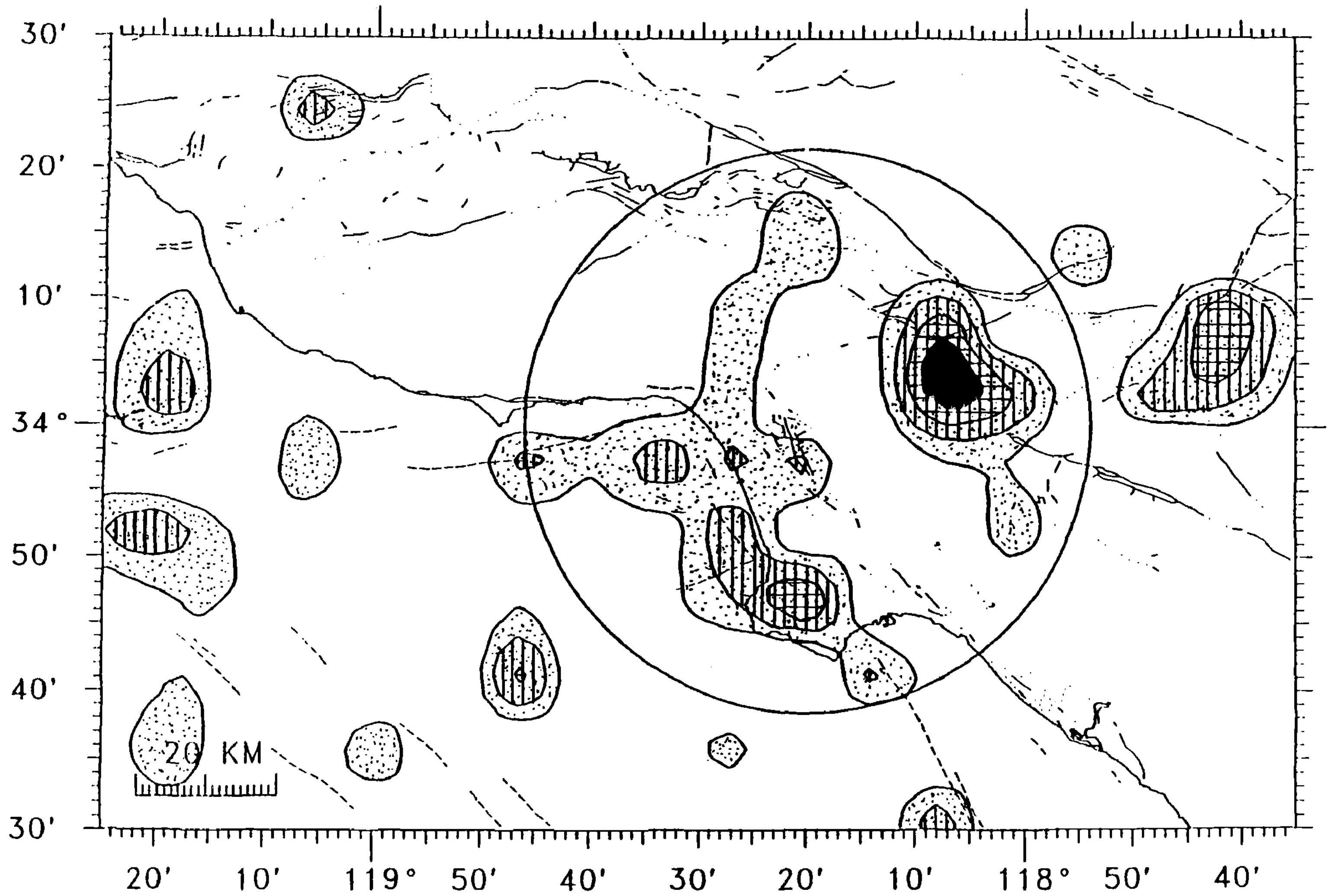

Figure 2

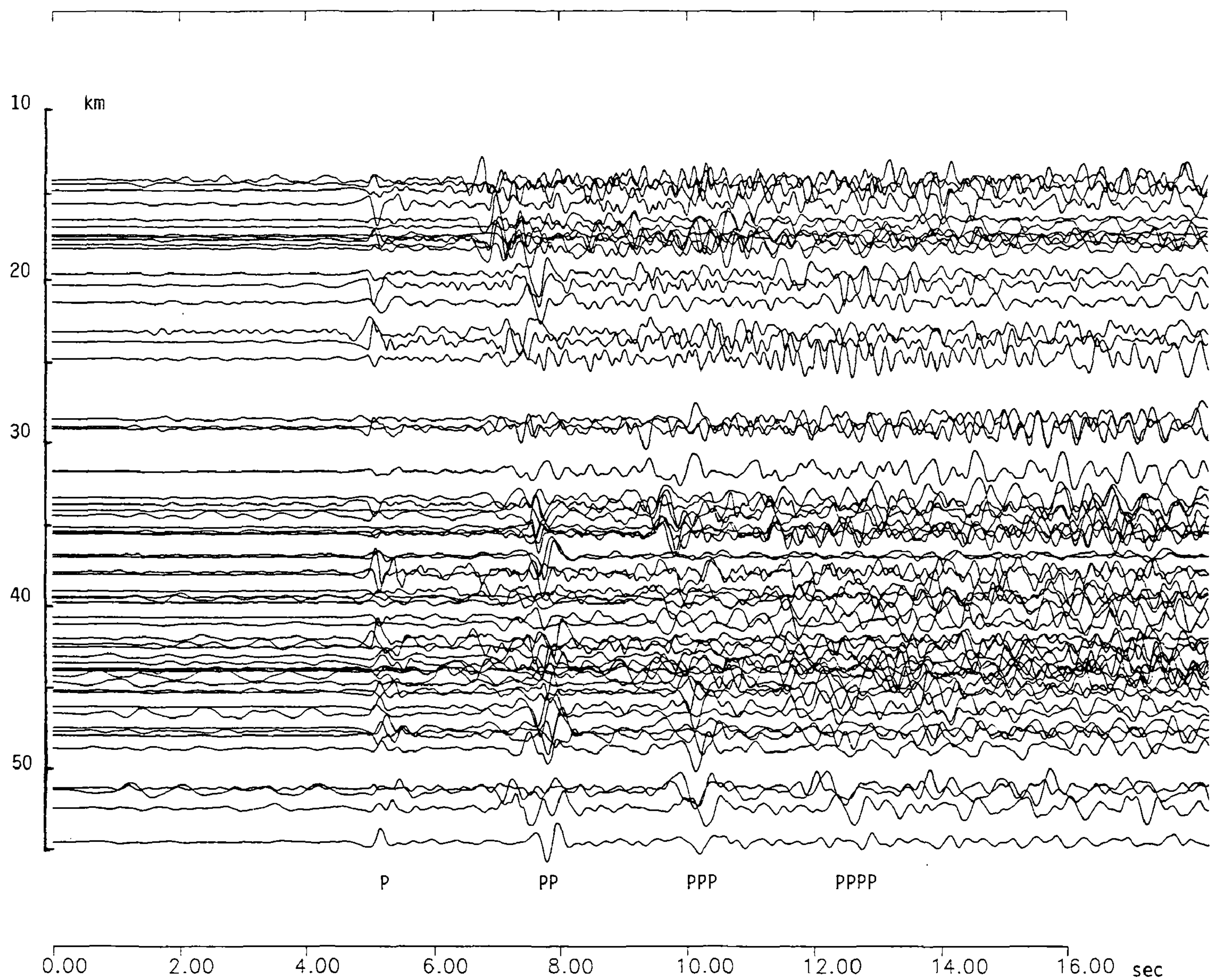
10
km
20
30
40
50
P
PP
PPP
PPPP
0.00
2.00
4.00
6.00
8.00
10.00
12.00
14.00
16.00
sec

ACTIVE SEISMIC STUDIES OF RECENT VOLCANIC SYSTEMS

9930-01496

David P. Hill

Branch of Seismology
U.S. Geological Survey
345 Middlefield Rd, MS 977
Menlo Park, CA 94025
(415) 329-4795

INVESTIGATIONS

For the past several years, this project has focused on the structure and seismo-magmatic processes beneath Long Valley caldera in eastern California. A substantial part of this effort has involved coordination of USGS monitoring, hazards assessment, and information dissemination activities associated with the ongoing unrest in the Long Valley-Mono Craters volcanic systems.

RESULTS

Mammoth Mountain earthquake swarm

Activity in the Long Valley region during the first half of 1989 was dominated by a persistent swarm of small earthquakes ($M < 3.5$) that began under Mammoth Mountain in early May and continues as this report is being written at the end of September. We have recorded a number of earthquake swarms under Mammoth Mountain since the seismic network became operational in mid-1982 but nothing that has sustained such a high rate of activity for so long (nearly four months at this writing). Most of these earlier swarms occurred in 1982 and 1983 and involved brief (a few hours) flurries of $M \leq 2$ earthquakes. Two of these earlier swarms included included a $M = 3$ event, one on September 15, 1983 the other on February 5, 1984. A modest increase in the rate of $M \approx 2$ events occurred during mid-July, 1984, and early September, 1985

The current activity began with several $M = 1$ events on May 4 followed by a gradual increase in both the rate of occurrence and in the size of the largest events -- much like an aftershock sequence running backwards. The activity rate picked up in early June and peaked on about June 12 with roughly 24 $M \geq 1$ and many more smaller events (see Figure S5). The largest event to occur in the sequence through the end of June was a $M = 3.3$ at 6:00 PM (PDT) on June 20 (a second $M = 3.3$ event occurred on August 1; these two $M = 3$ events are among the few in the sequence large enough to be locally felt so far). The activity rate during the last half of June fluctuated about the late May and early June levels.

Preliminary locations place most of these earthquakes beneath the southwest flank of Mammoth Mountain with a smaller number located beneath the north flank (Figures 1). Focal depths range less than 3 to about 9 km with most events clustering between 5 and 7 km beneath the southwest flank and shallowing to less than 5 km beneath the north flank.

Numerous spasmodic bursts (spasmodic tremor) have occurred with this activity. These bursts are characterized by a rapid-fire sequence of similar-sized earthquakes with overlapping coda. They became essentially a daily occurrence in mid June with individual bursts lasting for several tens of seconds to a few minutes. Similar bursts accompanied the earlier Mammoth Mountain activity as well as the recurring swarms in the south moat between 1980 and 1982. The data obtained from a temporary deployment of 12, three-component, digital GEOS stations around Mammoth Mountain from June 23 - 27 should provide some important new clues to processes generating these spasmodic bursts in addition to providing more precise information on the locations and focal depths of the swarm earthquakes. (Note: Spasmodic bursts are seldom, if ever, seen in purely tectonic environments. They are distinct, however, from the monotonous, low-frequency, wave-forms of harmonic [volcanic] tremor associated with subsurface magma movement. We have recorded no harmonic tremor either in this sequence or in any of the earlier Long Valley activity.)

The borehole dilatometer at Devils Postpile, which is within a few km of these earthquakes has shown unusual strain variations beginning in late April (see Malcolm Johnston's report). The amplitude of these deviations, however, amounts to only a few tenths of a microstrain. Several of the two-color geodometer lines show a change in trend that began earlier in the year, although it's not clear whether this change in trend, which corresponds to east-west compression across the caldera, is related to the Mammoth Mountain activity or to something under the resurgent dome (see John Langbein's report). Releveling of the L-shaped arrays during the first week in June reveals a small change in trend on the east component of the JEE array on the north side of Mammoth Mountain and the north component of the YMCA array 10 km to the east. None of the other deformation monitoring systems has shown any response that can be associated with this Mammoth Mountain activity.

In spite of the large number of earthquakes, the total energy associated with this swarm remains small with respect to May 1980 M=6 earthquakes or the January 1983 south-moat swarm. This current activity has our attention, however, because of its persistence, its magmatic signature (the gradual increase in intensity with time, an elevated b-value (b = 1.2±0.1), and bursts of spasmodic tremor), and because it is located near the southern end of the youthful Inyo-Mono volcanic chain.

[Background note: Mammoth Mountain itself has not erupted in more than 50,000 years. Several small explosion craters located on the north flank of the mountain, however, were produced by phreatic explosions about 500 years ago associated with the intrusion event that produced the Inyo Dome eruptions, the Inyo Craters phreatic explosions, and the "Earthquake Fault". The Red Cones (4 km south-southwest of Mammoth Mountain) lie further south along this same trend. These post-glacial, basaltic cinder cones are roughly 5,000 years old.]

REPORTS

Hill, D.P., (in press); Temperatures at the base of the seismogenic crust beneath Long Valley Caldera, California, and the Phlegrean Fields caldera, Italy: in P. Gasparini and R. Scarpa eds., Volcanic Seismology, Sprenger-Verlag.

FIGURE 1. Map showing epicentral locations of swarm earthqukes beneath Mammoth Mountain from May through July, 1989.

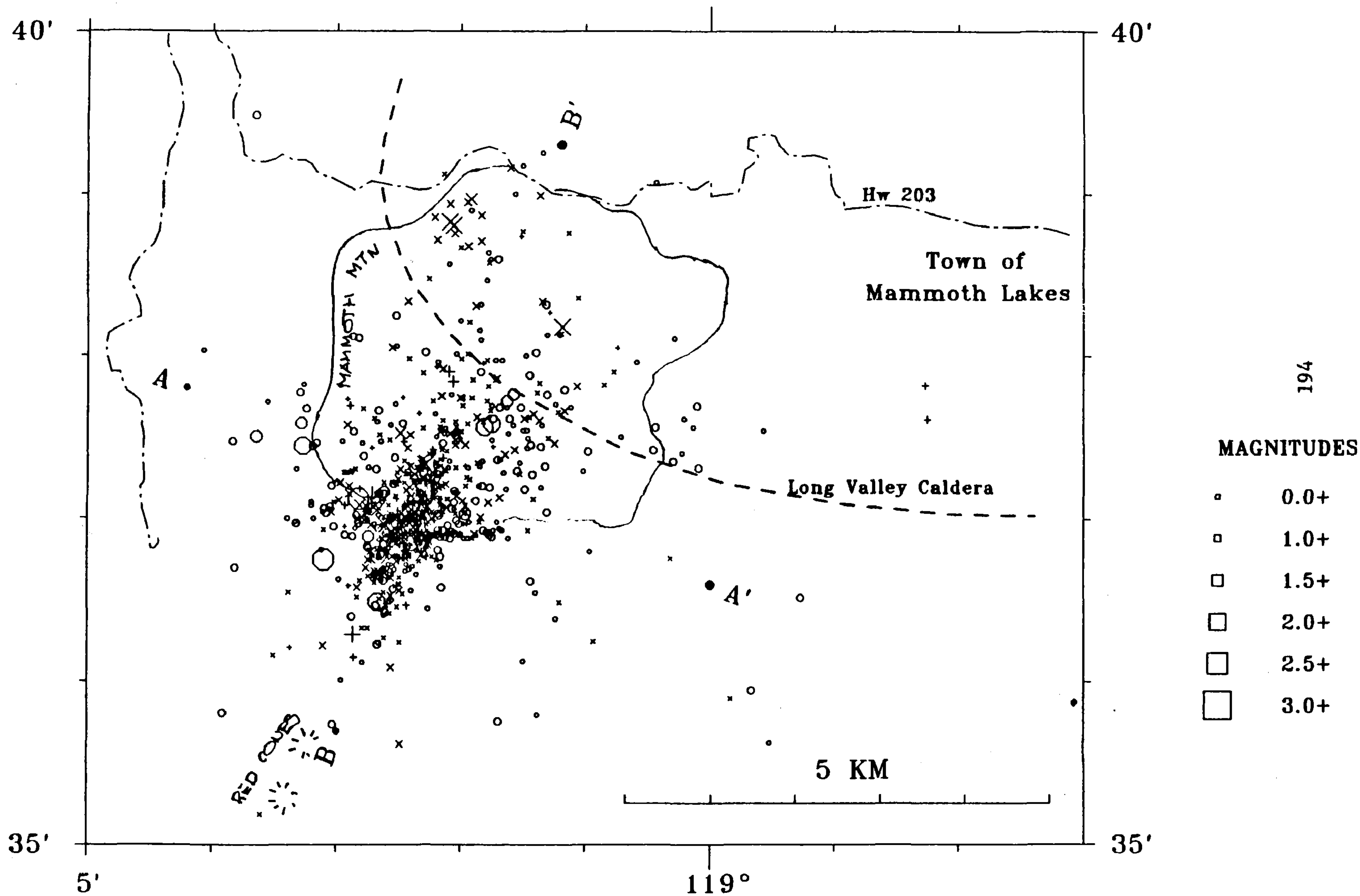

Instrument Development and Quality Control

9930-01726

E. Gray Jensen
Branch of Seismology
U.S. Geological Survey
345 Middlefield Road - Mail Stop 977
Menlo Park, California 94025
(415) 329-4729

Investigations

This project supports other projects in the Office of Earthquakes, Volcanoes and Engineering by designing and developing new instrumentation and by evaluating and improving existing equipment in order to maintain high quality in the data acquired by the Office.

Results

A joint effort by this project and Stanford University to modify 197 Seismic Group Recorders (SGR's) has been successfully completed. These instruments as received by Stanford almost a year ago are designed to record one channel of digital seismic data on a quarter-inch tape cartridge when triggered by a radio signal. Timing of data on each SGR and of seismic sources is synchronized by radio. This works well with seismic reflection experiments since distances between instruments are small and radio signals can usually reach each unit.

In order to permit operation in refraction experiments with units spread out over a couple hundred kilometers, it was decided to modify the SGR's to add a self-timed capability. A single circuit board (SGR Timer) using an 80C88 microprocessor and containing a temperature-compensated crystal oscillator for accurate timing was designed for this purpose. Each of the 197 units was modified by installing one of these boards in its interior, adding a battery-holding box to the exterior and by changing the program of the SGR's microprocessor.

In addition, five laptop computers were modified with similar circuit boards and programmed to act as programming units for the SGR Timers. These laptops allow operators to download a complete set of event times in a few seconds using only a few keystrokes. They also automatically synchronize the SGR Timers clock and permit easy measurement of clock drifts.

All these modifications were completed and tested in early September. The system was used to record four shot sequences in two deployments during the PACE 89 experiment in Arizona during September. The timer modification performed well in the field and the system is being readied for use in Kenya next year. Some improvements in laptop software and hardware are planned.

Three old photographic film seismic recorders (Develocorders) were completely overhauled and rehabilitated for use in Jordan. In addition, project personnel travelled to Jordan to evaluate the seismic network telemetry links and assist in system upgrading. Special modifications to master clocks and other portable clocks were made to permit delayed control of blasting and other triggering. Monitoring of the RefTek-based seismic network in Parkfield by a USGS CUSP system began earlier this year. Work has been done on eliminating noise problems from the system.

Routine maintenance of 16 stations at Yellowstone National Park was performed in August. As usual, numerous telemetry radios and seismometers were repaired, adjusted or calibrated and maintenance visits to microwave and CalNet seismic sites were made.

FAULT MECHANICS AND CHEMISTRY

9960–01485

C.–Y. King
Branch of Tectonophysics
U.S. Geological Survey
345 Middlefield Road, MS/977
Menlo Park, California 94025
(415) 329-4838

Investigations

[1] Water temperature and radon content were continuously monitored at two water wells in Parkfield, California.

[2] Water level was continuously recorded at six other wells in central California.

[3] Water temperature and electric conductivity were periodically measured, and water samples were taken from most of these wells and two springs in San Jose for chemical analysis.

[4] Geochemical research pertinent to earthquake prediction in China was reviewed with a visiting scholar, Zhang Wei from the Chinese State Seismological Bureau, in preparation for a review paper.

Results

The geochemical anomaly recorded at the Chabot well in Oakland on the Hayward fault beginning shortly before the 3 April 1989 earthquake of magnitude 4.9 about 55 km away (See last report) persisted. Figure 1 shows the updated data of temperature, sodium content, conductivity and water level, and rainfall data recorded nearby.

Figure 2 shows randon, temperature, flow rate, and barometric pressure data recorded at the Taylor well in Parkfield. Early problems associated with power interruption by UPS testings were solved in early August, and the monitoring has been smooth since then.

Reports

King, C.–Y. (1989). Gas–geochemical approaches to earthquake prediction: Proceedings of International Atomic Energy Agency Workshop on Radon Monitoring in Radioprotection, Environmental Radioactivity and Earth Sciences (in press)

Rydelek, P.A., Knopoff, L., and King, C.–Y. (1989). Comments on "Migration of historical earthquakes in California." by C.–Y. King and Z. Ma, *Pure and Applied Geophysics* (Submitted).

King, C.-Y., Basler, D., Presser, T.S., Evan, W.C., and White, D. (1989). Hydrogeochemical variations along Hayward fault and possible relation to earthquakes (abs.): *EOS (Transactions of American Geophysical Union)* (submitted).

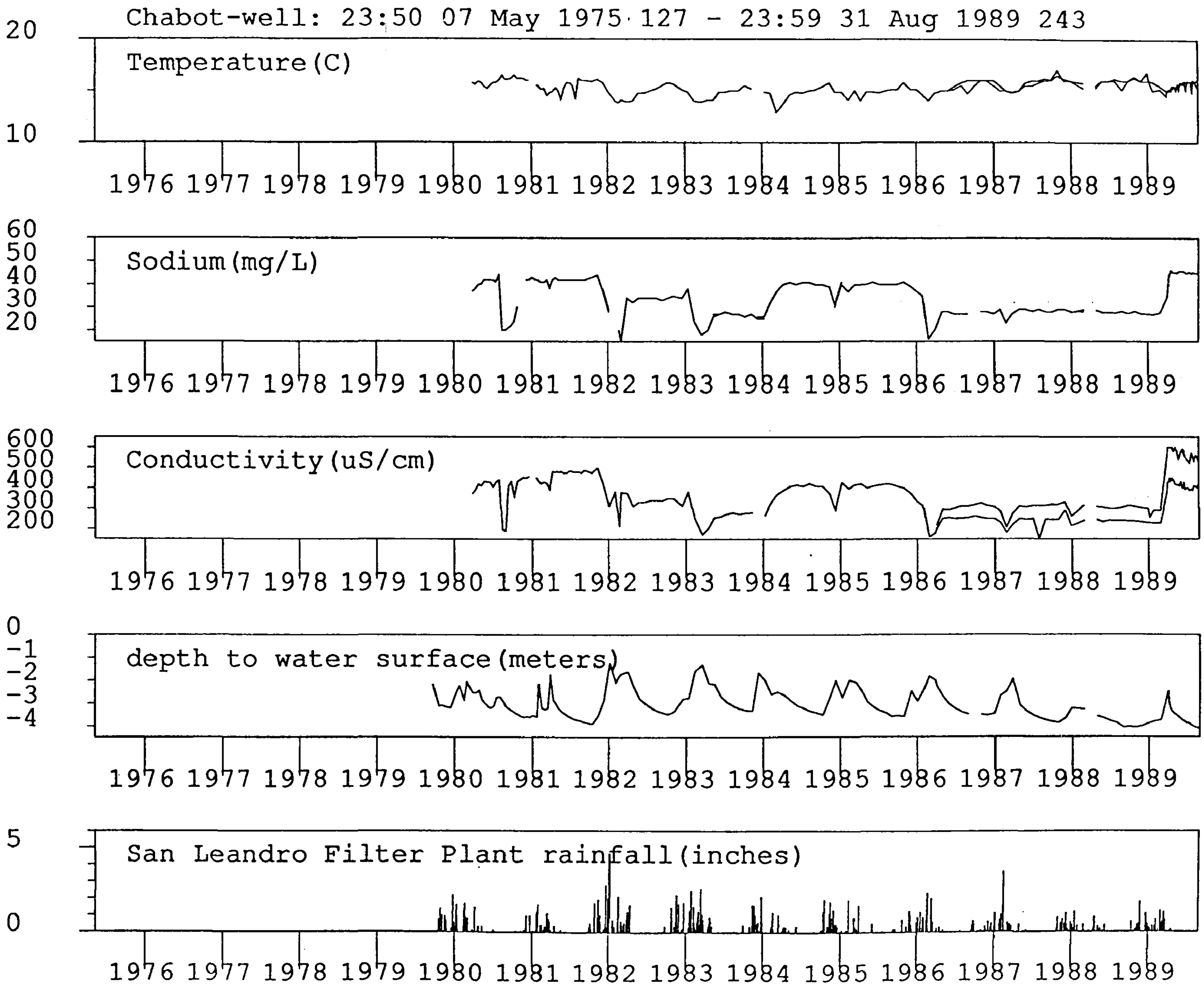
Chabot-well: 23:50 07 May 1975 127 - 23:59 31 Aug 1989 243
Temperature(C)
Sodium(mg/L)
Conductivity(uS/cm)
depth to water surface(meters)
San Leandro Filter Plant rainfall(inches)
1976 1977 1978 1979 1980 1981 1982 1983 1984 1985 1986 1987 1988 1989
20
10
60
50
40
30
20
600
500
400
300
200
0
-1
-2
-3
-4
5
0

Figure 1

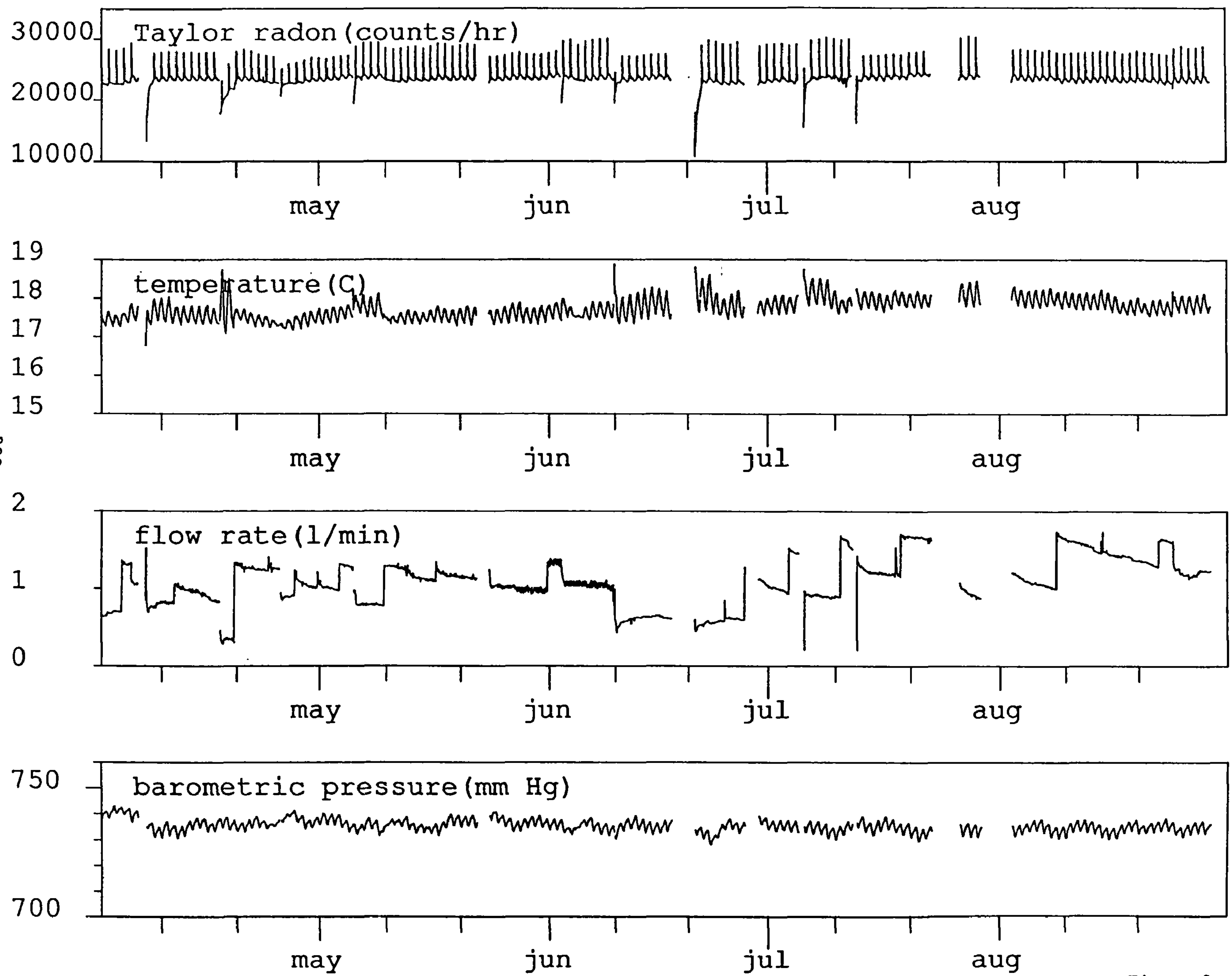
Taylor radon(counts/hr)
30000
20000
10000
temperature(C)
19
18
17
16
15
flow rate(l/min)
2
1
0
barometric pressure(mm Hg)
750
700
may
jun
jul
aug

Figure 2

CALIFORNIA AND HAWAII SEISMICITY STUDIES

Project 9930-03563
for the period May 1, 1988 through September 30, 1989

Fred W. Klein
Branch of Seismology
U.S. Geological Survey MS 977
345 Middlefield Rd.
Menlo Park CA 94025

Investigations

The overall objective is to look for long-term seismicity and tectonic patterns in the Northern California and Hawaii earthquake catalogs. The two catalogs are in very different states of self-consistency and usefulness for research, however. Accordingly, the Hawaiian work uses a completely reprocessed catalog and focuses on research. The Northern California effort presently involves cleaning up the raw phase data and developing methods for reprocessing this data into a self-consistent catalog. This reprocessing is necessary before many types of research become meaningful. The emphasis is on applying methods developed for Hawaiian processing and earthquake display to the California catalog.

The Hawaiian seismic investigation consists of a thorough study of earthquake focal mechanisms in the upper mantle beneath Hawaii. The goal is to determine the state of stress, nature of lithospheric flexure and interaction of the volcanic system with the lithosphere. This work includes a detailed study of the vertical magma conduit feeding Kilauea Volcano's shallow (3-7 km depth) magma reservoir. The seismically active conduit extends downward to about 55 km to the top of the magma source region. Earthquakes in the surrounding lithosphere below 15 km depth reflect deformation and stress imposed by the volcanic edifice above.

The work on the Northern California earthquake catalog is being shared by several colleagues in the branch. This project has assumed responsibility in several areas: (1) Develop a data base of seismic station data including a new systematic set of station codes and apply it to the reprocessing of the earthquake catalog. (2) Develop a computer file system or data base for storing both raw and processed earthquake phase data. (3) Develop and modify the HYPOINVERSE earthquake location program to handle the various tasks needed for Northern California processing. (4) Organize a system for recognizing earthquakes needing human reprocessing, dividing the catalog into regions of equal numbers of events to reprocess, and supervising individuals to reprocess each area. (5) Prepare earthquake animations for video presentations as needed on the Branch's Amiga computer.

These animations show the spatial distribution of earthquakes through animated movement and the time variation of seismicity with time-lapse map views. The animations have been used a) in research to visualize an earthquake catalog and look for patterns which are testable by more rigorous methods, b) for public display at the USGS open house, c) to demonstrate to VIP visitors the nature of seismicity observation and monitoring, d) to release video animation to the media illustrating important earthquakes and seismic zones, and e) to publish video tapes.

Results

The research on Kilauea's magma conduit suggests that the earthquakes require external sources of stress and are not simply generated by excess magma pressure, as with rift zone intrusions. Dramatic evidence for an external stress cause is the major drop in earthquake rate following the M=7.2 Kalapana earthquake in 1975. This event thus released stress in the entire volcanic system in addition to the rupture zone in Kilauea's south flank. Seismic gaps occur along the conduit centered at about 5, 13 and 20 km depths. The 3-to-7-km gap is the main magma reservoir, the 13 km gap appears to result from the layer of buried ocean sediments at the base of the volcanic pile, and the 20-km gap is present under the whole island. The latter may be a depth of low or "neutral" stress within the flexing lithosphere. Lateral extension is characteristic of the focal mechanisms within the volcanic pile (above the 13 km gap) and lateral compression occurs just below. Stresses are thus decoupled at the boundary of the volcanic pile with the underlying oceanic crust. Focal mechanisms below 20 km depth are similar to those in Kilauea's south flank and show southward motion of the upper block on a near-horizontal plane.

The reprocessing of the Northern California earthquake catalog is underway. Contributions from this project to date include: (1) A data base of seismic stations in and surrounding California has been assembled, including a time history of station gain. (2) The HYPOINVERSE location program now uses 24 crustal and station delay models assigned to different geographic areas. (3) Various routines to verify quarry blasts within the catalog and check for data completeness.

Reports

Klein, F.W., Multiple crustal models for earthquake location in Northern California and surrounding areas, U.S. Geological Survey Open File Report, in preparation, 1989.

Klein, F. W., User's guide to HYPOINVERSE, a program for VAX computers to solve for earthquake locations, U.S. Geological Survey Open File Report 89-314, 1989.

Klein, F. W., User's guide to five VAX FORTRAN programs for manipulating HYPOINVERSE summary and archive files, U.S. Geological Survey Open File Report 89-313, 1989.

Klein, F. W., Alan G. Lindh and Stephen G. Walter, Central California Earthquake Animation, January-June 1989, U.S. Geological Survey Open File Report 89-308, 1989.

Array Studies of Seismicity

9930-02106
David H. Oppenheimer
Branch of Seismology
United States Geological Survey
345 Middlefield Road - MS 977
Menlo Park, California 94025
415-329-4792

Investigations

1. Continue consolidation and clean-up of phase data of central California Seismic Network (CALNET) from 1969 through present.
2. Evaluate seismicity patterns along the Calaveras fault for ability to delineate segments which may slip during moderate earthquakes.
3. Investigate seismic budget in the Morgan Hill region.
4. Examine crustal seismicity along the Cascada arc.
5. Invert teleseismic traveltime data in central California for 3-D velocity variations in the crust and upper mantle.

Results

1. Progress continues to be made in the collection, organization, relocation, archiving, and documentation of all the CALNET earthquake data since 1969 (see previous Semi-Annual Reports). Main efforts were directed toward processing post-1983 RTP and CUSP data. All of the available phase data for the periods 1969–1985 and 1987–present are now merged and relocated with the best available local velocity model. Only ten months of data during 1986 remain to be processed. We anticipate that the entire catalog will be relocated and merged by the end of 1989. During the final phase of processing we will identify those earthquakes in the catalog that have poor location solutions or magnitudes. They will be removed from the catalog and assigned to conscripted volunteers for repair. The resulting data set will then be re-merged and relocated for one last time. The coda duration magnitudes will also be recomputed using more appropriate methods.

2. Previous semi-annual reports describe our findings on the potential for the occurrence of $M > 5$ earthquakes on the Calaveras fault. Efforts during this period were devoted primarily to revision of the manuscript. Additional Wood-Anderson seismograms from stations PAS, SBC, and TIN were digitized for the 9/5/55 $M5.5$ and 3/31/86 $M5.7$ earthquakes to demonstrate the dissimilarity of their respective waveforms to those written by the 10/26/43 $M4.9$ and 6/13/88 $M5.1$ Alum Rock earthquakes.

3. This research is being conducted with Geoff King of the U.S.G.S. in Denver. The intent is to assess the relative deformation occurring on the Calaveras fault to that occurring off the fault by 1) converting the double couple fault plane solutions to their moment tensor representations, 2) scaling the tensor by the equivalent scalar moment derived from coda duration estimates, and 3) summing the tensors within a given

region. Efforts have been directed primarily toward assembling a suite of over 1000 fault plane solutions of earthquakes occurring in this region since 1984. Substantial effort was also directed toward the development of computer code.

4. This research is being conducted with Craig Weaver of the U.S.G.S. and focusses on the distribution of crustal earthquake occurrence along the entire arc of the Cascades. Catalogs of earthquake hypocenters from Washington and Oregon located by the University of Washington were combined with catalogs of hypocenters near the Mendocino triple junction in California located by the U.S.G.S. Distinct variations in the distribution of crustal seismicity along the arc appear to coincide with the previously recognized variations in the distribution of volcanic events, suggesting that both the volcanism and seismicity are due to common tectonic processes. Geologic and geophysical data indicate that the interaction of crustal blocks may play a major role in dictating the style of deformation. The effect of the subduction process on the crustal seismicity is difficult to recognize. Instead, much of the seismicity appears to reflect the tectonics of the adjacent backarc provinces.

5. Work was begun with Harley Benz of the U.S.G.S. and George Zandt of L.L.N.L. to invert the teleseismic traveltime data recorded by the central California seismic network for 3-D velocity variations in the crust and upper mantle using the ACH block inversion method. Principal efforts during this period were directed toward assembling the data.

Reports

Oppenheimer, D. H., W. H. Bakun, and A. G. Lindh, The prospects for future $M > 5$ earthquakes on the Calaveras fault, California, submitted to *EOS*, in press, (Fall 1989 AGU meeting).

A. G. Lindh, D.H. Oppenheimer, and W. H. Bakun, Slip partioning of the Calaveras fault, California, into aseismic and seismic zones, submitted to *EOS*, in press, (Fall 1989 AGU meeting).

Yerkes, R.F., D.H. Oppenheimer, and W.H.K. Lee, Elsinore fault zone– seismicity *vs.* age of surface faults, submitted to *EOS*, in press, (Fall 1989 AGU meeting).

K.M. Shedlock, C.S. Weaver, D. Oppenheimer, and G.C.P. King, Seismic deformation in the Pacific northwest, submitted to *EOS*, in press, (Fall 1989 AGU meeting).

D.P. Hill, W.L. Ellsworth, M.J.S. Johnston, J.O. Langbein, D.H. Oppenheimer, A.M. Pitt, P.A. Reasenberg, and M.L. Sorey, Mammoth Mountain earthquake swarms, Long Valley caldera, California, submitted to *EOS*, in press, (Fall 1989 AGU meeting).

IGPP/UCR-89/33

Variations in Electrical Properties Induced by Stress Along the San Andreas Fault at Parkfield, California

Supported by the U.S. Geological Survey, Department of Interior under award number 14-08-0001-G1357

Stephen K. Park
Tien Chang Lee
Institute of Geophysics and Planetary Physics
University of California
Riverside, California 92521

Introduction

We are monitoring fluctuations of resistivity with telluric currents in Parkfield. The array uses grounded telephone lines as dipoles (Figure 1). We have recently completed a revised analysis of data between Day 60, 1988 to Day 240, 1989. The revised analysis involved selecting average eigenvectors for each dipole, rather than letting them vary daily. We project daily fluctuations of the telluric coefficients on these eigenvectors (Park and Lee, 1988), and previous results contained effects of both changes in the telluric coefficients <u>and</u> changes in the eigenvectors. The new results, shown here, have the fluctuations of the telluric coefficients only, which are related to the changes in resistivity. We also are now looking only at periods between 300 s and 7200 s.

Discussion of Data

Fluctuations of the telluric coefficients on channels 1, 3, 4, and 5 are small (Figure 2), with maximum variations below 1%. Note that data are smoothed with a 9 day average. Channels 2 (Figures 3 and 4) and 6 (Figures 5 and 6) show variations of several percent on the projection onto the minimum eigenvector, however. The fluctuations on channel 6 are very large (>10%) and we suspect a seasonal change is responsible for these fluctuations; this dipole is our shortest and is presumably more sensitive to shallow features. The fluctuations are smaller during the summer (compare days 150-240 in 1988 or 1989 to the rest of the record). Unfortunately, this dipole also spans the hypocentral location for characteristic earthquakes in Parkfield and we had hoped it would be one of our best. We cannot yet discount the possibility that these fluctuations are due to phenomena associated with stresses in the earth, however.

The fluctuations of the projection on the minimum eigenvector for Channel 2 are much more intriguing. Between approximately Day 195 and Day 125 in 1989 (Figure 4), this projection decreased by 2%, then increased by 5% and finally returned to its previous level. Significantly, this change is well above the level of seasonal or random fluctuations, as evidenced by Figures 3 and 4. We do not yet know why this occurred, and our next step is to correlate our results with the seismicity, hydrologic data, strain data, and geochemical data. We hope to find something else occurring during that time.

Sensitivity of Array

We recently completed an analysis of the sensitivity of our telluric array to changes of resistivity along the fault zone. This work, done with Dave Fitterman (USGS-Denver), showed that we are principally sensitive to fluctuations in the upper 6 km and within the array. We should be able to detect changes of a percent, however.

Conclusions

Results from the first two years show that our array is working and should detect perturbations of resistivity if they occur. All we need now is an earthquake!

References

Park, S.K. and T.C. Lee, Variations in electrical properties induced by stress along the San Andreas Fault at Parkfield, California, in Jacobson, M.J., National Earthquake Hazards Reduction Program, Summaries of Technical Reports, XXVII, USGS OF Rept 88-673, 242-247, 1988.

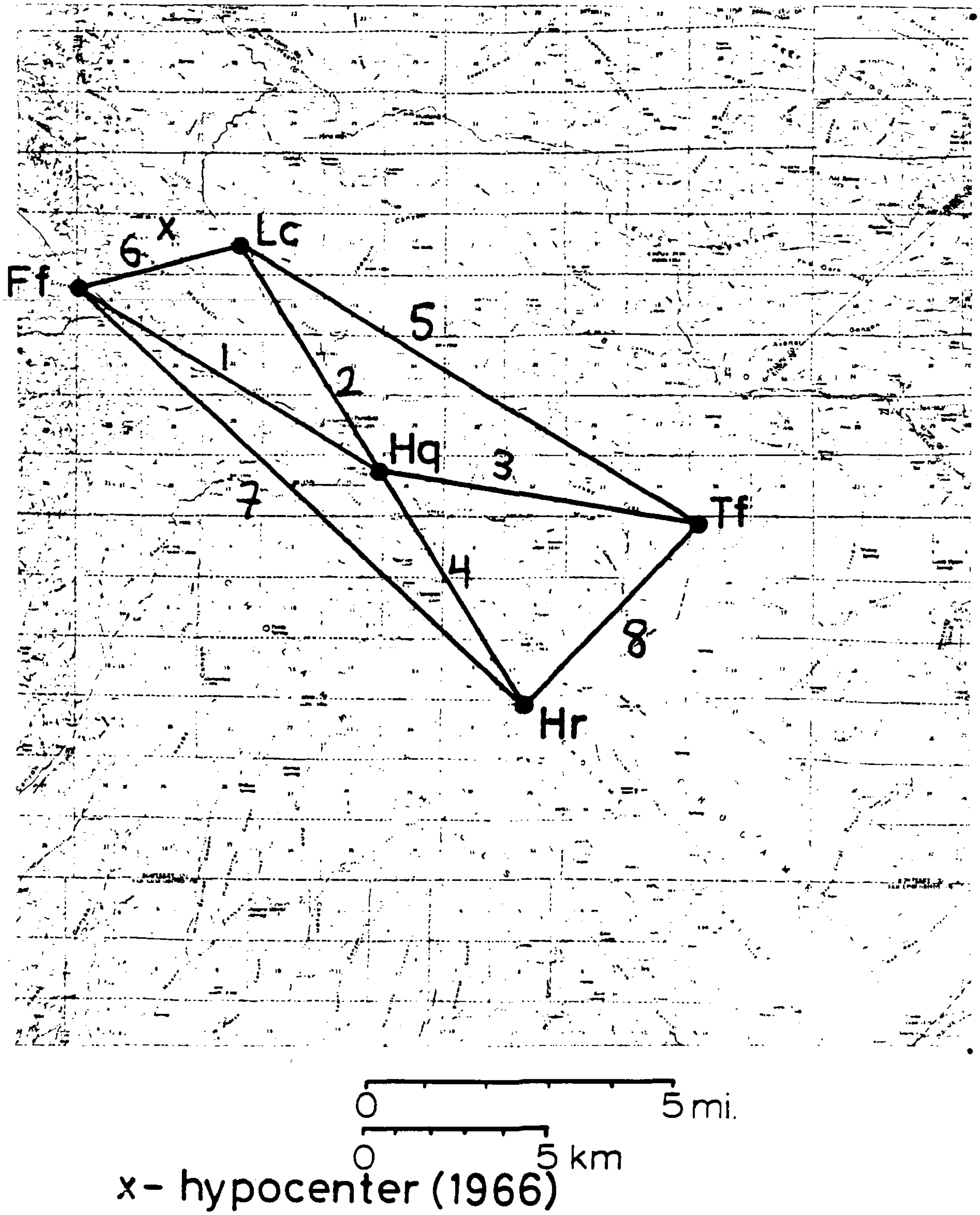

Figure 1 - Telluric monitoring array in Parkfield. Electrodes are marked with dots and the electrically created dipoles are shown with lines.

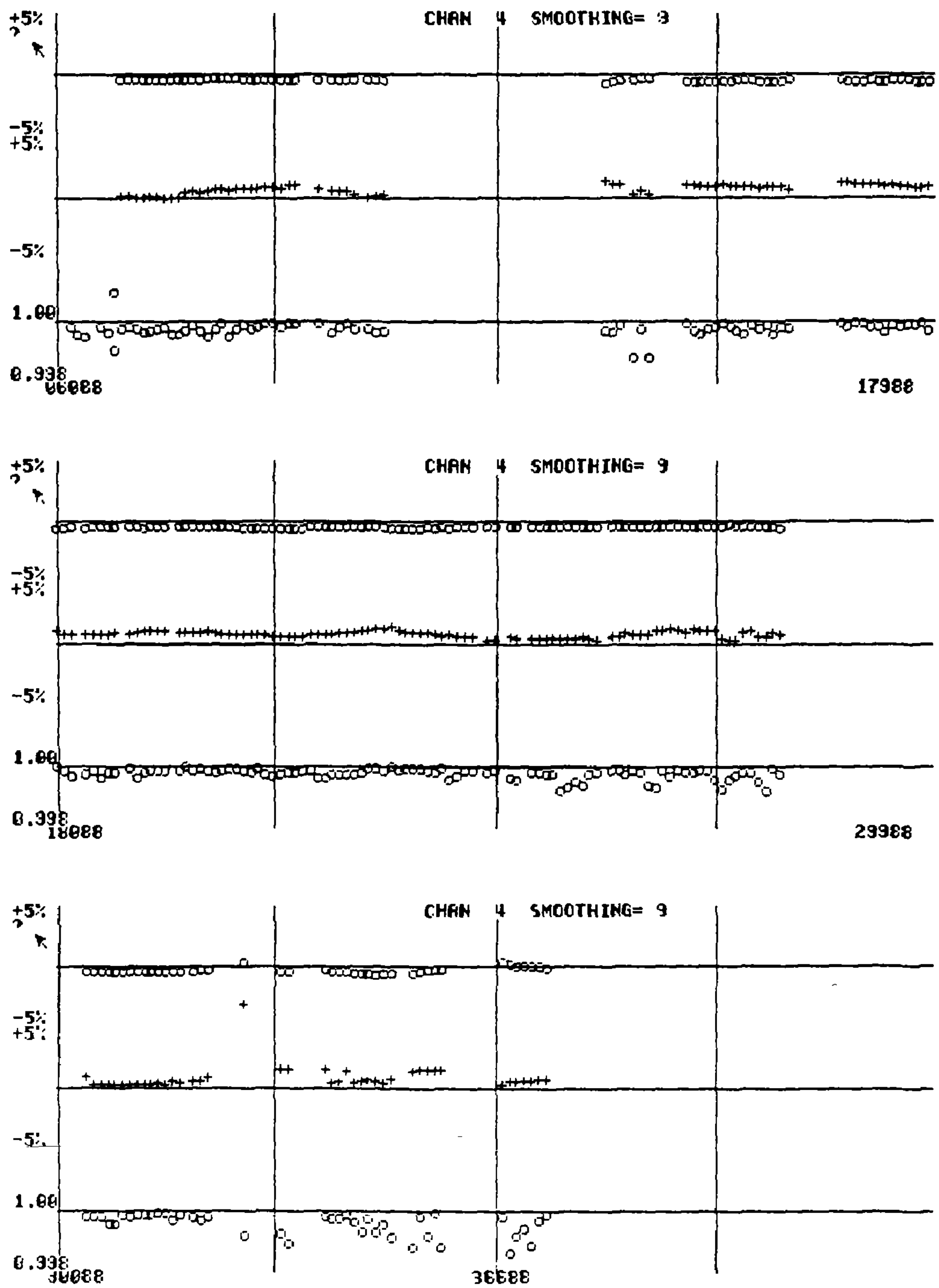

Figure 2 - Residual analysis for Channel 4 for 1988. The first plot is the projection of the residual on the major eigenvector and the second is the projection on the minor eigenvector. Projections are shown with a scale of +/- 5%. Coherencies between the predicted and measured Channel 4 signals are shown between .998 and 1.000. Gaps around Day 120 and Day 300 are due to loss of digitizer.

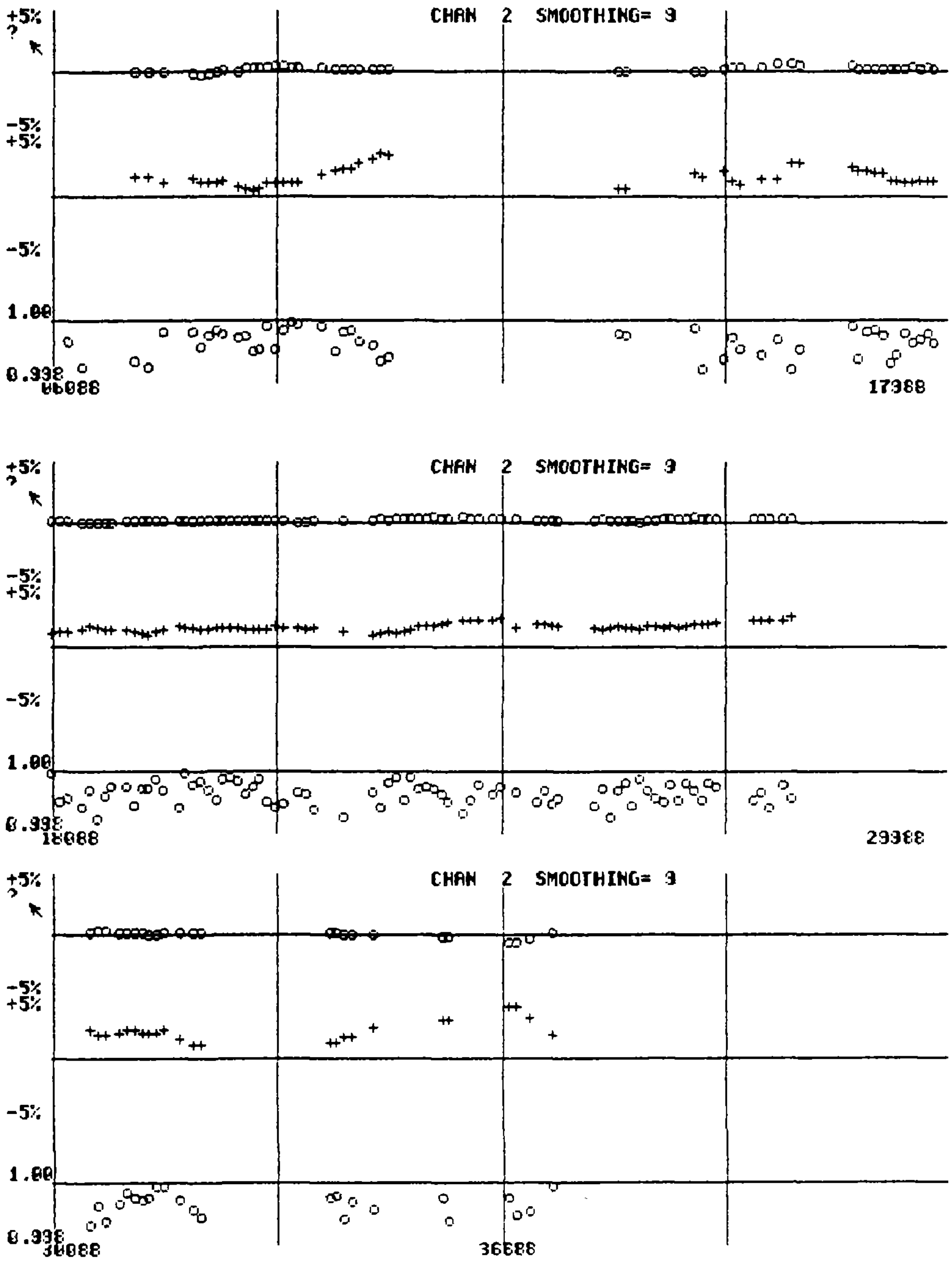

Figure 3 - Residual analysis for Channel 2 for 1988. See caption for Figure 2 for explanation.

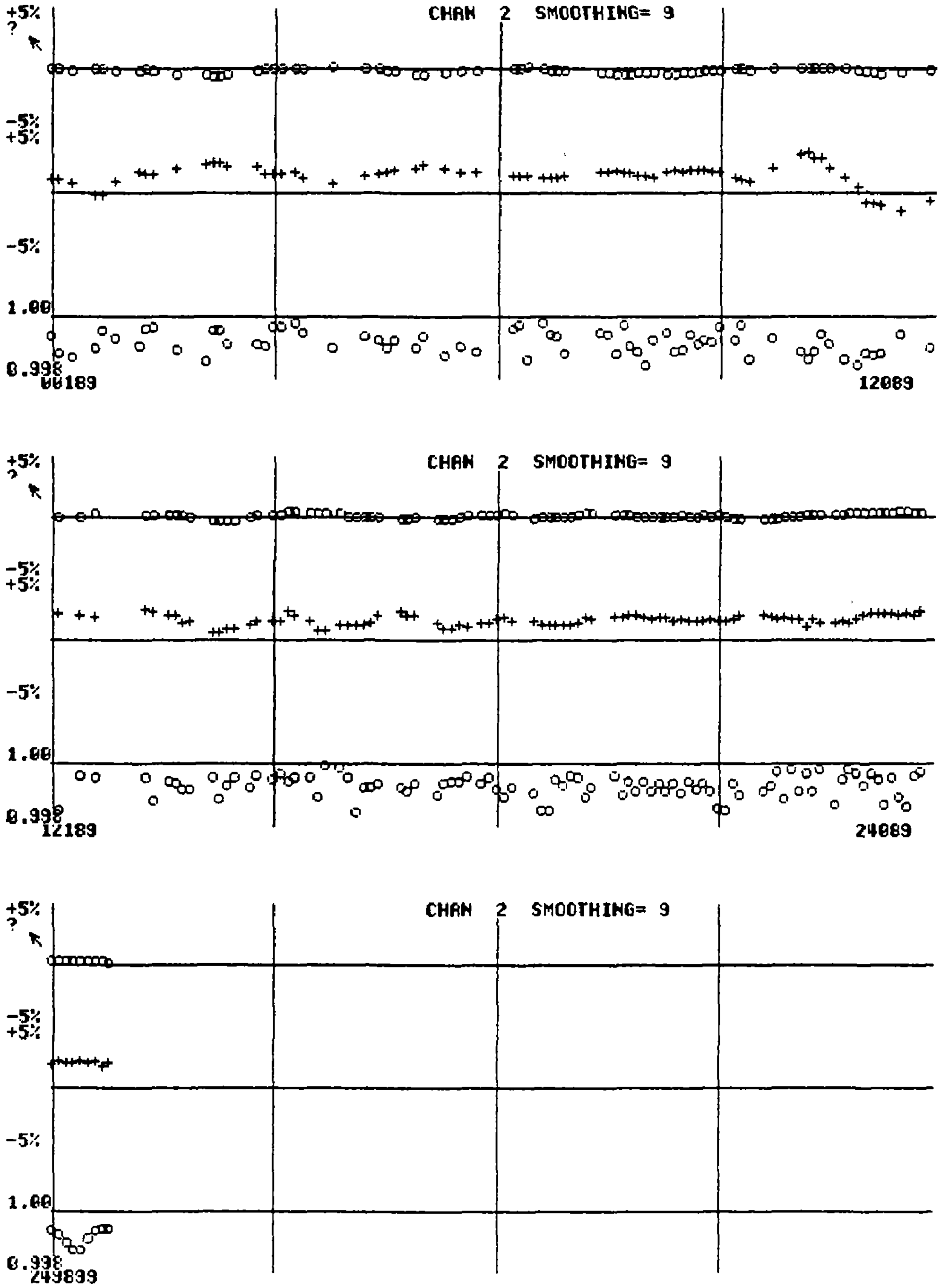

Figure 4 - Residual analysis for Channel 2 for 1989. See caption for Figure 2 for explanation.

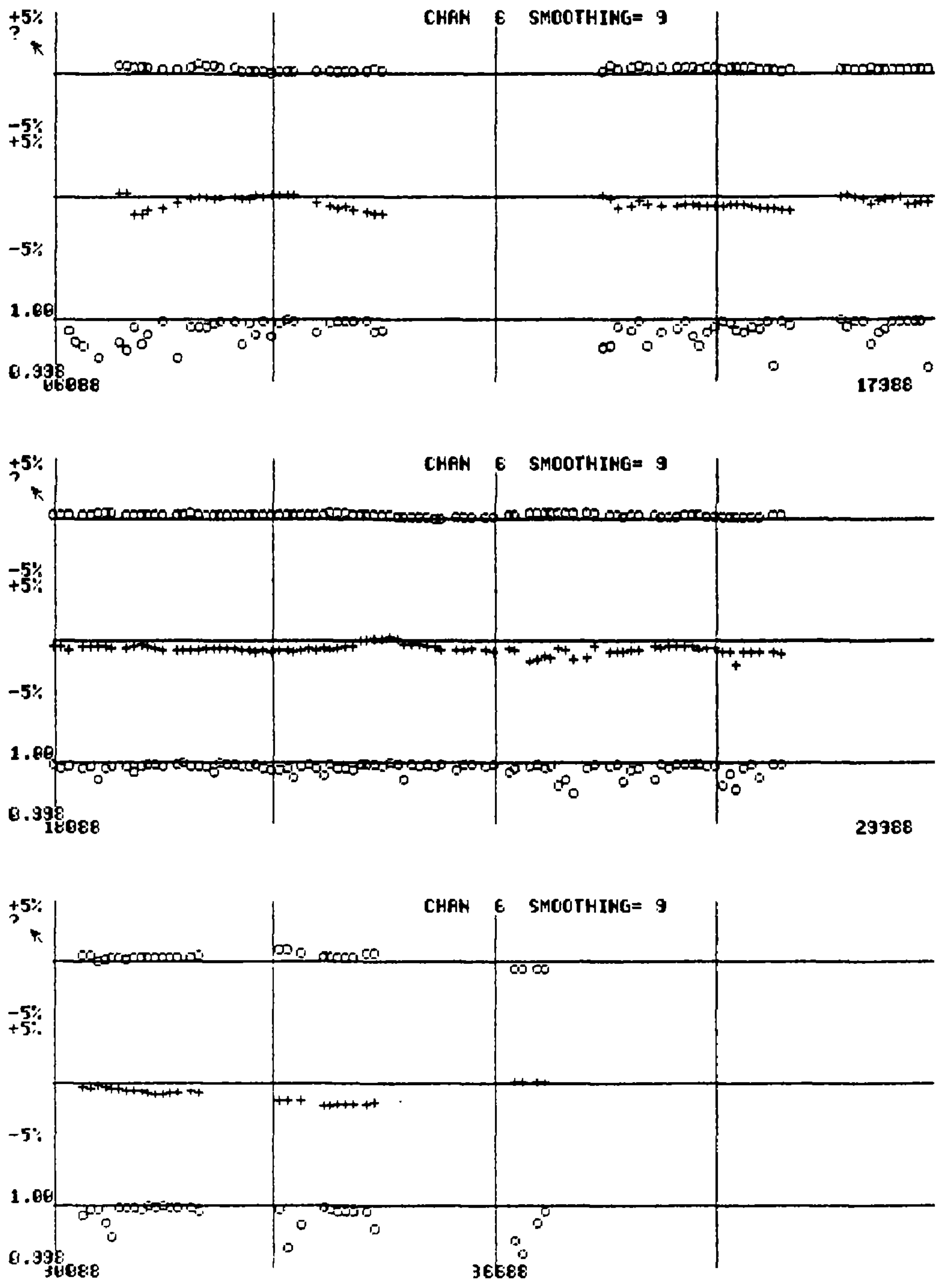

Figure 5 - Residual analysis for Channel 6 for 1988. See caption for Figure 2 for explanation.

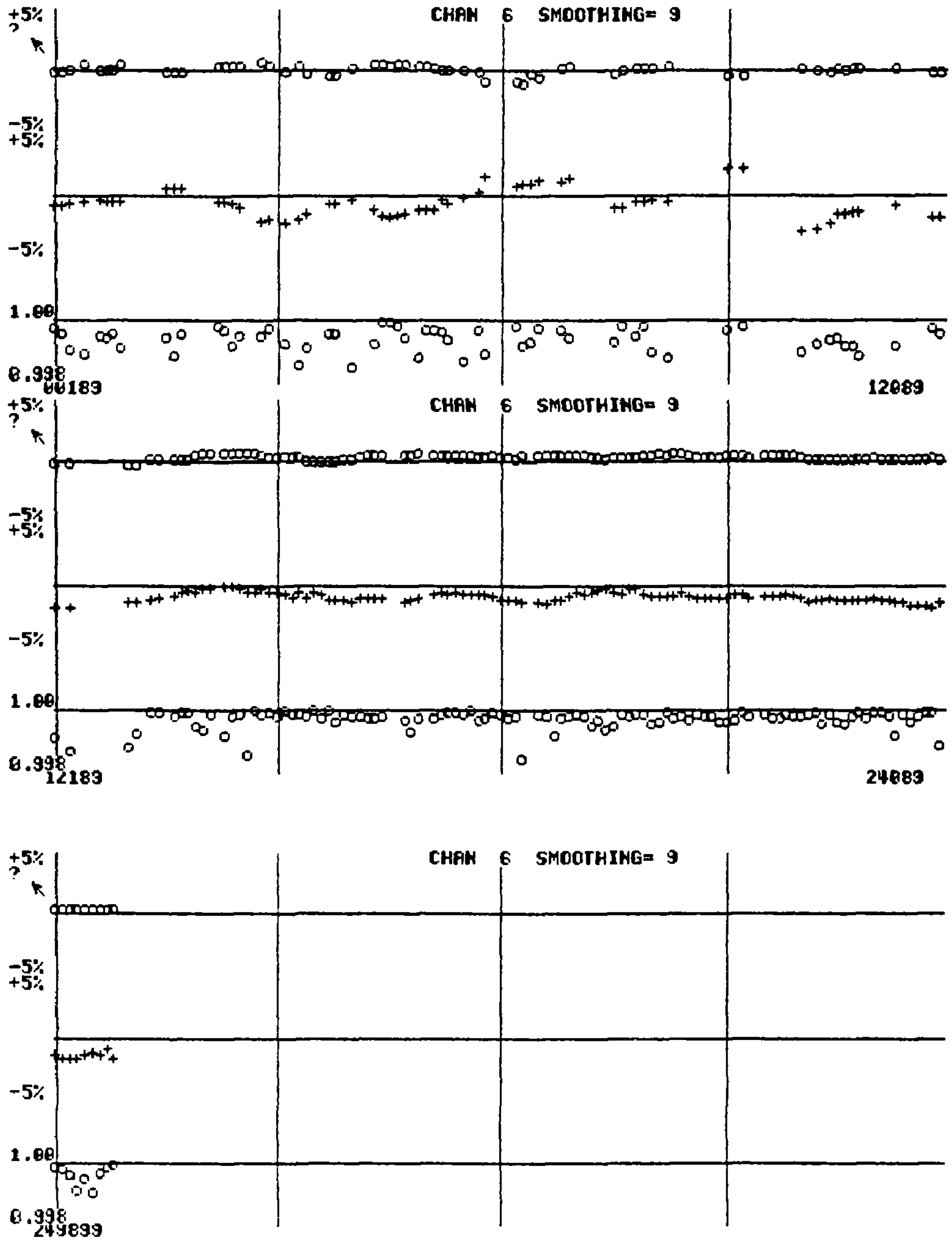

Figure 6 - Residual analysis for Channel 6 for 1989. See caption for Figure 2 for explanation.

CRUSTAL STRAIN

9960-01187

W.H. Prescott, J.C. Savage, M. Lisowski,
J.L. Davis, and J.L. Svarc
Branch of Tectonophysics
U.S. Geological Survey
345 Middlefield Road, MS/977
Menlo Park, California 94025
(415) 329-4860

INVESTIGATIONS

The principal subject of investigation was the analysis of deformation in a number of tectonically active areas in the United States.

RESULTS

1. Strain Accumulation near the San Andreas and Calaveras faults in the San Francisco Bay Area

Repeated measurement of several small aperture (2.5–7-km-wide) Geodolite trilateration networks (Figure 1) show a constant rate of deformation across the San Andreas fault in the San Francisco Peninsula, and an increase in the rate of deformation across the Calaveras fault near Milpitas after the 26 April 1984 $M_L = 6.2$ Morgan Hill earthquake.

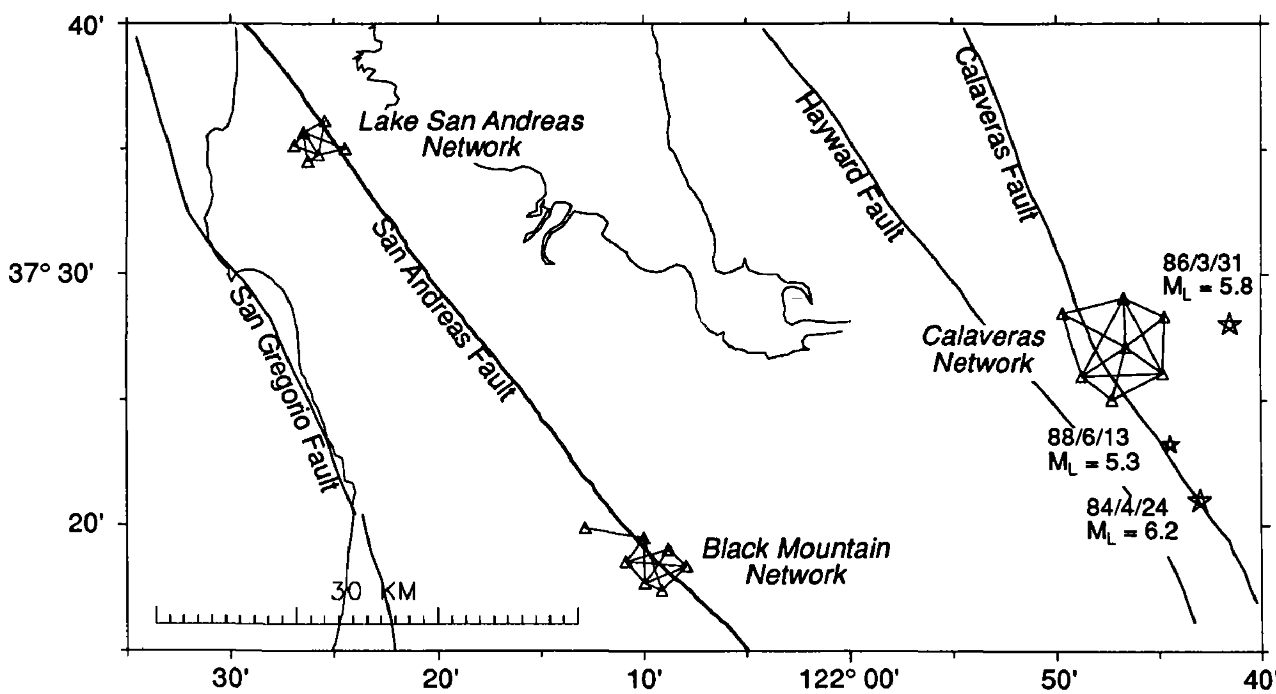

Figure 1. Map showing the location and configuration of small-aperture Geodolite trilateration networks in the San Francisco Bay Area. Stars mark the epicenters of the Morgan Hill (86/4/24), Mt. Lewis (86/3/31), and Alum Rock (88/6/13) earthquakes.

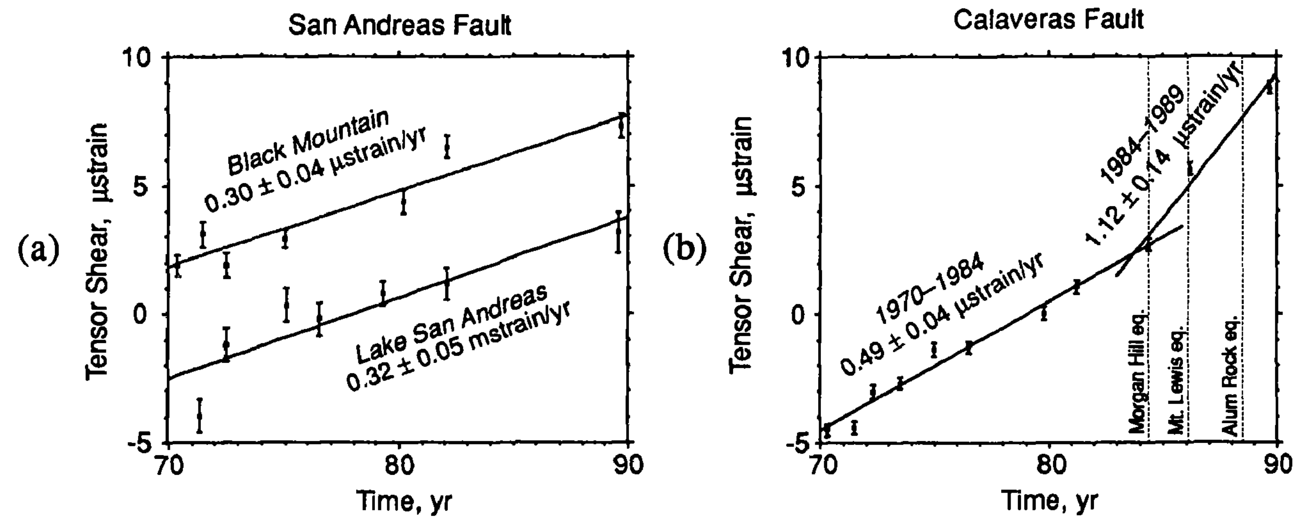

Figure 2. Plots showing the accumulation of right-lateral tensor shear strain parallel to the local strike of the (a) San Andreas and (b) Calaveras faults as a function of time. Linear fits to strain accumulation along with the calculated average rates of shear are shown in the plots. Dotted vertical lines in (b) mark the times of nearby earthquakes (See Figure 1 for epicenters).

Between 1970 and 1989, right-lateral tensor shear parallel to the local strike of the San Andreas fault accumulated at a constant rate of 0.30 ± 0.04 μstrain/yr in the 2.5-km-wide San Andreas network and 0.32 ± 0.05 μstrain/yr in the 2.5-km-wide Black Mountain network (Figure 2a). The San Andreas fault in both areas is believed to be locked, but if the deformation is from shallow fault slip (creep), a shallow slip rate of 1.1 ± 0.2 mm/yr in the Lake San Andreas network and 1.2 ± 0.2 mm/yr in the Black Mountain network could account for the observed line length changes.

The rate of right-lateral tensor shear strain observed in a 7-km-wide Geodolite trilateration network crossing the Calaveras fault increased from 0.49 ± 0.04 to 1.12 ± 0.14 μstrain/yr after the Morgan Hill earthquake (Figure 2b). These shear rates assume spatially uniform strain accumulation. Prescott *et al.* (*J. Geophys. Res.*, **86**, 10853–10869, 1981) suggested that shallow fault slip (creep) might account for some of the deformation across this section of the Calaveras fault. An alternative description of the deformation, in terms of fault slip and uniform strain accumulation, indicates a constant slip rate of 2.6 mm/yr between 1970 and 1989, and an increase in the shear rate from 0.26 ± 0.04 to 0.90 ± 0.25 μstrain/yr after the Morgan Hill earthquake. The observed increase in deformation might indicate an increased deep slip rate on the Calaveras fault (*i.e.*, more rapid loading) or shallow slip across other faults within the part of the network that does not cross the Calaveras fault.

2. Precision of Global Positioning System Observations: Broadcast Orbits versus Improved Orbits

Analysis of repeated GPS observations spanning two years from 1987 to 1989 suggests that at least for vectors up to about 40 km, current broadcast orbits provide a precision comparable to orbit-improved processing, about 0.2 ppm. We have analyzed about a dozen observations of a 31 km and a 43 km vector originating from Loma Prieta west of San Jose, California. The observations were made approximately monthly over the last 15 months. The data was processed with a slightly modified version of the Bernese software in several ways: 1) Using a multi-day fit to the broadcast orbits with biases free; 2) using improved orbits with a constant tropospheric delay with biases free and fixed; and 3) using improved orbits and a random walk troposphere. The improved orbits were calculated using data collected from tracking stations with well known coordinates located across North America. Our preliminary results suggest that varying the tropospheric model did not have a significant effect on the results. The bias-fixed solutions show either no improvement, or a small increase in the rms for the north and east components when compared to the bias-free solutions. The rms for the vertical component is slightly smaller in the bias-fixed solution. The comparison of broadcast-orbit and orbit-improved solutions produces a mixed result. For orbit-improved solutions, there is a significant improvement in the east component for the north-south line. For other components, the improvement is not as large, but the rms is slightly smaller when the improved orbits are used. These preliminary results are summarized in the following table.

Table 1. Comparison of broadcast-orbit solutions, improved-orbit-bias-free solutions and improved-orbit-bias-fixed solutions. All entries are given in millimeters.

Line and solution	North rms	East rms	Up rms	Length rms
Lp1-Allison (N-S, 43 km)				
broadcast-orbit	6.8	20.8	36.8	6.7
improved-orbit-bias-free	5.8	7.9	32.2	5.6
improved-orbit-bias fixed	6.7	9.4	31.7	6.8
Lp1-Eagle (E-W, 31 km)				
broadcast-orbit	7.1	8.4	35.5	8.6
improved-orbit-bias-free	4.2	7.1	39.3	7.3
improved-orbit-bias fixed	4.0	10.0	32.4	10.1

3. Strain Accumulation near the Mendocino Triple Junction, California

Measurements of the deformation of Geodolite trilateration networks near the Mendocino triple junction show a transition from northwest trending right-lateral shear associated with the San Andreas fault system to northeast trending contraction associated with the Cascadia subduction zone. Southeast of the triple junction right-lateral shear is distributed across a broad zone. Near Round Valley, located 50 km southeast of Cape Mendocino and 60 km from the San Andreas fault, right-lateral shear strain accumulated at an average rate of 0.41 ± 0.07 μradian/yr across a vertical plane striking N33°W±4° in the 1985 to 1989 interval. This shear strain rate across a zone 35 to 80 km east of the San Andreas fault indicates that about half of the estimated 34 mm/yr of relative plate motion across the San Andreas fault system is accommodated by the Garberville and Lake Mountain faults. Along the coast near Cape Mendocino, the right-lateral shear strain rate between 1981 and 1989 averaged 0.40 ± 0.04 μradian/yr across a vertical plane striking N44°W±4°, approximately parallel to the more westward trend of the San Andreas fault in this area. North of the triple junction between Cape Mendocino and Eureka, the deformation between 1981 and 1989 is roughly approximated by a 0.20 ± 0.04 μstrain/yr uniaxial N31°E±8° contraction. Additional evidence for strain accumulation north of the triple junction is from the comparison of 1941 triangulation with 1989 GPS. Angle changes between Cape Mendocino and Trinidad Head give an average shear rate of 0.26 ± 0.07 μradian/yr with the direction of maximum contraction N63°E±8°.

4. Deformation of Long Valley Caldera

The 40-line Geodolite network that spans the Long Valley caldera has been surveyed annually since 1983. A principal component analysis of the measurements indicates that the deformation is adequately described by a single mode. That is, the length of the i^{th} line at the time (t_j) of the j^{th} survey can be approximated by

$$L_{ij} = a_i C(t_j) + L_{i0}$$

where a_i and L_{i0} are constants for each line and $C(t)$ is a function of time. The common time function is closely approximated by

$$C(t) = (1.34 \pm 0.01) - (3.98 \pm 0.24) \exp\left\{ \frac{-(t - 80.0)}{(3.27 \pm 0.02 \text{ yr})} \right\}$$

Thus, the deformation rate appears to be decreasing exponentially with a decay time of about 3.25 yr. The overall pattern of deformation is generally a radial expansion directed outward from the center of the resurgent dome (see Figure 5 in *J. Geophys. Res.*, **93**, 13297–13305, 1988).

None of the 1989 measurements of the five lines into the station at the top of Mammoth Mountain appears anomalous. Thus, no deformation associated with the increased seismic activity beneath Mammoth Mountain, which began in May 1989, was detected in the September Geodolite survey.

5. Uplift along the Nankaido (Japan) Subduction Zone 1950–1985

The uplift indicated by tide gage recordings along the Nankaido subduction zone can be described as the superposition of an exponentially decaying relaxation following the 1946 Nankaido earthquake and a uniform secular uplift rate. The relaxation time for the postseismic relaxation appears to be about 4.7 ± 1.1 yr, and that relaxation is obvious at only a few of the 16 tidal stations studied. More remarkable than the postseismic relaxation is the linearity of the sea level change in the 1950–1985 interval. There is no evidence for a long-term (30 yr) relaxation in the 1950–1985 data, but, of course, a very long-term relaxation would be difficult to detect. Nevertheless, it is surprising just how constant the uplift rates are at both the 1946 Nankaido and 1964 Alaska subduction zones in the decades immediately following rupture.

6. The Hypsometer as a Pressure Standard

Although modern aneroid barometers are reliable and convenient, there is a need for a pressure standard such as a large-bore mercury barometer to detect drift in the aneroids. However, mercury barometers are very difficult to transport. An alternate standard is the hypsometer, where pressure is inferred from the boiling point of distilled water. A hypsometer can be easily constructed by installing a jacketed thermistor probe (Yellow Spring Institute Model 46008) in a Precision Scientific Company Model 92004 midget water still. The resistance of the thermistor is read with a Hewlett Packard Model 3468 multimeter using the 4-wire resistance configuration. The hypsometer was calibrated against a portable pressure standard at three different elevation (25 m at Menlo Park, 1260 m at Bishop, and 2400 m at Mammoth Lakes). The calibration was tested at 300 m elevation intervals between Menlo Park (25 m) and Tioga Pass (3045 m). The standard error in the difference pressure standard less hypsometer was about 5 Pa (0.05 mb = 0.04 mm). The drift rate of the hypsometer relative to a stationary mercury barometer over three years was about 3 Pa/yr.

REPORTS

Prescott, W.H., Davis, J.L., Svarc, J.L., 1989, Global Positioning System measurements for crustal deformation: Precision and accuracy, *Science*, **244**, 1337–1340.

California Seismicity Studies

9930-02103

Paul A. Reasenberg
Mark V. Matthews

Branch of Seismology
United States Geological Survey
345 Middlefield Road - MS 977
Menlo Park, California 94025
415-329-5002

Investigations

1. Worldwide comparison of earthquake sequences.

We have collected data for a worldwide comparison of earthquake sequences observed with regional networks. The sequences are being modeled in a fashion similar to that described in our recent *Science* report (Reasenberg and Jones, 1989). The study includes earthquake sequences from California, the Kanto-Tokai district, Japan, the Garm region, U.S.S.R., the Wasatch front, Utah, and Italy. Variations among clustering properties and earthquake sequence parameter distributions are being examined for these widely varying seismo-tectonic regimes. There are no results to report.

2. Recent seismicity changes in the Los Angeles area.

Recently, the Los Angeles metropolitan region has experienced numerous felt earthquakes. This increase has prompted Lucy Jones and I to focus attention on the detailed nature of the seismicity variations in the Los Angeles region. We have analyzed the Caltech/USGS earthquake catalog for the region within 25 miles of Los Angeles (Figure 1) since 1975. A preliminary study (Open-File Report) addressed two questions: 1) Has there been a significant change in the seismicity under Los Angeles?, and 2) What do such changes, when they occur, tell us about the present regional earthquake hazard? We found that a 2.9-year interval of significantly high seismicity rate, relative to the long-term rate for the region, began approximately March, 1986, and has continued to June, 1989. Additional work has focused on depth variations and changes in b-value for the region, and on the detailed spatial distribution of the seismicity surplus relative to the fault zones in the Los Angeles Basin.

Since mid-1987, 6 moderate earthquakes ($M \geq 4.5$) have occurred in Los Angeles area, the largest being the October 1, 1987, Whittier Narrows earthquake ($M_L = 5.9$). The rate of microearthquakes has also gone up. The rate of occurrence of independent earthquakes ($M \geq 2.3$) within 40 km of 34° 0.0' N, 118° 20.0' W between March 1966 and June 1989 is 75% greater than the rate between 1975 and February 1986. The increased activity is not concentrated at one site or in association with one fault, but has involved many different faults, including the Elysian Park and Torrance-Wilmington fold-and-thrust belts, the Raymond, Palos Verdes and Newport-Inglewood faults. It is, however, confined to the area around Los Angeles and cannot be seen, for instance, near the San Andreas fault.

In the same time period, the b-value has decreased, while the average depth of the hypocenters has increased. The b-value has decreased from a pre-1986 value of 0.92 to a present value of 0.75. The difference between the two values is close to the standard deviations in the values. The mean depth of faulting has increased from 7 km to 9.5 km and the lower quartile of the depth distribution has increased from 9 km to 13 km. This change has not involved an increase in the maximum depth of faulting but instead a greatly increased rate of activity in the bottom third of the seismogenic crust. This simultaneous change in three fundamental parameters of the seismicity distribution (rate, magnitude and depth) suggests a change in the underlying mechanism controlling microseismicity in the Los Angles basin.

3. Intense microearthquake activity beneath Mammoth Mountain, Long Valley, California

The seismic network under Mammoth Mountain became operational in August, 1982. The catalog of earthquakes in the Mammoth Mountain area detected and located with the network appears to be complete for magnitudes 1.2 and larger since that time. The seismicity observed under Mammoth Mountain since 1982 can be characterized by three distinct epochs of activity. From August, 1982 through 1985, the activity was dominated by small earthquakes ($M < 3.5$) occuring at a moderate and fairly uniform rate of 3.6 events ($M \geq 1.2$) per month. The largest earthquakes recorded during this epoch were two $M = 3.0$ events on September 15, 1983 and February 5, 1984. By the end of 1984 the activity diminished, however, save one intense swarm in August, 1985. During the next epoch, from January, 1986 through April, 1989, activity under Mammoth Mountain was relatively quiet, averaging only 0.7 events ($M \geq 1.2$) per month. The largest event in this period was a $M = 2.3$ earthquake on January 13, 1987.

The current epoch began with several $M = 1$ events on May 4, 1989, and was followed by an exponential-like increase in the rate of earthquakes that did not stop increasing until mid-June. The sudden onset of this intense activity was not preceded by any large earthquake, unusual swarm or change in rate of small earthquakes. The seismicity rate during the swarm peaked on June 12 at approximately 8.8 events ($M \geq 1.2$) per day. Since June 12, activity has generally fluctuated about an average rate of 4.3 events per day – a rate still more than 2 orders of magnitude greater than the level of activity prior to May. The current activity shows no signs of abating, and is characterized by surges lasting 1 to 2 weeks and reaching peak intensities of over 7 ($M \geq 1.2$) events per day. The largest earthquakes during the swarm were a $M = 3.3$ event at 6:00 pm (PDT) on June 20, and a $M = 3.2$ event at 7:17 pm (PDT) on August 1.

The magnitude distribution for earthquakes under Mammoth Mountain prior to the May, 1989 swarm is well-described by a Gutenberg-Richter relation with $b = 1.2 \pm 0.2$, a relatively high b-value for California seismicity but one fairly typical of volcanic seismicity. During the current swarm the average b-value remained the same ($b = 1.2 \pm 0.1$ for the period May - July, 1989). Insignificant fluctuations in b observed throughout the swarm (see Figure) show no obvious correlation with the major changes in earthquake rate.

The time history of hypocentral depth for *all* earthquakes ($M \geq 0.0$) – including the relatively deeper events to the southwest and the shallower ones to the northeast – was monitored throughout the swarm (see Figure). During the swarm the median depth fluctuated around 6 ± 1 km. A sudden deepening in median depth from approximately 5 to 7 km coincided with the onset of the swarm. A prominant and equally abrupt shallowing of the median depth from approximately 7 km to 5 km coincided with the onset of the intense mid-June surge. The median depth then equally abruptly plunged to approximately 6.5 km after the mid-June surge.

Reports

Reasenberg, Paul A. and L. M. Jones, Earthquake Hazard After a Mainshock in California, *Science*, 243, 1173-1176 (1989).

Jones, Lucile M. and Paul A. Reasenberg, The Application of Foreshocks to Real-Time Earthquake Hazard Assessment in Southern California, U.S.G.S. Open-File (redbook) report on U.S. - Japan Conference on Earthquake Prediction, Morro Bay, California, in press.

Jones, Lucile M. and Paul A. Reasenberg, A preliminary assessment of the recent increase in earthquake activity in the Los Angeles region, U.S.G.S. Open-File Report 89-162 (1989).

Jones, Lucile M., Paul A. Reasenberg and Egill Hauksson, Increased Earthquake Activity in the Los Angeles Basin, 1986–1989, (abstract), EOS, in press.

Hill, D.P., W.L. Ellsworth, M.J.S. Johnston, J.O. Langbein, D.H. Oppenheimer, A.M. Pitt, P.A. Reasenberg and M.L. Sorey, Mammoth Mountain earthquake swarms, Long Valley Caldera, California, (abstract), EOS, in press.

Figure Caption

Summary of seismicity under Mammoth Mountain. Earthquakes shown were located in the region 37:35 to 37:40, 119:00 to 119:10. (a) Stick plot of seismicity ($M \geq 1.2$) from August, 1982 through April, 1989. Scale on left is coda magnitude. (b) Cumulative number of events shown in (a). (c) Smoothed rate of seismicity shown in (a) obtained by a Gaussian smoothing kernel with width 0.2 years. (d) Expanded plot of seismicity ($M \geq 0.0$) for the swarm period May 1 – August 2, 1989. (e) Cumulative number of events shown in (d). (f) Smoothed rate of seismicity shown in (d) obtained with a Gaussian smoothing kernel with width 2 days. Broken line is mean rate for interval. (g) Time-history of depths of earthquakes ($M \geq 0.0$) for the period May 1 – August 2, 1989. Solid line is median depth of earthquakes; broken lines are upper and lower quartile depths. (h) Time-history of b-value (solid line) and its standard deviation (broken lines).

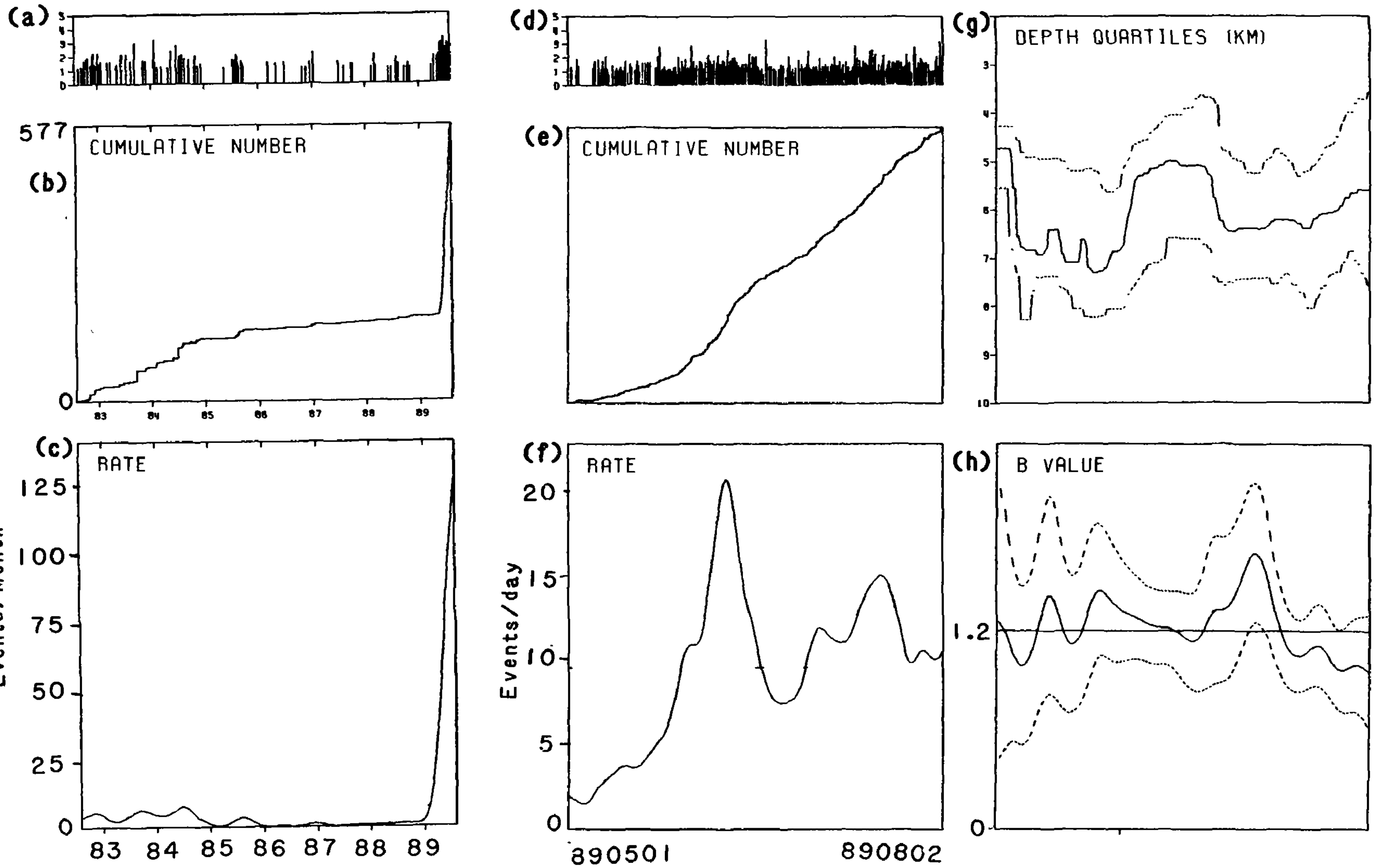
(a)
(b)
577
CUMULATIVE NUMBER
0
83 84 85 86 87 88 89
(c)
RATE
Events/month
125
100
75
50
25
0
83 84 85 86 87 88 89
(d)
(e)
CUMULATIVE NUMBER
(f)
RATE
Events/day
20
15
10
5
0
890501
890802
(g)
DEPTH QUARTILES (KM)
3
4
5
6
7
8
9
10
(h)
B VALUE
1.2
0

FLUID PRESSURE AND EARTHQUAKE GENERATTION

Project #9960-04451

Evelyn Roeloffs, Eddie G. Quilty
Branch of Tectonophysics
U.S. Geological Survey
345 Middlefield Road, MS 977
Menlo Park, CA 94025
(415)329-4833

Investigations:

1. Real-time monitoring and processing of water level data from Parkfield, California as part of the Parkfield Prediction Experiment.

2. Analysis of water level records and development of theoretical solutions to study response to fault creep, seismic waves, and barometric pressure. Searching of water level data for changes that may be related to to the earthquake generation process.

3. Water level monitoring in the Cajon Pass Deep Drillhole and other sites near the San Andreas fault between San Bernardino and Palmdale.

Results:

1. In cooperation with the USGS Water Resources Division, water level data from a network of 12 sites near Parkfield, California were collected throughout the reporting period. Water level data are processed in real time to remove tidal and barometric fluctuations, and the processed data are automatically screened for anomalous signals. A beeper monitoring system provides 24 hour a day automatic notification of water level anomalies.

2. A depth sensor was placed in the Cajon Pass Deep Drillhole in August, 1989. The data reflect the rise in water level as it reaches equilibrium with formation pressure. No earth tides or barometric fluctuations are present. In September, a telemetered water level monitoring site was re-established at the Crystalaire well, 3 km NE of the San Andreas fault zone and 6 km SE of the town of Palmdale, CA. Earth tidal fluctuations in this well have a peak-to-peak amplitude of 8 cm.

3. Re-examination of water level data from the Joaquin Canyon well in Parkfield shows that the coseismic water level drop caused by the August 4, 1985 Kettleman Hills (M 5.5) earthquake was preceded by a water level rise 3 cm in amplitude, beginning 5 days before the earthquake. This well has been monitored continuously since early 1986, and only one other unexplained water level change as large as the one preceding the 1985 Kettleman Hills earthquake has been observed. Further investigation of this possible earthquake precursor is underway.

4. We have estimated frequency-dependent transfer functions between barometric pressure and water level for 4 of the wells monitored near Parkfield. At one site

(Stockdale Mountain), the relationship between water level and barometer is strongly frequency dependent, but does not match existing models incorporating the effects of flow to the water table and of a finite diffusivity for air flow in the unsaturated zone. At the Gold Hill site, determination of a transfer function is complicated by the presence of other water level changes possibly due to tectonic strain. At all sites studied, using frequency-dependent transfer functions to remove barometric effects from water level data, instead of a single coefficient of proportionality, results in a significant reduction of variance.

Reports:

Liu, L.-B., E. Roeloffs, and X.-Y. Zheng, 1989, Seismically induced water level fluctuations in the Wali well, Beijing, China, *Jour. Geophys. Res., 94,* 9453-9462, 1989.

Quilty, E.G., and E. Roeloffs, Removal of barometric pressure response from water level data for selected wells near Parkfield, California (abstract), submitted for presentation at Fall 1989 meeting of the American Geophysical Union.

Roeloffs, E., S. Schulz-Burford, F.S. Riley, and A.W. Records, 1989, Hydrologic effects on water level changes associated with episodic fault creep near Parkfield, California, *Jour. Geophys. Res., 94,* 12,387-12,402, 1989.

Roeloffs, E., and E. Quilty, Groundwater level changes near Parkfield, California, before the August 4, 1985 Kettleman Hills earthquake (abstract), submitted for presentation at Fall, 1989 meeting of the American Geophysical Union.

Hydrogen and Other Non-Radon Geochemical Monitoring

9980-02773

Motoaki Sato* and J. Michael Thompson**
Branch of Igneous and Geothermal Processes
U.S. Geological Survey
* MS-959, Reston, VA 22092; ** MS-910, Menlo Park, CA 94025
(703) 648-6766, FTS 959-6766

INVESTIGATIONS

We continuously monitor soil hydrogen at 1.5 m depth along the San Andreas and Calaveras faults in central California. There are 7 monitoring sites in the Parkfield area and 5 sites in the Hollister area. Of the former sites, 6 sites now have duplicate sensors at about 50 feet separation.

We also continuously monitor water conductivity, dissolved CO_2, and dissolved H_2 in pumped water from two wells, one drilled into the San Andreas fault zone and the other about 500 m from the fault.

RESULTS (1 April 1989 - 1 October 1989)

Soil Hydrogen

1. Parkfield Area:

The data are summarily plotted in Fig. 1 (codes SC, MM, PK, TA, WK, GH, TW). No major anomalies have been recorded. At the end of September, the H_2 level at Twisselman Ranch began to rise. We will watch this development. At about June 10, a few sensors showed a quick increase and a substantial drop in the output signal. These were caused by injection of calibration gas into the ground. It is a new finding that the voltage drop after a positive peak is an artifact created by exposure to H_2 of some sensors (not all of them). This probably happens because of absorption of H_2 by the platinum-black catalyst. After an exposure to a high dose of H_2, somehow oxygen in soil electrochemically oxidizes the absorbed H_2, creating the reverse voltage. It is yet to be discovered why some sensors show this effect and some don't.

2. Holister Area:

Telemetered data from 3 sites (Melendy Ranch, Cienega Winery, and San Juan Bautista) are compiled also in Fig. 1. AT San Juan Bautista (SJ), there were a series of minor changes that began on July 8 and ended on August 9 (Fig. 2). A M 5.1 earthquake struck on August 8 near Los Gatos, about 50 km NW of this site, along the San Andreas fault. The San Juan Bautista site was the closest site in our limited network. The time-coincidence of the anomalous changes with the Los Gatos earthquake is convincingly good.

Melendy Ranch showed some minor anomalous changes in April and mid-May. There were several minor earthquakes (M 2 - 3) within 10 km of this site during this period.

The Shore Road site still have telemetry problem. Wright Road is off telemetry, and we have not retrieved the chartpaper of the on-site recorder.

Well-Water Geochemistry

The water geochemical monitoring suffered from the interuptions of the water supply caused by water line ruptures, sump pump shut downs, and rust clogging due to prolonged stagnancy. The monitored parameters were all severely affected by these water supply problems, precluding meaningful interpretatons. We have to install a flow meter at both Taylor Ranch and Miller Ranch to monitor the water supply changes. Until the installation of the flow meter, smooth operation seems hopeless.

Publications

Sato, M. (1989) Anomalous hydrogen emission along active faults and implications for earthquake triggering mechanism. Abstracts, 28th International Geological Congress. Washington, D. C., vol.3, p. 29-30.

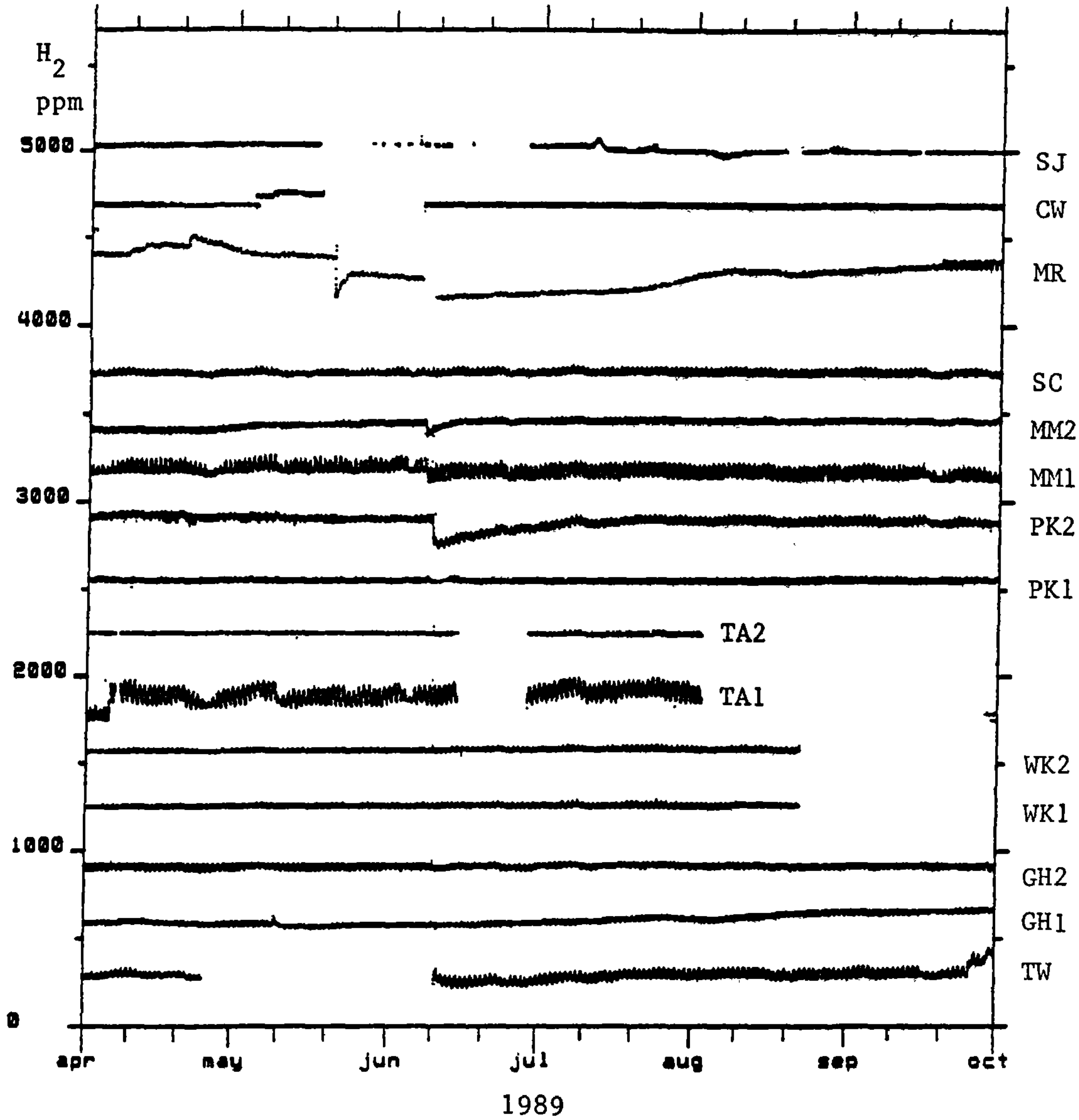

(Fig. 1) Soil hydrogen data recorded along the San Andreas fault between April 1 and October 1, 1989. The site codes are as follows:

Code	Site	Code	Site
SJ	San Juan Bautista	PK	Parkfield
CW	Cienega Winery	TA	Taylor Ranch
MR	Melendy Ranch	WK	Work Ranch
SC	Slack Canyon	GH	Gold Hill
MM	Middle Mountain	TW	Twisselman Ranch

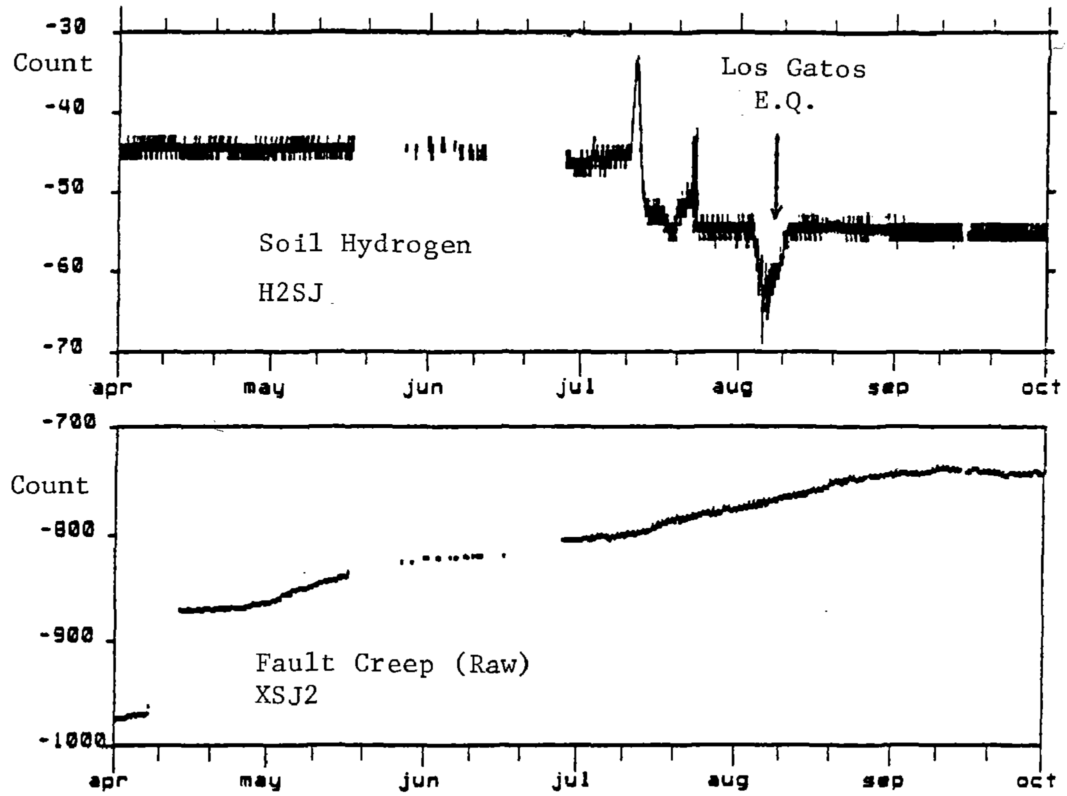

(Fig. 2) The soil hydrogen response to the 8 August 1989 Los Gatos earthquake (M 5.1) that occurred along the San Andreas fault about 50 km NW of San Juan Bautista. The creep data are shown to indicate that the precursory hydrogen anomaly was not artifact of telemetry.

Analysis of Seismic Data from the Shumagin Seismic Gap, Alaska

14-08-0001-G-1388

John Taber
Lamont-Doherty Geological Observatory of Columbia University
Palisades, New York 10964
(914) 359-2900

Investigations

Digitally recorded seismic data from the Shumagin seismic gap in the eastern Aleutian arc, Alaska, are analyzed for detecting space-time variations in the seismicity, focal mechanisms, and dynamic faulting parameters that could be precursory to a major earthquake expected in this seismic gap. The seismic results obtained from the network data are being integrated with with strong motion data, with crustal deformation data that are independently collected, with volcanicity data of nearby Aleutian volcanoes, and with teleseismic information to identify basic tectonic processes which may be precursory to a great earthquake.

Results

As the next step toward a detailed mapping of the variation of stress drops on the subducting plate interface within the Shumagin seismic gap, we have calculated dynamic (Boatwright, 1980) and Brune stress drops (Brune, 1970) for 5 moderate earthquakes within the Shumagin Gap. Analog strong motion records were digitized and then spectra were calculated. The angle of the fault plane was determined from the inversion of teleseismic body waves. Brune stress drop vs moment is plotted in the top of Figure 1 while the dynamic stress drops for the same events are plotted in the lower part of the figure.

The circles are for events that are all part of the same sequence in 1985, while the square represents an earthquake that occurred in 1987 at the opposite end of the Shumagin gap from the 1985 earthquakes. The 4 aftershocks of the 1985 mainshock (M_o=2.13x10^{25}) occurred within 35 days of the mainshock. All events were shallow thrusts along the plate interface. The 1987 event occurred at a similar depth to the 1985 sequence but appears to have a much higher stress drop. This difference in stress drop may relate to differences in coupling along the plate interface.

References

Boatwright, John, 1980, A spectral theory for circular seismic sources; simple estimates of source dimension, dynamic stress drop, and radiated seismic energy, **Bull. Seism. Soc. Am., 70,** 1-27.

Brune, J.N., 1970, Tectonic stress and the spectra of seismic shear waves from earthquakes, **J. Geophys. Res., 75,** 4997-5009.

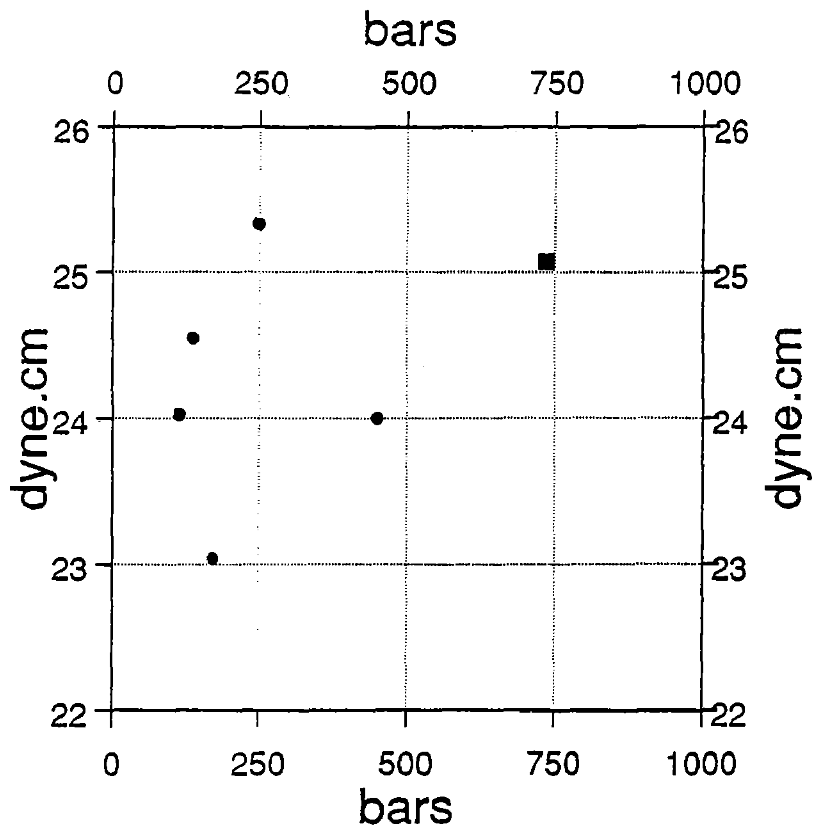

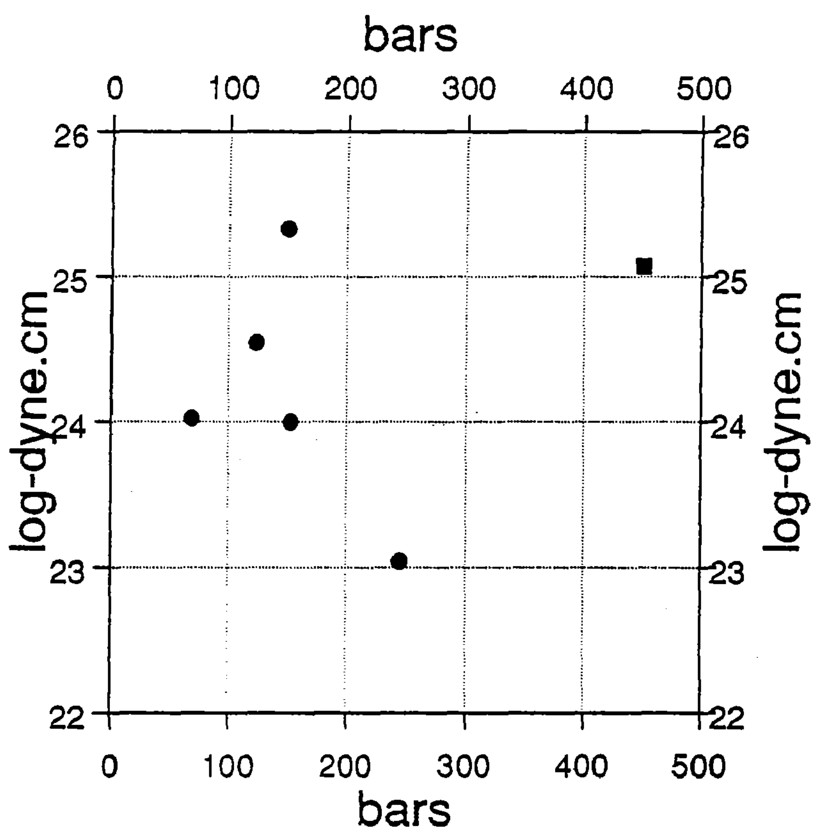

Figure 1. (Top) Brune stress drop vs moment for 5 events within the Shumagin seismic gap. (Bottom) Dynamic stress drops for the same events. Circles are a mainshock-aftershock sequence in 1985. Square is an event at a different location in 1987.

Piñon Flat Observatory: A Facility for Studies of Crustal Deformation

14-08-0001-G1178

Frank K. Wyatt, Duncan Carr Agnew,
and Hadley O. Johnson
Institute of Geophysics & Planetary Physics
Scripps Institution of Oceanography
University of California, San Diego
La Jolla, CA 92093
(619) 534-2411

This multi-year grant supports the operation of Piñon Flat Observatory (PFO) by providing half of the funding needed both for running the 160-acre facility and for maintaining the reference-standard instruments there. Matching funds are provided by a grant from the National Science Foundation. The work done at PFO includes establishing the accuracy of instruments designed for measuring various geophysical quantities by comparing results from them with data from the best available continuously recording deformation monitors. This comparison also allows accurate monitoring of strain and tilt changes in the area near the observatory, between the active San Jacinto fault and southern San Andreas fault systems (Figure 1: 30-year-conditional probabilities as reported by the USGS Working Group on California Earthquake Probabilities, *Open-File Report 88-398*, 1988). All of this effort is intended to foster development of precision instrumentation by providing a national facility for the long-term testing and operation of geophysical systems. The site continues to be utilized by about 20 different research teams with about 4-5 "graduates" per year and an equal number of new investigators.

For this report, we include some recent observations on the temporal and spatial distribution of strain in southern California. Figure 2 presents four year's of data from three systems monitoring strain over the Pinyon Flat area — systems of substantially different scale. Laser strainmeter data from the observatory's 732-m-long NW-SE sensor is shown both with ("Corrected Strain") and without the predictable solid-earth tides ("Residual"). Relatively frequent two-color geodimeter results are shown as solid squares with error bars for the 7-baseline ~4-km-wide network solution. (This data was kindly provided by Dr. John Langbein.) Finally, the periodic single-color Geodolite data (courtesy of Dr. Jim Savage) is shown as open squares along with its corresponding uncertainty for its 10-line, ~16-km-wide network. The important point here is that all three systems appear to be capturing the same long-term strain rate (shown as a dashed line for the geodetic data), despite the difference in averaging areas. This lends credence to the small-scale instrumental strain data, the geodetic techniques having already proven themselves, and suggests, at least in this NW-SE component, that the spatial pattern of surface deformation is relatively well behaved, even in an area as potentially complex as Pinyon Flat. The flat is located in the 2000-m-high Santa Rosa Mountains, half-way between the San Jacinto Fault system and the sea-level floor of the Coachella Valley. Figure 2 also identifies some particular events of interest in the laser strainmeter record. On this scale the strain associated with the Superstition Hills earthquake (labeled: #3) would seem of little importance, but expanding the record by 1000 yields a clear record of smoothly varying deformation immediately following the event, though nothing preceding it (Agnew and Wyatt, *Bull. Seism. Soc. Am.*, **79**, 480-492, 1989).

As we discussed in our previous report in this series, we have begun to look at the broader scale geodetic data for southern California using data collected by the USGS Crustal Strain group led by Dr. Will Prescott. Figure 3 presents our determination of the horizontal strain rate for networks of four stations (using the method of simultaneous reduction) along an east-west path across southern California. We plot the strain rates against distance from the San Jacinto Fault, along a line roughly perpendicular to the fault strike. The vertical error bars are 1σ intervals; the horizontal bars show the projected extent of each subnet, with the strain-rate plotted at the projected center of mass. Note that since many subnets share lines, the results should be somewhat correlated. To see how well these strain rates compare with geologically determined parameters for the faults crossed by the network, we computed strain rates for a fault locked to some depth and freely slipping below it. The dotted line shows the computed rates, which assume a locking depth of 10 km for all faults, and slip rates of 1 mm/yr for the Newport-Inglewood fault zone, 5 mm/yr for the Elsinore, 12 mm/yr for the San Jacinto, and 17 mm/yr for the San Andreas as given by Bird and Rosenstock (*Geol. Soc. of Am. Bull.*, **95**, 946-957 [1984]) and Millman and Rockwell (*GSA Cordilleran Section Guidebook on Neotectonics and Faulting in Southern California*, 159-166 [1986]). (The dotted line actually shows the integrated strain rate over 25 km, the average width of the USGS networks.) The model predictions roughly agree with the estimated rates. For the two geodetic subnets closest to PFO, the measured $\dot{EW}$ and $\dot{\gamma}_1$ strains are about equal, indicating that the north-south compressional rate ($\dot{\gamma}_1 = \dot{e}_{EW} - \dot{e}_{NS}$) is nearly zero. In contrast to the discussion above on strainmeters and geology this suggests local distortion in the deformation field near this end of the "Anza gap" on the San Jacinto fault. We are working on this.

As another means of investigating the overall character of deformation throughout southern California, we have computed the linear strain rate on each individual line in the network and plotted this against the value expected from the simple model described above. The result is presented in Figure 4 as a scatter plot. In the case of a perfect fit to the data this plot would show a straight line at a 45 degree angle. Overall the fit appears to be quite reasonable, especially for such a simple fault model. The plot also shows that the largest strain rate observed throughout the network (including fault crossing lines) is about 0.2 $\mu\epsilon$/yr.

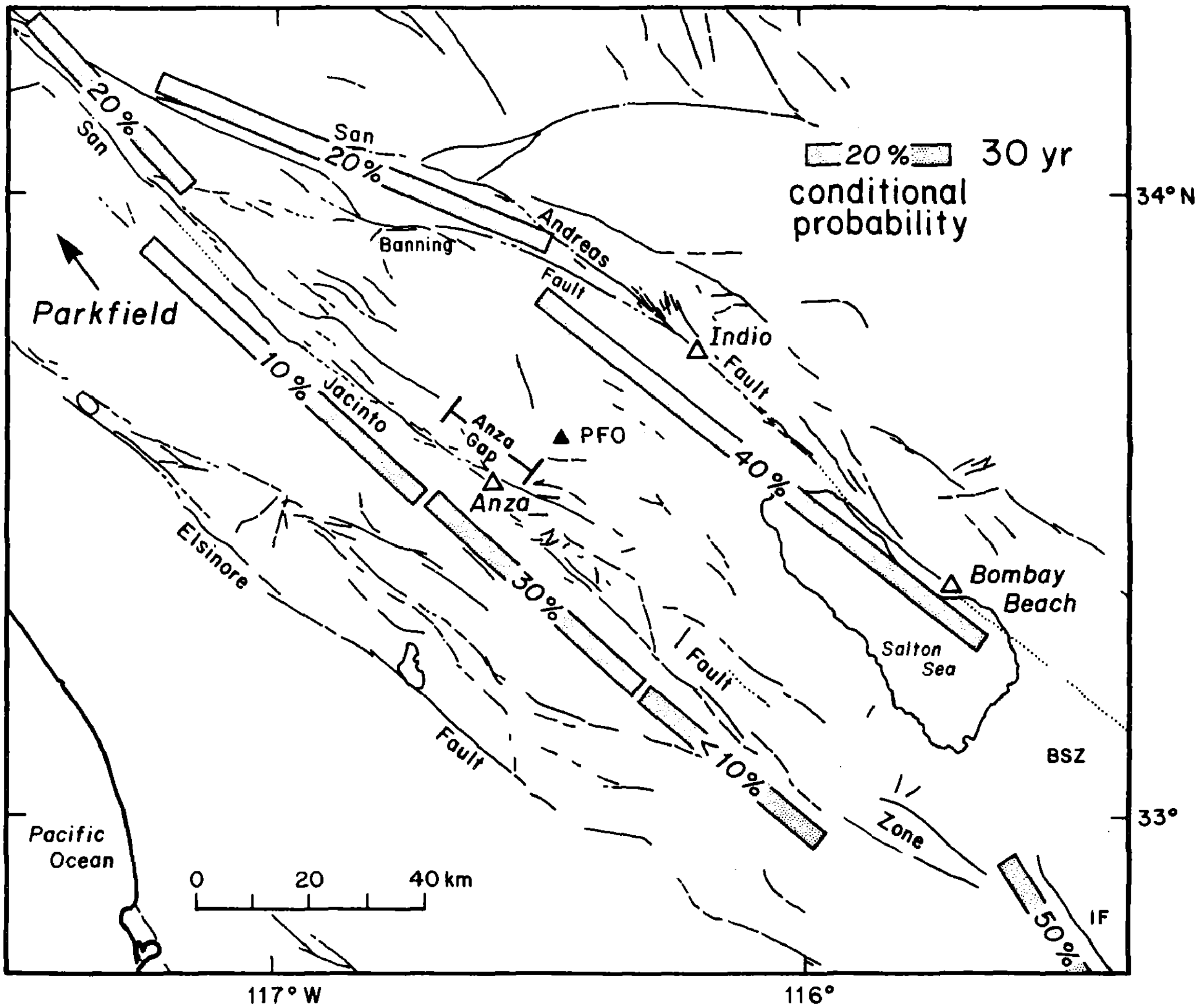
20%
30 yr
conditional probability
34°N
33°
117° W
116°
San
San
20%
20%
Andreas
Fault
Banning
Parkfield
Indio
Fault
40%
10%
Jacinto
Anza
Gap
PFO
Anza
30%
Elsinore
Fault
Fault
<10%
Bombay
Beach
Salton
Sea
BSZ
Zone
50%
IF
Pacific
Ocean
0
20
40 km

Figure 1.

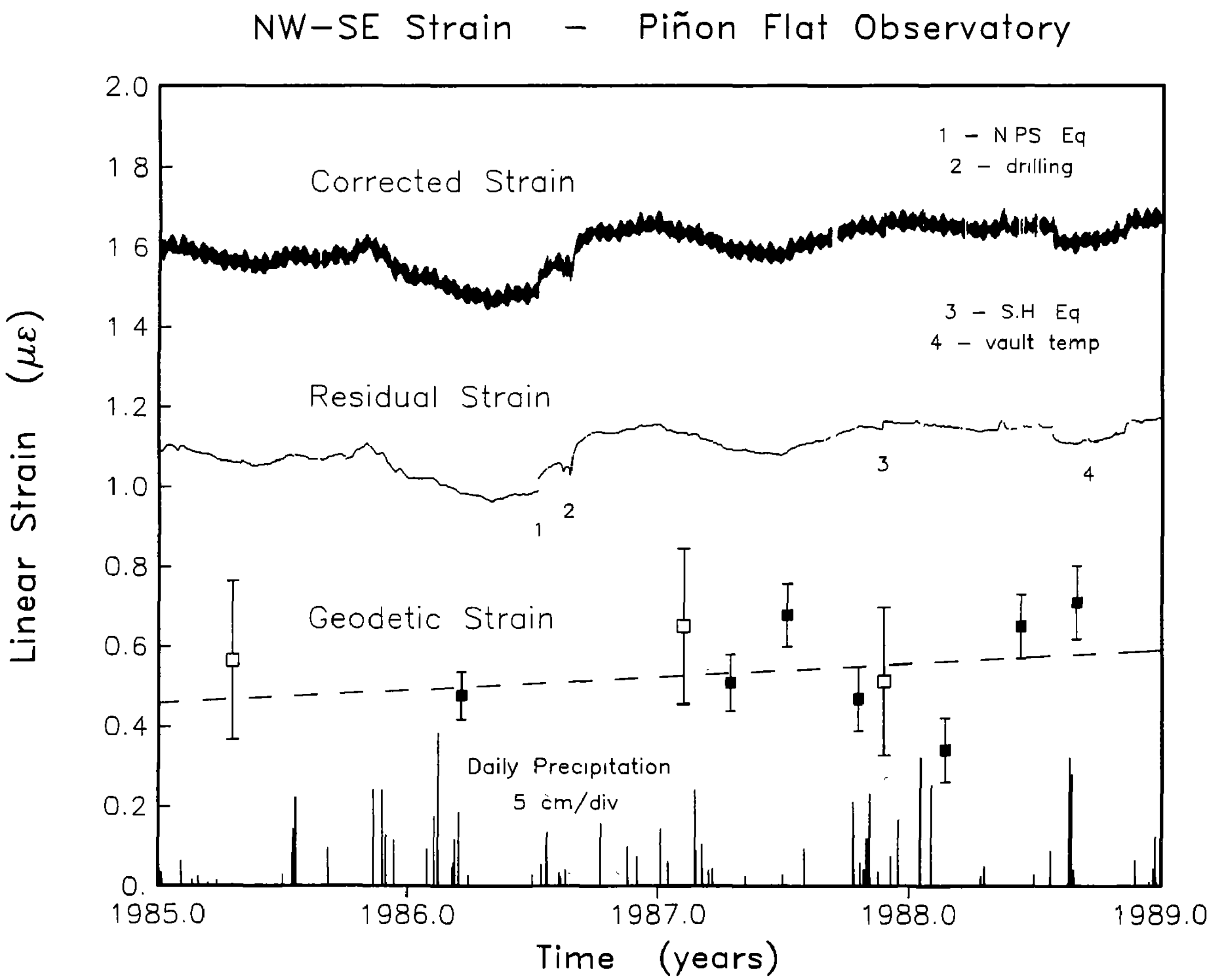
NW-SE Strain - Piñon Flat Observatory
Corrected Strain
1 - N PS Eq
2 - drilling
3 - S.H Eq
4 - vault temp
Residual Strain
Geodetic Strain
Daily Precipitation
5 cm/div
Linear Strain ($\mu\varepsilon$)
Time (years)
2.0
1.8
1.6
1.4
1.2
1.0
0.8
0.6
0.4
0.2
0.
1985.0
1986.0
1987.0
1988.0
1989.0
1
2
3
4

Figure 2.

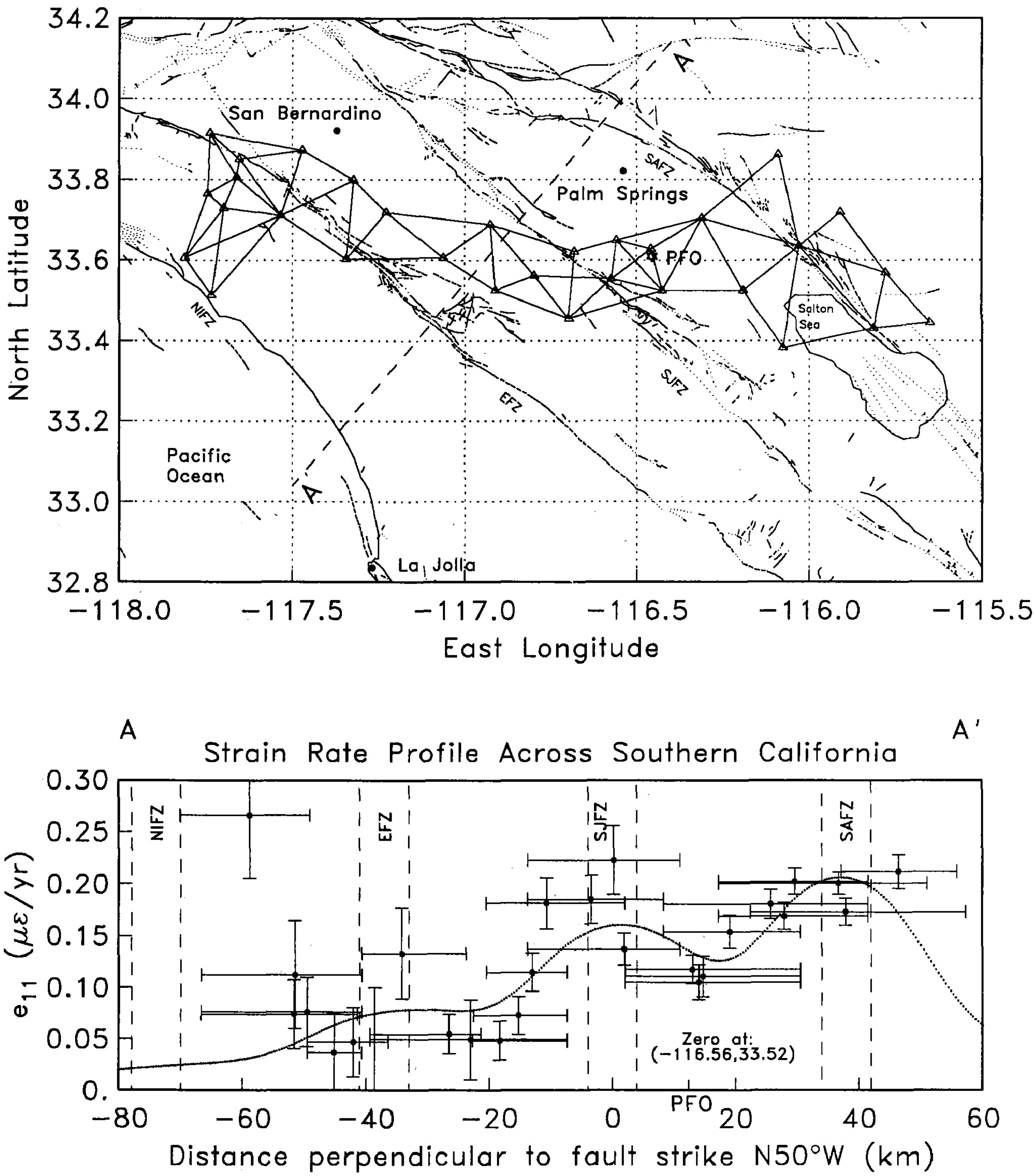
34.2
34.0
33.8
33.6
33.4
33.2
33.0
32.8
−118.0
−117.5
−117.0
−116.5
−116.0
−115.5
East Longitude
North Latitude
San Bernardino
Palm Springs
PFO
Salton Sea
Pacific Ocean
La Jolla
A
A'
SAFZ
SJFZ
EFZ
NIFZ
A
A'
Strain Rate Profile Across Southern California
NIFZ
EFZ
SJFZ
SAFZ
Zero at:
(−116.56,33.52)
PFO
e_{11} ($\mu\varepsilon$/yr)
0.30
0.25
0.20
0.15
0.10
0.05
0.
−80
−60
−40
−20
0
20
40
60
Distance perpendicular to fault strike N50°W (km)

Figure 3.

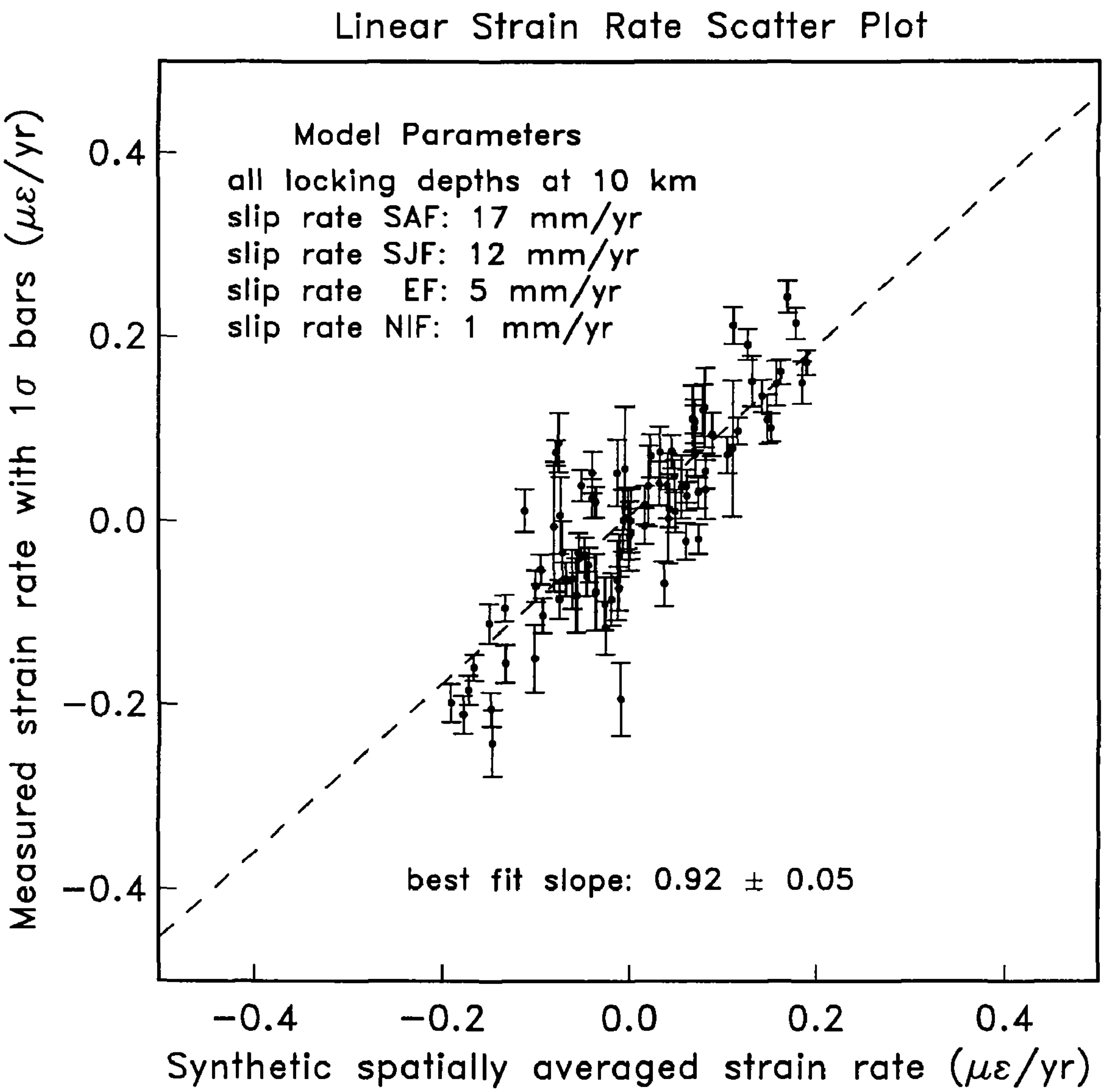

Linear Strain Rate Scatter Plot
Model Parameters
all locking depths at 10 km
slip rate SAF: 17 mm/yr
slip rate SJF: 12 mm/yr
slip rate EF: 5 mm/yr
slip rate NIF: 1 mm/yr
best fit slope: 0.92 ± 0.05
0.4
0.2
0.0
−0.2
−0.4
Measured strain rate with 1σ bars (με/yr)
−0.4
−0.2
0.0
0.2
0.4
Synthetic spatially averaged strain rate (με/yr)

Figure 4.

An Absolute Long-Base Tiltmeter with Vertical Anchoring

14-08-0001-G1336

Frank K. Wyatt, Hadley O. Johnson,
Mark A. Zumberge, and Duncan Carr Agnew
Institute of Geophysics and Planetary Physics
University of California, San Diego
La Jolla, California 92093-0225
(619) 534-2411

For long-base tiltmeters to be useful in crustal deformation measurement, they must be exceptionally stable, engineered for general use, and suitable for installation in a wide variety of locations. We have been working toward these ends for the past few years, with much of the emphasis on design and testing of the equipment. This year's grant supports work on field construction of the new tiltmeter systems, and for the monitoring and evaluation of these new systems against existing ones at Piñon Flat Observatory (PFO). The overall aims (some already reached) for our development program are:

- To develop an automated water-height gauge for dependable operation of a Michelson-Gale tiltmeter.
- To construct a low-maintenance instrument vault with sufficient environmental insulation to avoid the need for active temperature and humidity control.
- To produce instrument "anchoring" techniques that will allow near-surface long-base tiltmeters to provide highly stable results in a wide range of settings.
- To design these components, and other needed systems, to be available at a reasonable cost and operable without frequent skilled intervention.

Of these, reliably coupling the instrument to the earth is by far the most difficult problem—and one that affects not only tiltmeters, but strainmeters and geodetic monitoring programs as well. As a solution to this problem we have been evaluating optical-fiber interferometers; for tiltmeters this means using them as vertical anchors. These fiber systems measure the integrated strain (displacement) from depth to the surface, and so should provide the means to correct for any end-monument instability. Fibers can be installed in small-diameter, coarsely drilled holes and, being solid-state transducers, should be both long-lived (e.g., invulnerable to lightning) and generally maintenance-free.

We have also built a self-regulating water-height sensor which we installed in 1987, along with several test fibers, in a research vault along an extension of the original EW long-base tiltmeter at PFO; by connecting to the old instrument, we have used the records from it to estimate the stability of the new equipment. Our results show that the water-height gauge and vault design possess the needed stability, and that the optical fiber system is approaching that level. Although we still do not have the confidence we would like in the long-term stability of optical fiber, our experience to date is encouraging, provided some allowance is made for "settling in" of the system (see Figure 1, and previous reports in this series).

Under present funding, we have installed a second new instrument vault with 100-m-deep optical fiber anchoring at a site 550 m south of the first. Hydraulic conduit (15 cm pipe, half filled with fluid) has been installed between the two new vaults to form a North-South tiltmeter. This year of the program is thus focusing on construction, with testing, monitoring, and final evaluation planned for next year. Overall, this work should:

- Provide a new tiltmeter perpendicular to the existing one at PFO, allowing us to completely define vertical deformation at this tectonically interesting site.
- Allow, by virtue of the tiltmeter interconnecting the end-vaults, a needed test of relative fiber stability in two different settings, using different types of fiber.
- Give us additional hands-on experience in making this new technology work in a field environment and provide for documentation of it.

We expect that the new long-baseline tiltmeter, when combined with the original one, will provide an important record of surface deformations associated with dislocations on the nearby San Jacinto and San Andreas fault systems, and help in the interpretation of the other tiltmeters and geodetic leveling programs in the vicinity of the observatory.

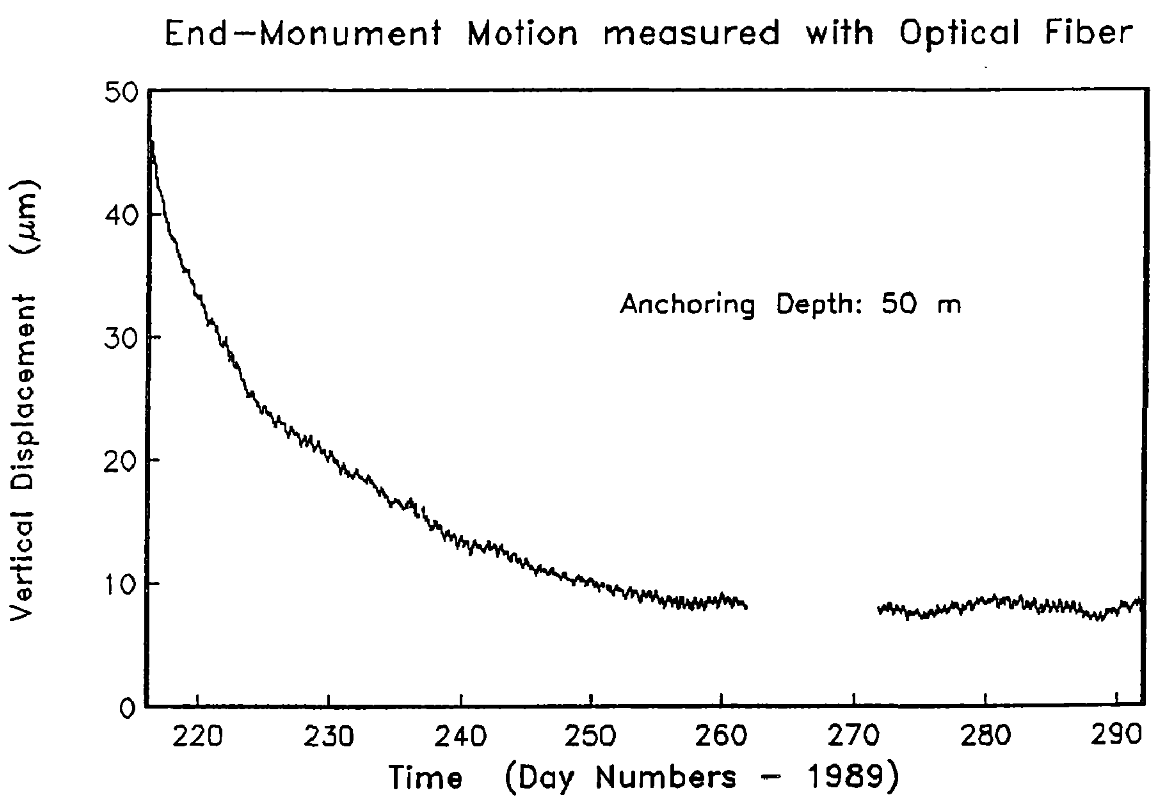

Figure 1.

Intraplate Stress and Deformation

9930-02669

Mary Lou Zoback
U. S. Geological Survey
Branch of Seismology
345 Middlefield Road, Mail Stop 977
Menlo Park, CA 94025
(415) 329-4760

Investigations

1. Continued compilation and analysis of global *in situ* stress data.

2. Analysis of the state of stress in the Pacific Northwest region using wellbore breakouts, earthquake focal mechanisms, and volcanic vent alignments.

3. Continued analysis of moderate-sized midplate earthquakes using independent stress data as constraints.

Results

1. More than 4500 stress orientation datapoints have now been compiled as part of the World Stress Map project of the International Lithosphere Program. The data are being stored in dBase IV on an IBM-PC compatible computer. A general database includes basic information for each data point (latitude, longitude, depth, quality, type of indicator, etc.) and a series of relational databases store detailed information (*e.g.*, P- and T-axes, seismic moment, stress magnitudes, standard deviations, etc.

The World Stress Map project was the subject of a day and a half symposium convened by Mary Lou Zoback and Sierd Cloetingh at the International Geologic Congress in July. Over 30 talks were given covering all aspects of tectonic interpretation of the data and using the data to constrain modelling of plate driving forces. Proceedings of the symposium will be published in a special issue of JGR along with additional papers by project participants who were unable to attend the symposium. Plans were made for a large-size (scale 1:30,000,000) color version of the World Stress Map to be published by the USGS to be compatible with the recently published USGS map entitled "World Map of Volcanoes, Earthquakes, and Plate Tectonics". Plans were also made for release of the entire stress database digitally through World Data Center A (for solid earth geophysics) at NOAA in Boulder, CO. Public release of the digital database is planned to coincide with publication of the JGR special issue.

Preliminary results and interpretations of the regional tectonic "first-order" stress fields have just been published in Nature (M. L. Zoback et al., Global Patterns of Tectonic Stress, October, 1989). Current analysis efforts include a detailed evaluation of the influence of major crustal structures and boundaries on the stress field in the upper, brittle crust. This is part of a broader effort to define so called "second-order" stress fields which result from local forces superimposed on the regional, plate-tectonic derived stress field. Rotation of the regional stress field in the vicinity of the continental slope is one example of a second-order stress field. In this case the sense of rotation is consistent with a superimposed extensional stress oriented perpendicular to the margin. Preliminary comparison of the stress data with major Precambrian province boundaries (continental building blocks) in North America indicate that the stress field in general is quite continuous across these boundaries.

2. Stress orientations inferred from analysis of wellbore breakouts, hydraulic fractures, and volcanic vent alignments are compared with earthquake focal mechanisms in the Pacific Northwest. Focal mechanisms considered are for crustal events of M $\geq$ 3.0 and are generally well-constrained by first motions. Available dipmeter logs from petroleum wells drilled in Washington state after 1970 were analyzed for breakouts. These data are supplemented with breakout data from Oregon (Werner *et al.*, 1988, EOS) and hydrofrac data from Hanford (Paillet and Kim, 1987, JGR). Volcanic alignments for vents younger than 1 m.y. were also determined.

A general pattern of NE to NNE compression extends from the coast to about 160 km inland north of about latitude 46°N. Breakouts from wells in the Coast Ranges of Washington and NW Oregon indicate a N30°E SH_{max}, consistent with a N31°E SH_{max} inferred from focal mechanisms along the St. Helen's seismic zone and a N27°E SH_{max} inferred from focal mechanisms in south Vancouver Island. An iterative inversion of focal mechanisms for events beneath the central Puget Sound Basin yields a well-constrained SH_{max} of N20°E. This is consistent with a N15°E SH_{max} inferred from breakouts in one well in the basin. These data confirm the influence of NE directed Juan de Fuca–North American plate convergence along this section of the Cascadia subduction zone and suggest a strongly coupled plate boundary.

Although focal mechanisms just east of Puget Sound show highly variable P axes orientations, data from the region east of the central axis of the Cascades north of 46°N consistently indicate a N-S S_{Hmax}, probably related to Pacific–North American plate interaction. Sparse focal mechanism, breakout, and geologic data south of 46°N to just north of the Mendocino triple junction suggests this N-S compression extends to the coastal region and indicates weak coupling with the subducted slab along this segment of the subduction zone.

3. Available stress data have indicated that many intraplate regions are characterized by a relatively uniform stress field. Well-constrained focal mechanisms in midplate north America have been analyzed using stress orientations independently derived from well-bore breakouts and hydraulic fracturing data. Earthquakes from a zone of high seismicity in southeastern Canada and New England have dominately reverse fault focal mechanisms. In contrast, earthquakes in the central and eastern United States nearly always show slightly oblique, but dominantly strike-slip focal mechanisms. Mechanisms in both regions have ENE-trending P axes.

The fundamental contrast in stress regime within a region characterized by a relatively uniform ENE S_{Hmax} orientation suggests a local source of stress variation.

The band of high seismicity along the S.E. Canada-U.S. border falls within the region of glacial rebound and suggesting a causal relationship. The expected upper crustal stress field in the rebounding region previously covered by the thick ice sheet is radial extension and circumferential compression (relative to a center point in Hudson Bay (T. James, 1989, oral communication). Interestingly, the seismicity level in the northern Great Lakes region, where the rebound-related circumferential stresses trend nearly orthogonal to the regional S_{Hmax}, is quite low.

However, superposition of rebound-related stresses does not by itself explain the contrast in stress regime between southeastern Canada and the central United States. Superposition of the rebound stresses in southeastern Canada would increase the magnitude of S_{Hmax} and lower the magnitude of S_{hmin} relative to the central United States; whereas, the observed thrust faulting requires that the magnitudes of both horizontal stresses must be increased above the vertical. An alternate interpretation is that the contrast in stress regime between southeastern Canada and the central United States may be reflecting a true plate-scale variation in relative stress magnitudes, possible related to the influence of resistive drag on the base of the plate.

Reports

Magee, M. E., and M. L. Zoback, 1989, Present state of stress in the Pacific Northwest: Eos (Trans. American Geophysical Union), in press.

Zoback, M. L., 1989, World Stress Map Project: Global patterns of stress and constraints on intraplate deformation, in Abstracts, 28th International Geologic Congress, v. 3, p. 449, Washington, D.C.

Creep and Strain Studies in Southern California

Grant No. 14-08-0001-G1666

Clarence R. Allen and Kerry E. Sieh
Seismological Laboratory, California Institute of Technology
Pasadena, California 91125 (818-356-6904)

Investigations:

This semi-annual Technical Report Summary covers the six-month period from 1 April 1989 to 30 September 1989. The grant's purpose is to monitor creepmeters, displacement meters, and alignment arrays across various active faults in the southern California region. Primary emphasis focuses on faults in the Imperial and Coachella Valleys.

During the reporting period, the alignment array across the Superstition Hills fault at IMLER ROAD was resurveyed, and nail-file arrays across the Imperial fault were resurveyed at ROSS ROAD and ANDERHOLT ROAD. Creepmeters were serviced at ROSS ROAD (5 times), HEBER ROAD, TUTTLE RANCH (3 times), SALT CREEK (4 times), MECCA BEACH, NORTH SHORE (4 times), and HARRIS ROAD. Slip meters were serviced at LOST LAKE, TWISSELMAN RANCH, AND JACK RANCH.

A new satellite-telemetered creepmeter was installed on 1 August at NORTH SHORE, replacing the former dial-gauge instrument there. This was a period during which we experienced unusual vandalism and mechanical problems with our creepmeter installations, particularly at ROSS ROAD and SALT CREEK.

A major time-consuming problem for us, not envisaged in the budget, has been caused by the transfer by NOAA/NESDIS of the data bank through which we receive our telemetered creepmeter data from DCS at Camp Springs, MD, to the DAPS computer system at Wallops Island, VA. The two systems are significantly different, requiring us to completely rewrite our software for receiving and archiving the creepmeter data. For financial reasons, we have necessarily had to delay completion of this software preparation, and we may, in fact, therefore be faced with gaps in data retrieval before funding for the new contract year arrives.

Results:

The reporting period was one of little activity except for continuing afterslip on the Superstition Hills fault. On 18-19 April, a classic 9-mm creep event occurred on the Imperial fault at ROSS ROAD, accompanied very locally by en-echelon cracks. The event took place over a 12-hour period, with most of the slip occurring in about 2 hours.

Tectonic Tilt Measurement: Salton Sea

14-08-0001-G1392

John Beavan
Lamont-Doherty Geological Observatory of Columbia University
Palisades, New York 10964
(914) 359-2900

Investigations

1. Historical water level recordings from three sites around the Salton Sea are being investigated to determine tectonic tilting, taking account of as many noise and error sources as possible.
2. The tectonic tilt so derived is being carefully compared with leveling data from the area.
3. LDGO-designed pressure-sensor gauges at five sites around the sea are being used to measure water level continuously, to investigate noise sources, to determine the level of detectability of tectonic tilt signals in the data, and to measure tectonic tilting.
4. A dense network of sites near the Southern San Andreas and northern Imperial Valley Faults is being surveyed annually to cm-level horizontal accuracy, using Global Positioning System (GPS) techniques (in cooperation with Dr. R. Reilinger of MIT).

Results (October, 1989)

1. Our paper on the historical 1952-87 tilt recorded by Salton Sea water level gauges was published (Hudnut & Beavan, JGR, 94, 9463-9476). Efforts continue to locate additional original information on the SB data from the late 1950's, a period of higher than average inferred tilt rate.
2. Four of the GPS stations are close to our water level sites. We are hoping to enhance the vertical accuracy of the GPS survey by introducing the 1 cm accurate inter-site height differences obtained from the water level data into the GPS analysis. The success of this effort will depend on being able to define the local geoid with sufficient accuracy. We have begun the task of analyzing GPS, water level and gravity data with this objective in view.
3. Data from the L-DGO water level sites (Fig. 1) continue to be collected. There have been a few data outages, which have been corrected in a timely fashion. One gauge (BPR) was removed due to recurrent silting at the site. Backup recorders using Onset TattleTale computers will be installed at the 3 remote sites late in 1989; these will prevent data loss due to telemetry outages.

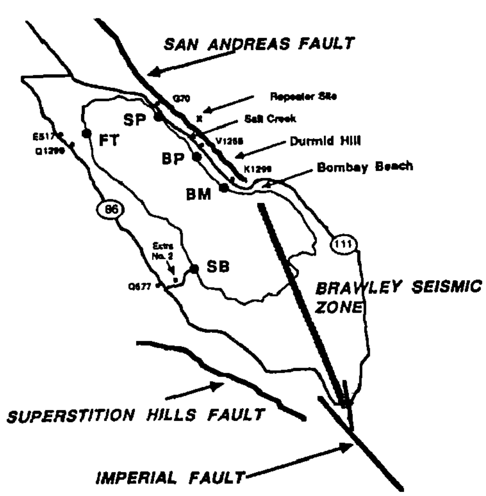

Figure 1. Map of the study region. Sea-level measurements using float or staff gauges have been made at FT and SB since 1950, and at SP since 1970. L-DGO continuous recording pressure gauges have operated at SP since May 1985, at SB since January 1986, at BP since December 1986, and at BM and FT since May 1987. The pressure gauge data are digitally telemetered, via the repeater site shown, to SP. There they are stored on disk, and can be accessed by modem. Datum control of the sea level gauges has been provided by leveling them to nearby NGS benchmarks; clockwise from SP, these are G70, V1255, K1299, Extra No. 2 and Q1299. The SB to FT baseline length is 35 km, FT to SP is 14 km.

Acceleration, Velocity, and Volumetric Strain from Parkfield GEOS Network

9910-02089

Roger D. Borcherdt, Malcolm J. Johnston, Allan Lindh
Branch of Engineering Seismology and Geology
345 Middlefield Road, MS 977
Menlo Park, California 94025
(415) 329-5619

Investigations

- o Maintain GEOS array near Parkfield, CA to serve as a strong-motion array to provide broad-band, high-resolution measurements of the mainshock as well as an array to provide measurements of pre-, co-, and post-seismic strain and displacement field pertubations for purposes of earthquake prediction.

- o Maintain up-to-date archive of all events recorded in anticipated rupture zone.

- o Develop theoretical basis and models to interpret colocated measurements of volumetric strain and seismic displacement fields.

Results:

- o An array of 15 stations has been maintained at 95 percent or greater reliability since July, 1987. An up-to-date digital data archive is being maintained and summarized in monthly internal USGS reports. (See previous reports for detailed description of the array.) Events recorded along Parkfield segment of study zone during time interval are summarized according to magnitude and depth.

Reports

Borcherdt, R.D., Johnston, M.J.S., Noce, T., Glassmoyer, G., aand Myren, D., 1988, A broad--band, wide dynamic range, strong-motion network near Parkfield, California, USA for measurement of acceleration and volumetric strain: *9th World Conference on Earthquake Engineering*, Proceedings, Tokyo-Kyoto, Japan, v. VIII, p. 125.

Johnston, M.J.S., Linde, A.T., and Myren, G.D., 1988, Earthquake strain steps, seismic moment and total earthquake moment, EOS, *Trans. Am. Geo. Un.*, v. 69, p. 401.

Johnston, M.J.S., Linde, A.T., Borcherdt, R.D., and Gladwin, M.T., 1988, Implications of high resolution strain measurements prior to moderate earthquakes in California, EOS, *Trans. Am. Geo. Un.*, v. 69, p. 1423.

Bakun, W. and Borcherdt, R. D., 1988, Criteria for the issuance of public warnings based on short-term earthquake predictions near Parkfield, California, USA: Proceedings, *Second U.S.-Japan Workshop on Urban Earthquake Hazard Reduction*, Tokai University, Shimizu City, Japan, in press.

Borcherdt, R., Holzer, T., Isenberg, J., Malin, P., Shakal, A., Spudich, P., Stepp, C., and Tucker, B., 1988, Strong-motion seismology prediction experiment in the near field of the predicted Parkfield earthquake: Proceedings, *9th World Conference on Earthquake Engineering*, Tokyo-Kyoto, Japan, in press.

(See projects (Borcherdt *et al.*, 9910-02689 and 9910-03009) for related reports.)

10/89

PARKFIELD TWO-COLOR LASER STRAIN MEASUREMENTS

9960–02943

Robert Burford
Branch of Tectonophysics
U.S. Geological Survey
345 Middlefield Road, MS/977
Menlo Park, California 94025
(415) 329–4850

and

Larry Slater
CIRES
University of Colorado
Boulder, Colorado 80309
(303) 492–8028

Investigations

Operation of the CIRES two-color laser geodimeter at the Carr Hill Observatory near Parkfield, California was continued during the period April 1 through September 30, 1989. Lines to permanent reflector sites that were monitored for length changes during this period are shown in Figure 1. Additional measurements were made occasionally to monumented points without permanent reflectors, including most of the reference marks adjacent to the permanent reflectors.

Results

Plots of detrended length–change histories for the 18 lines to permanent reflector points are shown in Figure 2a, b. Detrended changes for the period April 1, 1989 through September 1989 are shown in Figure 3a, b, and average rates of length change for the report period, as determined by linear least–squares approximation for each line, are given in Table 1. Average station velocities relative to Carr Hill for motion constrained to be parallel to the strike of the San Andreas fault zone are also given in Table 1 (negative values denote apparent left–lateral motion).

Short–term (6–month) rates of deformation for this report period are slightly biased by possible systematic scale errors that occurred during April–July, 1989 (Figure 3a, b).

Reports

Burford, R.O., L.E. Slater, P. Segall, J.O. Langbein, and P. Olds, 1986, Geodetic strain measurements and modelling of the earth's crust near Parkfield, California: *Proceedings of 5th Joint Panel Meeting, the U.J.N.R. Panel on Earthquake Prediction Technology*, June 16–19, 1986, Tsukuba, Japan, pp. 114–128.

Langbein, J.O., and R.O. Burford, 1989, Variations in fault slip and strain accumulation at Parkfield, California: Initial results using two-color geodimeter measurements, 1984–1988: *J. Geophys. Res.*, in press.

Table 1

Summary of Monitoring Results
Two–Color Laser Geodimeter Network at Parkfield
April 1, 1989 through September 30,1989

Permanent 2–Color Reflector Sites	Measurements Started	Location Relative to Car Hill	Average Extension Rate, mm/yr	Fault Parallel R.L. Station Velocities
1. Can	10/09/84	5.7 km N03°W	-11.94 ± 0.53	15.45 ± 0.69
2. Nore	08/13/87	1.1 km N44°E	-07.82 ± 0.26	[- - - - - - - -]
3. Table	10/09/84	6.2 km N69°E	-00.58 ± 0.64	$[-01.64^* \pm 1.81]$
4. Hunt	07/28/85	2.7 km S72°E	$+08.84 \pm 0.31$	10.25 ± 0.35
5. Mel–S	10/14/84	5.4 km S68°E	$+07.60 \pm 0.54$	08.48 ± 0.60
6. Turk	07/10/87	2.3 km S56°E	$+10.83 \pm 0.31$	11.26 ± 0.32
7. Gold	04/18/86	9.2 km S49°E	$+13.47 \pm 1.20$	13.57 ± 1.21
8. Creek	06/27/84	5.7 km S36°E	$+06.15 \pm 0.55$	$-06.19^* \pm 0.55$
9. Mason–W	06/26/84	6.3 km S11°W	$+01.90 \pm 0.67$	$-03.14^* \pm 1.11$
10. Todd	08/07/85	3.7 km S15°W	$+14.28 \pm 0.40$	$-25.87^* \pm 0.72$
11. Hog–S	07/25/84	5.0 km S62°W	$+01.99 \pm 0.48$	$[08.23 \pm 1.98]$
12. Lang	07/25/84	4.1 km N72°W	$+00.33 \pm 0.42$	00.38 ± 0.48
13a. Pomo	04/29/86	5.6 km N51°W	$+01.25 \pm 0.56$	01.27 ± 0.57
13b. Pitt**	10/09/84	5.7 km N47°W	$+04.05 \pm 1.25$	04.07 ± 1.25
14. Mid	08/23/84	5.0 km N43°W	-01.57 ± 0.45	$-01.57^* \pm 0.45$
15a. Mid–E	08/21/84	4.5 km N35°W	-33.41 ± 0.44	33.68 ± 0.44
15b. Buck	07/31/86	3.1 km N32°W	-14.42 ± 0.33	14.62 ± 0.34
16. Bare	10/09/84	4.8 km N12°W	-15.88 ± 0.47	18.30 ± 0.54

Note: (*) Indicates apparent left–lateral station movement (column 5)

[ ] Fault–parallel projection values in column 5 unreliable owing to orientation of line nearly normal to fault strike.

(**) Routine measurements discontinued after June, 1986.

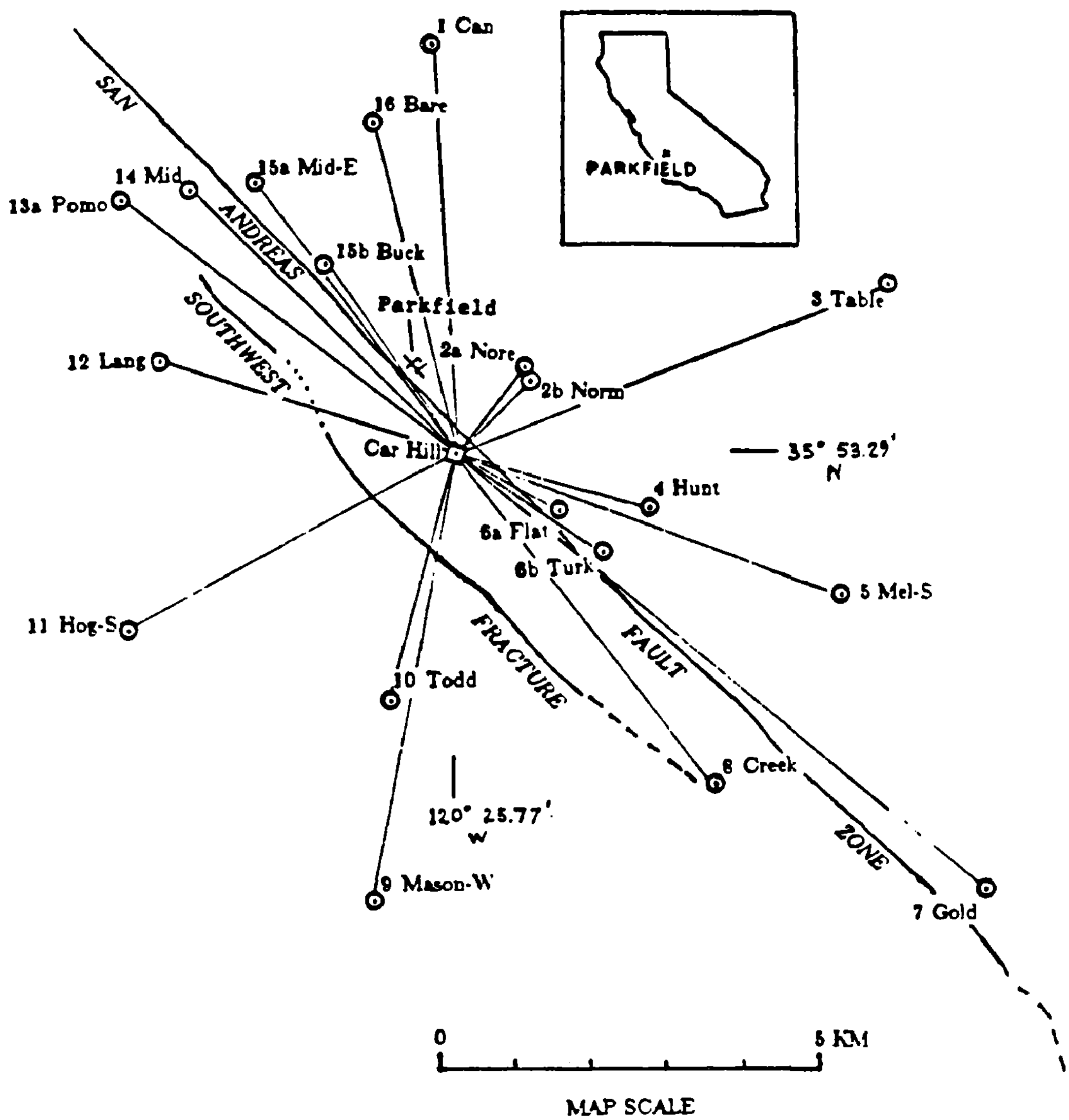

Figure 1. Two-color laser geodimeter network at Parkfield, California.

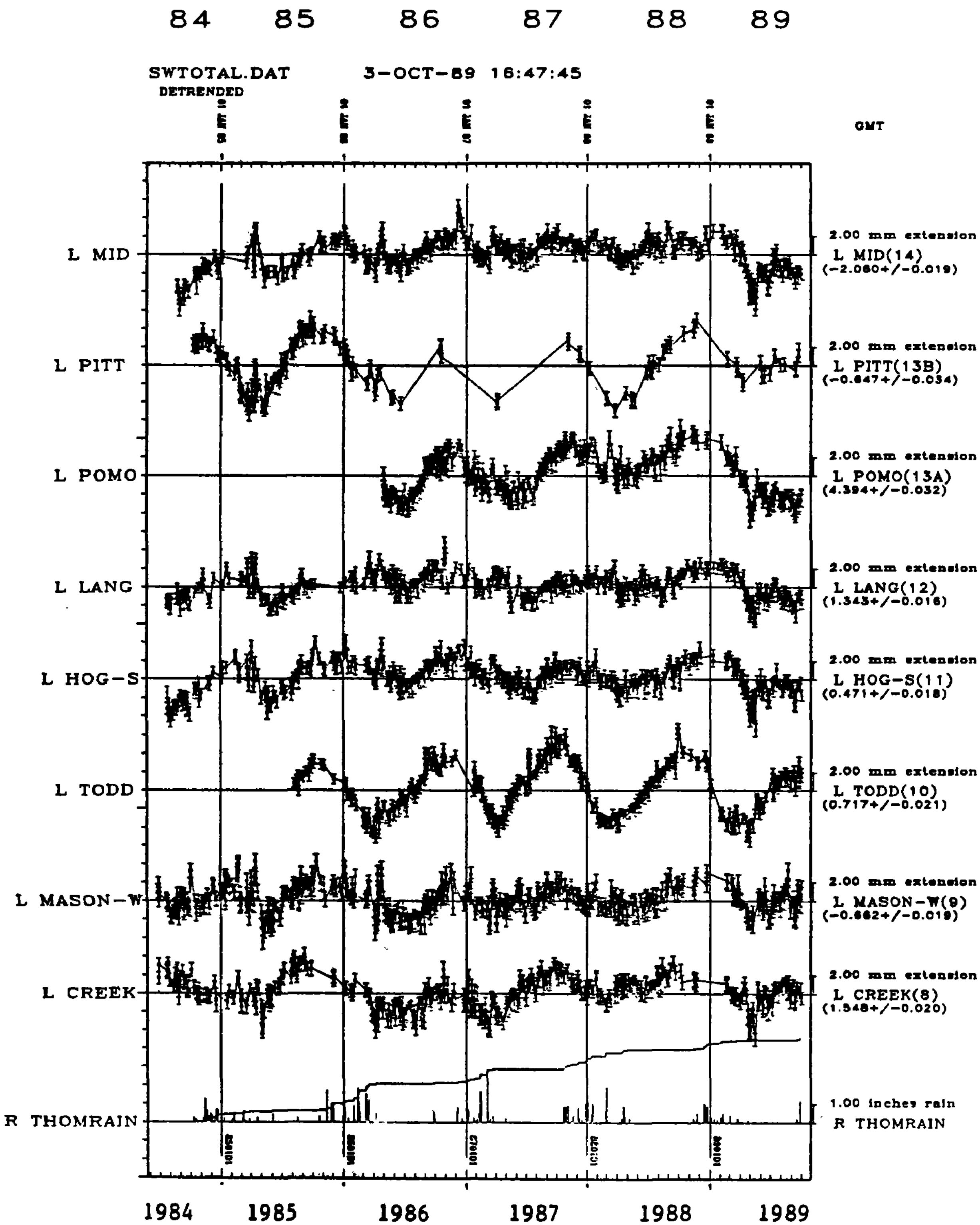

Figure 2a. Detrended 2-color data from the CarrHill network, Parkfield, for lines terminating in the block southwest of the main San Andreas fault.

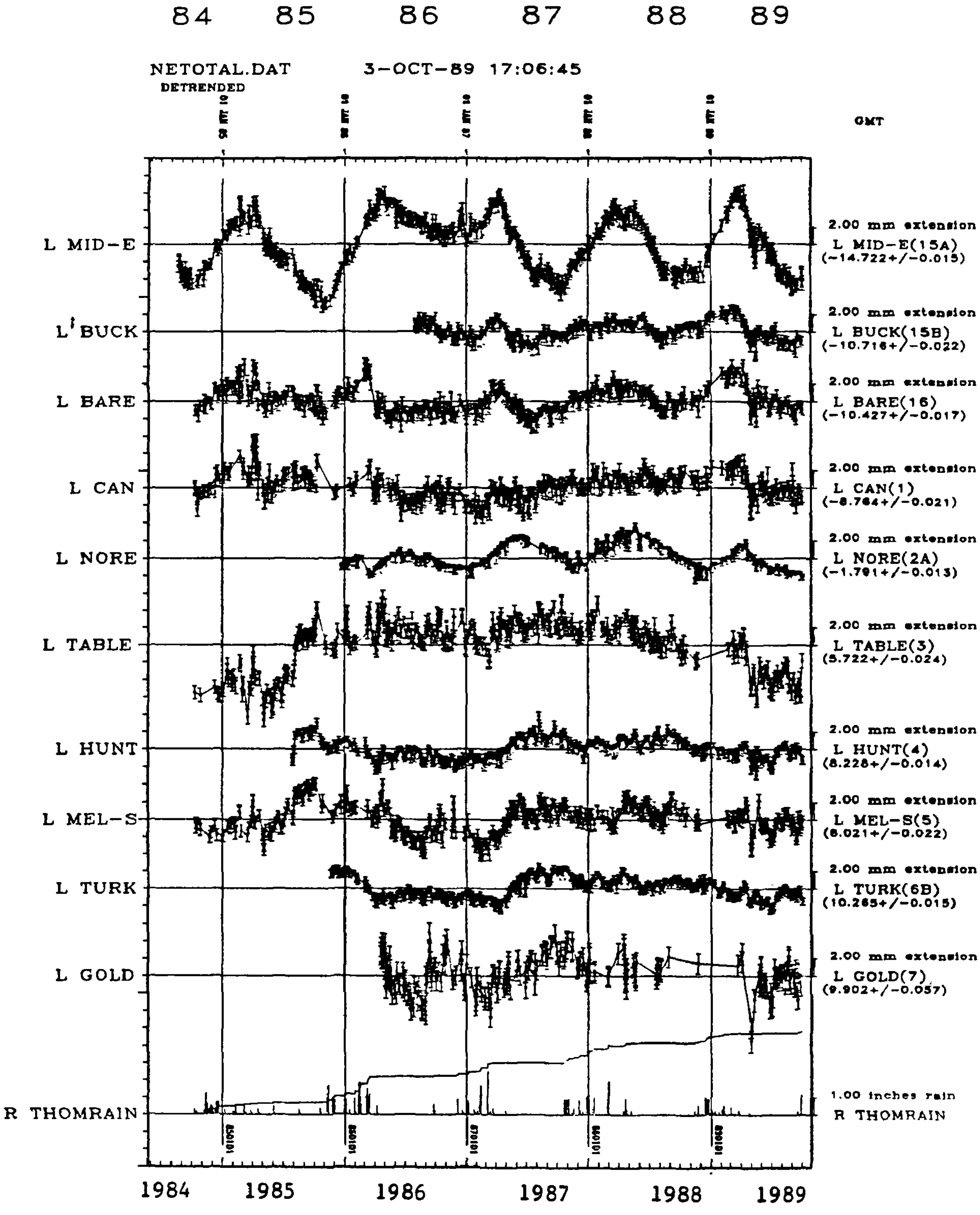

Figure 2b. Detrended 2-color data from the Carr Hill network, Parkfield, for lines terminating in the block northeast of the main San Andreas fault.

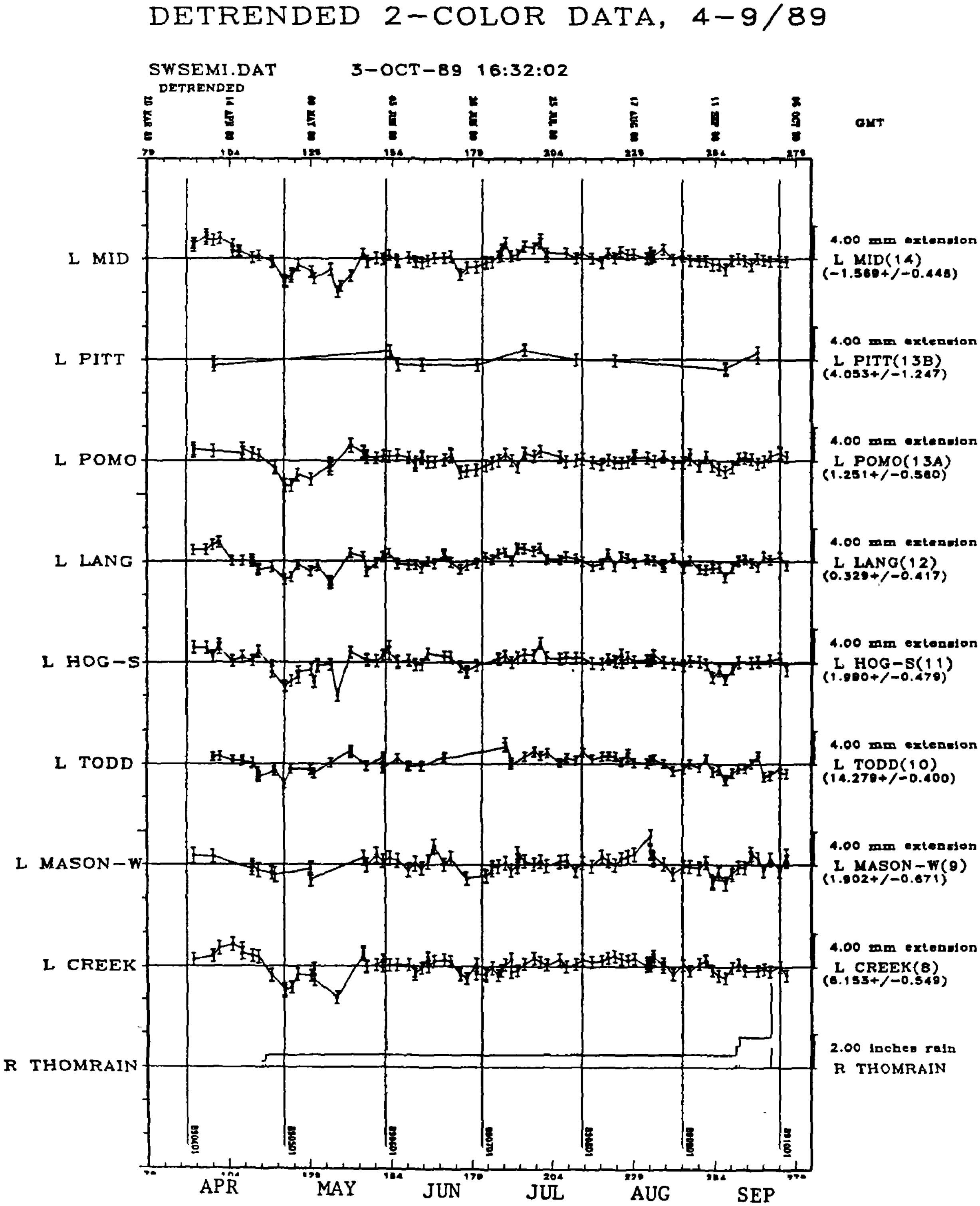

Figure 3a. Detrended 2-color data from Carr Hill network, Parkfield, April through September 1989, for lines terminating in the block southwest of the main San Andreas fault.

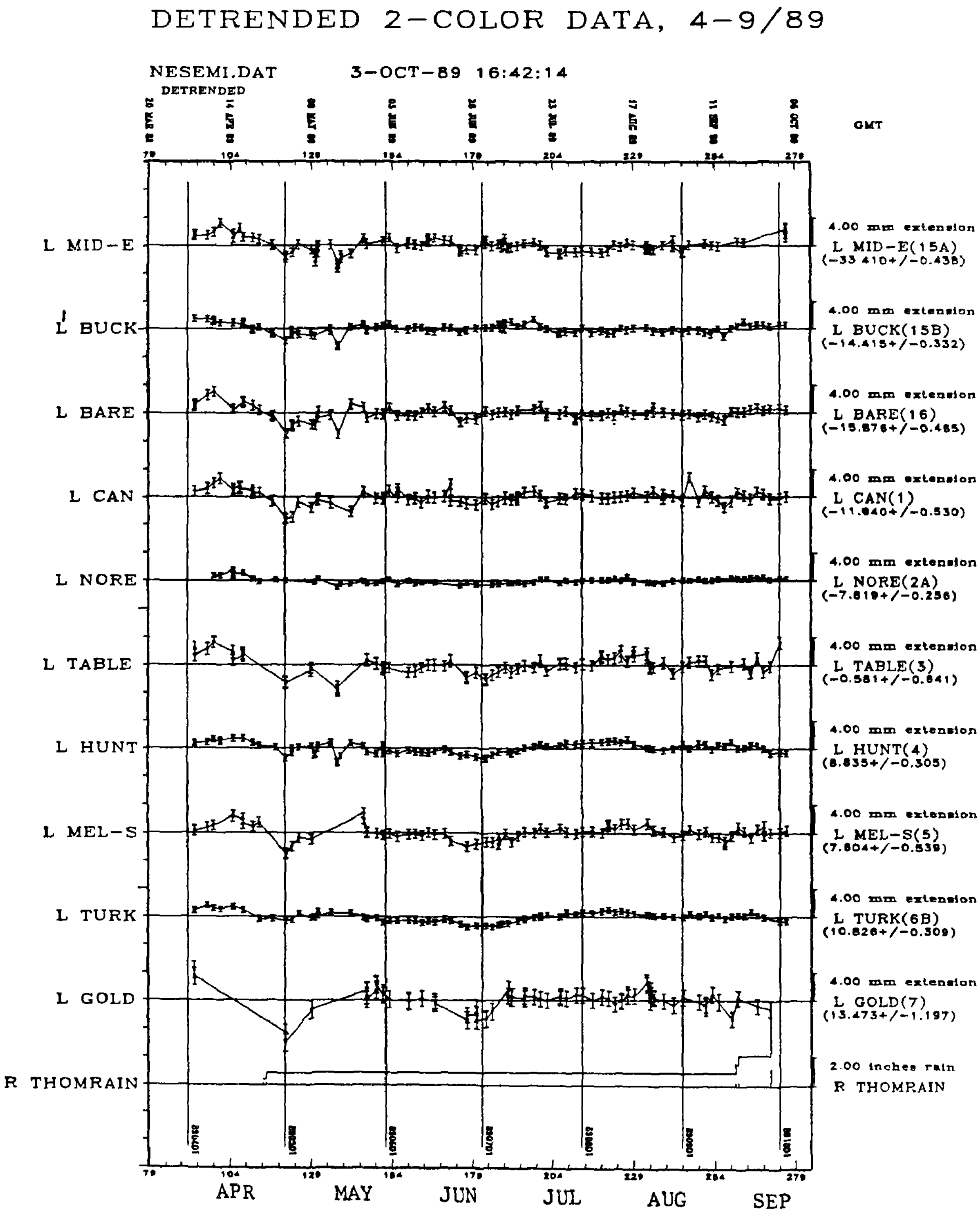

Figure 3b. Detrended 2-color data from Carr Hill network, Parkfield, April through September 1989, for lines terminating in the block northeast of the main San Andreas fault.

Seismic Studies of Fault Mechanics

9930-02101

William L. Ellsworth
Randall White and David Castillo

Branch of Seismology
U.S. Geological Survey
345 Middlefield Road - MS 977
Menlo Park, California 94025
415-329-4784

Investigations

1. Seismic strain release along the San Andreas fault system and in the western Basin and Range province.
2. High-resolution studies of microearthquakes near the hypocenter of the 1966 Parkfield earthquake.
3. Tectonics and state of stress within the San Andreas fault system in northern California.

Results

1. Analysis of a newly assembled catalog of M≥6 earthquakes in California, Nevada and Baja California (1852-1987) suggests that the deformation of the plate boundary due to historic seismicity conforms with the plate motion predicted by global models. The seismic deformation is determined by summing the moment tensors of the earthquakes (Kostrov's method) to obtain the average shear strain within the crustal volume that absorbs the intraplate motion. This three-dimensional shear may be related to plate motion through the projection of the seismic strain tensor onto the plate motion coordinate system. For M≥7 events within 150 km of the San Andreas fault the net seismic strain is dextral shear in an azimuth of N 43°W, which lies significantly to the west of the N 35-36° W direction derived from plate tectonics, and a N 2°E compression of one sixth the magnitude. M≥7 events in the Western Basin and Range Province gives nearly equal components of horizontal extension and horizontal shear, with the opening direction, N 59°W, agreeing well with geologic estimates. The shear component, dextral slip on a vertical plane striking N 13°W, reflects the large strike-slip displacement in nearly every historic event in this province. This strike-slip faulting reduces the net expansion of the Province toward the coast and increases the region's contribution to the plate motion to about ¼ of the total. Summing the seismic strain in both regions yields pure dextral shear on a plane striking N 36°W. Evidently, extension in the Western Basin and Range Province just compensates compression along the coast during this time period. Seismic slip within the total region contributed by the M≥7 earthquakes since 1857 correspond to a plate velocity of 2.2 cm/a. Integration of the observed frequency magnitude relation, $\log N = 5.9 - M_S$, gives a velocity up to twice as high, suggesting a strongly coupled plate boundary.

2. We have begun to investigate the spatial and temporal characteristics of the seismicity in the immediate vicinity of the hypocenter of the 1966 Parkfield earthquake. This is the zone that produced the foreshocks to both the 1934 and 1966 events, and is generally believed to be the probable locus of foreshocks (if any) to the next characteristic Parkfield earthquake. Most of the fault plane is aseismic in this region, with the best catalog locations suggesting several distinct spatial clusters of activity. Using digital waveform data from the Calnet, we are re-analyzing the events in this zone since 1984 when CUSP recording began. Using the joint hypocenter determination method on systematically re-analyzed P-wave arrivals, we observe a significant tightening in the size of individual hypocenter clusters on the fault plane.

   As the next step in the study, individual event clusters are being analyzed using precise cross-spectral timing procedures. We find that relative traveltimes can be measured to a precision of 0.001 s or better with the CUSP waveforms. Results for one pair of events from 1984 places them at a hypocentroidal separation of about 20 ± 5 m in the plane of the San Andreas fault. Ultimately, we hope to determine the precise geometry of each cluster and determine which events, if any represent repeated movement of the same part of the fault.

3. The objective of this study is to refine our understanding of the crustal structure, style of deformation and state of stress along the San Andreas fault system along its northernmost 150 km, between about the latitude of Clear Lake and the Cape Mendocino. The principal contemporary seismicity lie along the Maacama and Bartlett Springs fault zones. One-dimensional velocity modelling reveals a typical Franciscan crustal structure, with compressional velocities of 5.6 km/s near 5 km depth, increasing to 6.0 km/s at about 15 km. Focal mechanisms for well-constrained events range from right-lateral strike-slip to reverse, with one of the nodal planes approximately parallel to the average trend of the Maacama and Bartlett Springs faults (N 30°W). The 10-15 km wide band of hypocenters straddling each of these fault systems, together with the varied style of faulting, strongly suggests that slip is accomodated across a complex shear zone. The directions of the maximum horizontal compressive stress, inferred from P-axes in well-constrained focal mechanisms range from N-S to NE-SW. At the northern extreme of these fault systems, landward of the triple junction, the P-axes of crustal events undergo a marked transition indicating NW-SE compression. This stress re-orientation appears to be related to the influence of coupling between the subducting Gorda plate and the overriding North American plate.

Reports

Ellsworth, W. L., 1989, Implications of historic seismicity along the San Andreas fault system and in the Western Basin and Range for the accomodation of motion between the North American and Pacific Plates (abs.): Seismological Research Letters, v. 60, p. 23.

Continued studies of Extensive-Dilatancy Anisotropy in USA: III, modelling the effects of the Earth's surface on micro-earthquake wavetrains at Parkfield

14-08-0001-G1712

Russ Evans, Stuart Crampin and David C Booth
British Geological Survey,
West Mains Road,
Edinburgh EH9 3LA, Scotland, U.K.
(International +) 44 31 667 1000

Collaborating investigator - Peter E Malin, UCSB

Objective: To study microearthquake wavetrains obtained at the Varian well and the UCSB/UCB downhole seismometer stations at Parkfield - Firstly to identify the origins of the various components of the wavetrains using frequency-wavenumber and polarization techniques; Secondly to model the components using strong single-scattering, anisotropic and weak multiple scattering methods as appropriate.

Work to date: Evans visited UCSB in June, as planned, to familiarise himself with the available data from the Varian array and downhole networks. The practicalities of data exchange are proving a little more awkward than originally anticipated, as the Varian data is held on a microVAX system in CUSP format, so the capability of reading these data must be added to the BGS repertoire. A support proposal to the UK network authority for use of the JANET-Internet relay has been accepted, so remote access and file transfer between the Edinburgh and Santa Barbara machines has been established at no further cost to the project. This will enable limited data processing to be undertaken in near real time. A brief technical note summarizing the technical and organisational steps involved is in preparation and may be of interest to other UK and US groups wishing to set up similar communication.

In the course of his recent visit to California, Evans visited USC, San Diego and field sites, including KNW, of the Anza array, and held useful discussions on shear-wave polarization methods with a number of colleagues. The paper discussing recent results from Anza (Crampin et al., 1989) has been substantially revised and resubmitted to JGR.

Related activity: Evans, Crampin and Booth each presented papers on aspects of anisotropy and scattering related to micro-earthquake studies at the IASPEI meeting in Istanbul, during August. Following that meeting, X-R. Shih (University of Wisconsin) visited Edinburgh to collaborate with Booth on methods for interpretation of microearthquake seismograms.

Jonathan Lees at UCSB is analyzing travel-time data in the Parkfield area, and is employing tomographic inversion methods to determine Earth structure. BGS and Kandilli Observatory, Istanbul, have collected an extensive dataset of microearthquake records from a section of the North Anatolian Fault which displays some similarities to sections of the San Andreas. As a spin-off from the present project, we hope to collaborate in a parallel investigation of the travel-time data from this region.

Planned activity to March 1990: We expect that the coming half-year will see the principal effort on this programme. Evans is scheduled to make two extended visits to Santa Barbara, and Crampin a shorter visit in December 1989. We expect to have tangible results at the next reporting round.

References

Crampin, S., Booth, D.C., Evans, R., Peacock, S. & Fletcher, J.B., 1989. Changes in shear- wave splitting at Anza near the time of the North Palm Springs earthquake, *J.Geophys.Res.*, submitted.

Dense Seismograph Array at Parkfield, California

9910-03974

Joe Fletcher, Lawrence M. Baker, and Paul Spudich
U.S. Geological Survey
345 Middlefield Road
Menlo Park, California 94025
(415) 329-5628, (415) 329-5608, or (415) 329-5654

Investigations

1. Installation of the sensors and electronics. Troubleshooting any electronics problems.
2. Cataloging and analysis of data.

Results

1. The Parkfield Dense Array is a 14-element, short baseline seismic array situated on the Work Ranch near Parkfield, California (see Fig.1 for station locations). The maximum aperture of the array is about 1 km. Three-component force-balance accelerometers and velocity tranducers are digitized at each station at 200s/s by a 16-bit A/D for both high-dynamic range and broad frequency response. Data is telemetered in nearly realtime (within a few tenths of a second) to a central recording site where the events are recognized and written to disk on a MicroVAX-II.

During this period the array was installed in the field. We encountered two problems during the installation: timekeeping and network reconfiguration. Time code from a GOES receiver is broadcast to each site along a differential cable using the RS-422 protocol. Time is received at each station every second and a pulse at the end of the time code is used for synchronization. Gophers chewed through the small PVC-jacketed cable that was initially used and the timing cable was ultimately replaced with an armored cable. Nevertheless the time stamps put in the data packets by the data acquisition units were still very unreliable. The data acquisition units were not using parity to detect noise added in on the line and so the internal clocks were being reset with bogus time values. This problem has been mostly fixed with the addition of a new GOES receiver that also contains a stable internal clock so that meaningful time code will still be broadcast even if GOES cannot be recieved, by using parity sense on the data acquisition units, and by a change to the software that causes time to be reset only when good time code has been received several times in a row.

Telemetry of both data and commands is done using ARCnet, a local-area network adapted from the PC world. The ARCnet chip set accomplishes a number of tasks in hardware such as:

1). Acknowledgement of the successful transmission of data.

2). Ability to immediately sense the addition or removal of any station. No preconfigured number of stations

3). No master station.

4). CRC error detection within the data packets.

When the system senses a new station or the token (permission to transmit is given to each station in turn by the passing of a "token") is lost the system will undergo a "reconfiguration." During this time no data can be transmitted, so if the reconfiguration rate is high (more than once per second) then data can be lost. The reconfiguration rate appears to be sensitive to the quality of the earth ground at each site. Initially the system was kept floating, but some sites experienced a very high reconfiguration rate without a ground so all stations will now be grounded.

2). The first event was recorded on April 4, 1989, but the array was not working reliably until mid-June, when 13 of the 14 stations were operational and DC offsets had been mostly eliminated from the force-balance accelerometers. Records were obtained for 150 events up through Sept. 16, 1989. These events have trigger times that are roughly correlated with lists of events in central California such as the summary files from the routine processing of CALNET and the RTP. Other events were also recorded, many of which look like air waves (much slower apparent velocities than body wave arrivals) from gun shots. Both the Lake Elsman 1989 mainshock (M 5.2) and a large aftershock were recorded. Local events are rare but one example is shown in Figure 2. Figure 3 shows an event that appears to be from the Nevada Test Site.

Figure Captions

1). Map of the stations of the Parkfield Dense Array. The array is approximately due west of Gold Hill. The central recording house is on the main ridge uphill from the other buildings of the Work Ranch.

2). Seismograms for a event from the Parkfield section of the San Andreas fault. The trigger time is noted by the large numbers to right of the data. Small adjacent labels give the station name and whether the trace is from a vertical accelerometer (A) or a vertical velocity tranducer (V). Time is given across the top in seconds. The small numbers to the left give the maximum A/D counts for that trace. Time offsets of the P-wave arrival are not valid due to timing problems. Note that for this event which is a M_c 2.1 and has counts of approximately 2000 that the force-balance accelerometers have not registered any ground motion at unity gain.

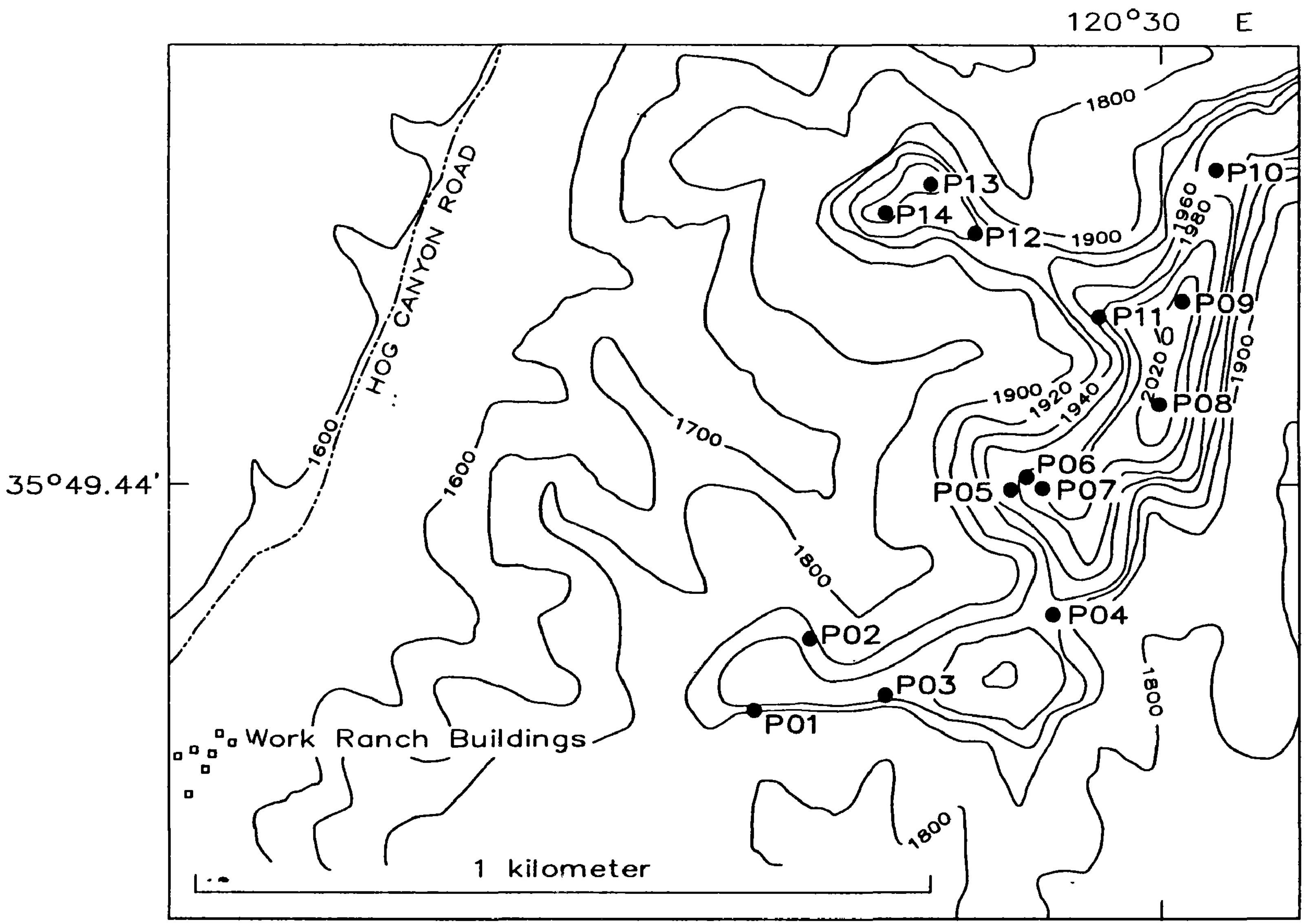
120°30 E
35°49.44'
HOG CANYON ROAD
1600
1700
1800
1900
1920
1940
1960
1980
2020
P01
P02
P03
P04
P05
P06
P07
P08
P09
P10
P11
P12
P13
P14
Work Ranch Buildings
1 kilometer

Figure 1

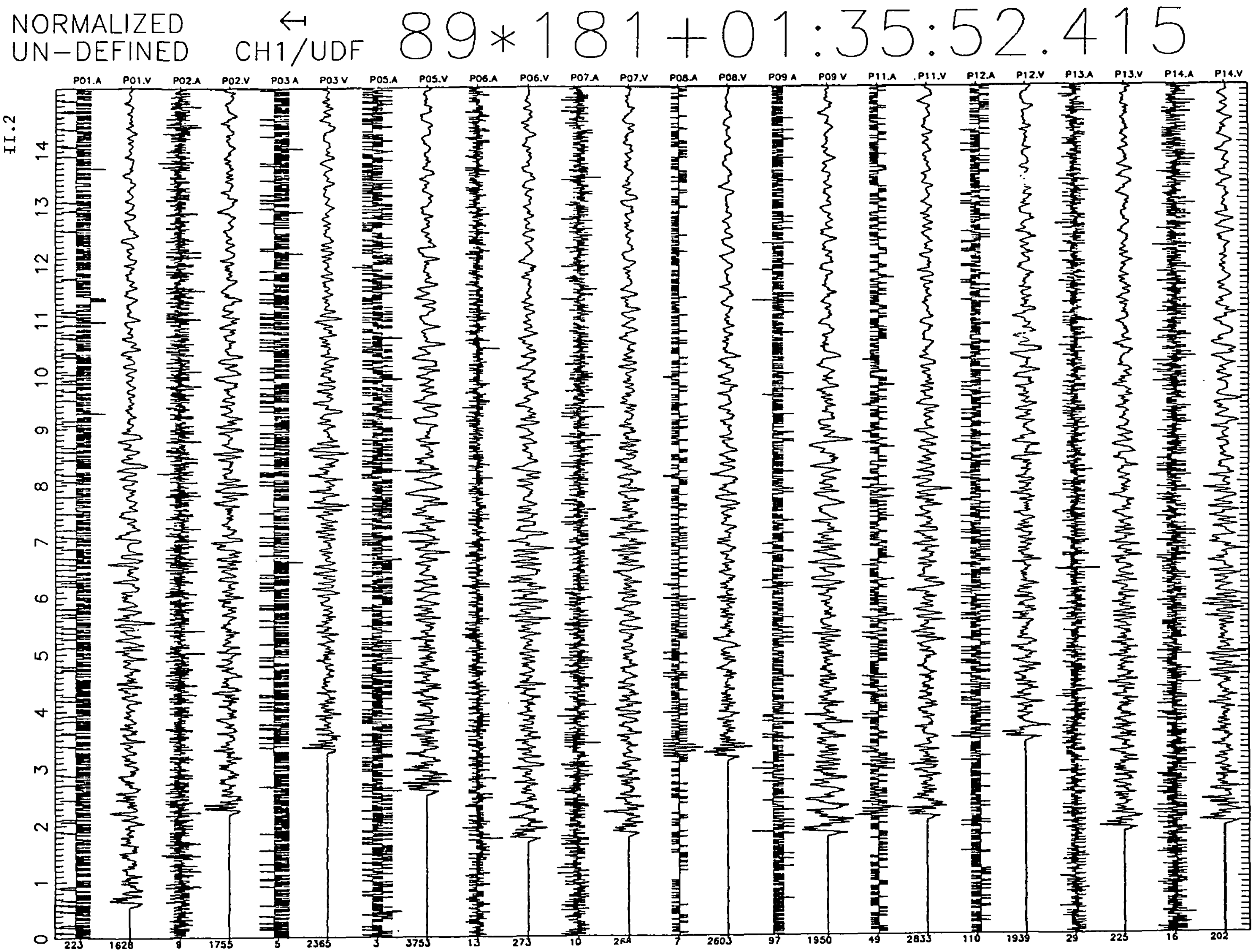
NORMALIZED
UN-DEFINED
←
CH1/UDF
89*181+01:35:52.415
P01.A P01.V P02.A P02.V P03.A P03.V P05.A P05.V P06.A P06.V P07.A P07.V P08.A P08.V P09.A P09.V P11.A P11.V P12.A P12.V P13.A P13.V P14.A P14.V
0 1 2 3 4 5 6 7 8 9 10 11 12 13 14
223 1628 9 1755 5 2365 3 3753 13 273 10 264 7 2603 97 1950 49 2833 110 1939 29 225 16 202

Figure 2

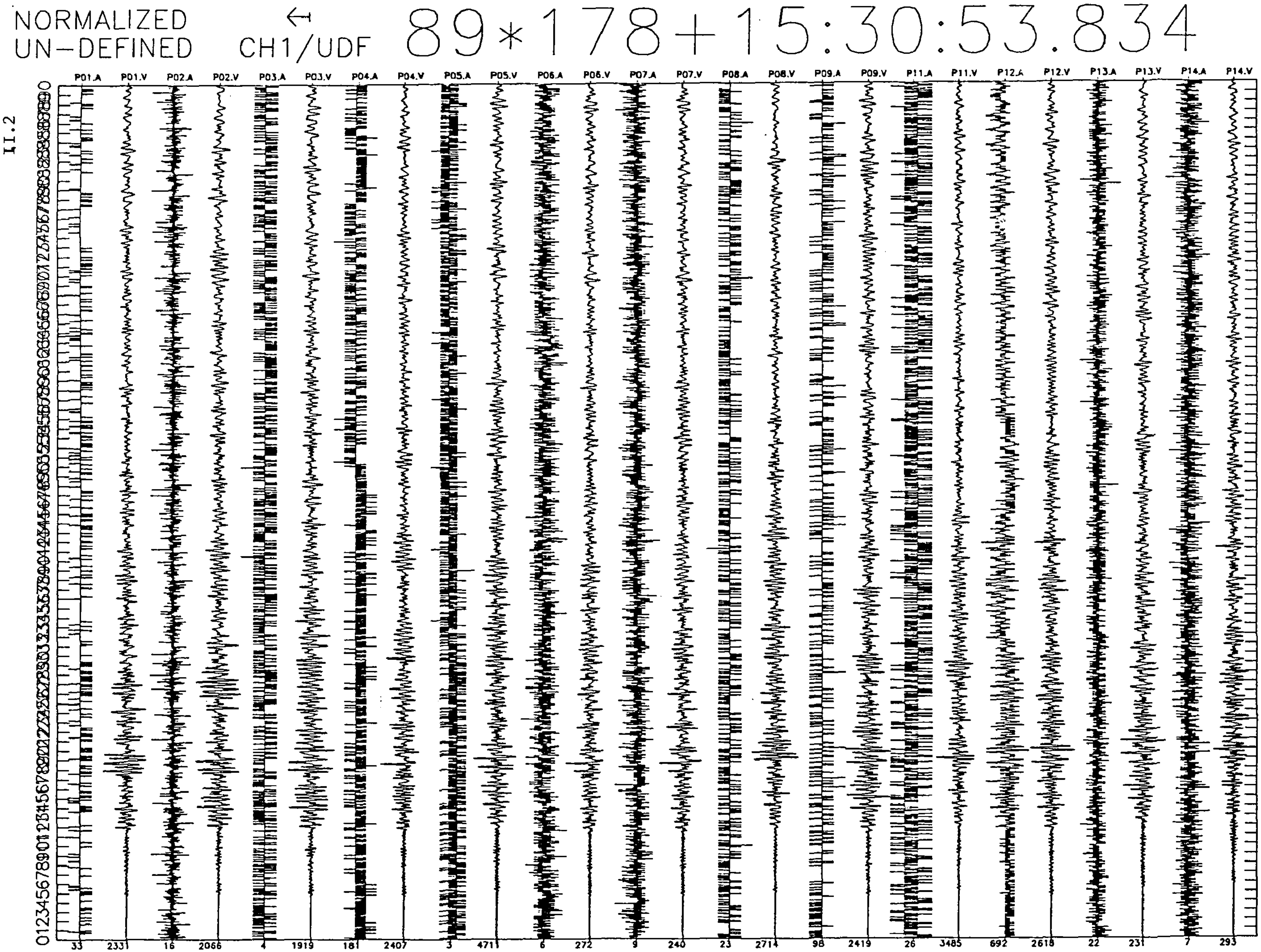
NORMALIZED
UN-DEFINED
CH1/UDF
89*178+15:30:53.834
P01.A P01.V P02.A P02.V P03.A P03.V P04.A P04.V P05.A P05.V P06.A P06.V P07.A P07.V P08.A P08.V P09.A P09.V P11.A P11.V P12.A P12.V P13.A P13.V P14.A P14.V
33 2331 16 2066 4 1919 181 2407 3 4711 6 272 9 240 23 2714 98 2419 26 3485 692 2618 22 231 7 293

Figure 3

Theodolite Measurements of Creep Rates on San Francisco Bay Region Faults

14-08-0001-G1676

Jon S. Galehouse
Dept. of Geosciences
San Francisco State University
San Francisco, CA 94132
(415) 338-1204

We began to measure creep rates on San Francisco Bay region faults in September 1979. Amount of slip is determined by noting changes in angles between sets of measurements taken across a fault at different times. This triangulation method uses a theodolite to measure the angle formed by three fixed points to the nearest tenth of a second of arc. Each day that a measurement set is done, the angle is measured 12 times and the average determined. The amount of slip between measurements can be calculated trigonometrically using the change in average angle.

We presently have theodolite measurement sites at 20 localities on ten active faults in the San Francisco Bay region (see Figure 1). Most of the distances between our fixed points on opposite sides of the various faults range from 50-275 meters. The precision of our measurement method is such that we can detect with confidence any movement more than a millimeter or two between successive measurement days. We remeasure most of our sites about once every two to three months.

The following is a brief summary of our results through 1 September 1989.

San Andreas fault - Since March 1980 when we began our measurements across the San Andreas fault in South San Francisco (Site 10), no net slip has occurred. Site 14 at the Point Reyes National Seashore Headquarters has averaged 0.7 millimeters per year of right-lateral displacement since measurements began in February 1985. Site 18 (not shown on Figure 1) in the Point Arena area has averaged 0.9 millimeters per year of right-lateral slip since January 1981. These results indicate that the northern segment of the San Andreas fault is virtually locked, with less than one millimeter per year of creep occurring.

Hayward fault (see Figure 2) - We presently have four sites on the southeastern portion of the Hayward fault and one site on the northwestern portion. We began measurements in September 1979 in Fremont (Site 1) and Union City (Site 2). Right-lateral slip is 4.5 millimeters per year in Fremont and 4.6 millimeters per year in Union City. Our results in the City of Hayward since June 1980 indicate 4.8 millimeters per year of right-lateral slip at D Street (Site 12) and 4.7 millimeters per year at Rose Street (Site 13). These data indicate that the southeastern portion of the Hayward fault is creeping at a rate slightly less than 5 millimeters per year.

Since we began measurements in San Pablo (Site 17) near the northwestern end of the Hayward fault in August 1980, the overall average rate of right-lateral slip has been 4.2 millimeters per year. Superposed on the overall slip rate in San Pablo are changes between some measurement days of up to nearly a centimeter in either a right-lateral or a left-lateral sense. Paradoxically, right-lateral slip tends to be measured during the first half of a calendar year and left-lateral during the second half. As shown on Figure 2, however, net slip on the Hayward fault in San Pablo has slowed to only about three millimeters per year of right-lateral displacement since July 1984.

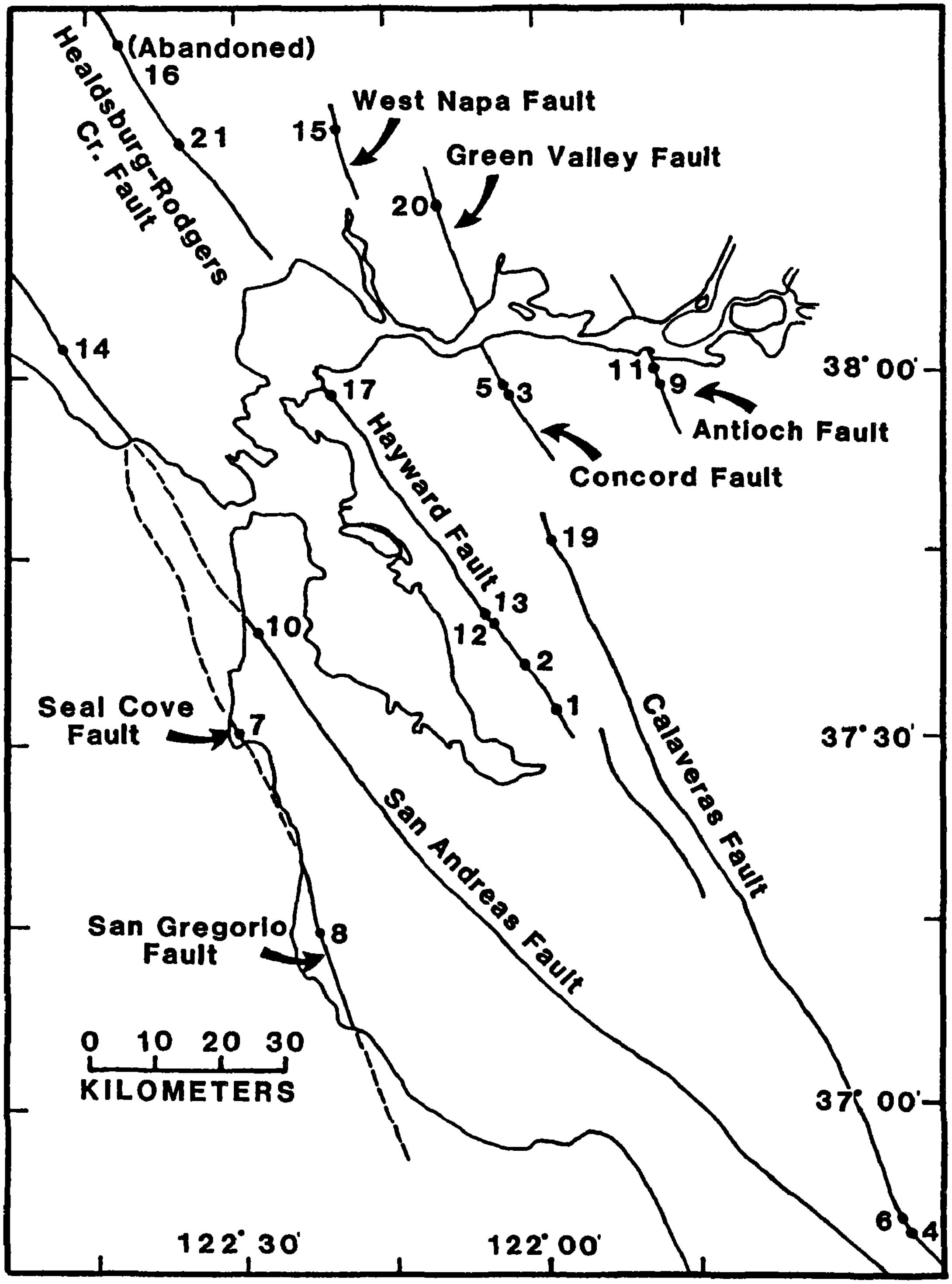

Figure 1. San Francisco State University Theodolite Measurement Sites

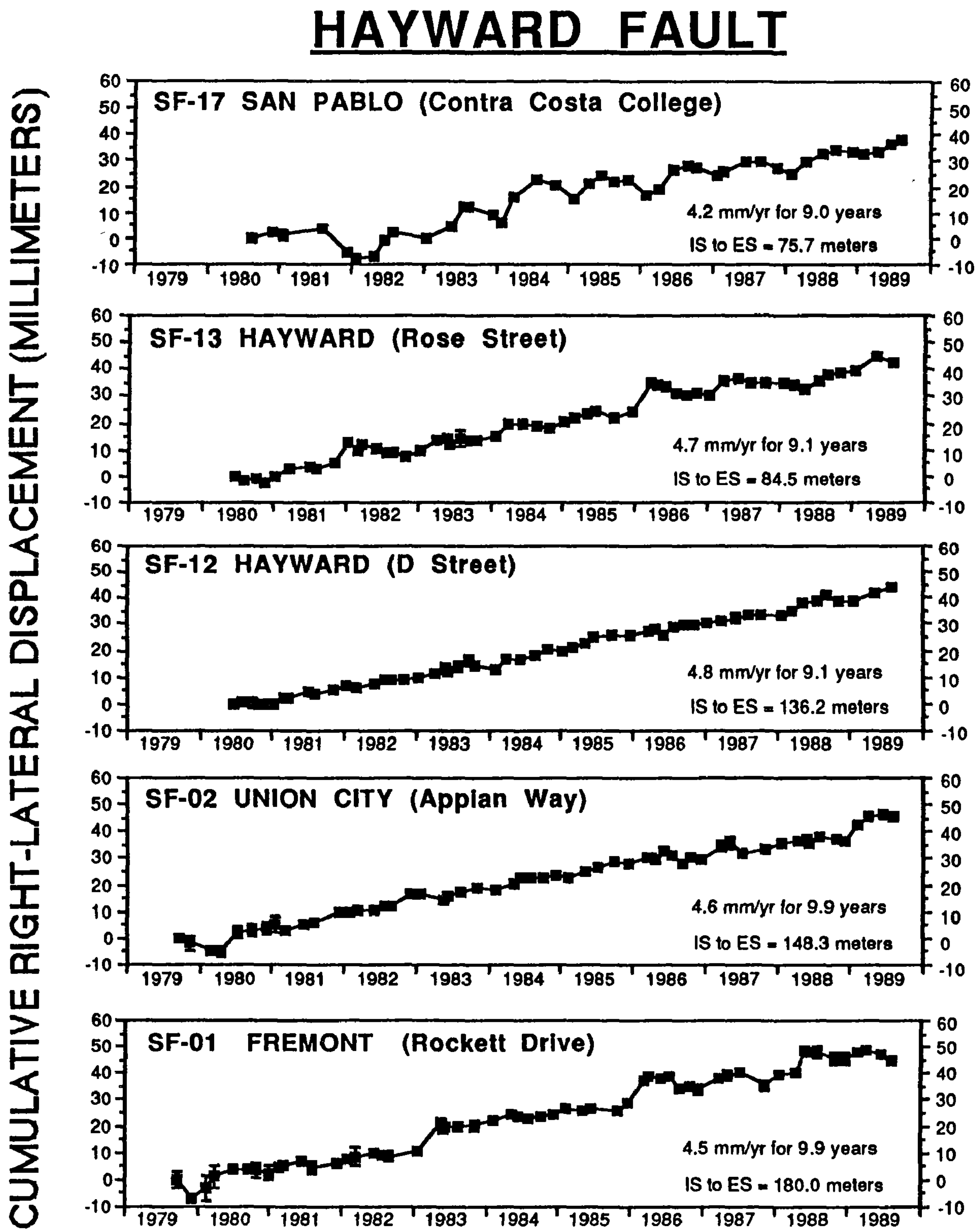

Figure 2. Hayward Fault Displacement

Calaveras fault - We have two measurements sites near the southeastern end of the Calaveras fault and one near the northwestern end. The rates of right-lateral displacement are considerably different at all three sites. The average rate of movement at Site 4 within the City of Hollister has been 6.8 millimeters per year since we began measurements in September 1979. Slip at this site is rather episodic, with most times of relatively rapid slip occurring early in a calendar year.

At Site 6 just 2.3 kilometers northwest of Site 4, the slip rate was rather constant from late 1979 to June 1984. Since then, however, fault displacement has been episodic. Virtually no net movement occurred for more than a year between late 1985 and late 1986. Overall, the average rate of right-lateral slip since October 1979 is 12.1 millimeters per year. This rate is the fastest of any of our sites in the San Francisco Bay region and is nearly twice as fast as that at our nearby Site 4 on the Calaveras fault. Inasmuch as the two sites are so close and the rates are so different, undetected movement may be occurring somewhere outside of our 89.7 meter-long survey line at Site 4 within the City of Hollister.

In contrast to the relatively high creep rates in the Hollister area, Site 19 in San Ramon near the northwesterly terminus of the Calaveras fault has shown very little net movement (only 0.3 millimeters per year) since we began measurements in November 1980.

Concord fault and Green Valley fault - We began our measurements at Site 3 and Site 5 on the Concord fault in the City of Concord in September 1979. We measured about one centimeter of right-lateral slip at both sites during October and November 1979. Following this, both sites showed relatively slow slip for the next four and one-half years at a rate of about one millimeter per year. In late Spring-early Summer 1984, both sites again moved relatively rapidly, slipping about seven millimeters in a right-lateral sense in a few months. The rate again slowed to about a millimeter per year for about the next three years, beginning in late August 1984. Between late November 1987 and late February 1988, the Concord fault moved about eight millimeters right-laterally. Since then the rate has again slowed down. It appears that characteristic movement on the Concord fault since at least 1979 is relatively rapid displacement over a period of a few months alternating with relatively slow displacement over a few years. Overall, the average rate of movement since late 1979 is 3.8 millimeters per year of right-lateral slip at Site 3 and 3.2 millimeters per year at Site 5.

Since we established Site 20 on the Green Valley fault in June 1984, measurements show an overall right-lateral slip rate of 4.2 millimeters per year. Although large variations tend to occur here between measurement days, our results suggest that the Green Valley fault behaves similarly to the Concord fault to the southeast, i.e., relatively rapid movement in a short period of time (months) alternating with relatively slow movement for a longer period of time (years). However, the one period of relatively rapid slip measured thus far on the Green Valley fault (early 1986) is midway between episodes of rapid slip on the Concord fault in 1984 and late 1987-early 1988. Continued monitoring of the Green Valley fault will help confirm its movement characteristics and rate and help determine if the Green Valley fault is actually the northwestward continuation of the Concord fault.

Other faults- The Seal Cove fault (Site 7) and the San Gregorio fault (Site 8) have shown very little net slip since November 1979 and May 1982 respectively. However, both sites (especially Site 8) often show large variations in the amounts and directions of movement from one measurement day to the next.

Much subsidence and mass movement creep appear to be occurring both inside and outside the Antioch fault zone and it is probable that these nontectonic movements obscure any tectonic slip that may be occurring. Site 9 has shown 1.6 millimeters per year of right-lateral slip since November 1982 and Site 11 has shown 0.7 millimeters per year of left-lateral slip since May 1980.

Both Site 16 and Site 21 on the Rodgers Creek fault have shown very little net slip (less than one millimeter per year) since August 1980 and September 1986 respectively. Seasonal and/or gravity-controlled mass movement effects are also present at both these sites and large variations occur from one measurement day to another. Site 16 had to be abandoned in early 1986 after 5.4 years of measurements because our line of sight became obscured.

Site 15 on the West Napa fault also shows large variations, but virtually no net movement has occurred since we began measurements in July 1980.

DEEP BOREHOLE PLANE STRAIN MONITORING
14-08-0001-G1376

Michael T Gladwin,

Department of Physics
University of Queensland
St.Lucia, 4067
AUSTRALIA.

ACTIVITIES

1. Retrieval of data from the five borehole tensor strainmeters in California (San Juan Bautista, Pinon Flat, and three at Parkfield) has continued. This data has been processed to account for station characteristics and analysed to obtain tensor strain components e_{xx}, e_{yy} and e_{xy}.

2. Regular reports have been provided to the monthly Parkfield review meetings, including data for the previous four months and comments on any anomolous strain signals observed.

3. A new procedure for calibration of the different instrumental components using both tidal response and long term borehole response is currently being developed.

4. Preliminary investigation of the San Juan Bautista instrument tensor strain data associated with the Loma Prieta earthquake of October 17, 1989 has been carried out.

RESULTS

1. Long term strain components of the San Juan data for the four years leading up to the Loma Prieta earthquake are shown in Fig.1. These data have been obtained by least square fitting of two exponentials to the raw data, a short term exponential of 100 day time constant (associated with curing of the expansive grout used in the instrument installation), and a 1200 day time constant exponential associated with migration of the surrounding strain field into the borehole.

When these two least squares fitted exponentials were removed from the data, the residuals for all three tensor components (see Fig 1) indicate a stability to better than 100 nanostrain over the whole of that period. There were no obvious precursors in the period immediately preceding the event. A change of gradient of Γ_1 and a fluctuation in the Γ_2 component occurred in the year prior to the event. Similar variations were noted on the SRL dilatometer. The significance of these signals is under evaluation.

2. A short term post seismic strain was observed (Fig 2), but represented less than 10% of the coseismic step. There was no obvious change of gradient associated with this event.

3. Modelling of the event is complicated by the fact that the station is almost on the nodal plane. This underlines the need for strain measurement sites in future arrays to be situated off the fault axis. The areal strain step computed

from the tensor instrument (and the direct SRL dilatometer step) agree in sense and magnitude though they both conflict with the predictions of a simple dislocation model for the presently determined fault parameters. More advanced modelling will follow after geodetic determination of the actual dislocation is completed.

4. For the Parkfield array, coseismic steps were also observed. These were consistently larger than expected from a simple model, and seem to indicate triggered local slip.

SAN JUAN TENSOR STRAIN

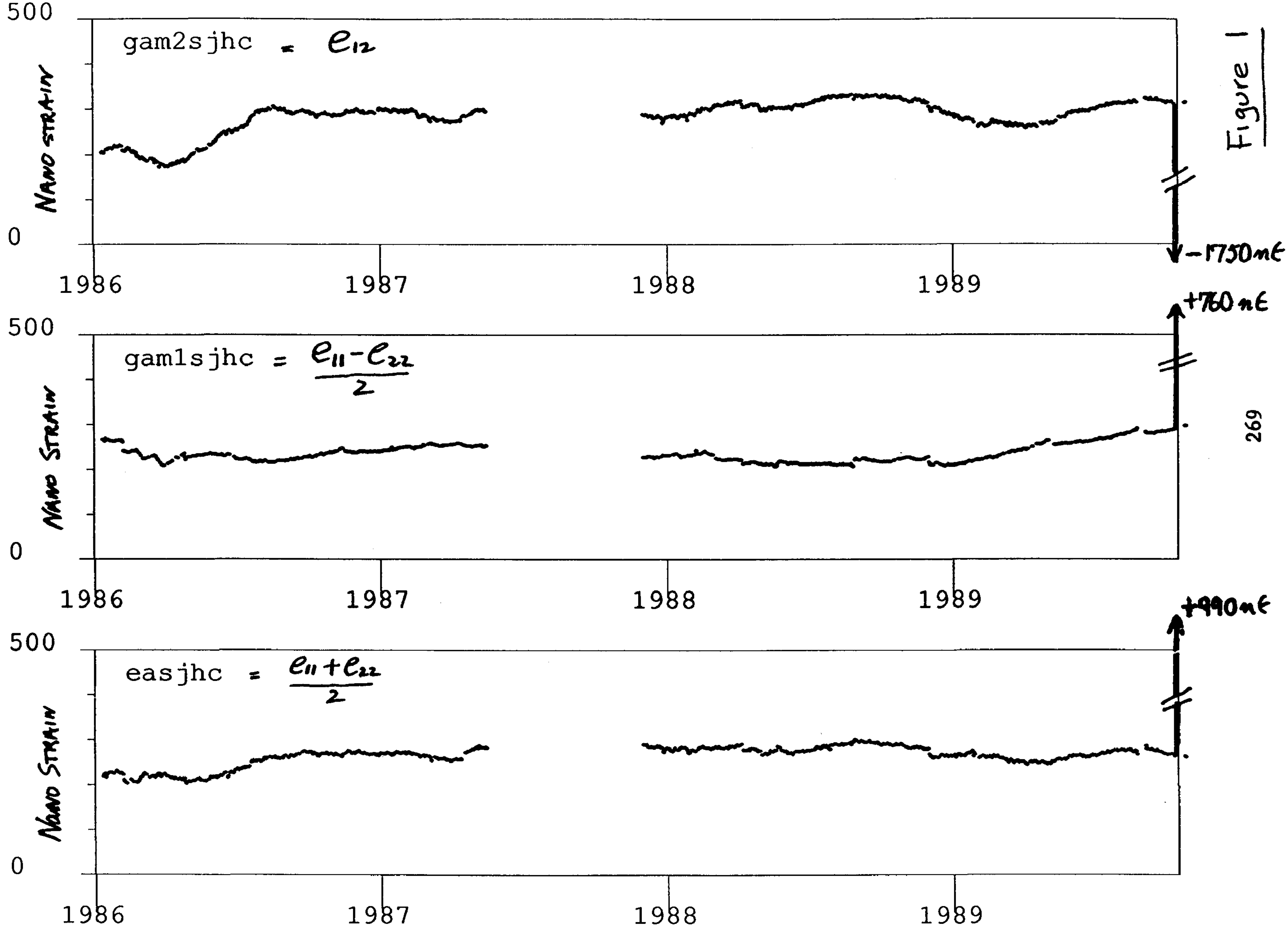

Figure 1

TENSOR STRAIN SAN JUAN BAUTISTA

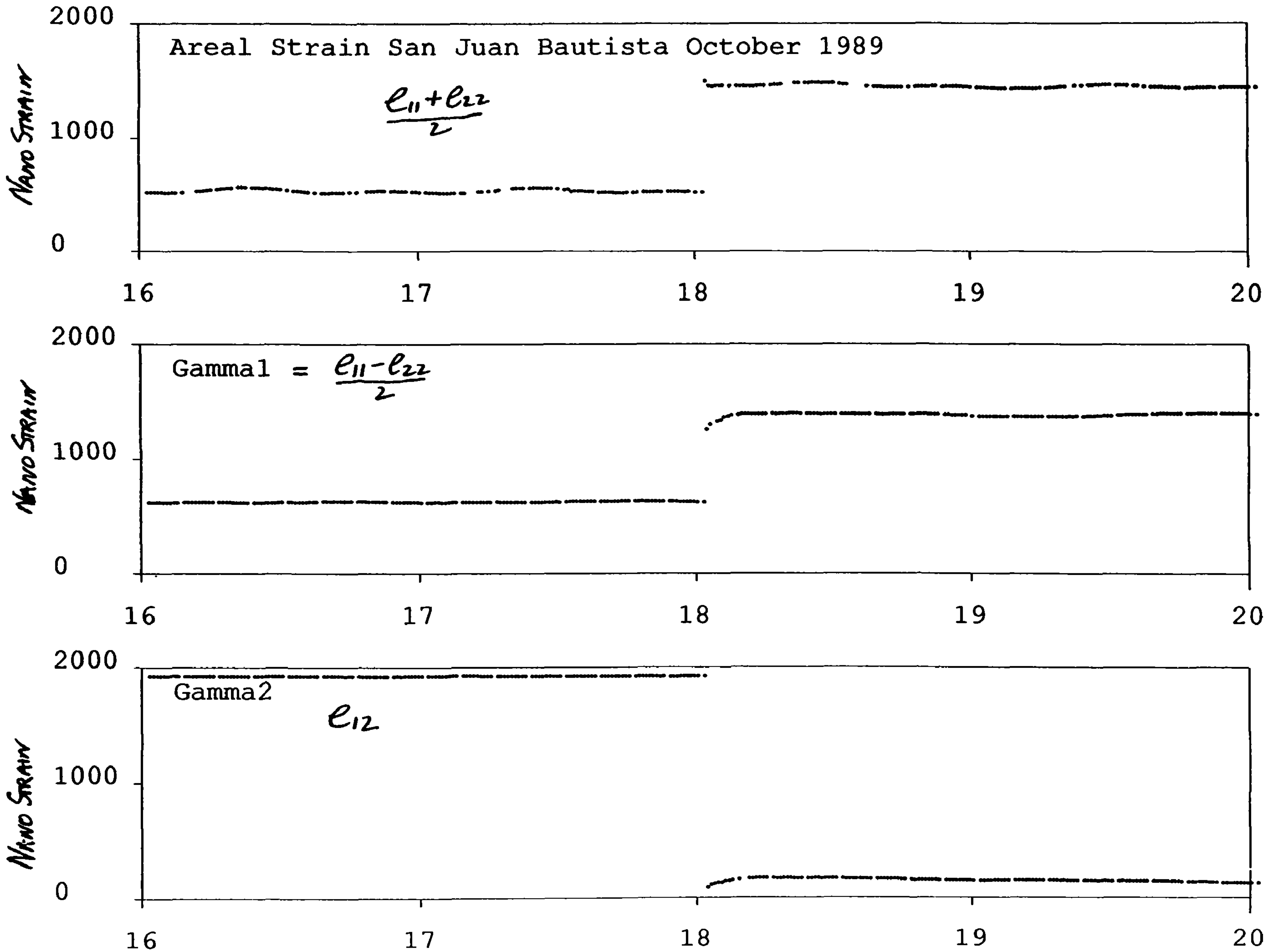

Figure 2

II.2

270

Parkfield Geophysics

9380-03074

Robert C. Jachens
U.S. Geological Survey MS 989
345 Middlefield Rd.
Menlo Park, CA 94025
(415) 329-5300

Investigations

1) Investigation continued on the regional geologic structure surrounding the Parkfield segment of the San Andreas fault through modeling of the magnetic and gravity fields. Structure northeast of the San Andreas fault in the area extending from Parkfield northwest for more than 60 km is reflected in large amplitude, coherent magnetic anomalies caused by large bodies of serpentinite. Two somewhat distinct anomalies dominate the magnetic field of the area, one over the serpentinite body exposed near New Idria, and the other along the San Andreas fault between 35°55' N. and 36°20' N. The source of the anomaly along the San Andreas is mostly concealed but the presence of isolated exposures of serpentinite within the anomaly area and the presence of a gravity low coincident with the magnetic anomaly suggest that this anomaly also is caused by a large mass of serpentinite. Two-dimensional modeling of the magnetic data was begun in an attempt to determine the subsurface structure.

2) In a study of potential interest to the Earthquake Hazards Reduction Program, a map of the depth to pre-Tertiary basement (thickness of Cenozoic cover deposits) was produced for the state of Nevada (Fig. 1). This map presents a quantitative representation of the response of the upper crust to extension over a large part of the Great Basin. The map was constructed from digital geologic information, gravity data, and well logs in an iterative scheme that separates the gravity field into a "basement" component and a "basin" component, the latter of which is inverted to yield the thickness of low-density cover. The accuracy of this map is critically dependent on the accuracy of the assumed variation of density with depth in the cover materials, a function which is reasonably well defined in the top 1 km, at least as a statewide average. For cover materials deeper than 1 km, density information was inadequate to define the variation with depth so a constant density contrast of -0.25 g/cm^3 was assumed. Therefore, although the shapes of the deep basins shown on Figure 1 probably are corrrect, the magnitudes of the depths may change as better density information becomes available.

Results

1) Modeling shows that both major magnetic anomalies are caused by sheet-like bodies of serpentinite. The New Idria body is thin along its north edge, thickens to the south, and attains its maximum thickness near its south-eastern end. The body is probably somewhat mushroom-shaped but a reliable estimate of its three-dimensional shape could not be made with the two-dimensional modeling techniques used in this investigation. More appropriate three-dimensional techniques are currently being developed.

Modeling of the large anomaly along the San Andreas fault suggests that its source is compound with major elements being an antiformal sheet 10-20 km wide, a dike-like body roughly 1 km wide that occupies the fault zone between 36°5' N. and 36°18' N., and other dike-like bodies including the one that feeds the serpentinite extrusion at Table Mountain. The antiformal sheet is truncated by the San Andreas fault along much of its length, probably reaches within 2 km of the surface at its peak, and may attain a maximum thickness in excess of 5 km. Along the north half of this anomaly, preliminary estimates suggest that in places the fault surface of the northeastern block is partly occupied by serpentinite that has an aggregate vertical extent of as much as 10 km. As in the case of the New Idria body, the quantitative estimates given above will be refined when the three-dimensional modeling techniques are perfected.

2) The map of depth to pre-Tertiary basement (Fig. 1) reveals patterns of deformation that are not readily apparent from the geologic and topographic maps of the state. Somewhat surprisingly, although about 80% of the state is covered by Cenozoic volcanic and sedimentary deposits, basins deeper than 1 km occupy only about 20% of the area. The deep basins do not form a connected pattern and numerous cross-structures can be seen in the elongate basins. Few deep basins occur south of 37° N. compared to the distribution in the rest of the state. The northwest corner of Nevada is anomalous in having a large area covered by a thick sequence of Cenozoic volcanic rocks. No pre-Tertiary basement is exposed in this area so the map was constructed on the assumption that the basement rocks seen around the edges of the area extend beneath it. However, the possibility exists that there are no pre-Tertiary rocks beneath this area.

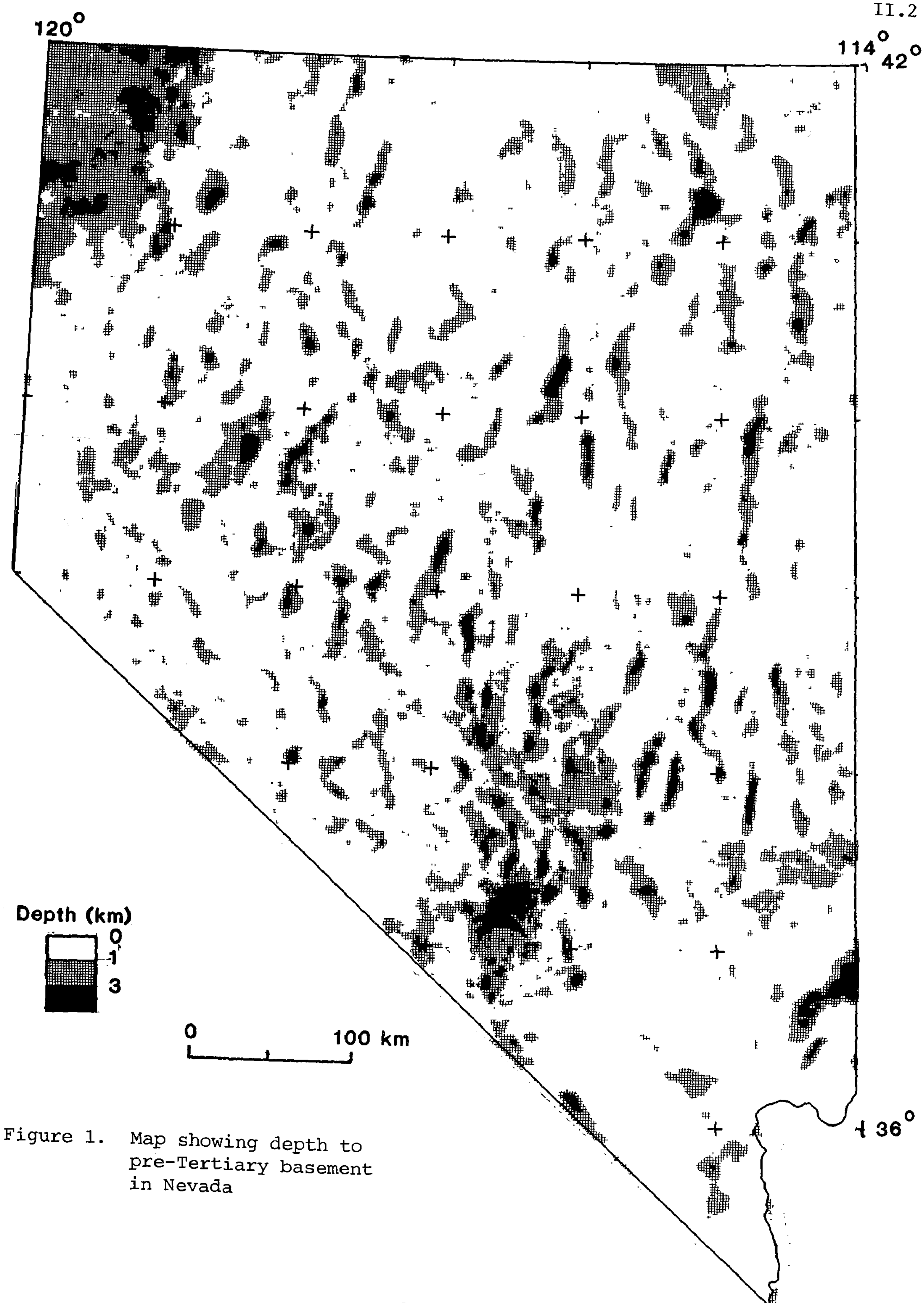

Figure 1. Map showing depth to pre-Tertiary basement in Nevada

TILT, STRAIN, AND MAGNETIC FIELD MEASUREMENTS

9960-2114
M. J. S. Johnston, R. J. Mueller, G. D. Myren
Branch of Tectonophysics
U. S. Geological Survey
Menlo Park, California 94025
415/329-4812

Investigations

[1] To investigate the mechanics of failure of crustal materials using data from both deep borehole tensor and dilational strainmeters and near surface strainmeters, tiltmeters, and arrays of absolute magnetometers.

[2] To develop physical models of incipient failure of the earth's crust by analysis of real-time records from these instruments and other available data.

Results

[1] **DEVIL'S PUNCHBOWL STRAIN TRANSIENTS**

A series of strain transients have been observed on the PUBS borehole strainmeter at the Devil's Punchbowl near the San Andreas fault in the southern Mojave Desert during June, July, and August 1989. Some of these strain transients are also detectable at the nanostrain level on the borehole strainmeter BBSS which is 17 km from the San Andreas. It is not clear what the source of these strain changes are although they are a cause for concern since signals of similar form occurred on the Isu Peninsular in Japan prior to the 1979 M = 7 earthquake.

[2] **MAMMOTH MOUNTAIN EARTHQUAKE SWARMS, LONG VALLEY CALDERA, CALIFORNIA.**

From mid-1982 through 1985, a dozen or so swarms of small earthquakes (M<3.5) occurred beneath Mammoth Mountain, a 200,000 to 50,000 year old cumulovolcano, standing on the southwestern rim of Long Valley caldera and along the southern extension of the youthful Mono-Inyo volcanic chain. These swarms involved brief, spatially clustered flurries of earthquakes beneath the flanks of the mountain, each lasting only a few hours to a day or so. Focal depths ranged from less than 4 km beneath the north flank to 6 km beneath the south flank, and focal mechanisms showing both normal and strike-slip solutions with the T-axes generally oriented in a WNW-ESE direction. Spasmodic bursts (rapid-fire sequences of similar-sized earthquakes with overlapping coda) were common in these swarms. Few earthquakes occurred beneath the mountain from early 1986 through early 1989. On May 4, however, two M=1 earthquakes beneath the south flank of the mountain marked the onset of a swarm that continues to the present (9/5/89). Aside from its longevity, noteworthy aspects of this persistent swarm include 1) an exponential-like increase in the rate of activity through the first month, 2) a vertically oriented, planar distribution of hypocenters at depths between 6 and 9 km with a NNE strike (roughly perpendicular to the average T-axis orientation for the swarm earthquakes), 3) recurring spasmodic bursts, 4) only two M>3 events (one on June 20 and the other on July 1) and a cumulative seismic moment through August 31 corresponding to a single M=4 earthquake, 5) a b-value of 1.2, 6) a solitary 18-km-deep event (M=2) beneath the north flank of the mountain with a "low-frequency" appearance on local seismic stations, and 7) sub-microstrain perturbations on the nearby borehole dilatometer leading heightened swarm activity by a few days and leading the onset of the swarm by about three weeks. Taken altogether, these aspects of the swarm point to a magmatic source for the modest but persistent influx of strain energy into the crust beneath Mammoth Mountain.

[3] **LOCAL DILATOMETER AND SEISMOMETER RECORDINGS OF THE M_L = 4.0 PARKFIELD EARTHQUAKE OF 25 MAY, 1989.**

On 25 May, 1989, a M_L = 4.0 near Parkfield, CA was recorded by our 14-station seismic array. It occurred near the center of the array and is the largest Parkfield earthquake to have been recorded in the 3-year history of this array. This array consists of 14 GEOS 16-bit digital recorders with triaxial FBA's and/or 1 Hz geophones. Six if the GEOS are recording volumetric strain from Sacks-Evertson borehole dilatometers. The 9-km deep event was recorded at 12 of the sites, including 5 of the dilatometer sites, at epicentral distances from 3 km to 25 km. The ultra-broadband (DC - 20 Hz) dilatometers show co-seismic DC strain offsets measuring from 1.2 to 42 nanostrain, which is up to 10% of the amplitude of the unfiltered straingram. By filtering out the high-frequency portion of the straingrams the DC offsets are seen to occur near the time of the S-wave arrival. Strain amplitudes recorded during the 2 seconds prior to the P-wave arrivals are less than 0.5 nanostrain at all sites. Comparison of the dilatometer records with seismometer records confirms that tha dilatometers respond to P waves but not S waves. The dilatometers do however respond to the reflected P waves resulting from the incidence of S waves upon the free surface. Observed strain amplitudes are consistent with downhole P-wave velocities of 1.1 to 1.6 km/s.

[4] **TRANSIENT EARTH STRAIN ASSOCIATED WITH NEAR-SURFACE CREEP NEAR PARKFIELD, CALIFORNIA**

Surface observations of aseismic fault displacement (fault creep) exhibit episodic behavior (creep events) whose sources are typically limited in extent and complex in character. Since 1984, more than 15 creep episodes on the San Andreas fault near Parkfield have been recorded on creepmeters located within an array of strainmeters in this region. The strainmeters are installed at distances of 0.6 km to 5.5 km from the fault and operate at a resolution of a few nanostrain at periods of a few hours to a few weeks. An example that illustrates the main features of simultaneous strain and creep observations occurred on August 18, 1986, when 1.5 mm of fault displacement was observed on the creepmeter XGH1 at Gold Hill near Parkfield, California. At this location, two borehole dilational strainmeters are installed at distances of 0.8 km and 1.15 km from the fault. Short-term strain changes preceding and during the creep event were of similar form on both strainmeters with peak amplitudes of 22 and 5 nanostrain, respectively. During the previous two weeks, however, longer-term strain transients of several hundred nanostrain occurred. The short-term data are consistent with a slip moment for the creep event of $2*10^{19}$ dyne-cm. If centered on the creepmeter, the patch that slipped could have been several hundred meters square. In general, strain transients associated with surface creep are usually, but not always, detected in the strain records from instruments within two kilometers of the fault and can be modeled with simple models of fault slip that involve a few millimeters of slip on fault patches with dimensions of several hundred meters (typical moments are 10^{19} dyne-cm). In some cases, strain changes are observed prior to the event that indicate the surface slip is triggered by deeper slip of longer duration. The occurrence of episodes of deeper slip could explain the general correspondence, over periods of months, between higher than normal number of creep events and higher rates of occurrence of moderate seismicity reported previously.

[5] BOREHOLE STRAIN ARRAY IN CALIFORNIA

A network of 15 borehole strainmeters along the San Andreas fault zone and in the Long Valley Caldera continue to be monitored and maintained. All instruments are installed at depths between 117-m and 324-m and all are between 1-km and 5-km from the the surface trace of the fault. High frequency dilatometer data in the frequency range 0.005 Hz to 100 Hz are recorded on 16-bit digital recorders with least count noise less than 10^{-11}. Low frequency data from zero frequency to 0.002 Hz are transmitted through the GOES satellite to Menlo Park, CA, using a 16-bit digital telemetry system. At the USGS in Menlo Park the data are displayed in "almost real time" and are continuously monitored with detection algorithms for unusual behavior. Least-count noise is about $5*10^{-12}$ for the on-site digital recordings, and about $2*20^{-11}$ for the satellite telemetry channels. Earth strain tides, strain transients related to fault creep and numerous strain seismograms from local and teleseismic earthquakes with magnitudes between -1 and 6 have been recorded on these instruments. Static moments and total earthquake moments are determined from the co-seismic strains and total strain changes observed with the larger events.

[6] CROWLEY LAKE AND SAN ANDREAS LAKE WATER LEVEL MONITORING

Water level monitoring sites have been installed on Lake Crowley in the Long Valley/ Mammoth Lakes region and San Andreas lake on the San Andreas fault just south of San Francisco. These data provide differential water level measurements (tilt) with a measurement precision of less than 1 mm on baselines of 5 to 8 kilometers. Monthly averages of the data from San Andreas lake between 1979 and 1989 indicate a tilt rate of 0.02 ± 0.08 microradians/yr (down S34°E)

[7] DIFFERENTIAL MAGNETOMETER ARRAY IN CALIFORNIA

We continue investigations of local magnetic fields and relationships to crustal strain and seismicity in the Parkfield region and in southern California. The network consists of 9 staions which are all sampled synchronously every 10 minutes and transmitted with 16-bit digital telemetry to Menlo Park, CA through the GOES satellite. Data are monitored daily with particular attention to the seven stations operating in the Parkfield region of central California.

Reports

Johnston, M. J. S., 1989. Review of magnetic and electric field effects near active faults and volcanoes in the U.S.A., Physics Earth Planet. Int., v57, 93-110.

Mueller, R. J., and M. J. S. Johnston, 1989. Large scale magnetic field perturbation arising from the May 18, 1980, eruption from Mount St. Helens, Washington, Physics Earth Plan. Int. v57, 111-121.

Silverman, Stan., Carl Mortensen, and Malcolm Johnston, 1989. A Satellite-based digital data system for low-frequency geophysical data, Bull. Seis. Soc. Am., **79**, 189-198.

Davis, P. M., M. J. S. Johnston, J. Dvorak, and D. Dzurisen, 1989. Electric and Magnetic Field Measurements on Mount St. Helens Volcano at Times of Eruptions 1980-1985, J. Geomag. Geoelec. (in press).

Linde, A. T., and M. J. S. Johnston, 1989. Source parameters of the October 1,1987 Whittier Narrows earthquake from borehole strain data, J. Geophysical Research, v94, 9633-9643.

Borcherdt, R. D., M. J. S. Johnston, and G. Glassmoyer, 1989. On the use of volumetric strainmeters to infer additional characteristics of short-period seismic radiation, Bull. Seis. Soc. Am., v79, 1006-1038.

Myren, Doug and Malcolm Johnston, 1989. Borehole dilatometer installation, operation and maintenence at sites along the San Andreas fault, California, U. S. Geological Survey Open File report (in press)

Mueller, R. J., and M. J. S. Johnston, 1989. Lake level observations to detect crustal tilt: San Andreas Lake, California, 1979-1989. Geophys. Res. Lett. v 16, 661-664.

Johnston, M. J. S. and A. T. Linde, 1989. Nucleation size and fault behavior for moderate earthquakes in California from high-resolution strain measurements. 1989 Rubey Colloquium, University of California, Los Angeles, May 9-11, 1989

D. P. Hill, W. L. Ellsworth, M. J. S. Johnston, J. O. Langbein, A. M. Pitt, P.A. Reasenberg and M. L. Sorey Mammoth Mountain Earthquake Swarms, Long Valley Caldera, California, Trans. Am. Geops. Un. (in press) 1989.

M. J. S. Johnston, A. T. Linde, and S. Schulz Transient Earth Strain Associated with Near-Surface Creep Near Parkfield, California. Trans. Am. Geops. Un. (in press) 1989.

G. Glassmoyer, R. D. Borcherdt, M. J. S. Johnston, and T. Noce, Local Dilatometer and Seismometer Recordings of the $M_L = 4.0$ Parkfield Earthquake of 25 May, 1989. Trans. Am. Geops. Un. (in press) 1989.

GEODETIC STRAIN MONITORING

9960–02156

John Langbein
Branch of Tectonophysics
U.S. Geological Survey
345 Middlefield Road, MS/977
Menlo Park, California 94025
(415) 329–4853

Investigations

Two–color geodimeters are used to survey, repeatedly, geodetic networks within selected regions of California that are tectonically active. This distance measuring instrument has a precision of 0.1 to 0.2 ppm of the baseline length. Currently, the crustal deformation is being monitored within the south moat of the Long Valley caldera in eastern California, near Pearblossom, California on a section of the San Andreas fault that is within its Big Bend section and on Middle Mountain near Parkfield, California. Periodic comparisons with the prototype, two–color geodimeter are also conducted near Parkfield, California. These intercomparison measurements serve as a calibration experiment to monitor the relative stabilities of the portable and prototype geodimeters.

Results

1. Instrumental Problems

As discussed in the last two semi–annual reports, I have estimated the offset in measured distances due to change in instrumentation due to failure of one of the portable, two–color geodimeters. To accomplish the task of estimating the offset, I have used the data from the periodic instrument calibration measurements at Parkfield and the frequent length measurements at Long Valley. The results from both data sets indicate that the offset is length dependent and are characterized by the functions shown in Figure 1. Furthermore, the periodic of calibration of the portable instruments with the observatory based, two–color geodimeter at Parkfield reveal that the Parkfield instrument failed in late spring 1989 and the subsequent repair yielded a 0.5 ppm in its length scale. The details of the data and the calculation are incorporated in an Open File Report.

2. Long Valley Caldera

The frequent measurements of line lengths within the Long Valley Caldera have shown some variations in strain rate over the past six months. In particular, the baselines that are most sensitive to inflation of the resurgent dome started to show compression in the early summer, 1989. However, lately these baselines have now started to extend.

In response to the continued swarm of earthquakes under Mammoth Mountain, we installed a small geodetic network southeast of the mountain. The two surveys in late August and late September 1989 show marginally detectable strain changes. A uniform strain model implies extension of 8.8±3.1 ppm/yr oriented N60W±16° and the orthagonal component shows $2.4/pm2.6$ ppm/yr.

3. Pearblossom

Results of measuring line–length changes at Pearblossom, California for the past nine years are plotted in terms of uniform strain changes in Figure 2. The dominant signal is the dextral shear strain across the San Andreas fault. As reported by Johnston elsewhere in this issue, the dilatometer that is located within the area of the Pearblossom network has detected a few extensional strain events during the summer of 1989. As illustrated in Figure 3, the two–color measurements made in June and September, 1989, show no anomalous changes relative to previous measurements. However, a more detailed examination of the length–change data reveal that the baseline in the southeast quadrant of the network compressed by 5.8±1.2 mm in three months and this would imply possible slip on a section of the San Andreas fault just to the southeast of the network.

To compare possible temporal/spatial relation of the strain changes in the Big Bend region of the San Andreas fault, we have initiated measurements of a 30 baseline network located just west of Palmdale. These baselines comprise a majority of the Palmdale network which has been measured infrequently since 1972 by Savage and Prescott using the single–color Geodolite. Comparison of the two–color data from Pearblossom and the Geodolite data from Palmdale have revealed some tantalizing correlations in shear strain. In particular, the decrease in shear strain rate followed by an increase in rate during late 1983 and through mid–1984 is apparent in both the Pearblossom and the Palmdale data. With better time resolution and higher precision from Palmdale, the possibility for correlation can be better explored.

Reports

Langbein, John, Testing for long–term stability of two–color geodimeters; January 1986 to August 1989, submitted as U.S. Geological Survey Open File Report, 1989.

Langbein, John, Burford, Robert O., and Slater, Larry E., Variations in fault slip and strain accumulation at Parkfield, California: Initial results using two–color geodimeter measurements, 1984–1988, *Journal of Geophysical Research*, in press 1989/1990.

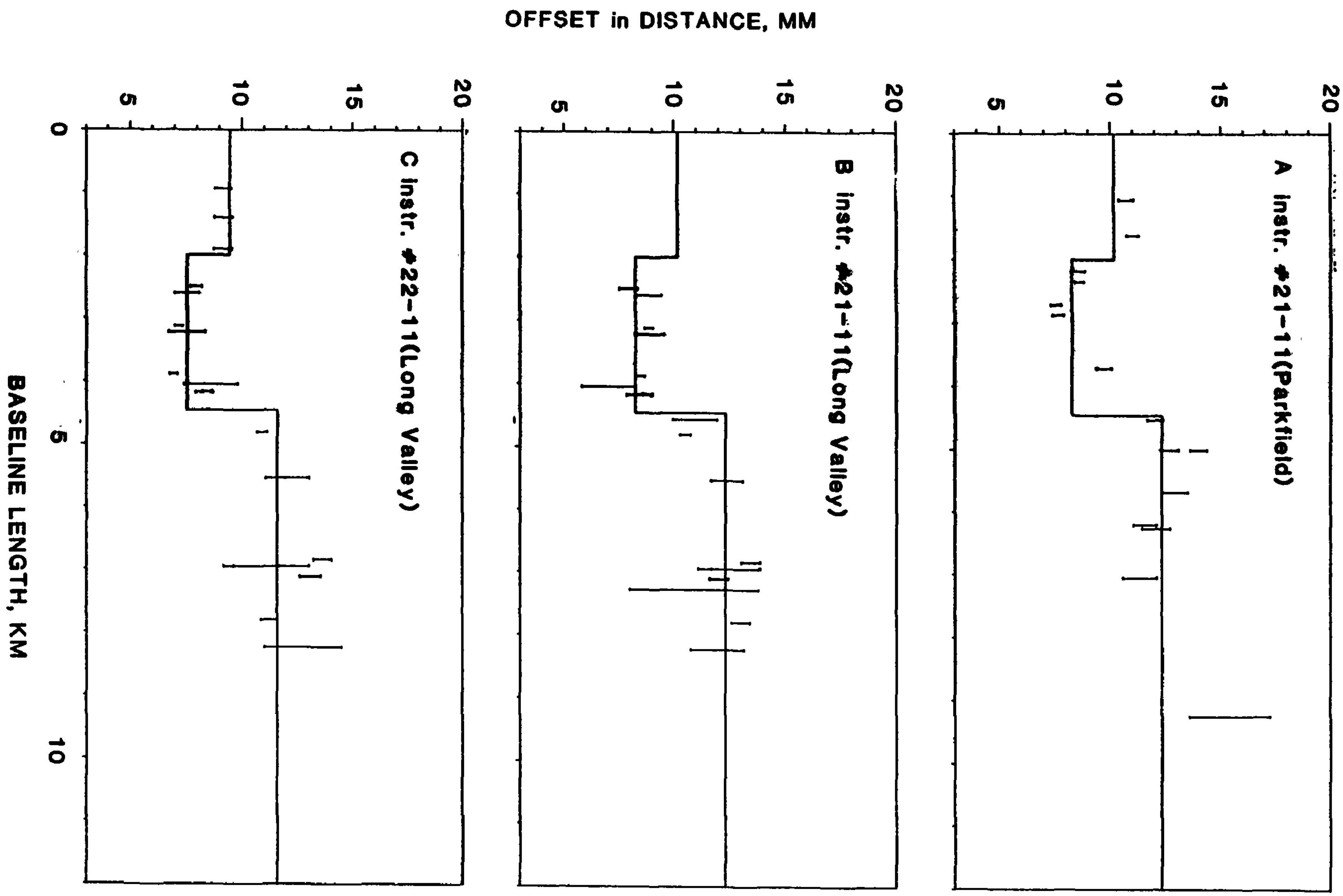

Figure 1. Estimates of the offset of two-color instruments #21 and #22 relative to #11 as a function of baseline length for the Parkfield and Long Valley data sets. Superimposed is the function showing the preferred model of offset in distance using the two instruments. Figure 1a shows for the Parkfield data the estimates of offset in distances of #21 relative to #11 that have been derived on the basis of the calibration data between mid-1987 and March 1989. The result in Figure 1b and 1c are for the offset of instruments #21 and #22 relative to #11 which have been derived from line-length changes measured in Long Valley. The estimates assume that the line-length changes are characterized by a second order polynomial in time.

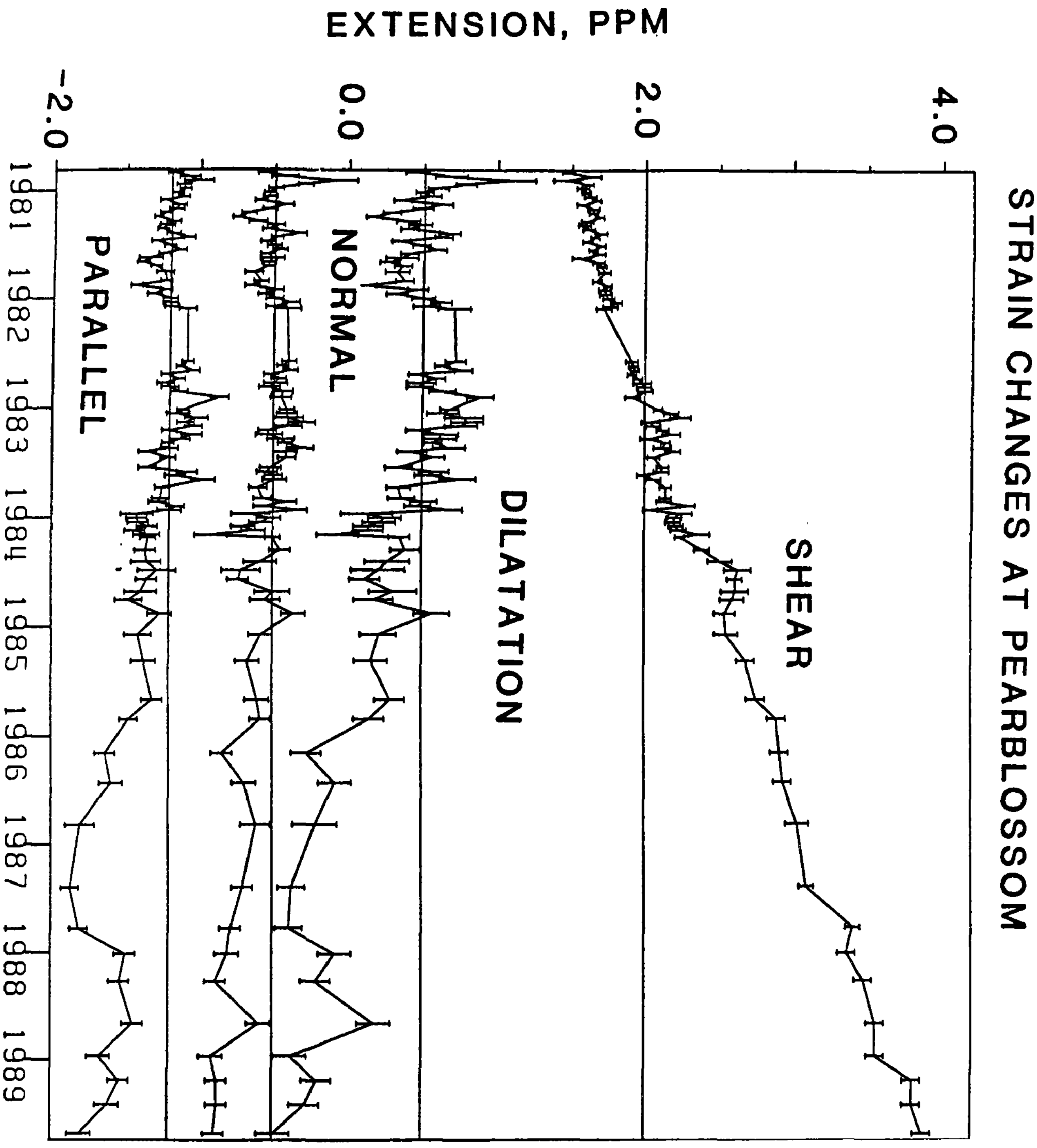

Figure 2. Strain changes inferred from nine years of line-length measurements taken near Pearblossom, California. Strains are rotated into a coordinate system parallel and normal to the local strike of the San Andreas fault (N65°W).

Microearthquake Data Analysis

9-9930-01173

W. H. K. Lee
U.S. Geological Survey
Branch of Seismology
345 Middlefield Road, Mail Stop 977
Menlo Park, California 94025
(415) 329-4781

Investigations

The primary focus of this project is the development of state-of-the-art computation methods for analysis of data from microearthquake networks. for the past six months I have been involved in:

1) Analysis of seismic waveform data of selected southern California earthquakes. This work is in collaboration with Bob Yerkes in an attempt to relate seismic focal mechanisms with known geological features.

2) A continued seismic study of explosive sources. Preliminary results are: (1) explosions at depths greater than 100 m were observed with more high-frequency signals than those fired near the surface, (2) quarry blasts were observed to have complex signal characteristics, even for the simplest (quadruple) quarry blast pattern, and (3) a single explosion at 100 m could be identified (because of its higher frequency signals) in the midst of a quarry blast if observations were made within a few kilometers, but identification could be difficult at greater distances.

3) An inexpensive 128-channel seismic data acquisition and recording system has been implemented using commercially available components and a 12 MHz IBM-compatible 286 or 386 PC. The total hardware and software cost is less than $10,000. The system can in real time (1) digitize 128 seismic channels at 100 samples per second, (2) display any set of 16 channels on a monitor screen, and (3) save the digital data on a hard disk, either event by event or continuously. In the event mode, the system also automatically picks first P-arrivals, and locates the source. This system is now monitoring signals from Central California Seismic Network stations, and has been performed reliably as designed.

   The hardware and software design is open-ended, and supports multiple (must be power of 2) of 16 channels. If the PC being used is faster than 12 MHz, then more channels can be digitized and/or the data sampling rate can be higher. There is also a direct trade off between the number of channels and the data sampling rate, e.g., decreasing the number of channels by a factor of 2 would allow a doubling of the sampling rate.

<u>Reports</u>

Tottingham, D. M., and W.H.K. Lee, 1989. XDETECT: A fast seismic data acquisition and processing program, U.S. Geol. Survey Open-File Report 89-205, 8 pp.

Lee, W.H.K., (editor), 1989. "Toolbox for Seismic Data Acquisition Processing, and Analysis", IASPEI Software Library Volume 1, Seismological Society of America, El Cerrito, 283 pp.

Lee, W.H.K., (editor), 1989. "Source Code Package for IASPEI Software Library Volume 1", Seismological Society of America, El Cerrito, 45 pp.

Lee, W.H.K., D. M. Tottingham, and J. O. Ellis, 1989, Design and implementation of a PC-based seismic data acquisition, processing and analysis system, IASPEI Software Library, Vol. 1, p. 21-46.

Parkfield Prediction Experiment

9930-02098

Allan Lindh, Andrew Michael, Cathy Aviles, and Barry Hirshorn
Branch of Seismology
Office of Earthquakes, Volcanoes and Engineering
345 Middlefield Road, Mail Stop 977
Menlo Park, California
(415) 329-4778
(FTS) 459-4778

Investigations

1. Coordination of activities in the Parkfield Earthquake Prediction Experiment.
2. Seismological research associated with the Parkfield Earthquake Prediction Experiment.
3. Analysis of USGS coda-duration measurements for magnitude determination.
4. Prepare weekly earthquake reports for Northern and Central California, distribute to press and public officials by FAX so that the reports are available on a timely basis.
5. Process RTP data to complete and final form on a daily basis.
6. Prepare on a timely basis merged monthly catalogs, including all CUSP and RTP data.
7. Continue ongoing work on long-term earthquake probabilities in California.

Results

1. A Real-time earthquake prediction experiment is underway at Parkfield.
2. The mechanics of the San Andreas fault at Parkfield and the Calaveras Fault near San Jose are better understood.
3. Weekly reports have gone out every Monday evening since February 1989.
4. Clean merged data is complete for January-August, 1989.

Reports

Aviles, C.A. and C.M. Valdes, 1989, Comparison of microearthquake source parameters in the preparation zone at Parkfield, California: 1977-1982 and 1984-1989, abstract, submitted to EOS.

Eberhart-Phillips, D. and A.J. Michael, 1989, Three-dimensional crustal velocity structure in the Parkfield, California region from inversion of local earthquake and shot arrival times, abstract, submitted to EOS.

Hirshorn, B.F., A.G. Lindh, and R.V. Allen, 1989, The shape of the earthquake coda in Central California; a new magnitude scale from the coda envelope, abstract, submitted to EOS.

Lindh, A.G., D.H. Oppenheimer, and W.H. Bakun, 1989, Slip partitioning of the Calaveras fault, California into Asesimic and Seismic zones, abstract, submitted to EOS.

Michael, A.J., 1989, Spatial patterns of aftershocks of shallow focus earthquakes in California and implications for deep focus earthquakes, Journal of Geophysical Research, 94, 5615-5626.

Michael, A.J. and B.R. Julian, 1989, Measuring the difference between two fault plane solutions, submitted to Bulletin of the Seismological Society of America.

Michael, A.J. and D. Eberhart-Phillips, 1989, Finding asperities without using seismicity patterns: results from Parkfield, California, abstract, submitted to EOS.

Nishioka, G.K. and A.J. Michael, 1989, A detailed seismicity study of the Middle Mountain zone at Parkfield, California, U.S.G.S. Open-File Report 89-546.

Nishioka, G.K. and A.J. Michael, 1989, A summary of a detailed seismicity study of the Middle Mountain zone at Parkfield, California, submitted to Bulletin of the Seismological Society of America.

Oppenheimer, D.H., W.H. Bakun, and A.G. Lindh, 1989, The prospects for future M>5 earthquakes on the Calaveras fault, California, abstract, submitted to EOS.

Attachments:

Following are the synopsis from each of the monthly Parkfield Data Review meetings held during the reporting period and the last weekly summary as an example.

MARCH 1989 PARKFIELD DATA SUMMARY

There were eighteen events in the Parkfield area in March. Twelve of these were northwest of Middle Mountain, five were in the MM alert box, and one was southeast of Middle Mt. Magnitudes ranged between 0.0 and 1.8, depths from 0.2 to 10.4 km.

There were two creep events during March. The first, a 0.88 mmRL event at XMM1(Middle Mt.) on 3/19, triggered a D-level alert by exceeding 0.5 mm in 30 minutes. The Carr Ranch creepmeter (CRR1) recorded a 2.4 mmRL event lasting over 5 days; no alert threshold was reached.

The two-color laser geodimeter is gradually moving back into full operation. To clarify last month's report, problems with the instrument's blue laser have affected only the frequency of measurements, not data quality. To the extent that lines have been measurable, results are reliable.

A D-level alert was triggered by a strain event at the Red Hills dilatational strain meter. The event was not seen on the closest instrument to this site (Jack Cyn), which is across the fault from the Red Hills instrument. However, only one past event has been detected simultaneously at the Jack Cyn and Red Hills instruments.

It was an uneventful month for the tiltmeters and magnetometers, as well as for water level, radon, and hydrogen measurements.

- J. Estrem

April 1989 PARKFIELD DATA SUMMARY

There were ten events in the Parkfield area in April. Seven of these were northwest of Middle Mountain, two were in the MM alert box, and one was southeast of Middle Mt. Magnitudes ranged between 0.8 and 1.5, depths from 2.1 to 10.9 km.

There were two D-level alerts based on two color geodimeter measurements. 4 mmRL of shallow slip occurred on the main fault near Carr Hill between the end of March and 15 April 1989, ending with a 2 mm step after 11 April. This sequence produced a D-level alert on 9 and 10 April (short term criterion). A D-level alert based on long-term fault-slip criterion began on 21 April and continues to the present (5-9-89). Tests are underway to confirm or eliminate the possibility of systematic instrumental error.

A D-level alert was triggered by a strain event at the Red Hills dilatational strain meter. The event was also picked up by the Jack Cyn instrument, just across the fault from the Red Hills instrument. Only one past event has been detected simultaneously at the Jack Cyn and Red Hills instruments.

There were no water level alerts during April. However, a strain event observed of the GH1 dilatometer beginning about April 1 appears to also have been recorded in the Gold Hill water well.

It was an uneventful month for the creepmeters, tiltmeters and magnetometers, as well as for radon and hydrogen measurements.

- J. Estrem

MAY 1989 PARKFIELD DATA SUMMARY

Allan G. Lindh and John Estrem

There were 35 earthquakes in the Parkfield area in May. Twenty of these were northwest of Middle Mountain, four were in the MM alert box, and 11 were southwest of Middle Mt. Magnitudes ranged between 0.0 and 4.0; depths from 0.1 to 11.4 km. <u>One event (M=1.8) in the alert box on May 5 caused a D-level alert. On May 25 there was a M=4.0 earthquake just south of the town of Parkfield, which resulted in a C level alert. Had this event been 10 km farther to the northwest in the Middle Mountain alert box, we would have had our first ever B level alert.</u>

There was one 0.58 mmRL creep event during May at XMM1 (Middle Mt). The event was coincident with a 3.2 cm drop in water level in the Middle Mt. well on May 14. Neither event triggered an alert. Coincident with the M=4.0 event, small coseismic steps were recorded at 9 of the 13 Parkfield creepmeters.

The M=4.0 earthquake also generated static steps on all dilatometer and tensor strain instruments. A preliminary inversion of these steps indicates a moment of 1.2E22 dyne-cm. The M=4.0 was also recorded at 13 of 15 GEOS stations and provided an invaluable test of the range of sensors recording on GEOS. Andy Michael and Cathy Aviles are preparing a report that will include as much of the data as possible for this event; please get in touch with Andy (415-329-4777) if you have any data to contribute. In addition to seismic recordings, interesting data from low-frequency instruments might consist of long term records (1-2 months for instance) spanning the event, or coseismic offsets, or both.

A D-level alert based on the long-term two-color geodimeter measurements that began on 21 April and persisted through most of May was caused by instrument malfunction and has been cancelled. There were no two-color alerts in May.

It was an uneventful month for the magnetometers, as well as for radon and hydrogen measurements.

JUNE 1989 PARKFIELD DATA SUMMARY

There were 13 events in the Parkfield area in June. Seven of these were northwest of Middle Mountain, five were in the MM alert box, and one was southeast of Middle Mt. Magnitudes ranged between 0.9 and 2.1, depths from 1.4 to 9.0 km. The rate at which earthquakes occurred in June was less than the previous month and less than the long-term average.

There were four creep events in June, three of which coincided with changes in nearby water wells. The first event, 0.42 mmRL at X461, had no corresponding change in any water wells. On 10 June, an 11.5 cm drop in water level in wmiw deep well occurred between creep events at Middle Mt. (0.37 mmRL, XMM1) and at Middle Ridge (0.70 mmRL, XMD1). No creepmeter alert thresholds were exceeded, but the water-level drop triggered a D-level alert for that network. A 0.42 mmRL creep event at XMM1 on 27 June was coincident with a small rise in the water level in wmiw well.

It was an uneventful month for the tiltmeters, magnetometers, strainmeters, and two color laser, as well as for radon and hydrogen measurements.

- J. Estrem

15 August 1989

July 1989 Parkfield Data Summary

There were 21 earthquakes of magnitude 0.6 and larger, located in the Parkfield area by the U.S.G.S. during the month of July -- none triggered an alert. As is usual, most of the activity was concentrated north of Middle Mountain; the six events within the Middle Mountain box were either too shallow, or too small, to trigger an alert. There were four events south of Middle Mountain on the 27th through the 29th, distributed from near Parkfield to near Cholame. These temporally clustered bursts of activity, distributed along the 20-30 km. length of the erstwhile rupture zone, remain an oft-noted and enigmatic feature of the Parkfield seismicity data.

UCSB located 59 earthquakes of magnitude -0.5 and larger using the Digital Downhole Seismic Network. There is generally good agreement between the two catalogs, when one allows for the differences in recording, processing, and detection thresholds, although as expected, magnitudes and depths often differ by considerable amounts.

The only alert of the month was a D-level alert associated with a large creep event which occurred beneath Middle Mountain on the 5th and 6th. This manifested as right-lateral offsets at the Middle Ridge (XMD1, 1.65 mm) and Varian (XVA1, 2.46mm) creepmeters. It was accompanied by strain changes at the Frolich site on the dilatometer (FR03, 3 ns) and the tensor strain meter (FLT, 4-5 ns). However no changes were seen on any of the other strain instruments, nor at the Middle Mountain water well (WMM3) which often sees offsets for large creep events; thus the event must have been centered between XMD1 and XVA1.

A very simple attempt to model this creep event in an elastic half-space produced a reasonable fit to the data with a 3.5 km long slip patch, 0.5 km wide (deep), with 1.6 mm of r.l. slip, extending from near XMD1 to just south of XVA1. I wish to emphasize the over-simplified and non-unique character of this model; it is a plausible, factor-of-two effort, and nothing more. The model is described in more detail in an appendix to this summary.

I cannot resist noting that the largest earthquake of the month at Parkfield was a shallow M2.0 on the 8th, just to the north of the Middle Mountain creepmeter. It has previously been noted that over the last few years, large Middle Mountain creep events have been followed in a disproportionate number of cases by M2 or larger events, within 5 days, within the MM3 alarm box (Michael and Roeloffs, unpublished data, 1989).

The other creep activity of interest was a pair of large events at the Gold Hill site (XGH1) on the 23rd (1.7mm) and the 27th (1.5mm); there is nothing obvious on the nearby Gold Hill dilatometer or water well. It is curious that this creep activity immediately precedes the sequence of four small earthquakes between Parkfield and Cholame that are described above.

WEEKLY EARTHQUAKE REPORT

for the San Francisco Bay Area
from the

UNITED STATES GEOLOGICAL SURVEY
Office of Earthquakes, Volcanoes, and Engineering
345 Middlefield Road, Menlo Park, CA 94025

Date: 10/02/89

To: AG LINDH USGS MENLO

Company:

Fax Phone Number: 5163

CC:

From: Allan G. Lindh and Barry F. Hirshorn

Subject: Seismicity for the week 25 September - 2 October 1989

# of Pages (including this cover sheet): 3

Message:

DISCLAIMER -- THIS IS NOT AN EARTHQUAKE PREDICTION OR WARNING!
The commentary provided with these map(s) is for INFORMATIONAL USE ONLY, and SHOULD NOT be construed as an earthquake Prediction Warning, or Advisory. Responsibility for such warnings rests with the Office of Emergency Services of the State of California.
PLEASE REMEMBER -- THIS IS PRELIMINARY DATA
Releasing these summaries on a timely basis requires that the data, analysis, and interpretations presented are PRELIMINARY. Of necessity they can only reflect the views of the seismologists who prepared them, and DO NOT carry the endorsement of the U.S.G.S. Thus while every effort is made to ensure that the information is accurate, nothing contained in this report is to be construed as an earthquake Prediction, Warning, Advisory, or official policy statement of any kind, of the U.S. Geological Survey, or the U.S. Government.
FURTHER INFORMATION IS AVAILABLE
If you have any questions, please call one of the people listed below for further information or clarification. We have provided at least one home number at which we can be reached at night or on weekends - please use it if ANY further clarification is required.

Pat Jorgensen,	Public Affairs	415-329-4011
Allan Lindh	Seismologist	415-329-4778 (415-941-8848 nights)
Rick Lester	Seismologist	415-329-4747

If you do not receive all pages, please call back immediately.

Voice:415-329-4778 Fax:415-329-5163

5pm 2 October 1989

SEISMICITY MAP of the SAN FRANCISCO BAY AREA
for the WEEK OF 25 September - 2 October 1989
from the U.S. Geological Survey, Menlo Park, CA.
prepared by Barry F. Hirshorn and Allan G. Lindh

This was a normal week for seismicity in the Bay area; for the seven day period ending at 12 noon (PDT) on Monday, 2 October 1989, the U.S. Geological Survey office in Menlo Park recorded 50 earthquakes of magnitude 1.0 and greater, within the area shown. The largest events of the week were a pair of M3.3 events on October 1st at 6:10am and 6:19am, that were located about 20km east of Vallejo. They were part of a small swarm that included 8 events of M1.9 and greater, at a depth of 10-15km beneath Grizzley Island in the Sacramento Delta; this is just north of a M4.0 event on the 22nd of June that was widely felt in the North Bay and Delta.

It was another light week on the Alum Rock segment of the Calaveras fault. There were only three events on this segment this week, and another five east of Mt. Hamilton, including a M2.5 on the 29th. There were no events on the Hayward fault, and just a single M1.3 on the San Andreas near Loma Prieta on the 26th.

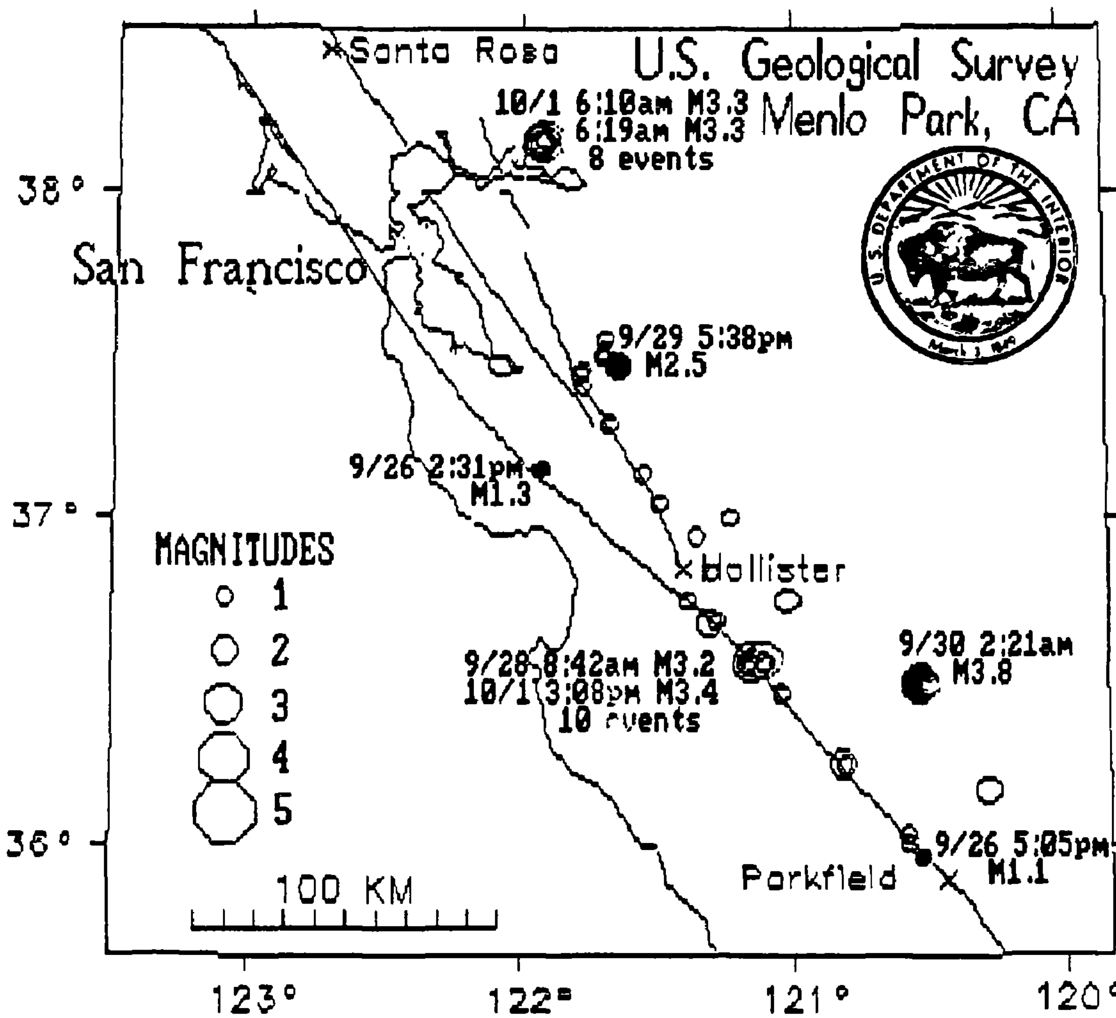

Most of the activity this week was south of the Bay. The largest event of the week in northern California was a M3.8 event on the 30th, near the western edge of the San Joaquin Valley northwest of Coalinga, in the sparsely populated Ciervo Hills. Closer to Coalinga there as a M2.3 event on the 30th.

Along the San Andreas south of San Juan Bautista there was a M3.4 event on the 1st near Bear Valley, east of the Pinnacles National Monument; ten events had occured near this location by noon on Monday. Farther south, there was a shallow M1.1 event beneath Middle Mountain, near Parkfield, on the 26th.

In the Sierra Nevada there was little activity this week, besides the usual scattering of small events in the Mammoth Lakes area. There was a M3.2 event at the Geysers on the 25th. In the northern Sacramento Valley, there was a M2.4 event 20 km southwest of Chico on the 27th.

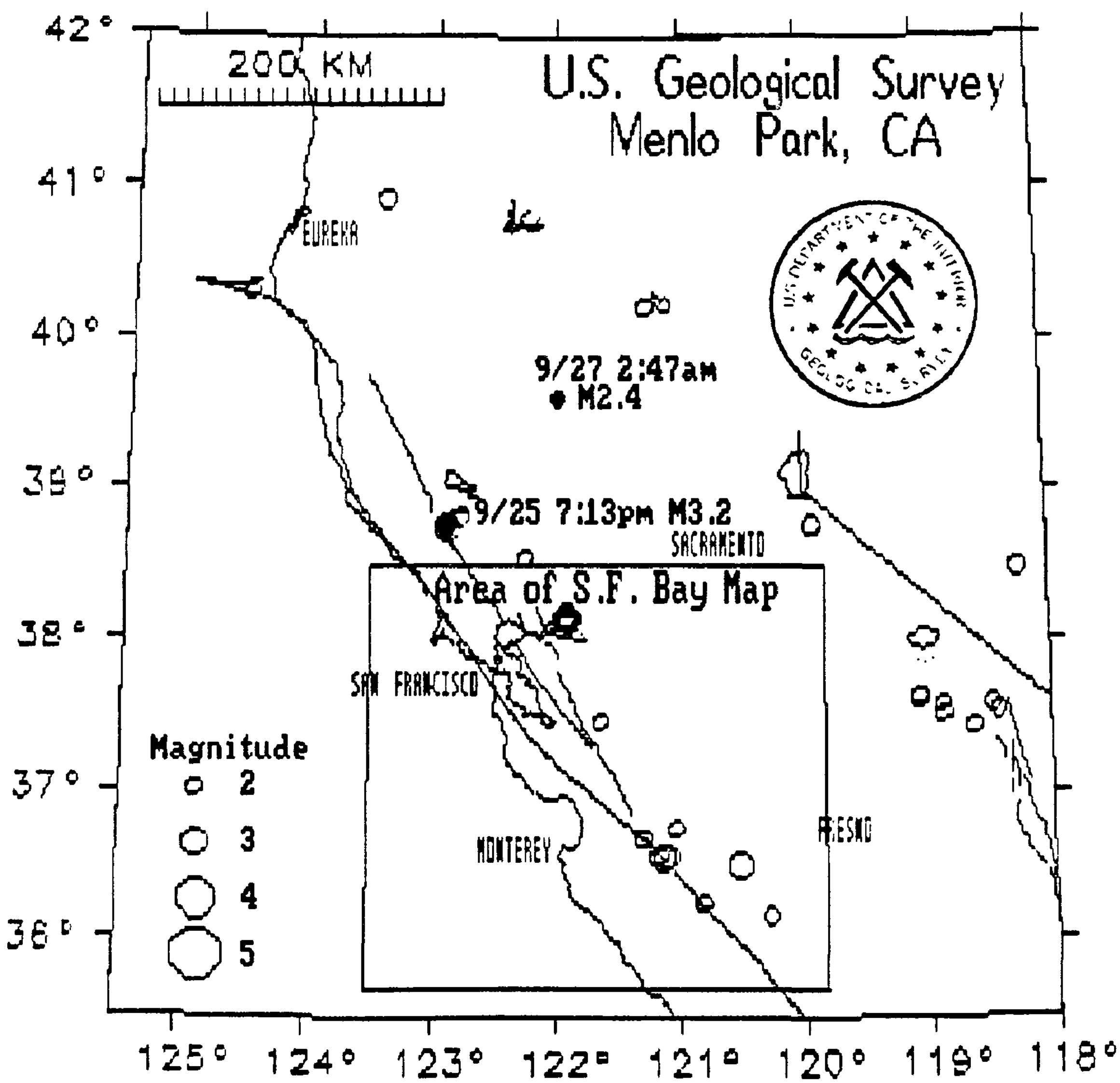

5 October 1989

August 1989 Parkfield Data Summary

There were 27 earthquakes of magnitude 0.9 and larger, located in the Parkfield area by the U.S.G.S. during the month of August; none triggered an alert. As is usual, most activity was concentrated north of Middle Mountain; the nine events within the Middle Mountain box were either too shallow, or too small, to trigger an alert. Six of them located in the 5 km deep cluster beneath XVA1, but not as a swarm -- the six events were distributed throughout the month. There were no events south of Middle Mountain.

UCSB located 60 earthquakes of magnitude -0.5 and larger using the Digital Downhole Seismic Network. There is generally good agreement between the two catalogs, when one allows for the differences in recording, processing, and detection thresholds, although as expected, magnitudes and depths often differ by considerable amounts, and the UCSB catalog contains a large fraction of events off the San Andreas fault that would not be included in the USGS list. There does appear to be a tendency for the USGS magnitudes to be about 0.5 units higher than those computed by UCSB.

The only alerts of the month were a series of D-level alerts associated with a large creep event which occurred beneath Middle Mountain on the 15th and the 16th. It began at XMM1 (0.9mm) at 0300gmt, and was accompanied by a 1.6 cm rise (-19 nstrain) in the deep interval at WMM3. Just over 24 hrs later their was a creep event at XMD1 (1.3mm), accompanied by a 13 cm water level drop (+156 nstrain) at WMM3. The evidence is consistent with a NW-SE propagation at just under 100m per hour; a very slight deflection at XVA1 is consistent with this trend. However since the strain signal at WMM3 consists of two discrete steps 26 hours apart, with little apparent deformation in-between, it may be more appropriate to model the deformation as failure of two discrete "asperities", or stuck spots.

Since the signals at XMM1, XMD1, and WMM3 all exceeded the criteria for D level alerts, they added up to a C alert, which ended at 0500gmt on the 19th. No seismicity was plausibly associated with the creep event.

No other changes were noted in the water well array, or strain nets. No significant changes occurred in the magnetometer or tilt data this month. The two-color laser is once more back in peak form, and no changes were noted in August. The Taylor Ranch geochemistry experiments continued to be troubled by operational difficulties, and no changes were noted in the hydrogen network.

We would welcome hearing from our esteemed colleagues, Steve Parks (UCR), Roger Bilham (U. of Colo.), and John C[illegible]son (U. of Alaska) concerning their Parkfield experiments. We look forward to a report next month on the Hog Canyon differential array, and on the Varian Well water pressure experiment.

Allan Lindh

Allan

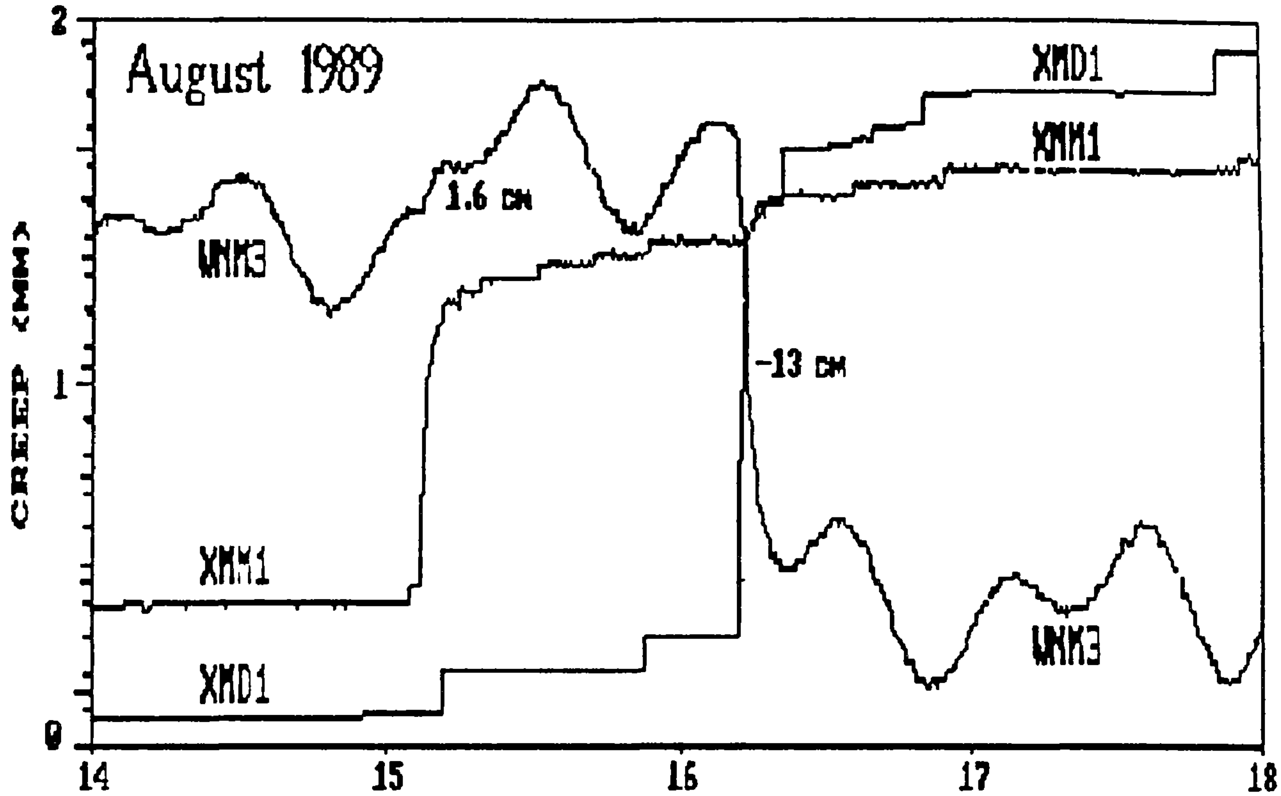
August 1989
XMD1
XMM1
1.6 CM
WMM3
-13 CM
XMM1
XMD1
WMM3
CREEP (MM)
2
1
0
14
15
16
17
18

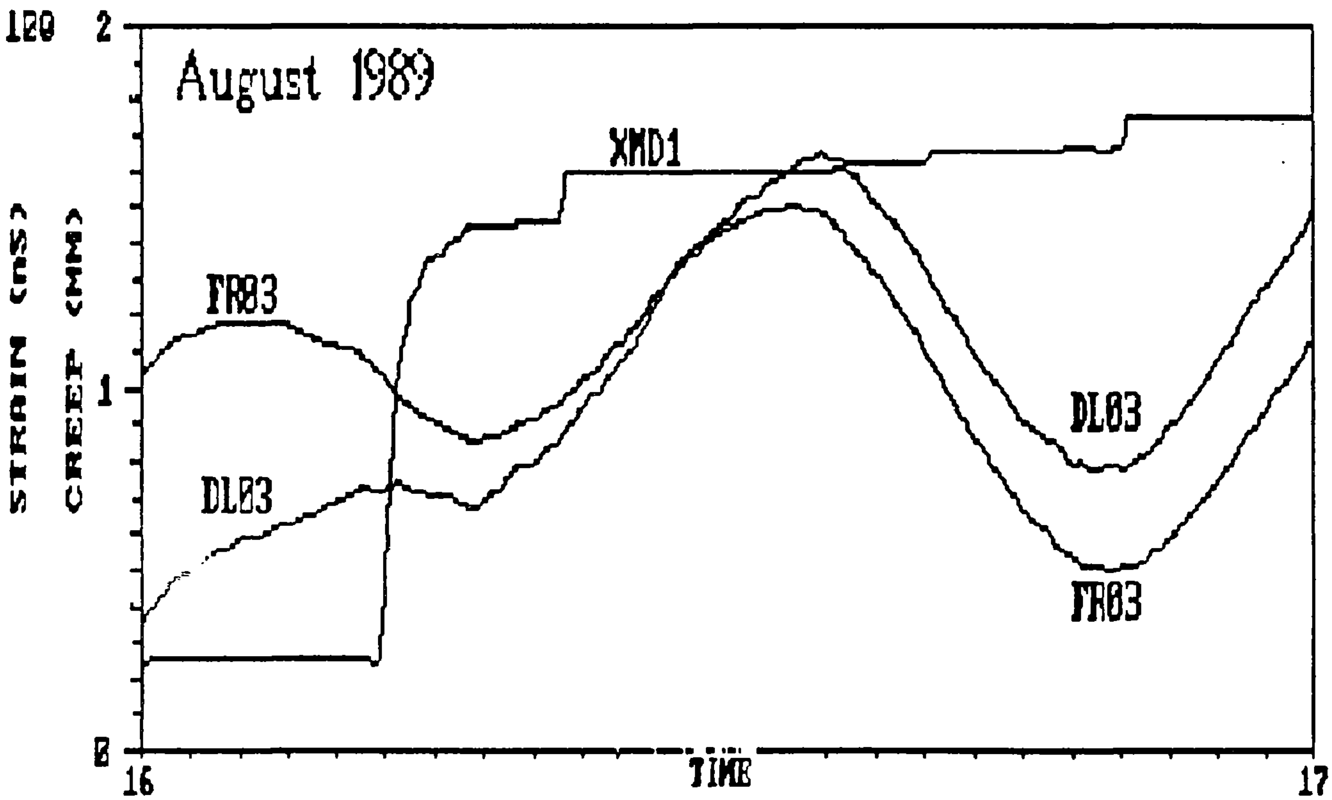
August 1989
XMD1
FR03
DL03
DL03
FR03
STRAIN (nS)
CREEP (MM)
120
2
1
0
16
TIME
17

Cooperative Downhole Seismology Project at Parkfield

USGS Grant # 14-08-001-G1375

P.E. Malin, J.M. Lees, and S.N. Blakeslee
Institute for Crustal Studies
University of California
Santa Barbara, CA 93106

Introduction.

In cooperation with the University of California Berkeley and the United States Geological Survey, we have continued to gather microearthquake data from the Parkfield segment of the San Andreas Fault (See Figure 1). The data are received on borehole seismometers and recorded with a triggered, central recording computer. The project has been going on for several years and currently (10/89) has a catalogue of 926 events of magnitude -0.75 to 1.25. Preliminary locations for events are found several times a week at UCSB. The moments, corner frequencies, and stress drops for each event are currently found at a single station using an automatic spectral integration procedure. After this step the data are ship to UCB and the USGS. At UCSB data reduction continues along two lines: (a) an empirical source parameter monitoring stream, reviewed every month, for potential changes in the physical state of the fault zone and (b) basic research in the physical state of the fault zone itself.

Investigations.

(a) Currently, the moment, corner frequency, and stress drops of each event as determined at the Vineyard Canyon station are catalogue. We have created cumulative moment diagrams for 3 boxes, one northwest of Parkfield, one at Middle Mountain, and one to the southeast. We are in the process of doing moment, corner, stress drop, and other waveform properties on all of the downhole recordings. We expect that averaging these values will yield a stable set of parameters that can be monitored by position on the fault for changes that can be related to the seismicity.

(b) We have complete and are preparing for publication two basic studies of the fault zone: (1) a tomographic inversion of P wave travel time perturbations and (2) a near source S wave attenuation study. (1). Tomographic inversion was applied to delay times from local earthquakes to image three dimensional velocity variations near Parkfield, California. The 25x20 square km region is represented by nearly cubic blocks of .5 km per side. P-wave arrival time observations from 551 crustal earthquakes, with depths of 0 to 15 km, were used as sources recorded at 8 stations of the Parkfield downhole array, producing 3135 rays covering the target region. A conjugate gradient method (LSQR) is used to invert the large, sparse system of equations. To diminish the effects of noisy data, the Laplacian is constrained to be zero within horizontal layers, providing smoothing of the model. The resolution is estimated by calculating impulse responses at blocks of interest and examining ray distribution plots. Estimates of standard errors are calculated by the jackknife statistical procedure. (2) We have developed a technique to measure seismic attenuation within an active fault-zone at seismogenic depths. Utilizing a pair of stations and pairs of earthquakes, spectral ratios are performed to isolate attenuation produced by wave-propagation within the fault-zone. This empirical approach, which is illustrated in Figure 2, eliminates common source, propagation, instrument and site effects.

In our approach we assume that the observed frequency spectrum, *A(f)*, can be described as the product of the earthquake source spectra, *EQ(f)*, with a number of transfer functions:

$$A(f) = I(f) \cdot R(f) \cdot P(f) \cdot F(f) \cdot EQ(f) \qquad (1)$$

The earthquake source spectrum, *EQ(f)*, will be controlled by the specifics of crack tip acceleration and deceleration during rupture. The instrumentation, *I(f)*, will introduce its receiver function into the final recorded signal. The propagation path, is divided into three distinct segments each with its own filtering effect: (1) the near-surface, *R(f)*, which can produce pronounced low-impedence amplification, high-frequency attenuation, and sinusoidal modulation due to near-surface multiples, (2) the country rock path, *P(f)*, which introduces both intrinsic losses and body wave scattering and finally (3) the fault-zone, *F(f)*, which will alter the spectrum in a way which will be determined by the following analysis.

Current understanding of these competing processes do not allow them to be explicitly modeled and eliminated. However, by obtaining multiple measurements of each of these effects they can be removed from the analysis empirically. The required redundancy of source and propagation effects can be obtained by recording a pair of earthquakes at a pair of stations. Diagrammed in figure 2 is a general, 1-dimensional case involving two stations and two earthquakes. For this geometry, the two earthquakes EQ_a and EQ_b are co-linear between the two stations, ST_1 and ST_2. Two earthquakes recorded by two stations will produce the following four spectra:

$$\begin{aligned}
A[ST_1, EQ_b] &= I_1 R_1 P_1 F_1 F_x EQ_b \\
A[ST_2, EQ_a] &= I_2 R_2 P_2 F_2 F_x EQ_a \\
A[ST_1, EQ_a] &= I_1 R_1 P_1 F_1 \; EQ_a \\
A[ST_2, EQ_b] &= I_2 R_2 P_2 F_2 EQ_b
\end{aligned} \qquad (2)$$

The four spectra can be combined as shown below:

$$\frac{A[ST_1, EQ_b]}{A[ST_1, EQ_a]} \cdot \frac{A[ST_2, EQ_a]}{A[ST_2, EQ_b]} = \frac{EQ_b F_x}{EQ_a} \cdot \frac{EQ_a F_x}{EQ_b} = F_x^2 \qquad (3)$$

This formulation separates fault-zone attenuation from country rock and near-surface losses. Although the technique does not require assuming a functional form for Q(f), a constant Q attenuation operator will approximately reproduce the type of attenuation commonly observed in seismic waves. A least-squares-determined line can then be fit to each log $F_{a,b}(f)$ and the slope of that line, c_1, is proportional to d/Q.

$$\begin{aligned}
\frac{\partial}{\partial f}\left[\log F_{a,b}\right] &= \frac{\partial}{\partial f}\left[\frac{-\log(e^1)\pi f d}{vQ}\right] = \frac{-1.36\, d}{vQ} \\
\frac{\partial}{\partial f}\left[\log F_{a,b} \cong (c_o + c_1 f)\right] &= c_1
\end{aligned} \qquad (4)$$

Thus, Q can be obtained by knowing *d*, the difference in propagation distance produced by the spatial separation between the events, and *v*, the velocity of the medium. The fault-zone propagation distance *d*, associated with $F_{a,b}(f)$ is $d(a,b) = (x_{b1}-x_{a1}) + (x_{a2}-x_{b2})$, where x_{b1} is the total distance from *event b* to station *1*.

Results.

(3) (See Figure 3). The cumulative moments as observed at VC for four boxes of events show periods of quiescence and activity in the time period of our monitoring. The largest swarm to take place occurred in the Frolich box near the beginning of our

study, and except for one period after day 770, has been relatively quiet. The largest event, a M=4) took place in the Gold Hill box near day 900, taking the cumulative moment off scale. At this time there appears to be no systematic relationship between the latter event and the character of the curves shown in Figure 3.

(b) (See Figures 4 and 5)

(1) (See Figure 4) The results of the tomographic inversion show correlation with some of the local geological and geophysical features. The largest velocity anomaly, a low at a depth of 2.5-3.5 km and a few km northwest of Parkfield, appears related to the largest gravity low within the study area. The velocity anomaly reverses sign in the layer below this depth, perhaps accounting for corresponding reflections observed on the Parkfield COCORP lines at this location. On the southwest side of the San Andreas the velocity contrasts of the Tertiary sediments and underlying Salinian basement can be seen. The sediments appear to cover a linear velocity feature paralleling the San Andreas fault and off set from it by several kms. This feature may correspond to the White Canyon fault, though to be an early branch of the San Andreas fault. More speculatively, the correlation of higher velocity features and seismic activity may indicate that, locally, earthquakes are occurring in more competent zones while aseismic slip takes place in slower, less competent, rocks.

(2) (See Figure 5) The technique for extracting fault zone attenuation was applied to a cluster of 19 earthquakes recorded by a pair of downhole instruments located within the San Andreas fault-zone, at Parkfield California. Over the 1-40 Hz bandwidth used in this analysis, amplitudes are found to decrease exponentially with frequency. Furthermore, the fault-zone propagation distance correlates with the severity of attenuation. Assuming a constant Q attenuation operator, the S-wave quality factor within the fault-zone at a depth of 5-6 kilometers is 31 (+7,-5). If fault-zones are low-Q environments, then near-source attenuation of high-frequency seismic waves may help to explain phenomenon such as f_{max}. Fault-zone Q may prove to be a valuable indicator of the mechanical behavior and rheology of fault-zones. Specific asperities can be monitored for precursory changes associated with the evolving stress-field within the fault-zone. The resolution of the technique is limited by the uncertainty in location and the travel time between earthquakes.

Fig.1. Epicenters and downhole stations at Parkfield CA. The moments, corners, and stress drops of events are currently calculated only at the VC station. All the stations shown were used in the tomography study. The two stations used in the attenuation study, MM and ED, are very near the trace of the San Andreas, and the line with brackets shows the limits of the attenuation study events.

Fig.2. This diagram shows the geometry of sources and stations which allows the filtering effect of the fault-zone to be isolated. In this study MM is used as station 1 and ED is used as station 2.

Fig.3 The top plot shows the cumulative moment of events in the different boxes along the San Andreas. The boxes are show in the lower half of the Figure as projected along the plane of the San Andreas Fault. Note the swarm near day 270 and the large event near day 900.

Figure 4 Tomographic inversion of Parkfield P-wave travel time residuals. The triangles correspond to the stations shown in Fig.1, the depth of the inversion layer in listed in the top left corner of each image, and the San Andreas, Table Mountain, Gold Hill, South West Fracture, and White Canyon Faults are indicated.

Fig.5. Each of the events in the brackets shown in Fig. 1 was paired with each other events to produce all possible source pairs. The transfer functions were then calculated, the slope of which is the attenuation along the propagation path. The slopes are plotted for all the event pairs verses distance. The average dependence of attenuation on propagation distance yields, Q_{fzone} = 31 (+5,-7).

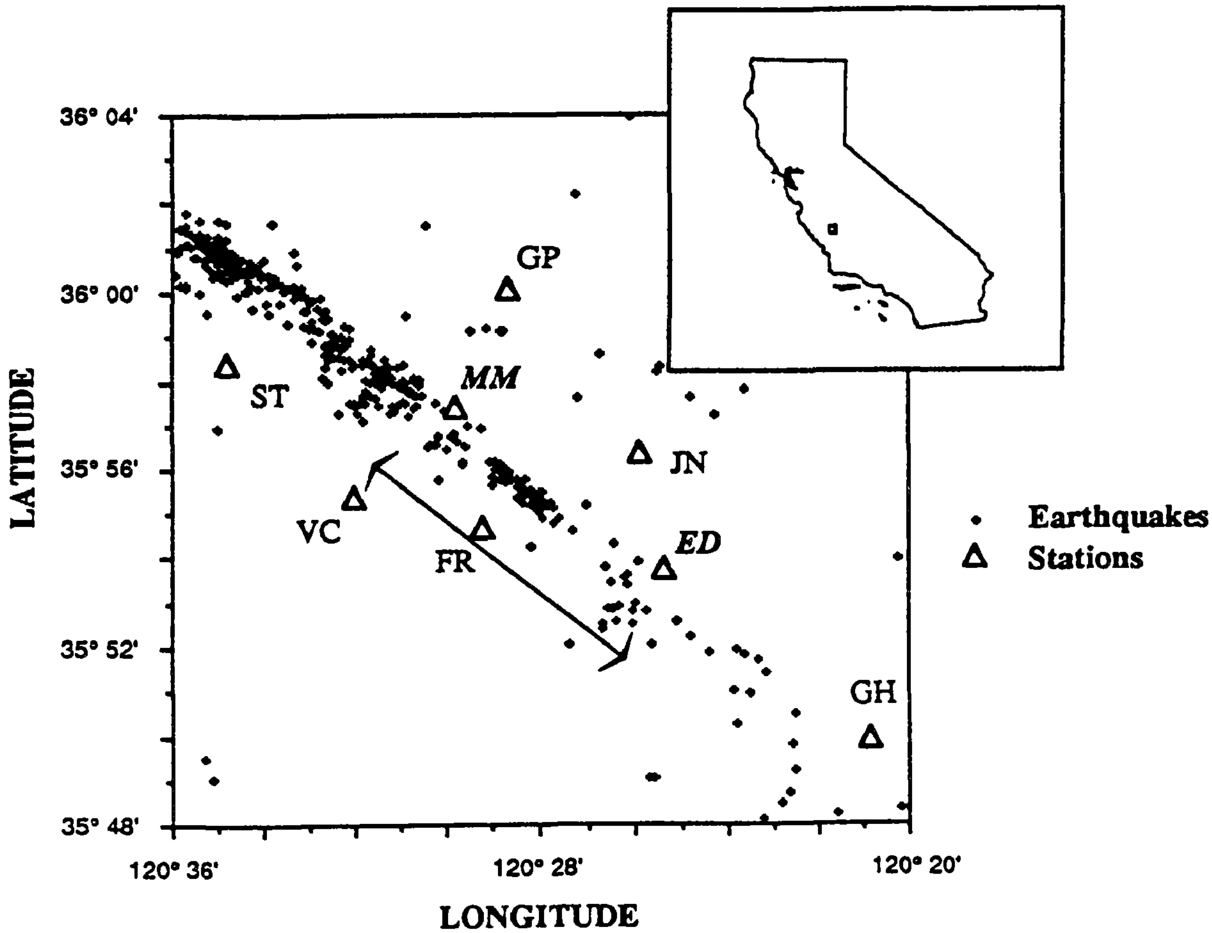

Figure 1. Map showing location of microearthquake activity at Parkfield CA., for two years. Shown as triangles are the downhole stations, the two stations used in this study are MM and ED which are very near to the active trace of the San Andreas Fault. The line from MM to ED represents the limits of the cross-section shown in figure 3

FIGURE 1

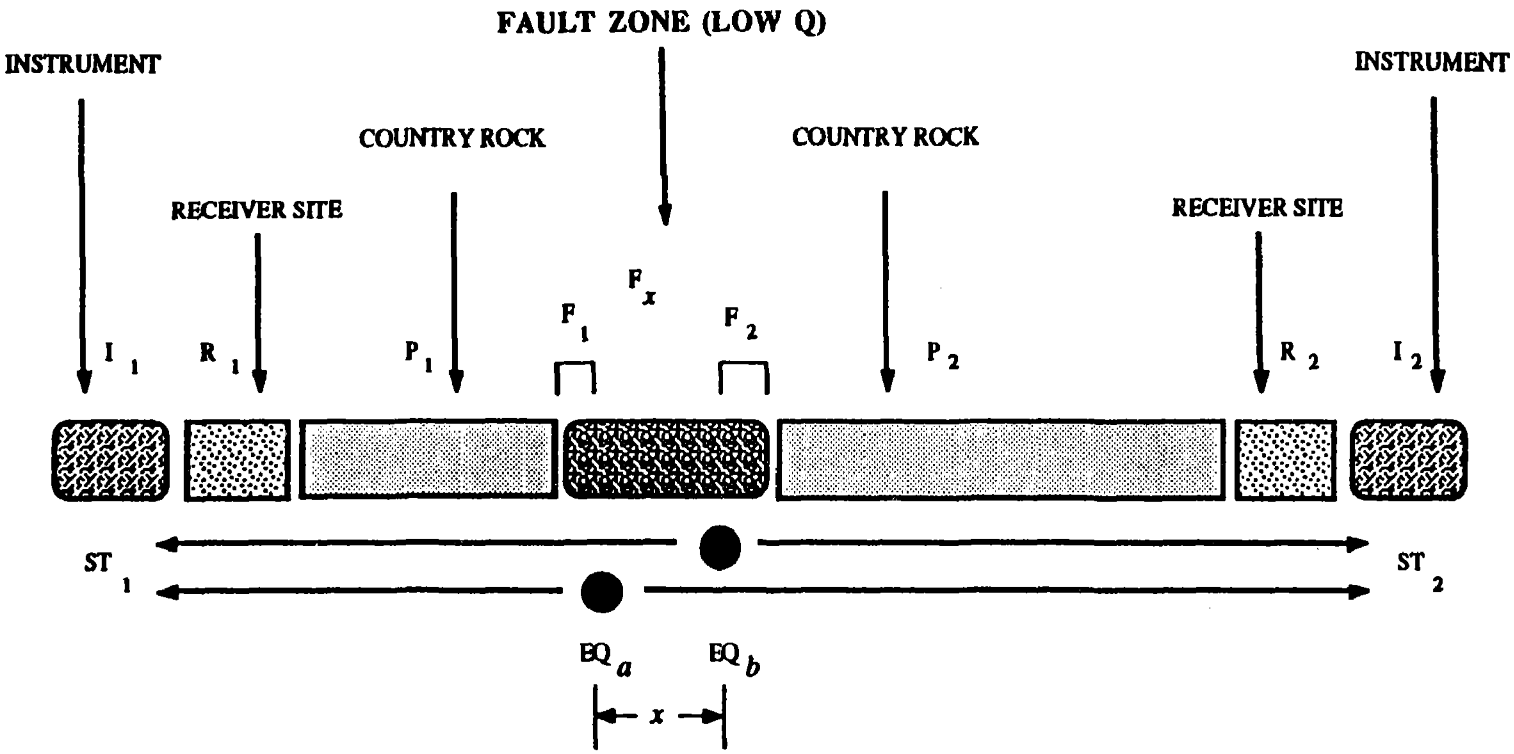

Figure 2. A pair of earthquakes recorded by a pair of stations will provide 4 spectra each of which reflects the source and transfer functions of the medium and recording system. This 1D diagram shows the geometry of sources and stations which allows the filtering effect of the fault-zone to be isolated. In this study MM is used as station 1 and ED is used as station 2.

FIGURE 2

CUMULATIVE MOMENTS FOR PARKFIELD REGIONS

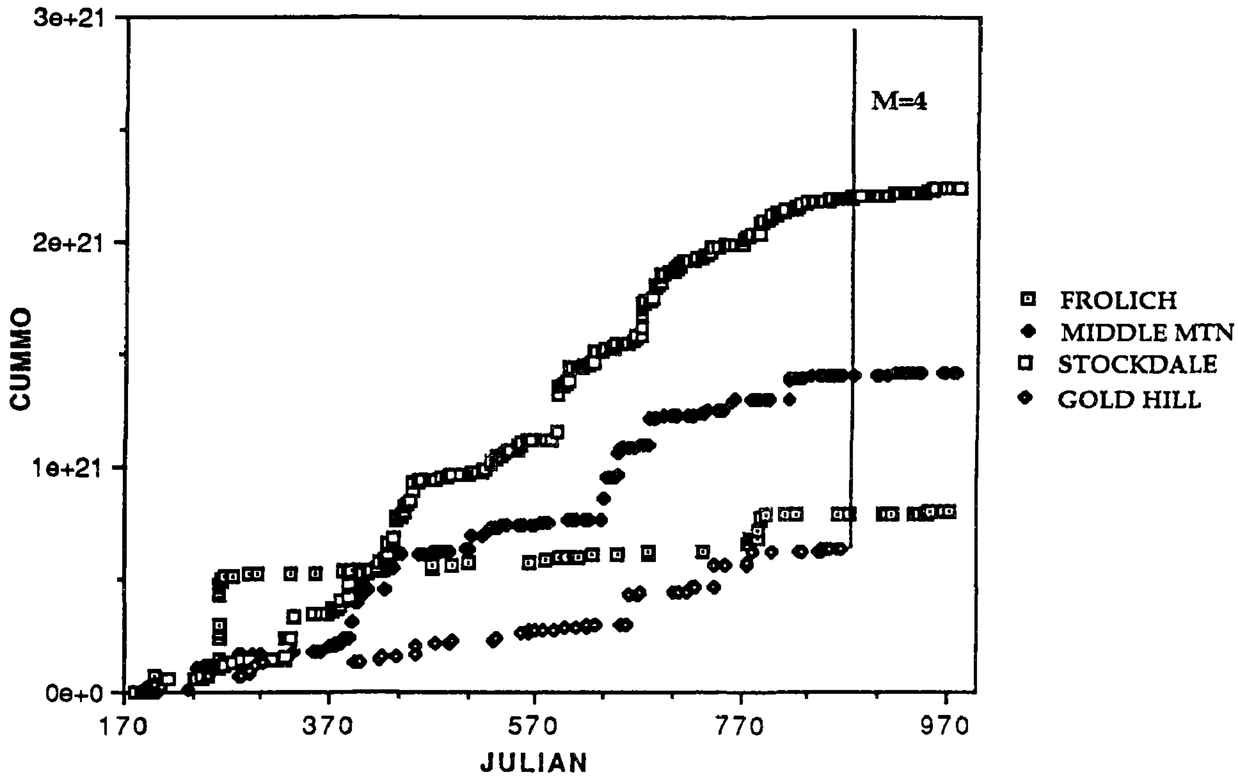

Fault Plane Cross Section

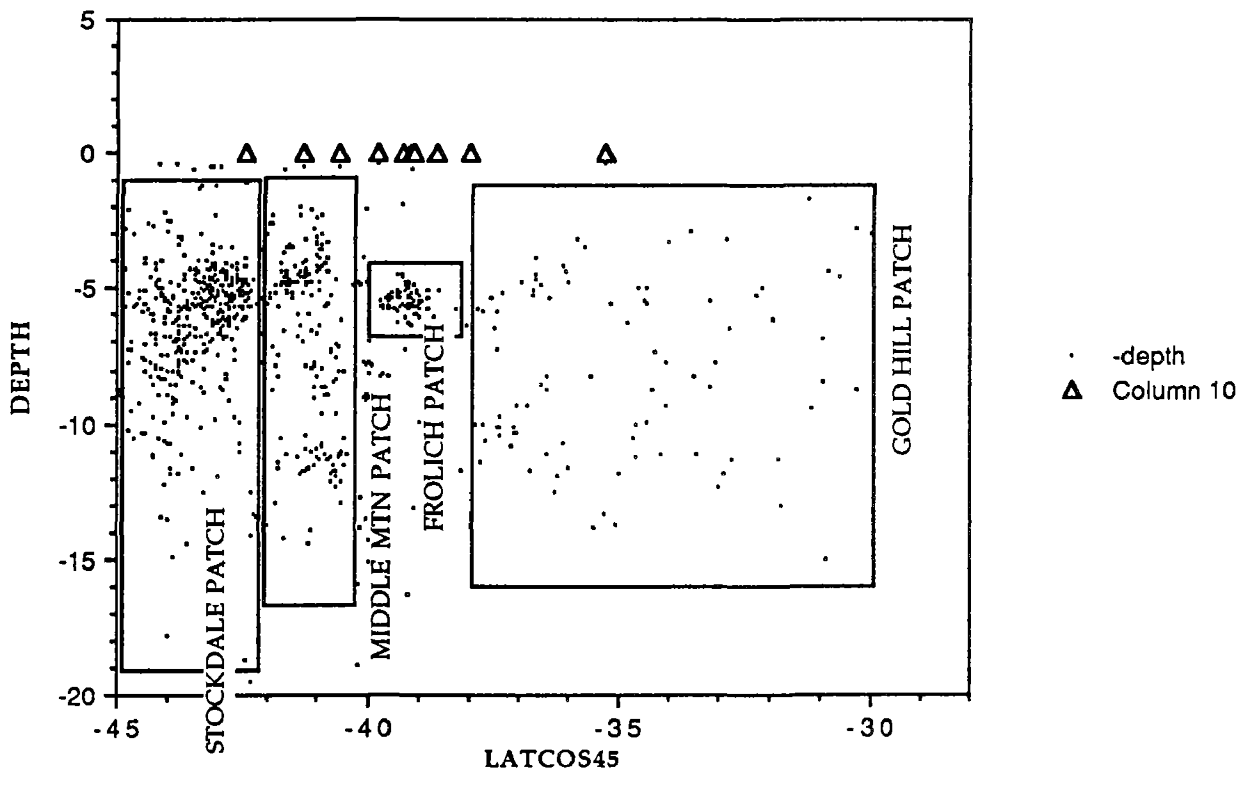

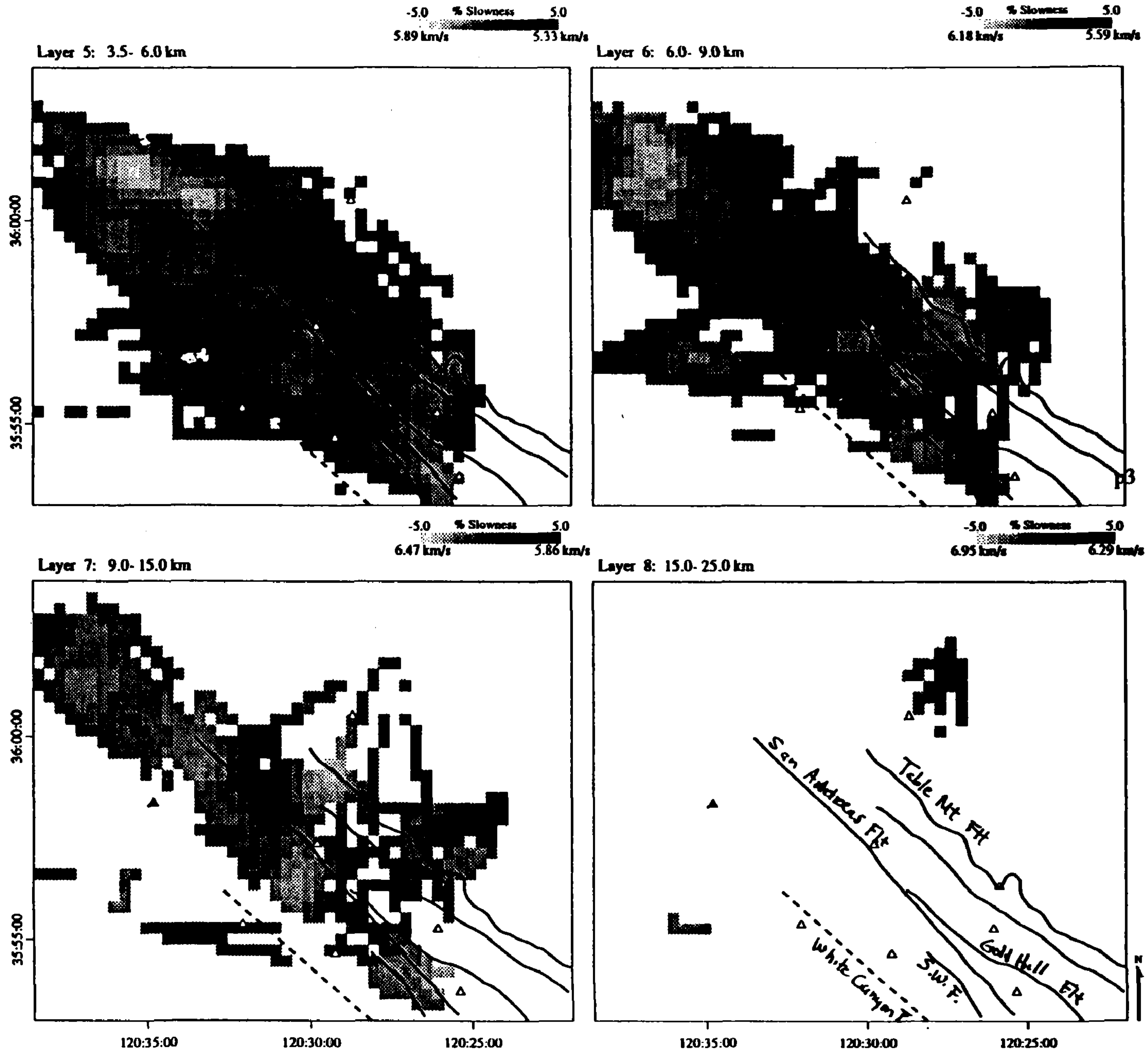
-5.0 % Slowness 5.0
5.89 km/s 5.33 km/s
Layer 5: 3.5- 6.0 km
-5.0 % Slowness 5.0
6.18 km/s 5.59 km/s
Layer 6: 6.0- 9.0 km
p3
-5.0 % Slowness 5.0
6.47 km/s 5.86 km/s
Layer 7: 9.0- 15.0 km
-5.0 % Slowness 5.0
6.95 km/s 6.29 km/s
Layer 8: 15.0- 25.0 km
36:00:00
35:55:00
120:35:00
120:30:00
120:25:00
San Andreas Flt
Table Mt Flt
Gold Hill Flt
S.W.F.
White Canyon F.
N

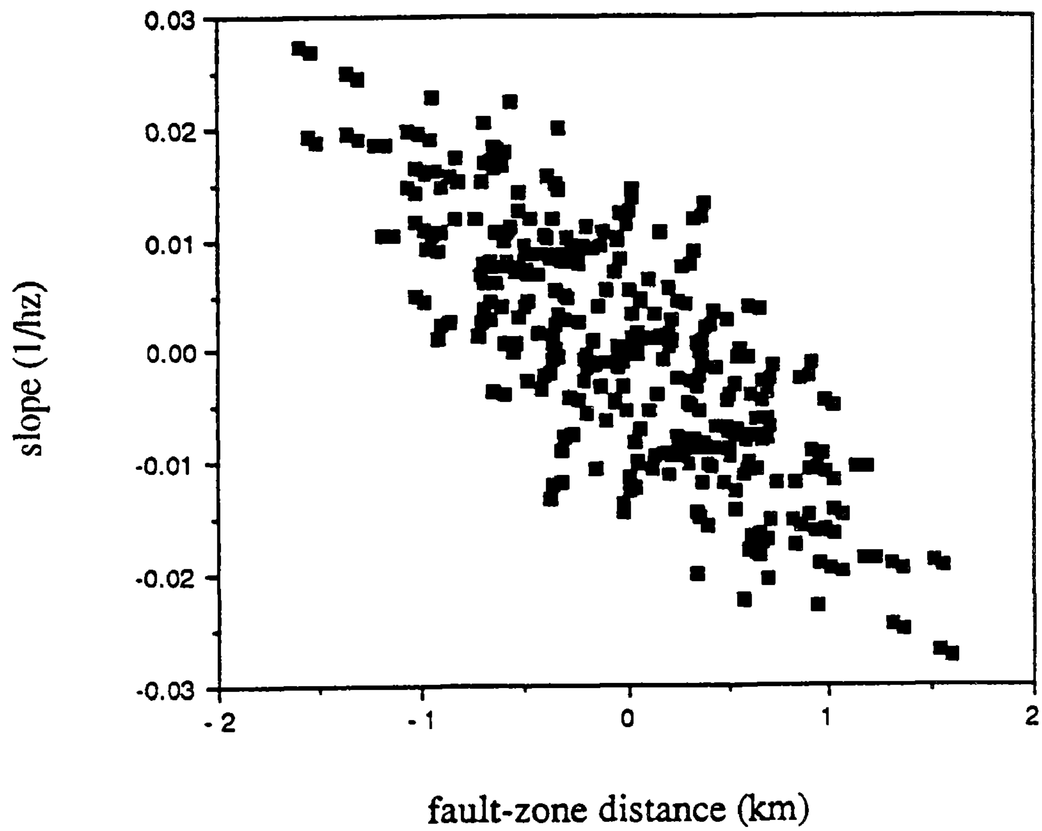

Figure. Each of the events was paired with all of the other events in the cluster, to obtain 342 fault-zone transfer functions. To quantify the severity of high-frequency attenuation, least-squares-determined lines were fit to each transfer function. The slopes of those lines are plotted as a function of propagation distance within the fault-zone. The dependence of attenuation on propagation distance is used to determine the fault-zone quality factor for S-waves; using all 19 events, $Q_{fzone} = 34 \pm 3$.

FIGURE 5

SEISMIC WAVE MONITORING AT PARKFIELD, CALIFORNIA

14-08-0001-G1703

T.V.McEvilly, R. Clymer, T.Daley, Wm Foxall, E. Karageorgi, A. Michelini
Seismographic Station
University of California
Berkeley, CA 94720
415/642-3977

INTRODUCTION

Three programs of seismic wave measurements continue: Earthquake recording with the high-resolution seismic network (HRSN), begun in December, 1986; controlled-source monitoring with HRSN, begun in June, 1987; and controlled-source monitoring with the Varian well vertical array (VWVA), begun in November, 1987.

The HRSN (Figure 1) consists of ten, 3-component, borehole seismometers surrounding the 1966 Parkfield epicenter. Data-acquisition features digital telemetry with 125-Hz bandwidth and 16-bit resolution, and can operate in external-trigger (*i.e.,* controlled-source) or event-trigger (earthquake) modes.

The VWVA extends to 1400-m depth at a site 2 km from the San Andreas fault (Figure 1), close to the nucleation zone of the expected magnitude 6 Parkfield earthquake. While tests done shortly after installation indicated that the entire array was functioning, failure of deep connecting cables soon eliminated sensors below 968m. There is no indication of further loss. The original November, 1987 tests provide a 'benchmark' vertical seismic profile (VSP) using the full string. The remaining instruments are adequate to proceed with all the proposed uses of the VWVA. The array is recorded on a Sercel 338 96-channel reflection system.

INVESTIGATIONS

1) Earthquakes. Local microearthquakes of magnitude about -1 to about +1.8 are continuously recorded. An improved velocity model and location procedure have been developed, which will allow analysis with high precision of all earthquakes in this area. Relocated events will then be used to study failure processes, fault zone structure, and material properties within the Parkfield nucleation zone.

2) Controlled-source monitoring with HRSN. The nucleation zone is illuminated on a nominally monthly schedule by the UCB shear-wave vibrator operated at eight source sites (Figure 1), generating three shear-wave polarizations at each site. Preliminary data reduction is accomplished at the University of California's Lawrence Berkeley Laboratory (LBL). Data analysis procedures are being developed to detect changes in velocity, attenuation, and anisotropy.

3) Controlled-source monitoring with VWVA.

- Analysis of local anisotropy and velocity structure using short-offset VSP's.
- Monitoring of seismic parameters by monthly illumination of the array from several of the HRSN source sites.

RESULTS

1) *Earthquakes.*

3-D Velocity Models

We have continued the development of three-dimensional models for P and S velocity in the Parkfield nucleation zone, using inversion techniques that allow full benefit of the high bandwidth and dynamic range of the HRSN data. We have tested the procedure 1) with synthetic travel-time models, and 2) by performing the inversion using two distinct datasets. The first dataset consists of the P and S onset readings from HRSN and from Parkfield-area USGS CALNET stations, providing a total of about 700 P and 300 S travel times. The second dataset consists of nearly 1300 P and 750 S onset readings from HRSN only in 1988. The results of the two inversions are very similar and their comparison provides an estimate of the uncertainties in the velocity determination. The final average rms residuals of the hypocentral locations was approximately 33 ms in both inversions.

The results suggest that:

1) There is a strong lateral velocity contrast across the fault trace (about 15%), for both P and S velocities. Higher velocities were resolved for the block southwest of the San Andreas fault, and lower velocities to the northeast;
2) A low velocity fault zone is revealed for both P and S velocities, more accentuated for the S, implying a higher than normal value of the Vp/Vs ratio along the fault trace at depth. We find Vp/Vs ratios of about 2.0 near the hypocenter of the 1966 main shock, and lower values elsewhere.

Present inversion work includes:

- Inversions for different time periods to search for temporal changes in the Vp/Vs ratio in the fault zone during the two years of operation of the HRSN;
- Development of a new inversion scheme that permits the parameterization of the velocity model using B-splines. This method will allow us to determine a velocity model and directly generate synthetic seismograms using dynamic ray-tracing (Cerveny, 1985). This method makes use of the entire waveform, and it will be usable in anisotropic media.

In other studies, we are 1) mapping structural characteristics of the fault zone, such as attenuation and scattering, and 2) obtaining a better understanding of the source mechanics of the microearthquakes through the study of their moment tensors and space-time migration patterns.

Source Mechanics

We have developed algorithms to generate ray-theoretical three-dimensional Green's functions for the velocity structure described above, in close collaboration with Ivan Pcencik of the Czechoslovakian Academy of Science in Prague. These are being used 1) in moment-tensor inversions for equivalent point sources of Parkfield microearthquakes, and 2) to investigate the effects of severe lateral heterogeneity on focal-mechanism solutions. It is also planned to investigate the use of these Green's functions in inversions for rupture time histories of larger Parkfield events.

2) Controlled-source studies - HRSN.

Twenty-two data sets have now been acquired, from June, 1987 to August, 1989. Preliminary processing of the field data produces edited, correlated, and stacked common-source files, *i.e.*, one source into all receivers for one month. New data go through this processing within a few days of acquisition.

Our basic working data sets for analysis are "time gathers": one source into one receiver, gathered across time, producing files of, at present, 22 similar traces. We have recently reorganized the entire data set into time gathers, producing files and displays for all 720 source-receiver combinations (24 sources into ten, 3-component receivers). The paths to be first analyzed in depth will be determined by visual scanning for anomalies, visual determination of signal-to-noise ratio, and the geometry of the path. Many of the gathers show surprising coherence of events across time to travel times as late as 10 to 12 seconds.

Several analysis tools are being developed to display key parameters of these data. Figure 5 shows relative travel-time variations of several events from several time gathers with a common source, analyzed with a cross-correlation, cross-coherence procedure for timing similar traces. Due to the common source, a common pattern of near-surface seasonal variations is clearly visible in the direct S and the 8-10 sec arrivals (labeled "M"). The P-waveforms are less stable (probably not surprising from an S-wave source), and the travel-time variations are noisier. We attempted to remove the seasonal variation by subtracting the average pattern for each event. The results (Figure 6) are stable to a few milliseconds in the S and M events.

3) Varian well.

The analysis of the initial VSP studies, showing up to 10% anisotropy in the vicinity of the well, is presently being submitted for publication.

The field work at Varian well was dealt a serious blow with the terminal failure of the borrowed recording system used there in the spring of 1989. We have recently arranged the loan of a more modern, 96-channel Sercel recording system from CGG American Services, Inc, which will see initial service in late October, 1989. The detailed multi-azimuth VSP survey planned for summer, 1989, will be accomplished in the spring of 1990, when access to sites will again be possible. Recording of the Varian well array during the monthly vibrating at HRSN sites will begin again in November, 1989.

The development of 3-D, generally anisotropic models continues, in cooperation with V. Cerveny, I. Psencik, and D. Gajewski. The results are being used in forward modeling of material properties at the Varian well.

Presentations

Michelini, A., Foxall W., and McEvilly. T.V., Three-dimensional velocity structure and high resolution seismicity in the Parkfield, California, nucleation zone, Abstracts of the 25th IASPEI General Assembly, Istanbul, August, 1989.

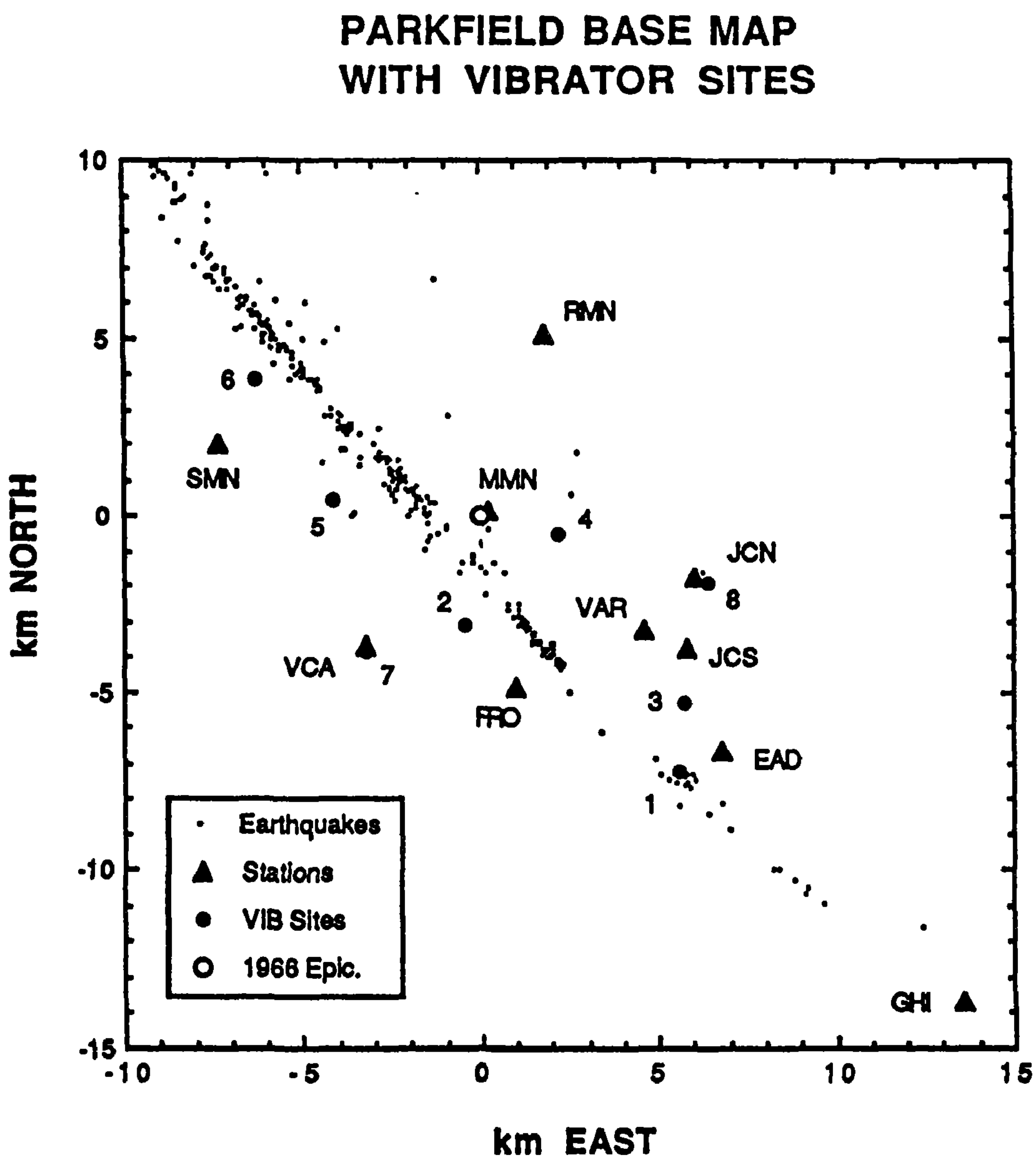

Figure 1. Parkfield high-resolution seismic network with vibrator sites. Varian well vertical array is labeled VAR. The origin of coordinates is the epicenter of the 1966 Parkfield earthquake.

P-VELOCITY; HRSN & CALNET; 75 EQ's

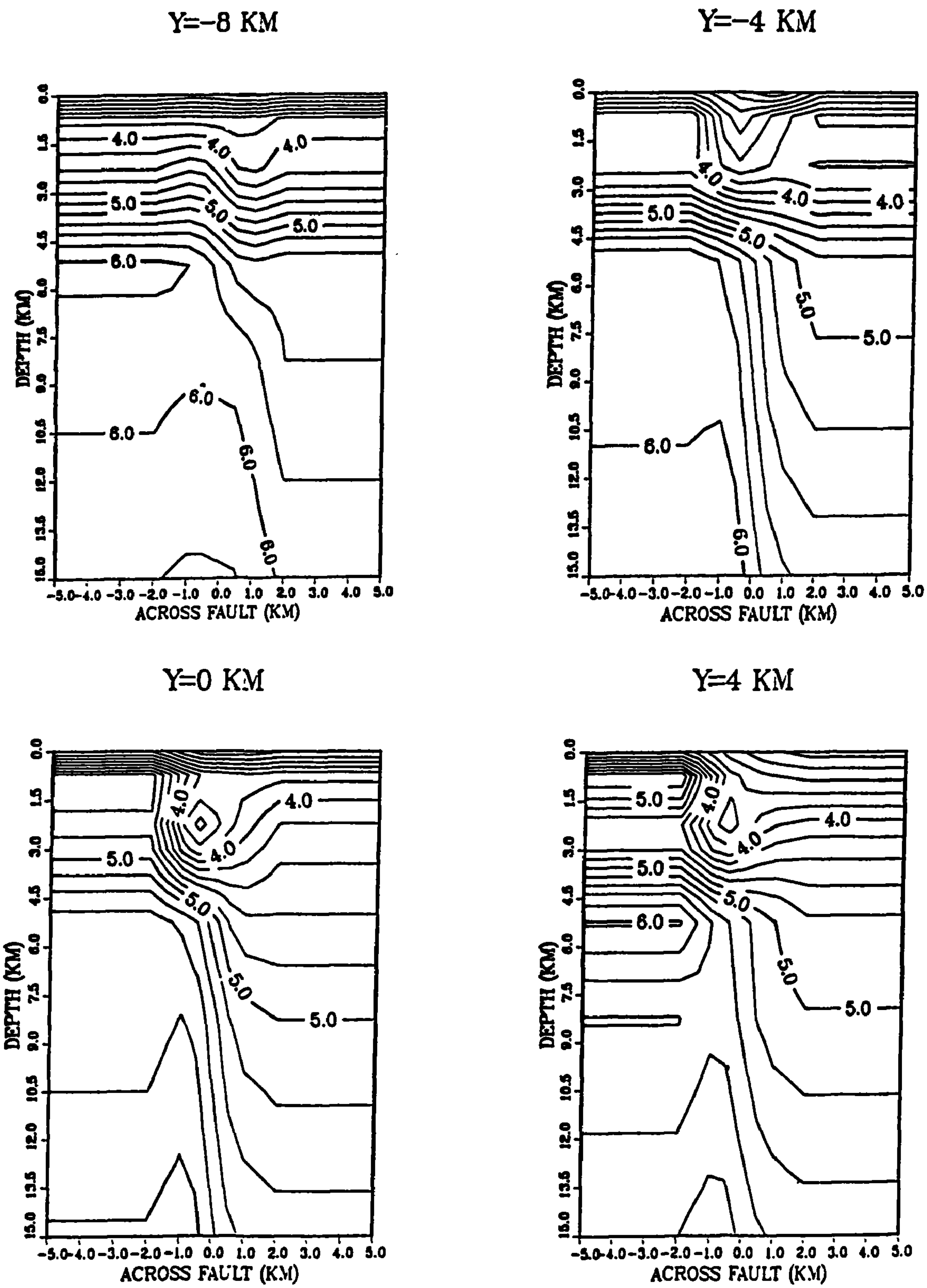

Figure 2. Three-dimensional inversion results: Cross-sections from southwest to northeast for P-velocity, determined using HRSN and CALNET arrival onsets. The Y-axis is along the surface fault trace, positive toward the northwest. The origin corresponds to the location of the 1966 main shock.

S-VELOCITY; HRSN & CALNET; 75 EQ's

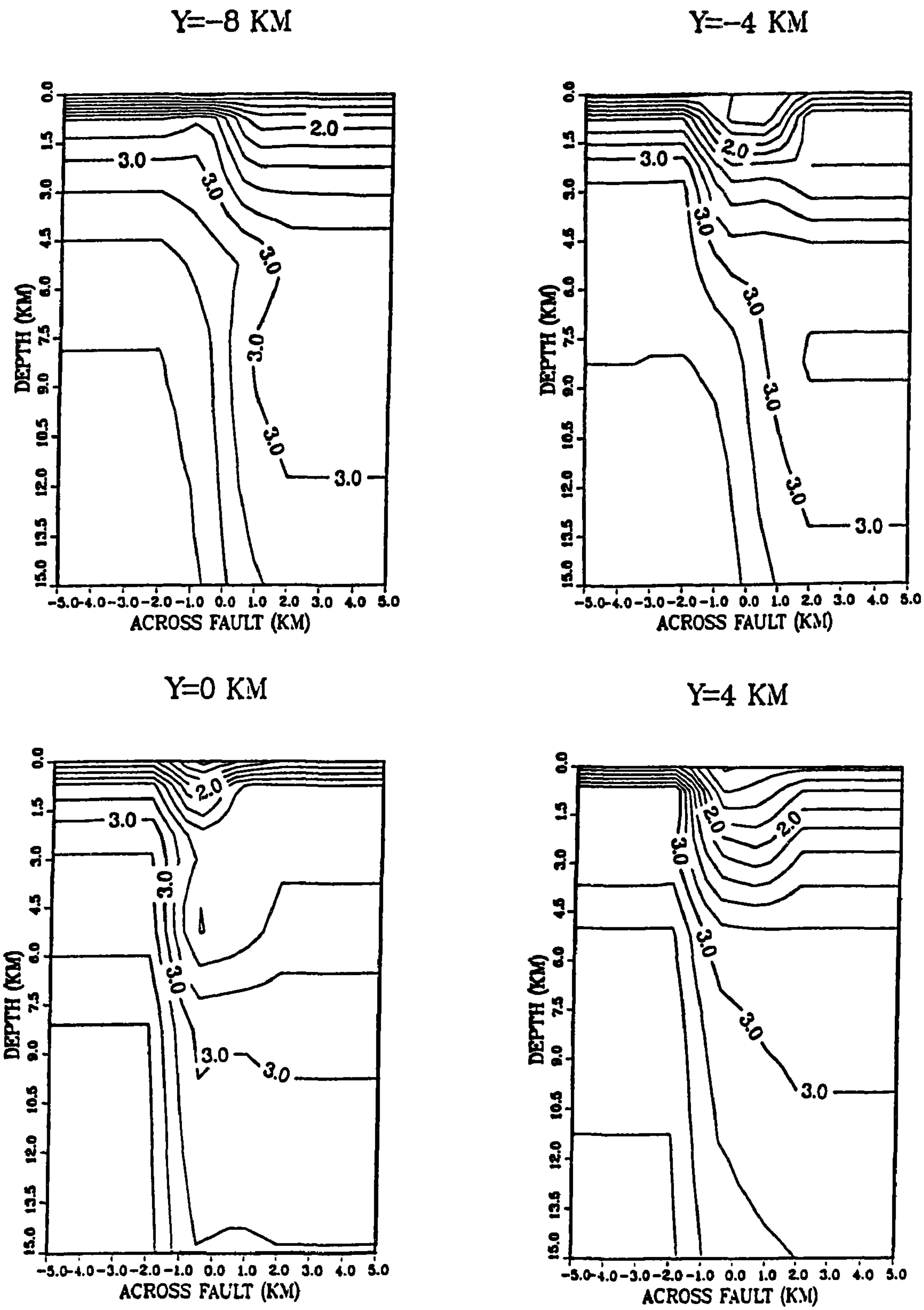

Figure 3. Three-dimensional inversion results: S-wave velocity.

Y=0 (Middle Mnt.); HRSN & CALNET; 75 EQ's

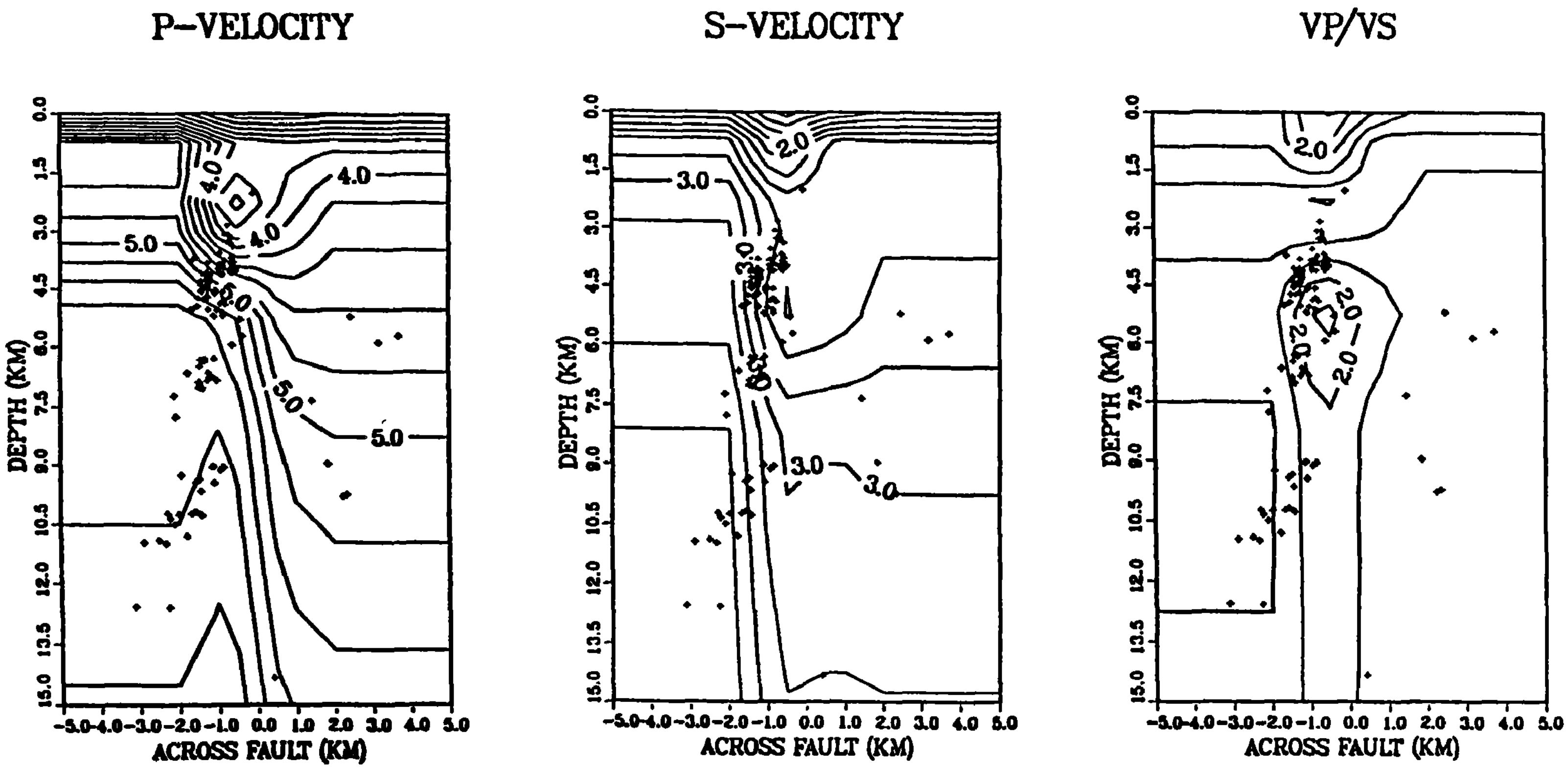

Figure 4. Three-dimensional inversion results: Cross-sections of P- and S-velocity and Vp/Vs-ratio at Y=0, with the seismicity within Y=±4 km.

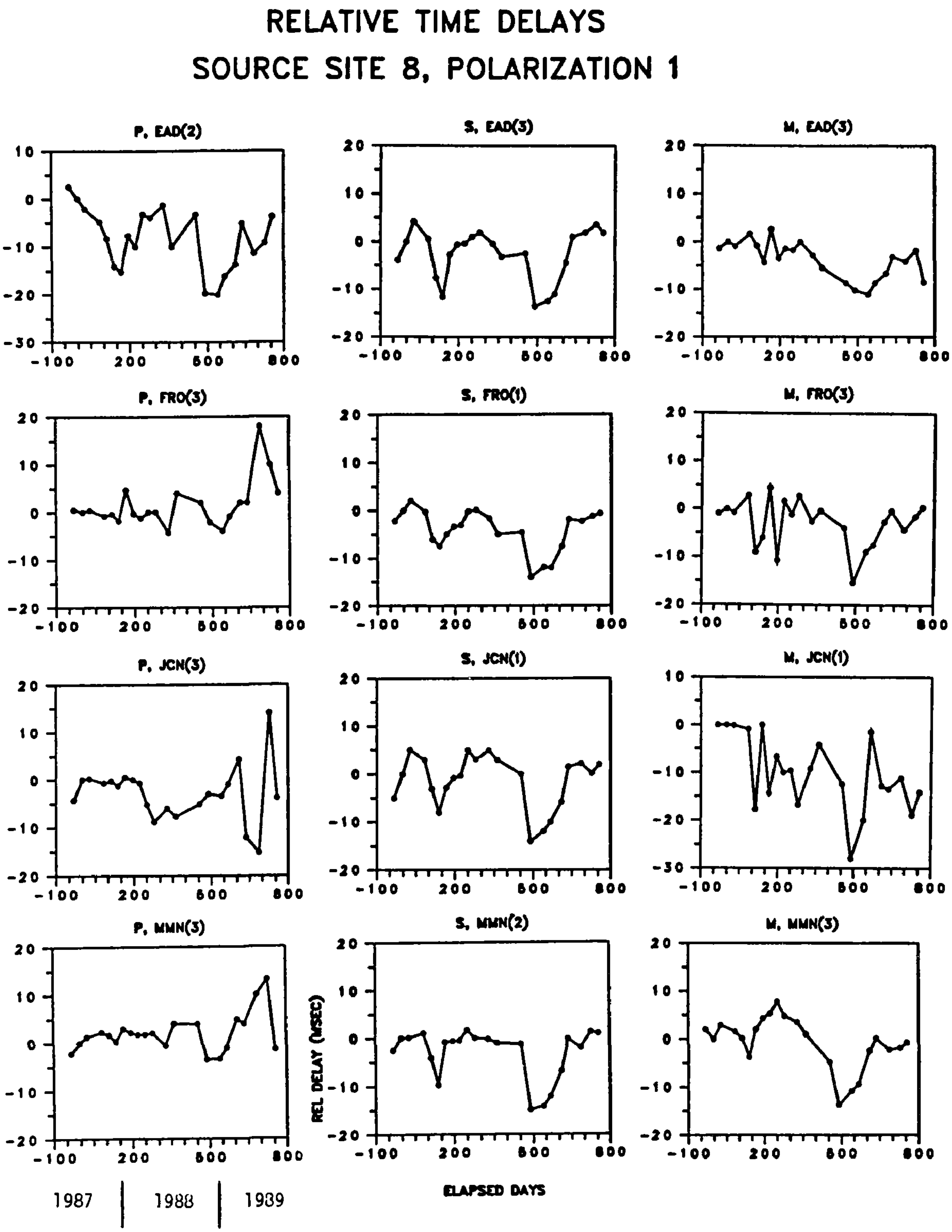

Figure 5. Travel-time variations at four receiver sites for direct P- and S-wave arrivals, and for an 8- to 10-sec event labeled "M". The data shown have a common source (vibrator site 8, Figure 1). Both axes are calibrated with respect to the chosen reference trace in the time gather, in this case, July, 1987.

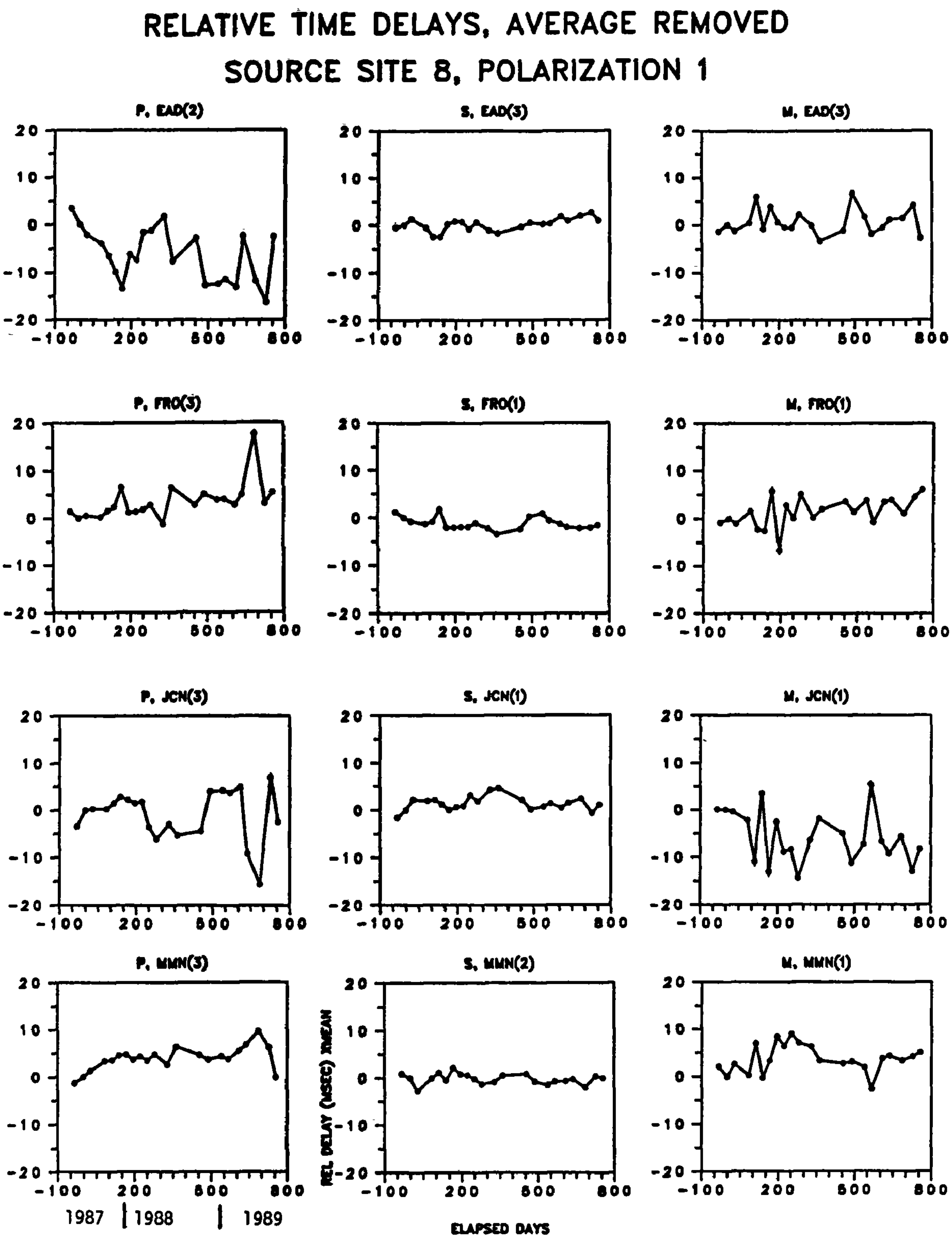

Figure 6. Time delays as in Figure 5. Estimated patterns of near-surface seasonal variations at the source have been removed.

EXPERIMENTAL TILT AND STRAIN INSTRUMENTATION

9960–01801

C.E. Mortensen
Branch of Tectonophysics
U.S. Geological Survey
345 Middlefield Road, MS/977
Menlo Park, California 94025
(415) 329–4856

Investigations

1. There are currently 135 Data Collection Platforms (DCP's) that transmit a variety of data through the GOES–6 spacecraft to the Direct Readout Ground Station (DRGS) in Menlo Park. Fifty–three of these DCPs transmit data at 10–minute intervals on an exclusively assigned random channel, which is being utilized under a special agreement with NESDIS. The remainder of the DCPs report at standard 3 or 4–hour intervals as assigned by NESDIS. This system transmits data from all types of low–frequency instruments including dilatometers, creepmeters, strainmeters, water–level meters, magnetometers, tiltmeters, and related measurements.

2. A system to backup the satellite telemetry system with non-volatile, solid–state memory and dialup or dedicated telephonic communications path has been developed. Included in this system is the capability to lock the DCP timing to a radio time standard. This feature will enable more efficient utilization of the assigned satellite bandwidth. This system is known as the Companion because of its interfacing role with satellite DCP's. The first five production models have been delivered and are currently being packaged and tested prior to field deployment.

3. A system has been developed that utilizes the emergency interrogate capability of GOES to switch the Sutron 8004 DCP to rapid reporting at random, frequent intervals. This adaptive random reporting is being interfaced with the Parkfield alert systems to test the feasibility of utilizing adaptive random reporting in earthquake prediction monitoring applications.

4. Networks of tiltmeters, creepmeters and shallow strainmeters have been maintained in various regions of interest in Califorina. A network of 14 tiltmeters located at seven sites monitor crustal deformation within the Long Valley caldera. Recently Roger Bilham of the University of Colorado and John Beavan of Lamont–Doherty installed a very long baseline tiltmeter in Long Valley. This project provided three DCP's to collect the data and return it to Menlo Park via GOES satellite. We also monitor the data received to keep track of deformation within the caldera, comparing results frequently with the USGS tiltmeter array. Other tiltmeters are located in the San Juan

Bautista and Parkfield regions. Creepmeters located along the Hayward, Calaveras and San Andreas faults between Berkeley and the Parkfield area are maintained in cooperation with the Fault Zone Tectonics project. A shallow strainmeter is located near Parkfield, while observatory type tiltmeters and strainmeters are sited at the Presidio Vault in San Francisco, and a tiltmeter is installed in the Byerly Seismographic Vault at Berkeley. Data from these instruments are telemetered to Menlo Park via the GOES satellite.

5. A system for remotely rezeroing and clamping a tiltmeter installed in a deep borehole is being developed, and two deep–borehole tiltmeters are being assembled.

6. A low–cost, short–haul digital telemetry system utilizing UHF radios, packet controllers and off–the–shelf digital data converters has been developed, tested, and is currently in use in Parkfield monitoring the tilt of monuments that support the reflectors that constitute the 2–color laser network. This system, components for which cost less than $1500 per site, automatically polls the remote sites and transfers the data to a computer file, calculating the mean and standard error in the process. The system, including the tiltmeters, can easily be removed and transported to other locations.

Analysis of Crustal Deformation Along the Southernmost Segment of the San Andreas Fault System, Imperial Valley, California: Implications for Earthquake Prediction

14-08-0001-G1679

R.E. Reilinger
Earth Resources Laboratory
Dept. of Earth, Atmospheric, and Planetary Sciences
Massachusetts Institute of Technology
Cambridge, Massachusetts 02142
(617) 253-7860

INVESTIGATIONS/RESULTS

This project involves using geodetic observations in conjunction with other geophysical and geological information to investigate contemporary tectonic processes along the southernmost segment of the San Andreas fault system. Our primary efforts during the present contract period include:

(1) Planning and carrying out (March 1989) a Global Positioning System survey in the Imperial Valley-Salton Trough region (Figure 1: with Caltech, and Lamont Doherty Geological Observatory).

(2) Initial reduction of the March 1989 static GPS observations using the Bernese software (Larsen/Reilinger).

(3) Initial reduction of the March 1989 kinematic GPS measurements and comparison with static observations on the same baselines (Jackson et al.).

(4) Investigation of the impact of Ionospheric disturbances on the March 1989 GPS measurements (Jackson et al.).

(5) Continuing analysis and interpretation of 1986 and 1988 GPS measurements in the Imperial Valley-Salton Trough with emphasis on regional strain accumulation and strain release associated with the 1987 Superstition Hills earthquakes (Larsen/Reilinger).

(6) Comparison of geodetic and geologic deformation in the Imperial Valley to investigate the age and average earthquake recurrence time on the Imperial-Brawley fault system (Larsen/Reilinger).

PUBLICATIONS

Jackson, M., R. Reilinger, K. Hudnut, L. Nel, B. Stephens, C. Quirion, and K. Mooyman, Preliminary results of a kinematic GPS survey across the Imperial fault, Imperial Valley, California, *EOS, Trans. Am. Geophys. Union*, submitted, 1989.

Jackson, M., R. Reilinger, M. Bevis, B. Perin, C. Rocken, B. Stephens, and H. Stowell, Impact of ionospheric effects on GPS campaigns in Southern California and the South Pacific, *EOS, Trans. Am. Geophys. Union*, submitted, 1989.

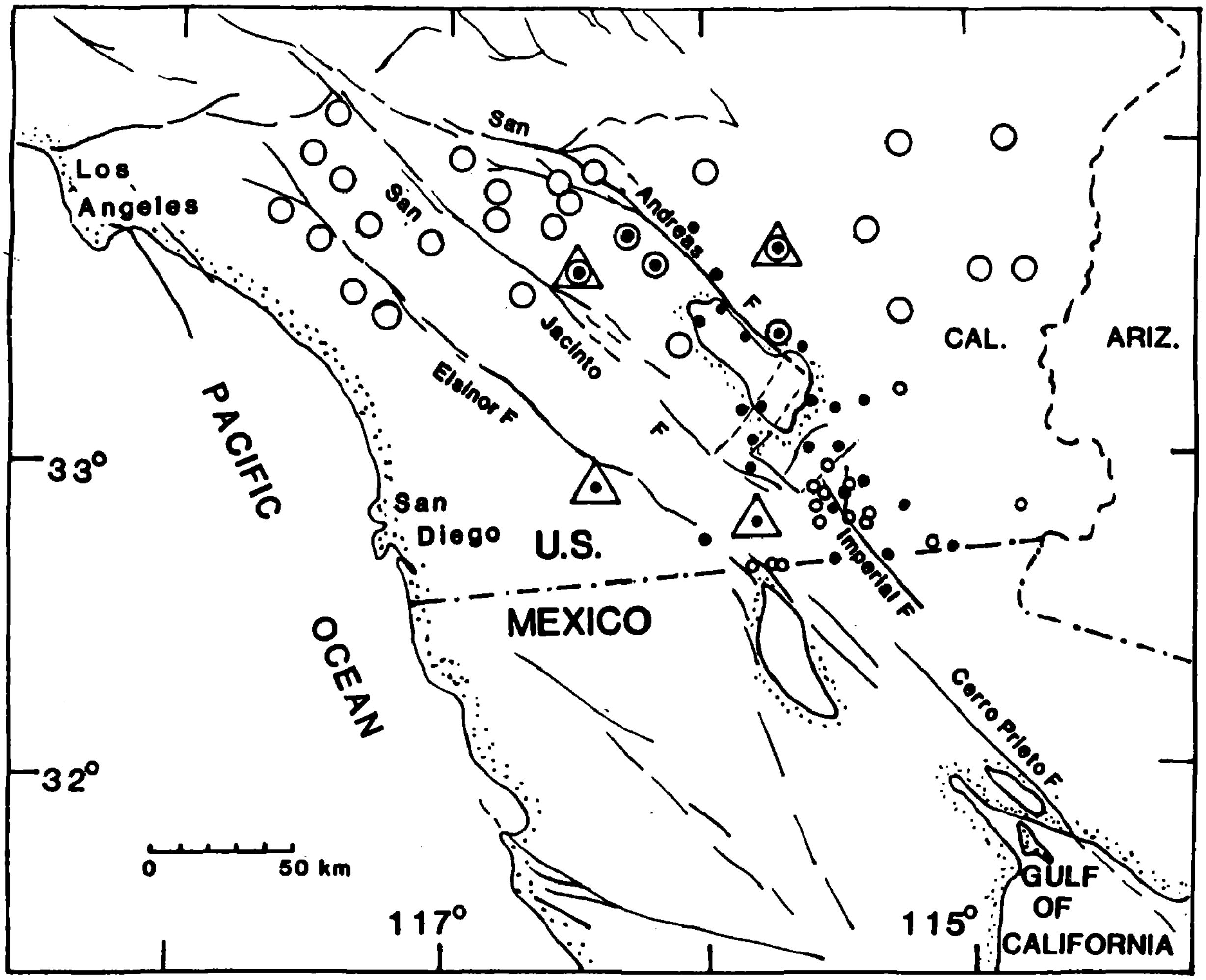

FIGURE 1. Map of the Imperial Valley-Salton Trough area showing major faults (including orthogonal, cross faults in the critical transition zone between the Imperial and San Andreas faults). Solid dots show GPS stations observed by our group during the March 1989 campaign. Small open circles are GPS stations observed in 1986 and 1988 which were not occupied this year. Large open circles are GPS stations established by Riverside County Flood Control District in March 1988. We established strong ties to this network and are cooperating with RCFCD on reduction of their 1988 observations (made with dual frequency TI receivers). Triangles show mobile VLBI sites occupied with GPS during the 1989 campaign.

MECHANICS OF FAULTING AND FRACTURING

9960-02112

Paul Segall
Branch of Tectonophysics
U.S. Geological Survey
345 Middlefield Road, MS/977
Menlo Park, California 94025
(415) 329–4861

Investigations

1. Study of the mechanics of earthquakes induced by artificially decreased pore-pressures.
2. Analysis of deformation and slip on the San Andreas Fault near Parkfield, California (with Mark V. Matthews).
3. Analysis of the deformation of Kilauea volcano and the 1975 M 7.2 Kalapana Earthquake (with Paul T. Delaney, HVO).

Results

1. Recent seismic studies have shown that earthquakes are occuring near oil and gas fields in Texas, Alberta, Canada, and at Lacq in southwestern France. Pore pressures in these fields have *declined* by several 10's of MPa. These earthquakes can not be explained by conventional models of induced seismicity, which require *increases* in pore pressure to destabilize faults. We have recently suggested (Segall, 1989, in press) that poro-elastic stresses resulting from production-generated decreases in pore pressure are responsible for earthquakes in these fields.

We have undertaken a collaborative study with J. R. Grasso (University of Grenoble) who is monitoring induced seismicity and deformation occurring above a major deep gas field at Lacq, in southwestern France. We have begun to aquire and assess the seismic, gas production, reservoir pressure, and repeated leveling data that are available for the Lacq field. This data should permit us to test the hypothesis that production-induced seismicity can be explained by poro-elastic stresses generated by fluid extraction.

2. A large component of the Parkfield prediction experiment involves collection of surface strain and displacement data in the vicinity of the 1966 rupture zone. We are investigating the idea of fitting "minimum norm" slip distributions to a given set of surface measurements. Ideally, the minimized norm has physical signifcance. It may, for instance, correspond to the elastic self-energy produced (conceptually) by back-slipping a fault from a nominal unstrained state. We continue to focus primarily on models for data collected by the two-color geodimeter at Parkfield. These models yield estimated slip distributions

by simultaneously inverting data measured on the entire two-color network. They provide explicitly for measurement error, seasonal variation, and local drift.

3. We have continued to examine misclosures in displacement solutions for the 1970, 1974 and 1976 EDM measurements on Kilauea in an attempt to quantify the measurement errors and weed out blunders. The 1974-6 epoch spans the M 7.2 Kalapana earthquake. Assuming the variance is $\sigma^2 = a^2 + b^2L^2$, where L is line length, we estimate a and b by maximum likliehood, extending the methods of *Segall and Matthews, J.G.R., 1988*. For the 1970-4 epoch $a \sim 5$ mm, and $b \sim 1 \times 10^{-6}$. The misclosures in the 1974-6 and 1976-82 data are larger, possibly due to unmodeled vertical deformation or rapid postseismic deformation during the 1976 survey. We have investigated the former possibility by extending the displacement calculations to include the effects of vertical motions. It appears that the vertical motions are significant in the line-length changes across the Halina Pali. Nevertheless there are still unusual changes that are unexplained, and may be due to blunders.

Reports

Segall, P., Earthquakes triggered by fluid extraction *Geology*, in press, 1989.

Segall, P., Earthquakes triggered by fluid extraction (abstract) *E.O.S.*, v. 709, p. 394, 1989.

Segall, P., and P.T. Delaney Horizontal deformation of Kilauea volcano, (abstract), I.A.V.C.E.I. General Assembly, Santa Fe, New Mexico June 25–July 1, 1989, p. 237, 1989.

Du, Yijun, A. Aydin, and P. Segall, Comparison of various inversion techniques applied to the 1983 Borah Peak earthquake, Fall AGU, 1989.

Martel, S.J., P. Segall, E.H. McKee, and B.D. Turrin, Late Cretaceous faulting in the Sierra Nevada Batholith, Fall AGU, 1989.

Low Frequency Data Network

Semi-Annual Report

S. Silverman, K. Breckenridge, J. Herriot
Branch of Tectonophysics
U. S. Geological Survey
Menlo Park, California 94025
415/329-4862
October 2, 1989

9960-01189

Investigations

[1] Real-time monitoring, analysis, and interpretation of strain, creep, magnetic, tilt and other low frequency data within the San Andreas fault system and other areas for the purpose of understanding and anticipating crustal deformation and failure.

[2] Enhancements to satellite-based telemetry system for reliable real-time reporting and archiving of crustal deformation data.

[3] Development and implementation of backup capablities for low frequency data collection systems.

[4] Specialized monitoring, including automated alerts, and display of data relevant to the Parkfield region.

Results

[1] Data from low frequency instruments in Southern and Central California have been collected and archived using the Low Frequency Data System. In the six months over over eight million measurements from over 100 satellite platforms have been received via satellite telemetry and subsequently archived by Low Frequency Network computers for analysis. The satellite telemetry system has been expanded to replace all instruments formerly monitored via telephone telemetry.

[2] The project has operated a configuration of an Integrated Solutions (ISI) V24S computer running under the UNIX operating system, with another ISI serving as data storgage backup. Data from the Network are available to investigators in real-time and software for data display and analysis is readily available. Tectonic events, such as creep along the fault, can be monitored while still in progress. Also, periodic reports are produced which display data collected from various groups of instrumentation.

[3] The project continues to use a five meter satellite receiver dish installed in Menlo Park for retrieval of real-time surface deformation data from California and South Pacific islands. The GOES geostationary satellite together with transmit and receive stations make possible a reliable realtime telemetry system. Further expansion of the number of platforms monitored is ongoing.

[4] The project continues to take an active part in the Parkfield Prediction activities. Software has been written to provide scientists with automated alerts for signals which may indicate anomolous tectonic activity. Kate Breckenridge is the associate monitor for Parkfield creep

events, which includes contact via paging system during periods of increased activity. Stan Silverman is the alternate monitor for Parkfield strainmeter data, which also includes contact via paging system for alerts. Also, data collection and computer operations are automatically monitored for abnormal activity and project members are paged for in the event of problems with either.

[5] The project has continued to provide real-time monitoring of designated suites of instruments in particular geographical areas. Terminals are dedicated to real-time color graphics displays of seismic data plotted in map view or low frequency data plotted as a time series. During periods of high seismicity these displays are particularly helpful in watching seismic trends. The system is used in an ongoing basis to monitor seismicity and crustral deformation in Central California and in special areas of interest.

Parkfield Area Tectonic Framework

9910-04101

John D. Sims
Branch of Engineering Seismology and Geology
U.S. Geological Survey
345 Middlefield Road, MS 977
Menlo Park, California 94025
(415) 329-5653

Investigations

1. Field investigations of structural and stratigraphic relationships between late Cenozoic sedimentary units and underlying Franciscan and granitic basement in central California with emphasis on the Parkfield-Cholame area.

2. Field investigations of late Holocene and historic slip rates in the Parkfield and Carrizo Plain segments of the San Andreas fault.

Results

1. Geologic mapping progressed and the Parkfield and Cholame 7½-minute quadrangles have been completed. The Parkfield Quadrangle is at Menlo-BTR and the Cholame Quadrangle is in the final stages of compilation. Work is progressing on the Stockdale Mountain 7½-minute quadrangle.

   These quadrangles along with those already publish delineate the complexitites of the San Andreas fault zone in the Parkfield segment. The San Andreas is shown to be composed of three segments that have been occupied as the "main" trace over the past 18-20 Ma.

2. A series of surveyed quadrilaterals have been established on the San Andreas, White Canyon, Red Hills, Gold Hill, and Gillis Canyon faults in the Parkfield-Cholame area—a total of 19 quadrilaterals. Fifteen quadrilaterals lie across the San Andreas, 2 on the White Canyon, and one each on the Red Hills and Gold Hill faults. These quadrilaterals are now being resurveyed every 2 months to gain background information on the sites prior to the next Parkfield earthquake.

3. We excavated 11 trenches (~330 m total length) in the summer of 1989 to examine offsets, search for evidence of individual events, and study the process of stream abandonment. The fault trace at the site is easily identified by geomorphic features. The site is characterized by a pair of offset modern streams, an older abandoned and infilled stream channel, and a pair of beheaded streams. Off-sets of the modern streams were measured by high precision surveys of their thalwegs. The thalweg of the SE larger stream is offset 17.4 ± 1.6 m, and the offset of the NW smaller stream is 15.8 ± 0.6 m. Excavations in the alluviated abandoned channel reveal that it is offset 101.9 ± 1.4 m from the smaller stream, its probable parent stream. Offset of the stream lengthened the channel without significantly altering its base level, and

aggradation proceeded. Filling of the channel occurred in four phases, the last ending just prior to establishment of the present pair of stream courses. One or two older abandoned and filled channels were revealed by the excavations NW of the younger abandoned channel.

The 1857 break varies from a single fracture with horizontal slickensides, to multiple vertical faults with gouge zones of 2 to 25 cm, to an indistinct zone of distributed shear up to 2 m-wide. Conjugate faults of the San Andreas fault have both normal and reverse sense and occur in groups which alternate in sense of movement along strike of the SAF. Deposits in the modern channels show evidence for 2 events; the 1857 and the penultimate event. Identification of events older than the penultimate event is uncertain. Detrital charcoal for C-14 dating is abundant in the sediments excavated; more than 320 samples were collected. All sedimentary units contained multiple charcoal samples and potentially can be dated. Radiocarbon analysis is now in progress.

Reports

Sims, J.D., 1989, Chronology of displ;acement on the San Andreas fault in central California: Evidence from reversed positions of exotic rock bodies near Parkfield, California: U.S. Geological Survey Open File Report 89-xxxx, 40 p.

Sims, J.D., Ito, Tanio, Hamilton, J.C., and Meier, D.B., in press, Late Holocene Record of Earthquakes and Slip on the San Andreas Fault in Excavations on the Carrizo Plain, Central California: American Geophysical Unioin, EOS, V. , P. -.

Semi-Annual Report XXIX

Modeling and Monitoring Crustal Deformation
9960–01488

Ross S. Stein & Wayne Thatcher
Office of Earthquakes, Volcanoes, and Engineering
U.S. Geological Survey
Branch of Tectonophysics
345 Middlefield Road, MS 977
Menlo Park, California 94025
415-329–4840
FTS 459–4840

Investigations

1. Study of the 4 August 1985 North Kettleman Hills Earthquake. Completed releveling in the epicentral region of the $M_L = 5.5, M_W = 6.1$ thrust event; relocated mainshock and aftershocks using 3–D velocity model and calculated error ellipsoids; determined focal plane solutions for foreshocks, mainshock, principal aftershocks. The objectives of the geodetic measurements are to deduce the fault geometry and slip, infer the relationship between the coseismic and long–term deformation, and to understand the relationship between this earthquake and the adjacent 1982 New Idria and 1985 Coalinga events to the north (Ross Stein, Göran Ekström, *Lamont-Doherty Geological Observatory*, Jerry P. Eaton, Donna Eberhart–Phillips).

2. Study of the recurrence characteristics of large interplate earthquakes and the influence of coseismic slip distribution on the mechanics of recurrence. Investigations include survey and synthesis of existing historical, seismological and paleoseismic information on earthquake recurrence. Geologic, geodetic and seismologic estimates of earthquake slip distribution are integrated with recurrence data wherever possible. Assessments of the precision and resolution of fault slip estimated by these different methods are needed both to evaluate the methods themselves and to judge the reliability of individual slip determinations.

Results

1. Broadband Seismic, Geodetic and structural analysis of the 4 August 1985 Kettleman Hills earthquake

The Kettleman Hills earthquake was depleted in higher frequency radiation, which led to a low local magnitude ($M_L = 5.5$) and small ground accelerations on local strong motion instruments. From long–period and broadband teleseismic data we determine a moment magnitude $M_W = 6.1$, and a source duration of 16 sec, 3-4 times the usual duration for an earthquake this size. Static deformation determined from a leveling network of 70 bench marks show a peak amplitude of 110 mm, and suggest a $M_W = 6.0$. Fault slip extended from the mainshock at the north end of Kettleman Hills North Dome, for 18 km to the south, which is 5 km from the south end of North Dome. Either a low angle thrust fault or a high angle reverse fault can satisfy the seismic and geodetic observations. A seismic reflection profile which runs across the anticline and is located over he main shock has been interpreted by Ann Meltzer (Ph.D. thesis, Rice University, 1989). The Mainshock and principal aftershocks appear concentrated at the leading edge of a 8–12 km deep low angle thrust fault, from which several high angle reverse faults emanate, and in the core of the anticline at shallower depths. The mainshock occurred 3 km east of the fold axis. Well–constrained focal mechanisms show compression on both low and high angle planes.

2. Rupture Sequence and Fault Geometry Beneath the 100–km–long New Idria–Coalinga–Kettleman–Lost Hills Segmented Fold Chain

During 1982–1985, a sequence of three $5.5 \leq M \leq 6.5$ earthquakes propagated from the north end to the center of a major fold axis bounding the eastern California Coast ranges, suggesting a 100–km–long active fault or group of faults underlies the folds. We have relocated the main shocks, their aftershocks, and the seismicity for the preceding 13 years using a 3–dimensional velocity model by D. Eberhart–Phillips; many of the 1st motion polarities were also timed by J.P. Eaton. All three main shocks are thrust or reverse faulting events which locate beneath or, at Kettleman Hills, lie several km east of the fold axis, at a depth of 7–12 km. The New Idria aftershocks align on a 60°-E dipping plane, suggesting that a high–angle reverse faulting event occurred there. At Coalinga and Kettleman Hills, the seismic and geodetic data do not permit discrimination of the fault surface from the nodal planes. Both the Coalinga and Kettleman folds uplifted during the earthquakes, indicative that at least part of the fold growth can be attributed to repeated earthquakes. The aftershock sequences show predominantly compressional mechanisms, with the shallowest events occurring within the cores of the folds. The aftershock zones abut or slightly overlap, and are separated by major offsets of the fold axes. Much of the background seismicity is concentrated at these echelon offsets in the fold axis, including a 1976 sequence that demarks the southern limit of the Coalinga rupture and the northern limit of the Kettleman Hill rupture. Identification of structural and seismic indices of fold discontinuities may be useful to deduce segment boundaries on blind thrust and reverse faults concealed by folds.

3. Patterns in Great Earthquake Recurrence on the San Andreas Fault and Their Implications.

The timing of prehistoric earthquakes on the Mojave segment of the southern San Andreas fault at Pallett Creek [*Sieh et al.*, *JGR*, **994**, 603, 1989] resembles that observed in the sequential rupture of individual circum–Pacific seismic gaps [*Thatcher, Nature*, in press, 1989]. In both cases, events are clustered in time and concentrated towards the end of the seismic cycle. Furthermore, the great California earthquakes of 1857 and 1906 were each preceded, in 1812 and 1838 respectively, by smaller events ($M \simeq$ 7-1/2) which occurred near the ends of the longer subsequent ruptures on fault segments that sustained the least amount of slip in 1857 and 1906. These patterns suggest that slip–deficient zones like the San Francisco Peninsula segment of the 1906 rupture and the Mojave segment of the 1857 earthquake are not filled early in the seismic cycle, as simple recurrence models would suggest. Instead, these zones are not expected to rupture until late in the current cycle of 300 to 400 year duration, implying a very low probability of $M < 7$ earthquakes on both of these segments during the next several decades. Although observations are too fragmentary to establish the mechanisms responsible for this behavior, the data are consistent with the notion that event timing is controlled by zones of concentrated high slip ('asperities') that lie outside the slip–deficient regions.

Reports published or submitted during this period (excluding abstracts):

Hauksson, E., and R.S. Stein, The 1987 Whittier Narrows earthquake: A metropolitan shock (Preface to Whittier Narrows earthquake Special Section), *J. Geophys. Res.*, 94, 9545–9547, 1989.

Lin, J., and R.S. Stein, Coseismic folding, earthquake recurrence, and the 1987 source mechanism at Whittier Narrows, Los Angeles Basin, California, in press *J. Geophys. Res.,* 94, 9614–9632, 1989.

Stein, R.S., C.T. Whalen, S.R. Holdahl, W.E. Strange and W. Thatcher, Reply to "Comment on 'Saugus–Palmdale, California, Field Test for Refraction Error in Historical Leveling Surveys,' by R.S. Stein, C.T. Whalen, S.R. Holdahl, W. Strange and W. Thatcher" and Comment on "Further Analysis of the 1981 Southern California Field Test for Leveling Refraction," by M.R. Craymer and P. Vaníček, *J. Geophys. Res.*, 94, 7673–7677, 1989.

Stein, R.S., Two hundred and fifty manuscripts before the mast: Reflections of an outbound editor (Editorial), *EOS*, 70, 729–731, 1989.

Thatcher, W., Tsunami wave seismology (News and Views Article), *Nature*, 340, 674–675, 1989.

Thatcher, W., Earthquake recurrence and risk assessment in circum–Pacific seismic gaps, *Nature* in press, 1989.

Thatcher, W., Order and diversity in the modes of Circum–Pacific earthquake recurrence, *J. Geophys. Res.*, submitted, 1989.

Thatcher, W., and M.G. Bonilla, Earthquake fault slip estimation from geologic, geodetic, and seismologic observations: implications for earthquake mechanics and fault segmentation, *U.S. Geol. Surv. Open–File Report* OFR 89–315, 386–399, 1989.

Northeast Striking Cross Faults, Detachments, Crustal Blocks and Strain Partitioning in Southern California: A Search for Changes in Seismicity and Focal Mechanisms Precursory to Major Earthquakes

USGS 14-08-0001-G-1688

Lynn R. Sykes and Leonardo Seeber
Lamont-Doherty Geological Observatory of Columbia University
Palisades, New York 10964

Objective:

For the past 5 years we have been studying the detailed distribution of earthquakes, focal mechanisms, rotations of small crustal blocks, N.E. striking cross-faults, the existence of shallow-angle detachment faults and premonitory changes before large earthquakes along the southern San Andreas and San Jacinto faults in southern California. Major emphasis has been given to the large tectonic knot centered near San Gorgonio Pass and to 2 recent earthquakes near the southern end of the Salton Sea. Little of the present seismic activity occurs on the major throughgoing faults themselves. Instead much of it is situated on secondary faults and detachments. Seismicity in the months before the 1986 North Palm Springs earthquake appears to be concentrated on a detachment fault that determined the lower limit of the rupture. Secondary cross-faults at the two ends of the rupture were active during the aftershock sequence. The purpose of this study is to use relocated hypocenters and single-event focal mechanisms to examine precursory changes in three regions near the San Jacinto and southern San Andreas faults that contain prominent cross-faults and detachment faults. One includes small earthquakes associated with a magnitude 6 event on a cross-fault near the southern end of the Salton Sea that was a short-term precursor to a larger event in 1987 on the Superstition Hills fault. A temporal sequencing of activity along NW and NE trending conjugate faults of the Brawley zone has been identified and is being examined in detail. Future changes in activity on the next cross fault to the north of the one that ruptured in 1987 could be a precursor to a larger event that would rupture the southern San Andreas. We have developed computer programs to automatically determine hundreds of focal mechanism solutions of high quality so as to examine in detail the hypothesis that the San Andreas is a weak fault.

Results:

Two large strike-slip ruptures 11.4 hours apart occurred on intersecting, nearly orthogonal, vertical faults during the November 1987 Superstition Hills earthquake sequence. This rupture was investigated in the paper "Cross-fault triggering in the November 1987 Superstition Hills Earthquake Sequence, Southern California" that was published in Geophysical Research Letters in February, 1989 by Hudnut, Seeber, and Pacheco. They show evidence that this sequence is the latest in a northwestward progression of earthquakes (1979, 1981, and 1987) rupturing a set of parallel left-lateral cross-faults that trend northeast between the Brawley seismic zone and the Superstition Hills fault. It is inferred that the observed northwestward progression of ruptures on cross-faults may continue. The next cross-fault expected to rupture intersects both the San Andreas fault and the San Jacinto fault zone. They hypothesize that slip on the cross fault decreased normal stress on the main fault and triggered main strand rupture after a delay that was caused by fluid diffusion.

The preprint "The interaction between secondary and master faults within the southern San Jacinto fault Zone, southern California" by Petersen, Seeber, Sykes, Nabelek, Hudnut and Armbruster shows evidence that a third of the moment radiated from the April 9, 1968 Borrego Mountain earthquake came from a subevent that occurred on a secondary fault. In addition, the April 28, 1969 Coyote Mountain earthquake may have occurred on a northeast cross-fault instead of along the mainstrand fault as was previously thought. They relocate seismicity (1981-1986) and identify a secondary fault (the Palm Wash fault) that is parallel to the mainstrand fault and appears to be activated by regional large earthquakes. Increased seismic activity in a location well off the master fault occurs in a three-month time window both subsequent and prior to activity on the master fault and may signal increased stress in the region.

An abstract "Stress orientation inferred from the kinematics of secondary faults within the San Andreas fault zone at Parkfield" by Seeber and Armbruster demonstrates the use of the focal mechanism program that automatically determines hundreds of mechanisms from the most well-constrained phase data. They show that near Parkfield almost half of the focal mechanisms have nodal planes that are not parallel to the San Andreas fault and are not ruptures on a master strand. They infer these ruptures to be on minor faults confined to the fault zone. If these faults are randomly oriented, their combined slip geometry define the direction of maximum compression on the San Andreas fault in the seismogenic depth range. The compression axis lies at about 55° with the San Andreas fault. This angle is consistent with friction laws derived from laboratory experiments.

Publications:

Bogen, N., and L. Seeber, Late Quaternary block rotation within the San Jacinto fault zone, southern California, submitted for publication, 1987.

Hudnut, K.W., L. Seeber, and J. Pacheco, Cross-fault triggering in the November 1987 Superstition Hills earthquake sequence, southern California, *Geophys. Res. Lett., 16*, 199-202, 1989.

Nicholson, C., L. Seeber, P. Williams, and L.R. Sykes, Seismicity and fault kinematics through the eastern Transverse Range, California: Block rotation, strike-slip faulting and shallow-angle thrusts, *J. Geophys. Res., 91*, 4891-4908, 1986.

Nicholson, C., L. Seeber, P.L. Williams, and L.R. Sykes, Seismic deformation along the southern San Andreas fault, California: Implications for conjugate slip and rotational block tectonics, *Tectonics, 5*, 629-649.

Pacheco, J., and J. Nabelek, Source mechanisms of three moderate southern California earthquakes of July 1986 (abstract), *EOS, Trans. AGU*, 67, 1091, 1986.

Petersen, M.D., L. Seeber, J. Nabelek, and K. Hudnut, The interaction between secondary and master faults within the southern San Jacinto fault zone, southern California, (abstract), submitted to *EOS, Trans. AGU*, 1989.

Seeber, L., and C. Nicholson, Block rotation along the San Andreas fault system in California: Long term structural signature and short term effects in the earthquake cycle, preprint, 1987.

Seeber, L., J.G. Armbruster, P. Williams, and L.R. Sykes, Faults antithetic to the San Andreas delineated by seismicity in the San Gorgonio Pass of southern California (abstract), *EOS, Trans. AGU, 67*, 1200 1986.

Seeber, L., J.G. Armbruster, M. Tuttle, Secondary faults associated with the 7 July, 1986 Palm Springs earthquake rupture on the San Andreas fault (abstract), *Seismol. Soc. Am. Abstracts with Programs*, pp. 20, 1987.

Seeber, L., and J.G. Armbruster, Secondary faults as agents for segmentation of the master strands in southern California (abstract), *IUGG Conference*, Vancouver, Canada, Aug. 17-22, 1987.

Seeber, L., and J.G. Armbruster, Stress orientation inferred from the kinematics of secondary faults within the San Andreas fault zone at Parkfield (abstract), *EOS, Trans, AGU, 69*, 1456, 1988.

Sykes, L.R., and L. Seeber, Great earthquakes and great asperities, San Andreas fault, southern California, *Geology, 113*, 835-838, 1985.

Williams, P., S. Fagerson, and K. Sieh, Triggered slip of the San Andreas fault after the July 8, 1986 North Palm Springs earthquake (abstract), *EOS, Trans. AGU, 67*, 1090, 1986.

Williams, P.L., L.R. Sykes, C. Nicholson, and L. Seeber, Seismicity and state of stress in the eastern Transverse Ranges: Implications of seismic potential of the southern San Andreas fault, California, submitted to *Tectonics*, 1989.

Nearfield Geodetic Investigations of Strain across Faults in Southern California

14-08-0001-G1690

Arthur G. Sylvester
Department of Geological Sciences, and
Marine Science Institute
University of California
Santa Barbara, California 93106
(805) 961-3156

Objectives: We have three objectives during the current funding period: 1) convert more of our existing leveling arrays into leveled alignment arrays by means of resurveys with a total station distance meter; 2) establish new, leveled alignment arrays across the southern end of the San Andreas fault and the northern half of the San Jacinto fault; and 3) locate and resurvey fault crossing arrays established in the 1960s by the U.S. Coast & Geodetic Survey and the California Division of Water Resources (CDWR).

The long-term, fixed purpose of this investigation is to search for and monitor the spatial and temporal nature of nearfield displacement across active and potentially active faults. Thus, we document pre-, co- and post-seismic displacement and aseismic creep, if any, especially where seismographic, paleoseismic and geomorphic evidence indicates current or recent fault activity. The geodetic arrays range in length from 300 m to 7000 m and are intermediate in scale, therefore, between the infrequent, regional geodetic surveys traditionally done by the National Geodetic Survey, and point measurements by continually recording instruments such as creepmeters, tiltmeters, and strainmeters. All leveling is done according to First Order, Class II standards, and horizontal surveys are done to First Order standards.

Results: We found and surveyed California Division of Water Resources bench marks in the following fault crossing arrays across the San Andreas fault: QUAIL, HUGHES, PALM, BARREL, and WRIGHT. Several bench marks have been obliterated in arrays QUAIL, HUGHES, and PALM. Sufficient bench marks exist in the HUGHES and PALM arrays to derive some indication of horizontal strain. All bench marks are present and in good condition at BARREL and WRIGHT, however, some of the lines of sight are blocked by the growth of large trees in the WRIGHT array. Preliminary comparison of our surveys with California Division of Mines & Geology surveys and with National Geodetic Survey results reveals little indication of horizontal strain during the last 15 years.

We learned that the California Division of Water Resources has continued annual resurveys of several of the arrays since the middle 1960s. The arrays they survey annually are COLT and RIALTO. They survey BARREL, PEAR, SANTA, and TEM every couple years. They have done parts of QUAIL and DEVIL on an infrequent basis. They have seen no appreciable changes in any of the arrays that can be related to tectonics. That is not surprising, because the arrays are across faults that have had no seismic activity in that time or that are known to creep.

The following leveling lines were releveled during the time period covered by this report: Cameron, Big Rock Springs, Una Lake, Mesa Valley, Caballo, Koehn Lake, Pallett Creek, Mina, McGee Creek, Kern Front, and all the arrays in the Parkfield area except the Gold Hill line across Cholame Valley. Interpretations of the results from two of the arrays, Cameron and Silver Canyon, are noteworthy. Cameron is a 738.5 m-long, L-shaped array consisting of 24 bench marks across the Garlock fault between Mojave and Tehachepi, almost coincident with the location of Caltech's alignment array. The array was surveyed in August 1986, July 1987 and in August 1989 (Fig. 1). Relative to the 1987 survey and to bench mark CM01, the east-west leg of the line south of the fault decreased in height about 1.5 mm. Although the height changes differ little from zero at the 1 sigma error level, the relative height change is consistent with the geomorphic, south-down sense of vertical displacement, and the displacement itself supports the Caltech observations of aseismic creep on that segment of the Garlock fault.

The Silver Canyon array (Fig. 2) contains 23 bench marks in an east-west line, 605 m-long, across the Owens Valley fault zone a few kilometers east of Laws. The line was established and surveyed in 1987, and has been resurveyed in 1988 and 1989. Bench marks east of the fault zone have risen nearly 3 mm in two years relative to bench mark SC01 at the west end of the line. The height change is consistent with the uplift of the White Mountains relative to Owens Valley. The fault zone has been the locus of small earthquakes since the 1986 Chalfant Valley earthquake (M 6.3) whose epicenter was about 10 km north of the leveling array. Thus, it cannot be established whether the observed displacement represents aseismic creep or strain release related to continuing aftershocks. In any event, the observed height changes are notable in that they represent one of the few observations of modern vertical displacement across faults in the Basin and Ranges. We intend to lengthen this array to characterize the displacement more carefully.

We releveled the array across the Hilton Creek fault in McGee Creek in mid-August. The line is 628 m-long with 29 bench marks, and it has been surveyed 11 times since it was established in July 1982. Data for the 1982, 1983, 1984 (two surveys), 1986, 1987, and 1989 surveys are plotted in Figure 3. Standard deviations of the surveys range from 0.02 mm to 0.5 mm; they are not plotted in Figure 1 to obviate clutter. Bench marks on the hanging wall (south of the fault), have risen and fallen simultaneously since 1982, but with a progressive upward increase to nearly 3 mm in 1989. Several earthquakes have occurred since the 1980 Mammoth Lakes earthquakes, and the observed displacement may represent the cumulative surficial strain release as a result of the earthquakes. The recent increase in earthquake activity in the Mammoth Lakes area has not noticeably affected the bench marks in McGee Creek The other noteworthy phenomenon in the leveling results is the subsidence of bench marks on the fault scarp relative to bench marks MC01 at the north end of the line on the hanging wall. The bench marks on the fault scarp are set only on small boulders, so we have previously interpreted this as the result of creep down the face of the fault scarp in response to annual free-thaw cycles. The other bench marks, being on much larger boulders set deeply in flat ground, are not affected by the downslope creep.

New Arrays: We established one new leveled alignment array and associated trilateration array. It was placed across the San Andreas fault near Littlerock where Dave Schwartz (USGS) conducted an extensive series of trench excavations. The leveled alignment array is 798 m-long with 19 permanent bench marks. The trilateration array consists of two doubly-braced quadrilaterals with an aperture from 100 to 200 m.

Grand Teton Project: The 22 km-long line across the Teton normal fault in Grand Teton National Park was resurveyed during the last few days of August and the first week of September. The line was established and first surveyed in August, 1988 in cooperation with the University of Utah and the National Park Service. The closure error for the 1989 survey is 12.25 mm, compared with 12.44 mm for the 1989 survey. The standard deviation in both surveys is 0.7 mm. Displacement across the fault from 1988 to 1989 was 8 mm, footwall down relative to the hanging wall.

Reports

Sylvester, A. G., 1989. Triggered vertical strain across active strike-slip faults in southern California. Abstracts Volume, 28th International Geological Congress, Washington, D. C., v. 3, 207-208.

Byrd, J. O. D., R. B. Smith, and A. G. Sylvester, 1989. Bench mark descriptions: 1st-order level line, Cascade Canyon to Deadman Bar, Grand Teton National Park, Wyoming. University of Wyoming - National Park Service Research Center Project 22. Department of Geology & Geophysics, 23 p.

Fig. 1. Height changes, CAMERON leveling array - 1986 to 1989.
Error bars - 1 sigma.

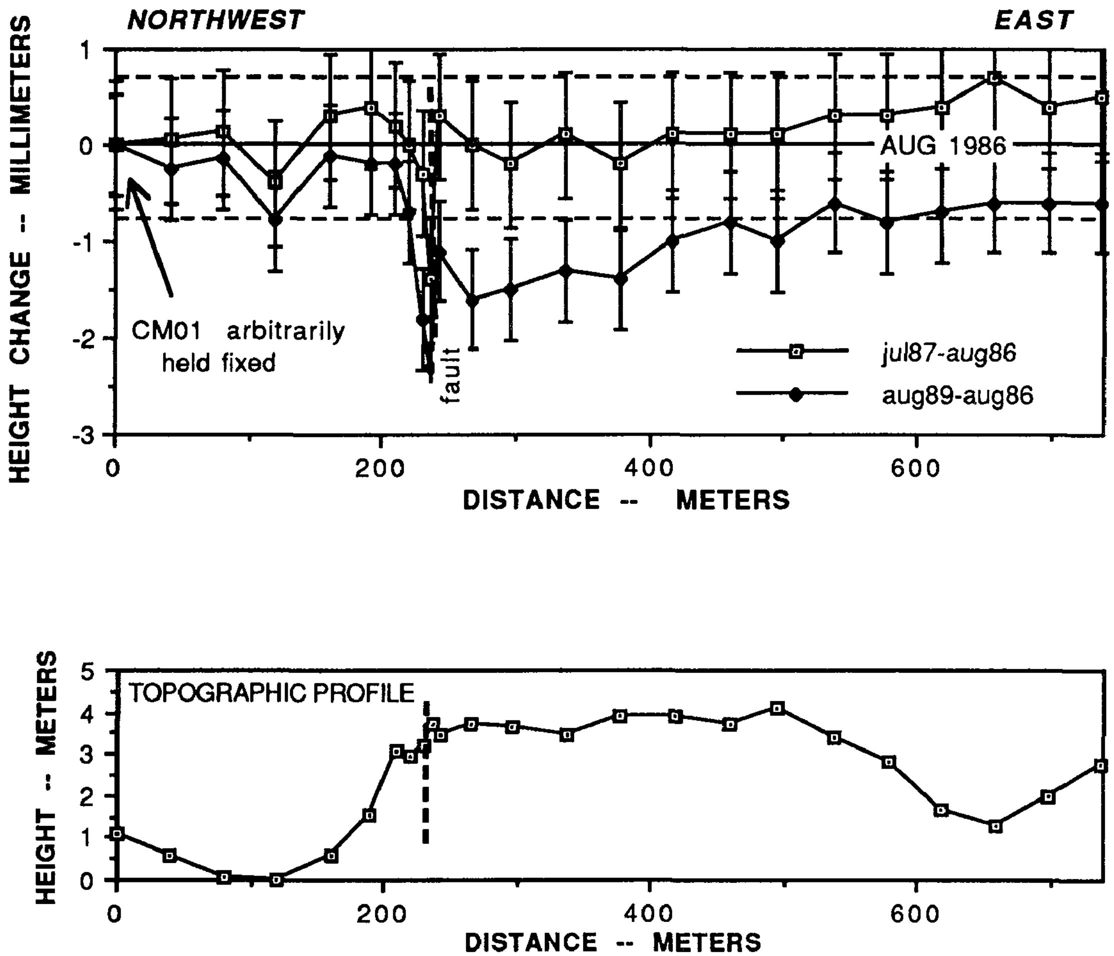

Fig. 2. Height changes, Silver Canyon leveling array - 1987 to 1989.
Error bars = 1 sigma.

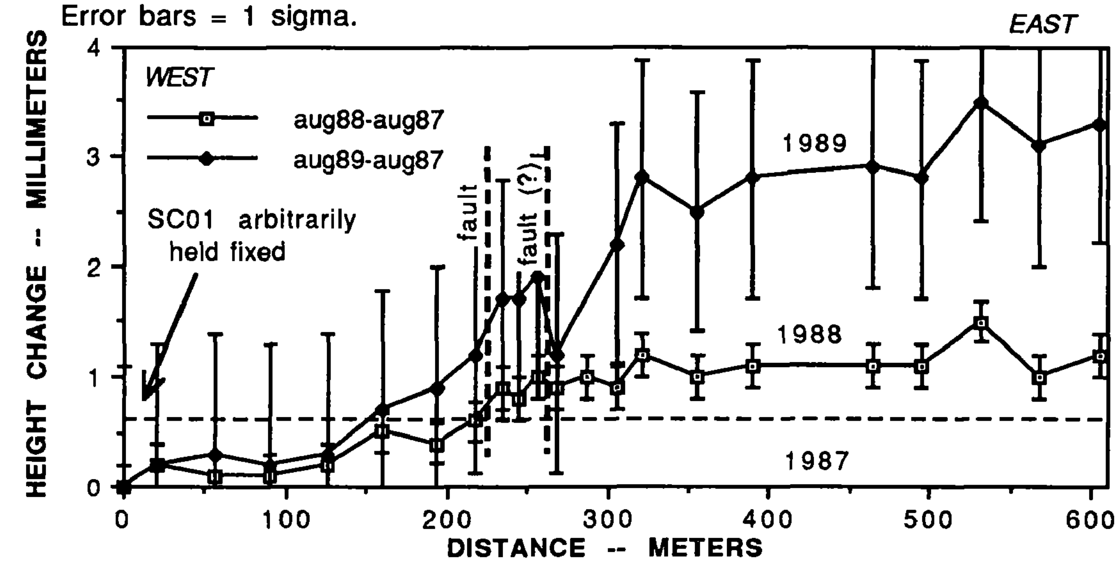

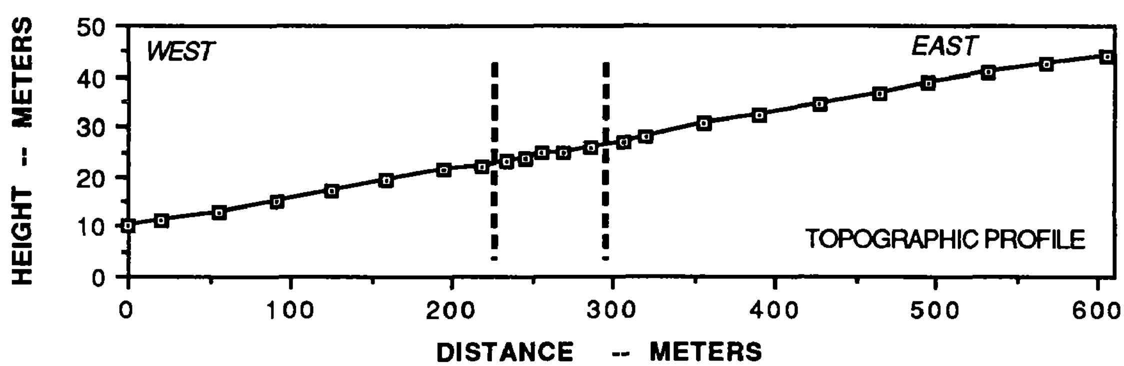

Fig. 3. Height changes, McGee Creek leveling array - 1982 to 1989.

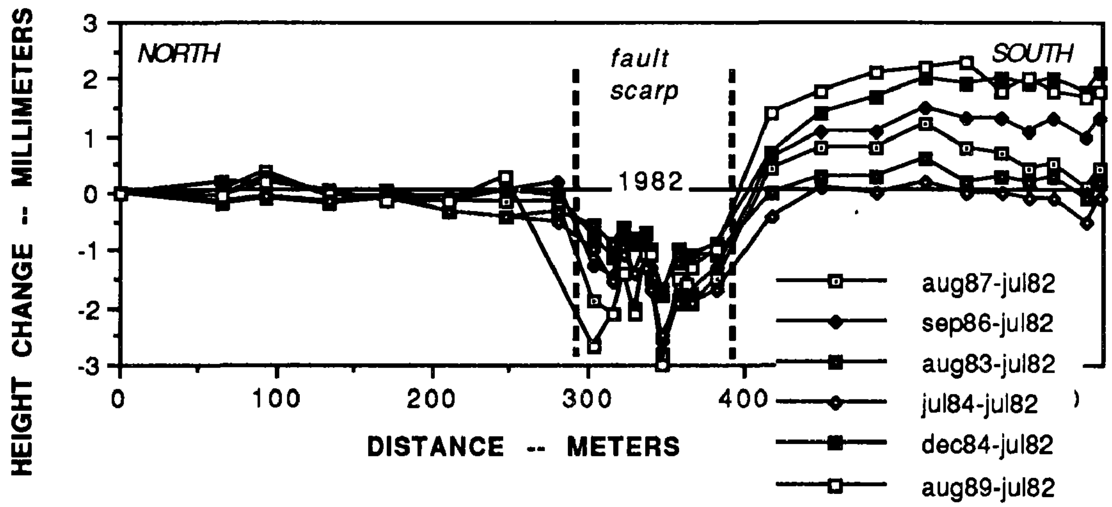

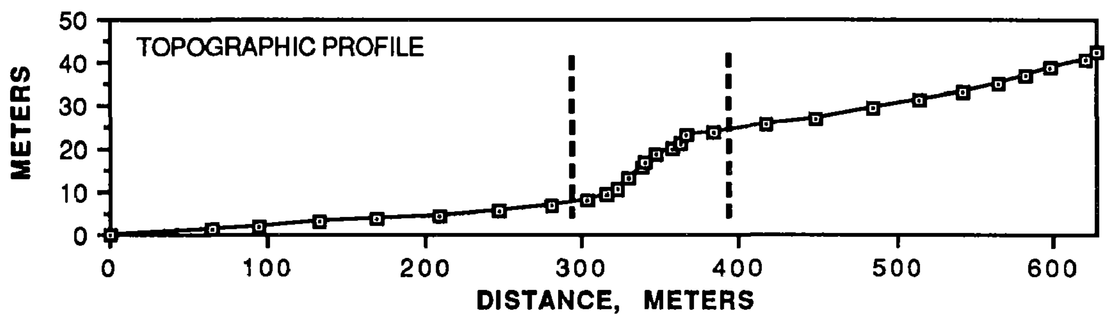

Piñon Flat Observatory: Cooperative Studies and Crustal Deformation Observatory Program

14-08-0001-G1197

Frank K. Wyatt, Duncan Carr Agnew,
and Hadley O. Johnson
Institute of Geophysics and Planetary Physics
Scripps Institution of Oceanography
University of California, San Diego
La Jolla, CA 92093
(619) 534-2411

This grant provides support for our collaborative studies with those investigators conducting research at Piñon Flat Observatory (PFO) under the auspices of the U.S. Geological Survey. In addition to collaboration, we also provide some direct assistance to the investigators in the form of (1) research and site-use coordination, (2) instrument operation and testing, (3) data logging, (4) preliminary data reduction, and, as results become available, (5) data analysis. The main purpose of this work is to evaluate instrumentation developed for the measurement of ground deformation, the idea being to simultaneously operate a number of continuously recording sensors, and small geodetic arrays, and thereby to identify the merits and limitations of the various techniques. Good progress has been made by evaluating the instruments in a common setting. Most of the studies currently underway are cooperative ones, with investigators forming their own associations for intercomparison of results.

Below we list the research groups sponsored by the USGS NEHRP who are currently active at the site, and with whom we are working. (For completeness this report includes some information from the Summary Report written earlier this year.)

Air Force Geophysics Laboratory (AFGL)

The borehole tiltmeters provided by the AFGL (partial sponsors of the overall cooperative program at PFO) continue to produce valuable data for comparison with the other nearby instruments. Last year we determined that the Arthur D. Little diamagnetic sensors used in these tiltmeters were troubled by aging of the sensors' incandescent bulbs. We replaced these with solid-state sources, with good results, and reinstalled one of these instruments at PFO in December 1988. The data since then has been quite good, though showing a relatively high secular drift. We intend to use the new results to test the surprising variability in the tidal tilts seen on the observatory's other tiltmeters (Wyatt *et al.* (1987), *EOS* **68**, 1247).

In the coming year we plan to add a second AFGL sensor at the site, in the 25-m-deep borehole that was previously monitored by an Askania borehole tiltmeter (discussed later). During its tenure, the Askania tiltmeter gave consistent results, even upon reinstallation at a different azimuthal orientation; we believe we know ground truth for this borehole, at least as recorded by an Askania tiltmeter. Discrepancies shown by the AFGL sensor will thus help us understand sources of error in borehole tilt measurements.

Carnegie Institution of Washington

This project involves recording data from three borehole volumetric strainmeters (CIA, CIB, and CIC). Two of these systems (CIB and CIC) are no longer operating, apparently because of cable-seal leakage at the instrument package which is cemented in place. From the beginning the data from all the sensors showed gradually slowing compression caused by curing of the cement around them. The initial compressional signal on CIA ended in late 1985, four years after installation, and was followed by expansion. The most obvious feature in recent times was an especially rapid expansion commencing in the fall of 1986, reversing abruptly to compression in early 1987, with (perhaps) a recovery to the earlier trend by 1988. Because of the other strain measuring systems at the site we know this 0.6 $\mu\varepsilon$ signal was not of broad extent. It is tempting to suggest that this event had some hydrologic cause, especially since the rapid expansion began just after the drilling of holes for some USGS seismometers, about 130 m away. However, the water-level data from the same borehole (which is open to within a few meters of the dilatometer) does not suggest any direct correlation between local pore-pressure and observed volumetric strain. The water level began falling before the dilatometer event began and reached an equilibrium level (despite disturbances from drilling and earthquakes) while it was still going on, remaining invariant during the 1987 swing in apparent strain. This stable record seems to rule out any simple diffusion of pore-pressure changes from the area of drilling as described by Kümpel (1988, *EOS*, **69**, 1193). A preliminary guess at explaining the strain record is that some external decrease in pressure around the time of the drilling diffused into the material around the dilatometer to cause an expansion. This external change must itself have diffused away over a longer time to cause the subsequent contraction, though a more gradual diffusion such as this would not explain the abrupt reversal seen in the strain data.

Joint Institute for Laboratory Astrophysics

Two ~30-m-deep borehole tiltmeters run by Dr. Judah Levine (in boreholes BOA and BOB) functioned well from their installation in early 1986, until November 1987, when a nearby lightning strike destroyed the electronics in these instruments (and all other electronics in the area). Two new sensors were reinstalled in the late spring of 1988, with one of these needing further replacement in the spring of this year (1989). As mentioned above, the data from these installations and the Askania tiltmeter show a surprising variability in their earth-tide response, and this is the subject of ongoing investigations. The earth tides, being roughly the same amplitude as the anticipated annual crustal tilt signal near a fault zone, but of relatively short period, are an important "calibration" signal.

In an attempt to understand better the reduction in borehole tilt noise with depth (ref: Wyatt *et al.* (1988), *JGR*, **93**, 9197-9201), a 120-m-deep fully cased hole, was prepared last year for a third JILA tiltmeter. Owing to a lack of funding, installation of an instrument in this hole was not completed until this summer.

Lamont-Doherty Geological Observatory

Dr. John Beavan's 535-m Michelson-Gale water-tube tiltmeter has produced excellent data since its refurbishment late in 1987. The secular tilt rate from this instrument seems now to be quite similar to the rate (0.10 μrad/yr down to the west) measured by the parallel UCSD long-base tiltmeter, and a detailed intercomparison is planned for next year.

Schiltach Observatory

This project involves deployment and evaluation of an Askania tiltmeter, loaned to us by Dr. Walter Zürn of the University of Karlsruhe. The sensor was first operated in a 25 m deep hole (borehole KUA). The instrument was installed on 1985:346 (only two weeks after cementing in the casing) and produced high-quality records until its failure from the lightning strike mentioned previously. With advice from Dr. Zürn we were able to dismantle, repair, and reinstall this instrument; it was put back into borehole KUA in the summer of last year (1988). This summer we removed the instrument for more work on its electronics after we observed a systematic change in its gain over the course of a year. This particular instrument is an early model, without active feedback electronics, so any instability in the electronics can easily translate to a gain change.

In parallel with this lab work we are completing work on a 120-m-deep borehole for this sensor; precise gyroscopic alignment in the hole has proven far more difficult than we originally imagined. Work in this fully cased borehole (called KUB) has been complicated by the need to deal with the rain of metal scale showering the borehole bottom; this scaling is caused by the instrument support wires scraping against the casing as equipment is raised and lowered.

University of California, Santa Barbara

This precise geodetic leveling project at PFO is part of the broader program of surveying conducted by Dr. Arthur Sylvester in southern and central California. The full quadrilateral of UCSB marks at PFO is surveyed at least yearly, tying in to most all the other long-baseline tiltmeter and geodetic experiments underway. During the latest occupations, the UCSB survey team has included repeated surveys of the new class A "bench mark farm" established by the NGS. We hope that long-term monitoring of these closely spaced monuments will help us to better understand the stability of this style of deeply anchored (9 m) reference mark.

University of California, San Diego

The original long-baseline tiltmeter that we operate at PFO has continued to operate well. A large (and disturbingly long-lasting) artifact was produced when a 115-m extension tube was added to this instrument late in 1986. This extension contained fluid of a slightly different density and the very slow mixing of these two fluids caused a "transient" tilt of nearly a year's duration. This year, under a two-year grant, we are completing the installation of a North-South long-base tiltmeter at PFO. This instrument is roughly perpendicular to the first one and shares an end-vault with the EW instrument. This grant is intended to support the completion of our long-baseline tiltmeter development and to continue our work on end-monument anchoring using optical fiber. Data from these orthogonal sensors will be most useful in evaluating other measurements made at or near PFO.

University of Queensland

The University of Queensland three-component borehole strainmeter, has continued to run with virtually no maintenance (except for occasional back-up battery changes). This instrument, designed by Dr. Michael Gladwin, and installed at a depth of 151 m is capable of measuring shear as well as areal strain, and so is largely immune to the effects of grout curing which control much of the long-period dilatometer record. Gladwin (1987, *USGS Open File Report 88-16*, 345-351) has presented the secular records from this instrument, and pointed out a surprising change in strain rate seen on it at the time of the North Palm Springs earthquake. Prior to this shock the rate of NS tensor shear strain (e_{12}, 1-axis east) was a large 0.6 $\mu\varepsilon$/yr, but after this earthquake it fell to less than 0.1 $\mu\varepsilon$/yr, a value more in keeping with local geodetic results. Surprisingly, during this same time period the areal strain e_A maintained a steady rate of -1.5 $\mu\varepsilon$/yr, indicating no gross change in the net compressional strain impressed upon the instrument by grout curing. We are studying this interesting change in response by comparing the data from this instrument with the laser strainmeter records from PFO and also with the geodetic measurements made over the site (see below).

U.S. Geological Survey – Crustal Deformation

Over the past few years several precise geodetic surveys have been made in the area around PFO. The longest-running of these is the Pinyon single-color Geodolite network, part of the larger Anza net, surveyed by the USGS Crustal Strain group of Drs. W. H. Prescott and J. C. Savage. This network (observed since 1973) serves as the low-frequency constraint on our continuous measurements, and shows that in one direction (EW) the strains over PFO are nearly equal to those occurring over the fault traces of the nearby San Jacinto and San Andreas Fault systems.

In 1986, Dr. J. Langbein set up a 2-color geodimeter network which extends across Pinyon Flat and is surveyed quarterly. This array spans 4-km distances, and so is intermediate in length scale to the 20-km lengths of the Geodolite network, and the ~500-m-long lines of the observatory instruments. As more surveys have been done, results from this 2-color network appear to be converging onto the long-running Geodolite values.

Also in 1986, Dr. R. Stein established a 14-km-long, reference-calibration leveling line (with a loop going through PFO) which is surveyed annually by an NGS crew. Results from this should prove valuable in interpreting the tilt observations made at PFO, though it will take several years for the leveling data to detect and constrain the near-fault tilt rates measured at the observatory.

Structure and Mechanics of Geometrical Barriers

14-08-0001-G1714

Ronald L. Bruhn
Dept. of Geology and Geophysics
University of Utah
Salt Lake City, Ut. 84112

Objective: This project is focussing on the geometrical properties of fault zones and how these properties affect rupture propagation during earthquakes. Jogs, bends and cross-fault intersections are observed sites of rupture initiation and arrest in some earthquakes, but not in others (Knuepfer, 1989). A major obstacle to applying seismic and paleoseismic data in hazards estimation is simply predicting how a specific type of fault structure will affect rupture propagation, and whether or not this effect will be consistent from one earthquake to the next. In order to investigate this problem we are studying the geometry, fluid transport characteristics and seismicity of fault structures in extensional and transtensional fault zones. Here we present preliminary results of a new structural study of the Lost River fault zone in Idaho, the site of the 1983 Borah Peak earthquake.

Lost River Fault Zone, Idaho: The 1983 Borah Peak, Idaho earthquake occurred in two segments of the Lost River fault zone (Crone et al., 1987). The earthquake was Ms = 7.3 and displacement was normal-oblique with a left-lateral component. Our previous work focussed on the southern end of the Thousand Springs segment, where the earthquake initiated (Susong et al., in press). During August, 1989 we studied the structure of surface scarps in the northern end of the Thousand Springs segment, where the earthquake rupture branched onto a west-northwest trending fault in the Willow Creek Hills, and we also studied the surface scarps in the Warm Spring segment, to the north (Fig. 1). Here we present a preliminary analysis of the data collected from the region of fault branching at the north end of the Thousand Springs segment.

Procedure: The trace of surface scarps along regions of irregular topography reflect the orientation of the fault plane in bedrock, even though the scarps are in unconsolidated materials. Fault scarps were surveyed with an optical rangefinder or tape, inclinometer and compass at intervals between 10m and 30m. The survey data were converted to cartesian coordinates and viewed in a three-dimensional graphics program that allows one to rotate the three cartesian axes and survey points through any desired angle. The survey data were rotated until approximately planar sections of the fault trace were identified, and the strike and dip of the planar sections were recorded. We took care to eliminate points associated with landsliding. At each survey point the scarps dipped at angles between 60° and 90° in the unconsolidated material, but estimates of fault dip determined from the three-dimensional properties of the survey points are usually between 25° and 50°. Two surveys are discussed here; one from the northern end of the Thousand Springs segment, and another from the southeastern part of the Willow Creek Hills (Fig. 1). This region is important because it was a branch point in surface faulting during the Borah Peak earthquake, and it is located near the end of the Thousand Springs segment.

Results: The northern end of the Thousand Springs segment forms an approximately planar surface that strikes 337° and dips 40° southwest (Fig. 2B). However, there is a large bump in the the fault plane (Fig. 2A, circles) that appears in the cross section view (Fig. 2B). The characteristics of this bump are best observed on a down-dip view of the fault plane, where a planar surface forms a straight line (Fig. 3, crosses). The bump is about 600 m long and about 80 m high. This bump is located adjacent to the region of complex surface cracking and faulting in the hanging wall, where rupture branching occurred during the Borah Peak earthquake (Fig. 1, dotted area).

The fault branch in the southeastern Willow Creek Hills is a complex, curviplanar surface. The fault plane decreases in dip from east to west, dipping on average about 42° south in the eastern part of the scarp (Fig. 4, crosses), but decreasing to about 26° south dip in the western part (Fig. 4, boxes). The western part of the scarp is complex, however, in that the topographically highest survey points occur on a steeply dipping, curviplanar surface that merges into the 26° dipping fault plane (Fig. 5, circles). The structure of the western part of the scarp is interpreted as a scoop, or "dust-pan shaped surface (Fig. 5C).

Implications: The bump in the Thousand Springs segment may be part of a structure, or one of a group of structures, that controlled the point of rupture branching and perhaps the termination of surface faulting on the Thousand Springs segment during the Borah Peak earthquake. There are several alternative ways to interpret the structural properties of the bump. 1) The bump may be the top of a much larger structure or "asperity" within the fault zone. 2) The bump may be one of several such bumps buried at depth within the fault zone. 3) The bump may reflect the maximum dimensions of a single structure or be the bottom part of a single structure that has been almost totally exhumed and removed by erosion during uplift of the footwall. In this latter case, the bump would occupy only a small part of the fault zone within the region of rupture branching and termination. The complex and discontinuous surface cracking and faulting in the hanging wall adjacent to the exposed bump may indicate that interpretation #1 or #2 should be preferred. The fault branch in the southeastern Willow Creek hills is twisted and forms a gently dipping fault surface near its western termination. We do not know if this near surface structure is representative of the fault plane at depth, or if it represents the complex tip of a much larger and deeper fault that has only partly propagated to the surface. We are incorporating work on the aftershock distributions of the Borah Peak earthquake to help in the interpretation of these newly discovered structural characteristics of faulting.

Notes: Field work done by R.L. Bruhn, Yang Zhu-en, Wu Daning, and W.A. Yonkee. Yang and Wu's participation was funded by a joint NSF-People's Republic of China research program in which Bruhn and Yang are Principal Investigators.

References

Crone, A.J., M.N. Machette, M.G. Bonilla, J.J. Lienkaemper, K.L. Pierce, W.E. Scott, and R.C. Bucknam (1987). Surface faulting accompanying the Borah Peak earthquake and segmentation of the Lost River fault, central Idaho, *Bull. Seism. Soc. Am.*, **77**, p. 739-770.

Knuepfer, P.L.K. (1989). Implications of the characteristics of end-points of historcal surface fault ruptures for the nature of fault segmentation, USGS Open-File Report **89-315** "Fault segmentation and controls of rupture initiation and termination", p. 193-229.

Susong, D.D., S.U. Janecke, and R.L. Bruhn (in press). Structure of a fault segment boundary in the Lost River fault zone, Idaho and possible effect on the 1983 Borah Peak earthquake rupture, *Bull. Seism. Soc. Am.*

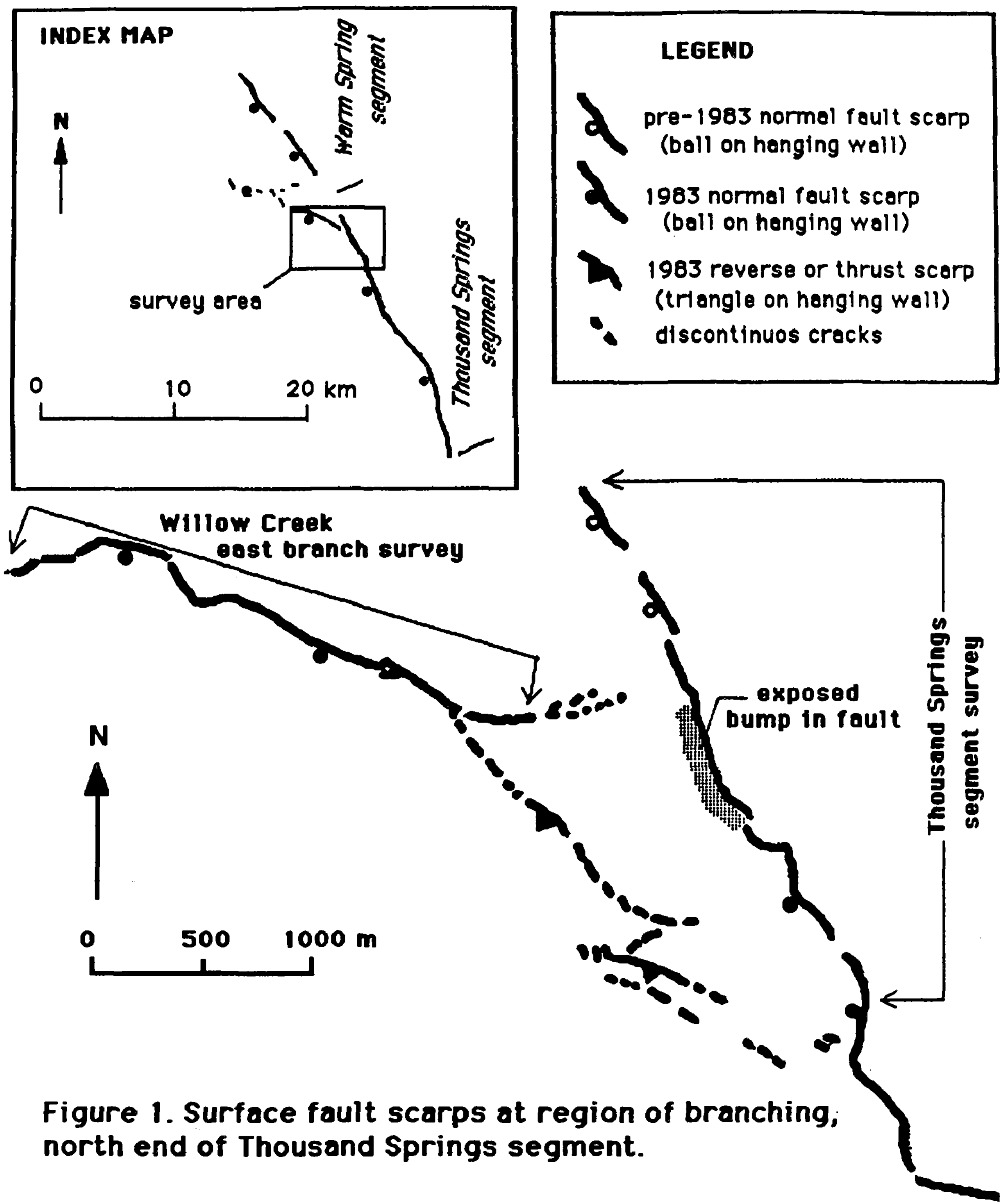

Figure 1. Surface fault scarps at region of branching, north end of Thousand Springs segment.

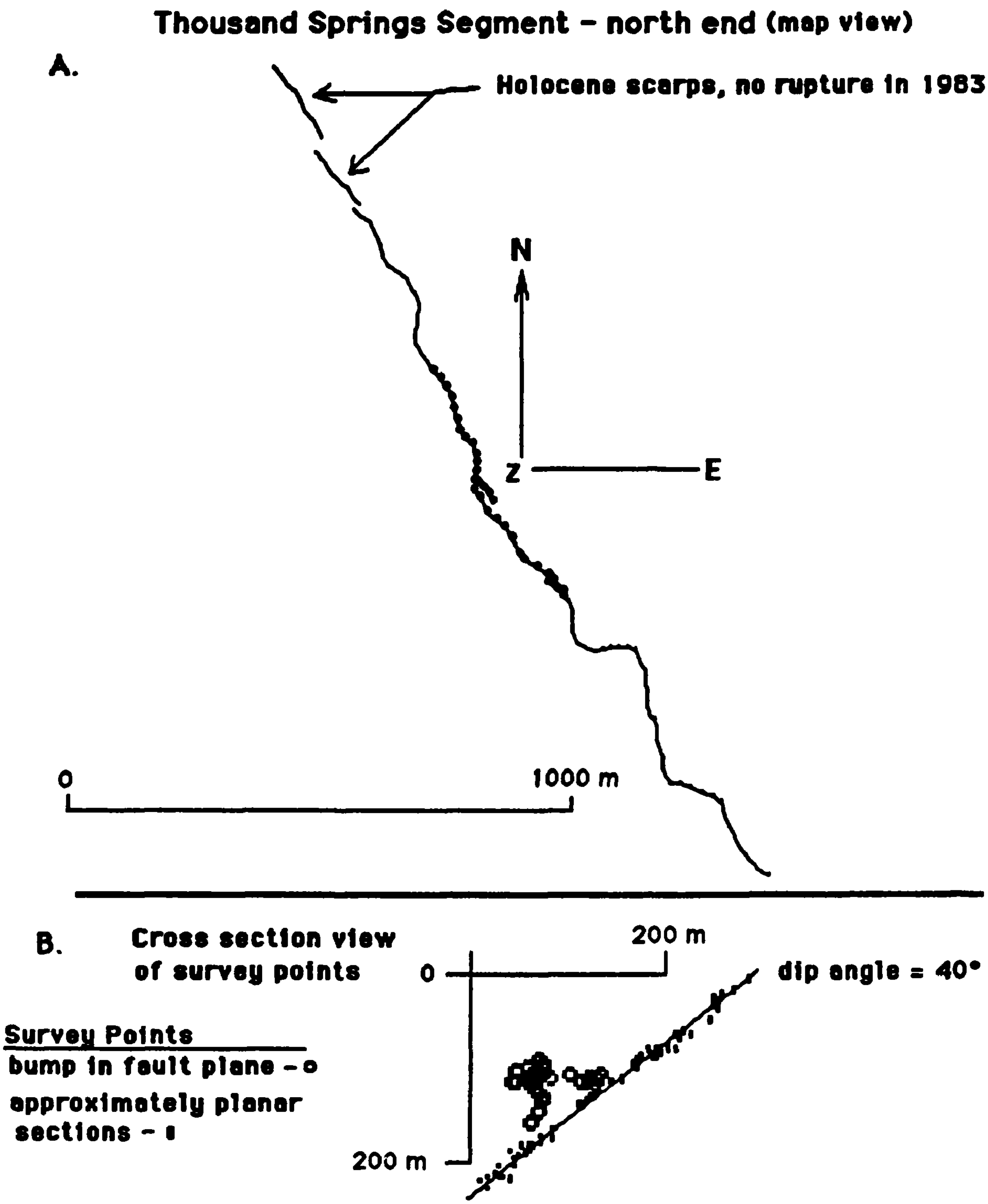

Figure 2.Thousand Springs segment survey and cross section.

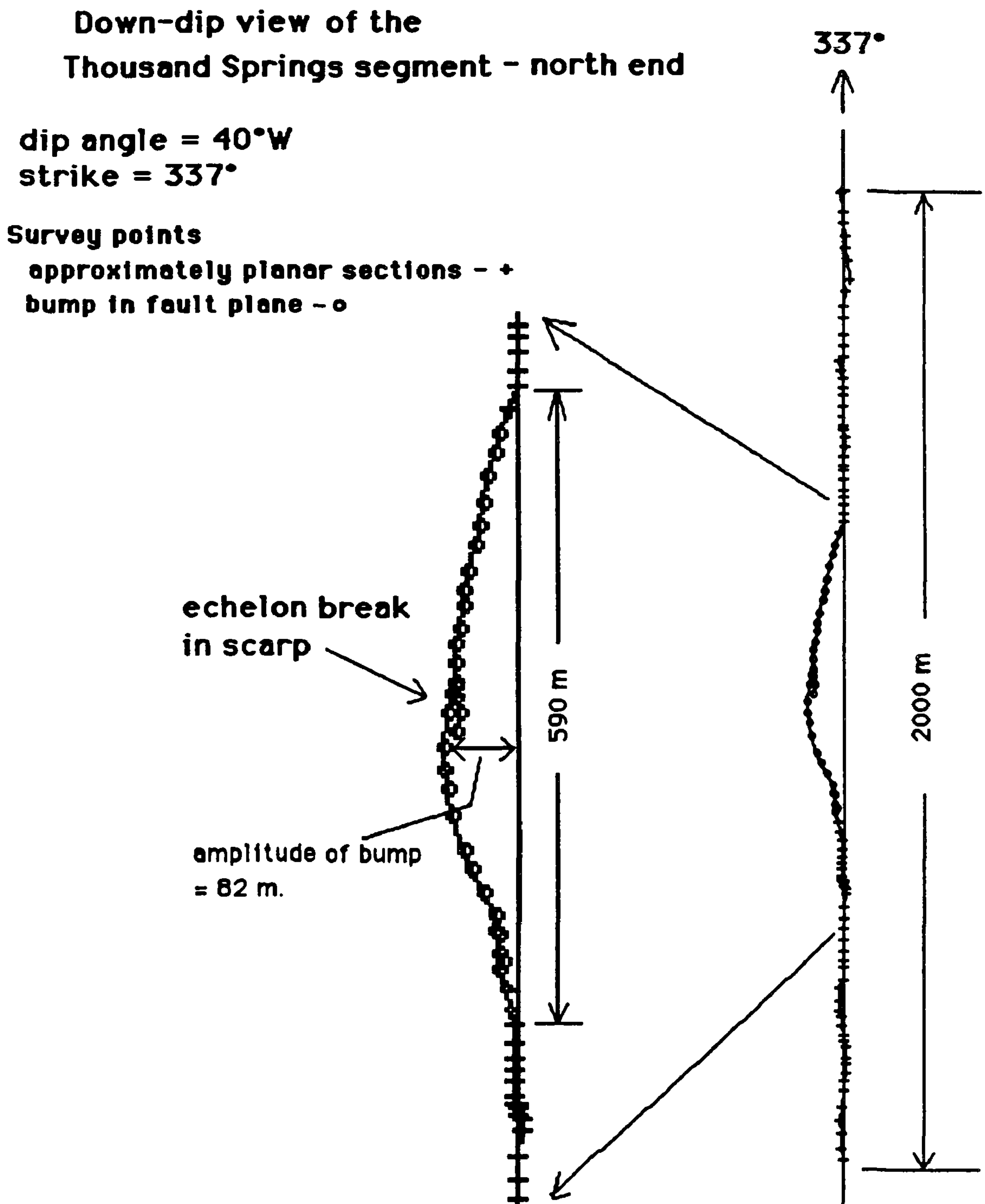

Figure 3. Down-dip view of Thousand Springs segment.

Figure 4. Willow Creek Hills Scarp - east branch

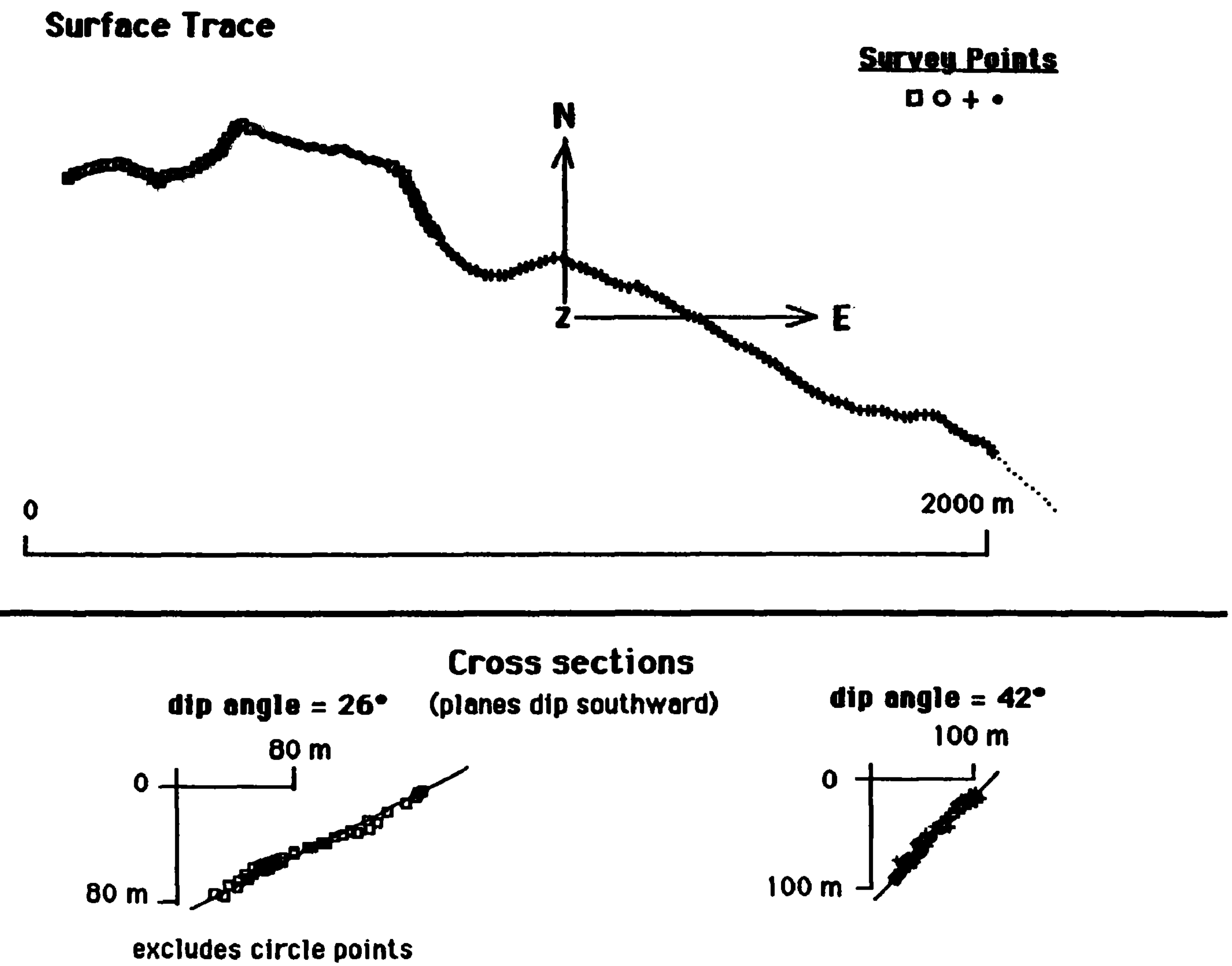

Figure 5. Willow Creek Hills Scarp - east branch (details of west end of rupture)

A. Cross section view - survey points at west end of rupture

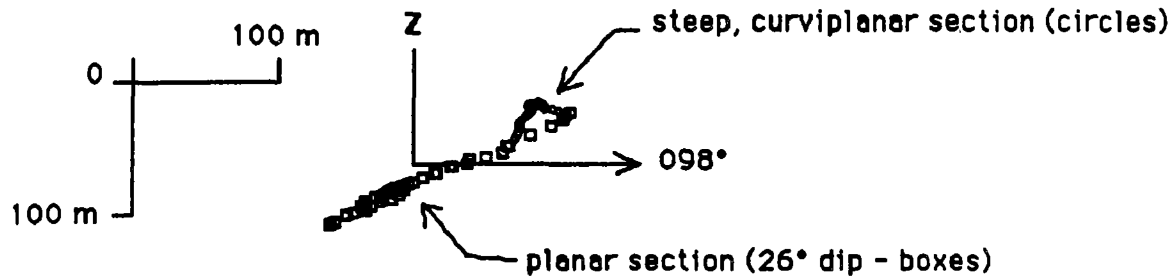

B. Survey points at west end of ruputure (perspective view)

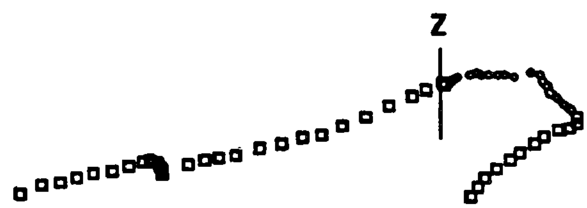

C. Interpretation of fault structure - west end of segment

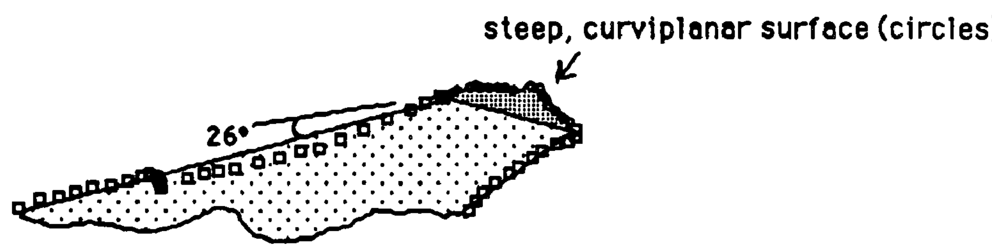

ROCK MECHANICS

9960–01179

James Byerlee
U.S. Geological Survey
Branch of Tectonophysics
345 Middlefield Road, MS/977
Menlo Park, California 94025
(415) 329–4841

Investigations

Laboratory experiments are being carried out to study the physical properties of rocks at elevated confining pressures, pore pressure and temperature. The goal is to obtain data that will help us to determine what causes earthquakes and whether we can predict or control them.

Results

Maps of recently active breaks along the San Andreas fault from Point Arena to Cajon Pass, California have been examined to compare the geometry of the fault zone in the creeping and locked parts. The fault was subdivided into 52 geometrically defined segments of uniform average trend, which were then grouped along strike into straight and curved sections. One of the straight sections is the creeping section between San Juan Bautista and Cholame in central California; the rest of the sections are locked. Many of the gross geometric characteristics of the individual segment, such as length, width, and stepover size, reflect their position in either a straight or curved section. The characteristics of the straight sections are those of a mature fault, whereas those of the curved sections are suggestive of youthful faulting, which is consistent with the tectonic interpretations of the curved sections.

The one section showing fault creep differs from all of the locked sections, in that (1) the recent breaks with a more westerly trend than the local strike of the fault zone predominate over those with a more northerly trend in the creeping section, whereas the opposite relationship holds in the locked sections; and (2) the more northerly traces make higher angles to the average trend in the locked sections than in the creeping section. Except for the abundance of westerly breaks in the creeping section, the fault patterns in the locked and creeping sections are consistent with the secondary shear patterns that develop in laboratory samples of fault gouge during frictional sliding experiments. An explanation that encompasses both the laboratory and field patterns and that also incorporates the sliding behavior has not yet been found; however, if the distinctive faulting characteristics of the creeping section can eventually be related to its sliding behavior, then those characteristics could be of use as indicators of seismic potential.

Reports

Moore, D.E., and Byerlee, J., 1989, Geometry of recently active breaks along the San Andreas fault, California, *U.S. Geological Survey* open file report 89-347, 72 p.

Moore, D.E., and Byerlee, J., 1989, Variations in fault zone geometry along the San Andreas fault, California, *Geol. Soc. Am.*, abstracts with programs v. 21.

Moore, D.E., Summers, R., and Byerlee, J., 1989, Location of deformation during stick–slip and stable sliding in granite, *Am. Geophys. Trans.* (EOS) v. 70.

Morrow, C., and Byerlee, J., (in press), Experimental studies of compaction and dilatancy during frictional sliding on faults containing gouge, *J. Structural Geol.*

Morrow, C., and Byerlee, J. (in press), Permeability of core samples from Cajon Pass scientific drill hole: Results from 2100 to 3500m depth, *J. Geophys. Res.*

Radney, D., Morrow, C., and Byerlee, J., (in press), Effective stress law for montmorillonite and illite clays, EOS, *Trans. Am. Geophys. Union.*

Lockner, D., and Byerlee, J. (in press), An example of slip instability resulting from displacement–varying strength, *PAGEOPH.*

Lockner, D., (in press), Crack interaction simulation using multi–scaling approach, *Am. Geophys. Trans*, (EOS).

Byerlee, J. and Lockner, D., (in press), Strength and stability of faults containing surface structure, *Am. Geophys. Trans.* (EOS)

Mechanics of Earthquake Faulting

9960-01182

James H. Dieterich
U.S. Geological Survey
Branch of Tectonophysics
345 Middlefield Road, MS/977
Menlo Park California 94025
(415) 329-2573

Investigations

1. Fault constitutive properties. Modification of the laboratory facility was undertaken to provide improved digital control and data acquisition capabilities for planned experiments over extreme range of fault slip rates. Constitutive formulations for fault slip under conditions of variable normal stress were evaluated using numerical simulations of laboratory experiments (with Mark Linker).
2. Nucleation and occurrence of earthquakes. Investigation of the effect of stressing history on earthquake rates was continued.
3. State of stress in active volcanoes. Finite element modeling of the possible factors controlling the evolution and state of stress for the Galapagos volcanoes was initiated with William Chadwick.

Results

1. Fault constitutive properties. To investigate the effects of variable normal stress on the resistance to sliding, we have performed frictional sliding experiments with 5x5 cm blocks of Westerly granite in a double-direct shear apparatus under servo-control. The observed variation in the frictional resistance in response to changes in normal stress mimic those observed in response to changes in imposed slip velocity. In particular, a sudden change in normal stress results in both a sudden and a transient change in the resistance to sliding. From analysis of several types of experiments in which the normal stress was changed during sliding, we conclude that earlier constitutive formulations with rate and state dependence can be generalized to represent sliding behavior when normal stress changes during slip. We adopt a version of the constitutive model proposed by Ruina [1980; 1983] as a simplification to our original formulation [*Dieterich*, 1979; 1981]:

$$\tau = \mu^* \sigma + A\sigma \; ln\,(V / V^*) + B\sigma \; ln(\theta / \theta^*)\,, \tag{1}$$

where μ^* represents a constant reference value of the coefficient of friction. When $V=V^*$ at steady-state, $\theta=\theta^*$, and $\tau=\mu^*\sigma$. The coefficients A and B are constitutive parameters that we estimate from laboratory measurements.

We find that the variable normal stress data may be represented by an evolution law for θ of the form:

$$d\theta = \left(\frac{\partial \theta}{\partial \delta} \right)_{\sigma = const.} d\delta - \left[\frac{\alpha\,\theta}{B\,\sigma} \right] d\sigma\,, \tag{2}$$

where α is a parameter determined by performing variable normal stress experiments.

The variation of θ with displacement is governed by the particular choice of $(\partial\theta/\partial\delta)_{\sigma = const.}$. Two laws for $(\partial\theta/\partial\delta)_{\sigma = const}$ have been proposed:

$$\left(\frac{\partial \theta}{\partial \delta} \right)_{\sigma = const} = \frac{1}{V} - \frac{\theta}{D_c}\,. \tag{3}$$

and

$$\left(\frac{\partial \theta}{\partial \delta} \right)_{\sigma = const} = \left[\frac{-\theta}{D_c} \right] ln \left[\frac{\theta\,V}{D_c} \right]. \tag{4}$$

(see Ruina [1980; 1983], Dieterich [1979; 1981]). The parameter D_c is the characteristic sliding distance for evolution of θ.

We have tested our proposed constitutive model with numerical simulations of the experiments. The numerical model employs the proposed constitutive relations and represents apparatus interactions as a spring and slider system. Figure 1 shows a simulation of a hold-pulse test. For the hold-pulse test illustrated in Figure 1, the constant load point speed of 1μm/s is interrupted by a one second load point hold. During the hold, the normal stress is pulsed from the nominal value of 5MPa to 7MPa (20% pulse) and to 9MPa (40% pulse). The normal stress pulse has a duration of 0.2seconds and begins 0.1seconds into the hold. This test severely taxes the evolution equation because θ evolves during the hold due to combined effects of a slip speed perturbation and normal stress perturbation. Evolution **law 1** employs (2) with (3) and evolution **law 2** employs (2) with (4).

2. Nucleation and occurrence of earthquakes. Closed form solutions for the rate of earthquake nucleation events have been applied to model the rate of earthquake occurrence under variable stressing conditions. During the report period, earlier solutions for a single stressing event were generalized to a sequence of events made up of stress steps and stressing rate changes. A study is planned to apply these solutions to model the effect of fault interactions on seismicity rates.

3. State of stress in active volcanoes. A finite element modeling effort of the internal structure and state of stress of the Galapagos volcanoes was initiated with NRC Postdoctoral Fellow William Chadwick. Goals of the study are to 1) evaluate the effects of intrusion, extrusion and gravity in controlling stress state and evolution of the volcanoes and 2) investigate the possible relationships of faulting to magmatic processes.

References Cited

Dieterich, J. H., Modeling of rock friction: 1 Experimental results and constitutive equations, *J. Geophys. Res., 84*, 2161-2168, 1979.

Dieterich, J. H., Constitutive properties of faults with simulated gouge, in: Mechanical Behavior of Crustal Rocks, edited by: N. L. Carter, M. Friedman, J. M. Logan and D. W. Stearns, *Geophysical Monograph 24*, 103-120, American Geophysical Union, Washington, D. C., 1981.

Ruina, A. L., Friction laws and instabilities: a quasistatic analysis of some dry friction behavior, Ph.D. Thesis, Brown University, Providence, R.I., 1980.

Ruina, A. L., Slip instability and state variable friction laws, *J. Geophys. Res., 88*, 10359-10370, 1983.

Reports

Biegel, R. L., C. G. Sammis and J. H. Dieterich, The frictional properties of a simulated gouge with a fractal particle distribution, *J. Structural Geol., in press*, 1989.

Chadwick, W. W., Jr., K. A. Howard and J. H. Dieterich, Why are there circumferential eruptive fissures on the Galapagos volcanoes (Abs.), in: IAVCEI General Assembly, *New Mexico Bureau of Mines and Mineral Resources Bull. 13*, 48, 1989.

Linker, M. F. and J. H. Dieterich, Effects of variable normal stress on rock friction: observations at 50 bars normal stress, *Submitted to J. Geophys. Res.*, 45, 1989.

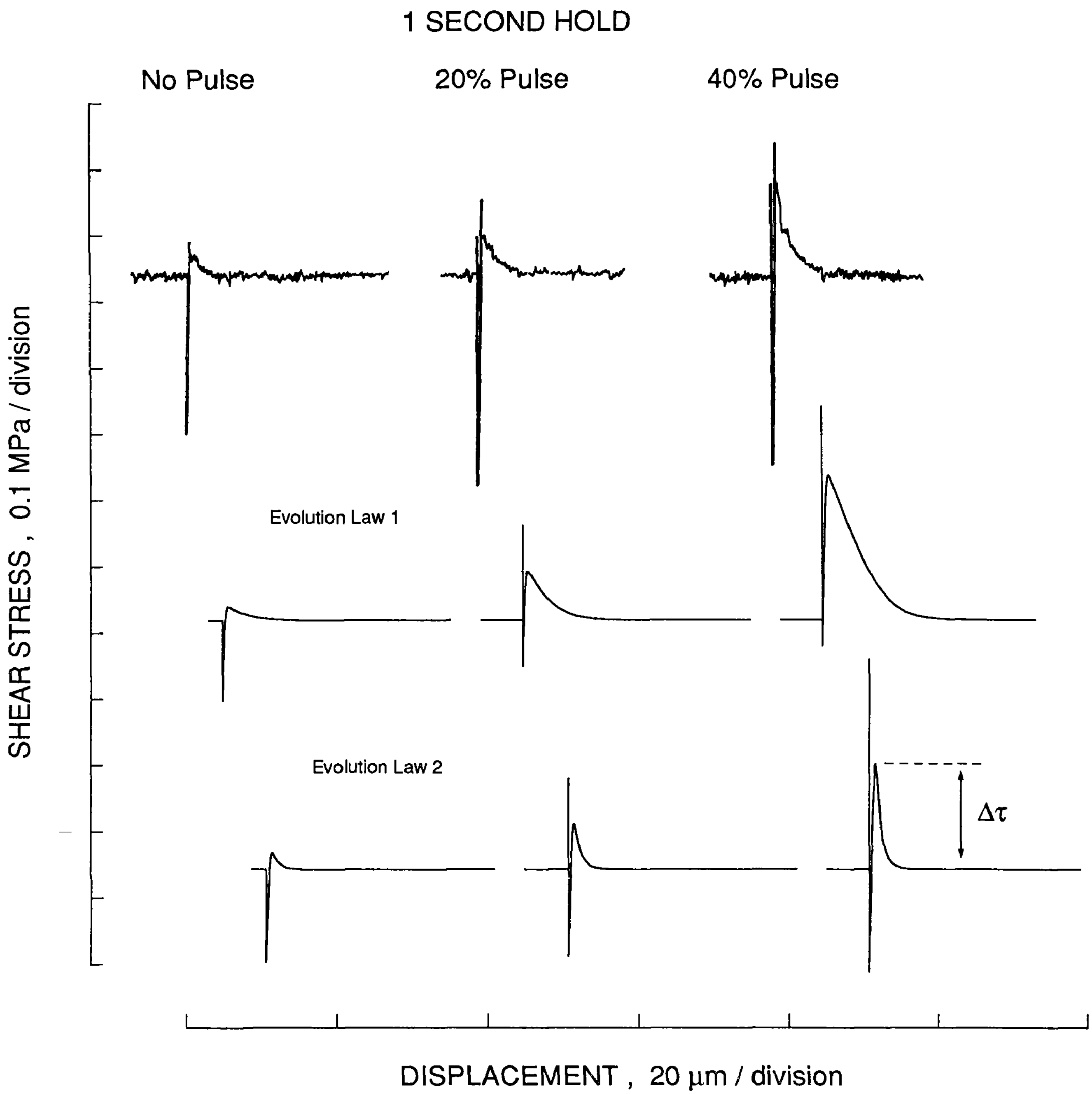
1 SECOND HOLD
No Pulse
20% Pulse
40% Pulse
Evolution Law 1
Evolution Law 2
Δτ
SHEAR STRESS , 0.1 MPa / division
DISPLACEMENT , 20 µm / division

The Physics and Mechanics of the Brittle-Ductile Transition

14-08-0001-G1340

Brian Evans and Joanne T. Fredrich
54-718
Dept. of Earth, Atmospheric, & Planetary Sciences
Massachusetts Institute of Technology
Cambridge, MA 02139

14-08-0001-G1352

Teng-fong Wong
Dept. of Earth & Space Sciences
State University of New York, Stony Brook
Stony Brook, NY 11794

Objectives: The physical mechanisms of semi-brittle rock deformation in the earth are poorly understood but are important for understanding seismogenic faulting and aseismic fault creep. We are conducting an integrated laboratory and observational study of the deformation mechanisms operating during the brittle-ductile transition, the micromechanics of semi-brittle flow, the effect of variations in pressure and temperature on the strength of rocks deformed in the semibrittle field, and the theoretical investigation of crack nucleation mechanisms in the semibrittle regime.

Acoustic emission measurements: An acoustic emission (AE) measurement system was designed and set up at Stony Brook by Takashi Yanagidani. The AE system, which utilizes PZT-7 transducers (of resonant frequency 1 MHz) and discriminators based on the original design of *Sondergeld* [1980], was used to investigate the micromechanics of grain crushing in porous sandstones. Contrary to our expectation, porosity reduction processes are very efficient in generating AE. Under hydrostatic loading, two stages of compaction with distinctly different AE activity, AE efficiency, and microstructures can be identified. Grain slip and rotation were probably the dominant micromechanical processes for porosity reduction in the first stage of compaction, while grain crushing was dominant in the second stage (see *Zhang et al.* [1989] for a detailed summary).

Brittle-Ductile Transition in Porous Rocks: We also investigated the micromechanics of the brittle-ductile transition of porous rocks using AE and microscopy measurements. The porosity and consolidation history of the sample have strong influence on the failure mode. The experimental results were compared with theoretical predictions of a fracture mechanics model formulated by *Sammis and Ashby* [1986] for cracks emanating from pores (see *Wong* [1989] for details).

Effect of Grain Size on Brittle and Semibrittle Strength in Carbonates: Conventional triaxial experiments and microstructural studies were performed on dense calcite aggregates with grain sizes ranging from 1.7 mm to 6 μm. The brittle fracture strength and macroscopic initial yield stress in the semibrittle field follow empirical Hall-Petch relations. The confining pressure at the brittle-ductile transition depends inversely on grain size, but the normalized stress $(\sigma_1-\sigma_3)/_3$ is nearly the same at the transition for the different rocks. We compared our experimental data to fracture mechanics models of brittle fracture [*Ashby and Hallam*, 1986] and the brittle-plastic transition [*Horii and Nemat-Nasser*, 1986] in compression. The first model predicts that small confining pressures will inhibit work softening behavior; but, localization in carbonates actually occurs for significantly higher values of confining pressure than those predicted. Although the second model predicts that the ratio $(\sigma_1-\sigma_3)/\sigma_3$ at the brittle-plastic transition scales with the inverse of the square root of the initial crack size (which appears to scale with grain size in these samples), we find that the transition occurs in the different calcitic rocks at a fixed value of the above ratio. The missing element from the model may be grain size-sensitive plasticity; a crude incorporation of such an effect better matches the experimental data (for further details see *Fredrich et al.* [1989]).

References:

Ashby, M. F., and S. D. Hallam, The failure of brittle solids containing small cracks under compressive stress states, *Acta Metall.*, *34*, 497-510, 1986.

Fredrich, J. T., B. Evans, and T.-F. Wong, Effect of grain size on brittle and semibrittle strength: Implications for micromechanical modelling of failure in compression, *J. Geophys. Res.*, submitted, 1989.

Horii, H., and S. Nemat-Nasser, Brittle failure in compression: Splitting, faulting and brittle-ductile transition, *Phil. Trans. Royal Soc. London*, *319*, 337-374, 1986.

Sammis, C. G., and M. F. Ashby, The failure of brittle porous solids under compressive stress states, *Acta Metall.*, *34*, 511-526, 1986.

Sondergeld, C. H., Effective noise discriminator for use in acoustic emission studies, *Rev. Sci. Instrum.*, *51*, 1342-1344, 1980.

Wong, T.-f. Mechanical compaction and brittle-ductile transition in porous sandstones, submitted to *Deformation Mechanisms, Rheology and Tectonics, Special Publication, Geological Society of London*, edited by R. S. Knipe, 1989.

Zhang, J., T.-f. Wong, T. Yanagidani, and D. M. Davis, Pressure-induced microcracking and grain crushing in Berea and Boise sandstones: Acoustic emission and quantitative microscopy measurements, *Mech. Mat.*, submitted, 1989.

High Frequency Seismic and Intensity Data

9910-03973
Jack Evernden and Jean Thomson
Branch of Engineering Seismology and Geology
U.S. Geological Survey
345 Middlefield Road
Menlo Park, California 94025
(415) 329-5627

Investigations:

1) Investigating via quantitative modeling of earthquake and explosion spectra the roles of elastic velocity structure, depth of focus and anelastic attenuation on the amplitude and spectral content of both compressional and shear phases (P_n, P_g, S_n and S_g–L_g, etc.) as a function of distance.

2) Investigating via large data sets the P-wave spectral content of earthquakes and explosions, the intent being to place in the literature a definitive analysis of this relationship.

Results:

Progress is slow but real on text under (1):

1) In EUS-like terrains, the crustal velocity model must be such as to display a Δ^{-2} fall-off for P_n from 150 to ~2000 km and a P_q/P_n amplitude ratio of 5 to 10. The code used does correctly predict a Δ^{-2} die off for P_n an abrupt velocity interface. However, modeling has shown such a die-off rate and amplitude ratio, even at high Q_α values, requires a zone several kilometers thick just above the Moho in which velocity increases by ~0.6 km/sec. A somewhat similar velocity increase to that in the EUS-like area above the Moho is required in WUS-like terrain (even with the lower Q_α values) to explain the $\Delta^{-3.5}$ rate of die-off of $P_{7.9}$. Also, explanation of the zero-intercept travel-time curve for P_q requires a low velocity zone of a few tenths of a km/sec at ~10 km depth in the crust, the velocity increase below that zone being constrained by the requirement to fit observed rates of die-off of P_g.

2) The work on 1) has taken longer than expected, so progress on this phase of the work has been very slow.

3) We will soon submit proposed maps for the San Mateo County series of Earl Brabb

for San Mateo County; also, we are developing a set of these maps for Central California. These maps express various parameters pertinent to ground motion expected as the result of a repeat of the San Francisco earthquake of 1906.

Mechanical Analysis of Large-Scale Folds Forming Above a Detachment

14 - 08 - 0001 - G1700
Raymond C. Fletcher
Center for Tectonophysics
Texas A & M University
College Station, TX 77843
(409-845-3251)

Objectives:

Several recent earthquakes in southern California have occurred on faults in the cores of large anticlines (e.g., 1983 M = 6.5 Coalinga earthquake, 1987 M = 5.9 Whittier Narrows eathquake). Mechanical modeling of large-scale folds formed above a basal detachment is being carried out to provide insight into the process of seismogenic faulting in this setting.

Investigations

1. Three-dimensional Folding. Folding in the Los Angeles Basin as well as elsewhere in California is not likely to closely conform to the special case of plane strain normal to the axis of a very nearly cylindrical fold. This is not even true in the central Appalachians, as illustrated by the simplified structural contour map on top of the Oriskany Sandstone for a portion of the Appalachian Plateau Province in southwestern Pennsylvania (Fig. 1a). The dominant structure is a series of NE-trending anticlines and synclines, but a striking EW cross-trend is clearly indicated by the alignment of anticlinal saddles and synclinal minima (arrow). Such a pattern can be simulated by the superposition of two sinusoidal waves (Fig. 1b) with the axis of the lower-amplitude wave (0.25 the higher amplitude) making an angle of 30° with the higher-amplitude wave. The primary structures are broken up in to obliquely-oriented anticlinal culminations and synclinal depressions. The same qualitative features are seen on the structural contour map. Low limb-dip folds with forms like this can be studied by the analysis under development. The solution provides the detailed distribution of stress and the growth rates of the structures.

In California, the interplay between compressional and strike-slip tectonics is apt to complicate the deformational history of large folds, and the variation in fold axis orientation and fold aspect ratio in map view is much greater than in the central Appalachians. We have consequently started work on the threatment of fully 3-dimensional folding. A thick-plate solution for the simplest case of the folding of a single layer of viscous fluid embedded in a viscous medium was initially obtained (Fletcher, 1989). The effect of the orientation of the fold axis to the direction of shortening and of the aspect ratio of the fold in map view on the low limb-dip growth rate has been determined. The extensions to nonlinear rheological behavior of the layers and to the detachment folding configuration are straightforward, and models of this type are currently under investigation. With these, we will be able to interpret patterns of minor structures and subsidiary fault sets on doubly-plunging folds or fold arrays where the regional deformation is some combination of in-plane shear and shortening.

2. Folding in a Layer With a Cohesive Coulomb Yield Condition. The pertinent mechanical behavior of layered rock masses in which large-scale folds form is a topic of some controversy.

In a simple model for folding above a detachment (Fletcher, in prep.), we have treated the strong surface layer as a plastic solid at yield, but with a yield strength independent of the mean stress. In this model, the strong layer is separated from a planar basal detachment by a weaker layer. Folding of the strong layer is accommodated by some combination of two processes: the flow of the weak layer into the cores of anticlines and thickening of the strong layer in the anticlinal cores. The latter occurs by localized faulting in natural structures, and may be related to the process of initiation of major thrust ramps.

To make this model more realistic, we will treat the strong layer as a cohesive Coulomb solid. The flow law considered spans the range between that obtained by using the yield condition as a plastic potential and that obtained by assuming isotropy and incompressibility (von Mises flow law) by means of a dilatancy factor. A tractable problem is achieved if we replace the linear rise in strength with depth with an exponential distribution fit to the values at the top and base of the layer. Results so far obtained show folding at longer dominant wavelength, but with little change in fold growth rates.

3. Deformation above a thrust ramp. A thrust ramp connecting two levels of detachment is a major type of thrust fault associated with large-scale folds. Structures formed by slip on shallow thrust ramps and the stress distributions in the vicinity of these slip surfaces have been estimated for weak slip surfaces separating viscous half-spaces (Kilsdonk and Fletcher, 1989). Figure 2 shows (a) a deformed initially square grid after a displacement of 1.5 ramp widths and (b) the maximum deviatoric stress distribution. Both media are linear viscous fluids. Currently, we are carrying out computations for nonlinear and anisotropic layers of finite thickness, taking into account gravity and sedimentation/erosion to provide simple mechanical models, including stress distributions, for a type of structure that has also been modeled kinematically.

<u>References</u>

Fletcher, R. C., Three-dimensional folding of a single viscous layer in pure shear, J. Structural Geology, accepted for publication.

Fletcher, R. C., Large-scale folding above a planar detachment, in preparation.

Kilsdonk, B., and R. C. Fletcher, An analytical model of hanging-wall and footwall deformation at ramps on normal and thrust faults, Tectonophysics, 160, 153 - 171, 1989.

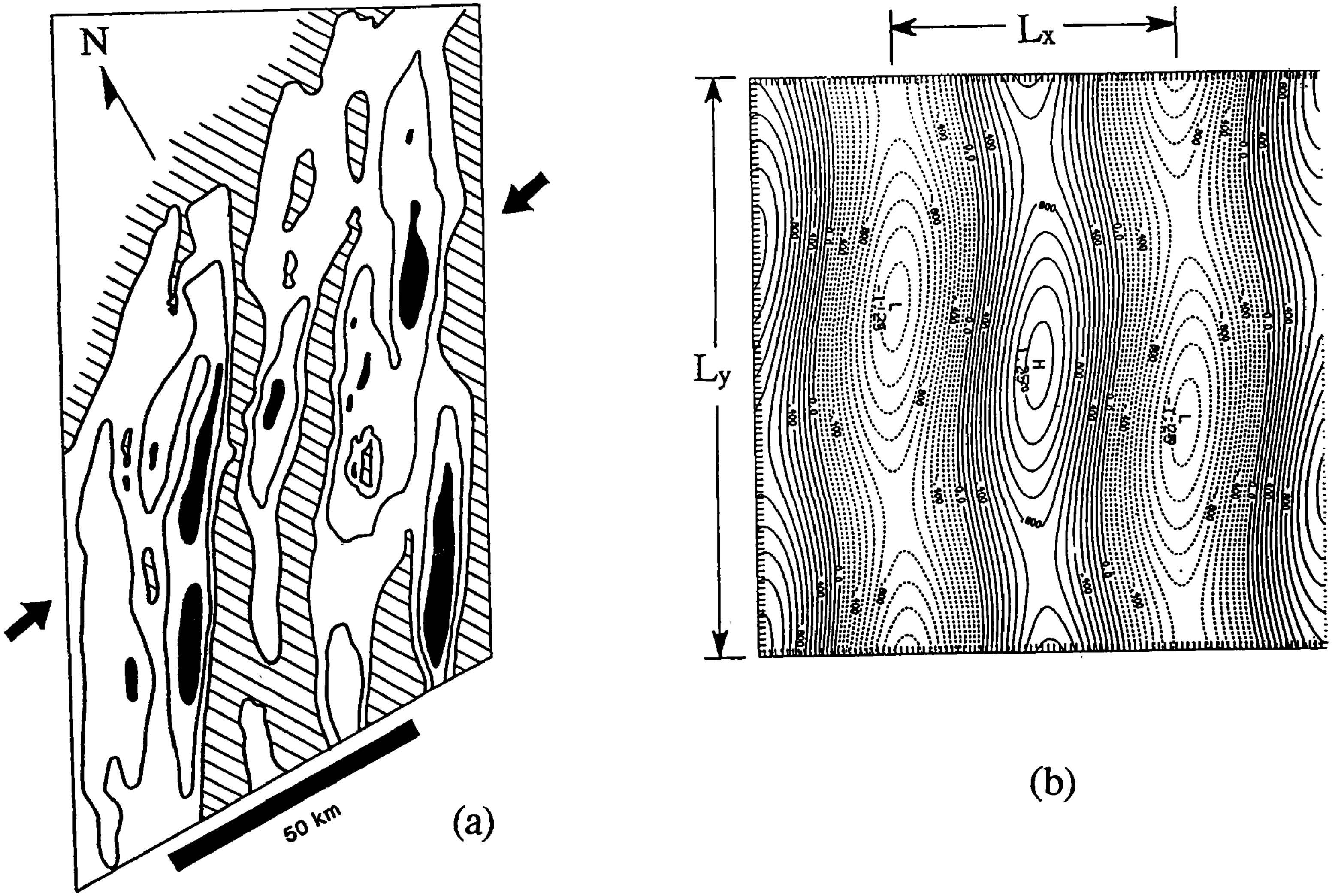

Figure 1. (a) Simplified structural contour diagram for a portion of the Appalachian Plateau Province in southwestern Pennsylvania. Contours are on top of the Oriskany Sandstone. The striped pattern is above -6500' and defines the anticlines; the -7000' contour is approximately the mean level of the surface, and the -7500 contour surrounds synclinal deeps (black). (b) Two superposed sine waves produce a pattern qualitatively similar to that on the structural contour map.

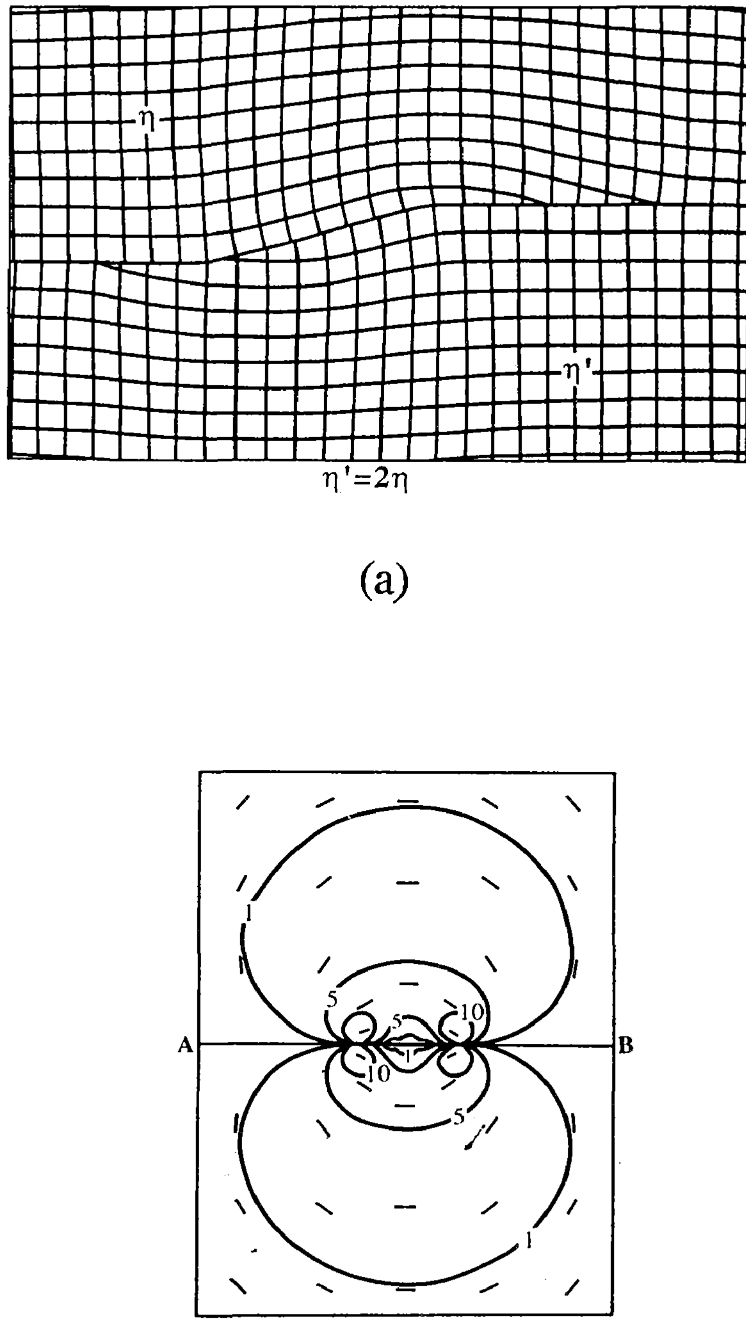

(a)

(b)

Figure 2. (a) Deformation of an initially square grid after 1.5 ramp widths of right-lateral displacement across a weak surface separating two isotropic viscous half-spaces. (b) Deviatoric stress in arbitrary units; the bars are in the direction of the minimum compressive stress. A-B is the level of the low-dip ramped sliding surface.

EXPERIMENTAL ROCK MECHANICS

9960–01180

Stephen H. Kirby
Branch of Tectonophysics
U.S. Geological Survey
345 Middlefield Road, MS/977
Menlo Park, California 94025
(415) 329-4847

Investigations

Polymorphic phase transformations and transformation faulting under stress were investigated in a new suite of experimental tests and a review of the literature on the interaction of non–hydrostatic solids was initiated.

As a part of a continuing study of the hydrothermal alteration of olivine under stress in sliding experiments, a controlled pore pressure capability was added to our 1 GPa gas apparatus and preliminary tests are favorable.

Tests were planned and a low–volume moist–argon pore–pressure system was designed to investigate the fracture of olivine at high temperatures and high gas pressure in order to simulate the physical conditions of intermediate depth earthquakes beneath Kilauea volcano and other volcanic craters.

Results

1. Polymorphic phase transformations under non–hydrostatic stress. Kirby and his colleagues previously reported the discovery of a new class of faulting connected with localized polymorphic phase changes in two mineral systems at conditions where the rates of bulk transformation were sluggish. This phenomenon has been confirmed by Harry Green and Pam Burnley in the Mg_2GeO_4 olivine → spinel transformation. They also show that lens shaped transformation flaws oriented normal to the maximum compressive stress, σ_1, are a key to the nucleation of these faults. In collaboration with Bill Durham of UCLLNL, we have renewed our investigation of the ice I_h → II transformation under stress with additional experiments to map the temperature–pressure–differential stress fields of bulk transformation and transformation faulting. Bulk ice I_h → II transformation is favored by high maximum normal stress and high temperature and occurs by the production and growth of lens–shaped transformation flaws oriented to σ_1. Differential stresses are bounded by a maximum principal stress criterion that is equivalent to the hydrostatic pressure P_t necessary to transform ice I_h to II. The bulk transformation experiments display a prominent yield drop that is presumably connected with the nucleation and growth of the transformation flaws that are observed in abundance in the samples. Transformation faulting, on the other hand, exhibits a failure criterion that is only weakly dependent on temperature and apparently independent of confining pressure and strain rate. These results are significant because transformation faulting is a leading candidate for the failure mechanism of deep earthquakes and the reconstructive phase transformations that occur in deeply subducting lithosphere have properties similar to the ice $I_h \rightarrow$ II transformation.

2. **Hydrothermal alteration weakening of experimental faults in olivine.** Sliding resistance of olivine sawcut samples in which small amounts of water are sealed is anomalously low and profuse dissolution and hydrothermal growth features are observed on the sliding surfaces. The new pore–pressure system has been tested and we are currently investigating the pore–pressure sensitivity of the weakening phenomenon.

3. **Brittle fracture of olivine rock at high temperature confining presssure and high gas pore pressure.** *Wilshire and Kirby*, (1989) have described partially healed shear fractures in mantle–derived ultramafic xenoliths and put forwawrd evidence that $C0_2$ H_20–rich volatiles released from ascending mafic magmas are important in the fracture process and deep seismicity beneath basaltic volcanic centers such as Hawaii. We plan to test this hypothesis by performing fracture tests on durite at elevated temperatures, confining pressures and gas pore pressures using a newly designed low–volume gas pressurization system.

Reports

Kirby, S.H., 1989, Transformation faulting and deep earthquakes., *Trans. Amer. Geophys. Union*, v. 70, in press.

Kirby, S.H., Durham, W.B. and Stern L.A., 1989, The ice Ih → II Transformation under non–hydrostatic stress: New observations relevant to the mechanisms of bulk transformation, faulting and deep earthquakes, *Trans. Amer. Geophys. Union*, v. 70, in press.

Wilshire, H. and Kirby, S.H., 1989, Dikes, joints and faults in the upper mantle, *Tectonophysics*, v. 161, p. 23–31.

Stressing, Seismicity and Rupture of Slip-Deficient Fault Zones

14-08-0001-G1367

J.R. Rice (P.I.) and R. Dmowska
Division of Applied Science and
Department of Earth and Planetary Sciences,
Harvard University
Cambridge, MA 02138
(617) 495-3445

1. Investigations

1.1 The influence of asperities in zones of large subduction earthquakes on the style of deformation and seismic behavior of the incoming oceanic plate, and of the slab at intermediate depths, has been studied for several areas - Andreanof Islands 1986, Kamchatka 1952 and southern Kuriles. The studies confirm the observability of large asperity distributions in the thrust contact zone from seismicity patterns of smaller earthquakes ($m_b \geq 5.0$) in the outer-rise and in the slab at intermediate depths.

1.2 A finite element code has been used to model stressing in a strongly coupled subduction zone (in the outer-rise, in the thrust contact zone and the slab underneath it, and in the downgoing slab at intermediate depths) during the earthquake cycle. The results (Rice and Stuart, 1989) provide consistent, but more detailed and accurate determinations of stressing than given in Dmowska et al., 1988.

1.3 Related finite-element studies have been initiated for strike-slip fault zones to explore the effects of constitutive parameters, and their variation with depth, on stress accumulation, the onset of fault instability, and the generation of possible earthquake precursors. The constitutive models for the fault zone and the adjacent crust are to include rate- and state-dependent frictional slip and creep, respectively; only the latter has thus far been incorporated in our finite element modeling.

2. Results

2.1 The current work is the outgrowth of our past studies into different aspects of the mechanics of subduction (Dmowska et al., 1988, Dmowska and Lovison, 1988). In the present work we have investigated the influence of large-scale fault inhomogeneities in large subduction earthquakes on the style of deformation and seismic behavior of the incoming oceanic plate, and slab at intermediate depths, during the earthquake cycle. The zones of large subduction events of Alaska 1964, Rat Islands 1965, Valparaiso 1985, Colombia 1979, Andreanof Islands 1986, and southern Kuriles have been searched for earthquakes with $m_b \geq 5.0$ if available and for as long time periods as possible. It has been found that in general the seismicity in the incoming oceanic plate clusters in front of asperities, defined as areas of highest seismic moment release in the main event and presumably of strongest locking in the interseismic period. It is usually lacking in areas adjacent to non-asperities, that is, to zones that slip during the main event but with appreciably smaller seismic moment release and possibly slip seismically/aseismically during the whole cycle. Similar behavior occurs in the downgoing slab at intermediate depths, where seismicity during the cycle clusters (but less strongly than in the oceanic crust) next to asperities and downdip from them. We infer that the locking of asperities causes higher stresses associated with the earthquake cycle itself to occur in areas adjacent to asperities, both updip and downdip from them, and that such stressing is much less pronounced in the areas adjacent to non-asperities. This opens the possibility of identifying the areas of highest seismic moment release in future subduction earthquakes, and carries implications for where the highest deformation and, possibly, precursory phenomena and/or nucleation of a future event might occur.

Part of the results will be presented in Dmowska and Lovison, 1989.

2.2 In collaboration with Dr. W.D. Stuart of USGS (Pasadena), we have used the ABAQUS finite element code to analyze stressing in and near a strongly coupled subduction zone during the earthquake cycle (Rice and Stuart, 1989). The stressing processes are modeled as uniform along strike (plane strain in a cut perpendicular to the trench line), and the earthquakes are considered as periodic with slip in each consistent with the long-term plate convergence rate accommodated at the margin. We solved for the fluctuating parts of the stress and displacement rate fields, i. e., the parts which average to zero over a cycle, and which are to be added to steady, long-term average tectonic fields to give the total stress and displacement rate. For this purpose, the ocean floor and subducting slab, and also the overriding continent, are assumed to respond elastically in stress fluctuations on the earthquake-cycle time scale, whereas the adjacent mantle is assumed to respond as Maxwell viscoelastic. The earthquakes are represented as sudden slips within a thrust contact zone that is otherwise locked. Our results provide a more detailed and accurate determination of stress fluctuations in the earthquake cycle than those that Dmowska et al. (1988) estimated using a simplified one-dimensional model. As in their work, we find that stress fluctuations throughout the cycle are consistent with seismicity variations in space and time as documented by them and in global surveys by Astiz et al.(1988) and Lay et al. (1989). We also predict variations in ground surface displacement rate with time throughout the cycle that show evidence of the mantle relaxation assumed in the modeling. For example, models with relaxation predict that during the latter half or so of the earthquake cycle, when the overall pattern of deformation in the continental plate is compressional, a localized region of unusually low compressional strain rate, or possibly even of slightly extensional rate, develops along the surface of the continental plate above and somewhat inland from the downdip edge of the locked thrust zone.

2.3 In our study of strike-slip fault zones we are investigating finite-element models that are consistent with constraints of geologic, geodetic, seismic, and heat flow data for fault segments along the San Andreas system, in California, and which draw on laboratory studies of frictional slip and creep for candidate fault zone and crustal materials. These studies are intended to address crustal loading and overall stress accumulation due to crustal driving by an underlying mantle shear flow, like in the work of Li and Rice (1987) and Fares and Rice (1988), while additionally incorporating Dieterich-Ruina style constitutive descriptions of frictional slip, so that instability can also be addressed. At the current level of these studies, slip on the fault is imposed kinematically while the surrounding crust and upper mantle are allowed to respond. Some solutions have been generated for a linear viscous rheology of the lower crust. An immediate further aim is to determine the degree to which the inclusion of power law creep in the lower crust couples the distribution of shear in the underlying mantle flow to the distrubution of surface deformation during earthquake cycles. For the linear lower crustal rheology, the surface deformation history is the same for all mantle flows which account for a given long term plate velocity, regardless of the detailed distribution of shear in those flows.

References

Astiz L., T.Lay and H.Kanamori, Large intermediate-depth earthquakes and the subduction process, Phys. Earth Planet. Inter., **53**, 80-166, 1988.

Dmowska R.,and L.C.Lovison, Intermediate-term seismic precursor for some coupled subduction zones, Pure Appl.Geophys.,**126**, N. 2-4, 643-664,1988.

Dmowska R. and L.C.Lovison, Influence of asperities in zones of large subduction earthquakes on style of deformation and seismic behavior of incoming oceanic plate and slab at intermediate depths - Alaska 1964, Rat Islands 1965, Valparaiso 1985 and Colombia 1979, submitted to 1989 Fall AGU meeting, San Francisco,December 4-8, 1989.

Dmowska R., J.R.Rice, L.C.Lovison and D.Josell, Stress transfer and seismic phenomena in coupled subduction zones during the earthquake cycle, J.Geophys.Res., **93**, NO. B7, 7869-7884,1988.

Fares N., and J. R. Rice, Crustal deformation modeling for San Andreas fault earthquake cycles, EOS, Trans. Am. Geophys. Soc., **69**, 149, 1988.

Lay T., L.Astiz, H.Kanamori and D.H.Christensen, Temporal variation of large intraplate earthquakes in coupled subduction zones, Phys. Earth Planet. Inter., **54**, 258-312, 1989.

Li V. C., and J. R. Rice, Crustal deformation in great California earthquake cycles, J. Geophys. Res., **92**, 11533-11551, 1987.

Rice J.R. and W.D.Stuart, Stressing in and near a strongly coupled subduction zone during the earthquake cycle, submitted to 1989 Fall AGU meeting, San Francisco, December 4-8, 1989.

Tse S. T., and J. R. Rice, Crustal earthquake instability in relation to the depth variation of frictional slip properties, J. Geophys. Res., **91**, 9452-9472, 1986.

ROCK DEFORMATION

9950-00409
Eugene C. Robertson
Branch of Geologic Risk Assessment
922 National Center, Reston, VA 22092
(703) 678-6792

Investigations

An experimental study has been made of the effect of stress and frequency on the elastic moduli and the energy dissipation in basalt, granite, and limestone samples. Part of the study included measurements of both dynamic and static moduli with a torsion pendulum and with a sinusoidally-cycled compression apparatus. An attempt was made to explain the ubiquitous observation that the dynamic modulus is larger than the static because of a relaxation phenomenon that produces a peak in the dissipation coefficient at some low frequency. The negative results from this attempt have led to an alternative model for the difference in moduli.

Results

In the torsion pendulum apparatus, a rod of rock was twisted in air to an initial deflection below failure (at about 0.001 strain), and then it was released to decay in free oscillations. Oscillations were monitored for frequency and voltage to obtain the dynamic rigidity, G_d, and the energy dissipation coefficient, Q^{-1}, with a precision of about 0.1 percent; in Figure 1 are shown the values of the beginning (maximum) G_d for each run under increasing stress increments. Static rigidity, G_s, was measured by incremental loading from slopes of the stress/strain (τ / γ) data. The differences, $(G_d - G_s)$, for the basalt, granite, and limestone samples ranged from 15 to 25 percent of the mean.

In the compression apparatus, dynamic experiments were made by programming the testing machine to apply a compressive load sinusoidally to the ends of cylindrical samples of the same rocks. Dynamic Young's modulus, E_d, was determined as the tangent of the stress/strain (σ / ϵ) curves. The static Young's modulus, E_s, was the slope of σ / ϵ curves from other experiments with continuous compressive loading. Again $E_d > E_s$, and the difference, $(E_d - E_s)$, ranged from 4 to 11 percent of the mean.

Closure of cracks has been called upon to explain the dynamic-static difference (for a review, see Simmons and Brace, 1965). Confining pressure causes the static modulus to increase faster than the dynamic,, and under 1 GPa pressure, it is within one percent of the dynamic (Simmons and Brace, 1965).

A possible explanation of the mechanism for the moduli difference was given by Zener (1948) with the expression,

$$\tan \delta = [(M_d - M_s)/M] \, [ft/1+(ft)^2] \qquad (1)$$

where δ is logarithmic decrement, and $\delta = \pi/Q$, f is frequency, $M = (M_d M_s)^{1/2}$ and is the mean of the dynamic and static moduli, and $t = (t_d t_s)^{1/2}$ and is the mean relaxation time. Data for equation (1) from tests on metals have showed peaks in δ at the break in slope between the moduli, M_d and M_s. The difference in moduli was accounted for as a relaxation at grain boundaries. An attempt was made to find such a peak in δ and a decrease in moduli at a frequency of 0.002 Hz, with a loading rate of about $10^{-6}\,sec^{-1}$, below the static loading rate of 10^{-4} to $10^{-5}\,sec^{-1}$.

The accessible frequency range of the torsion pendulum was only from 1 to 10 Hz, and thus it could not be used for observations at lower frequencies. However, the compression apparatus could be programmed to perform tests at frequencies of 1, 0.1, 0.01, and 0.001 Hz. As the hydraulic presss was large, it was relatively insensitive to deformation of the small samples, and adequate but not precise comparisons of moduli could be made. No decrease in the dynamic moduli, E_d, was found; they were very nearly the same, within a few percent, over the range of frequencies of 0.1 to 0.002 Hz under a dynamic stress range from 30 to 190 MPa. Furthermore, there was no indication of a log decrement peak in that range of frequency. My conclusion was that the relaxation peak explanation does not apply to these rocks in this range; such a relaxation has not been remarked in other dynamic investigations at frequencies to 0.001 Hz either.

It appears that the basic observation for the difference between the dynamic and the static moduli is that the static strain for a given stress is greater than the dynamic strain for that stress. As the static and the wave equations of the theory of elasticity are apparently equally valid, the explanation seems to be that there are two different properties of materials being tested by the two procedures. A simple model at the atomic scale utilizing the often-postulated cracks seems plausible. In the dynamic mode of deformation, the cracks open up, stretching the interatomic bonding, during the first part of the cycle and close back even closer during the second part of the cycle; the motion repeats through each cycle. In the static mode of deformation, the cracks open during the first increment of stress; they remain so until the next increment of stress is applied, when the cracks open farther, and so on for each stress increment. There is <u>no healing of interatomic bonds</u> in the static mode, whereas there is healing of bonds with every cycle in the dynamic mode. Thus, there is larger strain in the static deformation mode than in the dynamic, under the same stress; clearly, the M_d will be larger than M_s.

Examples of rehealing of bonds are found from the torsion pendulum experiments, shown in Figure 1. Each point represents a separate test. Referring to the first basalt test, the stress is raised from zero to a prescribed stress, (point 0 to point A); then a decay of the stress (from A to 0) occurs; in the second run, a repeat is begun to a new stress (from 0 to B). There is an accompanying fall and rise of the rigidity modulus in each cycle. The recovery of G_d to the initial G_o value within 0.1 percent <u>after each run</u> is evidence for a rehealing of the bonds across each crack that was opened up by the stress buildup. The rather large difference between G_d and G_s (up to 25 percent) may be explained by the tensile failure of the twisted rods of rock, on a spiral at 45^o to the shear stress.

As shown by Simmons and Brace (1965), M_s is still one percent less than M_d at 1 GPa pressure, at a pressure in the mantle below the Moho discontinuity. It is probably not possible to reconcile M_s with M_d in the earth's crust, and to use them interchangeably as has been tried by early investigators. The difference between the moduli can be quite large under low confining pressure in the shallow crust, and use of M_d for M_s in stress/strain calculations in earthquake fault problems is not more reliable than 25 percent.

References

Simmons, Gene, and Brace, W. F., 1965, Comparison of static and dynamic measurements of compressibility of rocks, Journal of Geophysical Research, v. 70, p. 5649-5656.

Zener, C., 1948, Elasticity and anelasticity of metals, University of Chicago Press, Chicago.

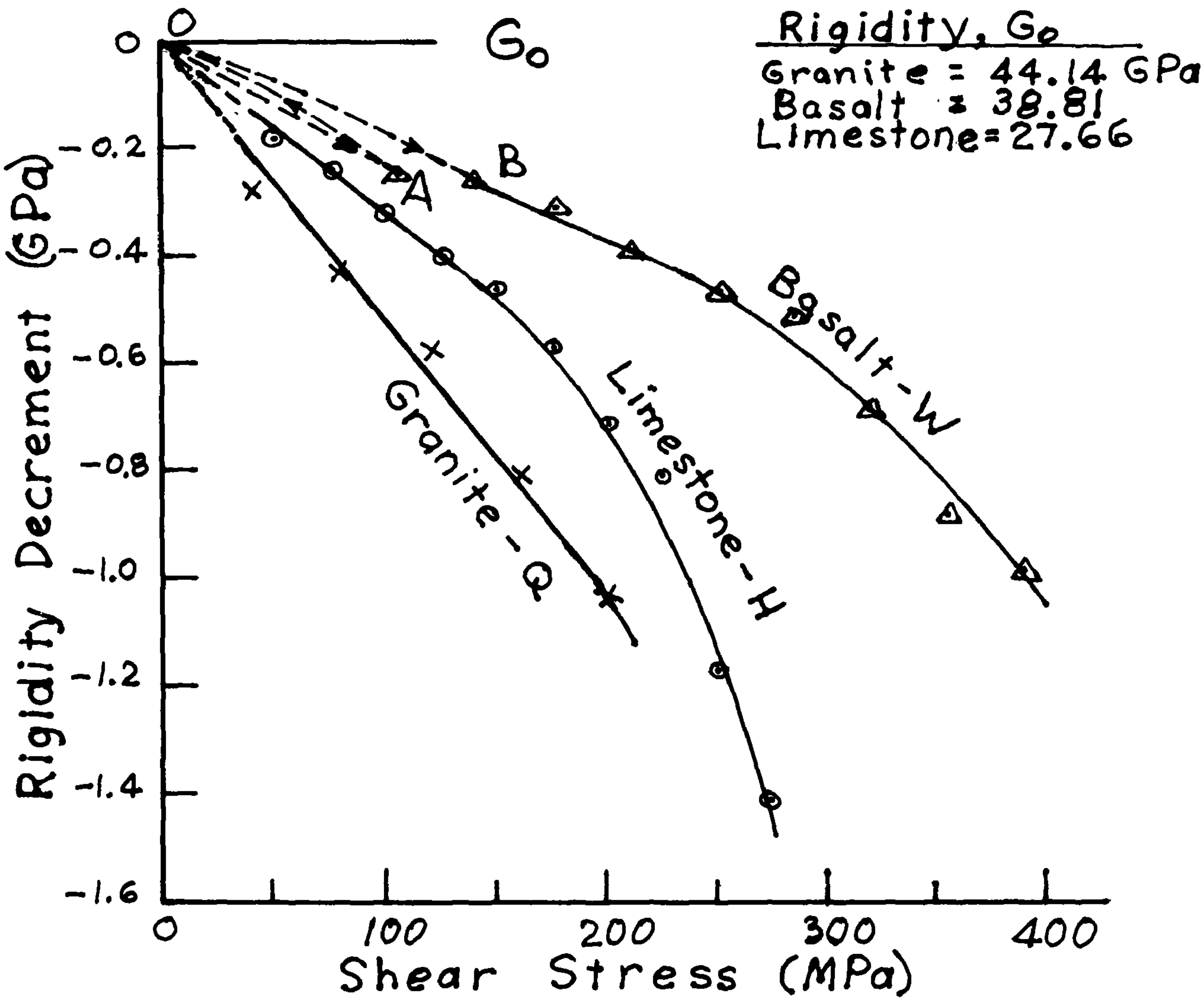

Figure 1. Maximum reductions in rigidity of three rocks in torsion experiments at specific stresses; G_0 is the recovery value for each rock after decay of each run.

Interpretation of Slip-Induced Water Well Level Changes at Parkfield

14-08-001-G1691

J. W. Rudnicki
Department of Civil Engineering
Northwestern University
Evanston, Il 60208
(312)-491-3411

(For period August 1, 1989 to September 15, 1989)

Objective

Properly calibrated water wells can function as inexpensive and sensitive strainmeters. Solutions predicting water well level changes due to slip are needed to infer fault slip history and distribution from observed water well level changes. Recent solutions for pore pressure changes induced by fault slip have demonstrated that the coupling between deformation and pore fluid diffusion can strongly affect the response of the well to slip, particularly if the well is close to the fault, and, consequently, the inference of fault slip from water well level changes. The objective of this study is to assess effects of coupling between deformation and diffusion on the inference of fault slip from observed water well level changes and to include these effects in the analysis of observed water well level changes at Parkfield.

Results

Initial efforts have focussed on the preparation of computer programs to evaluate the coupled-deformation diffusion solutions, to process water-well data from the Parkfield array, and to compare the solutions with the data. The relevant solutions include those for instantaneous and steadily moving shear dislocations on both permeable and impermeable planes (Rudnicki, 1987; Rudnicki and Roeloffs, 1989). These elemental solutions can be used to synthesize more elaborate distributions of slip.

References

Rudnicki, J. W., Journal of Applied Mechanics, **109**, 545-552, 1987.

Rudnicki, J. W. and E. A. Roeloffs, Journal of Applied Mechanics, in press, 1989.

Accurate Three-Dimensional Calculations for Advancing Slip Zones in the Earth's Crust

(Joint funding with NSF Grant EAR-8707392)

J. W. Rudnicki and L. M. Keer
Department of Civil Engineering
Northwestern University
Evanston, Il 60208
(312)-491-3411

(For period May 16, 1989 to September 15, 1989)

Objectives

Understanding the mechanism by which slip is transmitted from depth to the surface and along the strike of the fault from freely slipping to locked zones is of great importance for understanding the earthquake process and for possibly anticipating damaging events. A major impediment to more accurate and realistic analyses has been the difficulty of making calculations for three dimensional cracked bodies. We are doing three-dimensional analysis of slip zones (cracks) in an elastic half-space to determine stresses and surface deformations due to the advance of shear faults into locked, or more resistant portions, of the shallow crust. The goal of these studies is to understand three-dimensional geometric effects on the intensity of stressing near the edges of slip zones. Ultimately, we hope to develop theoretical models for the advance of slip zones into and around slip resistant portions of the fault, focussing particularly on the effects of nonuniformities in the advancing slip front.

Results

We are using the method of Lee et al. [1987], developed to analyze cracks in bimaterials. The method uses the integral representation for a distribution of body force and the elasticity solution for a point force near a bimaterial interface (free surface in the present application). The problem is then reduced to the solution of an integral equation for the unknown crack surface displacements over the two dimensional surface of the crack. Because the method uses the exact asymptotic form of the displacement field near the edge of the crack in discretizing the kernel of the integral equation, the results are accurate.

An auxiliary program uses the slip surface displacements to calculate displacements at the free surface since these are the quantities that are most easily observed. The method uses convolution of the displacements calculated for the slip surface with the Green's function for a unit point dislocation in a half space. The latter is calculated from Mindlin's solution for a point force in a half-space.

As a preliminary application of these programs, we calculated the stress intensity factors and surface displacements for an inclined circular shear cracks near a free surface. For numerical values consistent with the moment and geometry inferred by Lin and Stein [1988] for the Whittier Narrows earthquake from geodetic elevation changes by using a uniform rectangular dislocation model, the magnitude and distribution of the surface elevation changes agree well with the observed values. However, because the ratio of the depth of the slip zone to its size is relatively large (about 4.5) for the Whittier Narrows event, the stress intensity factors differ from their values in an infinite elastic body by only a few tenths of a percent. Calculations for shallower slip zones suggest that significant effects of the free surface on values of the stress intensity factors occur only when the ratio of the depth of a circular slip zone to its radius is less than two.

Recent efforts have concentrated on calculations for surface-breaking slip zones. Numerical values for the geometry have been chosen to be consistent with those inferred by Barrientos et al. [1987] for the Borah Peak earthquake: dip angle = 49° ($\alpha = 41^{\circ}$), fault length = 23 km, and fault width = 18 km. The slip zone was taken to be semi-elliptical with an area and aspect ratio equal to the rectangular zone used by Barrientos et al. The fault was subjected to a uniform shear stress drop.

Figures 1 and 2 show the variations in Mode II (in-plane shear) and Mode III (anti-plane shear) stress intensity factors (divided by $(\pi a)^{1/2}$, where a is the length of the minor semi-axis) as a function of θ, the angle measured from the direction perpendicular to the applied shear stress with $\theta=90^{\circ}$ corresponding to the down-dip direction. Figure 3 compares the observed and calculated surface displacements assuming the same average value of slip inferred by Barrientos et al., 2.2 m, and that the relation between the moment and stress drop is the same as for an isolated slip zone of the same geometry in an infinite elastic body. The calculated values of maximum uplift and downdrop are 0.28 m and 1.24 m compared with the observed values of 0.24 m and 1.39 m. The calculated stress drop is 3.15 MPa compared with the value of 3.0 MPa inferred by Barrientos et al.

The presence of the free surface causes a fault subjected to uniform shear stress drop to open, an effect noted in two dimensional problems by Dmowska and Kostrov [1973]. This tendency was suppressed in the calculations here by permitting only relative slip. The maximum compressive traction required to prevent opening is about 32% of the applied shear stress. Surprisingly, a small tensile stress (about 4% of the applied shear) is required on some portions of the fault. This results because preventing the crack from opening apparently tends to cause some portions of the slip zone to tend to interpenetrate.

References

Barrientos, S. E., R. S. Stein, and S. N. Ward, Comparison of the 1959 Hebgen Lake, Montana and the 1983 Borah Peak, Idaho, earthquakes from geodetic observations, Bull. Seismol. Soc. Am., **77**, 784-808, 1987.

Dmowska, R. and B. V. Kostrov, A shearing crack in a semi-space under plane strain conditions, Arch. Mech., **25**, 421-440, 1973.

Lee, J.C., Farris, T. N. and L.M. Keer, Stress intensity factors for cracks of arbitrary shape near an interfacial boundary, Engn. Frac. Mech., **27**, 27-41, 1987.

Lin, J. and R. S. Stein, Coseismic folding, earthquake recurrence, and the 1987 source mechanism at Whittier Narrows, Los Angeles Basin, California, Journal of Geophysical Research, **94**, 9614-9632, 1989.

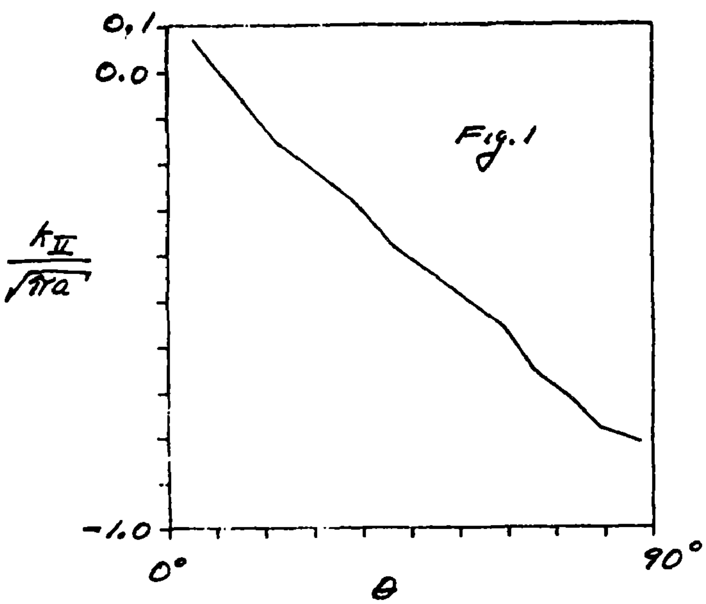

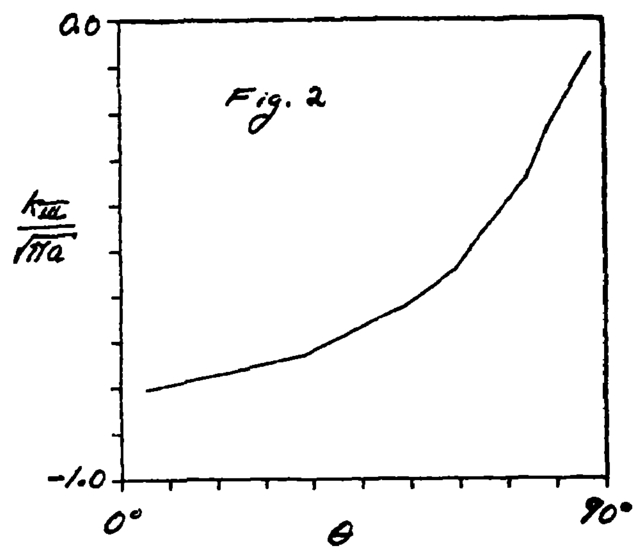

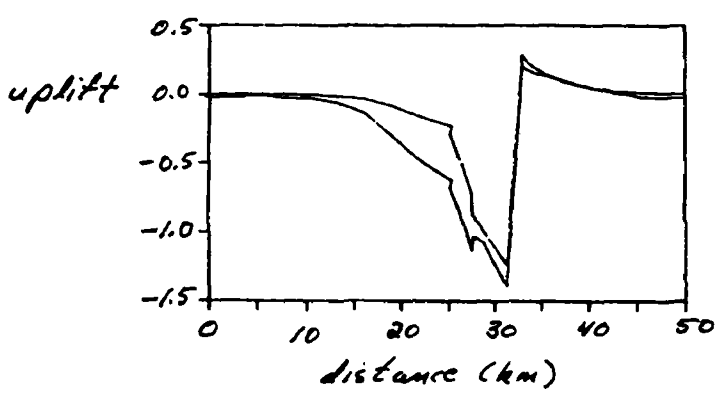

Figure 3

Heat Flow and Tectonic Studies

9960-01177

John H. Sass
Branch of Tectonophysics
U.S. Geological Survey
2255 North Gemini Drive
Flagstaff, AZ 86001
(602) 527-7226
FTS: 765-7226

Arthur H. Lachenbruch
Colin F. Williams
Branch of Tectonophysics
U.S. Geological Survey
345 Middlefield Road
Menlo Park, CA 94025
(415) 329-4879/4881
FTS: 459-4879/4881

Investigations:

A geothermal study of the Santa Maria Basin and environs is continuing. Fifteen idle oil wells have been logged, and more will be logged this fall. Samples are being collected for thermal conductivity determinations.

The long-term temperature monitor has been refurbished and moved to the USL-Pearson well at the San Andreas fault near Parkfield. Preliminary data collection is underway.

Studies of the Alaskan North Slope thermal regime are continuing.

Heat-flow studies from the Cajon Pass well are in the final phases of interpretation and manuscript preparation.

Hardware for the new digital data acquisition and reduction system has been purchased, and software development is underway.

Results:

Santa Maria Basin. The interdisciplinary USGS study of the Santa Maria Province in southern California provides an opportunity for the coordination of traditional heat-flow investigations with concurrent stratigraphic and tectonic studies. To date, 15 idle oil wells have been logged by the Geothermal Studies Project in the Guadalupe, Santa Maria Valley, Cat Canyon, Orcutt Hill, Lompoc, Zaca and Point Conception oil fields. In addition, commercial temperature logs have been obtained from 17 wells in the Cat Canyon and Santa Maria Valley oil fields. At least 7 more wells in the onshore Santa Maria Basin are targeted for logging, along with possible work in the Cuyama and offshore Santa Maria Basins.

With the exception of the Zaca and Pt. Conception sites, all of the temperature logs include data from thick (>1000 feet) sections of the Sisquoc Formation, a late Miocene - early Pliocene diatomaceous claystone which overlies the Monterey shale reservoir rock throughout the Santa Maria Basin. Thermal gradients within this formation range consistently between 45 and 60 deg C/km. While thermal conductivities have yet to be determined, typical values of sediment thermal conductivity (1.25 to 2.5 W/m K) suggest that heat flow in the Santa Maria Basin is consistent with typical values for the central California coast (approx. 70+ mW/m^2) rather than with the Ventura Basin to the south (approx. 50 mW/m^2). The apparent thermal differences between the Ventura and Santa Maria Basins may reflect differing sedimentation rates and histories, and the final results will likely have important implications for the thermo-mechanical properties of the large thrust faults and folds located within both basins.

Parkfield. The Project's Long Term Temperature Monitor (LTTM) was recovered from the Middle Mountain (VARN) well, refurbished at Menlo Park, and redeployed at a depth of 2600 feet in the USL-Pearson 1B (PRSN) well. This well is located approximately 1/2 mile west of the San Andreas fault and 15 miles northwest of Parkfield. It is thought that the monitor's thermal resolution (approx. 0.0002 deg C) will enable the observation and recognition of thermal variations associated with movement on the San Andreas fault. Hopefully, measurements from this well will be integrated with the existing network of Parkfield observations.

Cajon Pass. Two manuscripts are in preparation for a special JGR issue on the Cajon Pass Drilling Project. The first paper covers the details of heat-flow measurements in the drill hole, and the second paper summarizes the implications of those measurements for the thermo-mechanical behavior of the San Andreas fault.

Alaskan North Slope. As part of a continuing investigation of Arctic crustal heat flow and the near-surface thermal effects of climatic change, 26 wells in the Alaskan NPRA were re-entered and logged during July and August. The results will supplement existing investigations and help to launch new research into the relationship between shallow permafrost temperatures and the changing climate.

Data Acquisition and Reduction. Hardware purchases for the new acquisition system have been completed, and the development of new software is continuing. The new system should be deployed in late '89 or early '90.

Reports:

Lachenbruch, A. H., and McGarr, A., Stress and heat flow on the San Andreas fault: *U.S. Geological Survey Professional Paper,* in press, 1989.

Lachenbruch, A. H., and Morgan, P., Continental extension, magmatism, and elevation: Formal relations and rules of thumb: *Tectonophysics,* in press, 1989.

Langseth, M. G., Lachenbruch, A. H., and Marshall, B. V., Geothermal observations in the Arctic region: *Decade of North American Geology,* in press, 1989.

Osterkamp, T. E., and Lachenbruch, A. H., Current thermal regime of permafrost in Alaska and the predicted global warming in *Proceedings, Workshop on "Climatic Change and Permafrost: Significance to Science and Engineering":* American Society of Civil Engineers, in press, 1989.

Sass, J. H., 1988, Salton Sea Scientific Drilling Program: *Earthquakes & Volcanoes,* v. ***20,*** p. 156-160.

Micromechanics of Rock Friction

14-08-0001-G1668

C. H. Scholz
Lamont-Doherty Geological Observatory of Columbia University
Palisades, New York 10964
(914) 359-2900

Objective: To develop, from the micromechanics of contacting surfaces, a quantitative model of rock friction.

Investigations:

1. The first step in this project was to extend existing models to predict the elastostatic behavior of contacting surfaces subjected to both shear and normal loads under the conditions in which no slip occurs. This work has been completed and the model has been successfully tested experimentally. This work is reported in Yoshioka and Scholz (1989a,b).

2. The scaling of this problem from the laboratory scale to that of natural faults has begun to be addressed. A particularly vexing problem is that natural faults are fractal whereas laboratory measurements must be made with artificially ground surfaces. A simple model was made for contact of fractal surfaces. It was found that when the contact is subjected to normal load, long wavelength apertures close down whereas short wavelength apertures may remain open, so that a minimum mated contact size exists that is a function of normal stress. This defines a length scale which may be identified with the critical slip distance for seismic faulting. This work is reported in Scholz (1988).

3. The second phase of this project is to predict the initial friction at slip onset. A prerequisite is to obtain reproduceable friction behavior-- which has been notoriously hard to do. We have found that it is possible to obtain reproduceable data as long as the starting surfaces are reproduced-- that is, the unreproduceability of friction so often found in the literature seems to be due to variations in surface preparation. Our reproduceability seems, for practical reasons of surface preparation, to be at about 4%, which is considerably poorer than experimental precision but since we can measure the surface differences with the profilometer and account for it in the theory, this does not limit the level to which the theory can be compared with the experiments.

By subtracting out the response of the solid part of the sample and holder, we obtain a curve that corresponds only to the deformation and slip of the contacting surfaces. The following features are observed: i) partial slip of asperity contacts begins at low shear stresses and accelerates until ii) full slip begins at a pronounced yield point in the torque-twist curve, followed by iii) strong slip strengthening until, at about 1 mm slip, iv) a second yield occurs, which is followed by much weaker slip strengthening out to much greater slip (>2 cm).

Preliminary modelling indicates that we can predict the behavior out to and including the first yield point with a Mindlin-Deresiewicz formulation of the contact theory in which the topography model based on profilometry measurements is used as the input. Therefore, it appears that we will be able to predict initial friction if we have detailed knowledge of the surface topography.

4. To proceed further we must investigate slip induced damage and the buildup of asperity interlocking during sliding. Wear experiments have been carried out to study the first of these. These experiments were carried out with Westerly granite for several roughnesses and normal loads out to total slips of 2 m. A wear model was developed that combines an Archard-type wear model with our contact model. This model includes both the transient (running in) stage as well as steady-state wear. Comparison with the experimental results show that the theory correctly

predicts the effect of normal stress on wear but does not correctly predict the roughness effect. We believe this is due to our failure to correctly include the effect of asperity interlocking in the problem. The model has been reformulated to account for this effect, which can be evaluated with profilometry data, but we have not yet compared this with the experimental results.

Preliminary work has been carried out to determine if we can evaluate the evolution of the contact during slip with the transient pulse relaxation method. The technical feasibility has been confirmed but the method has not yet been tried in actual experiments.

References:

Scholz, C. H., The critical slip distance for seismic faulting, *Nature, 336*, 761-763, 1988.

Yoshioka, N., and Scholz, C. H., Elastic properties of contacting surfaces under normal and shear loads, 1: Theory, 2: Comparison of theory with experiment, *J. Geophysical Res.*, in press.

Systems Analysis of Geologic Rate Processes:
Stlyized Space-Time Models for California Earthquakes

9980-02798

Herbert R. Shaw and Anne E. Gartner
Branch of Igneous and Geothermal Processes, U. S. Geological Survey
MS-910, 345 Middlefield Road, Menlo Park, CA 94025
(415) 329-5245, 5209

Objective: We continue to explore the multifractal properties of the earthquake process. Following the lead of Shaw (1987a), analogies are drawn between the probability structures of earthquake recurrences in time and space and probability structures of coupled networks of oscillators, neural networks, and the "linguistics" (information theory) of natural codes (Shaw, 1987b).

Results: Our project has been proposing for several years that California earthquakes are more coordinated in space and time than is acknowledged in other studies of earthquake recurrence models. We came to this conclusion on the basis of quantitative studies of continent-scale faulting viewed as dendritic systems. A fractal perspective was an outgrowth of that view, and we have applied fractal concepts in our approach to California seismicity. A sequel to these studies was the outline of a probability model for earthquake recurrences based on the concept of interacting dendritic arrays. This model is analogous to dynamical interactions in neural dendrites, and the theory was referred to qualitatively as a "linguistic model of earthquake frequencies" (aspects have been reported in previous technical reviews of NEHRP). The word "linguistic" came from the notion that the probability structure of earthquake frequencies might resemble the frequency structure (or redundancy structure) found in language codes of various kinds (Shaw, 1987a).

The reason for positing this analogy is that earthquakes have some of the same attributes as words: (a) both come in a wide range of sizes, (b) both are individually composed of substructures, such as syllables and letters, (c) both have characteristic ranges of frequencies for different types of substructures (e.g., there are characteristic probabilities associated with letters and with words of different sizes in language codes and with earthquakes of different sizes in the Earth), and (d) both are organized in space and time according to some set of rules (syntax, punctuation, grammar). A message is the occurrence of an event of given size at a given time and place in the context of related events. Given a knowledge of related 'words' and their sequences, a message is completed by the event that fits best contextually. Even in the case of languages, however, there are always residual ambiguities where another word might also fit.

A message sequence is generally characterized by a particular mixture of small to large words. In either the case of language or of earthquakes, the message might run the gamut from total redundancy to total uncertainty. The former is periodic (like the Parkfield model of earthquake recurrences, or like verbal chants of repeated words), and the latter is nonperiodic and potentially random in space and time. To be both communicative and informative, languages have to be somewhere between these extremes. Typical English text is roughly 50% redundant; if it were much more redundant we wouldn't learn anything, and if it were much less redundant we wouldn't comprehend the message. The prevailing view of earthquake recurrences is analogous; some categories of events are thought to be relatively redundant (Parkfield-type), and others are thought to be beyond any reasonable expectation of predictability.

As a class, then, earthquake recurrences are made up of a mix with varying degrees of redundancy, not unlike the organizational properties of written text. Another common characteristic is that both language and earthquakes are the products of nonlinear dynamical mechanisms. It is now known with some certainty that the nonlinear dynamics of coupled systems (including networks) is capable of producing periodicity structures that are describable in terms of complex redundancy-uncertainty mixtures (e.g., Shaw, 1987b; Shaw and Chouet, 1989).

By contrast with the symbolic view of written languages, other codes, such as the genetic code, are associated with specific physical objects and recognizeable dynamical mechanisms. In such instances we can conceivably analyze how the system as a whole interacts, meaning there is some chance of seeing how the structure of word frequencies comes about in the context of network interactions among these mechanisms. This approach represents a central aspect of current neurological and immunological studies (e.g., Edelman, 1987). In some respects, the earthquake problem is simpler in terms of the variety of mechanisms and levels of feedback interactions, but the linguistic approach is hampered by the paucity of examples of characteristic word-frequency structures. The problem is something like the study of a few fragments of text in an alien language for which there are no dictionaries nor grammatical textbooks.

To illustrate the sample problem, the historic catalog of earthquakes in California (beginning in the year 1800) has roughly 500 events at magnitudes 5 and above. If each event is viewed as the analog of a word or group of words, it is easy to see how hampered we are by the paucity of 'text', unless the language as a whole has very few possible words and word combinations. This might occur if the words were limited to combinations of only a few letters. In the latter case, however, we might expect rather high redundancy. On the other hand, if the same kind of alphabet and syntax describes the behavior of small as well as large events, then the sample is orders of magnitude larger, and the above catalog is like a glossary that includes only words larger than some minimum number of letters. It might turn out that there are two or more alphabets at different magnitude levels, but this does not invalidate a linguistic approach. For instance, the genetic code is made up of at least two different alphabets.

It has to be admitted that, for some time to come, earthquake catalogs may not be large enough to demonstrate the existence of a seismic 'language'. Even so, the linguistic concept offers a framework against which to compare observed patterns, and that framework is inclusive of but more comprehensive than the approaches to recurrence relationships already being studied (e.g., studies of periodicity, of time- and/or magnitude-predictability, seismic gaps, seismic cycles, and so on, are subsets of more general probability methods such as those used in linguistic analyses).

Some workers feel that the generation of "characteristic earthquakes" is a different process from that of all other events, and the latter tend to be lumped as generalized foreshock-aftershock frequency patterns. This would imply two different types of text, two different languages, or perhaps a composite language with two or more alphabets. Initially, our approach has been to consider such unusual events to be special words within the body of a common language. They are analogous to the frequency structure of the very big, hence unusual, words in English.

One way to test the simpler sorts of linguistic notions is to see how the system-wide patterns of big and little earthquakes are similar or different. Such a study is begun by counting and plotting words of different sizes and their relative frequencies in a given spatial framework (e.g., on a map). This is the analog of the spatial, hence temporal, distribution of words in sentences and paragraphs. Epicenter maps, therefore, represent the first step in a linguistic analysis, but they usually lack information on chronological sequences. Of course, there are limitations to these analogies with written text, because writing is by definition arranged in some form of linear array both spatially and chronologically (earthquake distributions are more like conversations, where statements can dynamically interact and overlap).

The present status of this work is similar to the early stages of linguistic research in which workers spent a lot of time counting letters and words and the conditional probabilities that given a particular letter or word it would be followed by another particular letter or word, as in cryptography. One aspect is to provide a framework within which conditional probabilities can be calculated for event sequences oscillating among two or more localities.

If the linguistic study of earthquakes were to prove valid, presumably we would find that grammatical context offers the most powerful way to predict characteristic event sequences (letter and/or word combinations). Grammatical context means that given a relatively few sequences of events in a statewide or larger context, the next most likely kind of event would become automatically recognizeable (e.g., given the context of only a few letters or words, complete words and sentences in English can be completed with measurable confidence). It seems possible that such a context could be established within a linguistic framework characteristic of California, but we can not rule out the possibility that this context will have to include the Circumpacific seismic zones. There are indications that earthquake cycles in California oscillate in response to Circumpacific cycles (Shaw, 1987a).

In the work that forms the basis of this report we have plotted events in chronological sequence connected by lines (trajectories), subject to given magnitude cutoffs. Figure 1 is shown as an index map and guide to how such trajectories were drawn; for clarity we have shown only the largest post-1800 earthquakes in California and vicinity from CDMG catalogs (listed in the references). In other cases, time windows for sets of events range from a few months to the entire historical record. The shortest windows are for records that include events equal to or greater than M = 4 (6 months to a year for the period 1979-1982), and the longest is for those events equal to or larger than M = 6.7 (Fig. 1). The principal CDMG catalogs we have used have a cutoff at about M = 5 (pre-1900, and 1900-1974). The time windows we have used for most of the plots (after 1890) are at intervals of 2 to 10 years.

The choice of time window was based on numbers of events. Maps with more than about 30 or 40 events are hard to follow because of overprinting of trajectories. This factor in itself is a crude measure of redundancy associated with characteristic time windows. If there was little or no overprinting, the overall pattern would consist of a weave of line segments identified by dates and locations of epicentral end points and would look more like a map of a random walk or trajectories of Brownian motion.

The maps were plotted on orthogonal graph paper, where the coordinates give the latitudes and longitudes of epicenters. This was done to divorce the interpretations from preconceptions concerning location; correlations are illustrated using overlays, etc. Linear trends in these trajectories do not always correlate with specific fault geometries. Progressions in time are shown by arrows on the lines. Thus, the plots are epicenter maps in which trajectories have been added to highlight different types of evolution (jumps, spatial oscillations and/or stationarities, migrations, etc.). The purpose is to more clearly identify patterns of seismic energy release, above some threshold, from a two-dimensional perspective.

The chronological sequences in space (trajectories) form the basis for calculating conditional probabilities that given an event in one or more locations it (they) will be followed by an event in another location. This is a direct analogy with conditional probabilities in a sample of written text that a given letter will follow another letter or group of letters; there they are called digram probabilities, trigram probabilities, etc.

Suppose hypothetically that every time an event near Oroville was followed by an event near Brawley there was a high probability that the next event would occur near Coalinga but that this combination happened only once every fifty years or so. This sort of observation would remind us to keep an eye on event sequences in these localities (and any other combinations involving them), but it would permit us to classify this particular suite of event sequences among those with relatively low temporal probabilities of recurrence. On the other hand, suppose that the same relation applied to repetitions of events involving the sequence Eureka--Baja--SFBA (San Francisco Bay Area), and that this sequence occurred every two years or so. Obviously, estimates of short-term probabilities for events of intermediate size in SFBA are enhanced by a knowledge of the frequencies of occurrences of events near Eureka and in Baja California.

Some crude numerical observations of this kind have been made for events of M = 5 and larger. Because these maps are dominated by the smaller events in this range, the estimates refer to the relative frequencies of intermediate size earthquakes. For simplicity, we refer to three exterior domains (see Fig. 1) in terms of the directional symbols NW (Eureka vicinity), NE (western NV), and SE (Baja vicinity). Rough counts give a total of about 65 events in the NW zone, about 120 events in the SE zone, and about 100 events in the NE zone.

Events in the SFBA zone were preceded by events in one of these other three zones about 30 times (about half of the total in this zone; the others involved more complex paths involving other sites in the same zone and elsewhere). Of these 30 cases, the number of times each of the three zones was the precedent were about equal. That is, events in SFBA were preceded by an event in one of these zones about ten times in each case, giving ratios of about 1:7, 1:12, and 1:10, respectively, for preceding zones NW, SE, and NE. In other words, every time an event occurs in one of these other zones there is roughly an 8 to 14 percent chance that an event will occur in the SFBA zone before the next one in that zone. When it is also noticed that the temporal frequency of events in each of these three peripheral zones is roughly one per year, it is seen that this kind of observation offers potentially useful information for short-term predictions of intermediate-size events in the SFBA zone.

The above estimates are analogous to the digram probability that a given letter in the alphabet will be preceded by one of three other specific letters. A more restrictive test is to estimate the relative frequency that a given letter will be preceded by a given pair of two letters. Thus, it can be asked how often among the above counts was an event in the SFBA zone preceded by one of the six pairs of preceding sequences: NW--SE, NW--NE, SE--NE, SE--NW, NE--NW, and NE--SE? Of these six combinations, three appearto be dominant; these are the sequences SE--NE--SFBA (36%), SE--NW--SFBA (28%), and NE--SE--SFBA (20%). The other three sequences acount for the remaining 16%.

There are also sequences involving repeats within the SFBA zone and within each of the other zones, so a rigorous calculation of probabilities is much more complicated than this example. However, the above exercise tells us that not only can we get information about the probability of an event in a given zone from the frequency of events in other zones, but also that these estimates are increased or reduced by considering the frequencies of trajectory sequences among other zones that precede a given zone. For example, it would seem that an event in SFBA has a higher than average probability of occurrence when events occur successively in the Baja and western NV zones, in the Baja and Eureka zones, or in the western Nevada and Baja zones, in that order.

References:

Edelman, G.D., 1987, Neural Darwinism: The Theory of Neuronal Group Selection: N.Y., Basic Books, Inc.

Real, C.R., Toppozada, T.R., and Parke, D.L., 1978, Earthquake epicenter map of California: California Div. Mines and Geol., Map Sheet 39.

Shaw, H.R., 1987a, A linguistic model of earthquake frequencies applied to the seismic history of California: U.S. Geological Survey, Open-File Report 87-296, 129 p.

Shaw, H.R., 1987b, The periodic structure of the natural record, and nonlinear dynamics: Eos, Trans. American Geophys. Union, v. 68, p. 1651-1665.

Shaw, H. R. and B. Chouet, 1989, Singularity spectrum of intermittent seismic tremor at Kilauea Volcano, Hawaii: Geophys. Res. Letts., v. 16, p. 195-198.

Shaw, H.R. and Gartner, A.E., 1986, On the graphical interpretation of paleoseismic data: U.S. Geological Survey, Open-File Report 86-394, 92 p.

Sherburne, R.W., Boylan, R.T., and Parke, D.L., 1985, Seismicity of California, April, 1979 through October, 1982: California Geology, v. 38, p. 75-80.

Toppozada, T.R., Real, C.R., Bezore, S.P., and Parke, D.L., 1979a, Compilation of pre-1900 California earthquake history: California Div. Mines and Geol., Open-File Report OFR 79-6 SAC.

Toppozada, T.R., Real, C.R., and Pierzinski, D.C., 1979b, Seismicity of California, January, 1975 through March, 1979: California Geology, v. 32, p. 139-142.

Working Group On California Earthquake Probabilities, 1988, Probabilities of large earthquakes occurring in California on the San Andreas fault: U.S. Geological Survey, Open-File Report 88-398, 62 p.

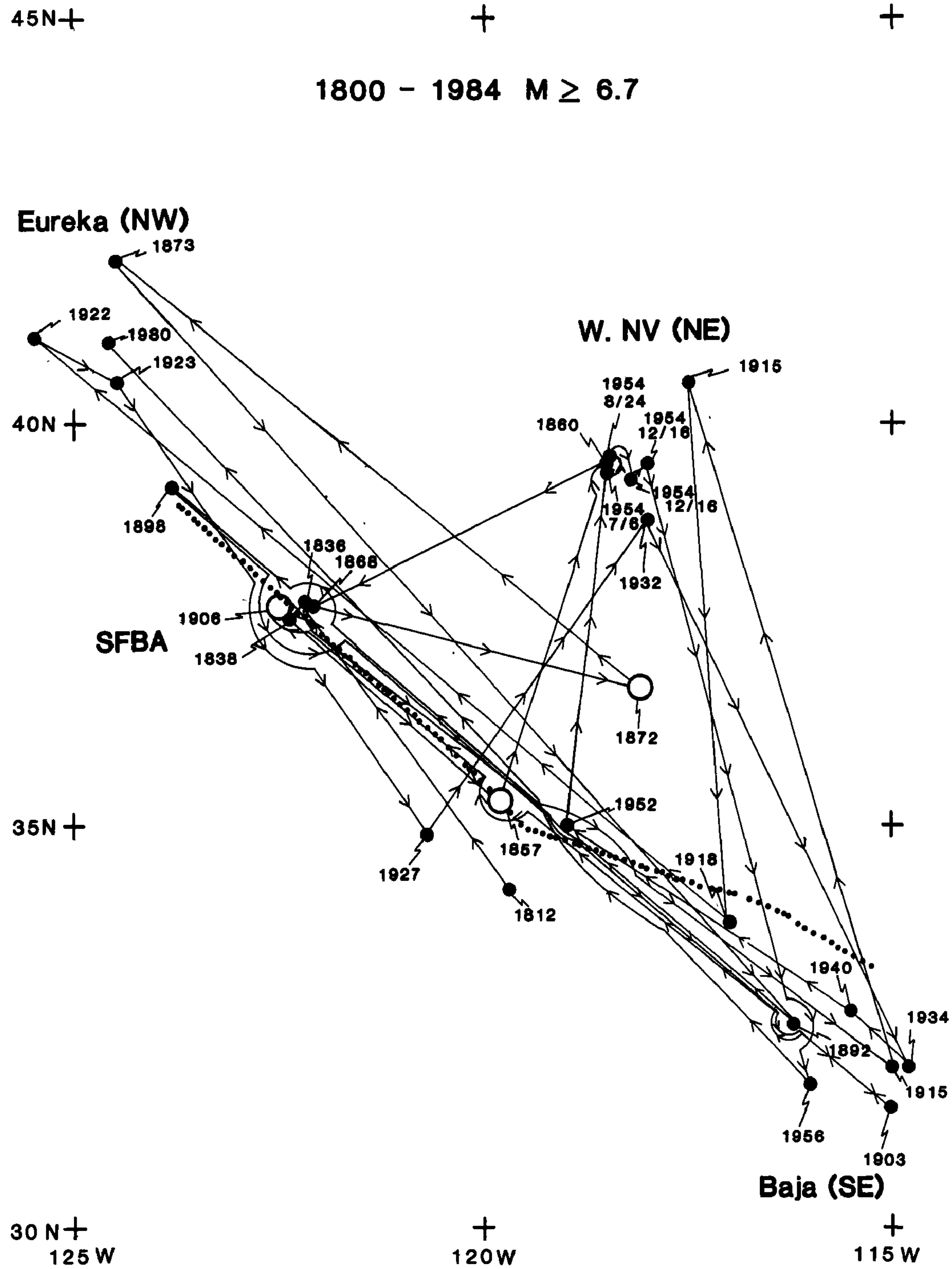

Figure 1. Index map drawn on orthogonal graph paper showing historic erathquakes in California and vicinity for magnitudes M > 6.6, and showing trajectories of temporal sequences (light lines with arrows). Open circles represent the three greatest earthquakes in the catalogs, having magnitudes of M ≈ 8. The general trend of the San Andreas fault system is shown by the dotted line.

FAULT PATTERNS AND STRAIN BUDGETS

9960-02178

Robert W. Simpson
Branch of Tectonophysics
U.S. Geological Survey
345 Middlefield Road, MS/977
Menlo Park, California 94025
(415) 329-4865

Investigations

Attempts to understand patterns of seismicity on the Calaveras fault have made it apparent that the Calaveras fault cannot be understood in any fundamental way unless it is viewed in the larger context of Bay Area faults. Mavko began such a study in 1982 by constructing a two-dimensional dislocation model of the Calaveras, Sargent, Busch, and San Andreas faults. He concluded that the distribution of earthquakes and creep required significant interactions between the various faults. I am building a three-dimensional dislocation model that will incorporate all of the important known tectonic elements in the Bay Area.

Results

The model will ultimately use on the order of 10^4 dislocation patches to simulate the faults and possible detachment surfaces. At best, it will be possible to infer information about the width of the shear zone at depth and the importance of horizontal decoupling surfaces in the regional tectonics. The models, although necessarily over-simple, may also permit us to keep a more quantitative accounting of the accumulations of stress within the system and to explore the effects of large earthquakes upon the equilibrium of the rest of the system. It will also be possible to explore the relation between uplift rates and topography as Bilham and King have done for the San Andreas fault farther to the south, and to predict rates of tectonic deformation and rotation for various blocks.

Present working models use about 1500 dislocation patches. Investigations have been slowed by a lack of disk space to hold the rather large files generated by such models. I hope that this project will evolve into a real interdisciplinary effort involving geologists, seismologists, modelers, geodesists and geophysicists.

MECHANICS OF LITHOSPHERE PLATES

9960-03419

William D. Stuart
Branch of Tectonophysics
U.S. Geological Survey
Pasadena, California 91106
818 405-7816

Investigations

Stressing Near a Strongly Coupled Subduction Zone

This study, with J. R. Rice and R. Dmowska, is an attempt to calculate time and space varying stress and deformation associated with repeated earthquake cycles at a subduction zone. Calculations are made with the ABAQUS finite element code for a vertical cross section in plane strain. In the model the lithosphere is elastic and the asthenosphere is Maxwell viscoelastic.

Locking of the Northern San Andreas Fault

This work is an attempt to explain why the north and south sections of the San Andreas fault are locked except for great earthquakes, whereas the central section has creep and small earthquakes. The problem is studied in terms of a two-dimensional plane stress model for faulting, and the fault is postulated to have a constitutive law wherein the rate of healing after an earthquake (*e.g.,* 1906 San Francisco) increases with effective confining pressure. Shear strain counteracts the healing. The pressure-dependent healing hypothesis is motivated by the suggestion of J. Byerlee that fault zone material can be viewed as a granular medium that becomes underconsolidated by deformation during an earthquake. A time-dependent boundary value problem is formulated and solved to simulate fault slip rate profiles, north to south, at successive times after an earthquake like the 1906 event. Effective confining pressure is assumed to vary along strike, being high in the currently locked northern section due to eastward traction applied across the Mendocino Fracture Zone by the subducting Gorda plate.

Results

Stressing Near a Strongly Coupled Subduction Zone

Results are described in the Semi-Annual Technical Summary by J. R. Rice.

Locking of the Northern San Andreas Fault

When the effective confining pressure on the central section of the model fault is several times less than on the neighboring sections, the neighboring sections become essentially locked in less than a year. The central section continues to creep at rates comparable to those observed on the San Andreas in central California. Another possible contribution to relatively low effective confining pressure on the creeping San Andreas may be high pore pressure, as suggested by Irwin and Barnes. Dislocations resulting from faulting associated with plastic flow of the Pacific plate around the bend in the San Andreas north of the Transverse Ranges might also decrease the effective confining pressure on the creeping section.

Reports

Stuart, W.D., Why the northern San Andreas fault has great earthquakes (abs.), AGU Fall Annual Meeting, 1989.

Rice, J. R., and W. D. Stuart, Stressing in and near a strongly coupled subduction zone (abs.), AGU Fall Annual Meeting, 1989.

Rupture geometries & kinematics of pseudotachylyte-bearing cataclastic strike-slip fault zones

14-08-0001-G1702

Mark T. Swanson
Department of Geosciences
University of Southern Maine
Gorham, Maine, 04038
207-780-5051

Investigations:

Continuing detailed mapping studies of Paleozoic strike-slip fault structures in the Cape Elizabeth Formation of coastal Maine have shown some intriguing structures, kinematic patterns and relationships. A 1.3 km long continuous coastal section at Two Lights State Park has been mapped at a scale of 1:300 using an airphoto base, three of the larger faults in these exposures have been mapped at a scale of 1:30, and a boudin field at a scale of 1:60 through photomosaic and grid mapping technique. The purpose of these studies is to better our understanding of the actual deformation mechanisms at work in accommodating paleoseismic displacements along these faults.

Observations:

Faulting in the Two Lights exposures has been accompanied by a diverse array of related structures (Swanson 1989b). The faults and related structures exhibit complex interrelationships that suggest they developed as a contemporaneous structural assemblage that varied through time. General characteristics of these faults and associated structures are as follows:

1.) The three larger faults with ~300 m outcrop lengths form an R-shear array adjacent to the more dominant Cape Elizabeth fault farther inland. Each fault has accommodated ~10 m of displacement but no linkage structures have developed between the faults. Each fault is shown to be made up of smaller en echelon segments that do show the details of linkage and strain accommodation across the offset-overlap zone. Linkages between smaller fault segments typically develop through contractional P-shear ramps, imbrication and duplex formation (Swanson 1988).

2.) The fault rocks are dominated by the production of cataclasite with no sign of mylonitization. Pseudotachylyte occurs in discontinuous fault-parallel veins of mm thickness, some with cm long orthogonal injection veins into the adjacent wall rock. Most veins occur within previously faulted host rock, crosscutting the cataclasites. Clasts of earlier pseudotachylyte can be observed in some cataclasite zones. Quartz and calcite cementation of the cataclasite and localized fault breccias is common. Deformation likely occurred under greenschist facies (and lower) metamorphism (abundant chloritization) at temperatures under 350^0 and depths of less than 10 km.

3.) Mesoscale adhesive wear features have been recognized that take the form of fault-bounded planoconvex lenses of wall rock adjacent to the main fault surfaces (Swanson 1989a). Adhesion during slip ruptures the sidewall resulting in both displacement and material transfer. These sidewall ripouts are generally in the 10 cm to 1 m slip-parallel length range. Direct observation of fault surfaces show remnant ripouts as thin fault-bounded patches, slightly elongate perpendicular to the slip direction. These fault patches are also slightly tilted during dextral shear due to rotation of the ripout slab along ramping contractional P-shears at the leading edge. Trailing mineralized tension fractures as well as leading and trailing localized mineralization are also common. The long-lived or permanent transfer of ripout or wear fragments creates significant geometric asperities with obvious restraining configurations. Subsequent ductile deformation of some of the larger ripout asperities is also apparent. Tensional fractures in the trailing fracture arrays have been deformed into sigmoidal configurations by clockwise rotation and reactivated with sinistral slip during dextral shear deformation. Multiple ripouts in nested arrays suggest persistence of the growing geometric asperities during repeated or continued slip that eventually leads to splay faulting in order to bypass the obstructions.

4.) Additional ductile and brittle-ductile deformation features in the adjacent host rock include a prominent F2 hinge-parallel ductile stretching lineation, dextral asymmetric shear band fabric and asymmetric foliation boudinage. The horizontal F2 hinge-parallel stretching lineation common throughout the Casco Bay area is defined in the Two Lights area by alignment of mineral aggregates, largely quartz grains in appropriate lithologies developed during ductile flow. The dextral shear band fabric is prominently developed in the more mica-rich layers and can be rather obscure, but still present in the more quartz-rich layers. The foliation boudinage is initiated intermittently as hinge-normal dilatant fractures, and parting surfaces mineralized with quartz and calcite. The veins are subsequently deformed by clockwise rotation, passive sinistral slip and elongation in dextral hinge-parallel dextral simple shear strain. Reoriented veins show consistent crosscutting relations with the younger less deformed veins at relatively high angles to the hinge-parallel lineation cutting the older more deformed veins at lower angles to the hinge-parallel lineation.

5.) The younger quartz-calcite veins show lesser degrees of rotation with no significant elongation and are typically several cm in width and upwards of 10 m in outcrop length. Some veins have been variably deformed into distinctly sigmoidal configurations with obvious rotation and sinistral slip. The youngest strictly planar veins often exhibt a sinistral oblique dilation. Most vein fractures are typically en echelon, strongly tapered, with relatively low length:width ratios. Some of the youngest fractures also exhibit short 20-50 cm veins that project orthogonally from the main vein with no observable cross-cutting relationships suggesting wall rock fracturing during inflation and fluid flow under relatively high hydrostatic pressures.

6.) The youngest fault structures in these exposures consist of conjugate sets of very planar faults that typically cut the entire width of the coastal exposures with up to 50 cm of displacement and develop with a rather small ~30^0 dihedral angle reflecting additional hinge-parallel extension.

Interpretation:

The fault structures under investigation appear to be part of a larger en echelon array representing an early stage of fault zone development. Abrasive wear is a dominant process related to the production of cataclasite but adhesive wear is also a significant process and a distinctive mesoscale deformation mechanism. These faults and related brittle-ductile deformation mechanisms and structures are interpreted to represent a paleoseismic zone with incremental coseismic slip events producing pseudotachylyte fault veins in cataclasite accompanied by an intervening bulk semi-brittle flow or creep through the development of shear band fabrics and asymmetric foliation boudinage. Faulting is also intimately associated with intermittent hydrofracturing of the adjacent rocks due to post-seismic dilatancy collapse and transient high hydrostatic fluid pressures. The apparent change in deformation mechanisms from ductile through brittle-ductile to dominantly brittle may be linked to progressive uplift and unroofing during deformation. The regional structural and tectonic framework suggests these faults and related structures may be related to the development of dextral transpression at a significant restraining bend and linkage complex in the regional Norumbega-Nonesuch River fault system. Investigations are continuing to define the spatial distributions of veins in relation to fault segments and to characterize the accompanying microstructural features and deformation mechanisms.

References:

Swanson, M.T. 1988. Pseudotachylyte-bearing strike-slip duplex structures in the Fort Foster Brittle Zone, S. Maine. *J. Struct. Geol.* **10,** 813-828.

Swanson, M.T. 1989a. Sidewall ripouts in strike-slip faults. *J. Struct. Geol.* **11,** in press.

Swanson, M.T. 1989b. Mesoscale Acadian deformation mechanisms during regional horizontal F2 hinge-parallel elongation and distributed dextral simple shear strain. *Geol. Soc. Amer. Abstr. with Prog.* **21,** in press.

STUDY OF THE CORRELATION BETWEEN WATER LEVEL FLUCTUATION AND RESERVOIR INDUCED SEISMICITY--PHASE I

14-08-0001-G-1713

Pradeep Talwani
Department of Geological Sciences
University of South Carolina
Columbia, SC 29208
(803) 777-6449

Introduction

Duke Power Company is constructing a pumped storage facility at Bad Creek in northwestern South Carolina. Construction on the project began a few years ago and all four dams are expected to be built by 1990. Bad Creek Reservoir will have a much smaller capacity than Lake Jocassee (Figure 1), although the depths of the two will be comparable. To generate electricity, water will flow through the one mile long tunnel onto the turbines located above Lake Jocassee. Water will be pumped back into Bad Creek when the demand for electric power diminishes. Due to the small reservoir capacity, the drawdown at Bad Creek is expected to be significantly larger and at a higher rate, than at other locations of reservoir induced seismicity (RIS). The objective of the research program is aimed at understanding the role of **rate** of lake level fluctuations on the nature of RIS.

Investigations

In the preimpoundment phase we began a two part study aimed at obtaining the background hydrological and seismological data. Figure 2 shows the locations of wells drilled by Duke Power Company to map the water table, a contour map of which is shown in Figure 3. After impoundment many of these wells will be submerged or under the dams. However, several wells surrounding the reservoir will be available for continued monitoring.

Figure 1 shows the locations of three permanent seismic stations in the Lake Jocassee/Bad Creek area. Data from these stations are telemetered to Jocassee Dam where they are recorded together with data from an additional station near Lake Keowee located to its South. Noise surveys were carried out at eleven sites in the vicinity of Bad Creek Reservoir, and three satisfactory sites were found.

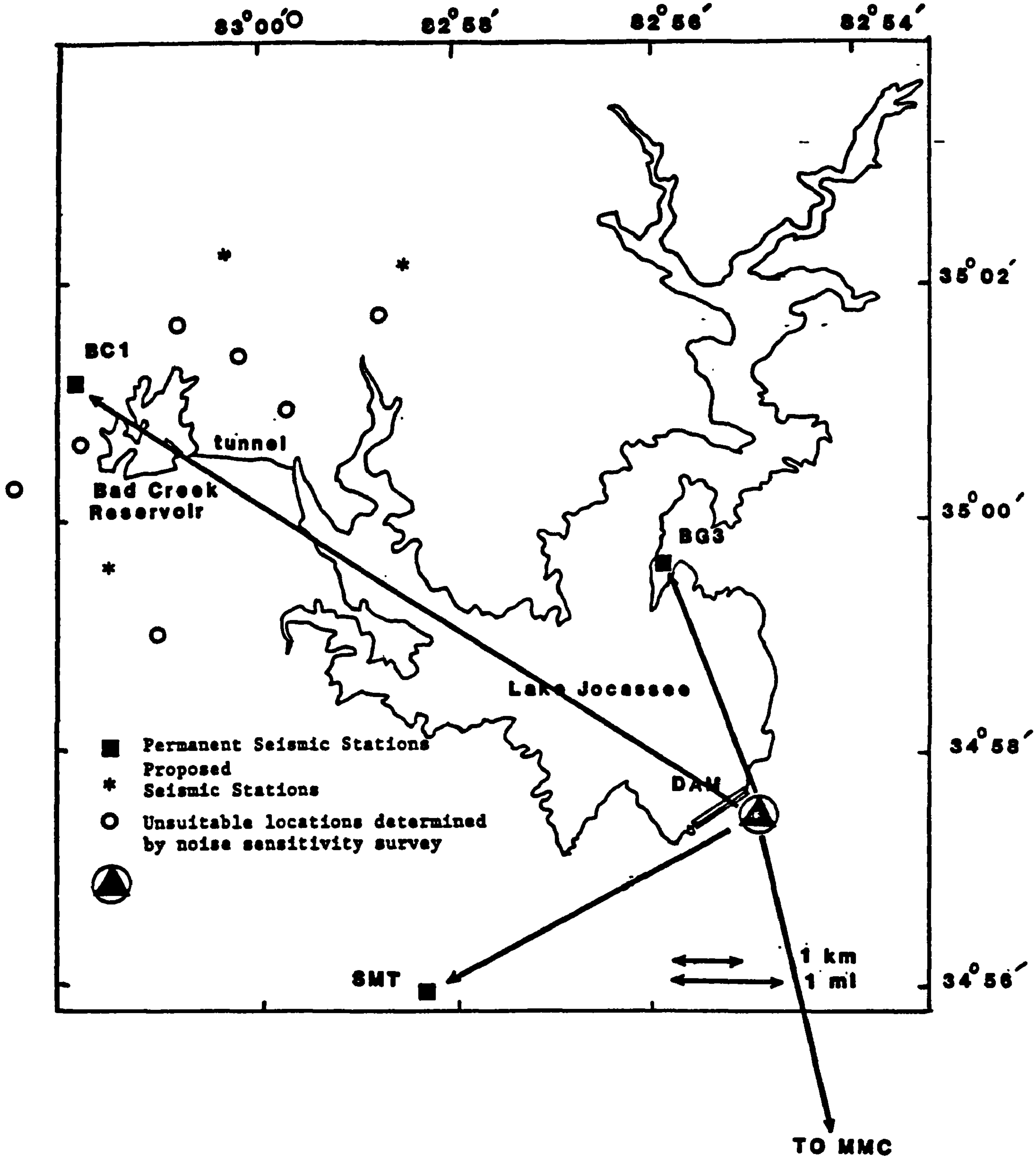

Figure 1. Location of current and proposed permanent seismic stations in the vicinity of Lake Jocassee and Bad Creek Reservoir.

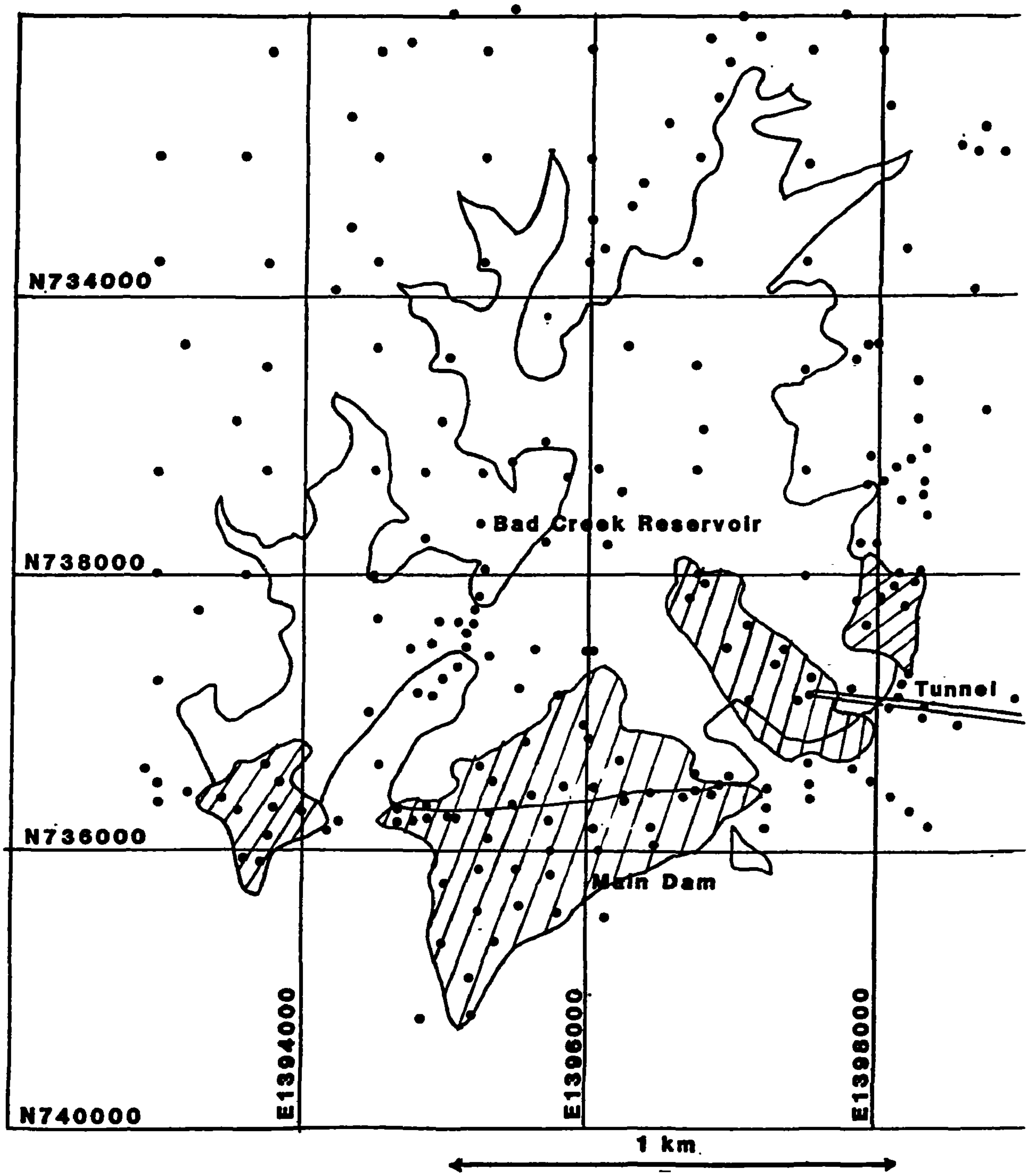

Figure 2. Shows locations of the four dams and observation wells drilled to map the ground water table. The expected outline of the reservoir when it is full is also shown.

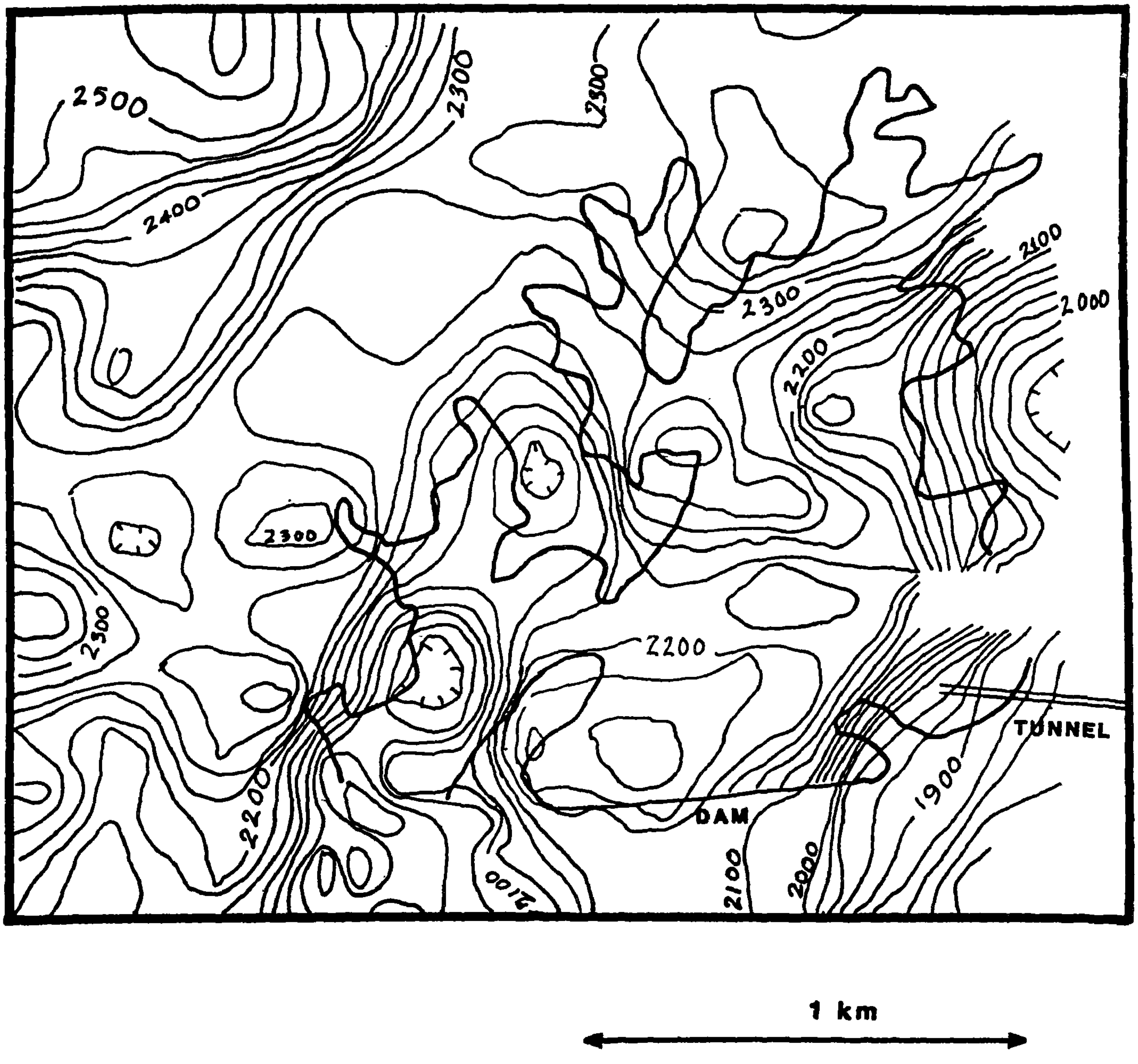

Figure 3. Contour map of elevation of ground water in feet above sea level. The anticipated outline of Bad Creek Reservoir is superimposed on the contour map.

Results

i. In the six month period, February 16 to August 15, 1989, we recorded 18 events with magnitudes less than 1.0 in the Bad Creek/Jocassee area.

ii. The contour map of the ground water level suggests very heterogeneous water elevations. The flow pattern following impoundment is expected to be extremely irregular and the monitoring wells will be selected to take this anticipated irregularity into account.

iii. Seismic noise surveys carried out over the summer of 1989 were seriously hampered by frequent thunderstorms. Of the eleven sites surveyed, three located on the property of Duke Power Company were found to be quiet and usable as permanent sites.

Planned Studies

Working together with Duke Power Company, we plan to identify observation wells for continued monitoring of the ground water. Additionally, we plan to install continuous monitors in a few selected wells.

Instead of telemetering seismic data to Columbia over 150 miles away, we are exploring the possibility of telemetering data to Jocassee Dam instead and recording it digitally. The data will then be called in by a PC in Columbia.

Reports

None.

EXPERIMENTS ON ROCK FRICTION CONSTITUTIVE LAWS APPLIED TO EARTHQUAKE INSTABILITY ANALYSIS

USGS Contract 14-08-0001-G-1364

Terry E. Tullis
John D. Weeks
Department of Geological Sciences
Brown University
Providence, Rhode Island 02912
(401) 863-3829

INVESTIGATIONS:

1. We have continued our studies of the constitutive behavior of serpentine.

2. We have completed a phase of our investigations into the frictional characteristics of granite and simulated granite gouge.

3. We have major technical improvements to our equipment under way.

RESULTS:

1. Because of the presence of serpentine in many faults, including the San Andreas and oceanic transforms, and the possible importance of serpentine in controlling the creep behavior of faults, we have continued our investigation of its frictional constitutive properties. Duplicate experiments at normal stresses of 25 and 50 MPa show consistent behavior as illustrated in Figure 1. The absolute magnitude of the velocity dependence is significantly larger than we find for other rock types, including granite. We find that at low slip velocity the behavior is velocity strengthening whereas at intermediate slip velocities there is a transition to velocity weakening. Preliminary experiments at higher normal stress (up to 150 MPa) indicate that the negative velocity dependence at intermediate velocities may become positive as the normal stress is increased. These results suggest that the velocity dependence of friction of serpentine is qualitatively similar to that of halite (results of Shimamoto, Logan and Chester). We tentatively conclude that the only conditions under which velocity weakening is found for serpentine is at low normal stress and intermediate slip velocities. This suggests that at nearly all crustal conditions, sliding of faults containing serpentine would be expected to show stable or aseismic sliding. In particular, our slowest experimental velocities approximate the average slip rate of the San Andreas Fault, and at these slip rates the velocity dependence appears to be positive at all normal stresses. This is in contrast to granite for which we find negative velocity dependence at low and intermediate slip rates. Although still preliminary, these findings support the speculation of Allen (1968) that serpentine may be responsible for the creeping behavior of the San Andreas fault in central California.

2. We have completed one phase of investigation of the velocity dependence of the friction of granite. It has been found previously that the presence or absence of simulated gouge (crushed granite) affects the sign and magnitude of **a-b** ($=d\mu_{ss}/d\ln V$), and that the frictional behavior evolves with displacement. It is important to resolve such questions because the velocity depen-

dence of steady state friction of rocks influences the stability of fault slip. To investigate these effects further, we slid Westerly granite in rotary shear at 25 MPa normal stress, room temperature, and velocities of 1 and 10 $\mu m\ s^{-1}$, both with and without layers of simulated gouge, to displacements up to 500 mm. It should be noted that some of the measurements on bare surfaces were made on unconfined samples and consequently have no errors caused by jacket friction. We are now in the process of implementing a sample design that will permit unconfined measurements on samples containing a layer of crushed granite simulated gouge.

We observe the following: 1) The frictional strength and **a-b** upon initiation of sliding depend strongly on the type of sample (bare or simulated gouge); 2) the coefficient of friction and **a-b** evolve over the first 10 to 20 mm to a relatively steady value; 3) the residual level of frictional strength depends on gouge layer thickness, with thinner layers being stronger; 4) after 50 to 100 mm of sliding on simulated gouge, **a-b** fairly abruptly becomes positive and, after about 300 mm frictional strength drops to quite low values. Observation 4) we have attributed to contamination of the sliding surfaces by Teflon from the sample jackets (which has been found in some of these samples), but this is still speculative. In detail, we observe that bare surfaces, which form about 0.1 mm of gouge, undergo a gradual rise in μ over ~20 mm of slip to ~0.75. A 1 mm layer of simulated gouge exhibits a peak in friction followed by a gradual drop to ~0.62 by 20 mm slip; a single run with a simulated gouge layer 0.3 mm thick showed μ of 0.70. Of more importance to stability of sliding, and earthquakes, is the evolution of **a-b**. Initially bare surfaces initially show **a-b** either positive or negative, but from 10 to 200 mm show a fairly constant value between -0.001 and -0.004. Simulated gouge initially shows positive **a-b** that evolves over 10 to 30 mm to a value of 0 to -0.0015. Thus, the velocity dependence of bare and gouge samples evolves from being quite different to being similar and negative in the displacement range of about 20 to 75 mm. Variations in surface roughness and particle size of simulated gouge also cause some initial differences that are eliminated by sliding to 10 to 20 mm. If the changes seen after 50 to 100 mm of slip are indeed caused by Teflon, then both bare surfaces and simulated gouge show velocity weakening after about 20 mm slip. This would mean that if granitic rocks along fault zones behave similarly, earthquakes might be expected to result during fault slip. This is in contrast to the behavior we find for serpentine in the same apparatus, as described above.

3. We are in the process of making a number of technological modifications to our equipment to allow better resolution, faster data collection, and more accurate measurements. We are converting to a Hewlett Packard data acquisition and computer system because it allows data to be collected with greater precision and at higher speeds; in addition, our existing DEC system has become unreliable and difficult to maintain. Because our sliding sample jackets could affect the data we are collecting, we have been assessing the possible role played by the Teflon and the O-rings in these jackets. As part of this we have been making internal measurements of the amount of eccentricity of our sample assembly and of the normal displacement of our samples. Occasional eccentricity may explain contamination of some samples by Teflon and we have begun to design a means of eliminating it. Measurement of normal displacement will help to determine the possible role of jacket compression on jacket corrections; it is also useful for measuring dilatancy during sliding. Dilatancy may affect frictional resistance- evaluation of its magnitude and evolution over large displacements is important in determining how much of the observed velocity dependence of frictional strength is caused by dilatancy and how much represents the intrinsic behavior of the material.

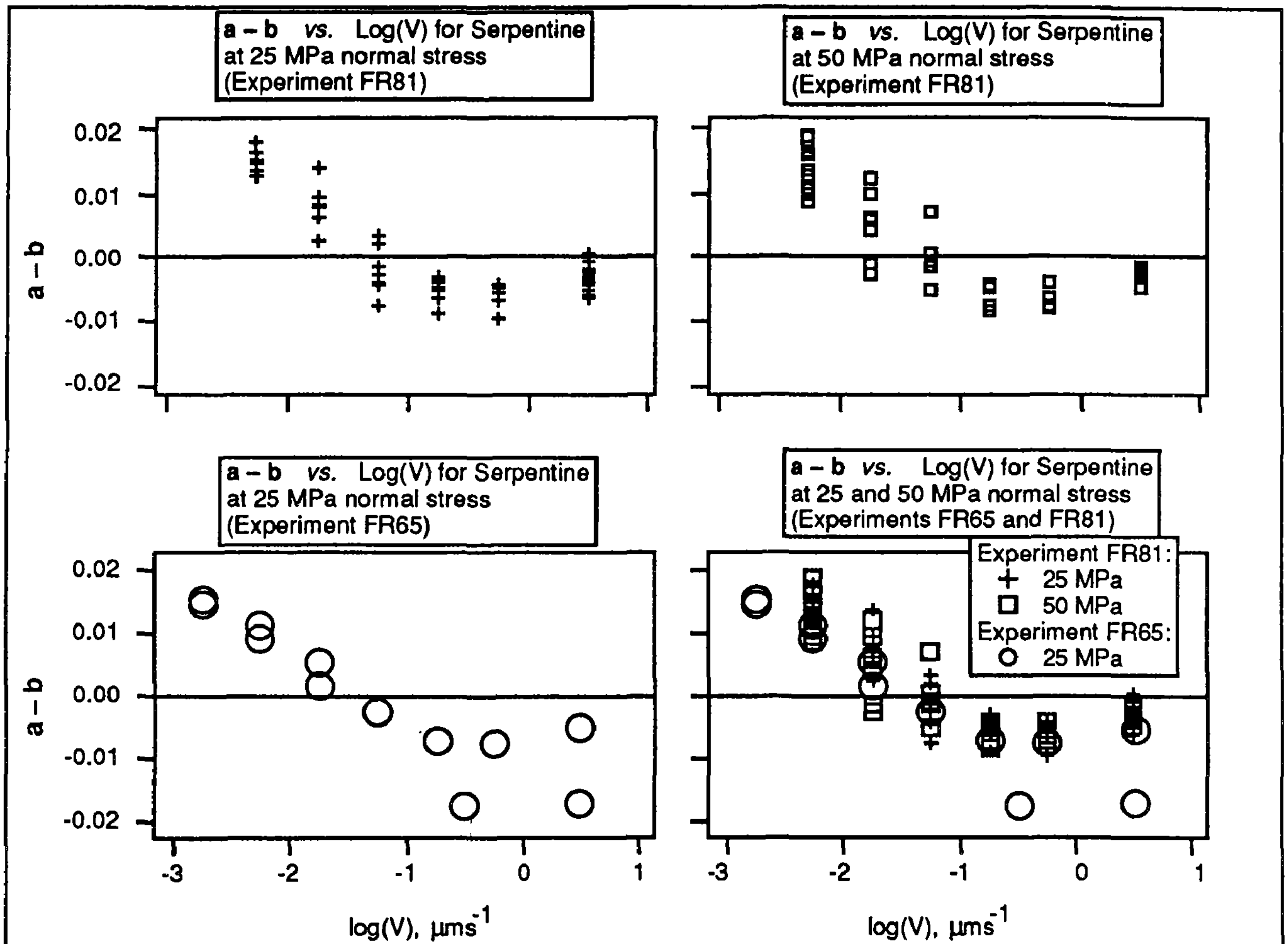

Figure 1. Comparison of velocity dependence of friction of serpentine at 25 MPa in two different experiments (FR81 and FR65), and at 25 and 50 MPa normal stress during the same experiment (FR81). These data have not been corrected for errors caused by jacket friction which we presently estimate to be ±0.001 to 0.002. The velocity dependence shown here is much larger than than we have measured for other materials. For instance, after 20 mm displacement, typical values of **a-b** for sliding on bare granite surfaces are -0.001 to -0.004 and for sliding on a layer of crushed granite simulated gouge are generally from -0.0015 to +0.001.

REPORTS:

Papers:

Lorenzetti, E.A., and T.E. Tullis, Geodetic predictions of a strike-slip fault model: implications for intermediate- and short-term earthquake prediction, *J. Geophys. Res., 94,* 12343, 1989.

Abstracts:

Blanpied, M. L., Weeks, J. D., and Tullis, T. E., Effects of sliding rate and shear heating on the velocity dependence of granite friction, submitted to AGU Fall Meeting, 1989.

Blanpied, M. L., Tullis, T. E. and Weeks, J. D., The velocity dependence of granite friction with and without simulated gouge, submitted to AGU Fall Meeting, 1989.

Regional and National Seismic Hazard and Risk Assessment

9950-01207

S.T. Algermissen
Branch of Geologic Risk Assessment
U.S. Geological Survey
Denver Federal Center, MS 966
Denver, CO 80225
(303) 236-1611

Investigations

1. On November 29-30, 1988, representatives of the Structural Engineers Association of California's Seismology Committee met with scientists and engineers of the U.S. Geological Survey to hear and discuss topical presentations related to the USGS's plans to produce a new generation of probabilistic ground motion maps. The overall goal was to identify the technical issues that need resolution so that they would not limit the application of the new maps in building codes and to forge a general agreement and plan for cooperation between the Seismology Committee and the USGS over the next several years.

2. Work on a new generation of probabilistic ground-motion hazard maps for the United States is proceeding along two parallel courses. One course follows a needs-assessment path that will provide engineering seismic design committees preliminary results of mapping new ground-motion parameters for a number of sites around the country so that the engineering community can determine which parameters best suit their needs for establishing sesimic design requirements for buildings. Input to these hazard evaluations, other than the new ground-motion parameters, is derived from the 1982 national ground-motion hazard maps for comparison with previous results.

3. Concurrently with investigation 2 above, work is continuing on reassessment of seismic source zones and seismicity, treatments of seismic parameter uncertainty and variability, and alternative procedures for incorporating site response into the national maps. Weekly meetings have been convened for the Hazard Assessment Group to review and discuss research progress and implementation concerning new seismic source zones, maximum magnitude estimates, earthquake recurrence rates, ground-motion attenuation and site response that, in the end, must be merged succesfully to create the new generation seismic hazard maps.

4. The computer program SEISRISK III (Bender and Perkins, 1987) for calculating probabilistic ground-motion hazard values has been adapted for use on personal computer systems. Documenting of the next-generation hazard evaluation program, FRIENDLY, continues as well as the concurrent development of a sophisticated graphics capability that will allow the analyst to call-up earthquake and geographic data displays interactively while in the program.

5. Work continues on the estimation of losses to dwellings in California using both deterministic (scenario) and probabilistic approaches. A new formulation is being investigated for determining the attenuation of Modified Mercalli Intensity with distance directly from primary observations of intensity. A new measure of the overall effect of an earthquake, called I_o', has been developed.

Results

1. Topical papers prepared by the Hazard Evaluation Group for the workshop "USGS's New Generation of Probabilistic Ground Motion Maps and their Applicaitons to Building Codes" were reviewed, revised and published in Open-File Report 89-364 (see "Reports").

2. Uniform hazard spectra are being calculated for 9 selected sites around the country. Return periods of interest in this study are 50, 100, 250, 500, 1000 and 2500 years for ground motion parameters of PHA (probabilistic horizontal acceleration), PHV (probabilistic horizontal velocity), and 5 percent damped pseudo-relative velocity (PSRVH) at periods of 0.1, 0.2, 0.5, 1, 2, and 4 seconds. The functional form used to model the scaling relationships between ground-motion, magnitude and distance is a variation of that of Campbell (1987):

$$lnY = a + bM + dln[R + c_1 exp(c_2 M)] - \alpha R + f_1 tanh[f_2(M + f_3)]$$

where Y is the strong-motion parameter of interest; M is earthquake magnitude; R is closest distance to seismogenic rupture in kilometers; α is the coefficient of anelastic attenuation per kilometer, and $a, b, ..., h_i$ are coefficients to be determined by the data. The equation was modified from Campbell (1987) to include the additional magnitude term, $f_1 tanh[f_2(M + f_3)]$, needed to model the magnitude dependence of PSRVH.

3. Regional geologic source zones for the eastern United States based on tectonic style and history, crustal ages and thickness, and related geological and geophysical properties are being documented. We assume that these regional differences in tectonic and crustal properties determine most regional differences in seismic activity rates and maximum magnitudes. For the western United States, a digital Quaternary fault data base is being compiled from available sources (Figure 1) to aid in seismic source zone evaluations for that region.

4. Since Bender and Perkins (1987) published the standard USGS program for seismic ground-motion hazard mapping, SEISRISK III, there has been increasing requests in the seismological and engineering communities for a version of the program adapted for microcomputers. The microcomputer version of SEISRISK III requires at least 640 KB of random access memory (RAM) and a mathematical co-processor for operation under DOS and at least 3 MB of RAM and a co-processor for operation under OS/2. Lesser quantities of RAM and the lack of a co-processor can be accomodated by some simple changes in the source code. However, operation with much less than 512 KB RAM is not possible under "native" DOS, that is, DOS loaded alone as opposed to the DOS "window" in OS/2. The lack of a co-processor also increases the required memory as well as increases the running time.

The program FRIENDLY is the next generation ground-motion mapping software and is designed to allow the analyst to rapidly test the effects on probabilistic ground-motion calculations of varying source locations, seismicity parameters, attenuation functions, etc. Therefore, the analyst is permitted to interactively enter source zone coordinates, to specify seismicity parameters (a and b-values, magnitude range, direction of faulting-if any), to specify boundary location uncertainty for each source, to enter an attenuation function, to define attenuation variability, to select sites (either single sites, a line of sites or a grid of sites) at which computations are to be performed, to specify time and probability levels of interest, and to indicate the type of output desired at the terminal (e.g., ground motions with a fixed probability of exceedance) and the type of output to be saved on a file. The dipping-plane rupture algorithm is an advanced version of that found in SEISRISK III and allows ruptures on articulated planes. That is, continuous ruptures are allowed across intersections of dipping planes if desired.

5. Probabilistic and deterministic loss models are being developed using Modified Mercalli Intensity as a measure of ground shaking. Intensity is being used because, at present, loss vulnerability relationships (replacement cost vs. ground shaking) are based on MM intensity. A related study was undertaken to define a quantity which can be derived from primary intensity observations which would represent a measure of earthquake-source energy in much the same way as does magnitude. That quantity is defined as I_o'. I_o' is interpreted as an intensity unique to a particular earthquake and respresentative of its overall size such that $I_o' \equiv M_s$, to the accuracy that either M_s or I_o' can be computed. A selection of earthquakes from the southern San Andreas fault province was used for a regional intensity attenuation relation:

$$I - I_o' = I - M_s = -0.006 - 0.496 log_{10}(1 + r/10)$$

where r is the source to site distance in kilometers. For 11 earthquakes in this province having a good distribution of intensity observations, regressions of I_o' on M_s and M_s on I_o' are

$$I_o' = (1.003 \pm 0.017)M_s \quad M_s = (0.994 \pm 0.017)I_o'$$

Therefore, to the accuracy that either M_s or I_o' can be computed, $I_o' \equiv M_s$ for Southern California in the range of $\approx 4.5 \leq M_s \leq\approx 7.7$.

Reports

Algermissen, S.T., 1990, Earthquake ground motion and economic losses in the Central United States [abs.]: American Association for the Advancement of Science Symposium, Earthquake Hazard and Risk in the Central United States, in press.

Algermissen, S.T., Hays, W.W., and Singh, J.P., 1989, Executive summary, *in* Hays, W.W., ed., Proceedings of conference XLVII - A workshop on "USGS's new generation of probabilistic ground motion maps and their application to building codes": U.S. Geological Survey Open-File Report 89-364, p. 1.

Algermissen, S.T., 1989, The U.S. Geological Survey program in probabilistic ground motion assessment, *in* Hays, W.W., ed., Proceedings of conference XLVII - A workshop on "USGS's new generation of probabilistic ground motion maps and their application to building codes": U.S. Geological Survey Open-File Report 89-364, p.10-11.

Algermissen, S.T., 1989, Basic probabilistic models used in hazard maps, *in* Hays, W.W., ed., Proceedings of conference XLVII - A workshop on "USGS's new generation of probabilistic ground motion maps and their application to building codes": U.S. Geological Survey Open-File Report 89-364, p. 90-91.

Arnold, E.P., in review, I_o': Relationships between macroseismic epicenter, attenuation and magnitude.

Arnold, E.P., 1989, Program Seisrisk III adapted to personal computers: U.S. Geological Survey Open-File Report (in press).

Bender, Bernice, and Perkins, D.M., 1989, Treatment of parameter uncertainty and variability in seismic hazard maps, *in* Hays, W.W., ed., Proceedings of conference XLVII

– A workshop on "USGS's new generation of probabilistic ground motion maps and their application to building codes": U.S. Geological Survey Open-File Report 89-364, p. 57-73.

Campbell, K.W., 1989, Proposed revisions to the Uniform Building Code – Issues related to the specification of ground motion, *in* Hays, W.W., ed., Proceedings of conference XLVII – A workshop on "USGS's new generation of probabilistic ground motion maps and their application to building codes": U.S. Geological Survey Open-File Report 89-364, p. 26-34.

Leyendecker, E.V., 1989, The design earthquake – Some issues for decision, *in* Hays, W.W., ed., Proceedings of conference XLVII – A workshop on "USGS's new generation of probabilistic ground motion maps and their application to building codes": U.S. Geological Survey Open-File Report 89-364, p. 15-17.

Perkins, D.M., 1989, Probabilistic seismic hazard assessment – Some trends in the USGS approach, *in* Second symposium on current issues related to nuclear power plant structures – Equipment and piping with emphasis on resolution of seismic issues in low seismicity regions, December 7-9, 1988, Orlando, Florida: Journal of Nuclear Engineering and Design, 20 ms. p., (in revision).

Perkins, D.M., 1989, How should the effect of site conditions be represented on probabilistic ground motion hazard maps? *in* Hays, W.W., ed., Proceedings of conference XLVII – A workshop on "USGS's new generation of probabilistic groundmotion maps and their application to building codes": U.S. Geological Survey Open-File Report 89-364, p. 35-38.

Rogers, A.M., 1989, The importance of geologic conditions on the level of strong shaking – Application to national probabilistic hazard maps: *in* Hays, W.W., ed., Proceedings of conference XLVII – A workshop on "USGS's new generation of probabilistic ground motion maps and their application to building codes": U.S. Geological Survey Open-File Report 89-364, p. 92-97.

Thenhaus, P.C., and Wheeler, R.L., 1989, A new generation of ground-motion hazard maps – Seismic source zones revisited, *in* Hays, W.W., ed., Proceedings of conference XLVII – A workshop on "USGS's new generation of probabilistic ground motion maps and their application to building codes": U.S. Geological Survey Open-File Report 89-364, p. 41-44.

Wheeler, R.L., and Thenhaus, P.C., 1989, Source zones and earthquake rates in the East, *in* Hays, W.W., ed., Proceedings of conference XLVII – A workshop on "USGS's new generation of probabilistic ground motion maps and their application to building codes": U.S. Geological Survey Open-File Report 89-364, p. 45-48.

References Cited

Bender, Bernice, and Perkins, D.M., 1987, SEISRISK III – A computer program for sesismic hazard estimation: U.S. Geological Survey Bulletin 1772, 48 p.

Campbell, K.W., 1987, Predicting strong ground motion in Utah, *in* Gori, P.L., and Hays, W.W., eds., Assessment of regional earthquake hazard and risk along the Wasatch Front, Utah: U.S. Geological Survey Open-File Report 87-585, v. II, p. L1-L90.

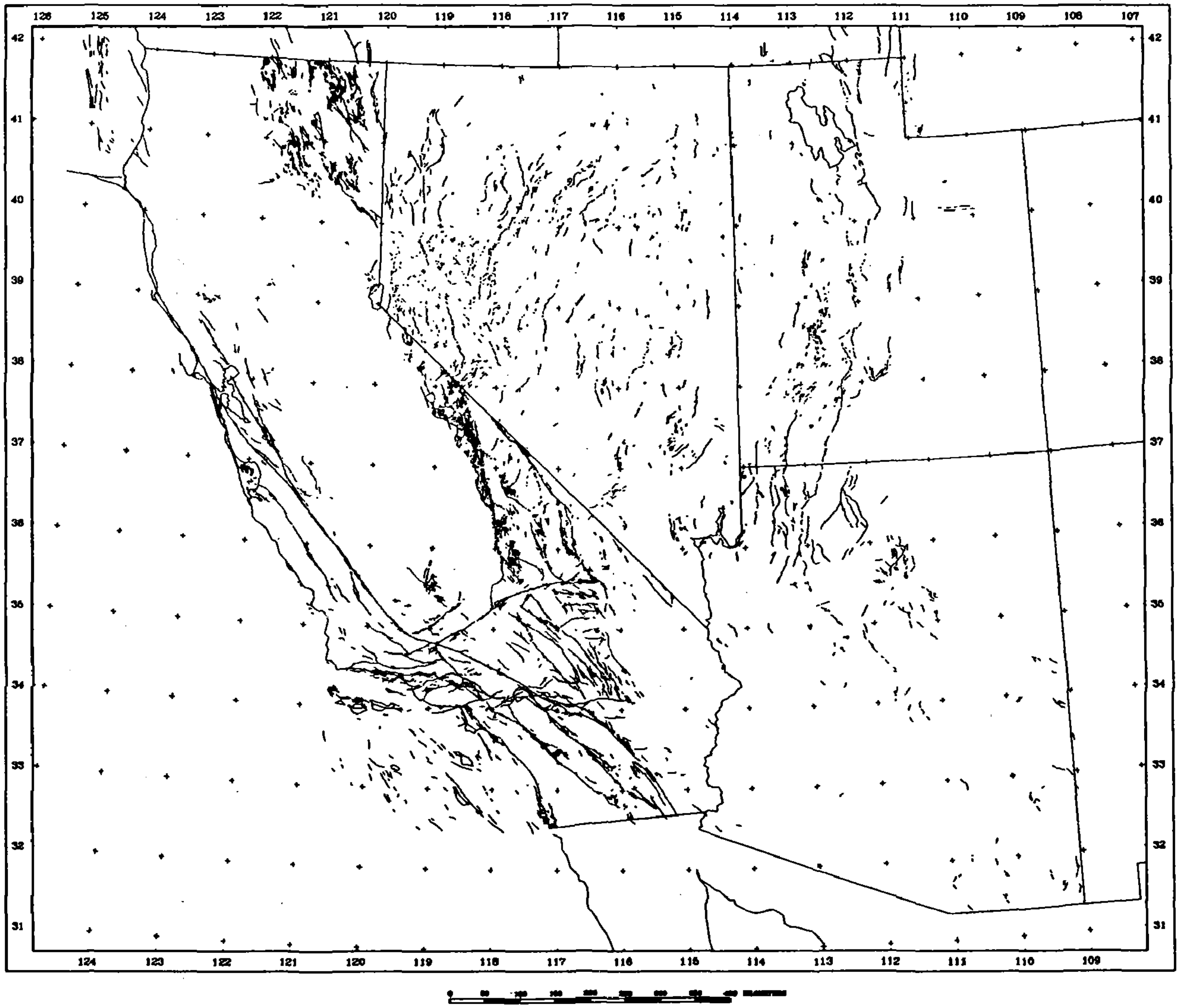

Figure 1. Preliminary map of Quaternary and suspected Quaternary faulting in part of the Western United States compiled in digital format from various sources.

REGIONAL AND LOCAL HAZARDS MAPPING IN THE EASTERN GREAT BASIN

9950-01738

R. Ernest Anderson
Branch of Geologic Risk Assessment
U.S. Geological Survey
Box 25046, MS 966, Denver Federal Center
Denver, CO 80225
(303) 236-1584

INVESTIGATIONS

1. Conducted field studies of range-bounding and transverse faults in the Mormon and East Mormon Mountains areas, Clark County, Nev.

2. Constructed cross sections of the upper crust in the Mesquite basin-Virgin Mountains-Beaver Dam Mountains areas and experimented with strain-field modeling of the largest structures in those areas.

3. Continued investigation of the tectonic geomorphology of northwest Greece.

4. Continued investigation of the structural control of drainage alinements in the Clover Mountains, Nevada-Utah.

RESULTS

1. Fault-slip measurements and selected detailed mapping in the Mormon and East Mormon Mountains show that north-striking range-bounding faults have significant components of sinistral strike slip, whereas east-west transverse faults lack evidence of uniform-sense strike slip and are mainly zones of structural accommodation for strong vertical tectonics and crustal attenuation. These results are the reverse of published results. The discrepancies indicate a need for reappraisal of some of the simplistic notions of uniform-sense lithosphere-penetrating simple shear that have been spawned in this area.

2. Our cross sectional strain-field modeling of zones of extreme uplift and subsidence analogous to that seen between Mesquite basin and the North Virgin Mountains reveals distributions of areas of compression and extension that are compatible with geologic maps and cross sections. The modeling does not include an early episode of tectonic denudation on low-angle faults. Instead, it indicates that the observed structural relief is consistent with evolution on a system of steep faults.

3. Completed and submitted for review an interpretive report in which the major aspects of the tectonic geomorphology of northwest Greece are shown, through an iterative process of boundary-element modeling, to be consistent with a small-plate motion vector for the adjacent north-central Mediterranean of $95° \pm 10°$. This vector is 75° anticlockwise of that previously reported for the area and thus has important implications for the regional kinematics.

4. Spectacularly straight drainages in the northern Clover Mountains, Nevada and Utah, owe their straightness to steep panels of disseminated and vein-type carbonate that makes interfluvial areas slightly more resistant to erosion than the areas occupied by the drainage channels. The carbonate was

apparently introduced from upward-circulating ground water, and its distribution was controlled by steep north- and northeast-striking fractures and joints. The carbonate currently resides above a siliceous igneous terrain from which it probably was not derived. Instead, it was deposited in the late Tertiary from a south-flowing, deeply circulating regional carbonate aquifer system that had its southward flow path impeded by the enormous Caliente caldera system. That caldera complexes can function as barriers to regional ground-water flow has important implications in the evaluation of hydrologic isolation of underground engineered facilities proposed for such a setting.

REPORTS

King, G.C.P., Sturdy, D.A., and Whitney, J.W., 1989, Determining plate-motion directions from active structures in northwestern Greece [abs.]: EOS [Transactions of the American Geophysical Union] (in press).

Anderson, R.E., and Christensen, G.E., 1989, Quaternary faults, folds, and selected volcanic features in the Cedar City 1° x 2° quadrangle, Utah: Utah Geological and Mineral Survey Miscellaneous Publication 89-6, 29 p.

Depth to Bedrock Map in the Greater Tacoma Area, Washington

9950-04073

Jane M. Buchanan-Banks
Branch of Geologic Risk Assessment
U.S. Geological Survey
David A. Johnston Cascades Volcano Observatory
5400 MacArthur Boulevard
Vancouver, Washington 98661
(206) 696-7996

Investigations

Depth to bedrock in the southern Puget Basin is being determined with data obtained from logs of deep water, oil, and mineral exploration wells collected from published and unpublished sources throughout the Tacoma and part of the Centralia 30′ by 60′ quadrangles (scale 1:100,000). Thickness of unconsolidated deposits beneath the seawater-sediment boundary is being determined with data from reconnaisance high resolution marine seismic surveys (Snavely and others, 1977) together with new multichannel data (Harding and others, 1988) in the Colvos Passage-Commencement Bay area.

Results

Collection of basic data and plotting of all wells with verified locations have been completed for all counties. Preliminary isopachs have been drawn for the southern and eastern parts of the map. Isopachs for the western and northern parts of the map will be drawn when analysis of marine seismic-reflection data is complete.

Various state, city, and county departments, and geologic consulting firms have been contacted regarding unpublished data on deep wells. Some deep wells located in a part of the map with little other deep data are being investigated. Attempts to obtain logs and to verify well locations continues.

Semiconsolidated to unconsolidated fluvial and lacustrine sedimentary rocks of Tertiary age crop out locally in parts of Pierce, Thurston, and King counties. These deposits cannot readily be distinguished in well logs from the overlying unconsolidated Quaternary deposits due to similarities in lithologies and degree of consolidation. Thus some thicknesses of unconsolidated materials on the map will include deposits that are considered to be Miocene in age.

Publications

Castle, R.O., and Buchanan-Banks, J.M., 1989, Vertical surface displacements along a part of the Newport-Inglewood zone of folds and faults, Los Angeles and Orange Counties, California: U.S. Geological Survey, Miscellaneous Field Studies Map MF 2088, 2 sheets.

Buchanan-Banks, J.M., Lockwood, J.P., and Rubin, Meyer, 1989, Radiocarbon dates for lava flows from northeast rift zone of Mauna Loa Volcano, Hilo 7 1/2′ quadrangle, island of Hawaii: Radiocarbon, v. 32, no. 2, 8 p.

References

Snavely, P.D., Jr., Gower, H.D., Yount, J.C., Pearl, J.E., Tagg, A.R., and Lander, D.L., 1977, High resolution seismic profiles in Hood Canal and southern Puget Sound, Washington: U.S. Geological Survey Open-File Report 77-195.

Harding, S.T., Barnhard, T.P., and Urban, T.C., 1988, Preliminary data from the Puget Sound multichannel seismic reflection survey: U.S. Geological Survey Open-File Report 88-698, 7 p.

PUGET SOUND PALEOSEISMICITY

9950-04484

Robert C. Bucknam
Branch of Geologic Risk Assessment
U.S. Geological Survey
Box 25046, MS 966, Denver Federal Center
Denver, Colorado 80225
(303) 236-1604

INVESTIGATIONS

1. Continued fieldwork at two sites of late Holocene uplift in the central Puget Lowland, Washington. The primary emphasis of the fieldwork was on refining stratigraphic relationships and the collection of samples for radiocarbon dating.

RESULTS

1. A trench was excavated across part of a raised beach bar and the adjacent lagoonal sediments on the landward side of the bar at Restoration Point on Bainbridge Island. The trench shows that the bar overlies 60 cm of silty sand that contains brackish water diatoms. The silty sand, which extends to within 20 cm of the present ground surface, overlies several meters of peat, the upper part of which has been dated as 1,770±70 yr B.P. Radiocarbon ages of subrounded fragments of carbonized wood that were collected from trench exposures of the upper part of the silty sand unit will more closely constrain the maximum age for the uplift of the platform and associated marine deposits at Restoration Point.

PUBLICATIONS

Bucknam, R.C., and Barnhard, T.P., 1989, Evidence of sudden late Holocene uplift in the central Puget lowland, Washington [abs.]: EOS [Transactions of the American Geophysical Union], v. 70 (in press).

QUATERNARY TECTONICS OF THE WICHITA FRONTAL FAULT SYSTEM, OKLAHOMA

9950-04419

Anthony J. Crone
Branch of Geologic Risk Assessment
U.S. Geological Survey
Box 25046, MS 966, Denver Federal Center
Denver, CO 80225
(303) 236-1595

INVESTIGATIONS

1. Continue analysis and interpretation of potential field data to clarify structural relations across the Wichita Frontal fault system in the area of the Meers fault.

2. Begin interpretation of industry seismic-reflection profile across the Wichita Frontal fault system.

3. Completed report on investigations of the late Quaternary history of the Meers fault in Comanche County, Oklahoma.

RESULTS

1. A series of 1:100,000 scale maps have been generated from digitized aeromagnetic data, and new (600 stations) and existing gravity data (collected, reduced, and compiled in cooperation with S.L. Robbins, Branch of Sedimentary Processes, USGS, Denver). Total magnetic field intensity reduced to the North Pole, horizontal derivative of the pseudogravity of this magnetic field, Bouguer and isostatic gravity anomalies, and horizontal derivative of the isostatic anomalies have been prepared in color and black-and-white contour maps for the Lawton 1:100,000 quadrangle. These maps help define the boundaries of blocks within the Wichita uplift, identify an area in the subsurface of folded and faulted high-density/susceptibility rock northeast of the Meers fault, and show possible splays of the Meers fault a few kilometers northwest of the end of the prominent Holocene fault scarp. In the same area, a 9,673-foot-deep well (the Standolind-#1 Perdosopfy), penetrated basalts and spilites of the Navajoe Mountain Group (Ham and others, 1964), which are likely sources of the strong gravity and magnetic signatures. The patterns of the magnetic signature and, to a lesser extent, the gravity signature suggest that the rocks northeast of the fault are deformed into broad folds. The pattern and orientation of these folds are consistent with the style of deformation that would result from left-lateral strike-slip movement on the fault. As reported previously, these maps (especially, the map of the horizontal derivative of the pseudogravity) show that the Meers fault splays in the subsurface a few kilometers northwest of the end of the Holocene fault scarp. These splays may be part of a structural barrier that divides the fault into separate rupture segments.

Preliminary models that simultaneously combine the gravity and magnetic data show a slight up-to-the-north displacement of the high susceptibility rocks near the southeastern end of Meers fault scarp. Earlier models based only on aeromagnetic data showed a clear down-to-the-north displacement of high susceptibility rocks near the northwestern end of the fault scarp. These relations imply that the subsurface rocks north of the fault are tilted or rotated in a scissor-like fashion.

Additional field studies will investigate the nature of a dike-like body immediately south of the Meers fault that has been identified by Purucker (1986) from aeromagnetic data and ground magnetic surveys.

2. We purchased 28.5 km of a 512-fold, non-exclusive, seismic-reflection line that extends across the Wichita Frontal fault system from the Anadarko basin to the Wichita uplift in conjunction with the Branch of Petroleum Geology (USGS, Denver). The line extends from near Apache, Oklahoma on the northeast to the foot of the Wichita Mountains near Lake Lawtonka on the southwest. These data have been almost completely reprocessed by personnel in the Branch of Petroleum Geology.

The reprocessed record sections show several prominent structural features associated with the Wichita Frontal fault system, including the thick, well-stratified Paleozoic sedimentary rocks in the Anadarko basin and truncated reflectors at the Mountain View fault. Along the southwestern half of the profile, a strong, continuous reflection is present on the upper 300 ms of the section. This reflection appears to be vertically displaced stepwise down-to-the-south across several faults within a distance of about 1.6 km. The major displacement in this reflector is very close to the scarp on the Meers fault and is estimated to have a throw of about 100 m, based on depth calculations using stacking velocities for the profiles. The down-to-the-south displacement of this reflection has the same sense of throw indicated by the topographic relief on the scarp. The biggest scarp is only 5 m high (Ramelli and others, 1987) compared to about 100 m of throw in the shallow subsurface. Southwest of the Meers fault, this reflection is flat-lying and continuous to the end of the record section.

In the area of the Meers fault, abundant refracted energy is present between the shallow reflection and 1.5 s. From 1.5 s to the bottom of the record section (5.4 s) reflections are discontinuous but appear to be subhorizontal to gently dipping.

3. Stratigraphic relations and radiocarbon ages of deposits exposed in trenches and excavations at five sites on the Meers fault help establish the timing, sense of slip, and style of deformation caused by Holocene surface faulting. Radiocarbon dating of soil-humus samples from these sites shows that the last surface-faulting occurred about 1,200-1,400 years ago. A comprehensive report describing these investigations is scheduled for publication in the Geological Society of America Bulletin in early 1990.

REPORTS

Crone, A.J., and Luza, K.V., 1990, Style and timing of Holocene surface faulting on the Meers fault, southwestern Oklahoma: Bulletin of the Geological Society of America.

Jones-Cecil, Meridee, and Crone, A.J., 1989, Constraints on the Anadarko basin-Wichita uplift boundary interpreted from aeromagnetic data, *in* Johnson, K.S., ed., Anadarko Basin Symposium, 1988: Oklahoma Geological Survey Circular 90, p. 228-232.

Robbins, S.L., Jones-Cecil, M., and Keller, G.R., Jr., 1989, Regional gravity of the Anadarko basin area and a more detailed look at the Wichita Frontal fault zone, *in* Johnson, K.S., ed., Anadarko Basin Symposium, 1988: Oklahoma Geological Survey Circular 90, p. 225-227.

REFERENCES CITED

Ham, W.E., Denison, R.E., and Merritt, C.A., 1964, Basement rocks and structural evolution of southern Oklahoma: Oklahoma Geological Survey Bulletin 95, 302 p.

Purucker, Michael, 1986, Interpretation of an aeromagnetic survey along the Wichita Frontal fault zone, *in* Gilbert, M.C., ed., Petrology of the Cambrian Wichita Mountains igneous suite: Oklahoma Geological Survey Guidebook 23, p. 129-136.

Ramelli, A.R., Slemmons, D.B., and Brocoum, S.J., 1987, The Meers fault--Tectonic activity in southwestern Oklahoma: U.S. Nuclear Regulatory Commission NUREG/CR-4852, 25 p.

SEISMICITY AND HYDROTHERMAL PROCESSES

9950-01574

W.H. Diment and T.C. Urban
Branch of Geologic Risk Assessment
U.S. Geological Survey
Box 25046, MS 966, Denver Federal Center
Denver, CO 80225
(303) 236-1574/1625

INVESTIGATIONS

1. Studied relations among seismicity, tectonism, and hydrothermal regime in the west moat of the Long Valley caldera, California.
2. Refurbished logging truck, logging system, and some logging tools. Calibrated temperature-sensing probes. Constructed and calibrated a multi-element thermistor cable for use in air-filled holes.
3. From 7/20/89 to 7/29/89, obtained temperature logs in some deep boreholes in the Long Valley caldera: PLV-1, PLV-2, RDO8, CW-1, CW-3, M-4, MLGRAP-1, and MLGRAP-2. Natural gamma-ray logs were obtained in: M-4, CW-3, MLGRAP-1 and MLGRAP-2.

RESULTS

Examples of the kind of information obtained this Summer are shown in figures 1 and 2. These wells were drilled in the Town of Mammoth Lakes as part of the Mammoth Lakes Geothermal Resource Assessment Project (MLGRAP).

The core was logged by Douglas Goodwin for The Town of Mammoth Lakes (California Division of Oil and Gas, Well Summary Report-Geothermal, 1988, A.P.I. Nos. 051-90120 and 051-90121). In the figures, his logs have been generalized as follows; White, glacial till. Dots, basalt. Vertical pattern, rhyolite. Horizontal pattern, tuff, cinders, ash, breccia, lapilli, and other volcanic rocks. Other symbols in figures are: W.L. (– – – –), water level. A, B, B1, B2, C (· — · — ·—) top (if not surface) and bottom of casing strings. T.D. (— – — – —), total depth drilled.

Temperatures were measured with a thermistor probe (time constant of 2 s in water) lowered at a rate of 3 m/min and recorded and plotted at 0.3 m intervals. Temperatures recorded in the air column are meaningless without further corrections, because the time constant of the probe is much longer in air than in water. Laboratory calibrations were made one month before logging and have not been repeated yet. So the results must be regarded as "preliminary", although the corrections are usually so small that they would not be evident at the scale shown.

Temperature gradients were calculated over 0.61 m intervals of depth. Note that the gradient scale is different for the two holes. The gradients are a bit "ratty" because of convection in the borehole (Diment, 1967; Urban and Diment, 1985). But, even when determined over 3 m intervals (not shown), the major features are preserved. Note that the gradients vary smoothly with depth when the gradient is negative.

Both holes (particularly MLGRAP-1) exhibit temperature "noses", that is, temperature maxima followed by minima with depth. These are common in the Long Valley caldera. In most cases, the temperature nose can be attributed to hot water flow along an aquifer of high permeability, which, in this environment, is usually an unaltered volcanic rock. Our thesis has been (Urban and others, 1987) that flow of hot waters through such zones results in hydrothermal alteration of these permeable zones to less permeable clays, and a consequent upward migration of flow with time. Perhaps we see this process in operation in MLGRAP-1. The temperature gradients above the nose (~ 150m) vary from positive to negative over small intervals of depth, although they were obtained 1.5 yr after drilling when we would have expected the drilling disturbance to have subsided. This is not strictly so when massive amounts of fluid have been pumped into permeable formations of large thickness (for example, Nathenson and others, 1979). In the case of MLGRAP-1, we suspect flow of water in the formation or along an imperfectly cemented annulus between hole and casing. Repeated logs would help resolve this problem.

The natural gamma-ray logs were obtained with a 2" scintillation tool good to about 85°C. The probe was calibrated on site using a gamma-ray source of known strength (1 count/s = 0.9 API units). Although the logs have not been corrected for casing thickness, cement, hole diameter and content, a strong correlation with lithology is evident. Development of a gamma-ray stratigraphy for the caldera might be useful.

Table 1.

Hole	MLGRAP-1	MLGRAP-2
Latitude (N)	37° 39.07′	37° 38.44′
Longitude (W)	118° 58.99′	118° 57.84′
Elevation (GL, m)	2450	2396
Depth (m)	468	491
Drilling started	12/12/87	11/26/87
Drilling completed	1/31/88	12/11/87

Determined capillary corrections for acid-etch inclinometry in glass tubes of various diameters to temperatures of 80°C (Urban and Diment, 1989a, 1989b) so that the inclinations of hot, small-diameter boreholes can be measured.

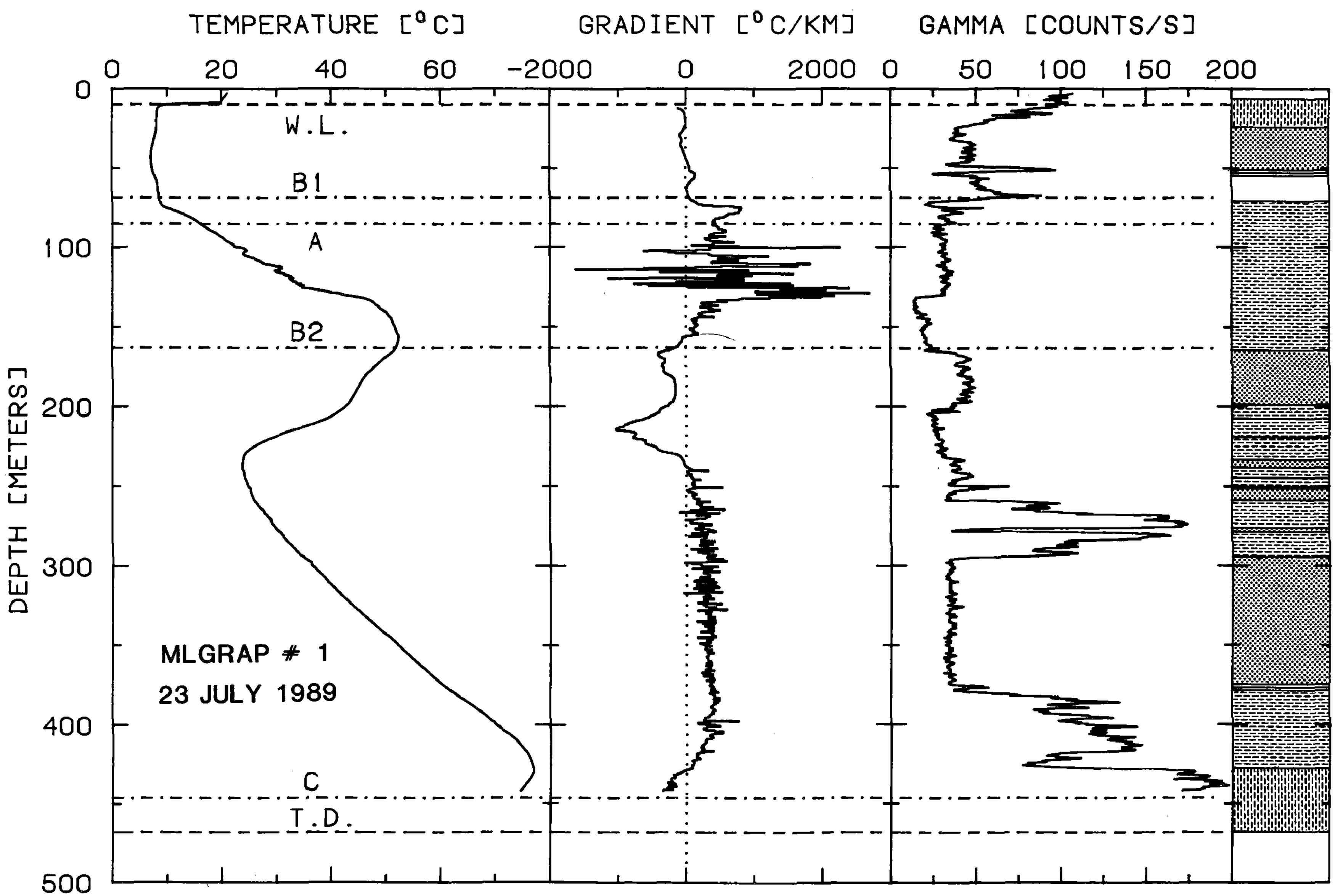
TEMPERATURE [°C]
GRADIENT [°C/KM]
GAMMA [COUNTS/S]
0
20
40
60
-2000
0
2000
0
50
100
150
200
DEPTH [METERS]
100
200
300
400
500
W.L.
B1
A
B2
C
T.D.
MLGRAP # 1
23 JULY 1989

Figure 1

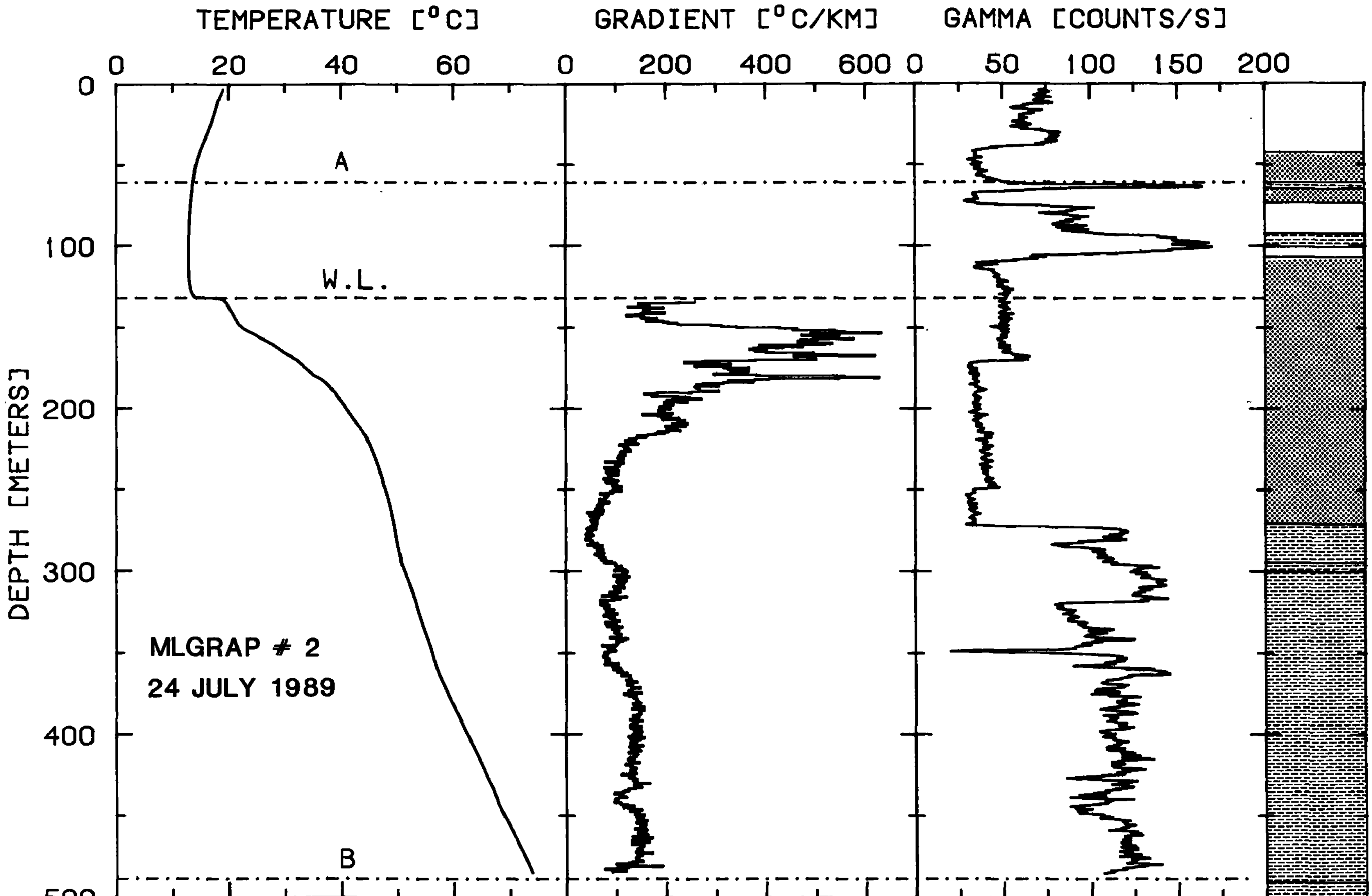
TEMPERATURE [°C]
GRADIENT [°C/KM]
GAMMA [COUNTS/S]
0
20
40
60
0
200
400
600
0
50
100
150
200
DEPTH [METERS]
0
100
200
300
400
500
A
W.L.
B
MLGRAP # 2
24 JULY 1989

Figure 2

Reports and References

Diment, W.H., 1967, Thermal regime of a large diameter borehole: Instability of the water column and comparison of air- and water-filled conditions: Geophysics, v. 32(4), p. 720-726.

Nathenson, M., Urban, T.C., and Diment, W.H., 1979, Approximate solution for the temperature distribution caused by flow up a fault and its application to tempertures measured in a drillhole at Raft River geothermal area, Cassia County, Idaho: Geothermal Resources Council, Transactions, v. 3, p. 477-480.

Urban, T.C. and Diment, W.H., 1985, Convection in boreholes: limits on interpretation of temperature logs and methods for determining anomalous fluid-flow: NWWA Conference on Surface and Borehole Geophysical Methods in Ground-Water Investigations, February 12-14, 1985, National Water Well Association, Worthington, Ohio, p. 399-414.

Urban, T.C., Diment, W.H., and Sorey, M.L., 1987, Hydrothermal regime of the southwest moat of the Long Valley caldera, Mono County, California, and its relation to seismicity–new evidence from the Shady Rest borehole (RDO8): Transactions, Geothermal Resources Council, v. 11, p. 391-400.

Urban, T.C. and Diment, W.H., 1989a, Capillary corrections for acid-etch inclinometry in boreholes for glass tubes ranging in diameter from 6–25 mm and over a temperature range of $4-80°C$, *in* Abstracts of Papers, Third International Symposium on borehole Geophysics for Minerals, Geotechnical, and Ground-Water Applications: Minerals and Geotechnical Logging Society, A chapter-at-large of the Society of Professional Well-Log Analysts, October 2-5, 1989, Las Vegas, Nevada, p. 20.

Urban, T.C. and Diment, W.H., 1989b, Capillary corrections for acid-etch inclinometry in boreholes for glass tubes ranging in diameter from 6–25 mm and over a temperature range of $4 - 80°C$, *in* Proceedings Third International Symposium on Borehole Geophysics for Minerals, Geotechnical, and Ground-Water Applications: Minerals and Geotechnical Logging Society, A Chapter-at-Large of the Society of Professional Well-Log Analysts, October 2-5, 1989, Las Vegas, Nevada, 28 p. (in press).

SEISMIC HAZARD STUDIES, ANCHORAGE, ALASKA

9950-03643

A.F. Espinosa
Branch of Geologic Risk Assessment
U.S. Geological Survey
Box 25046, Denver Federal Center, MS 966
Denver, CO 80225
(303) 236-1597

Investigations

1. Preparation of the surficial geologic map of the combined Anchorage B-8 SE and southernmost part of the NE quadrangles is complete and being reviewed without a prior field check, and preparation of the B-8 SW quadrangle is progressing prior to field check. Both maps include extensive introductory texts. Ongoing studies of gradients of lateral moraines, especially in the B-7 SW quadrangle is aiding in correlating geologic map units both within these areas and with type or reference deposits elsewhere in the region.

2. In cooperation with the Branch of Central Mineral Resources, Denver, results of previous field investigations of emergent tidal sediments and intercalated organic materials, from which paleoseismicity of the region may be interpreted, are being evaluated using about 34 radiocarbon dates received thus far. An additional suite of samples for radiocarbon analysis was collected in 1988 in order to clarify previous results. A paper intended for publication in the USGS Bulletin series is in preparation and nearing review phase.

3. A surficial geologic map of the Eklutna Valley, Municipality of Anchorage, is undergoing final preparation from existing manuscript maps for inclusion in a Water Resources Division (WRD), Alaska District, report on this new source of municipal water supply.

4. Focal-mechanism solutions and their distribution in Alaska and the Aleutian Islands for earthquakes which have occurred from 1927 through 1985 are being cataloged. A focal mechanism solution catalog is being prepared for publication.

5. Intensity attenuation relationships for different regions in Alaska are being determined from the Intensity-Magnitude Catalog released by scientists working in this project. Intensity-magnitude relationships for Alaska will also be determined with the above data base.

6. Surficial geologic manifestations of the Chilean Tectonic Subduction Zone were investigated in middle and southern Chile during part of the previous austral summer as part of a special grant. Sampling transects of several kinds of organic materials were completed, and their relation to submerged and emergent sediments is currently under study in cooperation with Branch of Central Mineral Resources geologists.

Results

1. The surficial geologic map of the Anchorage B-7 SW quadrangle has been completed and released in the USGS open-file series, 1989.

2. A surficial geologic map of the Nabesna B-6 quadrangle has been prepared by reinterpretation of previously developed material and transmitted to the Branch of Central Mineral Resources for inclusion in the GQ-series map of the area, and is presently undergoing final author revision.

3. Surficial geologic mapping for the combined Anchorage B-7 SE and part of the NE quadrangles is being reviewed.

Reports

Espinosa, A.F., Rukstales, K.S., and Udias, A., 1989, Focal mechanism solutions and their distribution in Alaska and the Aleutian Islands for earthquakes in Alaska and the Aleutian Islands: American Geophysical Union, Fall Meeting, San Francisco, Calif.

Espinosa, A.F., and Rukstales, K.S., 1989, Seismological mapping of the Wadati-Benioff zone and mode of subduction beneath western South America: IASPEI, 25th General Assembly Symposium, August 4, 1989, Istanbul, Turkey.

Espinosa, A.F., 1989, Seismic zonation methodology--A case study: Symposium On the Seismicity, Seismotectonics, and Seismic Risk of the Ibero-Magbrebian Region, April 1989, Madrid, Spain. [Invited paper].

Yehle, L.A., and Schmoll, H.R., 1989, Surficial geologic map of the Anchorage B-7 SW quadrangle, Alaska: U.S. Geological Survey Open-File Report 89-318, 33 p., scale 1:25,000.

Investigation of seismic-wave propagation for determination of crustal structure

9950-01896

Samuel T. Harding
Branch of Geologic Risk Assessment
U.S. Geological Survey
Denver Federal Center, M.S. 966
Denver, CO 80225
(303) 236-1572

Investigations

1. Research into the interpretion of seismic reflection data and the delineation of possible Holocene faults in Puget Sound.

Results

1. A number of possible Holocene faults have been found in the Puget Sound region. The criteria used to interpret a fault as Holocene is if the fault shows displacement of the sea floor and bedding in the young deeper sediments. The date of the sea floor is considered to be post Pleistocene and the reflectors (which seem to be continuous and not arising from a glacial lake) are assumed to be of Tertiary age. Thus the displacements seen on the sea bottom must have occurred in the Holocene. An example of one of these faults is shown in figure 1 which illustrates a fault that penetrates the sea bottom and also cuts Tertiary reflectors. While the data are not as clear as we would like it does show that there is definite Holocene faulting near Seattle.

Reports

Luzietti, E. A., and Harding, S. T., Reconnaissance shallow seismic reflection survey in the New Madrid seismic zone: Submitted to Fall Meeting, American Geophysical Union; approved by Director.

Luzietti, E. A., and Harding, S. T., Reconnaissance shallow seismic reflection surveys in the Reelfoot Rift seismic zone: U.S. Geological Survey Open-File Report; submitted for Branch approval.

Harding, S. T., Agena, W., Nichols, D., and Lee, M., 1989, Small-boat, multi-channel, high-resolution seismic-reflection survey in Puget Sound and the Strait of Juan de Fuca: Houston, Texas, Offshore Technology Conference, May 1-4, 1989, p. 593-598.

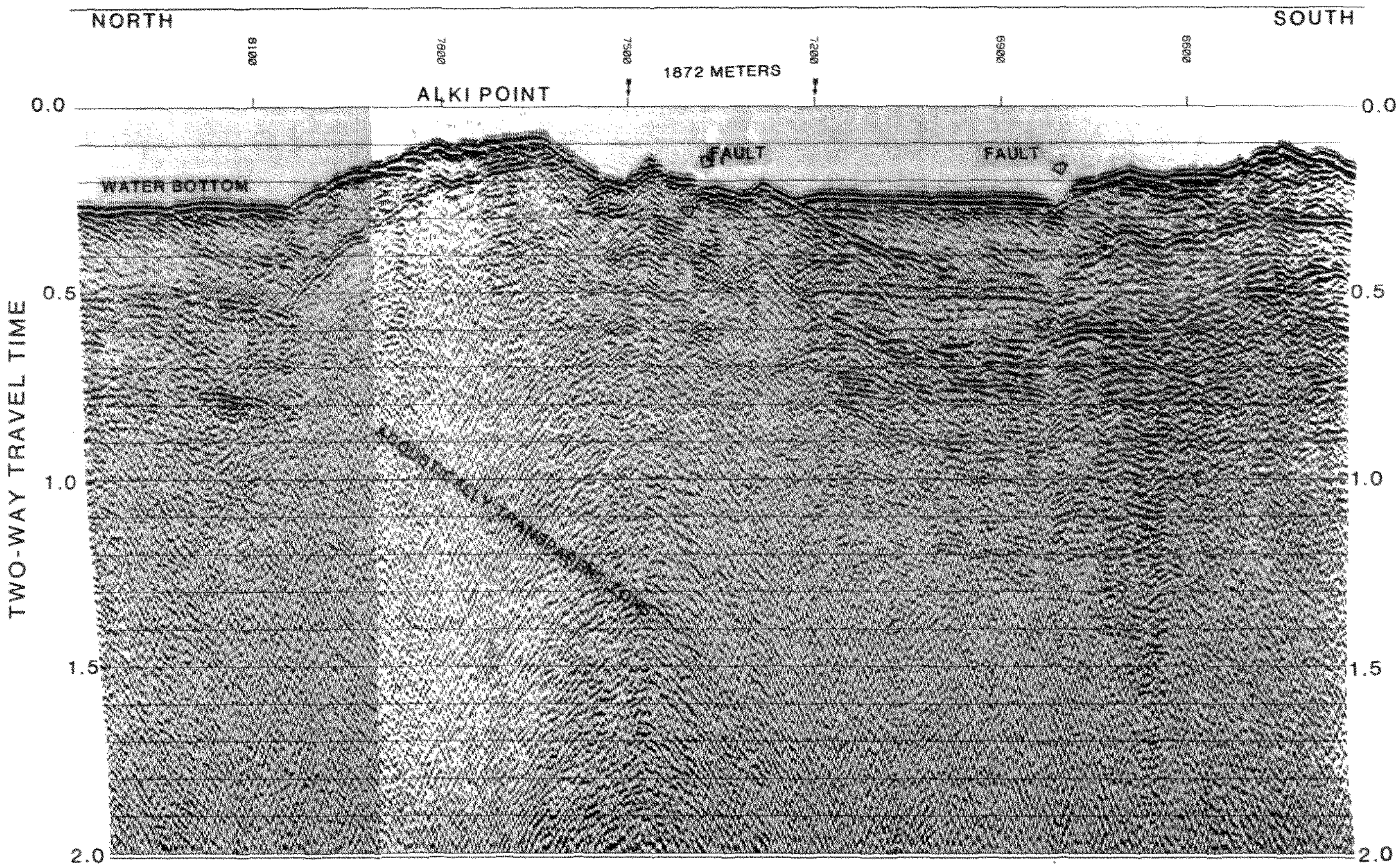

Figure l. Section of Line 5 showing two interpreted Holocene faults near Aiki Point, Seattle, Wash.

Analysis of Gravity Data for the Greater Portland Area

14-80-0001-G1675

Ansel G. Johnson & Paul T. Beeson
Geology Department
Portland State University
PO Box 751
Portland, Oregon 97207-0751
(503) 725-3022

Objectives: Gravity data has been collected in the Greater Portland area for many years. This study is designed to compile all available data into a single data set, and process all the data in a uniform manner. Contoured gravity maps are being produced at scales of 1: 250,000, and 1: 100,000, covering much of northwest Oregon and part of southwest Washington. Cross-sectional models are being produced to assist in determining the structure of the region. These models are incorporating recent surface and subsurface geologic information.

A 1: 250,000 scale Complete Bouguer gravity map has been generated shown as figure 1 using the 1967 Gravitational Formula. This map shows the gravity high over Oregon City which is created by high density Eocene basalts. The size of the basalt highland is being calculated and a northwest-southeast cross-sectional line is being modeled across this high. A second prominent feature shown by the map is the gravity low over Hillsboro. This feature is thought to be caused by a thick pile of lower density marine sediments.

Cross-sectional freeair modeling of the area is in progress with a regional model having been completed. The regional model shown as figure 2 was modeled to a depth of 50 Km and extended 100 Km on both ends beyond the primary area of interest to remove edge effects. Small scale details consisting of formations and structure are being added to the upper 5 Km of the model.

The final steps of the project will include the completion of the current line and a second modeled line across the southern end of the Portland Basin. Interpretation of the structures modeled will be completed. Final drafts of the maps produced will also be completed.

BOUGUER GRAVITY of the PORTLAND, OREGON AREA

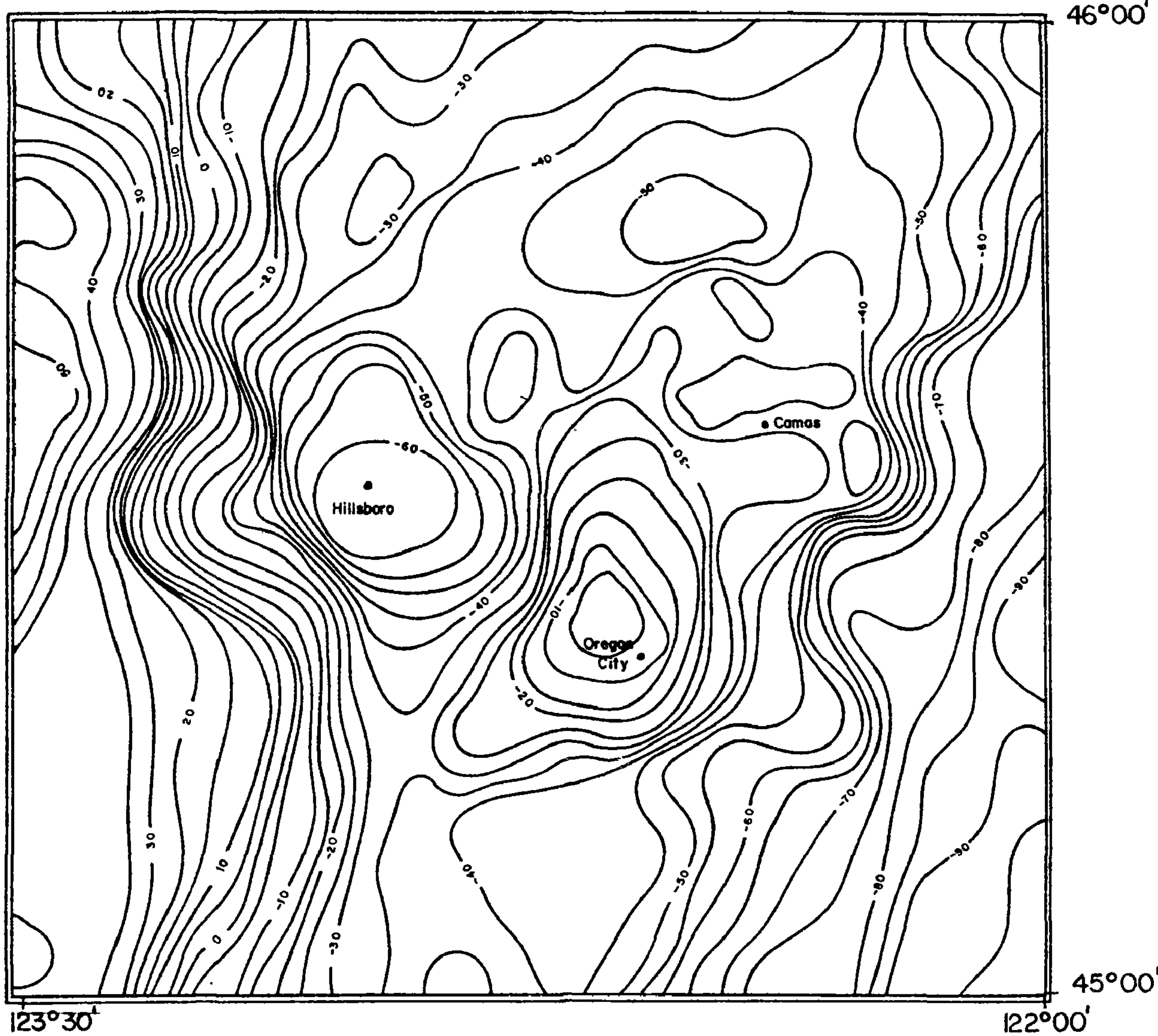

Figure 1

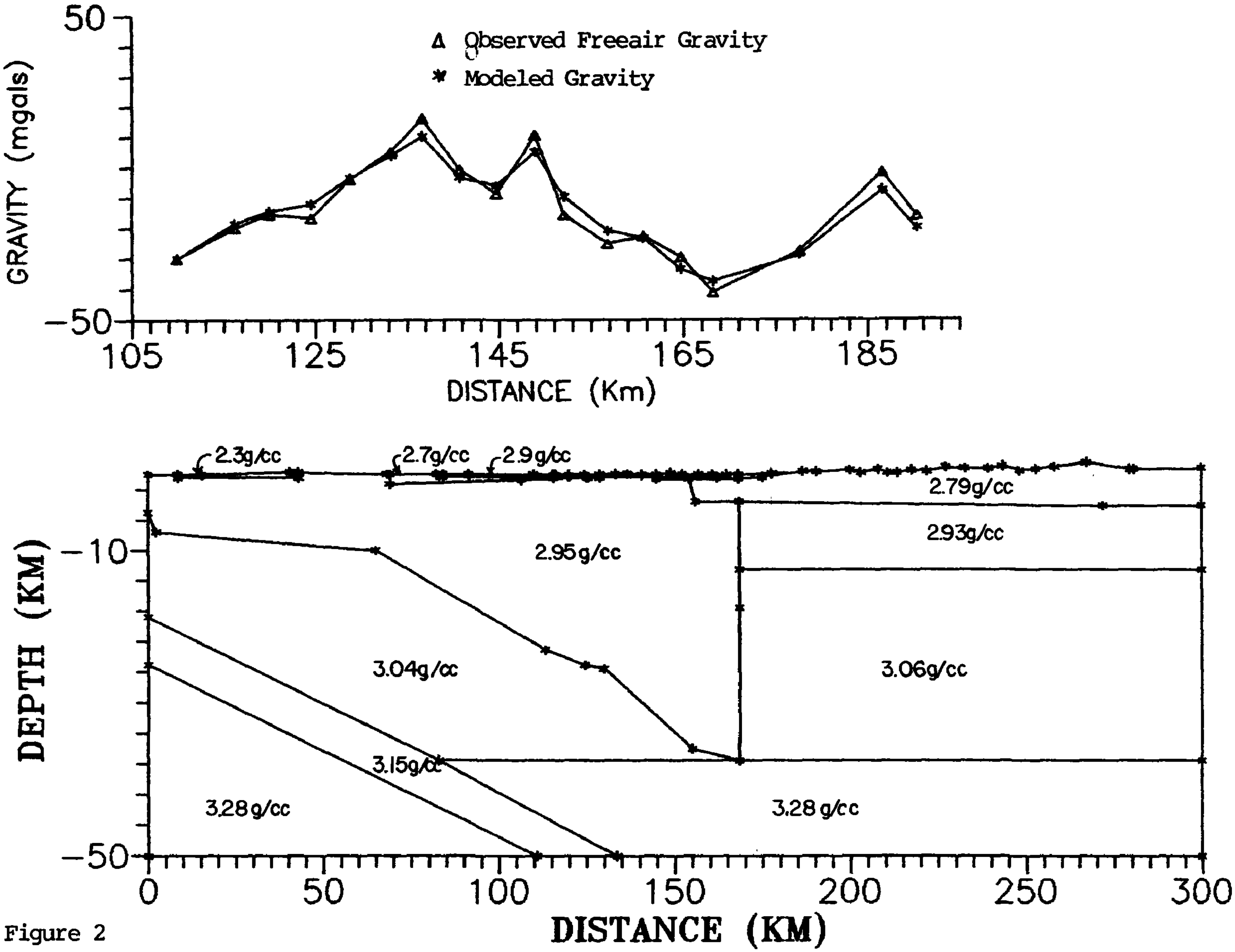
50
-50
GRAVITY (mgals)
Δ Observed Freeair Gravity
* Modeled Gravity
105
125
145
165
185
DISTANCE (Km)
2.3g/cc
2.7g/cc
2.9g/cc
2.79g/cc
2.93g/cc
2.95g/cc
3.04g/cc
3.06g/cc
3.15g/cc
3.28g/cc
3.28 g/cc
-10
-50
DEPTH (KM)
0
50
100
150
200
250
300
DISTANCE (KM)

Figure 2

JRBAN HAZARDS SEISMIC FIELD INVESTIGATIONS AND THE STUDY OF THE EFFECTS OF SITE GEOLOGY ON GROUND SHAKING

9950-01919

K.W. King and A.C. Tarr
Branch of Geological Risk Assessment
U.S. Geological Survey
Box 25046, Denver Federal Center, MS 966
Denver, CO 80225
(303) 236-1591; (303) 236-1605

INVESTIGATIONS

The objectives of this project are: (1) To improve the understanding of how shallow underlying geology affects ground motion, (2) to develop methods to investigate the geologic/engineering parameters of the shallow, upper 400 ft of the surface soils/geology, (3) to develop integrated techniques and methodologies for efficiently and effectively processing large quantities of digital seismic-response data, seismic reflection and refraction data, seismic and geological borehole data, and building response data, and (4) to produce relative ground-response maps for urban study areas.

Specific goals for this reporting period were: (1) To finalize the analysis of the Olympic seismic data and finalize a formal report on the ground-response-function research for the Olympia-Lacey urban area, (2) to finalize the analysis of the borehole velocity studies/ground response in the Wasatch area, (3) to begin preliminary analysis of the ground-response function of West Seattle, (4) to set up a seismic/vibration training course for the National Park, (5) to continue the implementation of geographic information systems (GIS) technology for seismic hazards map production in the Pacific Northwest study area.

RESULTS

(1) Olympia-Lacey area

Seismic-response data have been analyzed from approximately 80 sites in the Olympia-Lacey, Washington, area. The sites were selected, in cooperation with the Washington State Division of Geology and Energy Resources, according to known or suspected subsurface geology, documented seismic intensities from the 1949 and 1965 earthquakes, and the U.S. Geological Survey (USGS) drilling program. The energy source for the induced ground shaking was blasts from a large open-pit coal mine in the Centralia, Washington, area.

The most significant result of this study was the very good correlation between the 1965 intensity values and the ground-response functions (GRF) in the very narrow frequency band of 2-4 Hz. Good correlation was found between the GRF values and the surficial geology.

The downhole geophysical surveys in the Olympia-Seattle urban area were not completed because funding was not available. However, downhole geophysical data were obtained from three boreholes in the Olympia-Lacey area during the FY 1988 field season. The velocity data from the three boreholes have been analyzed and show similar correlations with GRF as did the Wasatch borehole data. The remaining three boreholes in Olympia and the two boreholes in West Seattle will be logged when additional funds become available.

(2) Puget Sound

Preliminary analysis of the limited seismic data indicates that relative spectral ratios of ground response generally compare well with observed Modified Mercalli (MM) intensities of the April 1965 Puget Sound earthquake; that is, higher spectral ratios are found near sites of higher MM intensity. Spectral ratios derived from several types of seismic sources are generally compatible, although reliable seismic response could not always be determined from coal-mine explosions. Thus far, microearthquakes near Seattle seem to provide the best spectral ratio data to date. A network of seismic systems was installed in the West and South Seattle areas to record small earthquakes for the development of GRFs for the area. Because funding restrictions did not allow maintenance of the sites, data were recovered from only four sites. The network has been moved to Northern Washington for other studies for another project. The data from the four sites have been given a preliminary analysis and will be the subject of a formal report in 1990. The eight portable seismic field systems were installed near Mt. Vernon, Washington, for an aftershock study program with Craig Weaver, USGS.

A cooperative building-testing project was completed with NBS. An eight-story building in Portland, Ore., and a seven-story building in Long Beach, Calif., was tested for engineering parameters. A report is in progress.

(3) National Park Service

The purpose of the seismic training of National Park personnel (requested and funded by NPS) was: (1) To help NPS develop a first-line vibration documentation program, (2) to develop an awareness of the seismic/vibration realm at specific parks, and (3) to develop cursory analytical capabilities.

A seismic-field testing (vibration) program was conducted on induced motions from helicopters. The program will continue into next fiscal year and will result in a published report.

(4) High-Resolution Shallow Reflections (HRSR)

Re-analysis was completed on past project data to help to improve the HRSR methods; that is, we re-analyzed the HRSR data from three field projects (two for BGRA, two for Water Resources Division (WRD)) as a means to improve the HRSR methods and analysis.

The HRSR methods were used in areas to study site-response and downhole-logging methods (Olympia-Wasatch), to detect sinkholes and related geologic structures in Alabama and Arizona. The analysis of the data appeared relatively successful. An improved method was developed to induce energy with a shotgun for the reflection surveys. A preliminary report was made using this analysis and the results are to be presented at the annual meeting of the Association of Engineering Geologists.

(5) Geotechnical Data Base

Production of a relative ground-response map for a large urban area requires the acquisition and analysis of many hundreds of pieces of seismic, geological, and geotechnical data. The rational organization and manipulation of so much data requires a data-base management system (DBMS) and a data-base structure that permits linking many types of data. Portability of the DBMS and data sets to several kinds of computers and ability to access the data base in the field suggested implementation on a microcomputer system.

Additional data from the Puget Sound studies have been added to the data base. All new data acquisition of ground-response and borehole studies uses the same software and data structures.

(6) Geographic Information System (GIS)

Production of a seismic-hazards map for an urban area requires integrating results of research (such as relative site response, landslide susceptibility, lifeline vulnerability) in a map format. GIS technology has shown promise in recent years as a powerful tool for spatial analysis and manipulation of data with geographical attributes. Because a seismic-hazards map is multi-disciplinary, an interdivisional investigation was established to use GIS technology in the production of preliminary seismic-hazards maps; this project took the lead in the investigation. A GIS project was established to integrate expertise and data sets to produce seismic-hazards maps expected from the Regional Earthquake Hazards Assessment of the Pacific Northwest urban hazards.

The hydrography, land use/land cover, and transportation digital data for the 1:100,000 Seattle and Tacoma quadrangles have been converted into ARC/INFO compatible form. Surficial geology of the southern half of the Tacoma quadrangle was completed. Several seismicity and geotechnical data sets have been transferred to the Urban Hazards Data Base.

Acquisition of digital cartographic data sets continues. Digital Line Graph (DLG) and Digital Elevation Model (DEM) data at 1:24,000 scale have been ordered for quadrangles encompassing Olympia (2), Tacoma (4), and Seattle (6); the two Olympia quadrangles have been received and added to the data base. SPOT images of the major urban areas of the Puget Sound have been acquired and will be analyzed with ERDAS software.

Installation of hardware and software for a BGRA GIS facility have been completed. The resources available include a SUN 3/60 workstation, Altek digitizing table, and a ARC/INFO software license.

PUBLICATIONS

Crane, Michael P., and Tarr, Arthur C., 1988, Application of GIS technology to assessment of seismic hazards in the Pacific Northwest (abs.): GIS/LIS'88, Houston, Texas.

King,K.W.,, Tarr, A.C., Carver, D.L., and Williams, R.A., 1988, Seismic ground response studies in Olympia, Washington and vicinity. (Director's Approval). (Submitted to BSSA).

King, K.W., and Williams, R.A., 1989, Seismic reflection profiling of subsurface cavities and related structures (abs.): Association of Engineering Geologists, Annual Meeting, 1989.

Williams, R.A., and King, K.W., 1989, Correlations between seismic shallow reflection, downhole, and ground response in the Salt Lake City, Utah, urgan area. (In review).

Williams, R.A., King, K.W., Carver, D.L., and Worley, D.M., 1988, A high-resolution seismic reflection profile at the Prince Ranch, South Dakota: U.S. Geological Survey Open-File Report 89-13.

QUATERNARY GEOLOGY ALONG THE WASATCH FAULT ZONE, UTAH
(Final Project Report)

9950-04182

Michael N. Machette
Branch of Geologic Risk Assessment
U.S. Geological Survey
Box 25046, MS 966, Denver Federal Center
Denver, Colorado 80225
(303) 236-1243

Michael N. Machette, Alan R. Nelson, and Stephen F. Personius have completed a 5-year investigation (FY 84-89) of the Wasatch fault zone (WFZ) in Utah. The principle goal of the project was to map, in detail, the Quaternary surficial geology along the WFZ on a large-scale topographic base using modern stratigraphic, geomorphic, and structural concepts, a well-calibrated stratigraphic framework, and modern paleoseismologic techniques. Establishing this data base for the Wasatch Front has allowed us and our colleagues to pursue detailed investigations of surface faulting, recurrence intervals, slip rates, and segmentation models, and to better evaluate the seismic hazards for the region. This final report summarizes our investigations and publications. A summary of the Holocene movement history of the WFZ and other significant results was included in the July 1989 Summary of Technical Reports.

INVESTIGATIONS

1. Mapping. Preparation of our four 1:50,000-scale strip maps of the WFZ is complete. These maps are being prepared in black and white (MF version) maps for immediate release, and in full color (I version) maps for release in about 2 years owing to preparation and printing time. Our maps include about 40 surficial geologic units that are subdivided on the basis of genesis (lacustrine, alluvial, glacial, eolian, and colluvial), facies, and age (early Holocene, mid to early Holocene, latest Pleistocene, late Pleistocene, and middle to early Pleistocene). In addition to description of more than 40 surficial mapping units, each map includes a fairly lengthy discussion of the Quaternary geologic history of the area as well as a discussion of the timing for movement on the WFZ as deduced from mapping, trenching, and dating studies. Tertiary through Precambrian bedrock is subdivided into 6-8 units that show important structural and lithologic information.

The four maps encompass four major segments of the WFZ; they are, from north to south: the Brigham City, Weber, Salt Lake City, and Provo segments. The maps show the surficial geology in 10- to 20-km-wide strips along the 40- to 70-km-long segments of the fault zone. The geology extends from the bedrock of the Wasatch Range into the lake-basin sediment of the adjacent valleys. Detailed (1:10,000-scale) geologic maps of trench sites and other areas of significance are included on each of the smaller scale strip maps.

2. Trenching investigations. In the summer of 1986, near the end of our mapping effort, we initiated a cooperative research program with the Utah Geological and Mineral Survey (UGMS), primarily with Bill Lund and his colleagues. We chose three main trenching sites: Brigham City, East Ogden, and American Fork Canyon. Three to five trenches were excavated at these sites to discern the time of most recent movement, times of prior movements, recurrence intervals, and slip rates. In addition, these sites were located along newly subdivided segments of the WFZ, thus testing our previous hypotheses about segmentation of the WFZ.

Preparation of summary reports describing the results of our trenching along the WFZ is continuing, albeit at a slow rate. These reports will be published by the UGMS and will include a complete listing of radiocarbon and thermoluminescence dates from our trenches and a systematic description of faulting events, slip rates, and recurrence intervals. These detailed reports provide the substantiating data for the conclusions and interpretations drawn in U.S. Geological Survey Professional Paper 1500-A (see item 5 and Reports). Personius has submitted the Brigham City trench report to the UGMS and is completing a similar report on the Pole Patch site, near Pleasant View, Utah. Machette has a rough draft of the American Fork Canyon site in Utah Valley, and Nelson is starting his report on the East Odgen site. Each of the authors has summarized his results in a field-trip guidebook for last year's GSA Annual Meeting (published as Utah Geological and Mineral Survey Miscellaneous Publication 88-1).

3. *Topical studies.* The 1983 Borah Peak, Idaho earthquake occurred about 1 month after the start of this project, and in retrospect, provided a rare opportunity to study what came to be accepted as a modern earthquake/faulting analog for the Wasatch fault zone. With a surface-wave magnitude of 7.3, this was the second strongest earthquake to strike the Intermountain Seismic Belt in historic time. Careful study of the surface rupturing revealed the types and persistence of segment boundaries, principles which were later applied to our studies of the WFZ. In addition, our studies of fault scarp morphology, both from the 1893 earthquake and from Holocene and late Pleistocene faults in the Eastern Basin and Range province, has helped to calibrate rates of fault scarp degradation and to better understand the processes involved.

4. *Dating techniques.* We were fortunate to collaborate with James McCalpin (Utah State Univ., Logan) and Steven Forman (Univ. of Colorado, Boulder) in the early stages of their experimental work on thermoluminescence (TL) dating of sediments. Sediment samples associated with fault-scarp-generated colluvium in our trenches at American Fork Canyon and East Ogden, which had been dated by radiocarbon analyses, was also dated with TL. Collectively, we have been able to date the silt-size fraction from organic soil (A) horizons, wind-blown silt (loess), the distal component of slope colluvium, and ponded sediment in the trenches. The useful range of dating seems to be about 500 years to >10,000 years, with a probable upper limit that may extend to 150,000 years depending on the natural radiation level in the sediment in the trenches. This collaborative research (through the USGS Grants Program) has been both extremely productive and successful.

5. *Summary report.* We completed an extensive revision of USGS Open-File Report 87-585 that now includes detailed discription of the WFZ, evidence for the times of faulting (abstracted from our trenching reports), and a lengthy discussion of dating techniques and dating control for our studies. This report constitutes Chapter A of USGS Professional Paper 1500 "Assessing Regional Earthquake Hazards and Risk along the Wasatch Front, Utah (volume 1). This manuscript has been abstracted in a recent open-file report and article for the *Journal of Structural Geology* by Machette and others (see reports).

REPORTS FOR THIS PROJECT (FY84-FY89)

Abstracts

Haller, K.M., 1987, Preliminary interpretation of segmentation of three range-front normal faults in southeastern Idaho and southwestern Montana: Geological Society of America Abstracts with Programs, v. 19, no. 5, p. 280.

Haller, K.M., 1988, Proposed segmentation of the Lemhi and Beaverhead faults, Idaho, and Red Rock fault, Montana--Evidence from fault-scarp morphology: Geological Society of America Abstracts with Programs, v. 20, no. 6, p. 418-419.

Jackson, M.E., Forman, S.L., and Machette, M.N., 1987, Dating of paleoseismic events using the thermoluminescence (TL) dating method--Preliminary results: EOS [Transactions of the American Geophysical Union], v. 68, no. 44, p. 1287.

Machette, M.N., 1987, Recent studies of the Wasatch fault zone, Utah--A review: Geological Society of America Abstracts with Programs, v. 19, no. 5, p. 317.

Machette, M.N., and Lund, W.R., 1987, Trenching across the American Fork segment of the Wasatch fault zone, Utah: Geological Society of America Abstracts with Programs, v. 19, no. 5, p. 317.

Machette, M.N., Personius, S.F., and Nelson, A.R., 1986, Late Quaternary segmentation and slip-rate history of the Wasatch fault zone, Utah: EOS [Transactions of the American Geophysical Union], v. 67, no. 44, p. 1107.

Nelson, A.R., and Personius, S.F., 1987, A nonconservative barrier to Holocene rupture propagation in the northern Wasatch fault zone, Utah, USA: International Union for Quaternary Research, 12th International Congress, Ottawa, Canada, Abstracts with Programs, p. 231.

Nelson, A.R., Klauk, R.H., Lowe, Michael, and Garr, J.D., 1987, Holocene history of displacement on the Weber segment of the Wasatch fault zone at Ogden, northern Utah: Geological Society of America Abstracts with Programs, v. 19, no. 5, p. 322.

Machette, M.N., Nelson, A.R., Personius, S.F., Schwartz, D.P., and Lund, W.E., 1988, The late Quaternary Wasatch fault zone, Utah--Evidence for segmentation, recent faulting, and clustering of earthquakes: Geological Society of America Abstracts with Programs, v. 20, no. 3, p. 177.

Personius, S.F., and Gill, H.E., 1987, Holocene displacement on the Brigham City segment of the Wasatch fault zone near Brigham City, Utah: Geological Society of America Abstracts with Programs, v. 19, no. 5, p. 326.

Wheeler, R.L., and Krystinik, K.B., 1987, Persistent segment boundaries on the Wasatch fault zone, central Utah [abs.]: Seismological Research Letters, v. 58, no. 1, p. 31.

Wheeler, R.L., and Krystinik, K.B., 1987, Persistent and nonpersistent segmentation of the Wasatch fault zone Utah: Geological Society of America Abstracts with Programs, v. 19, no. 5, p. 342.

Open-File and Administrative Reports

Machette, M.N., 1984, Preliminary investigations of late Quaternary slip rates along the southern part of the Wasatch fault zone, central Utah, *in* Hays, W.W., and Gori, P.L., eds., Proceedings of Conference XXV--A workshop on "Evaluation of regional and urban earthquake hazards and risk in Utah": U.S. Geological Survey Open-File Report 84-763, p. 391-406.

Machette, M.N., 1987, Changes in long-term versus short-term slip rates in an extensional environment, *in* Crone, A.J., and Omdahl, E.M., eds., Proceedings of Conference XXXIX--Directions in paleoseismology: U.S. Geological Survey Open-File Report 87-673, p. 228-238.

Machette, M.N., Lund, W.R., and Arabasz, W.J., 1986, Overview and comments on research progress--Tectonic and earthquake potential of the Wasatch Front area and other parts of Utah: U.S. Geological Survey Administrative Report, 1986 Earthquake Hazards Conference, Salt Lake City Utah, 13 p.

Machette, M.N., Personius, S.F., and Nelson, A.R., 1987, Quaternary geology along the Wasatch fault zone--Segmentation, recent investigations, and preliminary conclusions, v. 1, Chapter A, *in* Gori, Paula, and Hays, W.W., eds., Assessment of regional earthquake hazards and risk along hte Wasatch Front, Utah: U.S. Geological Survey Open-File Report 87-585, p. A1-A72.

Machette, M.N., Nelson, A.R., Personius, S.F., Schwartz, D.P., and Lund, W.R., 1989, Segmentation models and Holocene movement history of the Wasatch fault zone, Utah, *in* Schwartz, D.P., and Sibson, R.H., eds., Proceedings of Workshop XLV--Fault segmentation and controls of rupture initiation and termination: U.S. Geological Survey Open-File Report 89-315, p. 229-245.

Machette, M.N., Personius, S.F., Scott, W.E., and Nelson, A.R., 1986, Quaternary geology along the Wasatch Front--Evidence for ten fault segments and large-scale changes in slip rate on the Wasatch fault zone: U.S. Geological Survey Administrative Report, 1986 Earthquake Hazards Conference, Salt Lake City, Utah, 7 p.

Nelson, A.R., 1987, A facies model of colluvial sedimentation adjacent to a single-event normal-fault scarp, *in* Crone, A.J., and Omdahl, E.M., eds., Proceedings of Conference XXXIX--Directions in paleoseismology: U.S. Geological Survey Open-File Report 87-673, p. 136-145.

Wheeler, R.L., 1987, Boundaries between segments of normal faults--Criteria for recognition and interpretation, *in* Crone, A.J., and Omdahl, E.M., eds., Proceedngs of Conference XXXIX--Directions in paleoseismology: U.S. Geological Survey Open-File Report 87-673, p. 385-398.

Wheeler, R.L., 1989, Persistence of segment boundaries on Basin-Range normal faults, *in* Schwartz, D.P., and Sibson, R.H., eds., Proceedings of Conference XLV--Fault segmentation and controls of rupture initiation and termination: U.S. Geological Survey Open-File Report 89-315, p. 432-444.

Wheeler, R.L., and Krystinik, K.B., 1987, Persistent and nonpersistent segmentation of the Wasatch fault zone, Utah--Statistical analysis for evaluation of seismic hazard, *in* Hays, W.W., and Gori, Paula, eds., Assessment of regional earthquake hazards and risk along the Wasatch Front, Utah: U.S. Geological Survey Open-File Report 87-585, v. 1, p. B1-B124, Chapter B.

Journal Articles

Crone, A.J., and Machette, M.N., 1984, Surface faulting accompanying the 1983 Borah Peak earthquake, Idaho: Geology, v. 12, no. 11, p. 664-667.

Crone, A.J., Machette, M.N., Bonilla, M.G., Lienkaemper, J.J., Pierce, K.L., Scott, W.E., and Bucknam, R.C., 1987, Surface faulting accompanying the Borah Peak earthquake and segmentation of the Lost River fault, central Idaho: Bulletin of the Seismological Society of America, v. 77, no. 3, p. 739-770.

Forman, S.L., Machette, M.N., Jackson, M.E., and Maat, Paula, 1989, An evaluation of thermoluminescence dating of paleoearthquakes on the American Fork segment, Wasatch fault zone, Utah: Journal of Geophysical Research, v. 94, no. B2, p. 1622-1630.

Machette, M.N., 1987, Documentation of benchmark photographs that show the effects of the 1983 Borah Peak earthquake with some considerations for studies of scarp degradation: Bulletin of the Seismological Society of America, v. 77, no. 3, p. 771-783.

Machette, M.N., Nelson, A.R., Personius, S.F., Schwartz, D.P., and Lund, W.R., in press, Segment lengths, Holocene movement, and recurrence intervals along the Wasatch fault zone: Submitted to Journal of Structural Geology, 24 ms p., 4 figures.

Book Reports

Forman, S.L., and Machette, in press, Thermoluminescence dating, *in* Rosholt, J.N., ed., Chapter 17--Dating methods applicable to the Quaternary, *in* Morrison, R.B., ed., Quaternary non-glacial geology of the conterminous United States: Geological Society of America Decade of North American Geology, v. K-2.

Machette, M.N., editor, 1988, In the footsteps of G.K. Gilbert--Lake Bonneville and neotectonics of the eastern Basin and Range Province: Geological Society of America Guidebook for Field Trip 12, Utah Geological and Mineral Survey Miscellaneous Publication 88-1, 120 p.

Machette, M.N., 1988, Day 3--Stop 3, American Fork Canyon--Holocene faulting, the Bonneville fan-delta complex, and evidence for the Keg Mountain oscillation, *in* Machette, M.N., ed., In the footsteps of G.K. Gilbert--Lake Bonneville and neotectonics of the eastern Basin and Range province: Geological Society of America Guidebook for Field Trip 12, Utah Geological and Mineral Survey Miscellaneous Publicatin 88-1, p. 89-95.

Machette, M.N., 1988, Day 3--Stop 4, Exposures of transgressive and regressive sediment of the Bonneville lake cycle Dry Creek near Lehi, *in* Machette, M.N., ed., In the footsteps of G.K. Gilbert--Lake Bonneville and neotectonics of the eastern Basin and Range province: Geological Society of America Guidebook for Field Trip 12, Utah Geological and Mineral Survey Miscellaneous Publication 88-1, p. 96-99.

Machette, M.N., 1989, Slope-morphometric dating, *in* Forman, S.L., ed., Quaternary dating methods--A short course: Utah Geological and Mineral Survey Miscellaneous Publication, p. 30-42 (in press).

Machette, M.N., and Currey, D.R., 1988, Field trip road log for days 1, 2, and 3, *in* Machette, M.N., ed., In the footsteps of G.K. Gilbert--Lake Bonneville and neotectonics of the eastern Basin and Range province: Geological Society of America Guidebook for Field Trip 12, Utah Geological and Mineral Survey Miscellaneous Publication 88-1, p. 16-19, 48-51, and 74-77.

Machette, M.N., and Scott, W.E., 1988, Introduction, *in* Machette, M.N., ed., In the footsteps of G.K. Gilbert--Lake Bonneville and neotectonics of the eastern Basin and Range province: Geological Society of America Guidebook for Field Trip 12, Utah Geological and Mineral Survey Miscellaneous Publication 88-1, p. 7-14.

Machette, M.N., Personius, S.F., and Nelson, A.R., in press, Paleoseismology of the Wasatch fault zone--A summary of recent investigations, conclusions, and interpretations, *in* Gori, P.A., and Hays, W.W., eds., Assessing regional earthquake hazards and risk along the Wasatch Front, Utah: U.S. Geological Survey Professional Paper 1500, Chapter A, 150 p., Appendix, 21 figs., 4 tables.

Nelson, A.R., 1988, Day 1--Stop 3, The northern part of the Weber segment of the Wasatch fault zone near Ogden, Utah, *in* Machette, M.N., ed., In the footsteps of G.K. Gilbert--Lake Bonneville and neotectonics of the eastern Basin and Range province: Geological Society of America Guidebook for Field Trip 12, Utah Geological and Mineral Survey Miscellaneous Publication 88-1, p. 33-37.

Personius, S.F., 1988, Day 1--Stop 2, A brief summary of the surficial geology along the Brigham City segment of the Wasatch fault zone, Utah, *in* Machette, M.N., ed., In the footsteps of G.K. Gilbert--Lake Bonneville and neotectonics of the eastern Basin and Range province: Geological Society of America Guidebook for Field Trip 12, Utah Geological and Mineral Survey Miscellaneous Publication 88-1, p. 27-32.

Personius, S.F., in press, Paleoseismic analysis of the Wasatch fault zone at the Brigham City trench site, Brigham City, Utah: Utah Geological and Mineral Survey Special Studies, 46 ms p.

Sullivan, J.T., and Nelson, A.R., in press, Quaternary displacement on the Morgan fault--A backvalley fault in the Wasatch Range of north-central Utah, *in* Gori, P.A. and Hays, W.W., eds., Assessing regional earthquake hazards and risk along the Wasatch Front, Utah: U.S. Geological Survey Professional Paper 1500, Chapter J.

Wheeler, R.L., and Krystinik, K.B., 1987, Evaluating coinciding anomalies along a fault trace or other traverse--Simulations and statistical procedures: U.S. Geological Survey Bulletin 1802, 12 p.

Wheeler, R.L., and Krystinik, K.B., 1988, Segmentation of the Wasatch fault zone, Utah--Summaries, analyses, and interpretations of geological and geophysical data: U.S. Geological Survey Bulletin 1827, 47 p.

Wheeler, R.L., and Krystinik, K.B., in press, Persistent and nonpersistent segmentation of the Wasatch fault zone, Utah--Statistical analysis for evaluation of seismic hazard, *in* Gori, Paula, and Hays, W.W., eds., Assessing regional earthquake hazards and risk along the Wasatch Front, Utah: U.S. Geological Survey Professional Paper 1500, Chapter B.

Maps

Machette, M.N., 1989, Preliminary surficial geologic map of the Wasatch fault zone, eastern Utah Valley, Utah County and parts of Salt Lake and Juab Counties, Utah: U.S. Geological Survey Miscellaneous Field Studies Map, MF-2109, 70 ms p., scale 1:50,000.

Machette, M.N., in press, Surficial geologic map of the Wasatch fault zone, eastern Utah Valley, Utah County and parts of Salt Lake and Juab Counties, Utah: U.S. Geological Survey Miscellaneous Investigations Series Map, I-1095, scale 1:50,000.

McCalpin, James, 1989, Surficial geologic map of the East Cache fault zone, Cache County, Utah: U.S. Geological Survey Miscellaneous Field Studies Map, MF-2107, scale 1:50,000.

Nelson, A.R., and Personius, S.F., in prep., Preliminary surficial geologic map of the Weber segment, Wasatch fault zone, Weber and Davis Counties, Utah: U.S. Geological Survey Miscellaneous Field Studies Map, scale 1:50,000.

Nelson, A.R., and Personius, S.F., in prep., Surficial geologic map of the Weber segment, Wasatch fault zone, Weber and Davis Counties, Utah: U.S. Geological Survey Miscellaneous Investigations Series Map, scale 1:50,000.

Personius, S.F., 1988, Preliminary surficial geologic map of the Brigham City segment and adjacent parts of the Weber and Collinston segments, Wasatch fault zone, Box Elder and Weber Counties, Utah: U.S. Geological Survey Miscellaneous Field Studies Map MF-2042, scale 1:50,000.

Personius, S.F., in press, Surficial geologic map of the Brigham City segment and adjacent parts of the Weber and Collinston segments, Wasatch fault zone, Box Elder and Weber Counties, Utah: U.S. Geological Survey Miscellaneous Investigations Series Map MF-1979, scale 1:50,000.

Personius, S.F., and Scott, W.E., 1990, Preliminary surficial geologic map of the Salt Lake City segment and parts of adjacent segments of the Wasatch fault zone, Davis, Salt Lake, and Utah Counties, Utah: U.S. Geological Survey Miscellaneous Field Studies Map, 58 ms p., scale 1:50,000.

Personius, S.F., and Scott, W.E., in press, Surficial geologic map of the Salt Lake City segment and parts of adjacent segments of the Wasatch fault zone, Davis, Salt Lake, and Utah Counties, Utah: U.S. Geological Survey Miscellaneous Investigations Series Map, scale 1:50,000.

MISSISSIPPI VALLEY SEISMOTECTONICS

9950-01504

Frank A. McKeown
Branch of Geologic Risk Assessment
U.S. Geological Survey
Box 25046, MS 966, Denver Federal Center
Denver, Colorado 80225
(303) 236-9355

INVESTIGATIONS

1. Continued reprocessing of seismic-reflection profiles and integrated recently acquired drill-hole data with these profiles.

2. Completed detailed lithologic logs of the Dow Chemical #1 Wilson and the Dow Chemical #1 Garrigan drill holes.

3. Selected samples of cuttings from the Wilson and Garrigan drill holes for paleontological, geochemical, and petrographic studies.

4. Continued acquisition and editing of stratigraphic information from drill holes in the Upper Mississippi Embayment. Completed entering the information into a computer file and started plotting subcrop and structure contour maps.

5. Continued analysis and interpretation of seismic-refraction data.

6. Continued petrographic studies of cuttings and core from drill holes in the Upper Mississippi Embayment and Ozark Mountains.

7. Completed interpretation of 11 Mini-Sosie seismic-reflection profiles in part of the epicentral region of the New Madrid seismic zone.

RESULTS

1. Lithologic logs made by E. Glick and F. McKeown of the Wilson and Garrigan drill holes have provided the identity of the most prominent reflectors correlated by R. Hamilton and F. McKeown throughout 19 seismic-reflection profiles. Two of the reflectors, originally thought to be the tops of the Elvins Group and Lamotte Sandstone, are from lithologic boundaries that do not correspond closely with stratigraphic boundaries. These two reflectors are of particular importance because the early history of the Reelfoot rift and the later formation of the Blytheville arch can be interpreted from them. Biostratigraphic data for these stratigraphic units, which is not yet available, is important for the resolution of the history of structural events.

2. The computer file of stratigraphic information compiled by R. Dart is comprised of more than 400 published and unpublished records of municipal water-well and petroleum-exploration drill holes. In addition, some of these data have been combined with digitized selected depth sections of five lithologic units on the seismic-reflection profiles. Subcrop maps have been plotted on only the drill-hole data and on only the seismic-reflection data. A subcrop map using the combined data has also

been plotted. Structure contour maps of the lithologic units on the seismic-reflection profiles have been plotted.

3. Analyses of seismic-wave attenuation and velocities of seismic-refraction and seismic-reflection data by R. Hamilton and W. Agena show that the rocks within the Blytheville arch attenuate seismic waves severely and have lower velocities than rocks adjacent to the arch. Because much of the seismicity in the New Madrid seismic zone is within the arch, these investigators infer that the high attenuation and low velocities may be useful criteria to identify other potential seismic zones.

4. Synthesis by F. McKeown and R. Hamilton of current data on structure, stratigraphy, seismicity, petrography, seismic-reflection, geochemical, and sulfur-isotope data, provided by a multidisciplinary group of earth scientists, several of whom are in other Branches, results in a different explanation of the earthquakes in the New Madrid seismic zone than has heretofore been proposed. Briefly, the earthquakes are concentrated within the Blytheville and Pascola arches, because the composition and fabric of the rocks within them contrasts greatly with and are weaker than the rocks adjacent to them. The arches are the result of structural inversion of very deep sedimentary basins largely filled with very fine grained clastic sedimentary rocks and possibly evaporites. The inversion caused extreme deformation of the rocks and resulted in them having a distinct physical property domain favorable for nucleation of earthquakes.

REPORTS

Agena, W.F., Lee, M.W., Hamilton, R.M., and McKeown, F.A., 1989, Extended cross-correlation methods for deep crustal studies--A case study of the New Madrid area: EOS [Transactions of the American Geophysical Union], v. 70, no. 15, p. 466-467.

Dart, R.L., and Michael, J.A., 1989, Contour and subcrop mapping of the Paleozoic subsurface in the Upper Mississippi Embayment: Geological Society of America Abstracts with Programs, v. 21, no. 6, p. A206.

Diehl, S.F., and McKeown, F.A., 1989, Diagenesis and structural fabric of basal Cambrian rocks--The Dow Chemical #1 Wilson drill hole, Mississippi County, Arkansas: Geological Society of America Abstracts with Programs, v. 21, no. 6, p. A349.

Hamilton, R.M., and Agena, W.F., Seismic-wave attenuation and velocity anomalies in the New Madrid seismic zone: Geological Society of America Abstracts with Programs, v. 21, no. 6, p. A185.

Luzietti, E.A., and Harding, S.T., 1989, Reconnaissance shallow-reflection survey in the New Madrid seismic zone, northeast Arkansas and southeast Missouri [abs.]: EOS [Transactions of the American Geophysical Union], v. 70 (in press).

McKeown, F.A., and Hamilton, R.M., 1989, Origin of the Blytheville and Pascola arches in the Reelfoot rift and their relationship to the New Madrid seismic zone: Geological Society of America Abstracts with Programs, v. 21, no. 6, p. A148.

Database Management

9910-03975

Charles S. Mueller
Branch of Engineering Seismology and Geology
U. S. Geological Survey
345 Middlefield Road, MS 977
Menlo Park, California 94025
(415) 329-5646

Investigations

1. Development of techniques for data playback, processing, management, and export with emphasis on large datasets collected with portable digital event-recording seismographs (*e.g.*, GEOS).

2. Design and implement relational databases for strong-motion and aftershock/special-experiment data. The goal of the databases is to enhance researcher access to diverse Branch datasets.

Results

1. New datasets played back, processed, and archived:
   Armenia S. S. R. - aftershocks of 7 December 1988 earthquake (continued).

Reports

Borcherdt, R. D. (editor), 1989, Results and data from seismologic and geologic studies following earthquakes of December 7, 1988, near Spitak, Armenia S. S. R.:
Volume 1, U. S. Geol. Survey Open-File Report 89-163A, 188 pages
Volume 2, U. S. Geol. Survey Open-File Report 89-163B, 435 pages (seismograms)
Volume 3, U. S. Geol. Survey Open-File Report 89-163C, 479 pages (seismograms)
Volume 4, U. S. Geol. Survey Open-File Report 89-163D, 449 pages (seismograms)
Volume 5, U. S. Geol. Survey Open-File Report 89-163E, 407 pages (seismograms)

Rupture Characteristics of Large Earthquakes Along the Juan de Fuca Subduction Zone Using Historical Seismograms

14-08-0001-G1678

John L. Nábělek
College of Oceanography
Oregon State University
Corvallis, OR 97331
(503) 737-2757

Objective: The purpose of the study is to determine the rupture characteristics of the 1946 ($M = 7.3$) earthquake which occurred in the southern part of Vancouver Island. This is the largest earthquake to have occurred in this region during the seismometric era. The core of the analysis will be inversion and modeling of teleseismic body waves, but surface waves and regional phases will also be examined. The derived parameters will provide important constraints for the scaling characteristics of earthquakes in the Pacific Northwest.

Data Acquisition and Analysis: Several excellent teleseismic and regional seismogram recordings have been acquired and we are still gathering data from other stations that were in operation at the time of the earthquake. The available data are being digitized and we collecting information on the calibration of the instruments.

We have contacted Dr. Henry Hasegawa at the Geological Survey of Canada who has studied surface waves from this event previously and will cooperate with him on this project.

We have analyzed three recent earthquakes which occurred in the Nootka fault zone; the results are summarized in Figure 1. These smaller events will serve as a calibration for the wave propagation paths.

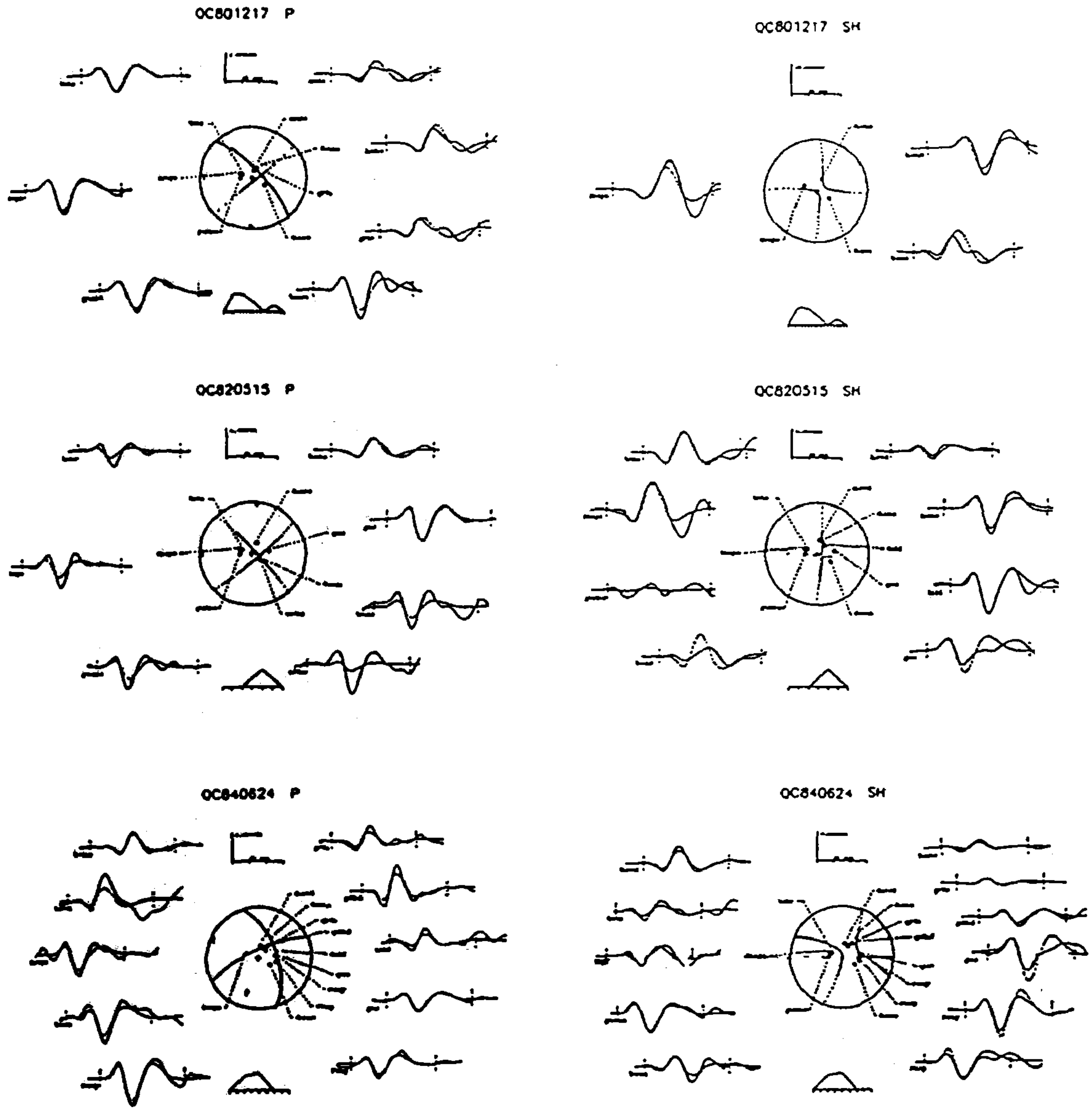

Event name	Orientation strike	dip	slip	Depth (Km)	Moment (dyne*cm)
801217	141.1	94.0	180.1	10.0	1.76e+26
820515	134.2	102.8	186.8	11.86	5.37e+24
840624	160.7	114.3	165.0	8.16	5.07e+24

Figure 1.

EARTHQUAKE RECURRENCE AND QUATERNARY DEFORMATION IN THE CASCADIA SUBDUCTION ZONE, COASTAL OREGON

9950-04180

ALAN R. NELSON, STEPHEN F. PERSONIUS, AND SUSAN RHEA

U.S. Geological Survey
Branch of Geologic Risk Assessment
MS 966, Box 25046
Denver, CO 80225
(303) 236-1596; FTS 776-1596

INVESTIGATIONS

There are three components to this project: (1) Nelson's study of coseismic changes in late Holocene sea level as revealed by salt marsh stratigraphy, (2) Personius' study of fluvial terrace remnants along major Coast Range rivers to determine style and rates of late Quaternary deformation, and (3) Rhea's study of river and drainage basin morphology in the Coast Range to determine relative rates of tectonic uplift.

RESULTS

Recurrence of Holocene earthquakes in central Oregon

Reconnaissance coring at many sites in the Coos Bay, Siuslaw River, Umpqua River, and Coquille River estuaries in south-central Oregon by Nelson shows that there is no consistent regional pattern of multiple, abruptly-buried, salt-marsh soils in the late Holocene sequence, like that reported along the southwestern Washington and northern Oregon coasts. Many sequences show a single buried soil at 0.8-1.5 m depth, which was apparently submerged abruptly in many areas and more gradually in others. The thickness, depth, and degree of development of soils in the few cores with multiple buried peats is highly variable, and there are very few sites where marshes appear to have been as extensive in the past 3000 years as they are today. These sequences resulted from the complex interaction of many processes. The processes included the rate and uniformity of Holocene relative sea-level rise, rate of sediment input (including unusual high tide, flooding, storm surge, and tsunamis events), tidal and river channel migration, compaction, differing effects of small-scale erosion and accretion at different sites, long-term and short-term rates of regional tectonism, and rates and styles of coseismic and aseismic deformation on local folds and faults.

The differences in the types of marsh sequences between northern and south-central Oregon suggest a possible segment boundary along the Cascadia subduction zone between 44°-45° N. Alternatively, the central and southern Oregon coasts may be on the western edge of a postulated north-south-trending zone of coseismic subsidence during great plate-interface earthquakes.

Late Quaternary deformation rates indicated by fluvial terraces in central Oregon

The purpose of this part of the project is to evaluate some of the longer-term (middle and late Quaternary) effects of subduction along the Cascadia subduction zone by examining the styles and rates of deformation of Quaternary deposits within the western Oregon Coast Range. The stratigraphy of fluvial terrace deposits and the distribution of terrace remnants show that the central part of the Oregon Coast Range has undergone, and is currently undergoing regional uplift. Rates of uplift calculated from both ^{14}C ages on early Holocene deposits and from TL analyses of fine-grained sediment are 0.2-0.6 mm/yr (Fig. 1). Fluvial deposits are very difficult to date using TL methods; our ages are some of first successful analyses from this type of fluvial sediment. Active Quaternary structures in the central Coast Range are rare, and none appear to have been active in the Holocene. If tilting due to growth of folds and faults in this region is continuing, it is at very low rates. Farther south, in the Coquille River area of the Cascadia fold and thrust belt of southern Oregon and northern California, rates may be higher, but the extensive floodplain of the Coquille is too young to have preserved evidence of Holocene deformation on local structures.

REPORTS

Grant, W.C., Atwater, B.F., Carver, G.A., Darienzo, M.E., Nelson, A.R., Peterson, C.D., and Vick, G.S., 1989, Radiocarbon dating of late Holocene coastal subsidence above the Cascadia subduction zone--Compilation for Washington, Oregon, and northern California: EOS [Transactions, American Geophysical Union], in press.

McInelly, G.W., Kelsey, H.M., and Nelson, A.R., 1989, Late Pleistocene and Holocene tectonic deformation of the Whiskey Run wave-cut platform in the Cape Arago-Coos Bay area, coastal Oregon: Geological Society of America Abstracts with Programs, v. 21, no. 5, p. 115.

Nelson, A.R., and Personius, S.F., 1990, Great earthquake potential in Oregon and Washington--An overview of recent coastal geologic studies and speculations on segmentation of the central Cascadia subduction zone: Proceedings of Nuclear Regulatory Commission 17th Water Reactor Safety Information Meeting, October 24, 1989, Rockville, MD, in press.

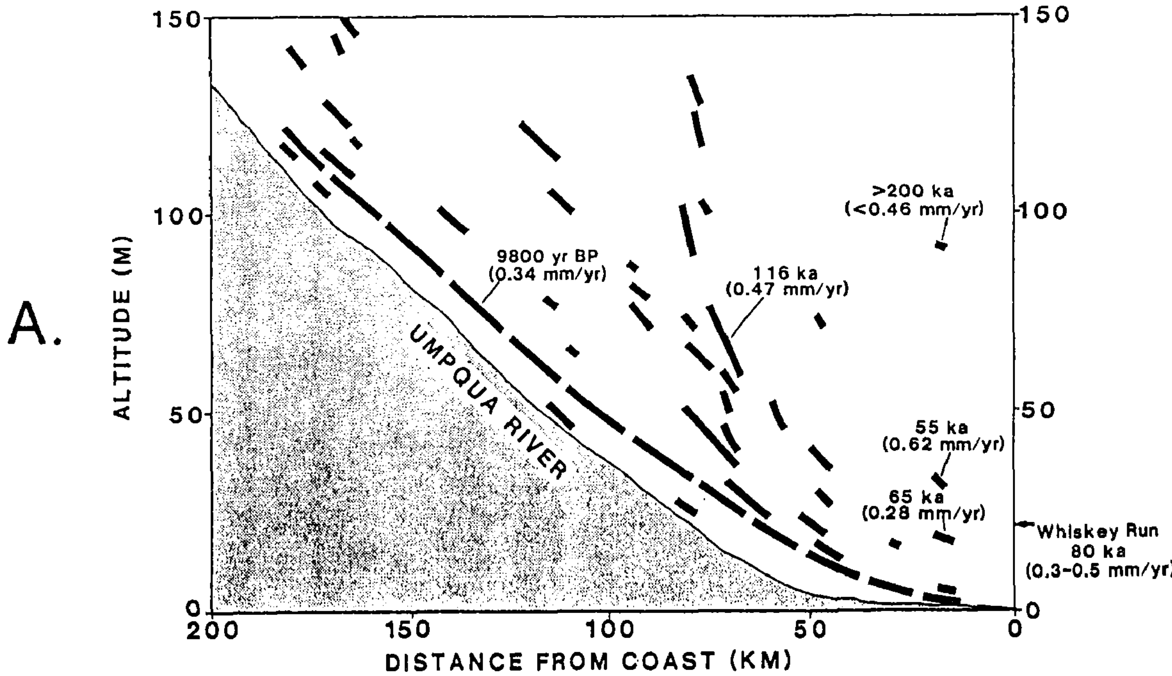

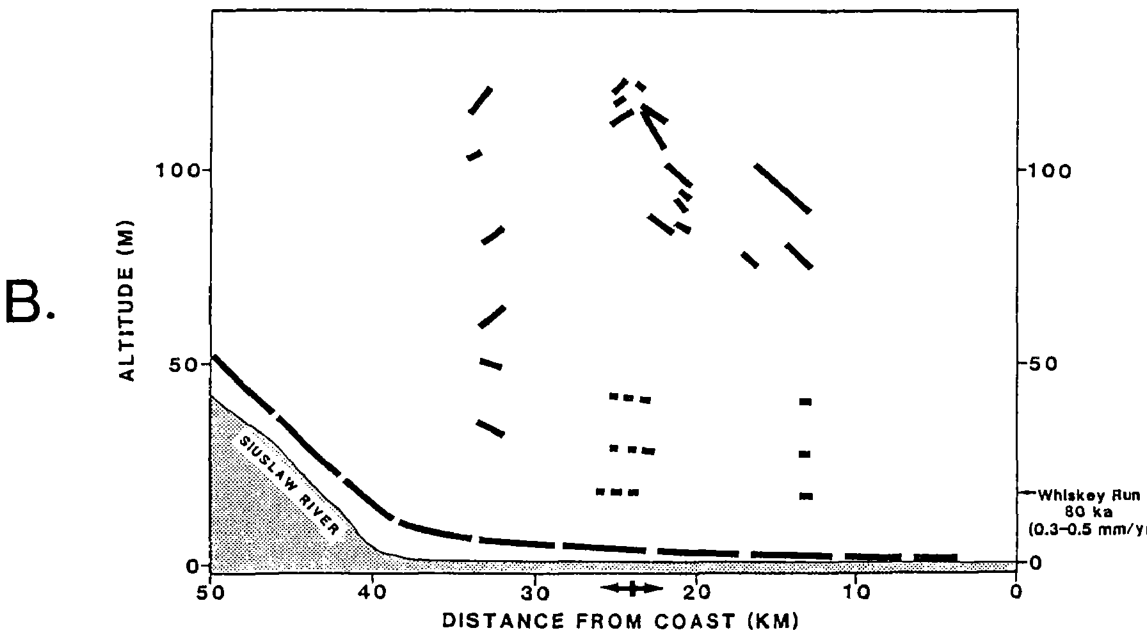

FIGURE 1. (A) Longitudinal profile of terraces along the Umpqua River, central Oregon Coast Range. Age estimates from thermoluminescence (TL) analysis are labeled "ka" (thousands of years ago); a single radiocarbon age is labeled "yr BP" (radiocarbon years before 1950). For comparison, the lowest marine terrace present near the mouth of the river (arrow) has been tentatively correlated with the Whiskey Run terrace near Bandon, Oregon, which has been dated by Muhs and others (submitted) at about 80 ka. Uplift rates calculated from the age determinations are shown in parentheses. Although some inconsistencies are apparent, the age data suggest regional uplift of 0.2-0.6 mm/ yr along this part of the Oregon coast. An intensive search for active structures along the Umpqua River was hampered by poor terrace preservation; active faults in particular could easily be undetected in the regions between terrace remnants. However, close examination of the more or less continuous early Holocene terrace revealed no evidence of latest Quaternary folding or faulting along the Umpqua River.

(B) Longitudinal profile of terraces along the lower part of the Siuslaw River, central Oregon Coast Range. Although no age data has been obtained on the pre-Holocene terraces, the position of the Whiskey Run terrace suggests that uplift rates along the Siuslaw River are similar to those along the Umpqua River. The most interesting aspect of the Siuslaw River profile is the clear expression of anticlinal folding of terrace remnants, coinciding with an anticline (double arrow symbol) in the underlying Eocene bedrock. We cannot determine if terraces below an altitude of about 50 m have been folded, because terraces are poorly preserved below this height. The age of the deformed terraces is unknown, but uplift rates from the nearby Umpqua River, and the presence of very well developed soils on the folded terrace deposits suggest they were probably formed well over 100 ka. The large area affected by the folding (over 20 km wide) suggests that these types of structures should be easy to detect on terrace profiles of other Coast Range rivers.

AN INTERACTIVE ENVIRONMENTAL/SOCIETAL PROCESS MODEL FOR THE ASSESSMENT OF VULNERABILITY TO EARTHQUAKES AND RELATED HAZARDS

9950-04477

SHERRY D. OAKS
Branch of Geologic Risk Assessment
U.S. Geological Survey
Box 25046, MS 966, Denver Federal Center
Denver, Colorado 80225
(303) 236-1600

Investigations

This study develops and tests a generalized, theoretical model for the assessment of vulnerability and resiliency to earthquakes and related hazards. The model can be applied globally, regionally, nationally, subnationally, locally, or to a specific site. In this study it is used for urban areas. The model includes geophysical, geotechnical, and engineering parameters and also includes key societal variables. The interrelationships between natural and technological hazards, and the environmental and societal processes that contribute to their occurrence, are analyzed. The ratio of vulnerability (V) to resiliency (R) is functionally dependent on interrelated environmental (E) and societal (S) systems $V/R = f_1 (E,S)$. E $[E = f_2 (e_g, e_b, S, \Delta^t)]$ is functionally dependent on the interconnected processes of the geosphere (e_g), the biosphere (e_b), and S. S $[S = f_3 (s, e, p, c, E, \Delta t)]$ is functionally dependent on the interrelated social (s), economic (e), political (p), and cultural processes (c) and E. The rate of change is represented by Δ^t.

Results

Standard measures of vulnerability from physical science and engineering, as well as from social science, were reviewed. Then, categories for determining vulnerability in each of the six main subvariables of the model (i.e. e_g, e_b, etc.) were determined from previous models and case studies. Quantitative data for the economic variable (e) were compiled from U.S. cities. Quantitative and qualitative data were analyzed for the environmental, social, political, and cultural components of the model for Salt Lake City, Utah. While the amount and structure of debt were important economic factors in the determination of vulnerability, other socially, politically, and culturally based economic factors such as access to credit or other economic resources were significant. Factors contributing to relative environmental stress, such as earthquake or other hazards, were important, but stress-causing societal factors, such as the amount of affordable housing, were highly significant. While type of structure was significant (i.e. unreinforced masonry, non-ductile concrete, etc.), maintenance of the structure was a primary element in determining vulnerability. Likewise density of structures was an important factor.

Reports

Oaks, S. D., 1989, Hazards and sustainable development: multiple considerations of environmental and societal factors. In Taller Internacional de Ecoturismo (in press).

Oaks, S. D., 1989, Community vulnerability to earthquakes and related hazards: environmental and societal factors. In Reconstruction After Urban Earthquakes (in press).

Oaks, S. D., and others, 1990, Disasters and Disturbance. (in press).

Data Processing, Golden

9950-02088

Robert B. Park
Branch of Geologic Risk Assessment
U.S. Geological Survey
Box 25046, MS 966, Denver Federal Center
Denver, CO 80225
(303) 236-1638

Investigations

The purpose of this project is to provide the day-to-day management and systems maintenance and development for the Golden Data Processing Center. The Center supports Branch of Geologic Risk Assessment with a variety of computer services. The systems include a PDP 11/70, a VAX/750, a VAX/780, two MicroVAX's, two SUN servers, 5 SUN workstations, and a PDP 11/34. Total memory is 40 mbytes and disk space is approximately 7 G bytes. Peripherals include four plotters, ten mag-tape units, an analog tape unit, two line printers, 5 CRT terminals with graphics, and a Summagraphic digitizing table. Dial-up is available on all the major systems and hardwire lines are available for user terminals on the upper floors of the building. Users may access any of the systems through a Gandalf terminal switch. Operating systems used are RSX11 (11/34's), Unix (11/70), RT11 (LSI's) and VMS (VAX's).

Results

Computation performed is primarily related to the Hazards program; however, work is also done for the Induced Seismicity and Prediction programs as well as for DARPA, ACDA, and U.S. Bureau of Reclamation, among others.

The data center supports research in assessing seismic risk and the construction of national risk maps. It also provides capability for digitizing analog chart recordings and maps as well as analog tape. Also, most, if not all, of the research computing related to the hazards program are supported by the data center.

The data center also supports equipment for online digital monitoring of Nevada and Colorado Western Slope seismicity. Also, it provides capability for processing seismic data recorded on field analog and digital cassette tape in various formats.

Simulating, Verifying, and Predicting the SH and P-SV Low Frequency Resonance in Salt Lake Valley

Grant No. 14-08-0001-G1518
Gerard T. Schuster
Mary Murphy
Harley Benz
Geology and Geophysics Dept.
University of Utah
Salt Lake City, Utah 84112

Objective. Salt Lake Valley (Figure 1) is in an area of high seismic risk. It is the objective of this study is to determine how deep basin structure controls the amplification of seismic ground motion along the valley floor. Is ground shaking primarily controlled by the upper 100 meters of strata, or is it influenced by a combination of near surface and deep basin structure resonance? We will attempt to answer this question by simulating two-dimensional elastic wave propagation in East-West cross sectional models of Salt Lake basin. A previous study (Hill, 1988) showed that SH resonance from deep (> 1 km) basin structure can play a major role in ground motion amplification.

Two–dimensional P–SV Wave Simulation Results. A second-order finite difference method is used to simulate P-SV wave propagation through 2-D models of Salt Lake Basin. The models are derived from two east-west cross-sections of Salt Lake Basin associated with the Northern and Central lines depicted in Figure (1). These models are derived from gravity, well log and seismic data within the valley. The source wavelet is a low frequency Ricker wavelet with a dominant frequency of 1.25 Hz.

Figure (2) depicts the synthetic horizontal and vertical displacement seismograms calculated at the basin surface for the northern basin model (Figure 2c). The source is a vertical displacement plane wave impinging from below. Results indicate that the greatest seismic amplification takes place over the deeper parts of the basin (between 20-30 km). Figure (4a) suggests an amplification factor of two to three for the plane wave source. The amplification factor tends to increase for line sources buried 15 km directly below the basin (Wasatch Line Source, Figure 4c) and buried at a depth of 10 km and offset 10 km west of the basin (Oquirrh Line Source, Figure 4b). It can also be shown that the the first two layers in Figure (4d) primarily influence the seismic amplification at the surface.

Figure (3) depicts the synthetic horizontal and vertical displacement seismograms calculated at the basin surface for the central basin model (Figure 3c). The source is a vertical displacement plane wave impinging from below. Results in Figure (5a) indicate a plane wave seismic amplification factor between 1-2 above the basin. Oquirrh and Wasatch line source responses in Figures (5b) and (5c) show even greater amplifications, with the Oquirrh source response showing dramatic amplification west of the basin.

In summary, our results suggest that resonance within the top two basin layers depicted in Figures (2c) and (3c) can account for seismic amplification factors between two to three. This assumes plane wave sources. Line sources buried west of the basin can further magnify the valley response relative to a bedrock site east of the basin. King et al. (1983) report amplification factors greater than 10 for measured site responses in the western part of the basin. The problem with correlating the observations of King et al. with our simulations is that the source for their seismic energy is an NTS blast in SW Nevada. We presently do not know how to accurately determine the incidence angle(s) or nature of this seismic energy as it impinges upon Salt Lake Valley.

Future Work. Future and ongoing work includes deriving a more accurate subsurface map of Salt Lake Basin (Radkins, 1990) and simulation of three-dimensional elastic waves in Salt Lake Basin (Olsen, 1991).

REFERENCES

Hill, J., 1988, A finite-difference simulation of seismic wave propagation and resonance in Salt Lake Valley, Utah; M.S. thesis, University of Utah, Salt Lake City, Utah.

King, K.W., Hays, W., and McDermott, P., 1983, Wasatch front urban area seismic response data report; USGS Open-File Report 83-452.

Murphy, M., 1989, Finite-difference simulation of seismic P- and SV-wave amplification in Salt Lake Valley, Utah; M.S. thesis, University of Utah, Salt Lake City, Utah.

Olsen, K., 1991, Simulation of three-dimensional elastic wave propagation in Salt Lake basin; PhD dissertation, Univ. of Utah, (in progress).

Radkins, H., 1990, Three-dimensional basin structure of Salt Lake Valley by seismically constrained 3-D gravity inversion; M.S. thesis, University of Utah, Salt Lake City, Utah.

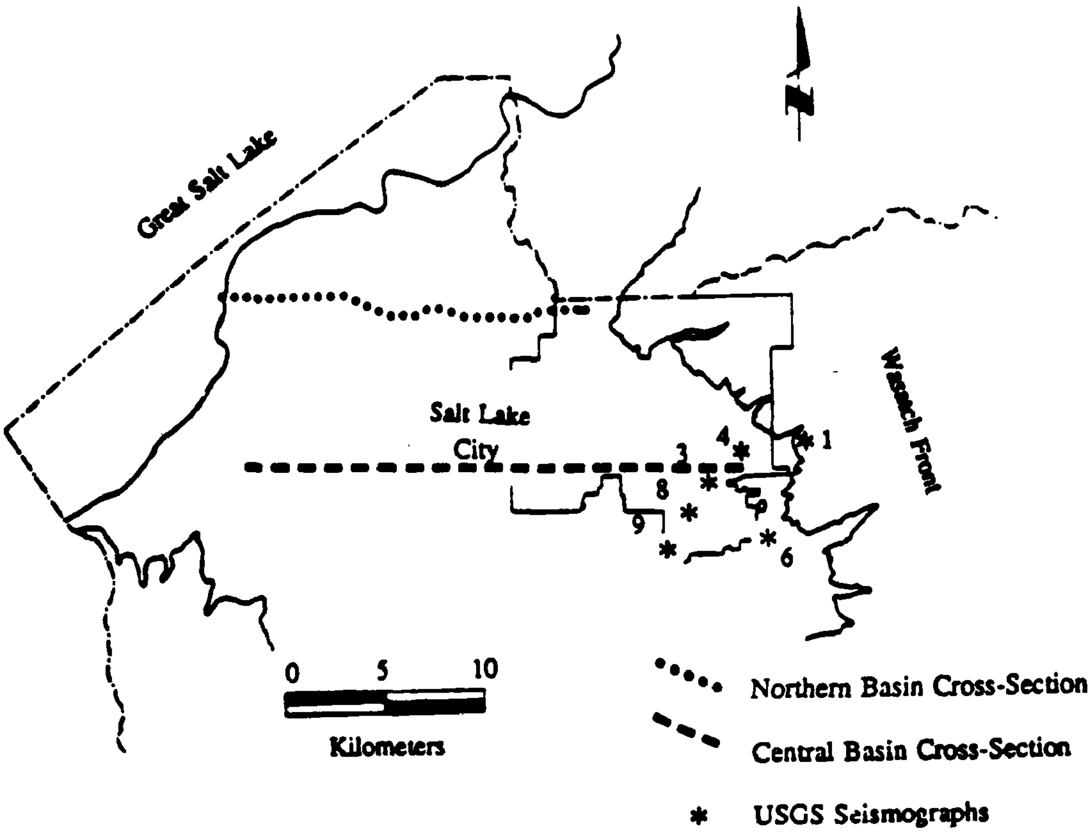

Figure 1. Map view of Salt Lake Valley.

Figure 2 (next page). Plane wave response of the Northern Basin cross-section resulting from an incident plane depicted in (2c). The basin is assumed to be homogenous in the N-S direction. "R" corresponds to the Rayleigh wave, and "P" corresponds to the direct P-arrival. Most of the seismic amplification occurs above the deep and intermediate parts of this assymetrical basin.

Figure 3 (next page). Same as Figure (2), except that the model is the Central Basin cross-section. "M" corresponds to multiple arrivals.

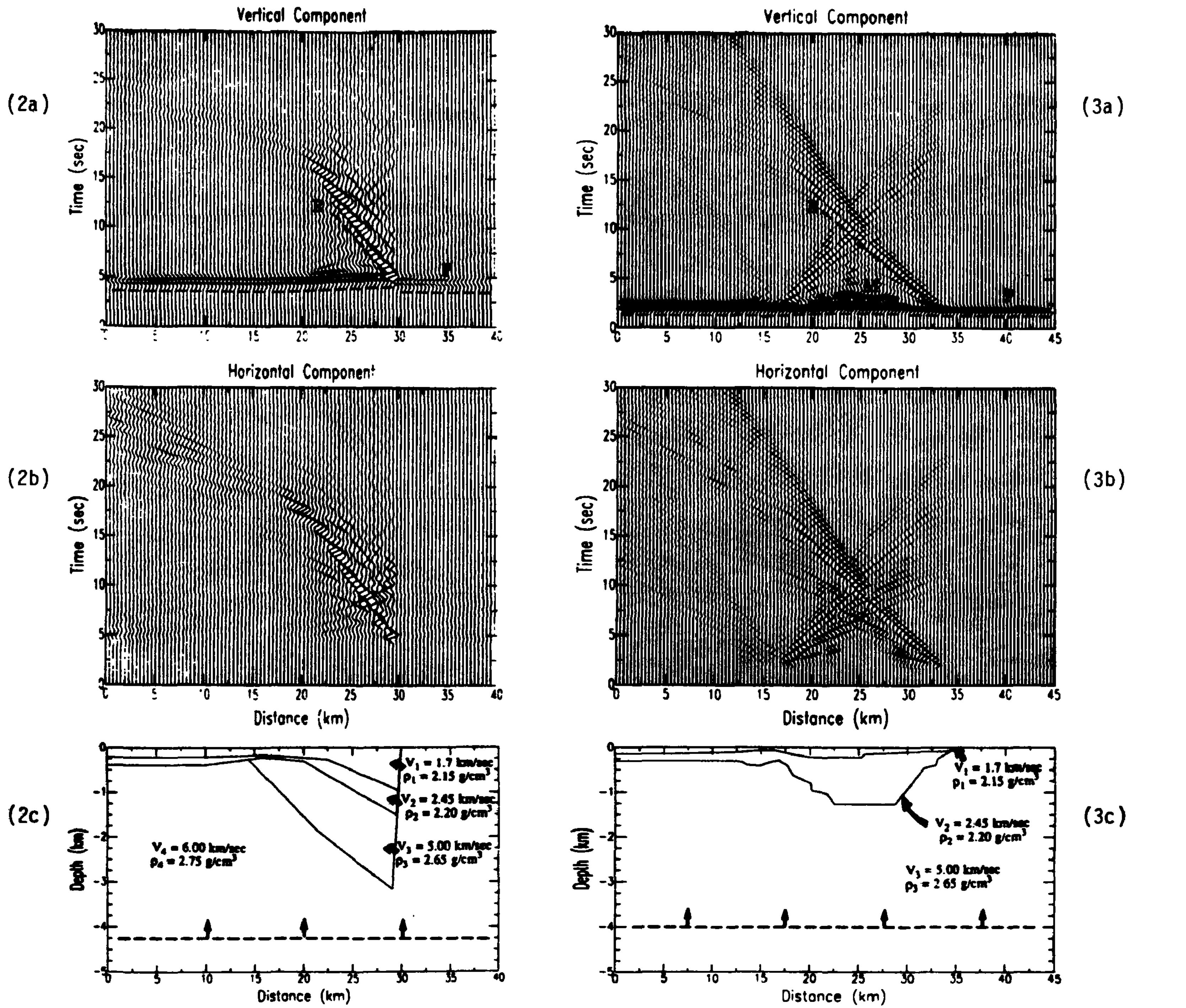

Vertical Component
Horizontal Component
(2a)
(2b)
(2c)
(3a)
(3b)
(3c)
Time (sec)
Distance (km)
Depth (km)
V_1 = 1.7 km/sec
ρ_1 = 2.15 g/cm^3
V_2 = 2.45 km/sec
ρ_2 = 2.20 g/cm^3
V_3 = 5.00 km/sec
ρ_3 = 2.65 g/cm^3
V_4 = 6.00 km/sec
ρ_4 = 2.75 g/cm^3

(a) (c)

(b) (d)

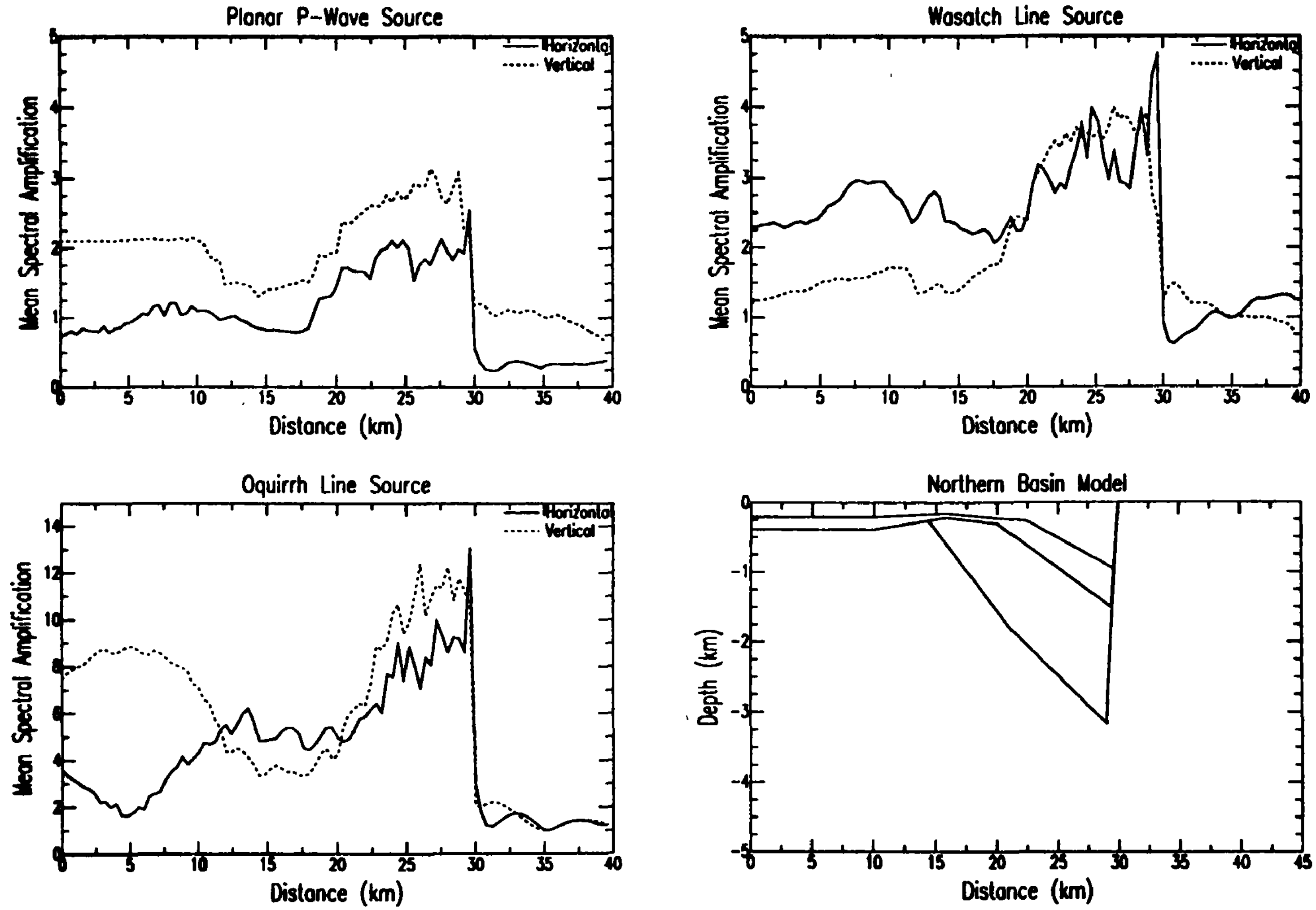

Figure 4. Mean spectral amplification ratios computed from the Figure (2) seismograms. The spectral ratios were computed by dividing the spectrum of the Figure (2) seismograms by the spectrum of the bedrock trace (i.e., the seismogram at the 40 km offset position). Note the artificial bias introduced by the quiescent nature of horizontal displacement at the 40 km location in Figure (2b). Thus the vertical component seismogram at the 40 km position was taken to be the bedrock trace for all calculations.

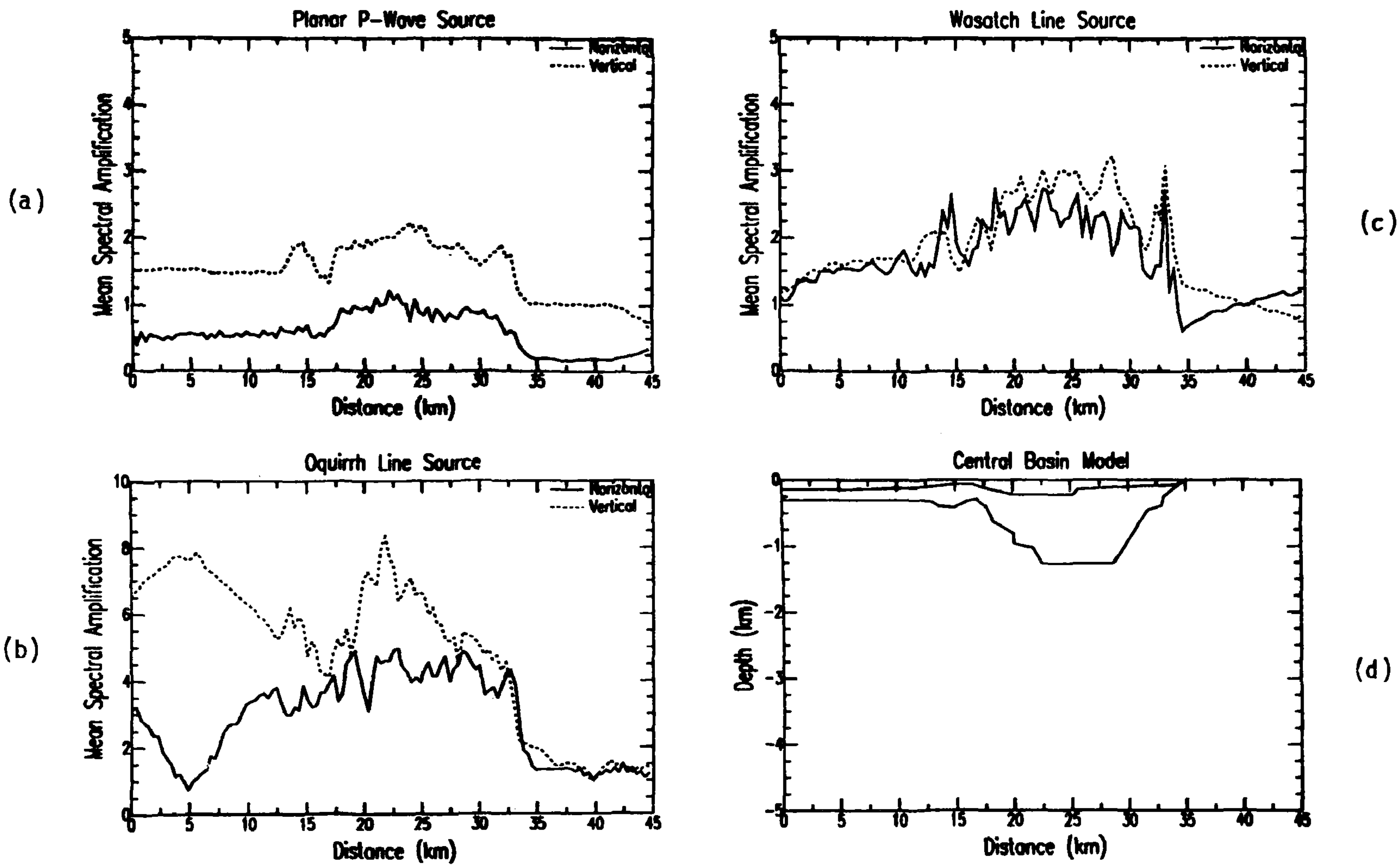

Figure 5. Same as Figure 4 except that the model is the Central Basin cross-section.

Deep Structural Complexity and Site Response in Los Angeles Basin

14-08-0001-G1684

Mrinal K. Sen*
Woodward-Clyde Consultants
566 El Dorado St.
Pasadena, CA 91101
(818)449-7650

(*Now at the Institute for Geophysics, University of Texas, 8701 Mopac Blvd., Austin, Tx 78759 , (512)471-0466)

OBJECTIVE : The objective of this project is to use geologic and seismologic information to develop seismic velocity structure in different parts of the Los Angeles Basin that can be used to predict strong ground motion in the basin.

INVESTIGATION AND RESULT:

The Los Angeles basin is characterized by its deep structural complexity and is the site of numerous earthquakes. In order to estimate strong ground motion, a detailed knowledge of the seismic velocity structure in the basin is required. We have been using a recently developed geologic model, well log data and recording of several small to moderate size earthquakes to derive seismic velocity structure in different parts of the basin. The models based on geology and other ancilliary informations are used as initial models for calculating synthetic seismograms and modified to model waveforms of the recorded seismograms. Reflectivity, asymptotic ray theory and finite difference methods are used to compute theoretical seismograms. We summarize below the results obtained from modeling of some of the events.

MODELING OF M_L=5.0 MALIBU, CALIFORNIA EARTHQUAKE OF JANUARY 19, 1989 RECORDED AT PASADENA :

A magnitude (M_L) 5.0 earthquake occurred under the Santa Monica bay near Malibu, california, at 0653 GMT January 19, 1989. The event was recorded well by the Caltech-USGS-USC network and the focal mechanism obtained from first motion reveals a thrust mechanism. The event was recorded well by Pasadena streckheisen instrument. Figure 1(a) shows the location of station, event and the focal mechanism. Since it is very difficult to model the broad-band data, the instrument response was deconvolved from the data and the data were high- pass filtered to frequencies above 0.5 Hz. Then the data were rotated to radial and tangential components. The data seem to rotate very well for we see very little p wave energy in the tangential component. We, therfore, carried out a synthetic seismogram modeling of this data using one-dimensional model. When the event and station locations are plotted (not shown here) on the basement contour map of Yerkes et al., we notice that the structure along this path is laterally varying; the basement being 5-6 km thick in the deepest part and then pinching out near Pasadena. Based on such geologic information and on ancilliary information on seismic velocities, we developed an initial one-dimensional model, computed synthetic seismograms and perturbed the model so as to match the synthetics with the observations. Our proposed model is displayed in Fig. 1(b). Our modeling results in a fairly simple model consisting of 6 km thick basin overlain by low-velocity sedimentary layers. The strong arrival appearing about 8 secs later than the direct arrival in the tangential component, is interpreted as the basin-reflected phase. The radial component obviously looks more complex than the tangential due to many converted phases. The comparison between the data and synthetics is shown in Fig. 1(c). We notice excellent agreement in peak amplitude and waveform in both radial and tangential component. We do notice some mismatches in the vertical component, which could probably be improved by changing the mechanism. However, the simple one dimensional model derived from waveform modeling seems to explain the wave propagation of this event very well.

MODELING OF AN M= 2.8 EARTHQUAKE RECORDED BY THE USC DOWNHOLE ARRAY IN THE BALDWIN HILLS, SOUTHERN CALIFONIA:

A three component downhole array consisting of 4.5 Hz seismometers deployed at the surface, 420m and 1500m depths, located in a deep abandoned oil well in the Baldwin Hills, Southern California is operated by the University of Southern California. The array recorded an M= 2.8 earthquake that occurred 0.9 km away from the array at a depth of 5.3 km on July 31 1986 (Hauksson, Teng and Henyey , 1987). The map (taken from Hauksson et al, 1987) showing the location of the array and the mechanism of the event is shown in Figure 2(a). Hauksson et al. (1987) analyzed these data set to study the site response, Q values and fmax. We have attempted to model these data using synthetic seismograms in order to derive detailed compressional and shear wave velocity structure of the sediments at that site of the basin. Since the earthquake was located very close to the array, it generated P and S rays travelling vertically up the downhole array and therefore this data set was best suited for this study. An interesting feature of this data set (Hauksson et al, 1987) is that the near surface site response results in amplification of the P wave by a factor of four and S waves by a factor of nine. The upgoing P and S waves and the surface reflected P and S waves can be easily identified in the data. Hauksson et al (1987) derived a gradient velocity model at the site using a sonic travel time curve. Their model was used as the initial P-wave velocity model; shear wave profile was derived from P-wave profile by using P to S travel time ratios. The velocity at depth below 1.5 km was assumed to be constant and was obtained from the arrival time of P and S waves at the deepest receiver. Forward synthetic seismograms were computed using the initial model and was then perturbed until an acceptable fit between the synthetics and the observations was obtained. Focal mechanism solution obtained by Hauksson et al. (1987) was used in the calculation. The final model and the comparison between the synthetics and the observations are shown in Figures 2(b) and 2(c) respectively. The model shows different gradient values of P and S wave velocities at different depths and thin layers of low P and S wave velocities near the surface to account for the amplification of P and S waves.

ANALYSIS OF SMALL AFTERSHOCKS OF OCT 1, 1987 WHITTIER NARROWS EARTHQUAKE:

Following the October 1, 1987 Whittier Narrows, southern California, earthquake (274 14:42 GMT; ML= 5.9), the U.S Geological Survey installed digital GEOS seismographs (Mueller et al. , 1988) at 32 temporary sites in the mainshock area in order to record aftershock motions over a broad range of magnitudes at small source to receiver distances. Hauksson and Jones (1989) obtained the location and focal mechanisms of most of these events using Caltech-USGS-USC network. We first discuss the analysis of peak ground accelerations (PGA) from 11 events (M_L = 2.2 to 3.5) recorded at most at 14 stations. The location of the events and the stations are shown in Figure 3(a). the plot of PGA vs hypocentral distance (Fig 3b) shows a wide variation in PGA. This may not be too surprising for we have events of different magnitudes and mechanisms and the L.A basin has a complex structure which is expected to affect wave propagation. The PGA recorded at a site depends upon magnitude, distance, site effect, source radiation pattern and propagation effect. In order to investigate the effect of these terms, we performed a regression analysis (using a code developed by N. A. Abrahamson at WCC) using the random effects model described by Brillinger and Preisler (1985). Since all of the sites in our data base have recordings of multiple earthquakes, we can estimate a correction factor for each site. The site effect is modelled as a simple scale factor and is included in the model by using random effects model. In the current application, the random effect is a site effect rather than an earthquake effect as used by Brillinger and Preisler. The resulting regression equation for the i-th site and j-th event is given by

$$\ln PGA = a + b\,M + c\,ln(r+h) + \phi\,F + \eta_i + \varepsilon_{ij}$$

where η_i and ε_{ij} represent the inter-site and intra-site variations with variances τ^2 and σ^2 respectively and F is a dummy variable that is 1 for thrust faults and 0 otherwise. The parameters as estimated by maximum likelihood are given below:

$a = 1.375$, $b = 1.672$, $c = -1.928$, $\phi = 0.213$, $\sigma = 0.653$ and $\tau = 0.261$

The regression analysis also results in site correction terms that are displayed in Fig. 3(a). We can then compute the theoretical PGA at all these sites using the regression equation and the residuals thus obtained are plotted against hypocentral distance in Fig 3(c). We next computed theoretical radiation pattern using the location and focal mechanisms obtained by Hauksson and Jones (1989). Fig 3(d) shows a plot of residual against radiation pattern. We do notice a linear trend with some degree of scatter; the cross-correlation coefficient being 0.367. Thus based on this analysis, we conclude that the PGA for these events at these sites is a result of a combination of radiation pattern and possibly the propagation effect.

We next discuss the results of modeling the waveform and amplitude of acceleration from an aftershock (Oct 11, 1987 22:34 M_L= 2.6) recorded along a profile AA. The location of the GEOS stations and that of the profile and the event are shown in Fig 4(a). This event was chosen because of its location very close to the profile (AA) along which Davis (1988) developed an improved geologic cross-section and five (maximum of all events) recording stations were available along this profile. The location, depth and mechanism of the event were taken from Hauksson and Jones (1989). The three-component data were first filtered to a maximum frequency of 3.5 Hz and were then rotated to radial and tangential components. The data rotated very well at this frequency and thus a two-dimensional modeling was justified.

An initial model was developed using the geologic cross-section of Davis upto a depth of 10 km below which Langston's model was used. The velocities to a depth of 10 km were taken from Vidale and Helmberger (1987). The model was then perturbed first by using an interactive 2-D ray-tracing code so as to obtain a fit in travel time between synthetics and observations. Then multifold path integral was used to construct synthetic seismograms for direct arrival only. Finally a finite-difference code was used to compute the complete seismograms. The final model along a profile AA is shown in Fig 4(b) and the comparison between observed and synthetic seismograms (SH component) is shown in Fig. 4(c). As seen in Fig 4(c), the waveform, polarity and peak amplitude of the observations can be simulated very well by finite-difference seismograms. The model also predicts the vertical and radial components (not shown) fairly well.

The strong arrival following the largest direct arrival at stations SVS and GAR is caused by multipathing of upgoing rays from source to receiver via the basin while the late arrivals are multiple reflections and scattering from the sedimentary layers. The stations to the north of the Raymond-Hill fault such as MIL and ECP show small phases following large simple arrivals. Initially we attempted to model this phase as reflection from the top of the low-velocity zone proposed by Langston (1989). Although the travel-time of first of these can be explained by slightly perturbing the depth to the top of the low-velocity zone, the amplitude of the reflection from this layer is too low compared to observations. However, these late arriving phases are modeled well as multiple reverberations from a thin sedimentary layer with a shear wave velocity of 0.9 km/sec and a thickness of 350 m lying to the north of the Raymond-Hill fault. We note that this thin layer was also predicted by modeling of Malibu event discussed earlier in the text.

REFERENCES:

Davis, T. L. (1988), Subsurface study of the late cenozoic structural geology of the Los Angeles Basin, final technical report to USGS.

Hauksson, E., Teng, T., and Henceyey, T. L. (1987), Results from a 1500m deep, three-level downhole seismometer array : site response, low Q values and fmax, BSSA, v77, no.6, 1883-1904.

Hauksson, E., and Jones, L. (1989), The Whittier Narrows earthquake sequence in Los Angeles, southern California : seismologic and tectonic analysis, in press, JGR.

Langston, C. A. (1988), Scattering under Pasadena, California, in press, JGR.

Muller, C., Dietel, C., Glassmoyer, G., Noce, T., Sembera, E., Spudich, P., and Watson, J., (1988), Digital recordings of the aftershocks of the 1 October 1987 Whittier Narrows, California earthquake, USGS open file report 88-868.

Sen, M. K., and Frazer, L. N., (1987). Synthetic seismograms using multifold path integral, Geophys. J. R. astr. Soc., 88, 641-671.

Vidale, J.E and Helmberger, D.V. (1987), Elastic finite difference modeling of the 1971 San Fernando, California earthquake, BSSA.

Yerkes, R. F., McCulloh, T. H., Schoellhamer, J. E., and Vedder, J. G., (1985), Geology of the Los Angeles Basin California, an introduction, USGS professional paper 420-A.

Malibu Earthquake January 19,1989

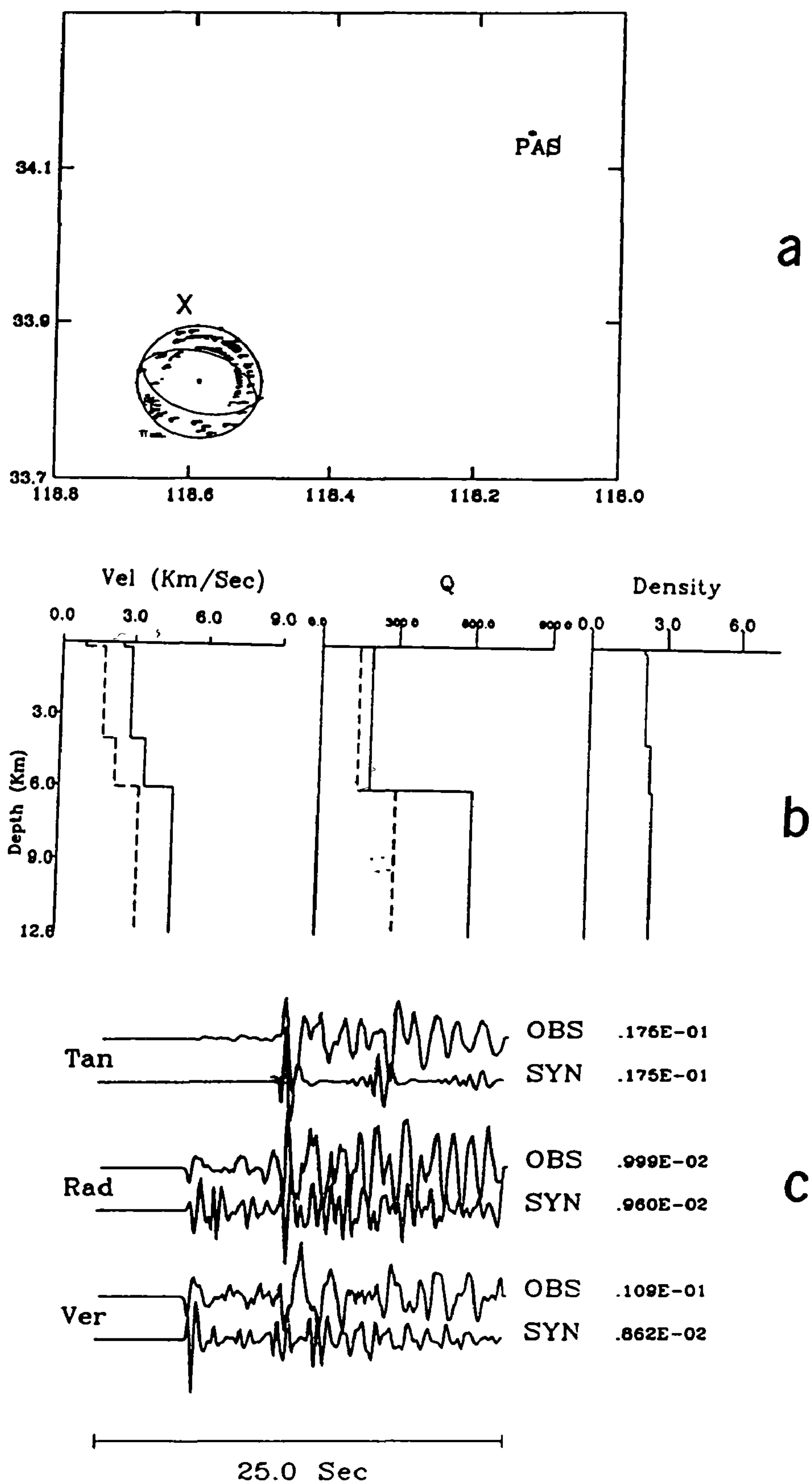

Figure 1. (a) Location of the event and the station, (b) Model obtained from forward modeling, (c) Comparison between synthetic and observed seismograms.

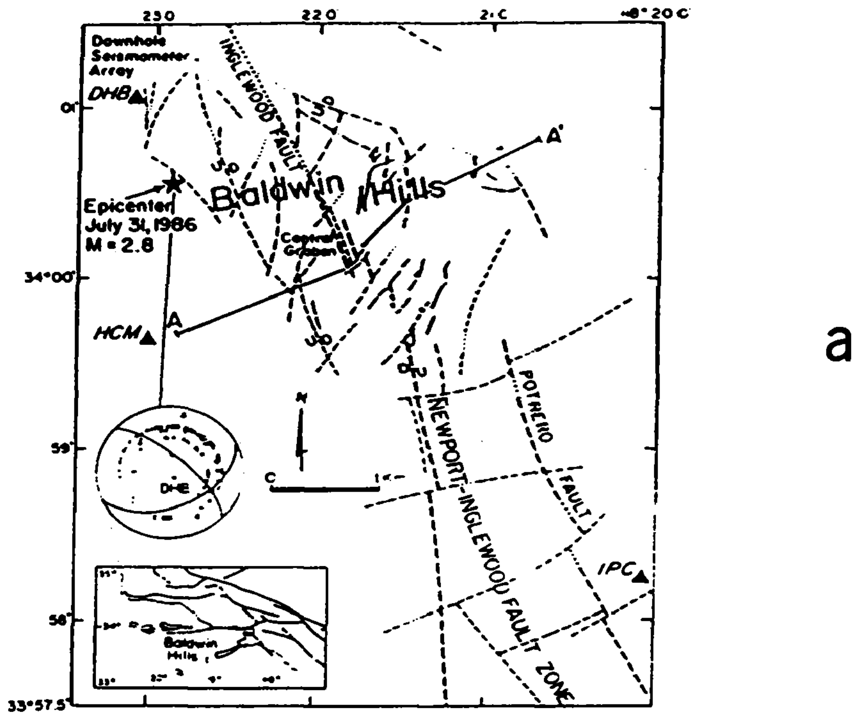

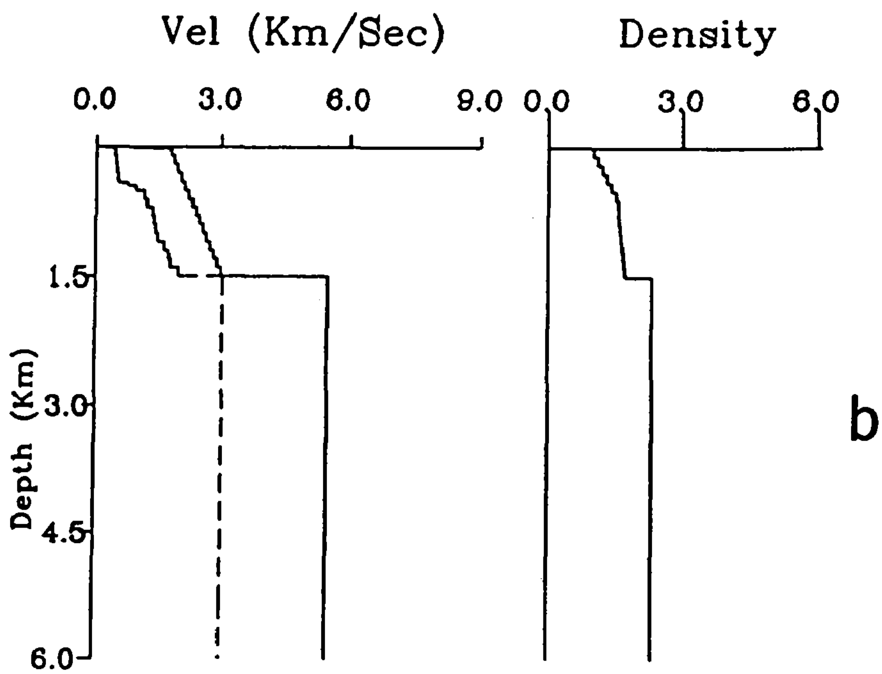

Figure 2. (a) Location of the array and the event (taken from Hauksson et al., 1987). (b) Model obtained from forward modeling.

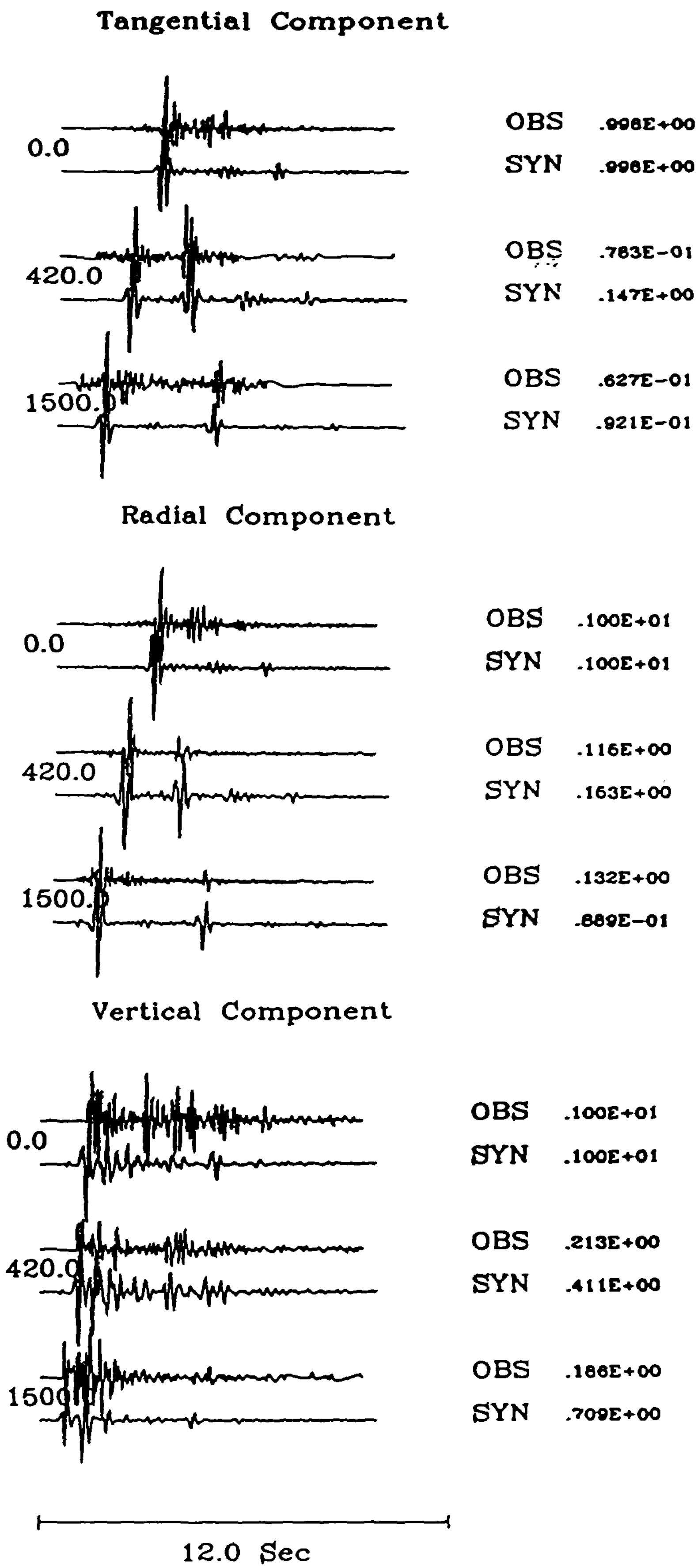

C

Figure 2 (c) Comparison between data and synthetics.

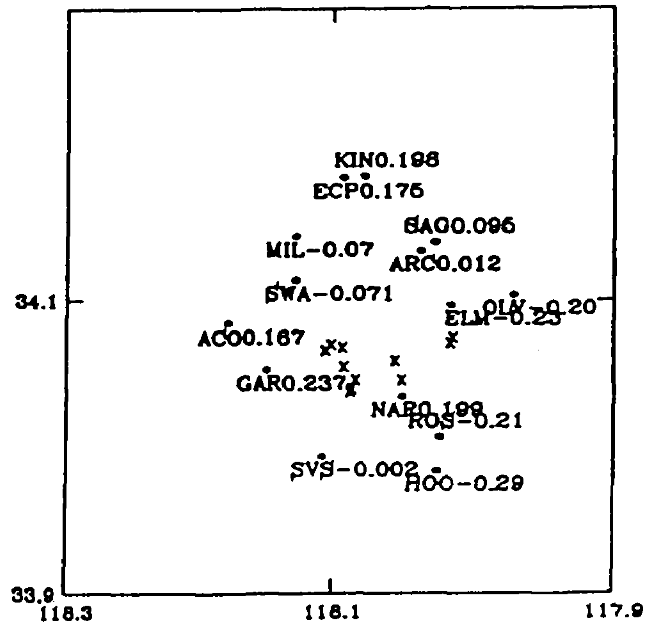

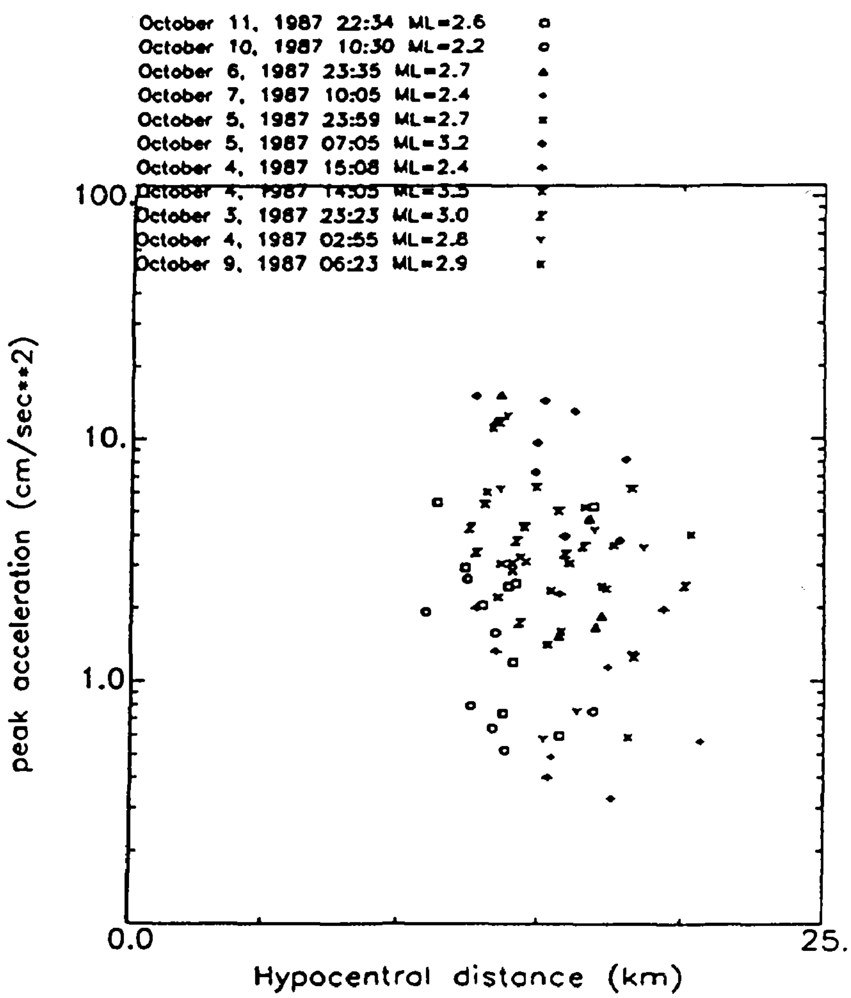

Figure 3. (a) Location of events and stations.
(b) Variation of PGA with distance.

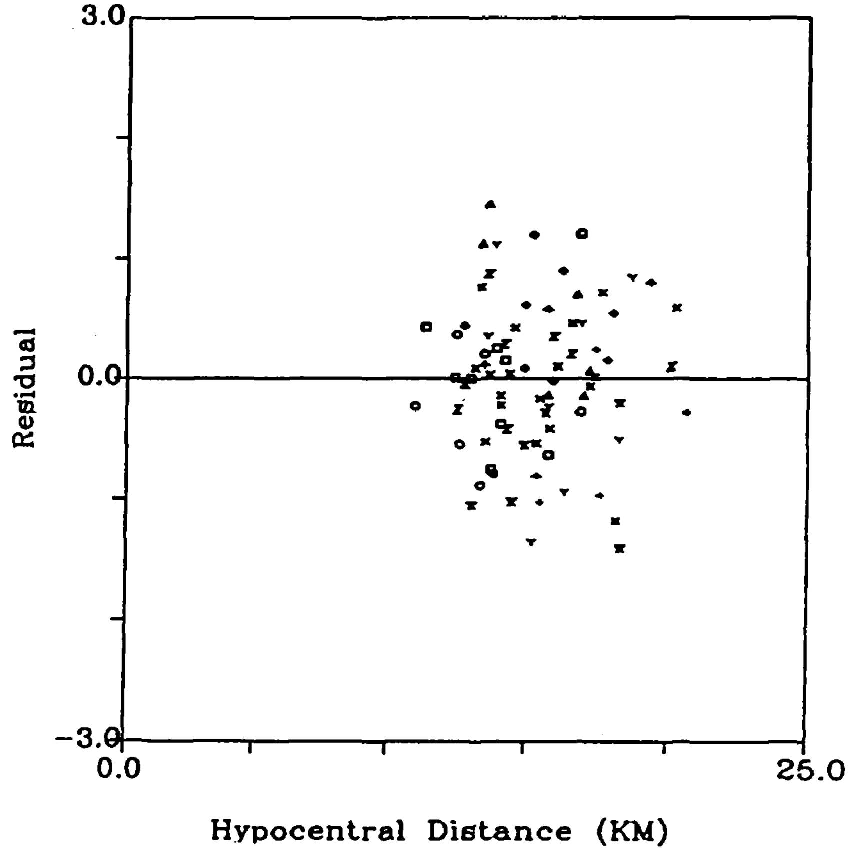

c

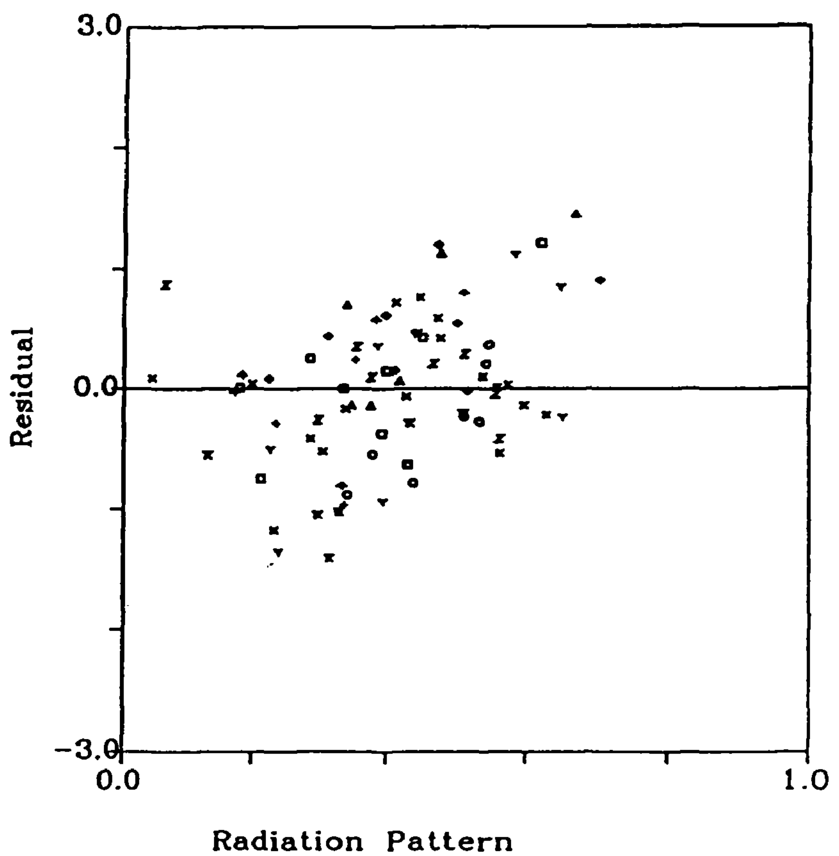

d

Figure 3. (c) Residual vs. distance.
(d) Residual vs. radiation pattern.

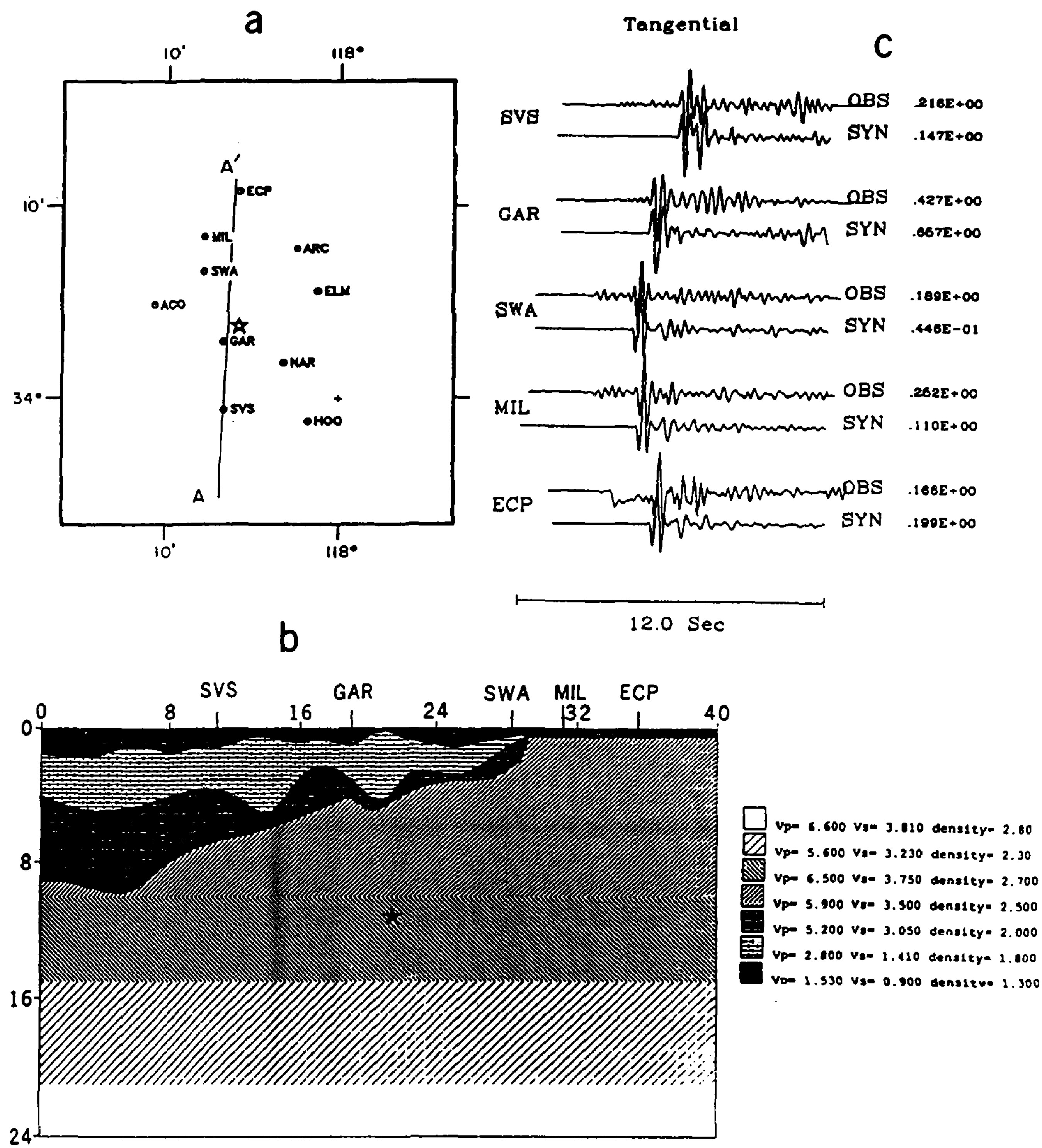

Figure 4. (a) Location of the event and the stations
(b) Model along a profile, (c) data vs. synthetics.

Simulation and Empirical Studies of Ground Motion Attenuation in the Seattle-Portland Region

14-08-0001-G1516

Paul Somerville and Brian Cohee
Woodward-Clyde Consultants
566 El Dorado Street, Suite 100
Pasadena, CA 91101

PHASE I: SUBDUCTION EARTHQUAKES

OBJECTIVE

The objective of the first phase of this project is to estimate strong ground motions for hypothetical M_w=8.0 subduction zone thrust earthquakes in the Puget Sound - Portland region using a simulation method. The use of strong motion simulation procedures is motivated by the complete absence of subduction earthquakes on the Cascadia subduction zone during historical time (and the consequent absence of strong motion recordings of such events), and the paucity of applicable strong motion recordings from other subduction zones.

APPROACH

We tested the simulation technique for large subduction earthquakes by modeling acceleration time histories and response spectra from the 1985 Michoacan (M_w=8.1) and Valparaiso (M_w=7.9) mainshocks. From the comparison between recorded and simulated ground motions, we estimated the modeling uncertainty associated with the simulation procedure. We then applied the simulation procedure to estimate ground motions in the Puget Sound - Portland region. Uncertainty in the source parameters of hypothesized subduction earthquakes on the Cascadia plate interface gave rise to uncertainty in the ground motion estimates. This parametric uncertainty was combined with the modeling uncertainty to obtain an estimate of the overall uncertainty in the ground motion estimates. This method of estimating the uncertainty in ground motion estimates derived by numerical modeling is described by Abrahamson and others (1989).

RESULTS

For periods less than 1 sec, the estimated response spectral values in the Puget Sound region for a M_w=8.0 subduction earthquake are about a factor of two larger than those of the 1949 Olympia and 1965 Seattle Benioff zone earthquakes. However, the duration of strong motion is expected to be significantly longer (50 sec vs. 10-15 sec), and the motions at periods longer than 1 sec are expected to be substantially larger.

PHASE II: BENIOFF ZONE EARTHQUAKES

OBJECTIVE

The objective of the second phase of this project is to estimate ground motions in the Puget Sound - Portland region resulting from earthquakes in the Benioff zone that lies within the subducted oceanic plate downdip of the subduction zone plate interface (depths greater than 40 km). Both the 1949 Olympia and the 1965 Seattle earthquakes were events of this type.

METHOD

Accelerograms from the 1949 and 1965 earthquakes, together with recent, well-calibrated velocity recordings of smaller earthquakes provide an empirical data base that will be used to define attenuation relations specific to this source zone. These will be compared with attenuation models derived from synthetic seismograms computed using crustal structure models appropriate to the Seattle-Portland region. We will examine the data to identify possible focussing and defocussing effects resulting from laterally-varying velocity structure. If such effects are observed, we will attempt to model them using synthetic seismograms computed in two-dimensional structure models.

PROGRESS

We have acquired calibrated velocity seismograms from 65 small (magnitude 1.2-4.5) earthquakes within the Benioff zone that were typically recorded by fifteen or more stations in the western Washington seismic network. We are currently analyzing wave propagation characteristics and the attenuation of ground motion in western Washington using these events. We are also modeling the strong motion recordings of the 1949 and 1965 events using finite source models, in order to develop realistic source models of large Benioff zone earthquakes. Corrected strong motion recordings from the 1976 Pender Island earthquake are being used as empirical source functions in this modeling procedure.

We are investigating wave propagation characteristics in a detailed two-dimensional model of the seismic velocity structure of the Cascadia subduction zone derived by the Lithoprobe project, and comparing them with those of a simplified one-dimensional model. The 1-D model is shown in the lower part of Figure 1, and the 2-D model is shown in Figure 2. Synthetic SH seismograms for a source depth of 18 km on the plate interface calculated using the two different models are compared in Figure 3. The seismograms for the 2-D structure were calculated using a finite difference technique, and include all arrivals. The seismograms for the 1-D model include just the direct and Moho reflected phases, and do not include radiation pattern. Although the 2-D calculation includes a large number of secondary arrivals that are not present in the 1-D calculation, the principal phases are comparable between the two calculations.

PUBLICATIONS

Abrahamson, N.A., P.G. Somerville, and C. Allin Cornell (1989). Goodness of fit for numerical strong motion simulations and uncertainty in numerical strong motion predictions, Manuscript in Preparation.

Somerville, P.G., M.K. Sen and B.P. Cohee (1989). Simulation of strong ground motions recorded during the 1985 Michoacan, Mexico and Valparaiso, Chile subduction earthquakes, *Seismological Research Letters*, **60**, p. 16; and manuscript in preparation.

Cohee, B.P. and P.G. Somerville (1989). Simulated strong ground motions for hypothetical Mw = 8 earthquakes on the Cascadia plate interface, *Seismological Research Letters*, **60**, p. 16; and manuscript in preparation.

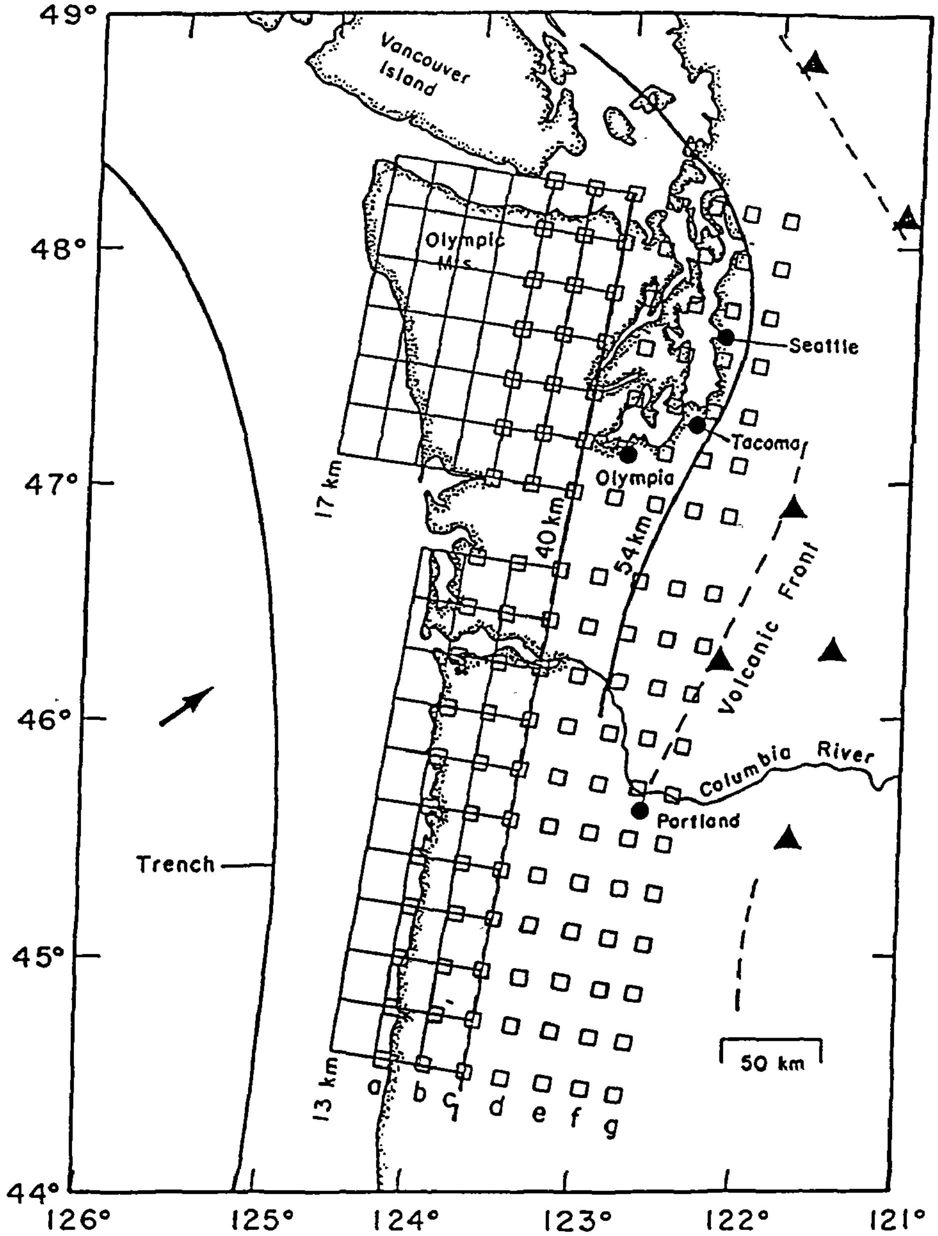

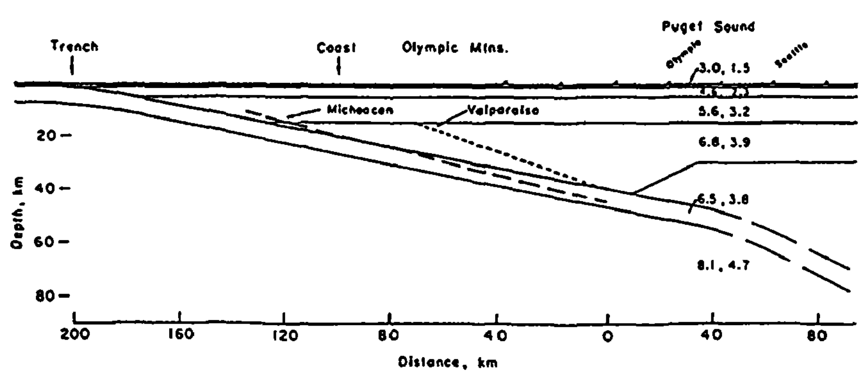

Figure 1. Geometry of the Cascadia subduction zone. (a) map view; (b) vertical section through the western Washington subduction zone, showing a simplified 1-D seismic velocity model.

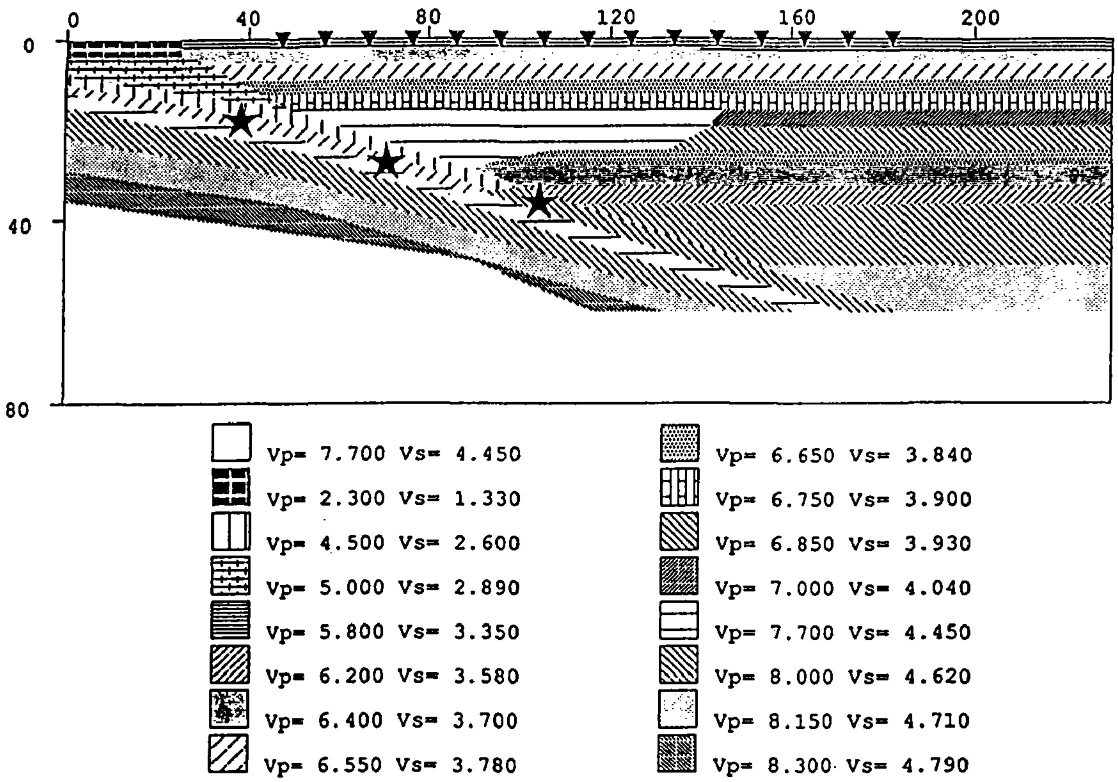

Figure 2. Seismic velocity model of the Cascadia subduction zone, modified from Clowes and others (1987).

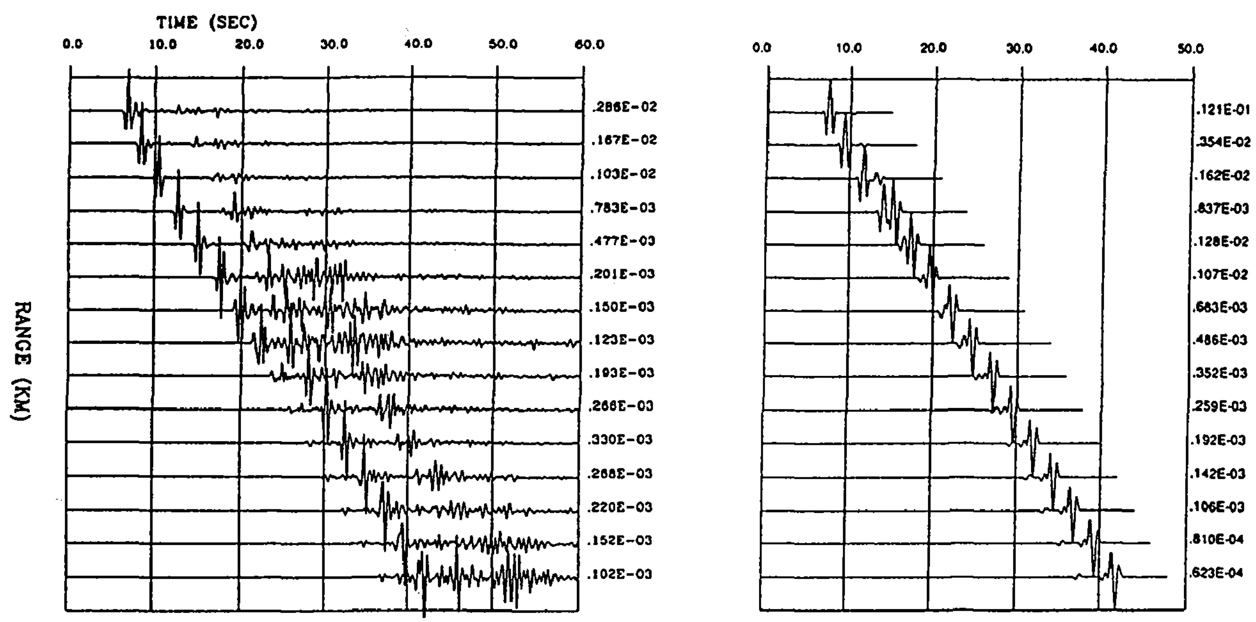

Figure 3. Comparison of profiles of SH synthetic seismograms across the subduction zone calculated for the 2-D model (left) and the simplfied 1-D model (right).

Quaternary Framework for Earthquakes Studies
Los Angeles, California

9540-01611

John C. Tinsley
Branch of Western Regional Geology
U.S. Geological Survey
345 Middlefield Road M/S 975
Menlo Park, California 94025
(415) 329-4928

Investigations

1. Geology and relative ground motion, Wasatch region, Utah:

Analysis of geologic and geophysical data from 43 sites in the Salt Lake Valley continues, and writing of interpretive reports is in progress. The studies involve comparisons among parameters including thickness of key stratigraphic intervals, degree of cementation of materials, shear-wave velocity, and soil index parameters in relation to alluvium-to-rock spectral ratios in two period bands (0.2-0.7 sec and 0.7-1.0 sec). (J. Tinsley, K. King, R. Williams, and D. Trumm).

2. Geology and relative ground motion, Puget Sound-Portland region:

In-situ studies of geologic and geophysical factors that correlate with relative levels of site response were underaken during late FY 88; the geologic factors have been analyzed further during the latter part of FY 1989 for the Olympia-Lacey, WA area (J. Tinsley, Menlo Park, CA; K.W. King, USGS, Golden, CO).

3. Regional Liquefaction Evaluation and Site Response studies, Los Angeles, CA; plans for FY 1990:

A. USGS scientists and program managers are negotiating a memorandum of understanding with the Planning Department of the City of Los Angeles to encompass Open-File publication of USGS regional liquefaction hazard mapping (surficial geology, shallow groundwater database, and derivative hazard maps, scale 1:24,000). The mapping is expected to be a point of departure for revisions to the earthquake hazards element of the City's general plan. This will complete the release of USGS data and USGS-compiled data mustered in connection with the regional evaluation of earthquake hazards by Tinsley and others, (1985), published in USGS Professional Paper 1360. (J. Tinsley/ D.M. Perkis, USGS, Golden, CO).

B. A ground shaking hazards map (scale 1:24,000) of the Los Angeles 7.5' quadrangle is also part of the foregoing MOU. The maps and supporting data overlays will be drawn according to the methodology of Rogers and others (1985).

Results

1. A contribution summarizing the results of the study of the Salt Lake Valley is being prepared; scheduled for completion by the end of calendar year 1989.

2. Kenneth W. King has recorded alluvium rock: rock spectral ratios at about 60 sites in the Olympia-Lacey area, using coal mine blasts as an energy source. Thirty (30) of these sites correspond to localities at which MMI (intensity) data are available from the earthquake that rocked the Puget Sound region in 1965. The variance in the spectral data closely mimics the variations in historical intensity, regionally and on a site-by-site basis. Geographically, the regional trends indicate that the spectral data are generally high at localities south of I-5, and tend to be lower to the north; exceptions to this generalization include sites in the harbor areas and sites located near the edges of embayments in proximity to cliffs. A limited number of sites were drilled during late FY 1988; the high response sites chiefly tend to be underlain by non-gravelly lithologies (chiefly sands and silts deposited as lacustrine deposits or deltas(?) in pro-glacial lakes) in relatively shallow basin settings; in contrast; the sites characterized by low alluvium: rock spectral ratios seem to occur on coarse, gravelly, cobbly, or bouldery late Pleistocene glacial outwash. These trends are expected to be mappable on the basis of driller's lithologic logs (where available) and published regional depth-to-bedrock maps; these inferred trends would be testable partly by making additional recordings in key areas, to see if the trends in the spectral ratios are conserved.

3. Nothing to report, as the Memorandum of Understanding is being negotiated.

Reports

Tinsley, John C., In press, Deterministic Ground Motion Mapping in the Portland-Puget Sound region: U.S. Geologicial Survey Open-File Report ___, Proceedings of Workshop on Earthquake Hazards of the Portland-Puget Sound region, convened Spring, 1989, 4 p.

References cited

Rogers, A.M., Tinsley, J.C., and Borcherdt, R.D., 1985, Predicting relative ground response: in Ziony, J.I., ed., Evaluating earthquake hazards in the Los Angeles region: U.S. Geological Survey Professional Paper 1360, p. 221-247.

Tinsley, J.C., Youd, T.L., Perkins, D.M., and Chen, A.T.F., 1985, Evaluating liquefaction potential in Ziony, J.I., ed., Evaluating earthquake hazards of the Los Angeles region, and earth science perspective: U.S. Geological Survey Professional Paper 1360, p. 263-316.

Seismic Reflection Investigations of Mesozoic Basins, Eastern U.S.

9950-03869

John D. Unger
Branch of Geological Risk Assessment
U.S. Geological Survey
922 National Center
Reston, VA 22092
(703) 648-6790

Ongoing Investigations

1. To consolidate and synthesize the available seismic reflection data that pertain to the internal and external structure of mesozoic basins, with special emphasis on the hypocentral areas of the present seismicity observed in South Carolina, New Jersey, New York, and Pennsylvania.

2. To use synthetic seismic reflection models of the basement structure along selected seismic reflection profiles as an aid to processing and interpreting these data and to develop better basement structural and velocity models for more accurate location of earthquake hypocenters.

3. To develop 2- and 3-dimensional Geographical Information System computer techniques to display, analyze, and interpret geological and geophysical data collected in and around Mesozoic basins and other seismogenic structures in the Eastern U.S., in order to better understand the tectonic history of the Appalachian orogen.

Results

This project continues data interpretation and analysis, which rely principally on the use of proprietary software from Dynamic Graphics Corp. (Interactive Surface Modeling and Interactive Volume Modeling) and ESRI (ARC/INFO). Research to date has resulted in promising possibilities for displaying interpreted seismic reflection data along with gravity, magnetic, and refraction information as three-dimensional models of the crust in and around Mesozoic basins. A key component of this process is the ability to integrate in-house software written on high resolution, color graphics workstations with the proprietary programs. This approach is expedited by being able to transfer data between the workstations and mini-computers, where these software packages reside, via high-speed networks.

Reports

Steward, David B., Unger, John D., Wright, Bruce E., Phillips, Jeffrey D., and Liberty Lee M., 1989, Geologic processes shown by the digitized Quebec-Maine-Gulf of Maine Global Geosciences Transect, Invited Poster, 28th International Geological Congress, Abstracts, v. 3, pp. 3-182.

Stewart, David B., Unger, John D., Wright, Bruce E., Phillips, Jeffrey D., Liberty Lee M., Spencer, Carl P., and Charlesworth, Phyllis, 1989, The digitization of the Quebec-Maine-Gulf of Maine Global Geosciences Transect, Invited Paper, 28th International Geologic Congress, Abstracts, v. 3, pp. 3-181.

Moench, Robert H., Boone, Gary M., Bothner, Wallace A., Boudette, Eugene L., Hussey, Arthur M., St-Julien, Pierre, and Unger, John D., 1989, Northern Appalachian Transect: Southeastern Quebec, Canada through Western Maine, USA; Field Trip Guidebook for the 28th International Geological Congress, Trip T358, American Geophysical Union, 52 pages.

Liberty, Lee M. and Unger, John D., 1989, Three-dimensional crustal modelling along a transect in the Northern Appalachians, Conference Proceedings, Third Annual Dynamic Graphics Users Conference, 15 pages; Director´s Approval, 6/29/89.

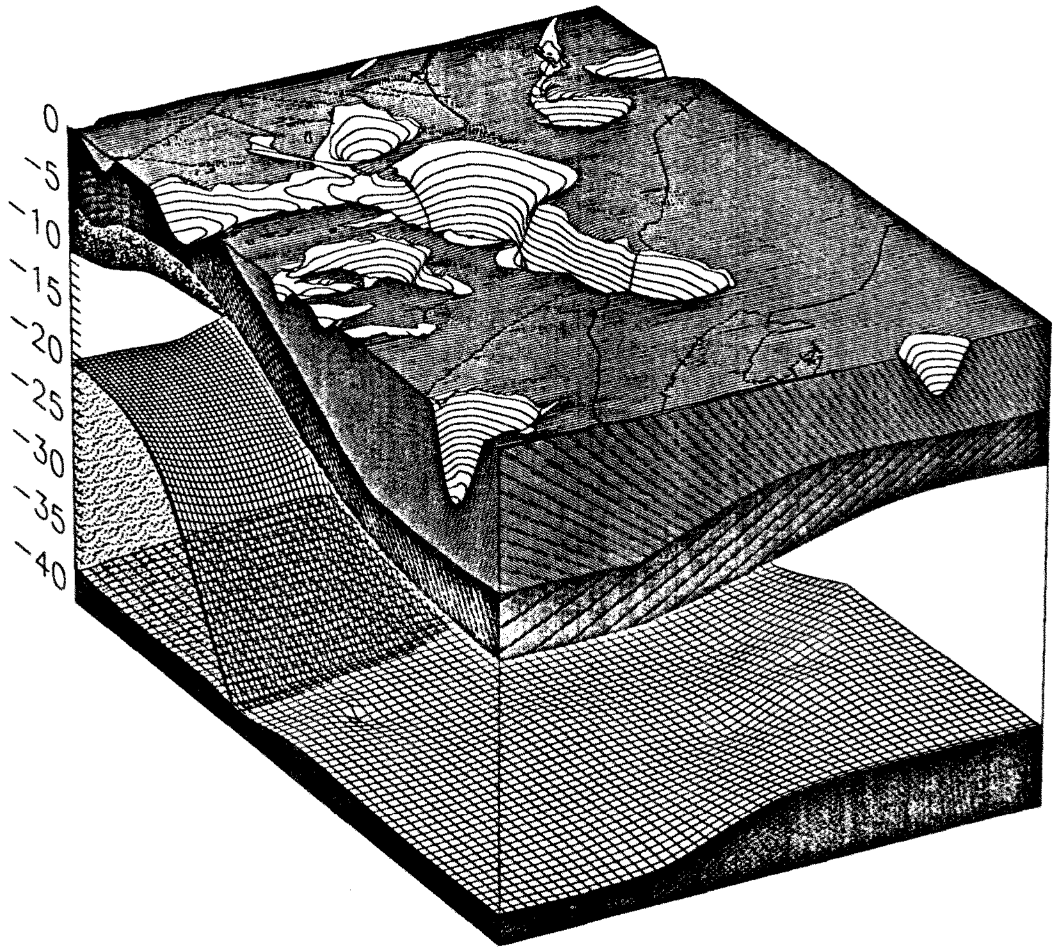

III.1

Block diagram of a 50 x 70 km area of the crust in the Appalachians of central Maine. The top layer of the model shows Cambrian - Devonian metasedimentary rocks cut by Devonian plutons, the bottoms of which are shown as contoured "holes" in the country rocks. The base of the model is the MOHO surface; the buried edge of the Grenville crustal rocks is shown in the lower left of the figure. The vertical scale is in kilometers. This model was created with ISM software.

Surficial Geology of the Oak City Area, Utah

9950-00638

David Varnes and Richard Van Horn (retired, volunteer)
Branch of Geologic Risk Assessment
U.S. Geological Survey
P.O. Box 25046, MS 966
Denver, Colorado 80225
(303) 236-1614

Investigations

With support of non-EHRP and personal funds, one week of fieldwork was accomplished in June, 1989. This was followed by a 2-day field conference to examine exposures and discuss differing views on the stratigraphic relations of Lake Bonneville deposits in the delta built by the Sevier River between Leamington and Delta, Utah. Members of the conference were:

C.G. (Jack) Oviatt, Kansas State University, supported by UGMS
Douglas Ekart, Oviatt's assistant
Fitzhugh Davis, Utah Geological and Mineral Survey (UGMS)
Donald Currey, Chairman, Dept. of Geology, University of Utah
Richard Van Horn, USGS, volunteer
David Varnes, USGS

The views of the first four are that the delta was deposited during the Provo-stage about 15,000 years ago. Varnes and Van Horn believe that only the upper part is that young and that the bulk of the delta is much older, with the base being 100,000 years or more in age. This controversy has considerable pertinence to assigning ages to deposits along the Wasatch Front, thus to determining recurrence intervals of faulting and hence assignment of seismic risk.

Oviatt has already published (Oviatt and Nash, 1989) a reinterpretation of the decades of work by Varnes and Van Horn, although he has not mapped to any significant extent in their area.

Results

Neither group changed its views.

Reference

Oviatt, C.G. and Nash, W.P., 1989, Late Pleistocene basaltic ash and volcanic eruptions in the Bonneville basin, Utah: Geological Society of America Bulletin, v. 101, p. 292-303.

A Search for Active Faults in the Willamette Valley, Oregon

14-08-0001-G1522

Robert S. Yeats
Department of Geosciences
Oregon State University
102 Wilkinson Hall
Corvallis, OR 97331-5506
503-737-2484

Investigations

Green-line mylars of 1:100,000 metric-series maps of the Willamette Valley have been ordered from USGS for the tectonic and geologic map which will be published in a forthcoming USGS professional paper on earthquake hazards in the Pacific Northwest. The components of this map were described in USGS Open-File Report 89-453.

Structure contours on key horizons (top Eocene Spencer Formation, top Columbia River Basalt) are being completed based on oil-exploratory well data and multichannel seismic lines. These data are being supplemented by water well logs. Tom Popowski spent the summer mapping the late Cenozoic geology of the west half of the Tualatin Valley west of Portland. The east half of the Tualatin Valley will be included in the geologic map of the Portland metropolitan area to be published by DOGAMI. Tom's work is focusing on the west half, one of the fastest growing areas in Oregon. Chris Goldfinger completed his mapping of the Corvallis fault, and he ran a gravity profile across the fault.

Bob Yeats testified before the Oregon legislature in favor of S.B. 955, which would assign additional responsibilities to DOGAMI to evaluate earthquake hazards. The bill was passed by the legislature without funds and signed into law by Governor Goldschmidt.

Results

Two of the major fault systems of western Oregon, the NE-striking Corvallis fault and the NNW-striking Portland Hills fault, are shown to be characterized by several major offsets. The offset pattern is in contrast to California, where both strike-slip and dip-slip faults are throughgoing, even though locally segmented. NW- and NE- striking faults, including many of the fault offsets, appear to be the same age. Some offsets on the Corvallis fault may by younger. The regional trends: NE for the Corvallis fault and NNW for the Portland Hills fault, formed in Miocene time or earlier. The marine Eocene section thins abruptly against the high side of the Corvallis fault, where Siletz River Volcanics are at the surface. The Portland Hills fault was a positive feature damming flow units of the Columbia River Basalt. However, the fault patterns have persisted into late Cenozoic time and are compatible with N-S maximum principal compressive stress (see discussion in Open-File Report 89-453) affecting previously-established crustal anisotropies.

There is relatively little expression of these faults in post-Columbia River Basalt sediments, implying a low slip rate, although pure strike slip (no vertical component) could lead to a higher slip rate than now suspected. If the pattern of offset faults persists to seismogenic depths, individual crustal earthquakes would be expected to be moderate to small.

Report

Yeats, R.S., 1989, Current assessment of earthquake hazard in Oregon: Oregon Geology, v. 51, no. 4, p. 90-91. (This report summarizes the findings of the 1989 Puget Sound/Portland Area workshop applicable to Oregon and issues a public warning about earthquake hazard in Oregon).

Liquefaction Hazard Mapping for the Seattle Urban Region Utilizing LSI

14-08-0001-G1695

T. Leslie Youd
Department of Civil Engineering
Brigham Young University
Provo, UT 94602
(801) 378-6327

Objective: Liquefaction, or more precisely, ground displacement caused by liquefaction is a major cause of earthquake damages. To fully assess earthquake hazards in a seismic region, such as the Seattle metropolitan area, maps showing liquefaction-induced ground failure potential are needed. The objective of this investigation is to develop techniques for mapping liquefaction-induced ground failure potential and field test and demonstrate the technique by compiling liquefaction hazard maps for part of the Seattle, Washington urban area.

Development of Criteria: The first six months of work on this project have been devoted to development of analytical models for predicting slope displacement at liquefaction sites. A computer code has been written for the analytical model of slope displacement proposed by Newmark. That model has been adapted to the case of a lateral spread moving on a liquefied layer. Synthetic time histories of ground shaking have been prepared which can be adjusted for magnitude of earthquake and distance from the seismic source. Preliminary analyses of displacement have been made using the Newmark model and the synthetic seismic records.

Liquefaction Severity Maps for the Seattle Urban Area: Contact has been made with Shannon and Wilson, Inc., Seattle, Washington, who are preparing liquefaction susceptibility maps for the Seattle North and South quadrangles. Arrangements have been made to examine the liquefaction susceptibility maps and obtain copies of the input data. This information will be used in the compilation of demonstration maps showing potential for liquefaction-induced ground displacement.

EARTHQUAKE LOSS ESTIMATION MODELING OF THE SEATTLE WATER SYSTEM

14-08-0001-G1526

Donald B. Ballantyne
Kennedy/Jenks/Chilton
33301 Ninth Avenue South, Suite 100
Federal Way, Washington 98003
(206) 874-0555

Objective: The Puget Sound region suffered magnitude 7.1 and 6.5 earthquakes in 1949 and 1965, respectively. USGS is currently evaluating potential for a magnitude 8+ earthquake in the region.

The Seattle Water Department (SWD), supplying water to over one million people, is the largest water supplier in Washington State, serving City residents as well as wholesaling water to 31 purveyors. While SWD has recently undertaken a project focusing on vulnerability of system structural components, their system has not been evaluated for operability following an earthquake.

This project is developing and applying techniques for estimating earthquake losses to the water system. The SWD system is being inventoried, and then modeled to estimate the loss of function based on the severity of ground shaking. Economic losses will then be estimated based on water loss and cost of repair. Secondary losses, such as business interruption, will be considered.

Data Collection and Review: Geological and seismological data being developed by USGS will be identified and used as applicable for input in the model. Ground motion attenuation study results, by Crouse, and liquefaction evaluation data, by Grant, both being funded by USGS, will be considered. Other liquefaction and landslide data collected, by Hopper, is being used. Existing applicable data will be collected and organized based on one mile square micro zones.

The system is being inventoried by line and node number, and facility category with all facilities located by coordinate. System operation parameters, such as flow and pressure, are being determined. Earthquake vulnerability data such as pipe and joint material type and structural design criteria are being gathered.

The pipeline database with over 8,000 pipe segments, maintained by the Seattle Water Department, is being used to identify pipe material and installation date. The database is particularly effective to calculate total pipe lengths of different pipe material for various earthquake intensity zones in the City.

Intensity data from the 1949 and 1965 earthquakes as well as intensity estimates made by USGS on their 1975 loss estimation study are being gathered. This intensity data is being plotted, and isoseismal zones established.

Water main failure data from the 1949 and 1965 earthquakes in the City of Seattle are being collected, plotted, and failure rates calculated for each isoseismal zone. Pipeline damage data in the 1985 Mexico City earthquake and 1987 Whittier Narrows Earthquake are also being gathered.

System Characterization: A system network computer model (Kentucky program) is being developed. System features important to vulnerability assessment, such as isolation valve locations, are being incorporated.

Hazard Definition: Hazards maps, divided into one mile square micro zones, will be prepared to facilitate input of data currently under development by USGS.

Component Vulnerability: Damage algorithms are being developed and/or updated for percent loss of function for categories of system components for varying earthquake scenarios. Scenarios will include magnitude 6.5 and 7.5 events similar to the 1965 and 1949 earthquakes, and a magnitude 8.5 subduction zone earthquake. Algorithm input will be based on site-specific geotechnical data, as well as structural and mechanical design of the facilities.

Failure rates for the 1985 Mexico City and 1987 Whittier Narrows earthquakes will be incorporated in the algorithms. The algorithm will be calibrated using 1949 and 1965 Seattle earthquake pipeline failure rate data. Previous algorithms for pipeline damage have identified and modeled all reported failures as breaks. This study differentiates between categories of failure, more closely modeling the system following an earthquake.

System Vulnerability: A system vulnerability model is being developed to modify input data files to KYPIPE, based on component vulnerability algorithms. As part of this model, system connectivity will be assessed to allow operation of KYPIPE. In previous models, system network connectivity analysis following an earthquake assumed that when a pipeline failure occurred, either the water would discharge freely from each end of the broken pipe, or the break must be isolated by closing all adjacent isolation valves. This study will utilize that same analysis for pipeline breaks, but will model leaks as flow demands on the system. The differentiation between leaks and breaks will significantly alter the model results. Earthquake parameters will be varied to establish operational criticality of each component.

Earthquake modeling criteria, such as location and configuration of seismic zones, magnitude, ground attenuation and liquefaction, will be varied to assess the sensitivity of the model.

Loss Estimation: The number of pipe failures will be estimated, and repair and water loss costs calculated. Losses from fire and business interruption will be considered.

Frequency and Survivability Profiles of Highway Bridges Along the I-5 Corridor Between Everett, Washington and Salem, Oregon

14-08-0001-G1698

Dr. Ralph Alan Dusseau
Wayne State University
5050 Cass, 1064 Mackenzie Hall
Detroit, Michigan 48202
(313)-577-3842

1.0 SUMMER FIELD TRIP

The principal objective during the first year of this project is to develop a comprehensive database for the approximately 1,000 bridges that are on and over Interstate Highways 5, 205, and 405 (I-5, I-205, and I-405) in western Washington State and northwestern Oregon. The data for this inventory was gathered during a 16-week field trip from May 16 to September 1, 1989. The information was taken from bridge design plans stored at the offices of the Washington State Department of Transportation in Olympia, Washington and at the offices of the Oregon Department of Transportation in Salem, Oregon. The segment of I-5 covered by the study begins at the Linn-Marion County Line south of Salem, Oregon and proceeds northward to the Snohomish-Skagit County Line north of Everett, Washington. The information assembled includes data such as bridge location, span lengths, connection details, soil boring logs, and the type and dimensions of the main members, the roadway deck, the supports, and the support foundations. Sufficient information was obtained about each bridge so that future users of this I-5 Bridge Database will be able to develop computer models of any bridge along the I-5 corridor based solely on the information contained in the database.

1.1 PRELIMINARY OBSERVATIONS

Appoximately 650 underpasses, overpasses, river crossings, and adjacent spans exist along I-5, I-205, and I-405 between the Oregon-Washington border at the Columbia River and the Snohomish-Skagit County Line north of Everett, Washington. Our current estimate is that over 90% of these bridges are either concrete box-girder bridges or precast pretensioned concrete girder bridges. While most of these bridges are three to five spans in length, some are massive viaducts with as many as 40 spans totaling a mile or more in length.

There are approximately 350 bridges along I-5, I-205, and I-405 in Oregon between the Linn-Marion County Line south of Salem, Oregon and the Oregon-Washington border. These bridges are a more uniform mix of concrete and steel construction compared with the bridges along the I-5 corridor in Washington State.

1.2 INVENTORY SHEETS

During the first few weeks of the field trip, the final versions of seven field inventory sheets (Figs. 1 to 7) were developed. These inventory sheets were used in various combinations to record all of the necessary information for each bridge that was inventoried in Washington State and Oregon during the summer field trip. Because of time and other constraints, inventories using these sheets were completed for about two-thirds of the bridges along the I-5 Corridor. Photocopies of the design plans for the remaining one-third of the bridges along the I-5 corridor have been and are being obtained. The pertinent information for these remaining bridges will be taken from the bridge design plans and recorded directly in the I-5 Bridge Database which is currently being developed at Wayne State University.

The information recorded on the field inventory sheets (Figs. 1 to 7) for each bridge can be divided into four categories based on how the data is indexed:

1. information that applies to the bridge as a whole, such as the number of spans, the compass bearing of the bridge, or the location;

2. data that pertains to a given span, such as the length of span one or the number of main members in span four;

3. information that is valid for a given support or support foundation, such as the height of support two or the footing thickness for support five;

4. data that is true across a segment of bridge or at the end of a bridge segment, such as the maximum cell width in the concrete box-girders between two specific points in the bridge or at a given point in the bridge.

For the latter category, the end-points of the segments involved do not necessarily coincide with support points. These segments may encompass a fraction of a span or several spans and are used in relation to either the bridge geometric properties (horizontal and vertical curves, deck tilt, and bent skew) or in relation to the concrete box-girder dimensions (where applicable).

Fig. 1 is the basic cover sheet that was used for all of the bridges that were inventoried in the field. This sheet contains: basic information that is true for the entire span, such as the compass bearing of the bridge and the bridge materials; data that is valid over segments of the bridge, such as the bridge geometric properties; data that is valid for spans one to six including the type and dimensions of the main bridge members; and data that is valid for supports and support foundations one to seven including the types and dimensions of the supports and the support foundations.

Fig. 2 is a continuation of Fig. 1 and was the required second page of information for all concrete box-girder bridges and for those precast pretensioned concrete girder bridges with more than six spans. Figs. 3 to 5 are continuations of Fig. 2 and were optional sheets that could be used one or more times in order to record all of the required information for either a concrete box-girder bridge or a precast pretensioned concrete girder bridge.

Fig. 6 is the second page that was used for steel plate-girder bridges or bridges having main members composed of steel wide-flange sections with steel cover plates, while Fig. 7 is the second page that was used for steel truss bridges. Figs. 6 and 7 have no designated span or support numbers and thus could be used multiple times if necessary in order to compile all relevant data on a given bridge. For unique structures, such as steel arches, design plans were obtained and will be used directly to record data in the bridge database without the need for specialized inventory sheets.

1.3 ADDITIONAL INVENTORY DATA

In addition to the data on the inventory sheets, other information was also gathered in the field. Photocopies were made of all bridge bearing and connection details, and of most soil boring logs. These photocopies will be permanently recorded on computer disks using a digitizing scanner. A number will be assigned to each bridge detail and to each soil boring log. These numbers will be recorded in the I-5 Bridge Database so that database users can find and examine the bearing and connection details and the soil boring logs that pertain to any of the bridges in the database.

2.0 PHOTOGRAPHS AND FIELD MEASUREMENTS

Because of time constraints, plans for photographing all 1,000 bridges along the I-5 corridor and for performing field ambient vibration measurements on selected bridges during the summer of 1989 have been postponed until the summer of 1990. During this second field trip, ambient vibration measurements will be taken on 30 to 50 typical bridges along the I-5 corridor in order to determine the natural frequencies and modes of vibration of these typical spans. This data will be extrapolated to estimate the natural frequencies of the other bridges along the I-5 corridor and this information will be added to the bridge database.

Also during this second field trip, 35mm slides will be taken of each bridge along the I-5 corridor and permanently recorded on a laser-disk. These images will be accessed using an IBM Infowindow hardware and software system with a Sony laser-disk player and selected third-party software. The eventual goal is combine the laser-disk images of each bridge with overlays containing the digitized images of the bridge details and the bridge soil boring logs, and with overlays containing pertinent information from the I-5 Bridge Database to create a comprehensive interactive visual presentation.

3.0 DATABASE FORMAT

The final format for the I-5 Bridge Database is currently taking shape and will include virtually all of the information recorded on the bridge inventory sheets (Figs. 1 to 7). The approximately 96 fields (columns) in the database are being arranged such that each record (line of information) will include information for one span, one support and support foundation, one segment with respect each bridge geometric property, and one segment of concrete box-girder. Thus a typical two-span bridge with three supports will utilize at least three records. The first record will include all of the data that is valid for the entire bridge, the information for span one, the data for support and support foundation one, the information for the first segments with respect to each bridge geometric property, and (where applicable) the data for the first segment of concrete box-girder. The second record will include all of the data pertaining to span two, support and support foundation two, the second segment for each bridge geometric property, and the second segment of concrete box-girder. The third record will include all of the information pertaining to support and support foundation three, the third segments for each bridge geometric property, and the third segment of concrete box-girder. Additional records, if needed, will include data pertaining to additional bridge segments for geometric properties and/ or to additional concrete box-girder segments.

The eventual goal is to convert all of the bridge geometric property data and the concrete box-girder dimensions, which are currently related to specific segments of bridge, into data that is applicable over a specific bridge span or at a given bridge support. Thus all of the data in the database would be related to either the bridge as a whole, a given bridge span, or a specific support and support foundation. This conversion will require the development of several computer programs for interpolation of the bridge geometric property data and the bridge concrete box-girder dimensions. While the result would be a database with entries that are either bridge, span, or support and support foundation specific, this would result in the loss of some data since any changes in the bridge geometric property data or in the concrete box-girder dimensions that occur within spans and between supports would be lost.

The software package that is currently being used to develop the I-5 Bridge Database is the dBASE IV program. The dBASE III+ program was used to create an initial version of the bridge database (prior to the field trip during the summer of 1989). With the recent release of the dBASE IV package, however, the decision was made to use this latest version of the dBASE series of programs to develop the final version of I-5 Bridge Database.

4.0 PUBLICATION PLANS

Abstracts dealing with the field inventory techniques that were used during the summer of 1989 have been submitted for possible inclusion in the Fourth U.S. National Conference on Earthquake Engineering and in the Third International Conference on Short and Medium Span Bridges. The final I-5 Bridge Database will be used to generate numerous graphs and charts pertaining to the type, size, distribution, and other parameters of the bridges in the database. These graphs will provide the basis for one or more journal papers that will be written and submitted after the I-5 Bridge Database is completed.

STAPLE HERE	BEARING	deg min sec		LOCATION		CONTRACT NO.	
BRIDGE NO.		YEAR APPR.		DATE	INIT	CHCK	PAGE 1 OF
MAIN MEMBER DESCRIPTION OR COMMENTS				MATERIALS DECK		MAIN MEMBERS	
				SUPP	ABUT	FNDTN	
INT. MAIN MEM.		EXT. MAIN MEM.		APPROACH DESCRIPTION OR COMMENTS			
MAX DECK THICK		MIN DECK THICK					
NO. MEMBERS #1		NO. MEMBERS #2		LEFT ABUT. EL.		RIGHT ABUT. EL	
MEM SPACING #1		MEM SPACING #2		LEFT BORING EL		RT. BORING EL.	
DECK WIDTH #1		DECK WIDTH #2		LEFT BORING NO		RT. BORING NO.	
RADIUS BETWEEN		LOCATION		RADIUS BETWEEN		LOCATION	
DECK TILT AT		LOCATION		DECK TILT AT		LOCATION	
BENT SKEW AT		LOCATION		BENT SKEW AT		LOCATION	
ROADWAY SLOPE		P.V.I.		ROADWAY SLOPE		CURVE LENGTH	

SPAN NUMBER--->	1	2	3	4	5	6	SPAN NO
SPAN LENGTH--->							<LENGTH

JOINT->	1	2	3	4	5	6	7
TYPE--->							
SEAT--->							
LOCA--->							
CLEAR->							
DETAIL>							
SUPPORT	1	2	3	4	5	6	7
TYPE--->							
NUMBER>							
WIDTH->							
SIZE--->							
HEIGHT>							
FNDTN TYPE->							
LENGTH>							
WIDTH->							
THICK->							

Figure 1. Field Inventory Sheets - General Cover Page for All Bridges

MAX. TOP WIDTH		MIN. TOP WIDTH		BRIDGE NO.		INIT		PG OF
MAX. BOT WIDTH		MIN. BOT WIDTH		UNIT NO.		FROM		TO
MAX. CELL WID.		MIN. CELL WID.		MAXIMUM CONCRETE THICKNESSES		MINIMUM CONCRETE THICKNESSES		
MAX. CELL HT.		MIN. CELL HT.		WALLS		WALLS		
NO. MEMBERS #1		NO. MEMBERS #2		BOTTOM SLAB		BOTTOM SLAB		
MEM SPACING #1		MEM SPACING #2		BORING ELEV.		BORING ELEV.		
DECK WIDTH #1		DECK WIDTH #2		ADD. BORING NO		ADD. BORING NO		
LOCATION #1		LOCATION #2		APPR. LOCATION		APPR. LOCATION		
RADIUS BETWEEN		LOCATION		RADIUS BETWEEN		LOCATION		
DECK TILT AT		LOCATION		DECK TILT AT		LOCATION		
BENT SKEW AT		LOCATION		BENT SKEW AT		LOCATION		
ROADWAY SLOPE		P.V.I.		ROADWAY SLOPE		CURVE LENGTH		

7	8	9	10	11	12	13	SPAN NO
							<LENGTH

JOINT-->	8	9	10	11	12	13	14
TYPE--->							
SEAT--->							
LOCA--->							
CLEAR-->							
DETAIL>							
SUPPORT	8	9	10	11	12	13	14
TYPE--->							
NUMBER>							
WIDTH-->							
SIZE--->							
HEIGHT>							
FNDTN TYPE-->							
LENGTH>							
WIDTH-->							
THICK-->							

Figure 2. Field Inventory Sheets - Second Page for Concrete Box-Girder Bridges and for Precast, Pretensioned Concrete Girder Bridges

MAX. TOP WIDTH		MIN. TOP WIDTH		BRIDGE NO.		INIT		PG OF	
MAX. BOT WIDTH		MIN. BOT WIDTH		UNIT NO.		FROM		TO	
MAX. CELL WID.		MIN. CELL WID.		BORING ELEV.		BORING ELEV.			
MAX. CELL HT.		MIN. CELL HT.		ADD. BORING NO		ADD. BORING NO			
NO. MEMBERS		NO. MEMBERS		APPR. LOCATION		APPR. LOCATION			
MEM SPACING		MEM SPACING		BORING ELEV.		BORING ELEV.			
DECK WIDTH		DECK WIDTH		ADD. BORING NO		ADD. BORING NO			
LOCATION		LOCATION		APPR. LOCATION		APPR. LOCATION			
RADIUS BETWEEN		LOCATION		RADIUS BETWEEN		LOCATION			
DECK TILT AT		LOCATION		DECK TILT AT		LOCATION			
BENT SKEW AT		LOCATION		BENT SKEW AT		LOCATION			
ROADWAY SLOPE		P.V.I.		ROADWAY SLOPE		CURVE LENGTH			

							SPAN NO
							<LENGTH

JOINT-->							
TYPE-->							
SEAT-->							
LOCA-->							
CLEAR-->							
DETAIL>							
SUPPORT							
TYPE-->							
NUMBER>							
WIDTH-->							
SIZE-->							
HEIGHT>							
FNDTN TYPE--> (ELEV)							
LENGTH>							
WIDTH-->							
THICK-->							

Figure 3. Field Inventory Sheets - Optional Page for Concrete Box-Girder Bridges and for Precast, Pretensioned Concrete Girder Bridges

BRIDGE NO.		INIT		PG OF

UNIT NO.		FROM		TO	UNIT NO.		FROM		TO
MAX. TOP WIDTH		MIN. TOP WIDTH			MAX. TOP WIDTH		MIN. TOP WIDTH		
MAX. BOT WIDTH		MIN. BOT WIDTH			MAX. BOT WIDTH		MIN. BOT WIDTH		
MAX. CELL WID.		MIN. CELL WID.			MAX. CELL WID.		MIN. CELL WID.		
MAX. CELL HT.		MIN. CELL HT.			MAX. CELL HT.		MIN. CELL HT.		
NO. MEMBERS		NO. MEMBERS			NO. MEMBERS		NO. MEMBERS		
MEM SPACING		MEM SPACING			MEM SPACING		MEM SPACING		
DECK WIDTH		DECK WIDTH			DECK WIDTH		DECK WIDTH		
LOCATION		LOCATION			LOCATION		LOCATION		

UNIT NO.		FROM		TO	UNIT NO.		FROM		TO
MAX. TOP WIDTH		MIN. TOP WIDTH			MAX. TOP WIDTH		MIN. TOP WIDTH		
MAX. BOT WIDTH		MIN. BOT WIDTH			MAX. BOT WIDTH		MIN. BOT WIDTH		
MAX. CELL WID.		MIN. CELL WID.			MAX. CELL WID.		MIN. CELL WID.		
MAX. CELL HT.		MIN. CELL HT.			MAX. CELL HT.		MIN. CELL HT.		
NO. MEMBERS		NO. MEMBERS			NO. MEMBERS		NO. MEMBERS		
MEM SPACING		MEM SPACING			MEM SPACING		MEM SPACING		
DECK WIDTH		DECK WIDTH			DECK WIDTH		DECK WIDTH		
LOCATION		LOCATION			LOCATION		LOCATION		

BORING ELEV.		BORING ELEV.		BORING ELEV.		BORING ELEV.	
ADD. BORING NO		ADD. BORING NO		ADD. BORING NO		ADD. BORING NO	
APPR. LOCATION		APPR. LOCATION		APPR. LOCATION		APPR. LOCATION	
BORING ELEV.		BORING ELEV.		BORING ELEV.		BORING ELEV.	
ADD. BORING NO		ADD. BORING NO		ADD. BORING NO		ADD. BORING NO	
APPR. LOCATION		APPR. LOCATION		APPR. LOCATION		APPR. LOCATION	
BORING ELEV.		BORING ELEV.		BORING ELEV.		BORING ELEV.	
ADD. BORING NO		ADD. BORING NO		ADD. BORING NO		ADD. BORING NO	
APPR. LOCATION		APPR. LOCATION		APPR. LOCATION		APPR. LOCATION	

Figure 4. Field Inventory Sheets - Optional Page for Concrete Box-Girder Bridges and for Precast, Pretensioned Concrete Girder Bridges

BRIDGE NO.		INIT		PG OF

UNIT NO.		FROM		TO	
MAX. TOP WIDTH		MIN. TOP WIDTH			
MAX. BOT WIDTH		MIN. BOT WIDTH			
MAX. CELL WID.		MIN. CELL WID.			
MAX. CELL HT.		MIN. CELL HT.			
NO. MEMBERS		NO. MEMBERS			
MEM SPACING		MEM SPACING			
DECK WIDTH		DECK WIDTH			
LOCATION		LOCATION			

UNIT NO.		FROM		TO	
MAX. TOP WIDTH		MIN. TOP WIDTH			
MAX. BOT WIDTH		MIN. BOT WIDTH			
MAX. CELL WID.		MIN. CELL WID.			
MAX. CELL HT.		MIN. CELL HT.			
NO. MEMBERS		NO. MEMBERS			
MEM SPACING		MEM SPACING			
DECK WIDTH		DECK WIDTH			
LOCATION		LOCATION			

UNIT NO.		FROM		TO	
MAX. TOP WIDTH		MIN. TOP WIDTH			
MAX. BOT WIDTH		MIN. BOT WIDTH			
MAX. CELL WID.		MIN. CELL WID.			
MAX. CELL HT.		MIN. CELL HT.			
NO. MEMBERS		NO. MEMBERS			
MEM SPACING		MEM SPACING			
DECK WIDTH		DECK WIDTH			
LOCATION		LOCATION			

UNIT NO.		FROM		TO	
MAX. TOP WIDTH		MIN. TOP WIDTH			
MAX. BOT WIDTH		MIN. BOT WIDTH			
MAX. CELL WID.		MIN. CELL WID.			
MAX. CELL HT.		MIN. CELL HT.			
NO. MEMBERS		NO. MEMBERS			
MEM SPACING		MEM SPACING			
DECK WIDTH		DECK WIDTH			
LOCATION		LOCATION			

UNIT NO.		FROM		TO	
MAX. TOP WIDTH		MIN. TOP WIDTH			
MAX. BOT WIDTH		MIN. BOT WIDTH			
MAX. CELL WID.		MIN. CELL WID.			
MAX. CELL HT.		MIN. CELL HT.			
NO. MEMBERS		NO. MEMBERS			
MEM SPACING		MEM SPACING			
DECK WIDTH		DECK WIDTH			
LOCATION		LOCATION			

UNIT NO.		FROM		TO	
MAX. TOP WIDTH		MIN. TOP WIDTH			
MAX. BOT WIDTH		MIN. BOT WIDTH			
MAX. CELL WID.		MIN. CELL WID.			
MAX. CELL HT.		MIN. CELL HT.			
NO. MEMBERS		NO. MEMBERS			
MEM SPACING		MEM SPACING			
DECK WIDTH		DECK WIDTH			
LOCATION		LOCATION			

Figure 5. Field Inventory Sheets - Optional Page for Concrete Box-Girder Bridges and for Precast, Pretensioned Concrete Girder Bridges

MAX TOP FL WID		MIN TOP FL WID		BRIDGE NO.		INIT		PG OF
MAX TOP FL THK		MIN TOP FL THK		COMMENTS			
MAX BOT FL WID		MIN BOT FL WID					
MAX BOT FL THK		MIN BOT FL THK					
MAX. WEB DEPTH		MIN. WEB DEPTH					
MAX. WED THICK		MIN. WEB THICK		ADD. BORING NO		ADD. BORING NO	
				APPR. LOCATION		APPR. LOCATION	
				BORING ELEV.		BORING ELEV.	
RADIUS BETWEEN		LOCATION		RADIUS BETWEEN		LOCATION	
DECK TILT AT		LOCATION		DECK TILT AT		LOCATION	
BENT SKEW AT		LOCATION		BENT SKEW AT		LOCATION	
ROADWAY SLOPE		P.V.I.		ROADWAY SLOPE		CURVE LENGTH	

							SPAN NO
							<LENGTH

JOINT->							
TYPE-->							
SEAT-->							
LOCA-->							
CLEAR->							
DETAIL>							
SUPPORT							
TYPE-->							
NUMBER>							
WIDTH->							
SIZE-->							
HEIGHT>							
FNDTN TYPE->							
LENGTH>							
WIDTH->							
THICK->							

Figure 6. Field Inventory Sheets - Second Page for Plate Girder Bridges

MAX. TOP CHORD		MIN. TOP CHORD		BRIDGE NO.		INIT		PG OF
MAX. BOT CHORD		MIN. BOT CHORD		COMMENTS				
MAX. PANEL WID		MIN. PANEL WID						
MAX. PANEL HT.		MIN. PANEL HT.						
TOP CHORD LENG		BOT CHORD LENG						
NO. MEMBERS #3		NO. MEMBERS #4		ADD. BORING NO		ADD. BORING NO		
MEM SPACING #3		MEM SPACING #4		APPR. LOCATION		APPR. LOCATION		
DECK WIDTH #3		DECK WIDTH #4		BORING ELEV.		BORING ELEV.		
RADIUS BETWEEN		LOCATION		RADIUS BETWEEN		LOCATION		
DECK TILT AT		LOCATION		DECK TILT AT		LOCATION		
BENT SKEW AT		LOCATION		BENT SKEW AT		LOCATION		
ROADWAY SLOPE		P.V.I.		ROADWAY SLOPE		CURVE LENGTH		

							SPAN NO
							<LENGTH

JOINT-->							
TYPE-->							
SEAT-->							
LOCA-->							
CLEAR-->							
DETAIL>							
SUPPORT							
TYPE-->							
NUMBER>							
WIDTH-->							
SIZE-->							
HEIGHT>							
FNDTN TYPE-->							
LENGTH>							
WIDTH-->							
THICK-->							

Figure 7. Field Inventory Sheets - Second Page for Steel Truss Bridges

Earthquake-Resistant Design and Structure Vulnerability

9950-04181

Edgar V. Leyendecker
Branch of Geologic Risk Assessment
U.S. Geological Survey
Denver Federal Center, M.S. 966
Denver, CO 80225
(303) 236-1601

Investigations

1. Work is in progress to examine, evaluate, and improve the estimation of casualties and aggregate monetary losses associated with the occurrence of earthquakes.

2. Work is continuing on improving measures of vulnerability of structures to damage, including the refinement of our understanding of earthquake damage and the applicability of the existing data base on earthquake damage.

3. Investigations continue for development/identification of cost-effective techniques for determining inventory at risk.

4. Work is continuing on damage survey procedures for collection and analysis of vulnerability data.

Results

1. Development of an improved and consistent loss-estimation methodology that can be applied in a uniform way on a regional basis for the estimation of losses throughout the United States is in progress. Application work has been done in Utah and work is progressing in California.

   Earthquake loss studies may be of the "deterministic" or "probabilistic" type, both types of studies have important uses. A scenario study might consider the consequences of one or more earthquakes; frequently this might be the largest likely earthquake. Such a study is very useful for purposes such as emergency planning. The probabilistic study considers both magnitude and frequency of occurrence and may be "more realistic" than the above "worst case" scenario. Both deterministic and probabilistic studies have been done in Utah and are planned for the Pacific Northwest, an area under current study in the Urban Hazards Program. Emphasis is being placed on developing the tools for use in loss studies rather than a complete assessment for the region. Accordingly, limited areas will be selected for conducting a detailed study of losses.

2. Examination of current vulnerability relationships is proceeding with a review of existing earthquake damage data bases including San Fernando and Coalinga. Plans for the collection of earthquake damage data following selected earthquakes have been made, including development of data

collection techniques. Improvement of vulnerability relationships, including parameter variability, depends heavily on the collection of earthquake damage data.

The 1983 Insurance Services Office (ISO) classification system is being used for the inventory survey of buildings and vulnerability relationships. This classification uses a system of 5 major classes as shown below:

Class 1: Wood frame structures
Class 2: All-metal buildings
Class 3: Steel frame buildings
Class 4: Reinforced concrete buildings, combined reinforced concrete and structural steel buildings
Class 5: Concrete, brick, or block buildings

This system was selected partly for existing data base compatibility and for its relative simplicity and ease of use by a lay person with a limited amount of training. However, recent classification systems such as the "Rapid Visual Screening Techniques" developed by the Applied Technology Council are being evaluated for use.

3. Development of inventory at risk is costly and is a major impediment to accurate loss estimates. A study of the critical elements of inventory needed for loss assessment in urban areas, including field inventory techniques is in progress. Plans for preparation of inventory training procedures are underway for trial use. Important strides have been made under the U.S.G.S. grant program and these results will be used where possible.

The data collection procedures are centered around (1) a simple system for classifying buildings, (2) the census tract as the basic area for data collection, and (3) machine read "mark-sense" sheets for compiling a computer data base. It should be noted that the procedures can be used for either inventory or damage surveys although there may be slight modifications between the two.

The census tract is being used as a data collection unit in order to simplify the inventory of buildings. Since census data provide a relatively accurate count of residential construction, this is one component of an inventory that does not have to be compiled in detail. The type of residential construction (type of frame, siding, etc.) can be determined by relatively simple statistical sampling. Other types of structures require additional inventory work. Additional extensive sampling is required in order to develop suitable inventories for structures other than dwellings.

Data collection procedures use "mark-sense" sheets which describe building class and various types of damage if it is a damage survey. The mark-sense sheets are preprinted forms with multiple choice responses that are filled out with a soft lead pencil. The "marks" by the soft lead pencil can be "sensed" by an optical scanning device and read into a computer data base.

A plan for an inventory in a limited portion of the Seattle urban area is being developed for using these techniques.

4. The methodologies under development for inventory and damage surveys were tested following the October 1, 1987 Whittier Narrows Earthquake. The survey procedures worked relatively well. Procedures are being revised as a result of this effort and are planned for field testing in FY90.

Reports

Leyendecker, E.V., Highland, L.M., Hopper, M.G., Arnold, E.P., Thenhaus, P.C., and Powers, P.S., 1988, Early Results of Isoseismal Studies and Damage Surveys for the Whittier Narrows Earthquake, Spectra, Earthquake Engineering Research Institute.

Leyendecker, E.V., 1988, Earthquake Damage to Commercial and Industrial Buildings, in Proceedings of Workshop on Earthquake Risk: Information Needs of the Insurance Industry: U.S. Geological Survey Open-File Report 88-669.

Algermissen, S.T. and Leyendecker, E.V., 1988, Estimation of earthquake Losses in the Puget Sound Area, in Proceedings of Conference XLII, Workshop on Evaluation of Earthquake Hazards and Risk in the Puget Sound and Portland Areas: U.S. Geological Survey Open-File Report 88-541.

Algermissen, S.T., Arnold, E.P., Steinbrugge, K.V., Hopper, M.G., Powers, P.S., 1988, Earthquake losses in central Utah, in Gori, P.L. and Hays, W.W., eds., Assessing regional earthquake hazard and risk along the Wasatch front, Utah, Part A: U.S. Geological Survey Professional Paper, (in press).

Historical Normal Fault Scarps -- Wasatch Front and Vicinity

9910-04102

David P. Schwartz
Branch of Engineering Seismology and Geology
U.S. Geological Survey
345 Middlefield Road, MS 977
Menlo Park, California 94025
(415) 329-5651, FTS 459-5651

Investigations

The project goal is to study historical and recent normal fault scarps in the Great Basin in order to calibrate geological techniques used to identify individual past earthquakes and the amount of displacement during each, quantify earthquake recurrence intervals, and evaluate earthquake recurrence models and fault segmentation models. Investigations have concentrated on 1) recurrence and segmentation along the 1983 Borah Peak, Idaho surface rupture and associated scarps of the Lost River fault zone, and 2) recurrence and paleo-displacements on the Wasatch fault zone at the Dry Creek site near the southern end of the Salt Lake segment and at the Mapleton and Rock Canyon sites on the Provo segment.

Results

1. Lost River fault zone, Idaho (with A.J. Crone, USGS, Denver).

   Trenches at Lower Cedar Creek, located near the south end of the MacKay segment of the Lost River fault zone, were re-cleaned and deepened. At this location the fault is expressed as a 9m-high scarp with associated graben that displace a surface tentatively assigned a Bull Lake age (140-150ka) based on geomorphic position and the degree of soil carbonate development. Topographic profiling indicates the net vertical tectonic displacement of this surface across the fault is 5.0-5.3 m. The trenches expose scarp-derived colluvium, loess, and two volcanic ashes (Mazama - 6850 years, Glacier Peak - 11,300 years). Mapping of the trench exposures indicates that the net tectonic displacement is the result of three events. The most recent event post-dates Mazama and pre-dates a charcoal-bearing organic layer in the distal part of the colluvial wedge from this event. Scott and others (1985) reported a bulk radiocarbon date of 4300 years from this layer, and we have collected charcoal for new dating. The penultimate event pre-dates Glacier Peak but post-dates stabilization of Pinedale (12-15ka) outwash surfaces. At present there are no constraints on the timing of the third event back, but relations between scarp colluvium and loess suggest it could be significantly closer in time to Pinedale than to Bull Lake.

If preliminary interpretations of the timing of events hold with additional analysis, the Lower Cedar Creek site will provide strong evidence for temporal clustering of earthquake activity. In this case, a long period of quiescence is followed by initiation of an active seismic cycle.

2. Wasatch fault zone, Utah, (with W.R. Lund, Utah Geological and Mineral Survey).

   No new field work was initiated during this report period.

Fault Segmentation: San Andreas Fault System

9910-03983

David P. Schwartz, Thomas E. Fumal, Ray J. Weldon, and Karin E. Budding
Branch of Engineering Seismology and Geology
U.S. Geological Survey
345 Middlefield Road, MS 977
Menlo Park, California 94025
(415) 329-5651 or (415) 329-5630

Investigations

The project goals are to: a) define segmentation and fault behavior models for the San Andreas fault between Wallace Creek and San Bernadino, and b) develop information on segmentation, recurrence intervals, and slip per events on major strands of the San Andreas system east and north of San Francisco Bay.

1. Trenching and mapping to develop new slip rate and recurrence data and define and quantify uncertainties in timing, displacement, and lateral extent of individual past earthquakes between Wallace Creek and San Bernardino.

2. Trenching and mapping along the Rodgers Creek fault zone to define slip rate, recurrence interval, and slip per event.

Results

1. Wrightwood site (Fumal, Weldon, Schwartz). Trenching and logging continued at Wrightwood between July and September. At this site coseismic deformation along the San Andreas fault is distributed over a 150-m-wide zone in which a variety of structural and stratigraphic relations are exposed that aid in defining and dating individual earthquakes. Our trenching and radiocarbon dating now provide reliable evidence for seven, and tentative evidence for three other, earthquakes during the past 1,300 years; other events can be observed in deposits dating back to 4,500 years B.P. The past three events, which occurred between 1460 A.D. and 1857 A.D. when this area was fairly dry, can be identified on the basis of fault scarps, colluvial wedges, fissure infills, and progressively tilled deposits in small graben. Earlier events, which occurred between about 700 A.D. and 1460 A.D. when the area was wet, are expressed by progressive folding of deposits above listric faults that produce marked angular unconformities and variations in stratigraphic thickness. Still older events are represented by downward growth of fault and fold complexity. Simple upward termination of faults does not appear to be a consistently reliable indicator of the timing of events.

Preliminary radiocarbon dating of eleven peaks indicates that the earthquake sequence at Wrightwood is similar to Pallett Creek, 25 km to the northwest, with regard to the number and timing of events during the past 1,300 years. At present our results are very similar to Sieh's 1979 initial revision of the Pallett Creek paleoearthquake chronology. The average recurrence interval at Wrightwood is about 130 years. We are in the process of obtaining precise radiocarbon dates to evaluate the degree to which earthquakes on this part of the San Andreas fault occur at regular intervals or are temporally clustered.

2. Rodgers Creek fault zone (Budding, Schwartz). Work was initiated along the Rodgers Creek fault zone (RCFZ), a major segment of the Hayward fault that extends at least 50 km from San Pablo Bay to about 10 km north of Santa Rosa. It has not produced a surface-faulting earthquake during at least the past 150 years. Five trenches were excavated 18 km north of San Pablo Bay at a site where the fault is expressed by a single-trace scarp across a late Holocene alluvial fan and by an offset gully and surface debris flow. The trenches exposed a sequence of coarse debris flow and fan deposits containing detrital charcoal with accelerator mass spectrometer ages ranging from 2395±50 to 1545±50 ^{14}C yr. B.P. Four buried channels correlated across the fault are right laterally offset 6-1/2 to 8 m and displaced 0.4 m vertically up to the east; they contain deposits with dendro-corrected ages of 1390 and 2115 yr B.P. Right slip during the most recent event measured at the gully and debris flow is 2.0 + 0.3/-0.2 m, suggesting the buried channel offsets represent the past 3-4 paleoearthquakes. With these data we have calculated a preliminary late Holocene slip rate of 3.25-6.3 mm/yr and a recurrence interval of 317-660 years. Because of measurement, dating, and elapsed time uncertainties, the slip rate is a <u>minimum</u> and the recurrence rate a <u>maximum</u>.

The RCFZ terminates on the south with a 6-km-wide right step to the Hayward fault; the north end is characterized by an 8-km right step to the Maacama fault and was the location of the M5.6 and 5.7 1969 Santa Rosa earthquakes. The RCFZ differs from the Hayward and Maacama faults by an absence of surface creep and a distinct absence of microearthquake earthquake activity and appears locked. With these observations and the new paleoseismicity data we suggest the RCFZ could be a source of the next M7 San Francisco Bay Area earthquake and must be considered in future probabilistic assessments of seismic hazard in the Bay Area.

Reports

Weldon, R.J., Fumal, T.E., and Schwartz, D.P., 1989, Paleoseismology of the San Andreas fault at Wrightwood, California - I. Setting and Structure (abs): EOS, AGU 1989 Fall Meeting.

Fumal, T.E., Weldon, R.J., and Schwartz, D. P., 1989, Paleoseismology of the San Andreas fault at Wrightwood, California - II. Recognition and timing of events (abs): EOS, AGU 1989 Fall Meeting.

Budding, K.E., Schwartz, D.P., Ostergren, C.L., and Hoirup, D.F., 1989, Preliminary slip rate and earthquake recurrence on the Rodgers Creek fault zone, northern California (abs): EOS, 1989 AGU Fall Meeting.

Development of Inventory and Seismic Loss Estimation Model for Portland, Oregon Water and Sewer Systems
USGS Grant No. 14-08-0001-G1694

Leon R.L. Wang, P.I.
Joyce C.C. Wang, Co-P.I.
Isao Ishibashi, F.A.
Department of Civil Engineering
Old Dominion University
Norfolk, Virginia 23529
(804) 683-3753

Donald Ballantyne, Co-P.I.
Kennedy/Jenks/Chilton
33301 Ninth Avenue S., Suite 100
Federal Way, WA 98003
(206) 874-0555

William M. Elliott, Co-P.I.
Bureau of Water Works
City of Portland
1120 S.W. 5th Avenue
Portland, OR 97204
(503) 796-7486

Objectives:

The purpose of this project is to develop methodologies for inventorying water and sewer systems and developing loss-estimation algorithms for damage to such lifeline systems under different levels of earthquake and ground shaking. This will be done by investigating two specific sewage drainage basins (Tanner and Fiske) in the City of Portland, Oregon. Each of these basins contains important water and sewage facilities. For geotechnical (soil liquefaction) study, the investigation covers a much larger area to insure its applicability.

Geotechnical (Liquefaction Susceptibility) Study

The liquefaction potential map was created by overlaying two previously prepared maps: (1) liquefaction susceptibility map which was developed based on surface geology, and (2) seismicity map which was obtained from historical intensity observations for a given earthquake scenario. The first map originally had five categories from Very High, High, Moderate, Low to Very Low. For the Portland area, however, its top category was only at the High classification. So it reduced to four categories. On the other hand the second map had 6 categories from 0.32g, 0.21g, 0.12g, 0.07g, 0.03g, to 0.00g for the scenario of M = 6.5 earthquake occurred at Central Portland area. The combination of two maps creates total 24 ranks (4 x 6) in terms of liquefaction potential. Based on engineering judgement and the comparison with the detailed liquefaction evaluation for individual boring logs, the following ranks were assigned as Very High, High, Medium High, Medium, Low and Very Low, six categories in all.

Figure 1 shows the liquefaction potential classification for the area under study in Portland, Oregon. When the detailed liquefaction map is compared with the above liquefaction potential map, those categories generally agree with each other. However, due to the local variation of soil conditions, it is impossible to obtain a one to one match. Therefore, it shall be noted that the above map shall be used only for preliminary assessment of the liquefaction potential. For an important building or structure, new borings at the site or at least nearby boring log should be used to carry out a detailed analysis for such project.

Inventory of Spatial Information by GIS Methodology:

The inventory of spatial information covers an area of approximately 105 square miles, which contain the major portion of Portland City water and sewer systems. Within the area, it has area, point, and linear types of information. The area type of information includes soil, seismic, block and parcel data. The point type information refers to concentrated water and sewer services facilities in large scale; and water and sewer pipeline joints and nodes in relatively small scale. The linear type of information pertains to water and sewer pipelines.

The graphic data inventory techniques in accordance with the GIS (Geographic Information System) general principles concern about the dynamic retrieval of data, the combination of graphic data into various functional maps and the elimination of data duplications within computer storage.

For example, the liquefaction potential map (Figure 1) contains 6 categories, which can be retrieved in whole or in separated manner. The map is derived from the combination of two maps which are seismic intensity and surface soil liquefaction susceptibility maps. On the map, there are major highway network and the boundaries of selected projects. Both of them are retrieved from a common factors map, which eliminates the duplications of data elements and assures the data integrity among various functional maps.

The common factors map first contains the concentrated facilities distinguished by function with their associated major attributes to be stored into relational database. Second, it has a layer of major water transmission lines linking the source reservoir with subsequent reservoirs, pumping stations, and tanks. Third, for a clarity in orientation, it has the regions major highway network and large water bodies. Fourth, it also indicates the two selected project areas for detailed pipeline inventories. And finally, it contains a map's basic components which are map legend, north arrow sign, scale ruler and frame outline. All of the above common factors can be totally or partially overlaid onto a functional map. The common factor map will not only enhance a map's legibility and also improve the coherent appearance and consistency among all studied maps.

Within a project area, the area type information includes street blocks and parcels. A parcel is defined as an area directly connected to one pipeline usually with valves on both ends. Under this definition, a parcel can be a combination of several parcels defined by a city assessor. Such an approach speeds up the coding process and serves the purpose for quickly identifying the affected area if a certain pipeline cannot function normally during a earthquake emergency situation.

The line type information within the project area is water and sewer serving pipelines. Each pipeline segment is identified by two end nodes such as valves and manholes respectively. A node and a pipeline's physical shapes store in graphic database and the associated attributes in text database as defined by FMSAC (Facility Management System for AutoCadd).

Concentrated Facilities Study

Concentrated water supply and wastewater facilities serving the Tanner and Fiske drainage basins were identified. A field evaluation survey was conducted to inventory the facilities. Concurrently, the project team was familiarized with system operation. Design and construction cost information was obtained from Portland Water Bureau staff.

Present value cost estimates were prepared for each of the identified concentrated facilities. Where available, actual construction costs were used and updated using the Engineering News Record Construction Cost Index. Many of the facilities were of old and cost information was not available. For those facilities, costs were estimated using EPA and Army Corp of Engineers cost estimating guides developed for planning level cost development.

Facilities were divided into categories of similar types of construction and site conditions. A total of 31 categories were identified. A loss curve was then developed for each category. ATC-13 approach [1] was used as a basis for loss curve development. The base curves were then modified considering the specific design, site conditions, age/design standard of facility, and previous studies performed on the particular facilities. The ASCE TCLEE Seismic Risk Demonstration Project report provided valuable information. The curves were then placed into a Lotus 123 spreadsheet lookup table format.

The present values for each facility component were then multiplied by the respective loss curve for each intensity, and losses estimated. Losses for components were summed for each facility.

The overall methodology is applicable to a variety of loss estimation projects. The loss curves, along with supporting documentation should be valuable to earthquake loss estimation projects particularly for water and wastewater systems.

Application to Federal Emergency Disaster Declaration

This task will describe how the inventory and loss estimate models can be used in the early stages of a disaster to provide critical data on amount of damage, and preliminary cost figures for repair and restoration. The following describe the declaration process, data needed and procedures for the application to Federal Emergency Disaster Declaration.

A. Disaster Declaration Process

The steps involved in the escalation of an incident such that local and state forces are unable to adequately respond leads to the declaration of either an emergency or a disaster that brings federal agency involvement into play. This step will describe the process and steps that are involved in bringing to bear federal resources.

B. Data Needs at Disaster Inception

The steps involved in immediate life-saving and rescue efforts are followed closely by the need for information on the type of damage and the extent of work necessary to restore first temporary and then permanent service. The importance of damage assessment at the earliest possible time and the relationship of the subject inventory and display models will be discussed.

The steps in repair and restoration and the need to prioritize among competing needs will be discussed. The ability of the models to produce outputs to aid in the disaster response process will be discussed.

C. Loss Estimates and Replacement Costs

The ability of the models to create loss estimates in advance of an incident will be discussed in that these activities can lead to a higher awareness of damages that are possible. The replacement costs for different facilities and components will be discussed more fully and the ways and means to determine replacement costs will be discussed.

D. Mitigation of Disaster Effects

A discussion of the current efforts of FEMA to encourage mitigation work by state and local agencies will be carried out. The use of the inventory and display model in identifying and prioritizing important facilities of the water and sewer infrastructure will be discussed. The role of local, state, and federal agencies in encouraging mitigation activities in hazard areas and the potential for funding through local sources, state grants, and federal participation will be discussed.

E. Field Trips to Interview Officials

To accomplish the proposed task, several trips to interview local, state and federal officials are planned. These include Program Administrator of Washington Division of Emergency Management, FEMA officials in Washington State (Region X), Administrator of Oregon Emergency Management Division, and the Portland Bureau of Fire, Rescue and Emergency Services.

[1] Christopher Rojahn and Roland L. Sharpe, "Earthquake Damage Evaluation Data for California," *Applied Technology Council Report*, No. ATC-13, 1985

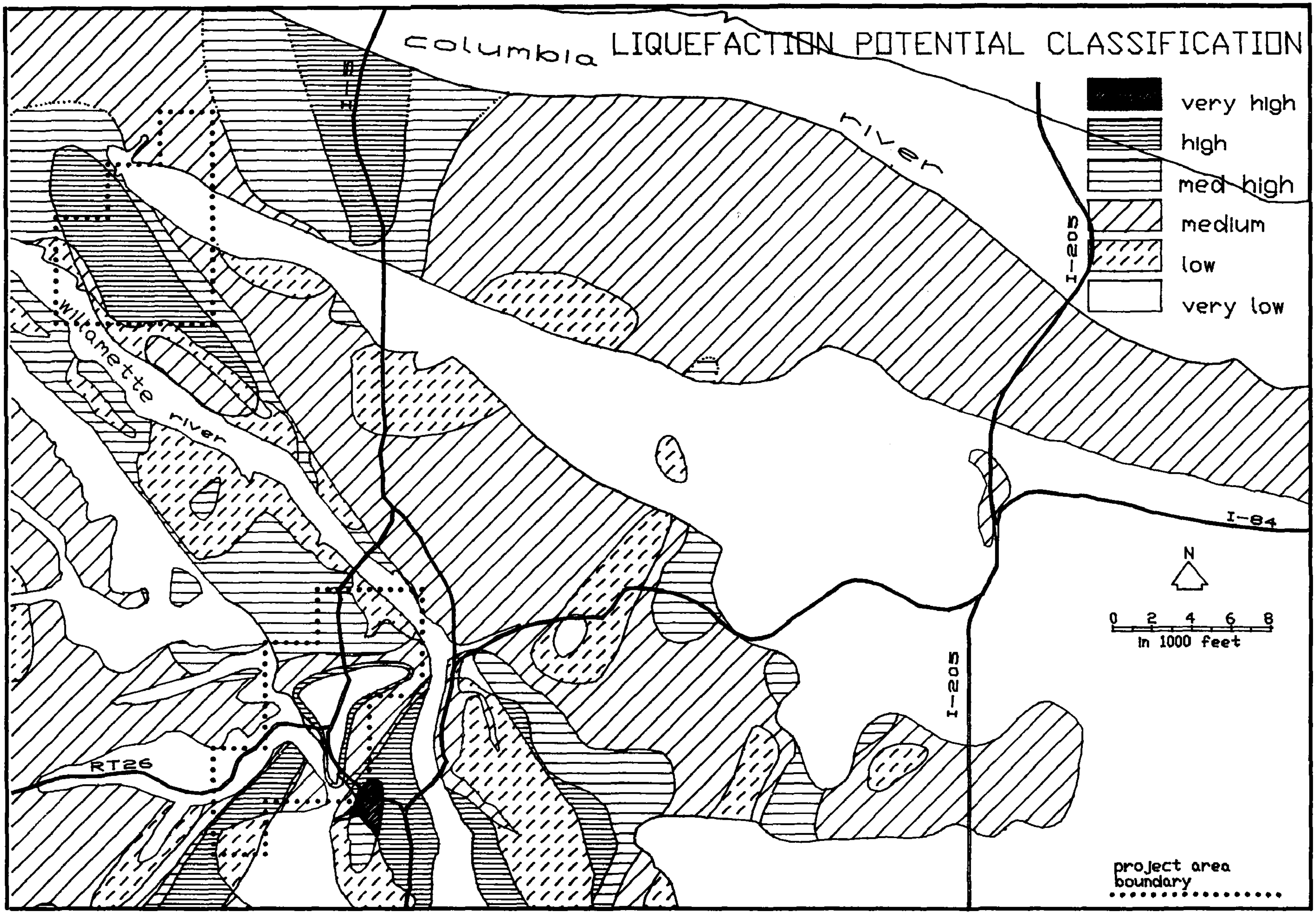

Figure 1: SOIL LIQUEFACTION POTENTIAL CLASSIFICATION

Earthquake Hazards Studies, Metropolitan Los Angeles-Western Transverse Ranges Region

9540-02907

R.F. Yerkes
Branch of Western Regional Geology
345 Middlefield Road, MS975
Menlo Park, California 94025
(415) 329-4946

Investigations and Results

1. Historic earthquakes (W. H. K. Lee and Yerkes).

(A) Reinterpreting all available seismograms for about 50 1984+ earthquakes in the Los Angeles basin-northern Santa Ana Mountains area to assist in identifying buried, southern tectonic boundary of Transverse Ranges.

(B) (Yerkes and D. H. Oppenheimer). Computed and mapped fault-plane solutions for Elsinore fault zone; prepared and submitted Fall AGU abstract on results. The Elsinore zone is a dominant physiographic feature of the Peninsular Ranges; it trends N. 50° W. for 215 km parallel to and 10-35 km southwest of the San Jacinto fault zone. Both the Elsinore and San Jacinto zones are considered parts of the San Andreas system, but only the San Jacinto has had large ($M_L \geqslant 6$) instrumentally-recorded earthquakes with fault-plane solutions. The Elsinore fault marks the steep, linear, northeast flank of the Santa Ana Mountains and traverses chiefly Mesozoic crystalline rocks. Southeast of Lake Elsinore the zone broadens progressively by diverging strands such as the Agua Caliente, Hot Springs, and Earthquake Valley faults. At the U.S.-Mexico boundary the zone is about 25 km wide, but farther south its course and extent are conjectural.

The geologically-inferred senses of motion on faults of the zone range from right lateral on vertical faults to reverse on gently southwest-dipping faults. Estimates of total right slip range from 10 km at the northwest to 5 km or less at the southeast. The inferred age of latest faulting is late Quaternary or Holocene along the west margin of the zone, the locus of the Elsinore fault s.s., but is pre-Quaternary along many central and eastern strands. Trilateration surveys of 1972-87 indicate that appreciable right-lateral shear strain is accumulating on the San Jacinto and southern San Andreas zones, but only slightly if at all on the Elsinore zone.

We computed single-event focal mechanisms for 127 earthquakes, $M_L \geqslant 6$, 1976-86, widely distributed along and across the Elsinore zone; 30 solutions, representative in both type and location, were mapped. About 125 solutions are consistent with right slip on typical northwest-trending faults or with left slip on several short, northeast-trending faults near lat. 33° N. P and T axes fit those of several large earthquakes long the San Jacinto zone, and Elsinore-zone seismicity appears to be consistent with the San Jacinto-zone tectonics. However, the distribution of many earthquakes along "pre-Quaternary" faults of the Elsinore zone indicates that the mapped pattern of most-recent surface faulting does not accurately depict the distribution of seismic activity.

2. Quaternary stratigraphy, chronology, and tectonics, southern California region (Sarna-Wojcicki). Not funded.

Reports.

Yerkes, R.F., Oppenheimer, D. H., and Lee, W. H. K., Elsinore fault zone--seismicity vs age of surface faults (abs.); submitted to fall AGU, September 1989.

Expert Synthesis and Translation of Earthquake Hazard Results —A Book for Non-Scientists in the Wasatch Front Region

14-08-0001-G1671

W.J. Arabasz and D.R. Mabey
Department of Geology and Geophysics
University of Utah
Salt Lake City, Utah 84112-1183
(801) 581-6274

Investigations:

This "implementation" project is part of the culmination of recent NEHRP focus on Utah's Wasatch Front region. The goals of the project are: (1) to coordinate with the scientific investigators who have worked in the Wasatch Front earthquake-hazards program—in order to develop a synthesis of important technical information, (2) to produce intermediate-level summaries from those discussions, and finally, (3) to "translate" the technical information into a book on the earthquake threat in Utah for non-earth scientists. The book is being designed to appeal to (i) the general public (who must encourage and support elected and appointed officials to make decisions on implementing earthquake-hazard-reduction measures), (ii) teachers and students, and (iii) decision-makers themselves.

Results: May 1-September 30, 1989

During the report period, efforts continued toward completing goals (1) and (2), and about one-third of the book writing (goal 3) was finished. A "consensus document" serving as a summary of available technical information on the earthquake threat in Utah has finally reached a stage where the judgment of scientists and engineers can be outlined in a non-controversial way—especially in terms of the ground-shaking hazard in the Wasatch Front region.

In September, a working group of eight scientists and engineers who have investigated Utah's ground-shaking hazard (A.M. Rogers, S.T. Algermissen, K.W. Campbell, D.M. Perkins, J.C. Pechmann, M.S. Power, J.C. Tinsley, and T. L. Youd) completed a consensus description of expected ground motions for the maximum earthquake on the Wasatch fault, the probabilistic ground-motion hazard for the region, and the effect of local site conditions on the ground motions of distant earthquakes. Revision of the consensus document for Utah's Wasatch Front earthquake hazards reduction program is now in its final stage.

A social scientist (Dr. Gary E. Madsen, Associate Prof. of Sociology, Utah State University) and a professional planner (Jerry Barnes, Director of the Salt Lake County Planning Division) have been involved in providing guidance for the book-writing project. The coincidental involvement of the PI's in extensive interactions with local governments is giving an extremely valuable perspective on the informational needs of the book's potential readers. The interactions relate to (i) the Utah Advisory Council on Intergovernmental Relations (dealing with a range of specific actions being recommended to city, county, and state officials to reduce earthquake hazards in Utah) and (ii) the Seismic

Safety Study Committee of the Salt Lake City Board of Education (dealing with the vulnerability of Salt Lake City schools to serious earthquake damage).

The scheduled completion of the book writing by December 31, 1989, has been impacted by an unanticipated but important development in Utah's state earthquake program. A major initiative is underway to solicit large funding from Utah's state legislature for a broad range of earthquake-related instrumentation—for network seismology, strong-motion seismology, the interfacing of network seismology with emergency management personnel, and GPS satellite geodesy. One of us (WJA) has undertaken the primary responsibility for the instrumentation initiative, including the recent convening of a "blue-ribbon" policy panel in August and the writing of multiple briefing documents for the panel. The latter, however, have direct value for the book writing insofar as they are illustrated, narrative compilations giving both a broad overview and specifics about all aspects of the earthquake threat in Utah. A no-cost extension of this project beyond December 31, 1989, is currently being requested for completion and printing of the book.

Strong Motion in San Bernadino and Riverside Counties from a Moderate Earthquake on the San Jacinto Fault

14-08-001-G1689

Ralph J. Archuleta
Institute for Crustal Studies and Department of Geological Sciences
University of California, Santa Barbara
Santa Barbara, CA 93106
(805) 961-4477

Objectives: The objective of this project is to compute strong ground motion at selected sites within 25 km of the northern San Jacinto fault assuming a moderate earthquake on this section. The earthquake source model is a spontaneously propagating stress relaxation on an inhomogeneously stressed fault. The dynamics of the rupture are modeled using a 3-D finite element code by which the slip rate is determined at a grid of points on the fault. The slip rate is convolved with numerical Green's functions computed from a discrete wavenumber/finite element code and integrated over the fault to produce strong motion at sites off the fault. Our assumption is that areas of the San Jacinto fault where other faults intersect and/or regions where the seismicity is low have higher yield stress than other parts of the fault.

Results: The quasidynamic rupture, i.e., a propagating stress relaxation with preassigned rupture velocity, finite element model has been tested on both a VAX11/750 at UCSB and a CRAY X-MP at the University of Illinois. Modifications of the source code to allow a spontaneous rupture under conditions of a slip-weakening fault constitutive law are in progress.

Near-Surface Lithologic and Seismic Properties

9910-01168

J.F. Gibbs and W.B. Joyner
Branch of Engineering Seismology and Geology
345 Middlefield Road, MS 977
Menlo Park, California 94025
(415) 329-5631 or (415) 329-5640

Investigations

Measurements of seismic velocity and attenuation to determine the effect of local geology on strong ground motion and to aid in the interpretation of seismic source parameters.

Results

1. Interpretation of data obtained from Lake Hemet borehole has been completed. P-wave and S-wave velocities are shown below:

Depth Interval	S-velocity	Depth Interval	P-velocity
0-17.5 m	220 m/s	0-5.0 m	(400) m/s
17.5-65.0 m	580 m/s	5.0-65.0 m	2030 m/s
65.0-100.0 m	1310 m/s	65.0-100.0 m	2460 m/s

The velocities interpreted from the downhole measurements provide a near-surface model for studying the seismic effects of alluvium over a bedrock surface. This site geology is common to many areas and a number of important structures are built or planned on similar near-surface materials.

2. We have logged the upper 120 meters of the borehole at Gilroy strong-motion station No. 2 for P- and S-wave velocities where the Coyote Lake, California earthquake was recorded. This hole which extends to bedrock (however was blocked at 120 meters) penetrates 180 m of Quaternary alluvium that is typical of what is present in many populated areas of California. The hole is ideal for the measurement of shear Q because it has plastic casing and because it was drilled more than eight years ago, enough time for the alluvium to settle firmly around the casing. The data has been processed, but the analysis has not been completed.

Reports

Lee, W.H.K., Gibbs, J.F., and Criley, E.E., 1989, A seismic study of explosive sources (abstract): San Francisco, A.G.U. fall meeting.

Experimental Investigation of Liquefaction Potential

9910-01629

Thomas L. Holzer
Branch of Engineering Seismology and Geology
U.S. Geological Survey
345 Middlefield Road
Menlo Park, CA 94025
(415) 329-5613

Investigations

1. Establishment and maintenance of an instrumented site in Parkfield, California, to monitor pore-pressure build-up in a sand undergoing liquefaction and strong ground motion during the predicted Parkfield earthquake.

2. Post-earthquake analyses of field data and pore pressure and downhole and surface ground motion records at the Wildlife liquefaction array from the November 23-24, 1987, Superstition Hills earthquakes.

3. Subsurface exploration of 1868 and 1906 Coyote Creek (San Jose, CA) liquefaction sites to find a location for a South Bay liquefaction array.

4. Cross-correlation analyses of horizontal acceleration records at the Downhole Array B in Lotung, Taiwan. Records from 3 earthquakes with magnitudes ranging from 5.4 to 7.0. The downhole array has recording sensors at depths of 6, 11, 17, and 47 meters. Consequently, the investigation has excellent controls on both the range of shaking amplitudes and the vertical distribution of wave motion.

Results

1. The Parkfield liquefaction array with 14 pore pressure transducers and 5 three-component force-balanced accelerometers was maintained. Recording systems consist of two CRA-1 film recorders and a GEOS digital recording system connected to five transducers to improve the dynamic range. Geotechnical laboratory testing of undisturbed soil samples taken in November 1987 was complete and the liquefaction potential from the laboratory tests is presently being compared to the field results. Analysis of seismic refraction tests conducted during initial site exploration revealed evidence for unsaturation beneath the water table. Since unsaturation reduces liquefaction potential, the refine of the technique offers the potential for improving liquefaction assessments.

2. Measurements of pore pressures in a silty sand undergoing earthquake-induced liquefaction are providing insight into how a deposit liquefies and behaves once liquefied. Analysis of the records reveal a strong dependence of liquefaction on peak acceleration, a dependence that is predicted well by conventional engineering methods. The strong-motion and pore-pressure records indicate that the liquefaction process began at 13.6 seconds after first motion. This time marks the arrival of the peak horizontal ground acceleration, a factor of two reduction in the average shear-wave velocity to 7.5-m depth, the onset of pore-pressure increase in the liquefying layer, the loss of phase coherence between the uphole and downhole acceleration time histories, and the divergence of recorded energy in the uphole and downhole accelerograms. The pore-pressure data, however, indicate that lithostatic conditions were not reached until 60 to 90 seconds, well after the earthquake ended. Although the delay may be an artifact of soil disturbance caused by transducer emplacement, the O records still permit analysis of the behavior of the deposit. Liquefaction began in the upper part of the silty sand and progressed downward; reconsolidation started at the base of the deposit and worked upward.

   Fourier transforms with small windows of the surface ground motion records could not pinpoint the time at which liquefaction occurred but did reflect gradual changes in frequency contents due to liquefaction. Cross correlation of the surface and downhole records showed a steady decline in the value of the cross-correlation coefficient beyond the 14-second mark which is consistent with the onset of liquefaction.

   Grain size distributions of sand boils generated during the 1981 Westmorland and 1987 Superstition Hills earthquakes were compared to distributions of the silty sand layer at the liquefaction array. These comparisons suggest that only the upper part of the deposit liquefied in 1981 and all of the deposit liquefied in 1987. These observations are consistent with liquefaction predictions based on field measurements of liquefaction resistance.

3. Cone and standard penetration testing at 1868 and 1906 liquefaction sites along Coyote Creek at the south end of San Francisco Bay discovered the liquefiable layer was a 7 -m thick channel sand that is confined beneath a 6-m thick finer grained layer. The deposit looks feasible for installation of a new liquefaction array. Geotechnical testing of the soils at the potential site were completed.

4. Variations in shear wave velocity were quite evident in the Lotung investigation. In general, the time shifts of maximum correlation for the weaker earthquake are shorter than the corresponding time shifts for stronger earthquakes. This indicates that shear wave velocity decreases with increasing magnitude. Even for a single earthquake (LSST#7), the first portion of SH-wave motion is shown to travel faster than the second portion does, suggesting definite nonlinear site re-

sponse due to strain-softening and/or pore-pressure build up.

Reports

Holzer, T.L., 1989, Detection of unsaturation beneath a water table by seismic refraction (abs.): Geological Society of America Abstracts with Programs, v. 21, no. 6, p. A41.

Holzer, T.L., 1989, Catastrophic collapse along fissures caused by withdrawal of ground water from unconsolidated aquifer systems (abs.): 28th International Geologic Congress, Abstracts, v. 2, p. 67.

Prandini, F.L., V.A. Nakazawa, and T.L. Holzer, 1989, Covered karst of Cajamar Town, Sao Paulo Brazil (abs.): 28th International Geologic Congress, Abstracts, v. 2, p. 63-64.

Youd, T.L., Y.K. Tang, J.C. Stepp, T.L. Holzer, and G.O. Jackson, 1989, A wedging system for downhole accelerometers: Earthquake Spectra, v. 5, no.4, p.

Assistance in Implementing Seismic Safety Programs in the Wasatch Region, Utah

14-08-0001-G1681

Martha Blair-Tyler
George G. Mader
William Spangle and Associates, Inc.
3240 Alpine Road
Portola Valley, California 94028
(415) 854-6001

Objective: The objective of the project is to assist state and local officials in Utah implement programs to increase seismic safety. To meet this objective, the project will provide local government officials access to expertise in earthquake hazard mitigation. More specific objectives include:

1. To transfer direct, practical experience with local government programs to mitigate earthquake hazards to at least one staff member or elected official in each county and major city along the Wasatch Front who can become a "champion" for earthquake safety within the jurisdiction.

2. To assist the county geologists to understand and respond to the information needs of local officials designing implementation programs.

3. To help state officials, especially in Utah Geological and Mineral Survey and Comprehensive Emergency Management, understand the problems, potentials and options for earthquake hazard reduction through actions of local governments and how the state can help.

4. To improve the general level of awareness and knowledge of local officials about the range of options available to improve earthquake safety.

Methods: The proposal calls for Martha Blair-Tyler and George G. Mader, two California urban planners who have extensive experience in earthquake hazard mitigation, to conduct workshops on local earthquake hazard mitigation programs and to offer assistance to local and state officials as requested. The idea is to facilitate transfer of relevant experience in mitigation from California to Utah through direct personal contact. The emphasis will be on local government programs and, particularly, land use measures which can reduce earthquake risks.

Progress May to October 1989: Efforts during the past six months include:

1. Meetings with County Geologists. Martha Blair-Tyler and George Mader spent July 10, 11 and 12 in Utah meeting with the county geologists and planners in their counties. We spent one full day in each county split between meeting with the planners and the geologists in their office and observing and photographing geologic hazards in the field. The trip had two objectives: 1) to encourage and support the county geologists and planners with interest and, where relevant, suggestions, and 2) to learn as much as possible about both the geologic hazards and land use planning tools in the three counties in order to prepare presentations tailored to

Utah. We took photographs throughout the three days in order to be able to illustrate our presentations with Utah examples of the hazards and, where possible, the mitigation techniques.

2. Utah League of Cities and Towns. On September 15, Martha Blair-Tyler made a presentation to a workshop session of the annual conference of Utah League of Cities and Towns. The session was organized by the Utah Chapter of the American Planning Association as part of its program to provide information to local government officials about planning issues. The presentation focused on various ways to reduce risk from specific earthquake hazards--surface faulting, ground shaking, landsliding, and liquefaction. The emphasis was on the ground failure hazards because they are most amenable to mitigation using land use planning techniques. Many of the slides from the July trip to Utah were used in the presentation to keep a Utah focus. Copies of the following publications were displayed and provided to all attendees who requested them:

   - California at Risk, Steps to Earthquake Safety for Local Government, 1988, California Seismic Safety Commission.
   - Putting Seismic Safety Policies to Work, 1988, Bay Area Regional Earthquake Preparedness Project.
   - Geology and Planning: The Portola Valley Experience, 1989, William Spangle and Associates, Inc.

   The number of attendees was disappointingly low, but those that attended expressed considerable interest in the subject. Surprisingly, more came from southern Utah than from the Wasatch Front. They were particularly interested in landsliding and geologic hazards that are not necessarily associated with earthquakes.

3. Questionnaire. A short questionnaire for local government officials was printed in the Wasatch Front Forum distributed in April. We received no responses. As noted in the last Summary Report, we received 6 completed questionnaires that were distributed at the Annual Workshop of the Wasatch Front Project in February. We have responded directly to the three that came from the county geologists and are working on direct responses to the other three.

4. Other Activities. We talked at some length with representatives of the Utah Chapter of the American Planning Association about conducting a workshop for planners on earthquake hazard reduction techniques. As of now, it does not look like this is going to happen. Planners we talk to seem to feel that they are well informed about what to do and that the need is to reach elected and appointed officials of local government.

Work Underway. We recently contacted several people with various state and local agencies in Utah to see how we might be of assistance. As a result we have a series of questions from the Geological and Mineral Survey and are in the process of conducting some research to provide answers. We are also working on responses to the questions from three cities in Utah and will be preparing the final project report.

Global Seismograph Network

9920-02398

Howell M. Butler
Branch of Global Seismology and Geomagnetism
U.S. Geological Survey
Albuquerque Seismological Laboratory
Building 10002, Kirtland AFB-East
Albuquerque, New Mexico 87115
(505) 844-4637

Investigations

The Global Seismograph Network (GSN) presently consists of 14 SRO/ASRO, 13 DWWSSN and 82 WWSSN type recording stations located in 58 countries and islands throughout the world. The primary objective of the project is to provide high-quality digital and analog seismic data for fundamental earthquake investigations and research, enhancing the United States capabilities to detect, locate and identify earthquakes and underground nuclear explosions in support of test ban issues. Technical and operational support is provided as required to keep the GSN operating at the highest percentage of recording time possible. This support includes operational supplies, replacement parts, repair service, modifications of existing equipment, installation of systems and on-site maintenance, training and calibration. A service contract provides technicians to perform the support requirements as well as special projects such as on-site noise surveys, site preparations, and evaluation and testing of seismological and related instrumentation.

The following on-site station maintenance activity was accomplished:

ANMO - Albuquerque, New Mexico - SRO - Eight maintenance visits
BCAO - Bangui, Central African Republic - SRO - Two maintenance visits
ANTO - Ankara, Turkey - SRO - One maintenance visit
GUMO - Guam Mariana, Islands - SRO - One maintenance visit
TATO - Taipei, Taiwan - SRO - One maintenance visit
TPM - Tepoztlan, Mexico - WWSSN - After many years of being inoperative, TPM was reactivated, calibrated and converted to the heated-stylus system.

Special Activity:

One Field Engineer was in China full time during this period assisting in maintenance and training of CDSN personnel.

One Field Engineer and one Computer Programmer was assigned full time to the IRIS project for testing and check-out of new equipment and the KS-54000 seismometer. ANMO was converted from a SRO to an IRIS II operating system during this period.

Three National Mapping Division personnel attended a 2-week training session on the operation and maintenance of the South Pole, Antarctic (SPA) WWSSN station.

Seventy-six WWSSN stations have been converted from photographic recording to thermal recording. Thirty-eight stations operate with six components. Six station, BKS, DUG, FVM, GSC, HON and LUB, continue with photographic recording.

Results

The Global Seismograph Network continues with a combined total of 109 WWSSN/SRO/ASRO/DWWSSN/IRIS stations. The main effort of this project, as funding permits, is to furnish the types of support at a level needed to keep the GSN at the highest percentage of operational time in order to provide the improved geographical coverage with analog and digital data from highly sensitive short-period and broadband seismic sensor seismograph systems.

U.S. Seismic Network

9920-01899

Marvin A. Carlson
Branch of Global Seismology and Geomagnetism
U.S. Geological Survey
Denver Federal Center
Box 25046, Mail Stop 967
Denver, Colorado 80225
(303) 236-1500

Investigations

U.S. Seismicity. Data from the U.S. Seismic Network (USSN) are used to obtain preliminary locations and magnitudes of significant earthquakes throughout the United States and the world.

Results

As an operational program, the USSN operated normally throughout the report period. Data were recorded continuously in real time at the National Earthquake Information Center's (NEIC) main office in Golden, Colorado. At the present time, 80 channels of SPZ data are being recorded at Golden on develocorder film. This includes data telemetered to Golden via satellite from both the Alaska Tsunami Warning Center, Palmer, Alaska, and the Pacific Tsunami Warning Center, Ewa Beach, Hawaii. A representative number of SPZ channels are also recorded on Helicorders to give NEIC real-time monitoring capability of the more active seismic areas of the United States. In addition, 18 channels of LPZ data are recorded in real time on multiple pen Helicorders.

Data from the USSN are interpreted by record analysts and the seismic readings are entered into the NEIS data base. The data are also used by NEIS standby personnel to monitor seismic activity in the United States and world wide on a real time basis. Additionally, the data are used to support the Alaska Tsunami Warning Center and the Pacific Tsunami Warning Service. At the present time, all earthquakes large enough to be recorded on several stations are worked up using the "Quick Quake" program to obtain a provisional solution as rapidly as possible. Finally, the data are used in such NEIS publications as the "Preliminary Determination of Epicenters" and the "Earthquake Data Report."

Development is continuing on an Event Detect and Earthquake Location System to process data generated by the USSN. We expect the new system to be ready for routine operational use during 1990. At that time, the use of develocorders for data storage will be discontinued. Ray Buland and David Ketchum have been doing the developmental programming for the new system. A Micro Vax III will be used as the primary computer of the Event Detect and Earthquake Location System.

Six stations of a pilot VSAT Network have been installed. Four of the stations are the former RSTN sites at McMinnville, Tennessee, St. Regis Falls, New York, Black Hills, South Dakota, and Red Lake, Ontario, which are now operated by the Branch of Global Seismology and Geomagnetism. The fifth site is the former AFTAC Array near Boulder, Wyoming, and the sixth site is at what was formerly the Newport Observatory, Newport, Washington, which is no longer a manned site. The data is transmitted via satellite to a shared Master Earth Station and on to the NEIC at Golden, Colorado, via AT&T long lines.

Earth Structure and its Effects upon Seismic Wave Propagation

9920-01736

George L. Choy
Branch of Global Seismology and Geomagnetism
U.S. Geological Survey
Denver Federal Center
Box 25046, Mail Stop 967
Denver, Colorado 80225
(303) 236-1506

Investigations

1. Effects of Earth Structure on Source Parameters. The NEIS now uses broadband data to routinely compute parameters such as depth from differential arrival times, radiated energy and arrival times of late-arriving phases. To assure the accuracy of source parameters derived from waveforms we are developing corrections for the effects of wave propagation in the Earth.

2. Use of Differential Travel-Time Anomalies to Infer Lateral Heterogeneity. We are investigating lateral heterogeneity in the Earth by analyzing differential travel times of phases that differ in ray path only in very narrow regions of the Earth. Because such phases often are associated with complications near a cusp or caustic, their arrival times can not be accurately read without special consideration of the effects of propagation in the Earth as well as additional processing to enhance arrivals.

3. Use of Body Wave Pulse Shapes to Infer Attenuation in the Earth. In previous work, we developed techniques to determine the depth- and frequency-dependence of attenuation in the Earth. Resolution of this frequency dependence requires analysis of a continuous frequency band from several Hz to tens of seconds as well as consideration of the contributions of scattering and slab diffraction to apparent broadening of a pulse. We are now in the process of documenting Q for surface events and for events at different depths.

Results

1. Effects of Earth Structure on Source Parameters. Body waves that touch internal caustics in the Earth are distorted in a way that can be mathematically corrected by Hilbert transformation. The correction for this pulse distortion has generally not been recognized in the practice of record interpretation. We are evaluating the effect on phases that are commonly read by analysts and the possible effect on tomographic inversions which take reported arrival times of body waves on face value.

2. Use of Differential Travel-Time Anomalies to Infer Lateral Heterogeneity. We have developed a source-deconvolution technique that resolves differential travel times of body waves near cusps and caustics. Application of this algorithm to PKP waves sampling the inner core suggests that

regional velocity variations exist within the upper 200 km of the inner core. The regional variations are consistent with those obtained from global inversions of absolute PKP times. We are reading high quality arrival times of PcP and branches of PKP, corrected for propagation effects. This accumulation of data can be used to determine if propagation phenomena have biased the catalog data which have been used to derive models of lateral heterogeneity.

3. Use of Body Wave Pulse Shapes to Infer Attenuation in the Earth. The frequency-dependent Q model of Choy and Cormier (1987) has been crucial to the practical implementation of some algorithms that are used to compute source parameters. It was incorporated into a semi-automated version of the algorithm of Boatwright and Choy (1986) for use by the NEIC in computing radiated energies of earthquakes with $m_b > 5.8$. This Q model also provided the crucial attenuation correction in the technique described by Choy and Boatwright (1988) and Boatwright and Choy (1989) which derives acceleration spectrum from far-field broadband data. We are now attempting to separate intrinsic attenuation from scattering in waveforms. We synthesize waveforms using a method that simultaneously models causal attenuation and source finiteness. Under the assumption that intrinsic attenuation can be described by minimum phase operators, we can attribute discrepancies in the waveforms to scattering.

Reports

Boatwright, J., and Choy, G. L., 1989, Acceleration spectra for subduction zone earthquakes: Journal of Geophysical Research (in press).

Boatwright, J., and Choy, G. L., 1989, Source spectra and stress drop of shallow thrust earthquakes obtained from teleseismic recordings [abs.]: in Abstracts of the 25th General Assembly of IASPEI, p. 242.

Choy, G. L., 1989, Interpretation of the earthquake mechanism from analysis of digitally recorded broadband seismograms [abs.]: Abstracts of the 25th General Assembly of IASPEI, p. 312.

Choy, G. L., and Bowman, J. R., 1989, The rupture process of a multiple main shock sequence--Teleseismic, local and near-field analysis of the Tennant Creek earthquakes of 22 January 1988: Journal of Geophysical Research (submitted).

Choy, G. L., and Kind, R., 1989, A preliminary broadband body-wave analysis of the Armenia S.S.R. earthquake of 7 December 1988 (in preparation).

Choy, G. L., and Presgrave, B. W., 1989, Broadband seismogram analysis--A. Deep earthquake of Honshu, Japan of 7 September 1988, and B. Nepal-India border region earthquake of 20 August 1988: in Semi-Annual Technical Report, U.S. Geological Survey Open-file Report 89-207, p. 11-15.

Sipkin, S. A., and Choy, G. L., 1989, Routine determination of seismic source parameters using digital data at the NEIC [abs.]: Abstracts of the 25th General Assembly of IASPEI, p. 282.

Reanalysis of Instrumentally Recorded United States Earthquakes

9920-01901

J. W. Dewey
Branch of Global Seismology and Geomagnetism
U.S. Geological Survey
Denver Federal Center
Box 25046, Mail Stop 967
Denver, Colorado 80225
(303) 236-1506

Investigations

1. Relocate instrumentally recorded U.S. earthquakes using the method of joint hypocenter determination (JHD) or the master event method, using subsidiary phases (Pg, S, Lg) in addition to first arriving P-waves, using regional travel-time tables, and expressing the uncertainty of the computed hypocenters in terms of confidence ellipsoids on the hypocentral coordinates.

2. Evaluate the implications of the revised hypocenters on regional tectonics and seismic risk.

Results

D. W. Gordon and P. K. Sims (CMR) are examining the relationship between seismicity and basement tectonics beneath the northern Great Plains (37°-49°N. latitude; 94°-105°W. longitude). The region under investigation contains Kansas, Nebraska, South Dakota, and North Dakota, and includes parts of adjacent states. Sims and Peterman (1986, Geology, v. 14, p. 448-491) have reported that the Precambrian basement in this region is composed of seven major terranes, which are separated in most cases by collisional suture zones. Orthogonal systems of structural lineaments with northwest and northeast trends crisscross these terranes. These linear structural elements have generally been interpreted as fracture zones or wrench faults. Some of the basement lineaments continue into the Rocky Mountains where they crop out in cataclastic or mylonite shear zones. Using regional earthquake catalogs and other seismological literature, we have reviewed data on historical and instrumental earthquakes having locations in the study area. We have considered all earthquakes with $I_{max} \geq$ III and/or $m_b \geq 3.0$. About 175 earthquakes which have occurred in the region since 1860 meet one of these criteria. In our reexamination of the historic data, we paid particular attention to the determination of the felt area associated with individual earthquakes, because, when taken by itself, maximum intensity is a notoriously poor estimator of relative earthquake size. We were able to make rough estimates of felt area for about 25 earthquakes for which felt areas had not previously been reported. Our review also disclosed over a dozen incompletely or vaguely documented earthquakes that were apparently widely felt. Most of these earthquakes occurred after 1900, and we believe that additional felt information associated with these shocks is recoverable. Using relationships between magnitude, maximum intensity, and felt area developed by Sibol, Bollinger, and Birch (1987, Bull. Seism. Soc. Am., v. 77, p. 1636-1654), we have estimated magnitudes (m_b) for the earthquakes considered. This analysis indicates that the historical record covering the study area is approximately complete down to the magnitude 3.5 level over the last 75 years. Our magnitude determinations imply the following magnitude-frequency relation:

$$\log N = 3.52\ (\pm\ 0.14) - 1.07\ (\pm\ 0.03)\ m_b,$$

where N is the annual frequency of earthquakes having magnitude equal to or larger than m_b.

Gordon (1989) has discussed preliminary comparison of seismicity and tectonics in the study region. Historical epicenters in the region exhibit spatial coincidence with Precambrian suture zones, rift zones, and inferred wrench-fault systems. The uncertainties associated with the epicenters ($\pm$ 10 to 20 km or more) and the lack of precise focal depths preclude correlation of individual earthquakes with specific faults, but clusters of historical and instrumental epicenters generally occur in areas of dense basement faulting. Epicenters that do not plot near mapped basement faults commonly plot near the along-trend projections of mapped wrench-fault systems, suggesting that these systems continue beyond their presently mapped limits.

Reports

Gordon, D. W., 1989, Historic seismicity and basement tectonics in the northern Great Plains, USA [abs.]: Seismological Research Letters, v. 60, p. 13.

Global Seismology

9920-03684

E. R. Engdahl
and
J. W. Dewey
Branch of Global Seismology and Geomagnetism
U.S. Geological Survey
Denver Federal Center
Box 25046, Mail Stop 967
Denver, Colorado 80225
(303) 236-1506

Investigations

1. Travel-Time Tables. Develop new standard global travel-time tables to locate earthquakes.

2. Arrival-Time Data. Develop a plan to establish an International Seismological Observing Period (ISOP)--a time interval during which there would be enhanced reporting of arrival time data.

3. Earthquake Location in Island Arcs. Develop practical methods to accurately locate earthquakes in island arcs.

4. Subduction Zone Structure. Develop techniques to invert seismic travel times simultaneously for earthquake locations and subduction zone structure.

5. Global Synthesis. Synthesize recent observational results on the seismicity of the earth and analyze this seismicity in light of current models of global tectonic processes.

Results

1. Travel-Time Tables. E. R. Engdahl was a Co-Convenor of a Workshop on Travel Tables and Earthquake Location Problems at the IASPEI General Assembly in Instanbul. This workshop was concerned with the construction of effective travel-time tables on both regional and global scales, with algorithms for earthquake location, and with the accuracy of estimated hypocenters.

Two working global travel-time models, developed according to recommendations of the IASPEI Sub-Commission on Algorithms, were presented: IASPR-based on upper mantle structure from Kennett (1988), lower mantle from Toy (1989), core after PEMC, and including static station corrections; and MD89PS--the spherically symmetric part of a spherically asymmetric Earth model, derived using travel times of P, PcP-P, PKP (AB, BC, DF), S, SKS, and SKKS-SKS (Morelli and Dziewonski), and with station corrections taken as a continuous function of position (Dziewonski and Morelli). These two models agreed in essential detail and are illustrative of the complexity in the class of models being developed. It was pointed out that a better fit to explosion travel times at regional distances could be made (Hales). Toy and Orcutt suggested that the present distribution of core phase data in the ISC catalog (1964-1986) was not adequate to resolve core structure. These radial Earth models will have a prescribed mode of interpolation and a specified scheme for the calculation of travel times for the various seismic phases. Such a scheme was presented by Buland and Kennett, and used by Engdahl to check the performance of the new models against a limited number of test events for which the origin times and hypocenters are well constrained. The models, IASPR and MD89PS, with and without station corrections, produced a significant shift in the travel-time baseline and a modest variance reduction in travel-time residuals when compared to JB.

On the problems of earthquake location and estimates of accuracy, there were a wide range of presentations. Shapira and du Plessis described a numerical procedure developed to assess hypocenter location errors. A new approach for analyzing travel-time residuals that can predict the impact of individual residual has on the estimated hypocentral vector was presented by Rabinowitz. Bruk and Kondorskaya demonstrated that stable station corrections can eliminate systematic errors in hypocenter location and thereby provide a more accurate error ellipsoid. Norikova and Rautian used numerical modeling to investigate the nature of systematic errors in hypocentral determination due to lateral inhomogeneity and to assess the accuracy of depth estimates as a function of epicenter location and station distribution. Dziewonski and Morelli proposed a scheme for earthquake location analogous to a joint hypocenter determination where the station correction incorporates a weighted averaging over source regions, thereby making it a continuous function of position. Bolt proposed using pattern recognition algorithms with broadband digital seismograms to characterize source location and mechanism parameters. Further presentations included an attempt to obtain a homogeneous catalog for the seismicity of the Italian region (Console, Giardini, and Veloná) and implications of well-constrained ridge earthquakes for global travel times and mantle structure (Bergman and Kong).

2. Arrival-Time Data. E. R. Engdahl was convenor of a joint IASPEI/Unesco Workshop on the International Seismological Observing Period (ISOP) at the IASPEI General Assembly in Istanbul. To set the tone for the workshop, T. Jordan presented the ISOP concept. The premises for an ISOP are: arrival-time data reported to international centers by the global network of ~1500 stations are providing fundamental new information about the Earth; the practice of seismology is changing and being revolutionized by digital seismology, by global communications, and by new algorithms and Earth models; and significant improvements to the existing data set can be achieved by increasing international cooperation. An ISOP would provide a time interval during which we would agree to enhance such international cooperation.

Jordan described objectives which could be realized by an ISOP: to compile arrival times of seismic phases, especially later phases; to improve the global data base; to strengthen the infrastructure of international seismology; to educate young scientists; to foster the widespread use of 3-component, broadband systems; to encourage observatory initiatives; and to increase national sources of support for observatories. In addition, Jordan outlined initiatives that might be taken during an ISOP and described elements of an organizational plan.

D. Doornbos and R. Haddon demonstrated the scientific gains that could be expected from an ISOP. Highlighted were experiments to determine details of Earth structure and to detect lateral heterogeneity using short-period arrival-time data. M. Bergman reviewed the performance of the present global reporting network using ISC data and reported on an unassociated phase experiment. The inadequacies of later phase reporting and the global distribution of reporting stations was evident. O. Kulhanek and A. Plesinger described manuals and procedures which could be implemented at observatories to improve seismological analyses. W. Smith and J. Berrocal described the opeation of typical networks and addressed the role of regional data centers. E. R. Engdahl described how the development of a new global travel-time model would enhance the identification of later phases during an ISOP. Some improvement in phase identification algorithms also would be needed, as evidenced by current practice at the ISC (A. Hughes). E. Bergman presented a simply parameterized weighting scheme for ISOP event selection, producing workloads which vary within reasonable limits around a desired average. It was determined that a 3-year ISOP experiment with a workload near one event per day would provide a good sample of global seismicity. Finally, B. Presgrave described the manner in which data flow from the stations to NEIC and ISC might be implemented under an ISOP.

A general meeting followed during which an organizational structure, operational plan, and time table were discussed. It was decided to establish a list of ISOP correspondents representing individual observatories, networks, or countries. A need for workshops to explain the ISOP program and to train analysts was recognized. M. Hashizume announced that Unesco would support these type of activites in developing countries. A time table was developed that included, in the first two years, submission of proposals, development of a Science Plan, development of an Organizational Plan, emplacement of an ISOP Committee and a full-time Coordinator. There would follow a planning period to include worshops, culminating at the end of 1991, after the IUGG Assembly in Vienna. ISOP would officially commence in 1992. An Executive Committee was pointed (E. R. Engdahl, Chairman) to coordinate applications for funds, to develop planning documents, and ultimately to oversee the daily operation of an ISOP.

3. Earthquake Location in Island Arcs. J. W. Dewey attended the International Tsunami Symposium and Workshop, Novosibirsk, USSR, as representative of the National Earthquake Information Center (NEIC) of the U.S. Geological Survey. He reported on planned upgrades in NEIC instrumentation and analysis procedures that may help tsunami-warning agencies improve the speed and accuracy of tsunami forecasts. Considering the goals of the present project, it is evident from papers presented at the symposium that modeling of tsunami generation is attaining a high level of sophistication, and one may anticipate that errors in hypocenters that define the spatial configuration of tsunamigenic sources will come to have a significant impact on the modeling. The modeling results depend on depth of the source, depth of seawater above the source, and elastic properties of the medium in which

the source occurs. Forty-kilometer errors in routinely determined epicenters and tens of kilometers errors in routinely determined focal depths, both of which are characteristic of some subduction zones such as the Aleutian Islands, might cause modeling results to be inappropriate to the observations they are intended to match.

4. Subduction Zone Structure.

A technique for the inversion of seismic travel-time residuals has been developed at the USGS and University of Cambridge for resolving a laterally inhomogeneous velocity structure, assuming an anomalous region of limited spatial extent. The inversion is formulated as the solution to the non-linear least-squares problem. The slowness in the anomalous region is expressed as

$$s(r, \theta,\phi) = \sum_{k=1}^{m} c_k w_k(r,\theta,\phi)$$

where w_k is a continuously twice-differentiable function of position. Therefore the problem of travel-time inversion for velocity (or slowness) can be recast as the inversion for the coefficients c_k, as seen by

$$\delta T_i = \int_{\Gamma_i} \delta s \, dl_i$$

and,

$$\delta T_i = \sum_{k=1}^{m} \delta c_k \int_{\Gamma_i} wk(r,\theta,\phi) dl_i$$

where the integral over Γ_i means the integral over the raypath associated with the ith ray. The solution is obtained by using ray tracing to find the raypaths and inverting using Marquart-Levenberg iterative damped least-squares.

The ray tracing techniques used require the slowness model to be a continuous, twice-differentiable function of position. This leads naturally to its expression in terms of cubic spline functions, which have continuous second derivatives. Two possible choices for the spline functions are the cardinal-spline $C_4(x)$ and the B-spline $B_4(x)$. However, the cardinal-spline is non-zero over the entire interpolation region, thus forcing the evaluation of the slowness, for some arbitrary position x within the interpolation region, to involve the summation over all the spline functions,

$$s(x) = \sum_{k=1}^{N} c_k C_{k,4}(y).$$

where

$$y = \frac{x}{\Delta x} + 1$$

and Δx is the knot point spacing. The B-spline however is only non-zero over four-consecutive intervals, allowing the evaluation of the slowness to involve only the summation over four B-splines,

for x such that: $x_i < x < x_i+1$

$$s(x) = \sum_{k=i-3}^{i} c_k B_{k,4}(x).$$

This naturally leads to great computational savings while completely specifying the slowness in the region of interpolation.

Two ray tracing methods have been employed for use in calculating the raypath as required in the inversion. First, the shooting method, solves the two-point raypath problem which requires the solution i_{r0} and z_0 to be found for the two simultaneous, generally non-linear equations

$$\theta_f(i_{r0}, z_0) = \Theta$$

$$\phi_f(i_{r0}, z_0) = \Phi$$

where (θ_f, ϕ_f) are the coordinates of the end point of the ray and (Θ, Φ) are the desired coordinates of the end point. These can be solved by the Newton-Raphson iterative technique, for example. However, the solution can be strongly deviant from the desired solution depending on the initial choice of i_{r0} and z_0.

Second, the bending method, considers the two-point raypath problem as a boundary-value problem to be solved using Fermat's principle and the calculus of variations. That is, the problem ca be expressed as

$$T = \int_{\alpha(a)}^{\alpha(b)} sF d\alpha = \text{Extremum}$$

where the ray path has been parameterized in terms of a the single parameter $\alpha : r = r(\alpha)$, $\Theta = \Theta(\alpha)$ and $\phi = \phi(\alpha)$. The problem posed in this manner occurs frequently in the calculus of variations and can be solved by finding solutions to the corresponding set of Euler's differential equations. The solution is obtained by an iterative scheme which has no guarantee of converging. However, the limit of any converging series must be a valid ray path. The bending method is found to be favorable in regard to the computational labor it requires.

5. Global Synthesis. Nothing new to report.

Reports

Ekström, G., and Engdahl, E. R., 1989, Earthquake source parameters and stress distribution in the Adak Island region of the central Aleutian Islands, Alaska: Journal of Geophysical Research (in press).

Engdahl, E. R., Billington, S., and Kisslinger, C., 1989, Teleseismically recorded seismicity before and after the May 7, 1986, Andreanof Islands, Alaska, earthquake: Journal of Geophysical Research (in press).

Schwartz, S. Y., Dewey, J. W., and Lay, T., 1989, Influence of fault plane heterogeneity on the seismic behavior in the southern Kurile Islands arc: Journal of Geophysical Research, V. 94, P. 5637-5649.

Systems Engineering

9920-01262

Gary Holcomb
Branch of Global Seismology and Geomagnetism
U.S. Geological Survey
Albuquerque Seismological Laboratory
Building 10002, Kirtland AFB-East
Albuquerque, New Mexico 87115
(505) 844-4637

Investigations

Engineering development to improve the quality of seismic instrumentation.

Results

A new method for calculating the system self noise from data obtained during side-by-side seismometer evaluations was developed and tested on both artificially computer generated test data and on test data from actual sensor outputs. This method evaluates the system self noise directly thereby avoiding the need to define a system signal to noise ratio in terms of the coherence between the outputs of the two systems under test. An Open-File Report detailing these procedures and examples of the methods performance was written and released.

An extensive series of measurements of system parameters was conducted on several seismic sensor systems which were submitted for USGS evaluation as a result of a RFP to procure sensors for the National Seismic Network. The results of these measurements are being analyzed at the present time; they will become part of the technical evaluation of individual manufacturers' proposals.

Probabilistic Earthquake Assessment

9920-01506

Stuart P. Nishenko
Branch of Global Seismology and Geomagnetism
U.S. Geological Survey
Denver Federal Center
Box 25046, Mail Stop 967
Denver, Colorado 80225
(303) 236-1500

Investigations

1. Continued probabilistic evaluation of large and great earthquake hazards associated with seismic gaps in the circum-Pacific region.

2. Evaluation of the probabilities for damaging earthquakes in the central and eastern United States.

3. Improvement of methodology for calculating probabilistic earthquake hazard evaluations.

Results

1. Regional investigations of large and great earthquake hazards for the Queen Charlotte-Alaska-Aleutian, southwest Pacific, and Peruvian seismic zones have been conducted by Nishenko and Jacob (1989), McCann and Nishenko (1989), and Beck and Nishenko (1989) and are either in press or in preparation at this time.

2. Probabilistic estimates for the occurrence of damaging (i.e. $m_b \geq 6.0$) earthquakes in the eastern and central United States are presently being investigated by Nishenko and Bollinger (1989). These estimates are based on regional return times inferred from local network data, catalogs of eastern and central U.S. seismicity since 1727, and paleoseismic data. Preliminary results indicate that the conditional probability for an event of m_b 6 or larger in this region is at the 40-60 percent level for the next 30 years (i.e. 1989-2019).

3. The "generic" characteristic earthquake recurrence model of Nishenko and Buland (1987) has been extended in Buland and Nishenko (1989) to provide a marginal distribution for recurrence intervals which is independent of the uncertainty in the median recurrence interval. This permits the estimation of a <u>single</u>, preferred value for the conditional earthquake forecast probability. This marginal distribution also allows utilization of the additional information that the expected event has not yet occurred to update both the conditional probability and expected date of the next event.

Reports

Beck, S., and Nishenko, S. P., 1989, Variations in the earthquake rupture mode along the central Peru subduction zone (in preparation).

Buland, R., and Nishenko, S. P., 1989, Preferred earthquake forecasts and conditional earthquake prediction: Bulletin of the Seismological Society of America (submitted) 24 p.

McCann, W. R., and Nishenko, S. P., 1989, Seismic potential and seismic regimes of the southwest Pacific (in preparation).

Nishenko, S. P., and Bollinger, G. A., 1989, Forecasting damaging earthquakes in the central and eastern United States (in preparation).

Nishenko, S. P., and Jacob, K.H . Jacob, 1989, Seismic potential of the Queen Charlotte-Alaska-Aleutian seismic zone: Journal of Geophysical Research (in press).

Nishenko, S. P., and Buland, R, 1987, A generic recurrence interval distribution for earthquake forecasting: Bulletin of the Seismological Society of America, v. 77, p. 1382-1399.

Global Seismograph Network Evaluation and Development

9920-02384

Jon Peterson
Branch of Global Seismology and Geomagnetism
U.S. Geological Survey
Albuquerque, New Mexico 87115-5000
(505) 844-4637

Investigations

Continued planning activities and associated studies in support of the IRIS/USGS program to upgrade the global seismograph network and for deployment of broadband systems in the Soviet Union.

Results

Detailed IRIS/USGS plans for upgrading the global seismograph network (GSN) were documented in a report intended for distribution to stations that will be asked to participate in the program. The report includes a comprehensive description of system design and current plans for network deployment and operation. A final review of the joint IRIS/USGS Technical Plan in underway. Preliminary documentation has been prepared on the IRIS-type GSN system that will be installed at Garni, Armenia, sensor systems have been ordered, and an application has been made for an export license.

Reports

Peterson, J, 1989, The china digital seismograph network: *U.S. Geological Survey Yearbook 1988*, 68-71.

Peterson, J. and C.R. Hutt, IRIS/USGS plans for upgrading the global seismograph network: *U.S. Geological Survey Open-File Report 89-471,* 46 p.

Digital Data Analysis

9920-01788

Stuart A. Sipkin
Branch of Global Seismology and Geomagnetism
U.S. Geological Survey
Denver Federal Center
Box 25046, Mail Stop 967
Denver, Colorado 80225
(303) 236-1506

Investigations

1. Moment Tensor Inversion. Apply methods for inverting body phase waveforms for the best point-source description to research problems.

2. Other Source Parameter Studies. Apply methods for inverting body phase waveforms for distributed kinematic and dynamic source properties.

3. Aftershock Source Properties. Examine mainshock and aftershock source properties to study the mechanics of aftershock occurrence.

4. Significant Historic Earthquakes. Study the effects of large historic earthquakes at subduction boundaries to infer the characteristics of interplate thrust faulting.

5. Earthquake Recurrence Statistics. Use earthquake recurrence statistics and related parameters to better understand the earthquake cycle and study how they can be used for prediction and forecasting purposes.

6. Broadband Body-Wave Studies. Use broadband body phases to study lateral heterogeneity, attenuation, and scattering in the crust and mantle.

7. NEIC Monthly Listing. Contribute both fault-plane solutions (using first-motion polarity) and moment tensors (using long-period body-phase waveforms) for all events of magnitude 5.8 or greater when sufficient data exists. Contribute waveform/focal-sphere figures of selected events.

Results

1. Moment Tensor Inversion. A paper listing the moment-tensor solutions for 426 moderate-to-large size earthquakes occurring from 1984 through 1987 is in press. A study of the 24 November 1987 Superstition Hills earthquake and its largest foreshock has been published. We find that the foreshock had a depth of 8 km, a scalar moment of 2.3×10^{18} Nm (M_w 6.2) and a best double-couple mechanism of strike 217°, dip 79°, rake 4° with a non-double-couple component of 4 percent. The mainshock was a complex event, consisting of at least two sub-events, with a combined scalar moment of 1.0×10^{19} Nm (M_w 6.6), a depth of 10 km, and a mechanism of strike 303°, dip 89°, rake -180°. A study of the 7 December 1988 Armenian Earthquake is in preparation. The preliminary results indicate that the rupture consisted of two,

and possibly three, subevents occurring at a centroidal depth of 5 km. The orientation of the mechanism changed during the rupture process, beginning as a thrust, but ending with strike-slip motion.

2. Other Source Parameter Studies. The results of a joint inversion of teleseismic P waveforms and strong-motion velocity data observed during the 1985 Michoacan, Mexico, earthquake, have been published. Two major shallow zones, and possibly a third smaller more downdip region, were involved in the rupture of the plate interface. The area between the two large shallow sources exhibited relatively little slip during the 1985 earthquake. This area coincides with the aftershock zone of the 1981 Playa Azul earthquake, suggesting that most of the strain that had accumulated within this portion of the plate boundary had been released in 1981. The inversion method has recently been modified to include the derivation of rupture time along the fault. This nonlinear procedure in now being implemented in the analysis of teleseismic and near-source data of the 1978 Tabas, Iran, earthquake.

3. Aftershock Source Properties. Work is continuing on the comparison of aftershock locations with distribution of fault slip derived from observed waveform data, especially for interplate thrust events. One such comparison, conducted for the Michoacan, Mexico, earthquake, suggests that subduction-zone thrust earthquake sequences may behave similarly to normal-interplate and intraplate events. That is, aftershock activity tends to occur mainly outside of, or near the edges of, the mainshock source regions.

4. Significant Historic Earthquakes. A study of the intensities and damage observed during a large earthquake in northern Panama on 7 September 1882 has been published. The results suggest that the earthquake was a great ($M \sim 8$) underthrusting event that occurred at or near the boundary between the Panama "block" and the Caribbean plate.

5. Earthquake Recurrence Statistics. A paper has been submitted for publication in which the "generic", characteristic earthquake, recurrence interval, probability density function model has been extended to provide a marginal distribution for recurrence intervals which is independent of the uncertainty in the median recurrence interval. This permits the estimation of a single preferred value for the conditional earthquake forecast probability. A new determination of the seismic potential of the Queen Charlotte-Alaska-Aleutian seismic zone is in press.

6. Broadband Body-Wave Studies. A data set of relatively broadband shear-wave data has been assembled for the purpose of studying deep discontinuities in the Earth. Another data set is being assembled for the purpose of identifying near-receiver scattering of seismic waves. Software for both studies is being developed. Preliminary results indicate that, when deconvolving an instrument response, unless one is explicitly takes into account the properties of the filters being used, either bias or increased uncertainty in the results can be introduced, especially when taking integral measures of the displacement pulse.

7. NEIC Monthly Listing. Since January 1981, first-motion fault-plane solutions for all events of magnitude 5.8 or greater have been contributed to the Monthly Listings. Since July 1982, moment-tensor solutions and waveform/focal-sphere plots have also been contributed. In the last six months, solutions for approximately 73 events have been published. An atlas of European seismicity is in preparation. Special maps showing the seismicity of Algeria, Indonesia, and the southwest Pacific Ocean have been made for the Office of Earthquakes, Volcanos, and Engineering.

Reports

Buland, R. P., and Nishenko, S. P., 1989, Preferred earthquake forecasts and conditional earthquake prediction: Bulletin Seismological Society of America (submitted).

Massé, R. P., and Needham, R. E., 1989, National Earthquake Information Center-- NEIC: Earthquakes and Volcanos (in press).

Mendoza, C., and Hartzell, S. H., 1989, Slip distribution of the 19 September 1985 Michoacan, Mexico, earthquake--Near source and teleseismic constraints: Bulletin Seismological Society of America, v. 79, no. 3, p. 655-669.

Mendoza, C., and Nishenko, S. P., 1989, The north Panama earthquake of 7 September 1882--Evidence for active underthrusting: Bulletin Seismological Society of America, v. 79, no. 4, p. 1264-1269.

Needham, R. E., and Sipkin, S. A., 1989, Teleseismic source parameters of the 7 December 1988 Armenian earthquake [abs.]: EOS (American Geophysical Union, Transactions) (in press).

Nishenko, S. P., and Jacob, K., 1989, Seismic potential of the Queen Charlotte-Alaska-Aleutian seismic zone: Journal Geophysical Research, (in press).

Sipkin, S. A., 1989, Moment-tensor solutions for the 24 November 1987 Superstition Hills earthquakes: Bulletin Seismological Society of America, v. 79, no. 2, p. 493-499.

Sipkin, S. A., and Choy, G. L., 1989, Routine determination of seismic source parameters using digital data at the NEIC: in Abstracts, 25th IASPEI General Assembly, Istanbul, Turkey, p. 282.

Sipkin, S. A., and Lerner-Lam, A. L., 1989, Some caveats regarding broadband deconvolution [abs.]: EOS (American Geophysical Union, Transactions) (in press).

Sipkin, S. A., and Needham, R. E., 1988, Moment tensor solutions estimated using optimal filter theory--Global Seismicity, 1984-1987: Physics of the Earth and Planetary Interiors (in press).

Seismicity and Tectonics

9920-01206

William Spence
Branch of Global Seismology and Geomagnetism
U.S. Geological Survey
Denver Federal Center
Box 25046, Mail Stop 967
Denver, Colorado 80225
(303) 236-1506

Investigations

Studies carried out under this project focus on detailed investigations of large earthquakes, aftershock series, tectonic problems, and Earth structure. Studies in progress have the following objectives:

1. Determine the maximum depth and degree of velocity anomaly beneath the Rio Grande Rift and Jemez Lineament by use of a 3-D, seismic ray-tracing methodology (W. Spence and R. S. Gross).

2. Explore the consequences of the slab pull force acting at the zone of plate bending that is downdip of the lower end of an interface thrust zone (W. Spence and W. Z. Savage).

3. Develop a tectonic model for the Carpathian arc, Romania (G. Purcaru and W. Spence).

Results

1. The Jemez lineament is the most active volcanic feature in the southwestern United States. It is the southeastern tectonic boundary of the Colorado Plateau, it extends about 800 km from the Raton-Clayton volcanic field in northeast NM to the San Carlos volcanic field in AZ, and it crosses the Rio Grande rift at the Jemez Mountains. The lateral variations in P-wave velocity in the upper mantle beneath the central Jemez lineament and the central Rio Grande rift were investigated using teleseismic P-wave delays measured at a 23-station seismic network. The inversion used a method of damped, least-squares and velocity interpolations within a three-dimensional grid of points, rather than using blocks of fixed P-wave velocity. To a depth of about 160 km, the upper mantle P-wave velocity beneath the Rio Grande rift and Jemez lineament is 4-6 percent lower than beneath the High Plains Province. While lateral variations showing low P-wave velocity in the upper mantle beneath the Rio Grande rift were not resolvable, the inversion shows a primary trend of 1-2 percent lower P-wave velocity underlying the Jemez lineament, at the depth interval of about 50-160 km. This result extends at least from Mt. Taylor through the Jemez volcanic center and through the Rio Grande rift. Three independent calculations of resolution indicate that these results are well-resolved. The most likely interpretation is that there are additional concentrations of partial melt in the upper mantle beneath the Jemez lineament but not

beneath the Rio Grande rift. This interpretation is consistent with the much greater volume of volcanism during the last 4.5 m.y. originating with Jemez lineament than originating with the Rio Grande rift. This result implies that the present volcanic potential of the Jemez lineament greatly exceeds that of the Rio Grande rift.

2. Interface thrust zones typically have dips in the range 8-15°, whereas lithospheres that are subducted into the mantle typically have dips in the range 40-70°, giving an average dip increase in the mantle of about 45°. These dip increases often occur within 40-60 km of plate length. These zones of sharp dip increases (slab bends) have not been given much attention because generally they lack large earthquakes. This is in sharp contrast to the well-studied zones of bending beneath oceanic trenches where there are frequent normal-faulting earthquakes. It has been noted by Ruff and Kanamori (1983) that great, interface thrust earthquakes terminate their downdip ruptures at the updip part of mantle slab bends. Spence (1987) showed that the slab pull force is the primary force that causes shallow, subduction earthquakes. Spence also interpreted the mantle slab bends as a pivot for the summed slab pull force of the more deeply subducted plate. In this study, we model the stress distribution in the mantle slab bend, acting under a slab pull load. We find that the observed lack of earthquakes in the mantle slab bend is due to ductility there. However, the strength of the work-hardened ductile portion of the slab bend is more than sufficient to transmit the slab pull load into the shallow subduction zone.

3. In the Vrancea region of the southeastern Carpathian arc, earthquakes extend to depths of 200 km, and have magnitudes as great as 7.5. Although tectonic reconstructions for this concave-westward arc are not definitive, especially for pre-Miocene time, we know that westward subduction at the Carpathian trench has terminated from northwest to southeast. Oceanic lithosphere is completely subducted and continental lithosphere is at the arc. Seismicity is most pronounced at the southeastern corner of the arc. Based on a variety of evidence, we propose a new tectonic model with a continuous subducted lithosphere, in which: (1) above 40 km depth the subducted lithosphere has a shallow dip; (2) between 40 and 70 km depth the dip of subducted plate steepens to near vertical; (3) the bending of the subducted plate is mostly aseismic; (4) the m_B 7.5 earthquakes at depths of 100-160 km result from downdip plate extension; (5) this extension results from the sinking of plate at depths of 100-160 and deeper; (6) stresses due to the sinking of deeply-subducted plate are communicated updip past the zone of plate bending into the shallow-dipping part of the plate; and (7) stresses in the shallow-dipping plate are communicated to the overriding plate and lead to broad regional deformation there.

Reports

Spence, William, and Gross, R. S., 1989, A tomographic glimpse of the upper mantle source of magmas of the Jemez lineament, New Mexico: Journal of Geophysical Research (submitted).

United States Earthquakes

9920-01222

Carl W. Stover
Branch of Global Seismology and Geomagnetism
U.S. Geological Survey
Denver Federal Center
Box 25046, Mail Stop 967
Denver, Colorado 80225
(303) 236-1500

Investigations

Ninety-nine earthquakes in the United States and Puerto Rico, were canvassed by a mail questionnaire for felt and damage data. Thirty six of these earthquakes occurred in California, 22 in Alaska, and 36 in seventeen other states. Hypocenters for United States earthquakes for the period April 1, 1989 to September 30, 1989, have been computed and published in the Preliminary Determination of Epicenters (PDE). Compilation is continuing on a history of earthquakes in the 50 states.

Results

Six earthquakes caused damage during this period. A maximum intensity of VI-VII was given to an event on August 2 in the southern San Francisco Bay area which damaged chimneys in parts of Santa Clara and Santa Cruz counties. One in the San Jose area on April 3 caused minor damage (intensity VI), and two in Los Angeles on April 7 and June 12 also caused minor damage (intensity VI). The other two occurred in Hawaii and Missouri. The damage from the Hawaii earthquake on June 26 was mostly from broken windows. The Missouri earthquake on April 27 cracked exterior brick walls.

United States Earthquakes, 1985, has been completed and is in CTR for review. United States Earthquakes, 1986, is currently being compiled and is about 50 percent complete.

The Earthquake Data Base System has been updated through the current PDE and through March 1989, Monthly Listing. Data is available on paper, tape, or floppy disk. Contact Glen Reagor at (303) 236-1500 for details.

Reports

Brewer, Lindie, 1989, The intensity of the July 21, 1986, Chalfant Valley, California, earthquake: U.S. Geological Survey Open-File Report 89-135, 24 p.

Data Processing Section

9920-02271

John Hoffman
Branch of Global Seismology and Geomagnetism
U.S. Geological Survey
Albuquerque Seismological Laboratory
Building 10002, Kirtland AFB-East
Albuquerque, New Mexico 87115
(505) 844-4637

Investigations

1. IRIS/USGS Data Collection Center. The Incorporated Research Institutions for Seismology (IRIS) have designated the Albuquerque Seismological Laboratory (ASL) to be the data collection center (DCC) for a new global network of digitally recording seismograph stations. A new data processing system has been installed at the ASL, a new data format has been developed and new code to process the data is in the final stages of completion.

2. Data Processing for the Global Digital Seismograph Network. All of the data received from the Global Digital Seismograph Network (GDSN) and other contributing stations is regularly reviewed and checked for quality.

3. Network Volume Program. Data from the GDSN stations and other contributing networks are assembled into network volumes which are distributed to regional data centers and other government agencies.

Results

1. IRIS/USGS Data Collection Center. IRIS will install a network of 50 or more digital recording seismograph stations around the world during the next several years. All of the data from this network will be forwarded to the DCC located at the ASL. As part of this program, IRIS funded much of the new hardware required by the DCC to process this large amount of data. A part of this hardware was an optical laser jukebox memory system which can automatically select any of 50 optical platters each of which can store up to 3.2 gigabytes of seismic data. During the past 6 months an additional 4-1/2 years of network-day tapes have been archived on these optical platters. This makes a total of 8 years of global seismic digital data (approximately 50 gigabytes) which is available as online storage in the jukebox. An estimated 35 gigabytes of seismic data remain in our tape library and will be added to the optical storage system during the next 6 months. The optical platters on which this seismic data is archived have an estimated shelf life of 100 years.

2. Data Processing for the Global Digital Seismograph Network. During the past 6 months, 547 digital tapes (158 SRO/ASRO, 214 DWWSSN, 110 CDSN, 65 IRIS-1) from the GDSN and other contributing stations were edited, checked for quality, corrected when feasible and archived at the ASL. The Global Digital Network supported by the USGS is presently comprised of 13 SRO/ASRO stations, 14 DWWSSN stations and one IRIS-1 station. In addition,

there are 10 contributing stations which include Glen Almond, Canada, the five stations from the China Digital Seismograph Network, and four IRIS-1 stations. Effective September 1989 data from four Russian stations (OBN, ARU, GAR, KIV) and from four IRIS/IDA stations (ESK, NNA, PFC, RPN) will be processed at the ASL and archived on the optical jukebox storage system.

3. Network Volume Program. The network volume program is a continuing program which assembles all of the data recorded by the Global Digital Seismograph Network, plus all the various contributing stations mentioned in previous paragraph, for a specific calendar day or days onto one magnetic tape. This tape includes all the necessary station parameters, calibration data, transfer functions, and time-correction information for each station in the network. Copies of these tapes are distributed to several university and government research groups for detailed analysis. These tapes are assembled approximately 60 days after real time in order to provide a sufficient time frame for recording the data at the stations and forwarding this data to the ASL.

National Earthquake Information Service

9920-01194

Waverly J. Person
Branch of Global Seismology and Geomagnetism
U.S. Geological Survey
Denver Federal Center
Box 25046, Mail Stop 967
Denver, Colorado 80225
(303) 236-1500

Investigations and Results

The Quick Epicenter Determinations (QED) continues to be available to individuals and groups having access to a 300-baud terminal with dial-up capabilities to a toll-free watts number or a commercial telephone number in Golden, Colorado. The time period of data available in the QED is approximately 3 weeks (from about 2 days behind real time to the current PDE in production). The QED program is available on a 24-hour basis, 7 days a week. From April 1, 1989, through September 30, 1989, we have had approximately 11,509 log-ins. Several communications links have been established on computer networks. The QED's are now transmitted on a daily basis to a scientific bulletin board operated by Dr. Francis Wu at the State University of New York at Binghamton. This bulletin board is accessible worldwide by anyone who is connected to BITNET, a university-based computer network. Phase data and epicenter computations are now being exchanged on a regular basis via DECNET/SPAN between NEIC and the Istituto Nazionale di Geofisica (ING) in Rome and the Centro Cultura Scientifica Ettore Majorana (CCSEM) in Erice, Sicily, and via BITNET between NEIC and the Universidad Nacional Autonoma de Mexico (UNAM). Data exchange via computer network is currently being established via TYMNET between NEIC and the Department of Scientific and Industrial Research in New Zealand, the Australian Bureau of Mineral Resources, and Ottawa, Canada. All these network links have been established using the GEONET gateways at Menlo Park (SPAN), Denver (TYMNET), and Reston (BITNET). New communication links have been established: ORPHEUS, Bernard Dost at University of Utrecht (transmitting, QED, PDE, and alarm earthquakes); IRIS, Steve Malone at University of Washington (alarm earthquakes); the University of Bergen, Norway (bulletin). Also, preliminary contacts have been made with the University of Chile (Santiago) and with CSEM (Strasbourg, France). All of the above communication links are using BITNET.

Telegraphic data are now being received from the USSR on most larger earthquakes. These data are being received from the Central Seismological Observatory, Obninsk, through an agreement set up by John Filson and O. E. Starovoit.

Data from the People's Republic of China via the American Embassy continue to be received in a very timely manner and in time for the PDE publication. We continue to receive four stations on a weekly basis from the State Seismological Bureau of the People's Republic of China. The Bulletins with additional data are now being received in time for the Monthly. Data are now being received from New Zealand by computer. Special efforts are being made to receive more data from the Latin American countries on a more timely basis. We have rapid data exchange (alarm quakes) with Centre Seismologique European-Mediterranean (CSEM), Strasbourg, France, and Instituto Nazionale de Geofisica, Rome, Italy, and Sicily, and data by telephone from Mundaring Geophysical Observatory, Mundaring, Western Australia and Japan Meteorological Agency (JMA).

The Monthly Listing of Earthquakes is up to date. As of September 30, 1989, the Monthly Listing and Earthquake Data Report (EDR) are completed through May 1989. A total of 12,730 events was published for 1988. Total number of events published through May 1989 was 6,965. Solutions continue to be determined when possible and published in the Monthly Listing and EDR for any earthquake having an m_b magnitude $\geq$ 5.8. Centroid moment tensor solutions from Harvard University continue to be published in the Monthly Listing and EDR. Moment tensor solutions are being computed by the U.S. Geological Survey and are also published in the above publications. Waveform plots are being published for selected events having m_b magnitudes $\geq$ 5.8. Beginning with the month of October 1985, depths for selected events were obtained from broadband displacement seismograms and waveform plots published in the Monthly.

The Earthquake Early Alerting Service (EEAS) continues to provide information on recent earthquakes on a 24-hour basis to the Office of Earthquakes, Volcanoes, and Engineering, scientists, news media, other government agencies, foreign countries, and the general public.

Forty-one releases were made from April 1, 1989, through September 30, 1989. In the United States, the most significant earthquakes were a magnitude 6.2 in Hawaii on June 26; a magnitude 5.3 in central California on August 8; and a magnitude 6.9 south of Alaska on September 4, 1989. The most significant foreign earthquakes were a magnitude 6.2 in Sichuon Province, China, on April 15 and September 22; a magnitude 7.1 in Mexico on April 25; a magnitude 8.3 in the Macquarie Island region (the largest ever to occur in that area); and two magnitude 6.3 earthquakes in Ethiopia on August 20 and 21 (probably the largest to occur in that area).

Reports

Monthly Listing of Earthquakes and Earthquake Data Reports (EDR); six publications from December 1988 through May 1989. Compilers: W. Jacobs, L. Kerry, J. Minsch, R. Needham, W. Person, B. Presgrave, W. Schmieder.

Person, Waverly J., Seismological Notes: Bulletin of the Seismological Society of America, v. 79, no. 3, July-August 1988; v. 79, no. 4, September-October 1988.

Preliminary Determination of Epicenters (PDE); 35 weekly publications from April 27, 1989, numbers 14-89 through 36-89. Compilers: W. Jacobs, L. Kerry, J. Minsch, R. Needham, W. Person, B. Presgrave, W. Schmieder.

Quick Epicenter Determination (QED) (daily): Distributed only by electronic media.

Monthly Listing of Earthquakes, v. 60, no. 2, April-June 1989 (Microfiche): Seismological Research Letters, Eastern Section, SSA. Compilers: W. Jacobs, L. Kerry, J. Minsch, R. Needham, W. Person, B. Presgrave, W. Schmieder.

Person, Waverly J., "Earthquakes and Volcanoes," v. 20, no. 3, January-February 1988; v. 20, no. 4, March-April 1988; v. 20, no. 5, May-June 1988.

Seismic Review and Data Services

9920-01204

James N. Taggart
Branch of Global Seismology and Geomagnetism
U.S. Geological Survey
Denver Federal Center
Box 25046, Mail Stop 969
Denver, Colorado 80225
(303) 236-1506

Investigations

This project distributes copies at cost of filmed seismograms from the Worldwide Standardized Seismograph Network (WWSSN), the Canadian Standard Network (CSN), and various stations with historical (pre-1963) records. In addition, the project receives the original WWSSN analogue seismograms for photography, and afterward returns them to the stations.

Results

We completed technical review, quality control, and photography on 410 station-months of seismograms from the WWSSN during this reporting period. The Geological Survey of Canada also furnished 72 station-months of high-quality filmed CSN seismograms, but we received no additional historical seismograms.

We supplied filmed seismograms at cost to 77 requesters during Fiscal Year 1989, including nine standing orders for WWSSN microfiches and two standing orders for CSN 35mm microfilm. Altogether, the requesters received 1,318,400 filmed seismograms on 444 reels and 69,900 microfiches of various kinds. Two full-time contract employees and Juanita Severe, working half-time, handled this work.

The duplication and mailing of the second half of the station-month sets of the standing orders for FY 1989 should be completed by mid-November. This was the final year of the three-year contract to photograph the WWSSN seismograms. The Requests for Proposals for the subsequent three-year contract were mailed in late September and some interruption in the contract services is inevitable.

We ran tests on our special-design flatbed microfiche camera with historical seismograms from the Hawaiian Volcano Observatory (HVO) network. High-quality images, comparable to those of the WWSSN records, were obtained of the HVO photographic paper records. Images of the smoked paper records were unsatisfactory because the camera has no illumination from underneath.

Taggart spent most of this reporting period selecting sites and handling much of the correspondence for the U.S. National Seismograph Network.

Computer and Data Analysis Services

9920-04151

Madeleine Zirbes
Branch of Global Seismology and Geomagnetism
U.S. Geological Survey
Denver Federal Center
Box 25046, Mail Stop 967
Denver, Colorado 80225
(303) 236-1506

Investigations

1. NEIC Monthly Listing. Contribute waveform data for all events of magnitude 5.8 or greater when sufficient data exists.

2. Network Day Tape Support. Develop, distribute and support FORTRAN programs to access network-day tapes and station tapes.

3. SEED Support. Develop, distribute and support software for the Standard for the Exchange of Earthquake Data (SEED) format.

4. Event Tape Production and Distribution. Produce and distribute event tapes.

5. Event CD-ROM Production and Distribution. Produce and distribute event CD-ROM data.

Results

1. NEIC Monthly Listing. Since July 1982, digital waveform plots have been contributed to the Monthly Listings. USGS fault-plane and moment tensor solutions, and broadband data have also been incorporated into the focal sphere plots.

2. Network Day Tape Support. FORTRAN software to read and extract digital data from station tapes (1976-1979) and network day tapes (1980-1987) has been developed and distributed to the research community worldwide. Users are supported on a variety of computers.

3. SEED Support. A new Standard for the Exchange of Earthquake Data (SEED) has been created and tapes are now being produced (1988 to present) and distributed by the Albuquerque Seismic Laboratory. FORTRAN software has been developed to read and extract the digital data from the SEED tapes and this software is being made available to the research community.

4. Event Tape Production and Distribution. Event tapes have been produced from network day tapes for data from 1980 through 1986 for all events with magnitude 5.5 or greater. These tapes are distributed to 25 institutions worldwide, along with a waveform catalog that provides a visual display of the data available for each event.

5. Event CD-ROM Production and Distribution. Data from the event tapes are reformatted and sent to a CD-ROM mastering facility for replication. Four volumes have been produced, covering 1980 through 1984. The CD-ROMs are being distributed to over 200 Universities across the United States and geophysical research institutes worldwide. Retrieval software, SONIC (C) and CDRETRV (FORTRAN), has been developed for the IBM/PC/AT/386 compatibles and distributed. It allows easy access to the digital data.

Reports

Zirbes, M., and Moon, B. J., National Earthquake Information Center waveform catalog July 1986: U.S. Geological Survey Open-File Report 86-660G.

Zirbes, M., National Earthquake Information Center waveform catalog August 1986: U.S. Geological Survey Open-File Report 86-660H.

Zirbes, M., National Earthquake Information Center waveform catalog September 1986: U.S. Geological Survey Open-File Report 86-660I.

Zirbes, M., National Earthquake Information Center waveform catalog October 1986: U.S. Geological Survey Open-File Report 86-660J.

Zirbes, M., National Earthquake Information Center waveform catalog November 1986: U.S. Geological Survey Open-File Report 86-660K.

Zirbes, M., National Earthquake Information Center waveform catalog December 1986: U.S. Geological Survey Open-File Report 86-660L.

General Earthquake Observation System (GEOS)
General Analysis and Playback Systems (GAPS)

9910-03009

Roger D. Borcherdt
Branch of Engineering Seismology and Geology
U.S. Geological Survey
345 Middlefield Road, MS 977
Menlo Park, California 94025
(415) 329-5619

Investigations

1. Complete construction and development of 100 portable, broad band, high-resolution digital data acquisition systems for use in a wide variety of active and passive seismic experiments.

2. Develop Program Plan for Large Array Seismic Observations **(LASO)**

3. Develop PC-based capabilities for retrieval, processing, and archival of large volumes of GEOS data.

4. Conduct Eurasian Seismic Studies Program.

Results

1. The following design modifications for 55 new GEOS systems are in final testing stages:

    a.) Expanded data buffer (1 M/sample) design by M. Kennedy.
    b.) Extended gain with improved noise for amp/filter board by J. van Schaack and G. Jensen.
    c.) New tape controller for new 16 Mbyte tape cartridges by Phoenix Data, Inc.
    d.) Software drivers for mag tape controller by G. Maxwell.
    e.) Software for RS 232 for use in satellite, radio, and telephone telemetry and data transfer to field computer by G. Maxwell.
    f.) Software for incorporating design modifications, teleseismic trigger, and field playback are being pursued by G. Maxwell.
    g.) Completion of the 55 new GEOS units is expected by January 1990. Testing of first article is in progress but has been slowed by limited personnel resources.

2. An extensive scientific plan for management of a Large Array Seismic Observation program was developed and presented to office management by the **LASO** executive committee (R.D. Borchert, chair, M. Celebi, J. Filson, H.M. Iyer, M. Johnston, W. Mooney, A. Rogers.

3. GEOS maintenance laboratory under direction of J. Sena together with field support of G. Sembera and C. Dietel has facilitated the execution of several experiments during the report period, including experiments at Parkfield, Anza, Armenia, and teleseismic and refraction experiments near Pace, Arizona.

4. Significant efforts have been devoted to planning for the Eurasian Seismic Studies Program in conjunction with J. Filson and D. Simpson. PC-based data playback and analysis capabilities have been developed in conjunction with W. Lee and E. Cranswick. Selectable Omega/WWV timing capabilities for GEOS have been developed in conjunction with G. Jensen. Hardware and sensors required for deployment have been acquired for shipment on Oct. 28, 1989.

Reports

Glassmoyer, G. and Borcherdt, R.D., 1989, Source parameters and effects of bandwidth and local geology on high-frequency ground motions observed for aftershocks of northeastern Ohio earthquake of 31 January, 1986: submitted to the Bulletin of the Seismological Society of America.

Borcherdt, R.D. (editor), 1989, Results and data from seismologic and geologic studies of the earthquakes of December 7, 1988 near Spitak, Armenia, U.S.S.R.: U.S. Geological Survey Open-File Report 89-163, vols. I-V, 1958 p.

Borcherdt, R.D., Glassmoyer, G., Der Kiureghian, A., and Cranswick, E., 1989, Effect of site conditions on ground motions in Leninakan, Armenia, U.S.S.R. in Borcherdt, R.D. (editor), 1989, Results and data from seismologic and geologic studies of the earthquakes of December 7, 1988 near Spitak, Armenia, U.S.S.R.: U.S. Geological Survey Open-File Report 89-163A, v.1, 188 p.

Borcherdt, R.D., Simpson, D., Langer, C., Sembera, G., Dietel, C., Cranswick, E., Mueller, C., Noce, T., Andrews, M., and Gasssmoyer, G., 1989, Seismological investigations (objectives and field experiments), in Borcherdt, R.D. (editor), 1989, Results and data from seismologic and geologic studies of the earthquakes of December 7, 1988 near Spitak, Armenia, U.S.S.R.: U.S. Geological Survey Open-File Report 89-163A, v. 1, 188 p.

Borcherdt, R.D., Maxwell, G., Sena, J., Kennedy, M., Jensen, G., and van Schaak, J., 1989, Instrumentation used for seismological investigations -- Digital recording systems in Borcherdt, R.D., (editor), 1989, Results and data from seismologic and geologic studies of the earthquakes of December 7, 1988 near Spitak, Armenia, U.S.S.R.: U.S. Geological Survey Open-File Report 89-163A, v.1, 188 p.

Agbabian, M.S., Borcherdt, R.D., Der Kiureghian, A., Filson, J.R., Krimgold, F., Lew, H.S., Mileti, D.S., Noji, E., O'Rourke, T., Schiff, A., Simpson, D., Sharp, R.V., Wyllie, Jr., L.A., Yanev, P.I., Armenian earthquake reconnaissance report: Jour. Earthq. Eng. Res. Inst., Spec. Suppl. Aug. 1989, 175 p.

Borcherdt, R.D., Celebi, M., Filson, J., Iyer, H.M., Johnston, M., Mooney, W., Rogers, A., 1989, A program for Large Array Seismic Observation (LASO): U.S. Geological Survey Administrative Report, 116 p.

(See projects (Borcherdt et al., 9910-02089, 9910-02689) for related reports.

National Strong-Motion Network: Data Processing

9910-02757

A.G. Brady
Branch of Engineering Seismology and Geology
345 Middlefield Road, MS 977
Menlo Park, California 94025
(415) 329-5664

Investigations

1. Processing data from Whittier Narrows and Superstition Hills earthquakes, including the determination of long-period limits.

2. Selection, purchase, and software improvement for PC network in various staff offices within the Branch.

3. Cataloging of all USGS strong-motion records for 1986.

Results

1. Continuing work on the strong-motion records from the Whittier Narrows earthquake shows that the signal-to-noise ratio is the prominent factor in the determination of suitable long-period limits for individual records. All records closer than 40 km have been digitized, half of those between 40 and 60 km, and none beyond 60 km. In some cases only, reliable 4-sec content can be seen out to 30 km, and 1/2-sec content out to 60 km.

2. User guides to help others in the project and in the Branch have been written for commercial software packages installed in the newly acquired IBM AT compatables: communicating with the ST68K digital recorders via CrossTalk; using the PacerLink network between PC's and the VAX's; using the Branch PC software library; and detecting computer viruses.

3. The annual report describing all strong-motion records recovered in a single year is now called a "Catalogue of U.S. Geological Survey Strong-Motion Records, 19--" and its Table 1 lists all important parameters obtainable from the original record: earthquake epicenter and magnitude, station name and location, trigger and S-T times, and component directions, peak acceleration and duration.

Report

Brady, A.G., 1989, Processing digitally recorded seismic strong-motion accelerations - with a review and comparision, in Iai (ed.), 1988, Proceedings of the 2nd workshop on processing of seismic strong-motion records (part 2): Tokyo, Japan, IASPEI/IAEE, 375 p.

Porcella, R.L., and J.C. Switzer, 1989, Catalogue of U.S. Geological Survey strong-motion records, 1986: U.S. Geological Survey Circular 1032, 37 p.

Brady, A.G., 1989, Analysis of structural response records during the Whittier Narrows earthquake, 1 October 1987: Proc., 21st Joint Meeting UNJR Panel on Wind and Seismic Effects: Tsukuba, Japan, in press.

National Strong-Motion Network: Engineering Data Analysis

9910-02760

A.G. Brady and G.N. Bycroft
Branch of Engineering Seismology and Geology
345 Middlefield Road, MS 977
Menlo Park, California 94025
(415) 329-5664 or (415) 329-5665

Investigations

1. Buildings with extensive instrumentation, triggering records from the October 1, 1987, magnitude 5.9, Whittier Narrows, California, earthquake have been studied. The most interesting is a seven-story moment-resisting steel-frame building in Norwalk, 15 km from the epicenter, with ground-level accelerations of 0.2 and 0.3 g, and roof accelerations of 0.41 g. We consider the building's response to be split between translations in the two orthogonal horizontal direction, torsion about a central vertical axis, in-plane bending of the floors, and rocking about the shorter horizontal axis, even though the low frequency resonant modes might well contain combinations of these motions.

2. The analysis of the results from field testing of soil-structure interaction theories continues, using tests on instrumentation pads and pedestals at Jenkinsville, South Carolina, the El Centro, Calif., Differential Array, and Camp Parks, Calif.

Results

1. Taking suitable combinations of the recorded accelerations, filtering out unwanted low-frequency content, and integrating for displacement permit a clear representation of the onset and dissipation of the motions with time. Ground level records at 30 m and 131 m from the building, considered to be "free field," show that the low frequency (0.7 to 2 Hz) modes include amplification at ground level in the building between 1.0 and 1.2, while at the higher mode frequencies, up to 5 Hz, the building reduces the earthquake input motion to 0.6 to 0.8 of the "free field" motion.

2. Soil structure interaction is certainly an important factor affecting recorded accelerograms, particularly peak values, for some specific combinations of earthquake ground motion and instrumentation pad.

Reports

Brady, A.G., 1989, Analysis of structural response records during the Whittier Narrows earthquake, 1 October, 1987: Proc., 21st Joint Meeting, UJNR Panel on Wind and Seismic Effects, Tsukuba, Japan, in press.

Bycroft, G.N., and A.G. Brady, 1989, Tests of soil structure interaction theory, submitted to BSSA.

Branch of Engineering Seismology and Geology Computer Project

9910-02085

Howard Bundock
Branch of Engineering Seismology and Geology
U. S. Geological Survey
345 Middlefield Road, MS 977
Menlo Park, California 94025
(415) 329-5621, FTS 459-5621

INVESTIGATIONS

The objectives of the Branch of Engineering Seismology and Geology Computer Project are to:

Maintain a strong capability for the processing, analysis and dissemination of all strong motion data collected on the National Strong Motion Network and data collected on portable arrays;

Support research projects in the Branch of Engineering Seismology and Geology by providing programming and computer support including digitizing, graphics, processing and plotting capabilities as an aid to earthquake investigations;

Manage and maintain computer hardware and software so that it is ready to process data rapidly in the event of an earthquake.

The Center's facilities include a VAX 8250 running VMS version 5.02 and a VAX 11/750 computer operating under VMS Version 4.6, a PDP 11/70 running RSX-11M+ and a PDP 11/73 computer. The Center's computers are part of a local area network with other branch, OEVE, Geologic Division, and ISD computers, and we have access to computers Survey-wide over Geonet. Project personnel join other office branches in the support of the OEVE VAX 11/785.

Investigations during the last six months of FY89 included preparation for and upgrade to version 5.0 of the VMS operating system software on Branch and Office computers. The project has also worked with other Branch representatives to install a new Local Area Network including personal computers for Branch scientists, mainly for word processing and spreadsheet capabilities. The project has been involved in the installation and testing of a dense array of earthquake sensing and recording devices and the related computer system near the San Andreas fault in Parkfield, CA. The project has also installed an 8mm cassette tape drive on the Office VAX for backup and archiving. The project continues its support of the OEVE VAX 11/785 project. We have worked with computer specialists in other branches in planning a move of all computer hardware into space provided in an enclosed area in the same building. As an ongoing policy, we have kept our hardware up to current revision levels, and operating system, network, and other software at the most recent versions.

RESULTS

As a result of these and previous investigations, the project has:

Upgraded to VMS version 5.0-02 on its VAX 8250 and version 4.6 on the Office computer, prepared further for upgrade to version 5.0

With other Branch representatives, began installation of a Local Area Network for IBM PC clones and Apple IIse microcomputers.

Assisted in the installation of the Parkfield Dense Array,

Installed a new tape drive for use of Branch and Office scientists,

Purchased and readied for installation a Power Distribution Unit to be used when computer equipment is moved,

Managed and maintained the OEVE VAX 11/785,

Managed, maintained, updated Branch and Office computer system hardware and software.

REPORTS

None

Instrumentation of Structures

9910-04099

Mehmet Çelebi
Branch of Engineering Seismology and Geology
U.S. Geological Survey
345 Middlefield Road, MS 977
Menlo Park, California 94025
(415) 329-5623

Investigations:

1. The process of selection of structures to be recommended for strong-motion instrumentation has continued in Orange County, Hawaii, and Puget Sound (Seattle), Reno (Nevada), and Puerto Rico. This effort has also been extended to Salt Lake City.

2. The process to design instrumentation schemes for selected structures has continued. Applicable permits for a structure in Anchorage, Alaska, have been obtained. Current efforts are being make to obtain permits for structures in Hawaii, Seattle, and Orange County.

3. The process of implementation of instrumentation for those structures for which instrumentation schemes have been designed has been completed in Boston and in San Bernardino, California. The strong-motion recording systems in these buildings are now operational. Records have been obtained from the recently instrumented structure in San Bernardino and the 1100 Wilshire Building in Los Angeles. Salt Lake City and County Building is now instrumented in cooperation with the city of Salt Lake City. The building is the first building being retrofitted by base isolation. Non-destructive dynamic testing of the building is to be carried out progressively to evaluate the dynamic characteristics of the building before and after being rehabilitated by base isolation.

4. The minimal instrumentation in a building in Alhambra, Southern California has been upgraded to contain extensive instrumentation to acquire sufficient data to study complete response modes of the building.

5. Agreements have been made with UCLA to convert the wind-monitoring system in the Theme Buildings in Los Angeles (previously financed by NSF) into a strong-motion monitoring system. Plans are being made to implement the conversion.

6. Studies of records obtained from instrumented structures are carried out. In particular, the records obtained during the October 1, 1987 Whittier Narrows earthquake from the 1100 Wilshire Finance Building (Los Angeles), the Bechtel Building (Norwalk), and the Santa Ana River Bridge (base-isolated) are being investigated. Papers and open-file reports are prepared.

7. An externally funded project on behalf of International Atomic Energy Agency (IAEA) was performed in Lima, Peru. A test reactor was temporarily instrumented to obtain its response characteristics. A preliminary and a final report have been submitted. The results indicate use of low-level motions in identifying dynamic characteristics of structures.

Results:

1. The Hawaii committee on strong motion instrumentation of structures has completed its deliberations and a draft report is being prepared.

2. A final report of the Puget Sound (Seattle) advisory committee for strong-motion instrumentation has been completed.

3. Papers resulting from study of records obtained from structures are prepared.

4. A special session on Seismic Monitoring of Structures was organized and chaired during the ASCE Structures Congress (May 1989) in San Francisco.

5. A session was chaired during the SMIRT (Structural Mechanics in Reactor Technology) Conference, Anaheim, Calif., August 1989.

Reports:

Çelebi, M., Bongiovanni, G., Safak, E., and Brady, G., 1989, Seismic response of a large-span roof diaphragm (paper accepted for publication in *Earthquake Spectra).*

Çelebi, M., Safak, E., and Maley, R., 1989, Some significant records from instrumented structures in California--USGS program: Proc., ASCE Structures Conference, San Francisco, May 1989.

Çelebi, M., 1989, Seismic monitoring of structures--objectives and analyses of records from structures: U.S.-Japan Panel, (Wind and Seismic Effects), May 1989.

Safak, E. and Çelebi, M., 1989, A method to estimate center of rigidity using vibration recordings: paper accepted for publication in ASCE.

Çelebi, M., Safak, E., and Youssef, N., 1989, Analyses of recorded responses of a unique building in Los Angeles to motions caused by Whittier Narrows earthquake of October 1, 1987: *U.S. Geological Survey Open-File Report 89-542*.

Çelebi, M. *et al.*, 1989, Seismic response of a nuclear test reactor building: Proc., SMIRT Conf., Anaheim, Calif., vol. K1.

STRONG-MOTION INSTRUMENTATION NETWORK DESIGN, DEVELOPMENT, AND OPERATIONS

9910-02764, 9910-02765

Ed Etheredge, Ron Porcella, and Dick Maley

Branch of Engineering Seismology and Geology
345 Middlefield Road, MS 977
Menlo Park, California 94025
(415) 329-5667

Investigations

The Strong-Motion laboratory, in cooperation with federal, state, and local agencies and advisory engineering committees, designs, develops, and operates an instrumentation program in 41 states and Puerto Rico. Program goals include: (1) recording of potentially damaging ground motion in regional networks, and in closely spaced sensor arrays; and (2) monitoring the structural response of buildings, bridges and dams using sensors placed in critical locations. The present coordinated network consists of approximately 1,000 recording units installed at 600 ground sites, 28 buildings, 5 bridges, 56 dams, and 2 pumping plants.

New Instrumentation

An extensive 15-channel structural instrumentation system was installed in the 13-story steel-frame BP Exploration Headquarters Building in Anchorage, Alaska. Sensors were located at the 8th and 14th (penthouse) levels, in the basement, and at a free-field site 215 feet from the structure. The system configuration is designed to record torsional motion, translation modes in the long-axis direction, and rocking at the foundation level.

An extensive 12-channel structural instrumentation system was installed in a 12-story steel-frame building in Alhambra, California. Sensors were located on the 6th and 12th levels to record torsional and translational motions, at the 3rd level where there is a change in framing, and in the basement. This building was previously instrumented with three accelerographs that recorded the 1971 San Fernando earthquake and the 1987 Whittier Narrows earthquake.

A moderate 3 accelerograph system was installed in the 13-story steel-frame Veterans Administration (VA) Hospital in Memphis, Tennessee. This was a cooperative project between the VA and the USGS and was prompted by a recommendation of the New Madrid Region Structural Advisory Committee. Instruments are located at the basement, 8th and 14th (roof) levels.

An existing moderate 2 accelerograph system in the Anchorage Hilton was expanded to include three more units, using instruments relocated from interior Alaska. Accelerographs are now sited at the following levels, basement, 6, 13, 19, and 22 (roof).

Three Dunstan ortho-quad accelerometer modules were installed on the containment wall of the Northern Los Angeles Test Facility for hazardous waste disposal. The sensors are located at critical junctures in the shear wall to measure sudden latero-vertical strain movements. The signals are transmitted by a regression facsimile unit to the nearby headquarters building for integration into a status quo early alert system.

Two SSA-1, solid state recording digital accelerographs were installed on the crest and downstream of the Corps of Engineers Sacramento District's Warm Springs Dam in northern California. The instruments will eventually be fitted with modems to provide remote access to evaluate or set the instruments parameters and to retrieve recorded data.

An instrumentation project was recently completed for the Metropolitan Water District of Southern California (MWD) and included the following additions:

Station	Site	Instrumentation
Los Angeles Area		
Palos Verdes Reservoir	Crest	SMA-1 accelerograph in a standard fiberglass housing.
Orange County Reservoir	Crest	SMA-1 accelerograph in a standard fiberglass housing. Interconnected with abutment instrument.
Garvey Reservoir	Crest	SMA-1 in a standard fiberglass housing.
San Joaquin Reservoir	Crest	SMA-1 in a standard fiberglass housing. Interconnected with a USGS accelerograph installed in a small concrete block building on the abutment.
Riverside		
Mills Filter Plan	Basement	SMA-1 in the Administration Building.
California Arizona Border		
Gene Wash Dam	Crest	SMA-1 in small fiberglass housing.
Copper Basin Dam	Crest	SMA-1 in small fiberglass housing.

Accelerographs Removed

Alaska
- Cantwell
- Talkeetna
- Trims Camp
- Slana

The above instrumentation has been installed in the Anchorage Hilton.

- Anchorage - Art Institute

destroyed by flooding.

California
Martinez VA Hospital
Palo Alto VA Hospital
These older digital systems have become non-operational. Temporary SMA-1's have been installed at each location pending funding by the VA for new equipment.

Hawaii
Wahaula
Building destroyed by lava flow.

Recent Earthquake Records

April 3, 1989 MS=4.7
Northeast of San Jose, California, on the Calaveras Fault

Ground records were obtained at four stations, two on the Calaveras fault, and at two instrumented structures, Anderson Dam and the I-280/101 interchange bridge in San Jose. A peak ground acceleration of 0.16 g was recorded on the abutment of Cherry Flat Reservoir

April 7, 1989 ML=4.6
Northern area of Newport Beach, California

Strong-motion data was recovered from a Santa Ana ground station, 0.19 g, and from 8-story twin towers in Newport Beach Center where maximum accelerations were 0.43 g on the ground and 0.66 g on the second floor. The level of shaking exceeded what would normally have been anticipated from a ML=4.6 earthquake.

June 12, 1989 ML=4.5
Los Angeles area

Strong-motion records were recovered at 12 stations: 6 dams, 3 buildings, 2 ground sites, and 1 filter plant. Peak ground accelerations occurred at a Los Angeles rock site, 0.15 g, and at the Garvey reservoir abutment, 0.16 g. Records from buildings include 1111 Sunset, Los Angeles, where peak accelerations were 0.18 g respectively at the basement, 4th floor, and 8th level (roof).

June 26, 1989 MD=6.2
40 km south of Hilo, Hawaii

Strong-motion records were obtained from 15 ground stations all located on the Big Island of Hawaii. The peak acceleration was 0.21 g at Pahoa, 20 km from the epicenter.

Miscellaneous Earthquakes

Numerous other minor records were recovered between 1 April and 30 September 1989 from California, Alaska, and Hawaii.

Structural Analysis
9910-02759

Erdal Şafak and Mehmet Çelebi
Branch of Engineering, Seismology, and Geology
U.S. Geological Survey
345 Middlefield Road, MS 977
Menlo Park, California 94025
(415)-329-5648, FTS 459-5648

Investigations

1. Implementation of structural instrumentation and design of instrumentation schemes for structures selected by instrumentation advisory committees.
2. Development of methodologies and computer software to analyze ground motion and structural vibration recordings.
3. Analyses of seismic response data obtained from instrumented structures during the October 1, 1987 Whittier Narrows earthquake.

Results

1. In accordance with the recommendations made by advisory committees, three new buildings have been instrumented, BP Exploration Headquarters Building in Anchorage, Alaska, a steel-frame building in Alhambra, California, and the VA Hospital in Memphis, Tennessee. Also the instrumentation at the Hilton Hotel in Anchorage, Alaska has been extended by putting three more units.
2. A method and a computer software have been developed for identification of structures by using recordings of dynamic motions during earthquakes. The method is based on the prediction-error approach and the discrete-time modal analysis technique. Also, an algorithm has been developed to detect and identify torsional and rocking vibrations in buildings.
3. A complete set (21 channels) of response data was obtained from the 33-story Wilshire Finance Building, Los Angeles, during the October 1, 1987 Whittier-Narrows earthquake. This data has now been analyzed, and the behavior of the building during the earthquake has been determined. The building is very unique because of its cross-section, which is a rectangle up to the twelfth story, and a triangle thereafter. Another structure analyzed by using the data from the same earthquake is the Santa Ana River Pipeline Bridge, located near Riverside. The bridge carries the pipeline that provides water to half of Southern California's 13 million people. This bridge was retrofitted with elostameric bearings for base isolation, prior to the earthquake.

Reports

Şafak, E. and Brady, G.A., 1989, Recorded seismic response of a base-isolated steel bridge carrying a steel water pipe, *Earthquake Behavior of Burried Pipelines, Storage, Telecommunication, and Transportation Facilities*, ASME, PVP-Vol.162.

Şafak, E., 1989, Modeling, identification, and control of dynamic structural systems: Part I- Theory, and Part II- Applications (two papers), *Journal of Engineerin Mechanics*, ASCE, in print (both will appear in the November 89 issue).

Şafak, E. and Çelebi, M., 1990, Method to estimate center of rigidity using vibration recordings, *Journal of Structural Engineering*, ASCE, in print (will appear in the January 90 issue).

Çelebi, M., Şafak, E. and Youssef, N., 1989, Analyses of recorded responses of a unique building to motions caused by the Whittier-Narrows earthquake, *Open-File Report*, USGS (in print).

Çelebi, M., Şafak, E. and Youssef, N., 1989, Torsional response of a unique building, *Earthquake Engineering & Structural Dynamics*, submitted for publication.

Physical Constraints on Source of Ground Motion

9910-01915

D. J. Andrews
Branch of Engineering Seismology and Geology
U.S. Geological Survey
345 Middlefield Road, MS 977
Menlo Park, California 94025
(415) 329-5606

INVESTIGATIONS

Looking for nonplanar features in earthquake sources.

RESULTS

Strong motion records from the Superstition Hills earthquake are being inverted to find a source with slip on more than one fault plane.

REPORT

D. J. Andrews, 1989, Mechanics of fault junctions: *Journal of Geophysical Research*, v. 94, p. 9389–9397.

Ground Motion Prediction for Critical Structures

9910–01913

D. M. Boore
W. B. Joyner

Branch of Engineering Seismology and Geology
U. S. Geological Survey
345 Middlefield Road, MS 977
Menlo Park, California 94025

Investigations:

1. Study the source scaling of earthquakes in the Northwest Territories of Canada.

Results:

The sequence of earthquakes that began in October, 1985, near the Nahanni River, Northwest Territories, Canada, provides an exceptional opportunity to study the variation with magnitude of the source spectra from intraplate earthquakes. We study the spectral scaling for the 7 largest events, using P waves recorded at stations of the Western Canada Telemetred Network (WCTN), the Eastern Canada Telemetred Network (ECTN), and the Global Digital Seismograph Network (GDSN). These earthquakes range in size from M=4.8 to M=6.8. We compare predictions from various source-scaling models with observed spectral ratios and source acceleration spectra for the suite of events. The spectral ratios show a strong azimuthal dependence, which is probably due to differences in the focal mechanisms or rupture characteristics of the events. Taking the average of the ratios from individual GDSN stations as the best representation of the spectral ratios, an ω-squared model with a constant stress parameter or one that increases slightly with moment magnitude gives a simultaneous fit to both the spectral ratios and to the absolute spectra. The high-frequency spectral levels, by themselves, imply a somewhat stronger dependence of the stress parameter on moment than found from fitting the overall spectra. The stress parameters for the scaling laws are less than 35 bars for earthquakes as large as M=7. Recently proposed scaling laws in which the corner frequency is proportional to the inverse quarter root of seismic moment for an ω-squared model are not consistent with the data and neither are ω-cubed models.

The spectral scaling for the sequence of Nahanni earthquakes may not be representative of intraplate magnitude scaling in general, since there is some evidence that aftershocks do not exhibit the same scaling as main shocks. The high-frequency spectral levels of the aftershocks of both the Nahanni and the 9 January 1982 Miramichi, New Brunswick, earthquakes imply stress parameters that increase with magnitude. By contrast, the spectral levels for a series of main shocks in eastern North America show less magnitude dependence of the stress, and generally higher stress levels, when compared to aftershocks of the same magnitude.

Reports:

Boore, D. M. and G. M. Atkinson (1989). Spectral scaling of the 1985-1988 Nahanni, Northwest Territories, earthquakes, *Bull. Seism. Soc. Am.* (in press).

Boore, D. M. and W. B. Joyner (1989). The effect of directivity on the stress parameter determined from ground motion observations, *Bull. Seism. Soc. Am.* (in press).

29 September 1989

Anelastic Wave Propagation

9910-02689

Roger D. Borcherdt
Branch of Engineering Seismology and Geology
U.S. Geological Survey
345 Middlefield Road, MS 977
Menlo Park, California 94025
(415) 329-5619

Investigations:

Interpretation of colocated measurements of scalar volumetric strain and vectorial seismic displacement fields to infer additional characteristics of anelastic seismic wave fields.

Results:

Volumetric strain meters (Sacks-Evertson design) are installed at 15 sites along the San Andreas fault system, CA, to monitor long-term strain changes for earthquake prediction. Deployment of portable broad-band, high-resolution digital recorders (GEOS) at several sites extends the detection band for volumetric strain to periods shorter than 5×10^{-2} seconds and permits the simultaneous observation of seismic radiation fields using conventional short-period pendulum seismometers. Simultaneous observations establish that the strain detection bandwidth extends from periods greater than 10^{7} seconds to periods near 5×10^{-2} seconds with a dynamic range exceeding 140 db. Measurements of earth-strain noise for the period band, 10^{7} to 10^{-2} seconds, show that ground noise, not instrument noise, currently limits the measurement of strain over a bandwidth of more than eight orders of magnitude in period. Comparison of the short-period portion of earth-strain, noise spectra (20 to 5×10^{-2} secs) with average spectra determined from pendulum seismometers, suggest that observed noise is predominantly dilatational energy. Recordings of local and regional earthquakes indicate that dilatometers respond to *P* energy but not direct shear energy that straingrams can be used to resolve superimposed *P* and *S* waves for inference of wave characteristics not permitted by either sensor alone. Simultaneous measurements of incident *P*- and *S*-wave amplitudes are used to introduce a technique for single-station estimates of wave field inhomogeneity, free-surface reflection coefficients and local material velocity. Estimates of these parameters derived for the North Palm Springs earthquake ($M_{\omega}5.9$) are respectively for the incident *P* wave 29°, -85°, 1.71, 2.9 km/s and for the incident *S* wave 17°, 79°, 0.85, 2.9 km/s. The empirical estimates of reflection coefficients are consistent with model estimates derived using an anelastic half-space model with incident inhomogeneous wave fields.

Reports

Borcherdt, R.D. and Glassmoyer, G., 1989, An exact anelastic model for the free-surface reflection of P and S-I waves: *Bull. Seismol. Soc. Am.*, 79, 842-859.

Borcherdt, R.D., Johnston, M.J.S., and Glassmoyer, G., 1989, On the use of volumetric strainmeters to infer additional characteristics of short-period seismic radiation: *Bull. Seismol. Soc. Am.*, 79, 10,106-10,230.

(See projects (Borcherdt, 99190-02089 and 9910-03009) for related reports.)

10/89

Excitation and Propagation of High-Frequency Seismic Waves

9910-04482

A. Frankel

Branch of Engineering Seismology and Geology
U.S. Geological Survey
345 Middlefield Rd., MS 977
Menlo Park, CA 94025
(703) 648-4119

Investigations

1. Develop methods to separate the shear-wave attenuation of the crust caused by anelasticity from that produced by scattering.
2. Study the high-frequency seismic response of sedimentary basins using 2-D and 3-D finite-difference wave propagation codes.
3. Document and quantify the effects of near-surface attenuation on high-frequency seismic waves.
4. Use tomographic inversion methods to invert strong-motion data from major earthquakes for dynamic rupture parameters (e.g., rupture velocity, sub-event location and timing).

Results

1. I have used an energy-flux model of seismic coda to develop methods for estimating the scattering and anelastic Q in the crust. In several data sets, we observe that high-frequency energy is enriched in the seismic coda relative to the direct arrival. This enrichment increases with increasing travel distance. We quantify this observation and use it to determine the scattering Q of the crust. We also observe that the relative high-frequency coda decay with lapse time is less than the relative high-frequency amplitude decay with propagation time for direct waves. We apply this observation to estimate the anelastic attenuation in the crust. Using these methods we find that L_g wave attenuation in New York State is caused about equally by scattering and anelasticity. For South Africa, we infer that S-wave attenuation over local distances is caused primarily by scattering.

2. I have applied 2-D and 3-D finite-difference codes to investigate the seismic response of the Leninakan basin in Armenia. The city of Leninakan suffered substantial damage during the 1988 Armenian earthquake. This study is being undertaken in cooperation with R. Borcherdt and John Filson of the USGS and John Vidale of the University of California, Santa Cruz. The 2-D results indicate the importance of body wave to surface wave conversion at the edges of the basin. These surface waves propagate slowly across the basin, substantially increasing the duration and amplitude of strong shaking, relative to sites outside the basin. A large phase after the S-wave observed in aftershock recordings from Leninakan is probably such a S to surface wave conversion. I have written a 2nd order, 3-D elastic-wave algorithm for the finite-difference code provided by J. Vidale and R. Clayton. In addition, I have developed a program that inserts a propagating earthquake source into the 3-D finite difference grid. This code accepts an arbitrary slip-velocity history along a planar fault and is presently under test. Initial 3-D simulations of the Leninakan basin show how surface waves are generated at the sides and corners of the basin, producing very complicated patterns of displacement within the basin.

Reports

Frankel, A., A. McGarr, J. Bicknell, J. Mori, L. Seeber, and E. Cranswick, Attenuation and scattering of high-frequency shear waves at local and regional distances in South Africa, New York State and southern California, *EOS Trans. Amer. Geophys. Union,* **70** , 401, 1989.

Frankel, A. and L. Wennerberg, Rupture process of the M_S 6.6 Superstition Hills earthquake determined from strong-motion recordings: application of tomographic source inversion, *Bull. Seism. Soc. Amer.,* **79** , 515-541, 1989.

Frankel, A. and L. Wennerberg, Microearthquake spectra from the Anza, California seismic network: site response and source scaling, *Bull. Seism. Soc. Amer.,* **79** , 581-609, 1989.

Frankel, A., Effects of near-surface attenuation on the short-period waveforms and spectra of earthquakes and explosions, *EOS Trans. Amer. Geophys. Union, in press.*

Frankel, A., J. Filson, R. Borcherdt, and J. Vidale, Numerical simulations of strong ground motions in the Leninakan basin produced by the 1988 Armenian earthquake and its aftershocks, *EOS Trans. Amer. Geophys. Union, in press.*

Precise Velocity and Attenuation Measurements in Engineering Sesimology

9910-02413

Hsi-Ping Liu
Branch of Engineering Seismology and Geology
U. S. Geological Survey
345 Middlefield Road, MS 977
Menlo Park, California 94025
(415) 329-5643

Investigations

Water-saturated estuarine deposits (bay mud) underlie parts of San Francisco bay and the present and former marshlands that border the bay. Population growth in the metropolitan San Francisco area has led to an intensified building development of the former marshlands. This project is presently concerned with two field studies that will provide parameters characterizing the earthquake engineering properties of the bay mud.

1. The seismic shear-wave velocity and attenuation properties at low strain amplitudes are to be determined *in-situ* by active seismic measurements using shear-wave generator and borehole geophones. The measured values are used to determine the upper bound of the shear modulus and the lower bound of the attenuation factor in strong-motion calculations.

2. The decrease in shear strength of bay mud, a thixotropic material, as a result of strong ground shaking ($\sim$ 0.5 g acceleration) will be measured using an air gun and a seismic cone penetrometer. The air gun will be used as the strong-motion excitation source; a seismic cone penetrometer will be used to determine the shear strength and shear-wave velocity of the bay mud after a given number of strong ground-motion cycles. The purpose of this experiment is to determine the magnitude of the loss of strength in bay mud as a result of strong ground shaking.

Results

1. A surface shear-wave source (Liu *et al.*1988) has been used in conjunction with two three-component geophones embedded at 10.36 m and 16.56 m depths for the measurement of shear-wave velocity and anelastic attenuation in the San Francisco bay mud. Shear-wave rise times of seismograms recorded at these two depths are interpreted by computing synthetic seismograms using the model of a horizontal point force acting on the surface of an anelastic half-space (Liu 1989) which yield the bay mud anelastic seismic quality factor. Work is in progress to process the twenty independent measurements — it takes forty-eight hours of CPU time on a VAX computer to process each measurement. Numerical value of the bay mud anelastic seismic quality factor will be given in the next semi-annual report.

2. Work accomplished in this report period include obtaining permits for the Ravenswood Test Site in Menlo Park, California and construction of a loading frame and a 1/2-ton-force power source for a penetrometer. The thrust of the power source is generated by a DC motor driving a ball-bearing screw.

References Cited

Liu H.-P., R. E. Warrick, R. E. Westerlund, J. B. Fletcher, and G. L. Maxwell, 1988, An air-powered impulsive shear-wave source with repeatable signals, *Bull. Geol. Soc. Am.,* , **78**, 355–369.

Liu, H.-P., 1989, Calculation of zero-offset vertical seismic profiles generated by a horizontal point force acting on the surface of an anelastic half-space, submitted to *Bull. Seismol. Soc. Am.*.

Report

Liu, H.-P., 1989, A method for determining shear-wave anelastic attenuation using the inhole configuration, *Geophysics*, in press.

Scaling of Seismic Sources

9910-04488

Art McGarr and John Bicknell
Branch of Engineering Seismology and Geology
345 Middlefield Road, MS 977
Menlo Park, California 94025
(415) 329-5645 or (415) 329-5625

Investigations

Seismic source parameters measured from surface records are compared to those from underground records in deep South Africa's gold mines to determine whether reported scaling transitions are a consequence of wave propagation or are due to corresponding scaling changes in the source processes.

Results

1) Source parameters from surface records of events with moment magnitude less than 3 have been contaminated by wave propagation effects. These attenuation and site effects lead directly to the strong scaling changes measured. The underground data indicate a weaker scaling change. When wave propagation effects are removed from the surface records (using either a Green's functions approach or a generalized inversion to separate source and site spectra), the surface results agree with the underground data.

2) A detailed Q structure has been produced by this analysis for both the Klerksdorp and Carletonville mining areas. In both areas, the vast majority of the attenuation is occurring in the near surface. Spectral ratios indicate near surface Q's of well under 100 for both P and S waves. Underground Q's are much higher, of the order of 1500 for both P and S waves. Over the short hypocentral distances to the underground sites, then, wave propagation effects, except for geometric spreading, are almost nil.

3) The fitting of synthetic seismograms to locally-recorded, broad-band, wide dynamic-range seismic data is a very effective means of determining both seismic source parameters and focal mechanisms of mine tremors. Using data from a single three-component surface station, in conjunction with a seismic location network, a comprehensive description of the seismic source process can be obtained by the trial and error calculation of synthetic seismograms, for a point source in a homogeneous half-space, until the ground motion observed at the surface is matched. This methodology was applied to two tremors located in the Vaals Reefs Gold Mine, near Klerksdorp, South Africa, and was used to relate these events to the geological and mining situation in the environs of each hypocenter.

Reports

McGarr, A., and Bicknell, J., 1989, Synthetic seismogram analysis of locally-recorded mine tremors, in Maury, V., and Fourmaintraux D., eds., Rock at great depth, v.3, in press.

Modeling Earthquake Cycles with a State Variable Friction Law

9910-04475

Paul G. Okubo

Branch of Engineering Seismology and Geology
U. S. Geological Survey
345 Middlefield Road, Mail Stop 977
Menlo Park, California 94025
(415)329-5682

Investigations

Calculations of theoretical models of dynamic rupture on faults governed by laboratory-derived rate- and state-dependent frictional fault constitutive relations. The effects of variable fault initial stress distributions and fault properties on rupture behavior and seismic radiation are considered.

Results

1. Computer programs to compute and display far-field seismic radiation have been completed.

2. Rupture models that demonstrate the effects of non-uniform initial stress and non-uniform fault state, and fault roughness have been computed. The findings are:
   a. Strong non-uniformity of initial stress is associated with lower-average rupture velocity. In the models calculated, spectral content of seismic radiation is closely associated with properites of the stress nonuniformity.
   b. Initial fault state can be interpreted loosely in terms of fault strength. When a seismological asperity is surrounded by stronger fault regions, *i. e.*, when fault state is higher outside of the asperity, dynamic overshoot of the rupture of the asperity is reduced. The overall spectral shape is affected: seismic moment is smaller and high frequency spectral content is greater than that for the rupture of the same asperity, when the entire fault including the asperity is assigned the same value of fault state variable.
   c. Seismic radiation from rupture on a rougher fault is lower in high-frequency spectral content than from smoother faults. There is a source f_{max} which is related to fault roughness.

Reports

Okubo, Paul G., Body wave pulse shapes from in-plane shear ruptures with state variable friction (abstract), submitted to 1989 Fall Meeting of the American Geophysical Union.

INDEX 1

INDEX ALPHABETIZED BY PRINCIPAL INVESTIGATOR

INDEX 2

INDEX ALPHABETIZED BY INSTITUTION

U.S. Geological Survey	Mueller, C. S.	438
U.S. Geological Survey	Nelson, A. R.	441
U.S. Geological Survey	Nishenko, S. P.	525
U.S. Geological Survey	Oaks, S. D.	444
U.S. Geological Survey	Obermeier, S. F.	92
U.S. Geological Survey	Okubo, P. G.	569
U.S. Geological Survey	Oppenheimer, D. H.	203
U.S. Geological Survey	Park, R. B.	445
U.S. Geological Survey	Person, W. J.	536
U.S. Geological Survey	Peterson, J.	527
U.S. Geological Survey	Prentice, C.	138
U.S. Geological Survey	Prescott, W. H.	213
U.S. Geological Survey	Reasenberg, P. A.	217
U.S. Geological Survey	Robertson, E. C.	365
U.S. Geological Survey	Roeloffs, E.	221
U.S. Geological Survey	Safak, E.	556
U.S. Geological Survey	Sass, J. H.	373
U.S. Geological Survey	Sato, M.	223
U.S. Geological Survey	Schwartz, D. P.	491
U.S. Geological Survey	Schwartz, D. P.	493
U.S. Geological Survey	Segall, P.	317
U.S. Geological Survey	Sharp, R. V.	99
U.S. Geological Survey	Shaw, H. R.	378
U.S. Geological Survey	Silverman, S.	319
U.S. Geological Survey	Simpson, R. W.	385
U.S. Geological Survey	Sims, J. D.	321
U.S. Geological Survey	Sipkin, S. A.	528
U.S. Geological Survey	Spence, W.	531
U.S. Geological Survey	Stein, R. S.	323
U.S. Geological Survey	Stewart, S. W.	39
U.S. Geological Survey	Stover, C. W.	533
U.S. Geological Survey	Stuart, W. D.	386
U.S. Geological Survey	Taggart, J. N.	539
U.S. Geological Survey	Tinsley, J. C.	466
U.S. Geological Survey	Unger, J. D.	468
U.S. Geological Survey	Van Schaack, J.	48
U.S. Geological Survey	Varnes, D. J.	471
U.S. Geological Survey	Weaver, C. S.	49
U.S. Geological Survey	Weems, R. E.	105
U.S. Geological Survey	Yerkes, R. F.	499
U.S. Geological Survey	Zirbes, M.	540
U.S. Geological Survey	Zoback, M. L.	237
Utah State University	McCalpin, J.	140
Utah, University of	Arabasz, W. J.	4
Utah, University of	Arabasz, W. J.	501
Utah, University of	Bruhn, R. L.	338
Utah, University of	Schuster, G. T.	446
Utah, University of	Smith, R. B.	101
Washington, University of	Bourgeois, J.	119
Washington, University of	Crosson, R. S.	8
Washington, University of	Crosson, R. S.	57
Wayne State University	Dusseau, R. L.	477
Woodward-Clyde Consultants	Sen, M. K.	452
Woodward-Clyde Consultants	Somerville, P.	462

★U.S. GOVERNMENT PRINTING OFFICE: 1990 -786- 58739103